

Hanford Double-Shell Tank Thermal and Seismic Project - Buckling Evaluation Methods and Results for the Primary Tanks

TC Mackey

Richland, WA 99352

U.S. Department of Energy Contract DE-AC27-99RL14047

EDT/ECN: ECN-724428 -R0 UC:

Cost Center: Charge Code:

B&R Code: Total Pages: 304

Key Words: Double-Shell Tank, Tanks, DST, Seismic, Thermal, Buckling, J Bolt.

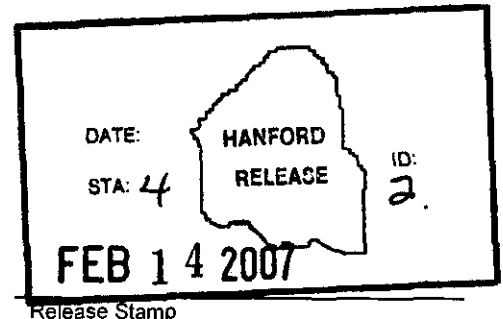
Abstract: This revision is to include the independent reviewer comments shown in Appendix D. Revisions to the buckling analyses in response to the review comments are contained in this Executive Summary and in Sections 5.6, 6.3, 6.4.1, 6.4.3, 7.1, 7.2, and 8.0 of this report.

TRADEMARK DISCLAIMER. Reference herein to any specific commercial product, process, or service by trade name, trademark, manufacturer, or otherwise, does not necessarily constitute or imply its endorsement, recommendation, or favoring by the United States Government or any agency thereof or its contractors or subcontractors.


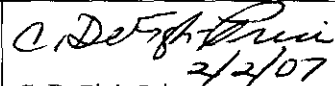
Printed in the United States of America. To obtain copies of this document, contact: Document Control Services, P.O. Box 950, Mailstop H6-08, Richland WA 99352, Phone (509) 372-2420; Fax (509) 376-4989.

RE JAL
Release Approval

2-14-2007
Date



Approved For Public Release

Tank Farm Contractor (TFC) RECORD OF REVISION		(1) Document Number: RPP-RPT-28967	Page 1
(2) Title: Hanford Double-Shell Tank Thermal and Seismic Project – Buckling Evaluation Methods and Results for Primary Tank			
Change Control Record			
(3) Revision	(4) Description of Change – Replace, Add, and Delete Pages	Authorized for Release	
		(5) Resp. Engr. (print/sign/date)	(6) Resp. Mgr. (print/sign/date)
1 RS	Incorporate ECN-724428 Rev. 0	 TC Mackey 2/2/07	 C. DeFigh-Price 2/2/07

SUBCONTRACTOR CALCULATION REVIEW CHECKLIST

Page 1 of 1

Subject: Hanford Double-Shell Tank Thermal and Seismic Project – Buckling Evaluation Methods and Results for the Primary Tank

The subject document has been reviewed by the undersigned.
The reviewer reviewed and verified the following items as applicable.

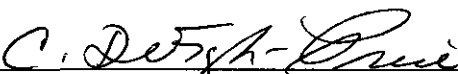
Documents Reviewed: RPP-RPT-28967 Rev. 1

Analysis Performed By: M. Rinker et.al.

- Design Input
- Basic Assumptions
- Approach/Design Methodology
- Consistency with item or document supported by the calculation
- Conclusion/Results Interpretation
- Impact on existing requirements
- _____

TC Mackey 
Reviewer (Print/Sign)

2/1/07
Date

C. DeFigh-Price 
Organizational Manager (Print/Sign)

2/1/2007
Date

**Pacific Northwest
National Laboratory**

Operated by Battelle for the
U.S. Department of Energy

Hanford Double-Shell Tank Thermal and Seismic Project – Buckling Evaluation Methods and Results for the Primary Tanks

K. I. Johnson J. E. Deibler
S. P. Pilli M. W. Rinker
N. K. Karri

January 2007

Prepared for
CH2M HILL Hanford Group, Inc.
in Support of the
Double-Shell Tank Integrity Program



Prepared for the U.S. Department of Energy
under Contract DE-AC05-76RL01830

DISCLAIMER

This report was prepared as an account of work sponsored by an agency of the United States Government. Neither the United States Government nor any agency thereof, nor Battelle Memorial Institute, nor any of their employees, makes **any warranty, express or implied, or assumes any legal liability or responsibility for the accuracy, completeness, or usefulness of any information, apparatus, product, or process disclosed, or represents that its use would not infringe privately owned rights.** Reference herein to any specific commercial product, process, or service by trade name, trademark, manufacturer, or otherwise does not necessarily constitute or imply its endorsement, recommendation, or favoring by the United States Government or any agency thereof, or Battelle Memorial Institute. The views and opinions of authors expressed herein do not necessarily state or reflect those of the United States Government or any agency thereof.

PACIFIC NORTHWEST NATIONAL LABORATORY

operated by

BATTELLE

for the

UNITED STATES DEPARTMENT OF ENERGY

under Contract DE-AC05-76RL01830



This document was printed on recycled paper.

Hanford Double-Shell Tank Thermal and Seismic Project – Buckling Evaluation Methods and Results for the Primary Tanks

K. I. Johnson J. E. Deibler
S. P. Pilli M. W. Rinker
N. K. Karri

January 2007

Prepared for
CH2M HILL Hanford Group, Inc.
in Support of the
Double-Shell Tank Integrity Program

Pacific Northwest National Laboratory
Richland, Washington 99352

Executive Summary

This report documents a detailed buckling evaluation of the primary tanks in the Hanford double-shell waste tanks (DSTs), which is part of a comprehensive structural review for the Double-Shell Tank Integrity Project. This work also provides information on tank integrity that specifically responds to concerns raised by the Office of Environment, Safety, and Health (ES&H) Oversight (EH-22) during a review of work performed on the double-shell tank farms and the operation of the aging waste facility (AWF) primary tank ventilation system.

The current buckling review focuses on the following tasks:

- Evaluate the potential for progressive J-bolt failure and the appropriateness of the safety factors that were used for evaluating local and global buckling. The analysis will specifically answer the following questions:
 - Can the EH-22 scenario develop if the vacuum is limited to -6.6-inch water gage (w.g.) by a relief valve?
 - What is the appropriate factor of safety required to protect against buckling if the EH-22 scenario can develop?
 - What is the appropriate factor of safety required to protect against buckling if the EH-22 scenario cannot develop?
- Develop influence functions to estimate the axial stresses in the primary tanks for all reasonable combinations of tank loads, based on detailed finite element analysis. The analysis must account for the variation in design details and operating conditions between the different DSTs. The analysis must also address the imperfection sensitivity of the primary tank to buckling.
- Perform a detailed buckling analysis to determine the maximum allowable differential pressure for each of the DST primary tanks at the current specified limits on waste temperature, height, and specific gravity.

Based on the J-bolt loads analysis and the small deformations that are predicted at the unfactored limits on vacuum and axial loads, it is very unlikely that the EH-22 scenario (i.e., progressive J-bolt failure leading to global buckling of the tank under increased vacuum) could occur.

Based on the buckling analysis contained in this report, the current limits on the maximum vacuum level of 6-inch w.g. for the AY, AZ, SY, AN, and AW tanks and 12-inch w.g. for the AP tanks are acceptable given the current lack of corrosion in the tanks and the expectation that the maximum waste temperature will not exceed 250°F. These limits are predicated on maintaining the minimum allowable waste level at 6 inches for the AY, AZ, SY, AN, and AW tanks and 12 inches for the AP tanks to preclude bottom uplift from occurring. For this analysis, the occurrence of maximum tank vacuum was classified as a service level C, emergency load condition.

Previous buckling evaluations of the double-shell primary tanks used the analysis method in ASME Code Case N-284-1, which is based on the buckling of a constant thickness cylindrical shell with unsupported length, L . The cylindrical shells of the DST primary tanks do not have constant wall thicknesses, and they do not have clearly defined lines of support due to the varying wall thicknesses and the upper and lower knuckle geometries.

The present buckling analysis used large displacement finite element analysis to predict the limiting vacuum load for the DST primary tanks under combined axial and vacuum loads. The detailed finite element analysis included models of the AY and AP tanks. The AY results are also representative of the AZ, SY, AW, and AN tanks because they have very similar wall thickness distributions. The current buckling evaluation method uses the ASME NB-3213.25 stiffness reduction method to conservatively estimate the vacuum and axial load limits on the primary tank. Comparison with N-284-1 calculations showed that Pacific Northwest National Laboratory's (PNNL's) large displacement method better accounts for the effect of the wall thickness variation on the limiting vacuum and axial loads. The finite element analysis also predicts that the tank deformations are small at the limit loads and they increase stably at loads beyond the limit loads. A large matrix of analyses was run that covers the expected range of axial forces and vacuum loads on the primary tanks. Influence functions were then fit to the limit load data to allow calculating the limiting vacuum and axial loads for all reasonable combinations of axial load, corrosion allowance, specific gravity, and waste height.

An ANSYS® thermal model was developed that is directly node-to-node compatible with the ANSYS DST structural model. The ANSYS thermal model supports the tank buckling analysis by allowing easy prediction of tank stresses due to different combinations of thermal and operating loads. This capability was required to calculate the allowable net vacuum loads as a function of the waste height and temperature. The ANSYS thermal model includes the effects of radiation and convection in the annulus and the dome space, and the thermal solution compared very closely with the previous TEMPEST thermal results. The two temperature solutions also gave very similar stresses throughout the thermal transient.

Influence functions were also developed to estimate the applied axial force in the primary tank wall, which is required for evaluating buckling of the primary tank. The ANSYS thermal and structural models were used to predict the axial thermal stresses in the wall of the primary tanks for a large matrix of waste height and temperature conditions. Analyses were conducted for both the AY and AP tank models. The axial forces for the applied load components were curve fit to allow estimating total axial force as the sum of the following loads:

- Differential thermal expansion
- Gravity
- Surface loads
- Concrete thermal degradation and creep
- Seismic excitation
- Effect of hydrostatic waste pressure on the confined axial force.

The J-bolts that anchor the primary tank dome to the adjacent concrete dome were evaluated to the methods of ASME Section III, Division 2, Subsection CC-3730, which covers the design of steel liners backed by concrete and their anchorage systems. The axial and shear forces in the J-bolts increase linearly as the axial force in the tank wall increases. The J-bolt forces do not change significantly with the application of increased vacuum. The finite element analysis shows that increasing the vacuum to levels that exceed the current limits by at least a factor of 1.67 will not cause progressive tensile failure of the J-bolts as was postulated by the EH-22 panel. The typical operating load condition includes axial

® ANSYS is a registered trademark of ANSYS, Inc., Canonsburg, Pennsylvania.

compression in the wall of the primary tanks. Under these conditions, the finite element analysis shows that all the J-bolts are in compression whether they are at or away from the buckling instability (wrinkle).

Therefore, under typical operating conditions, J-bolt pullout cannot occur as was postulated by the EH-22 panel. The maximum J-bolt shear and axial forces are observed in the outer ring of J-bolts near the haunch for both the AY and AP primary tanks.

For the unlikely case of zero axial compression, the J-bolts are under a small amount of tension due to increasing vacuum and the Poisson's effect associated with the tensile hoop stress from the hydrostatic waste pressure. The combined loads were calculated to be less than 30% of the allowable loads for all cases considered in this review.

The more probable failure mode is shear failure of the outermost J-bolts. Table 6.5 in Chapter 6 of this report shows that the only case where the shear reaction force is predicted to exceed the J-bolt load limit is for the AY tank with no corrosion at a waste temperature of 350°F. However, the tank waste is not expected to exceed 200°F during future operations. If the calculations are repeated for a conservative maximum future temperature of 250°F, then the J-bolt shear demand/capacity ratio is only 0.81. Therefore, it is not expected that the combined operating and seismic loads will jeopardize the structural integrity of any of the J-bolts. Since the J-bolts are not predicted to fail, then it is highly unlikely that the EH-22 scenario could occur.

A buckling evaluation was also performed to calculate the allowable vacuum limits for the DST primary tanks. The safety factors for the ASME Section III service levels are applied to calculate the allowable tank vacuum limits. Each service level has required factors of safety for local and global buckling:

	Factors of Safety	
	Local Buckling	Global Buckling
Level A = Normal operating conditions	2.0	2.4
Level B = Upset conditions	2.0	2.4
Level C = Emergency conditions	1.67	2.0
Level D = Faulted conditions	1.34	1.61

An Excel™ spreadsheet was constructed to perform the above calculations and apply the safety factors. The spreadsheet was used to evaluate each of the DST primary tanks for their current operating conditions (waste temperature, height, and SpG) and corrosion allowances of 0.000, 0.060, and 0.100 inch. The calculated vacuum limits for the specified 0.060 inch corrosion allowance are greater than the current vacuum limits for all of the tanks except the AP tanks. The current AP vacuum allowable is 12-inch w.g. compared to the calculated allowable of 10.53 inch w.g. This vacuum limit is based on global buckling assuming a minimum waste height of 12 inches. The calculations show that although the AP tank is slightly thicker in the upper tank wall, this is not enough to double the vacuum limit compared to the other tanks.

Additional cases were analyzed with corrosion levels from 0.000 to 0.120 inches and a more realistic maximum waste temperature of 250°F for future operations. The calculated allowable vacuum limits for the AY, AZ, SY, AW, and AN tanks are above the current vacuum limit of 6 inch w.g. for all the cases. The allowable vacuum limit for the AP tank is above the current 12-inch w.g. limit for corrosion allowances of 0.000 to 0.025 inches. Therefore, the minimum wall thickness for buckling in the AP tanks is estimated to be 0.475 inch in the upper section of the primary tank wall.

The corrosion allowance for the AY, AZ, SY, AW, and AN tanks was also increased to identify the maximum value where the calculated vacuum limit was nearly equal to the 6-inch w.g. vacuum limit. The maximum allowable corrosion for these tanks was estimated to be 0.120 inch. Therefore, the minimum wall thickness for buckling in these tanks is estimated to be 0.255 inch in the thinnest upper section of the primary tank wall.

The spreadsheet provides a convenient tool for quickly calculating the applied loads, the vacuum and axial load limits, and the code-based allowable vacuum loads. The buckling evaluation method contained in this work uses curve fitting to condense many detailed analyses into a quick evaluation tool. As such, it includes necessary conservatism in the influence functions to ensure that the applied loads are not under-predicted or that the unfactored vacuum limit is not over-predicted for the range of input parameters that define the tanks. In addition, the ASME stiffness reduction method used to calculate the limiting vacuum and the axial loads is also judged to be conservative. The finite element results show that the unscaled tank deformations are barely visible on the tank geometry at the ASME limits for vacuum and axial loads. The models also predict that stable deformation will occur beyond these limits. Therefore, the buckling evaluation tool provides a conservative evaluation of the DST primary tanks. In cases where the calculated allowable vacuum is predicted to be below the current vacuum limit, then additional, more detailed analysis would be required to qualify the tank for the higher vacuum limit.

Tank farms operations staff recently reviewed all of the Occurrence Reports from 1990 to the present. This information will be released in the next revision of RPP-11413, *Technical Basis for the Ventilation Requirements Contained in Tank Farm Operating Specifications Documents*, authored by L. Payne. No incidents were found where the primary tank differential vacuum has exceeded the 6-inch w.g. maximum. Therefore, not only are the tanks able to withstand the expected loads without buckling, there are no recorded occurrences where the maximum vacuum has been achieved. There are also safety systems and operating procedures in place to ensure that the maximum vacuum loads are not achieved in future operations.

Subsequent to the initial publication of this report, an independent review of the Double-Shell Tanks (DST) Thermal and Operating Loads Analysis (TOLA) combined with the Seismic Analysis was conducted by Dr. Robert P. Kennedy of RPK Structural Mechanics Consulting and Dr. Anestis S. Veletsos of Rice University. Revision 1 is being issued to document their review and to address their comments. The results of these clarifications and additional analyses do not affect the conclusions of the original report. The independent reviewer comments are included in Appendix D. Revisions to the buckling analyses in response to the review comments are contained in this Executive Summary and in Sections 5.6, 6.3, 6.4.1, 6.4.3, 7.1, 7.2, and 8.0 of this report.

Appendixes A, B, and C contain examples of the ANSYS finite element model input files used in this study.

Appendix E contains an independent review of the methods used to calculate the vacuum limits on the DST waste primary tanks. The review specifically confirms the correct calculation of the axial tank force, the unfactored vacuum limit at incipient buckling, and the application of the safety factors for the ASME Service Levels A, B, C, and D.

Appendix F summarizes buckling evaluations from the body of this report that address the resistance of the Hanford double-shell waste primary tanks to buckling when in the full condition. These results were compiled in response to a question by CH2M HILL staff regarding the potential for primary tank buckling to occur when the tank is full and being drawn down during waste treatment efforts.

Contents

Executive Summary	iii
1.0 Introduction and Background	1.1
1.1 Background and Findings.....	1.1
1.2 Organization of the Buckling Evaluation Report	1.2
2.0 Assessment of Buckling Evaluation Methods for the DST Primary Tanks.....	2.1
2.1 ASME Code Case N-284-1 Method for Evaluating DST Primary Tank Buckling.....	2.1
2.2 Sensitivity of Critical Buckling Loads to the Size and Number of Tank Imperfections....	2.11
3.0 Buckling Evaluation Method for the DST Primary Tanks Based on Large Displacement Instability Analysis	3.1
3.1 Vacuum Limit Equations for the AY Primary Tank	3.13
3.2 Vacuum Limit Equations for the AP Primary Tank	3.19
3.3 Comparison of Buckling Evaluations Using ASME N-284-1 and the DST Primary Tank Specific Method	3.21
4.0 ANSYS Thermal Model of the Double-Shell Waste Tanks	4.1
4.1 Comparison of Previous Double-Shell Tank Thermal Models	4.1
4.1.1 TEMPEST Model.....	4.1
4.1.2 GOTH_SNF Model	4.2
4.1.3 P/THERMAL Model.....	4.5
4.1.4 Summary of the Previous DST Thermal Models and the Objectives of the Buckling Analysis	4.5
4.2 ANSYS Thermal Model.....	4.6
4.3 Comparison of the ANSYS and TEMPEST Results.....	4.8
4.4 Calculated Boiling Temperatures for the Different Double-Shell Waste Tanks.....	4.13
5.0 Influence Functions for Calculating the Applied Axial Force on the Primary Tank Wall	5.1
5.1 Axial Compression in the Primary Tank Wall Due to Concrete Thermal Degradation and Creep	5.2
5.2 Differential Thermal Expansion Forces for Current Operating Conditions	5.5
5.3 Axial Load Components Due to Gravity.....	5.9
5.4 Axial Load Components Due to Surface Loads	5.9
5.5 Axial Load Component Due to Waste Hydrostatic Pressure	5.11
5.6 Axial Load Component Due to Seismic Excitation	5.12
5.7 The Total Axial Force in the Primary Tank Wall	5.13
6.0 Evaluating the J-Bolt Anchors Under Axial Tank Compression, Vacuum, and Seismic Loads	6.1
6.1 J-Bolt Evaluation Criteria.....	6.1
6.2 J-Bolt Force Evaluation.....	6.3
6.2.1 AY Tank with 0.3-Inch Wall Foreshortening and a 25-Inch Waste Height.....	6.5

6.2.2	AY Tank with No Tank Wall Foreshortening and 25 Inches of Waste	6.8
6.2.3	AY Tank with No Tank Wall Compression and 400 Inches of Waste.....	6.12
6.2.4	AP Tank with 0.3 Inches of Tank Wall Foreshortening and 25 Inches of Waste	6.14
6.2.5	AP Tank with 0.0 Inches of Tank Wall Foreshortening and 25 Inches of Waste	6.15
6.2.6	AP Tank with 0.0 Inches of Tank Wall Foreshortening and 400 Inches of Waste	6.16
6.3	Correlating J-Bolt Limit Loads with the Equivalent Linear Elastic Axial Force in the Primary Tank Wall	6.18
6.4	Addressing the EH-22 Findings on the Potential for Progressive J-Bolt Failure and the Appropriate Safety Factors for Evaluating Local and Global Buckling.....	6.23
6.4.1	Can the EH-22 Scenario Develop if the Vacuum is Limited to -6.6 Inch Water Gage by a Relief Valve?	6.23
6.4.2	What is the Appropriate Factor of Safety Required to Protect Against Buckling if the EH-22 Scenario Can Develop?.....	6.24
6.4.3	What is the Appropriate Factor of Safety Required to Protect Against Buckling if the EH-22 Scenario Cannot Develop?.....	6.24
7.0	Buckling Evaluation of the DST Primary Tanks	7.1
7.1	Elastic Buckling	7.1
7.2	Plastic Buckling	7.8
8.0	Summary and Conclusions	8.1
9.0	References	9.1
	Appendix A – Seismic Model Primary Tank Knuckle Stress Evaluation.....	A.1
	Appendix B – Description of ACI-349 Demand/Capacity Calculations	B.1
	Appendix C – Software Acceptance	C.1
	Appendix D – Reviewer Comments and Discussion	D.1
	Appendix E – Independent Confirmation of PNNL’s Use of N-284-1 Safety Factors in Computing the Double-Shell Primary Tank Allowable Vacuum Level Governed by Buckling.....	E.1
	Appendix F – Buckling Resistance of the DST Primary Tanks Under Internal Vacuum When in the Full Condition	F.1

Figures

2-1	Cross-Section View of the Hanford DST Primary Tank Designs	2.2
2-2	Predicted First Eigenvalue Buckling Mode for a Uniform Cylinder with Fixed Displacements, Added at the Top and Bottom Edges of the Cylinder	2.4
2-3	Predicted First Eigenvalue Buckling Mode for the AY Primary Tank Geometry with Fixed Displacements at the Tangent Points of the Top and Bottom Knuckles	2.5
2-4	Predicted First Eigenvalue Buckling Mode for the AY Primary Tank Geometry with Fixed Displacements and Rotations at the Tangent Points of the Top and Bottom Knuckles	2.5
2-5	Predicted First Eigenvalue Buckling Mode for a Uniform Cylinder Loaded with External Pressure and Fixed Displacements, Added at the Top and Bottom Edges of the Cylinder	2.8
2-6	Predicted First Eigenvalue Buckling Mode for a DST Cylinder with External Pressure Loading, Plus Fixed Displacements, Added at the Top and Bottom Edges of the Cylinder	2.9
2-7	Predicted First Eigenvalue Buckling Mode for a Uniform Cylinder with Fixed Displacements, Added at the Top and Bottom Edges of the Cylinder	2.10
2-8	Predicted First Eigenvalue Buckling Mode for a DST Cylinder with Fixed Displacements, Added at the Top and Bottom Edges of the Cylinder	2.10
2-9	Uniform Cylinder with Imperfections	2.13
2-10	AY Tank with Imperfections	2.13
3-1	Double-Shell Primary Tank Model Used in the Large Deflection Buckling Analysis	3.2
3-2	Loads Applied to the Large Deflection Buckling Model	3.2
3-3	Effect of Increasing Dome Load on the Axial Stress in the AY Primary Tank	3.3
3-4	Load Deflection Curve for Increasing Vacuum Load Applied to the Large Displacement Tank Buckling Model	3.3
3-5	Displaced Shape of the AY Model at the Limit Vacuum Defined by the ASME Slope Reduction Method	3.5
3-6	Contour Plot of the Maximum Surface Stress in the Upper Knuckle of the AY Tank	3.5
3-7	Stress Strain Curves for A515-65 Steel	3.8
3-8	Load Deflection Curves of the AY and AP Primary Tanks Under Axial Compression Alone	3.9
3-9	Surface Stress in the Upper Knuckle Region of the AY Tank at the Maximum Axial Compressive Load	3.9
3-10	Surface Stress in the Upper Knuckle Region of the AY Tank at a Dome Deflection = 1.0 Inch	3.10
3-11	Load Deflection Curves for the AY Primary Tank Under Axial Compression for a Range of Yield Strengths and Wall Thicknesses in the Nominal 0.5 Inch Wall Section	3.11
3-12	Nonlinear Load Deflection Curves for the AY Tank Plus the Linear Elastic Projected Stiffness, Showing the Definition of the Equivalent Linear Elastic Compressive Force	3.11
3-13	Nonlinear Load Deflection Curves for the AP Tank Plus the Linear Elastic Projected Stiffness, Showing the Definition of the Equivalent Linear Elastic Compressive Force	3.12

3-14	Calculated Vacuum Limit Versus Waste Heights for a Range of Axial Compressive Loads	3.13
3-15	Axial Compression Scale Factor of Adjusting the Vacuum Limit for the AY Primary Tank.....	3.14
3-16	Wall Thickness Scale Factor for the AY Tank	3.15
3-17	Specific Gravity Scale Factor for the AY Tank	3.16
3-18	Comparison of the Analytical Equations for Vacuum Limit with the Discrete Valued Predicted with Large Deformation Finite Element Analysis.....	3.17
3-19	Effect of Wall Thickness and Yield Strength on the Axial Limit Load for the AY Primary Tank.....	3.18
3-20	Effect of Wall Thickness on the Axial Limit Load for the AP Primary Tank.....	3.18
3-21	Typical Displacement Shape of the AY and AP Primary Tanks at the Axial Limit Load	3.19
3-22	Comparison of the PNNL Large Displacement Buckling Evaluation Method with the ASME N-284-1 Method	3.22
3-23	Comparison of the PNNL Large Displacement Buckling Evaluation Method with the ASME N-284-1 Method	3.22
3-24	Comparison of the PNNL Large Displacement Buckling Evaluation Method with the ASME N-284-1 Method	3.23
4-1	TEMPEST DST Model Configuration.....	4.2
4-2	GOTH_SNF DST Model Configuration	4.3
4-3	P/THERMAL DST Model Configuration	4.4
4-4	Example Waste Temperature Transient Showing the Limiting Waste Surface Temperature.....	4.9
4-5	TEMPEST Temperatures Mapped onto the ANSYS DST Model	4.9
4-6	ANSYS Thermal Solution with Bulk Waste and Waste Surface Boundary Temperatures.....	4.10
4-7	ANSYS Contour Plot Showing Temperatures Around and Beneath the Tank for a Waste Depth of 422 Inches.....	4.10
4-8	ANSYS Contour Plot Showing Temperatures Around and Beneath the Tank for a Waste Depth of 144 Inches.....	4.11
4-9	Comparison of the TEMPEST and ANSYS Temperature Predictions at the Inside Surface of the Concrete Tank	4.11
4-10	Comparison of the TEMPEST and ANSYS Temperature Predictions at the Outside Surface of the Concrete Tank	4.12
4-11	Comparison of Maximum Meridional Membrane Stresses During Heatup for the TEMPEST and ANSYS Temperature Distributions	4.12
4-12	Vapor Pressure Data Used to Estimate the Boiling Temperature of Different Tank Wastes	4.14
5-1	Relationship of Maximum Axial Thermal Expansion Force During the Heatup Cycle in the AY Primary Tank Wall for a Range of Waste Heights and Temperatures.....	5.6
5-2	Relationship of the Steady State Axial Thermal Expansion Force in the AY Primary Tank Wall for a Range of Waste Heights and Temperatures	5.7
5-3	Relationship of the Maximum Axial Thermal Expansion Force During the Heatup Cycle in the AP Primary Tank Wall for a Range of Waste Heights and Temperatures	5.8

5-4	Relationship of the Steady State Axial Thermal Expansion Force in the AP Primary Tank Wall for a Range of Waste Heights and Temperatures	5.9
5-5	Comparison of the Axial Force Components in the AY Primary Tank Wall Due to the Different Tank Loads	5.10
5-6	Comparison of the Axial Force Components in the AY Primary Tank Wall Due to the Different Tank Loads	5.10
5-7	Axial Force in the Primary Tank Wall Due to Waste Hydrostatic Pressure.....	5.11
5-8	Effect of Specific Gravity on Axial Force in the AY Tank Wall	5.12
5-9	Meridional (axial) Membrane Stress in the AY Tank Wall for the Four Different Combinations of Soil and Concrete Properties.....	5.13
5-10	Stiffness Scale Factors to Estimate the Seismic Axial Force for the AY and AP Tanks with Different Corrosion Allowances.....	5.14
6-1	Buckling Model Showing the Location of the J-Bolts Attached to the Tank Dome	6.2
6-2	Axial Force Variation Along the Outermost J-Bolt Circle for Increasing Tank Wall Foreshortening.....	6.5
6-3	Shear Force Variation Along the Outermost J-Bolt Circle for Increasing Tank Wall Foreshortening.....	6.6
6-4	Axial Force Variation Along the Outermost J-Bolt Circle with Increasing Vacuum Load and a Constant Wall Foreshortening of 0.3 Inch	6.6
6-5	Shear Force Variation Along the Outer Ring of J-Bolts with Increasing Tank Vacuum and a Constant Wall Foreshortening of 0.3 Inch	6.7
6-6	J-Bolt Axial Load Histories for Increasing Tank Wall Foreshortening Followed by Increasing Vacuum Load.....	6.7
6-7	J-Bolt Shear Load Histories for Increasing Tank Wall Foreshortening Followed by Increasing Vacuum Load.....	6.8
6-8	Axial Force Variation Along the Outermost J-Bolt Circle as a Function of Internal Vacuum for Zero Axial Foreshortening	6.9
6-9	Shear Force Variation Along the Outermost J-Bolt Circle as a Function of Internal Vacuum for Zero Axial Foreshortening	6.9
6-10	Combined Tensile and Shear J-Bolt Force Evaluation for the Case with Zero Axial Compression and Increasing Vacuum Load.....	6.10
6-11	Axial Force Histories for Zero Axial Compression and Increasing Vacuum Load.....	6.10
6-12	Shear Force Histories for Zero Axial Compression and Increasing Vacuum Load	6.11
6-13	Combined Tensile and Shear J-Bolt Force Evaluation for the Case with Zero Axial Compression and Increasing Vacuum Load.....	6.11
6-14	Axial Force Histories for Zero Axial Compression, 400-Inch Waste Height, and Increasing Vacuum Load.....	6.12
6-15	Shear Force Histories for Zero Axial Compression, 400-Inch Waste Height, and Increasing Vacuum Load.....	6.13
6-16	Combined Tensile and Shear J-Bolt Force Evaluation for the Case with Zero Axial Compression, 400-Inch Waste Height, and Increasing Vacuum Load.....	6.13
6-17	Axial Force Histories for the AP Tank with 0.3 Inch Axial Compression, 25-Inch Waste Height, and Increasing Vacuum Load	6.14

6-18	Shear Force Histories for the AP Tank with 0.3 Inch Axial Compression, 25-Inch Waste Height, and Increasing Vacuum Load	6.14
6-19	Axial Force Histories for the AP Tank with Zero Axial Compression, 25-Inch Waste Height, and Increasing Vacuum Load	6.15
6-20	Shear Force Histories for the AP Tank with Zero Axial Compression, 25-Inch Waste Height, and Increasing Vacuum Load	6.15
6-21	Combined Shear and Axial Forces for the AP Tank with Zero Axial Compression, 25-Inch Waste Height, and Increasing Vacuum Load	6.16
6-22	Axial Force Histories for the AP Tank with Zero Axial Compression, 400-Inch Waste Height, and Increasing Vacuum Load	6.17
6-23	Shear Force Histories for the AP Tank with Zero Axial Compression, 400-Inch Waste Height, and Increasing Vacuum Load	6.17
6-24	Combined Loads for the AP Tank with Zero Axial Compression, 400-Inch Waste Height, and Increasing Vacuum Load	6.18
6-25	J-Bolt Shear and Axial Force Distributions for the AY and AP Tanks	6.19
6-26	J-Bolt Shear Force Due to Horizontal and Vertical Seismic Loads	6.19
6-27	Maximum J-Bolt Force vs. the Equivalent Linear Elastic Axial Force for the AY Tank with Corrosion Allowances of 0.00, 0.06 and 0.10 Inches	6.20
6-28	Maximum J-Bolt Force vs. the Equivalent Linear Elastic Axial Force for the AP Tank with a Corrosion Allowance of 0.000 Inches	6.21
6-29	Maximum J-Bolt Force vs. the Equivalent Linear Elastic Axial Force for the AP Tank with a Corrosion Allowance of 0.060 Inches	6.22
6-30	Maximum J-Bolt Force vs. the Equivalent Linear Elastic Axial Force for the AP Tank with a Corrosion Allowance of 0.100 Inches	6.22
7-1	The Axial Distribution of Hoop Stress in the Primary Tank Wall Due to Thermal + Operating + Seismic Loads	7.9

Tables

2-1	Summary of Design Data and Operating Limits for the DST Primary Tanks.....	2.2
2-2	Comparison of Eigenvalue Critical Buckling Loads for the Approximate Uniform Cylinder and the AY Primary Tank Geometry.....	2.4
2-3	Summary of the Eigenvalue Buckling Comparisons of the Uniform Cylinder and the DST Primary Tank Geometry for Axial, Hoop, and Combined Axial and Hoop Loads.....	2.7
2-4	Comparison of the Construction Imperfection Tolerances Specified in ASME NE-4220 and the AY Tank Construction Specifications	2.12
2-5	Matrix of Imperfection Sizes That were Simulated.....	2.12
2-6	Summary of the Critical Buckling Loads for the Sensitivity Study on the Number and Size of the Tank Imperfections.....	2.14
3-1	Large Deformation Tank Analyses for the AY Vacuum Limit Equations	3.6
3-2	Large Deformation Tank Analyses for the AP Vacuum Limit Equations.....	3.7
3-3	Yield Strength at Temperature for the Primary Tank Steels	3.8
3-4	Summary of Maximum Dome Displacements and Maximum Equivalent Linear Elastic Compressive Forces for the AY Primary Tank	3.12
3-5	Summary of Maximum Dome Displacements and Maximum Equivalent Linear Elastic Compressive Forces for the AP Primary Tank	3.13
3-6	Excel® Spreadsheet for Calculating the Vacuum Limit of the AY Primary Tank.....	3.17
3-7	Excel® Spreadsheet for Calculating the Vacuum Limit of the AP Primary Tank	3.20
3-8	Buckling Evaluation Cases for Comparing the N-284-1 Method with the PNNL Large Displacement Buckling Evaluation Method.....	3.21
3-9	ASME N-284-1 Calculated Section Properties and Allowable Stresses	3.21
4-1	Example Vapor Pressure Data from Ogden et al. (2002) for Tank AY-102	4.13
4-2	Estimated Boiling Temperature for the 28 Double-Shell Tanks	4.14
5-1	Load Conditions for the Baseline DST Analysis.....	5.1
5-2	Example Creep and Thermal Degradation Calculations	5.4
5-3	Estimated Axial Force Due to Creep and Thermal Degradation of the Elastic Modulus for a Range of Tank Waste Temperatures and Waste Heights	5.5
5-4	Matrix of Waste Tank Models That were Analyzed to Estimate the Axial Thermal Expansion Forces for the AY Tank Design.....	5.6
5-5	Matrix of Waste Tank Models That were Analyzed to Estimate the Axial Thermal Expansion Forces for the AP Tank Design	5.7
6-1	J-Bolt Force Limits from ASME Section III, Division 2, Subsection CC-3730	6.2
6-2	F_y and F_u Relationships for J-Bolts.....	6.3
6-3	Calculation of the J-Bolt Allowables for Combined Loads and Tension and Shear Only Loads	6.4
6-4	Summary of Allowable J-Bolt Forces for Normal and Abnormal Loads.....	6.5
6-5	Summary of the Applied Equivalent Linear Axial Force and the Maximum Equivalent Linear Axial Forces for the Buckling Evaluation of the Current Operating Limits	6.23

7-1	Calculation of Axial Applied Force for the AY Primary Tank	7.2
7-2	Calculation of Unfactored Vacuum Limit for the AY Primary Tank.....	7.3
7-3	Evaluation of the Allowable Vacuum Limit for the AY Tank Based on the ASME Section III Service Level Safety Factors	7.4
7-4	Summary of the DST Primary Tank Buckling Evaluations for the Specified Maximum Operating Conditions.....	7.5
7-5	Summary of DST Primary Tank Buckling Evaluations for a Range of Corrosion Allowances and Operating Conditions	7.6
7-6	Reevaluation of Plastic Buckling for the DST Primary Tanks.....	7.10

1.0 Introduction and Background

This report documents a detailed buckling evaluation of the primary tanks in the Hanford double-shell waste tanks (DSTs). The analysis is part of a comprehensive structural review for the Double-Shell Tank Integrity Project. This work also provides information on tank integrity that specifically responds to concerns raised by the Office of Environment, Safety, and Health (ES&H) Oversight (EH-22) during a review (in April and May 2001) of work being performed on the double-shell tank farms, and the operation of the aging waste facility (AWF) primary tank ventilation system (CH2M HILL 2002).

1.1 Background and Findings

The EH-22 review team assessed the adequacy of the nuclear facility hazard analysis by performing an essential system review of the AWF primary tank ventilation system. Several concerns with the hazards analyses performed on the AWF tanks were identified with respect to potential non-conservative assumptions in the tank structural analysis, analysis of scenarios involving high efficiency particulate air (HEPA) filter failure, and the potential for tank airlift circulators to over-pressurize tanks and negate the requirement for sub-atmospheric tank operation. With respect to the tank structural analysis for vacuum reported in HNF-1838, *Assessment of Project W-030 Relief Valve Pressure Setting on Internal Vacuum Specification Limits for AY and AZ Tank Farm Primary Tanks* (Julyk 1997), the EH-22 panel had the following findings:

- The AY/AZ tank structural analysis for vacuum conditions is potentially non-conservative. A structural analysis on the AY/AZ primary tanks (the inner shells of the double-shell tanks) determined the ability of the tanks to withstand all negative pressures associated with operation of the ventilation system. A single vacuum relief valve on each tank protects against excessive vacuum and would limit vacuum to -6.6-inch water gage (w.g.). Normal operating vacuum is -1.0- to -3.0-inch w.g.
- The structural analysis was based on an American Society of Mechanical Engineers (ASME) Code Case N-284-1, *Metal Containment Shell Buckling Design Method, Class MC, Section III, Division 1*, that addressed tank buckling due to vacuum (ASME 1995). This Code Case required that the factor of safety used for the local buckling failure mode be increased by 20% when local buckling would lead to a total collapse failure mode. The higher safety factor was not used in the analysis, based on the assumption that total collapse would not occur because the primary tank wall is supported through structural interaction between the primary tank steel shell dome, the secondary tank reinforced concrete dome and connecting embedded J-bolts. The review team identified that this assumption was probably invalid. The load path would initially be only through the outer ring of J-bolts, because the primary tank dome would likely peel away from the underside of the concrete dome because of the downward pull of the buckling sides. Each succeeding inboard bolt circle could assume load only after the outboard bolts had failed, and thus the J-bolt failures would be progressive until complete detachment of the steel dome from the concrete dome, with the resultant total collapse of the primary tank. The J-bolts or their attachments were the unanalyzed weak link in the load path. Therefore, the factor of safety that was used is potentially non-conservative with respect to the ASME Code Case requirements.

The first finding by the EH-22 panel describes the focus of the previous analysis and simply states that it may be non-conservative. No specific recommendations are given in the first finding that require further

analysis or review. The second finding details the panel's concerns regarding non-conservative assumptions in the analysis and it postulates that progressive J-bolt failure may occur which could cause local buckling (and local J-bolt failure) to progress to global buckling. The J-bolts or their attachments were identified as the unanalyzed weak link in the load path.

The allowable vacuum with regard to buckling under combined vacuum and axial stress is sensitive to the compressive axial membrane stress in the tank vertical wall. The axial stress results from: 1) dead loads (soil overburden, concrete structure, and self weight of the primary tank), 2) waste hydrostatic pressure, 3) differential thermal expansion between the primary steel tank and the concrete tank, 4) concrete creep down loads on the primary tank with time, and 5) seismic loads. Variations in these conditions can lead to high axial compressive stress in the primary tank vertical wall. The buckling analysis in Julyk (1997) relied on the tank stresses reported in the ASA Phase III analysis (see Appendix A of Rinker et al. 2004) that considered only a limited number of load cases. Scaling functions were used by Julyk to estimate the tank axial membrane stresses for load combinations other than those specifically evaluated in the Phase III analysis.

Because of the concerns raised by the EH-22 panel and the approximate nature of the stress solutions used in the previous buckling analysis, the current buckling review focuses on the following tanks:

- Evaluate the potential for progressive J-bolt failure and the appropriateness of the safety factors that were used for evaluating local and global buckling. The analysis will specifically answer the following questions:
 - Can the EH-22 scenario develop if the vacuum is limited to -6.6-inch w.g. by a relief valve?
 - What is the appropriate factor of safety required to protect against buckling if the EH-22 scenario can develop?
 - What is the appropriate factor of safety required to protect against buckling if the EH-22 scenario cannot develop?
- Based on detailed finite element analysis, develop influence functions to estimate the axial stresses in the primary tanks for all reasonable combinations of tank loads. The analysis must account for the variation in design details and operating conditions between the different DSTs. These variations include operating temperature, waste level, primary tank material thickness, creep of the secondary concrete tank, secondary tank concrete degradation, waste specific gravity and soil overburden. Note that from a buckling perspective the worst condition is when the waste level is low, the waste specific gravity is low and the temperature is high. Note also that the compressive stresses are secondary, driven by differential thermal expansion and creep down of the concrete. The analysis must also address the imperfection sensitivity of the primary tank to buckling.
- Perform a detailed buckling analysis to determine the maximum allowable differential pressure for each of the DST primary tanks at the current specified limits on waste temperature, height, and specific gravity.

1.2 Organization of the Buckling Evaluation Report

This report is organized in the following manner. Following this Introduction and Background chapter, Chapter 2 compares the buckling analysis method in the ASME Code Case N-284-1 (used in the previous tank buckling analyses) with detailed finite element analysis of the specific geometry of the DST primary

tanks. The analysis also evaluates the sensitivity of the calculated critical buckling loads to the number and size of the geometric imperfections that are assumed.

Chapter 3 presents an alternate buckling evaluation method based on large displacement finite element analysis of the DST primary tanks. Limit values on internal vacuum and axial compression loads are defined using an ASME criterion for establishing structural collapse loads. Influence functions are developed to calculate the unfactored limit loads (vacuum and axial compression) as a function of the applied axial force, corrosion allowance, waste height, and specific gravity. Different influence functions are presented for tanks with thickness distributions comparable to the AY primary tanks (including AZ, SY, AN, and AW) and the AP primary tanks.

Chapter 4 describes the ANSYS thermal model that was developed to provide temperature solutions from which to estimate the differential thermal expansion stresses for different waste heights and temperatures. The modeling methods are checked by comparing the ANSYS temperature solutions with previous results from the TEMPEST code.

Chapter 5 details the development of influence functions for estimating the applied axial forces in the primary tank, which are necessary for estimating the limit vacuum. The influence functions were implemented in Microsoft Excel™ to allow easily estimating the applied force as continuous functions of the tank-specific operating parameters. Separate influence functions were developed for the AY and AP tank thickness distributions.

Chapter 6 presents a detailed analysis of the J-bolt shear and normal forces that are predicted for the possible loading conditions on the primary tank. The analysis estimated the maximum allowable axial compression in the tank wall that corresponds to the J-bolt allowable forces for normal (operating) and abnormal (operating + seismic) loads. Chapter 6 also addresses the concerns of the EH-22 panel and recommends the appropriate safety factors for the buckling analysis.

Chapter 7 uses the buckling criteria developed in Chapter 3 and the influence functions for estimating the applied loads (Chapter 5) to calculate the allowable vacuum loads for each of the DST primary tanks at the currently specified operating limits on waste heights, temperatures and specific gravities.

Chapter 8 summarizes the conclusions of this buckling analysis.

Appendix A contains examples of the ANSYS finite element model input files used in this study.

Appendix B contains the ANSYS input and post processing files for buckling analysis of the AP and AY primary tanks under combined axial compression and vacuum loads.

Appendix C includes ANSYS model input files for estimating the individual contributions of various load components (gravity, surface loads, hydrostatic loads and differential thermal expansion loads) to the total meridional stress in the tank wall. Input files for the ANSYS DST thermal model are contained here.

Appendix D documents an independent review of the Double Shell Tanks (DST) Thermal and Operating Load (TOLA) and Seismic analyses that was conducted by Dr. Robert P. Kennedy of RPK Structural Mechanics Consulting and Dr. Anestis S. Veletsos of Rice University. Their review included an evaluation of the initial release of this report on the potential for buckling of the DST primary tanks.

Appendix E documents an independent review that confirmed the correct calculation of the axial tank force, the unfactored vacuum limit at incipient buckling, and the application of the safety factors for the ASME Service Levels A, B, C, and D.

Appendix F summarizes buckling evaluations from the body of this report that address the resistance of the Hanford double-shell waste primary tanks to buckling when in the full condition. These results were compiled in response to a question by CH2M HILL staff regarding the potential for primary tank buckling to occur when the tank is full and being drawn down during waste treatment efforts.

2.0 Assessment of Buckling Evaluation Methods for the DST Primary Tanks

2.1 ASME Code Case N-284-1 Method for Evaluating DST Primary Tank Buckling

Buckling of the primary tank is of concern due to compressive stresses that occur in both the meridional and hoop directions. Meridional (axial) compression results from differential thermal expansion between the primary tank and the concrete over-structure, plus creep-down of the concrete structure over time. Hoop compression results from net vacuum loads in the tank. These loading conditions (displacement controlled in the meridional direction and load controlled in the hoop direction) are unique compared to the vacuum-induced stresses in typical free-standing storage tanks, and are a direct result of the unique design of the underground double-shell waste storage tanks.

The buckling evaluation method defined in Code Case N-284-1, *Metal Containment Shell Buckling Design Methods*, of the American Society of Mechanical Engineers (ASME) Boiler and Pressure Vessel Code, Section III, Division 1 (ASME 1995) has been used in previous evaluations of the DST primary tanks because it considers the interaction of independent levels of compressive stress in both the meridional and hoop directions. By comparison, the ASME Code Case N-530 method (ASME 1994) that is described in the Brookhaven report, BNL 52361 (Bandyopadhyay et al. 1995), only addresses buckling of thin-walled tanks loaded with hoop tension. The N-530 method is not applicable to tanks subjected to vacuum loads.

The N-284-1 method provides an acceptance criteria with respect to buckling instability for defining the allowable loads for a given tank design. The method is based on theoretical critical buckling loads (hoop and axial limit stresses) that are adjusted by knockdown factors to account for geometric imperfections, the height of the tank, the radius-to-thickness ratio, and material plasticity. The intent of these calculations is to accurately estimate the actual bifurcation buckling load for a specific tank geometry. These loads are then reduced by safety factors (specified for four different service levels) to set the allowable combination of axial compressive load and tank vacuum. The bifurcation buckling solutions and knockdown factors used in N-284-1 are for simplified geometries that are intended to conservatively apply to typical storage tank geometries. This section reviews the analytical basis for N-284-1 and compares the solutions with finite element models that include the specific geometric features of the DST primary tanks.

Although the DST designs vary somewhat between tank farms, the primary tanks typically consist of a 75-foot-diameter by 34-foot-high cylindrical portion that is connected to a flat bottom through a 1-foot-radius lower knuckle (Figure 2-1). The wall thickness of the tank cylinder is graduated to counteract the hydrostatic stress of the contain waste (see Table 2-1). The tanks are capped by a shallow spherical dome that transitions to the cylindrical section through a radiused upper knuckle. The dome is attached to the concrete over-structures with J-bolts that are imbedded in the concrete. The total height of the tank is approximately 46.8 feet.

The formulas presented in Section 1710 of ASME Code Case N-284-1 are based on the buckling of a constant thickness cylindrical shell with an unsupported length, L . The length, L , is defined between

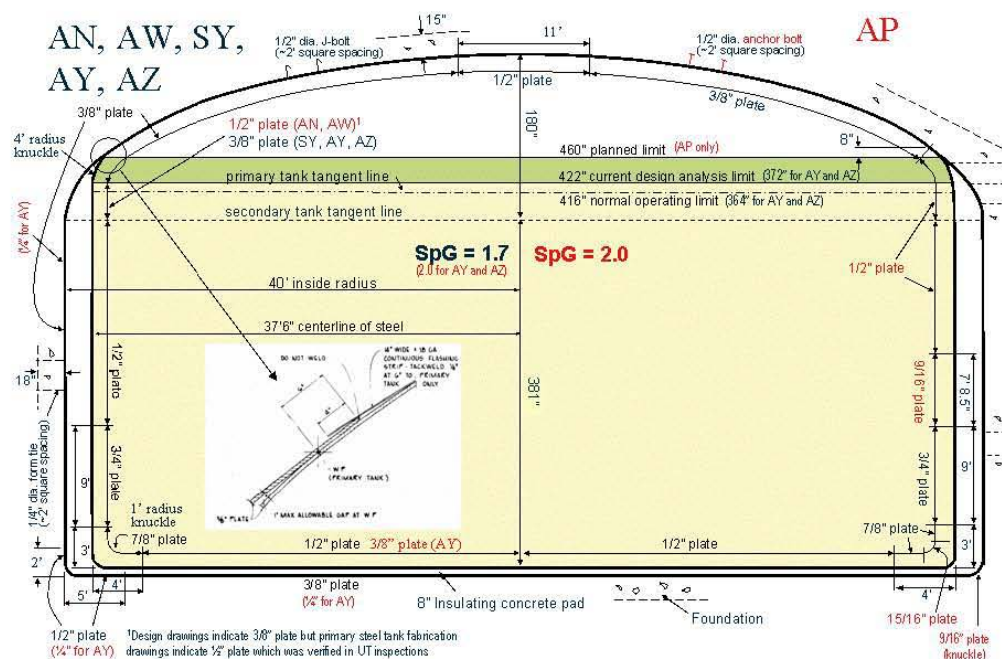


Figure 2-1. Cross-Section View of the Hanford DST Primary Tank Designs

“lines of support that provide sufficient stiffness to act as bulkheads.” In previous analyses, L has been defined as the vertical distance from the waste-free surface to the tangent point between the upper knuckle and the dome. The wall thickness used in the N-284-1 equations was then calculated as the weighted average over this length. However, the primary tank cylindrical shell does not have a constant wall thickness, and it does not have clearly defined lines of support due to the upper and lower knuckles.

Table 2-1. Summary of Design Data and Operating Limits for the DST Primary Tanks

Design Data and Operating Limits	The Different Tank Farm Designs			
	AY/AZ	SY	AW/AN	AP
Primary Tank Thickness, inches				
Upper Haunch	0.375	0.375	0.375	0.5
Vertical Wall, Top	0.375	0.375	0.5	0.5
Vertical Wall, Mid	0.5	0.5	0.5	0.563
Vertical Wall, Bottom	0.75	0.75	0.75	0.75
Lower Knuckle	0.875	0.875	0.875	0.9375
Max Allowable Waste Temp., F	350	250	350	210
Max Historical Waste Temp, F	247/263	155	135/150	118
Yield Strength @ Room Temp, ksi	32	35	50	45
Ultimate Strength, ksi	60	65	70	70
Sm at Max. Allow Temp, ksi	18.6	21	21.3	21.7
Sm at Max Hist Temp, ksi	19.2	21.4	21.7	21.7
Specified Max. Waste Height, inch	370	422	422	422
Maximum Specific Gravity	1.7	1.7	1.7	2

Therefore, finite-element-based, eigenvalue buckling models were constructed to compare the bifurcation buckling loads for the theoretical approximation and the actual tank geometries. Additional models were also constructed to investigate the sensitivity of the results to the imperfection size and the number of imperfections. The ANSYS input files for this work are listed in Appendix A.

First, a model was constructed to confirm that the ANSYS finite element code could accurately predict the eigenvalue buckling mode of a uniform thin-walled cylinder. The model was constructed using the basic dimensions of the AY primary tank in the DST bounding model ($R = 450$ -inch, average wall thickness = 0.507 -inch, height = 460 -inch). A 180° arc was modeled to ensure that the minimum eigenvalue was not increased artificially by simulating too small a section of the tank. Symmetry boundary conditions were applied to the cut edges of the 180° model. The critical buckling loads predicted by ANSYS were compared against the theoretical buckling stress used in N-284-1:

$$\sigma_{\varphi L} = 0.605Et / R \quad (2.1)$$

This is equivalent to the equation derived in Timoshenko and Gere (1961) for a cylindrical shell that is uniformly compressed and assumed to buckle symmetrically with respect to the axis of the tank (i.e., the cylinder ends are simply supported, but they remain circular). Table 2-2 lists the predicted critical buckling load in the uniform cylindrical wall from the finite element model. The table shows that the critical buckling load predicted by the finite element model (with the end displacements fixed to remain circular) matches the theoretical value within 0.1%. Therefore, the ANSYS solution reproduces the theoretical buckling solution very accurately. Figure 2-2 shows the predicted mode shape from the ANSYS uniform cylinder buckling model.

Next, the actual primary tank geometry and wall thickness variation of the AY design were substituted into the model to compare the critical buckling load and the resulting buckling mode shape with that of Figure 2-2, the uniform cylindrical approximation assumed in the ASME N-284-1 evaluation. Table 2-2 gives the eigenvalue buckling load for the AY tank geometry with the in-plane displacements of the cylinder ends fixed. These are the same end-constraints assumed in the theoretical solution. The critical load for this case is only 20.7% of the theoretical buckling load for the uniform cylindrical tank section assumed in N-284-1. Figure 2-3 shows that the corresponding buckling mode shape is confined to the upper section of the tank with the thinnest wall (0.375 -inch minus the 0.060 -inch corrosion allowance = 0.315 inch). The AY primary tank model was also run with the in-plane displacements and the edge rotations fixed, which closely approximates the actual conditions of the primary tank. The eigenvalue buckling load for this case is 34.1% of the theoretical buckling load, and the buckling mode shape is again confined to the top thinnest course of the tank wall (Figure 2-4).

Table 2-2. Comparison of Eigenvalue Critical Buckling Loads for the Approximate Uniform Cylinder and the AY Primary Tank Geometry

No.	Top and Bottom Edge Constraints	Total Buckling Load for a 360° Cylinder (lb)	Percent of the Theoretical Buckling Load in N-284-1
1	Theoretical buckling solution – Ends fixed to remain circular ($\sigma_{cr}=0.605 Et/R$)	2.883E+07	100
	ANSYS uniform cylinder model		
2	Ends fixed to remain circular	2.885E+07	100.1
	ANSYS AY primary tank geometry		
3	Ends fixed to remain circular	5.962E6	20.7
4	Ends fixed to remain circular + top and bottom edge rotations fixed to approximate the primary tank conditions	9.831E6	34.1

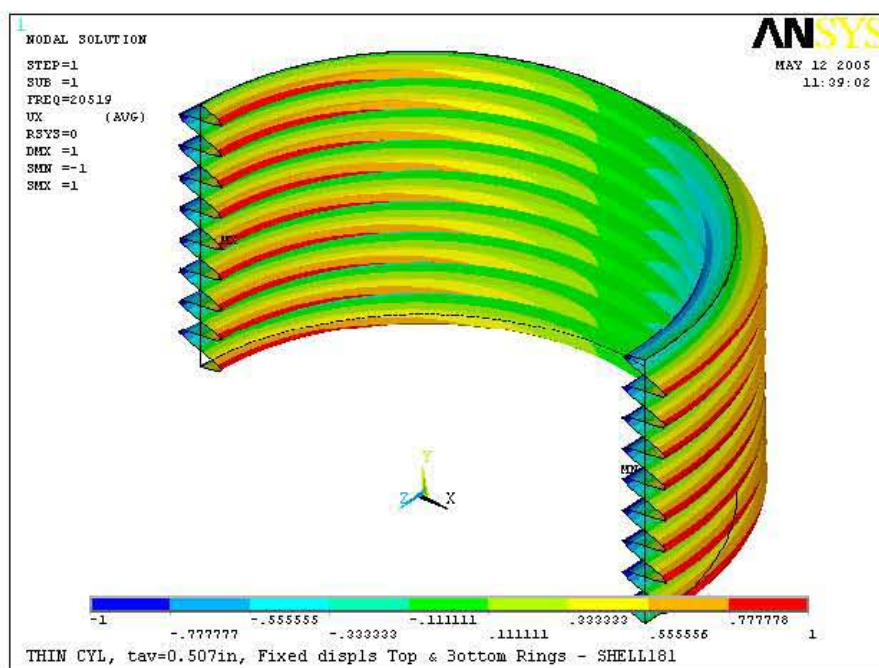


Figure 2-2. Predicted First Eigenvalue Buckling Mode for a Uniform Cylinder with Fixed Displacements (in the plane of the cylinder), Added at the Top and Bottom Edges of the Cylinder

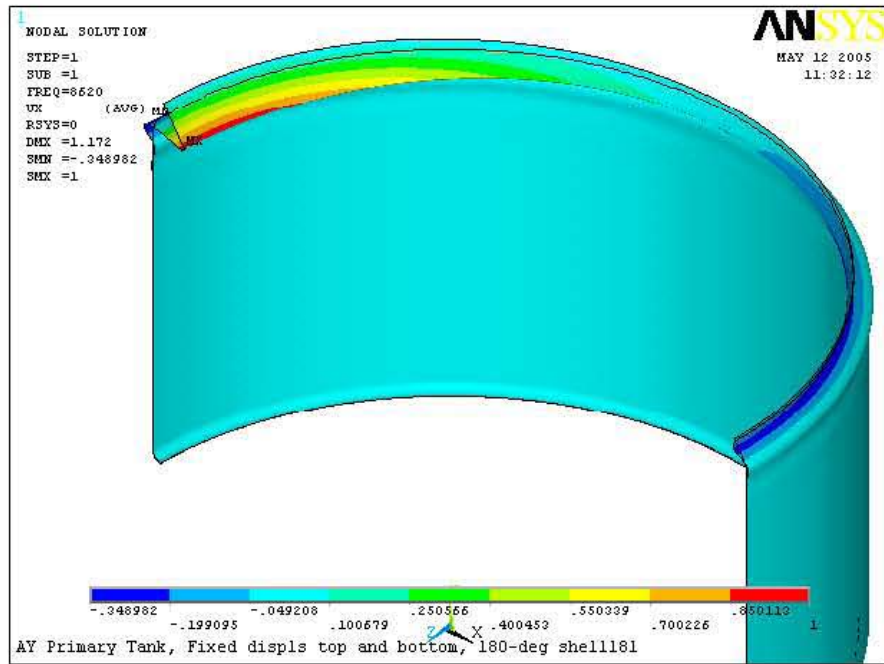


Figure 2-3. Predicted First Eigenvalue Buckling Mode for the AY Primary Tank Geometry with Fixed Displacements (in the plane of the cylinder) at the Tangent Points of the Top and Bottom Knuckles

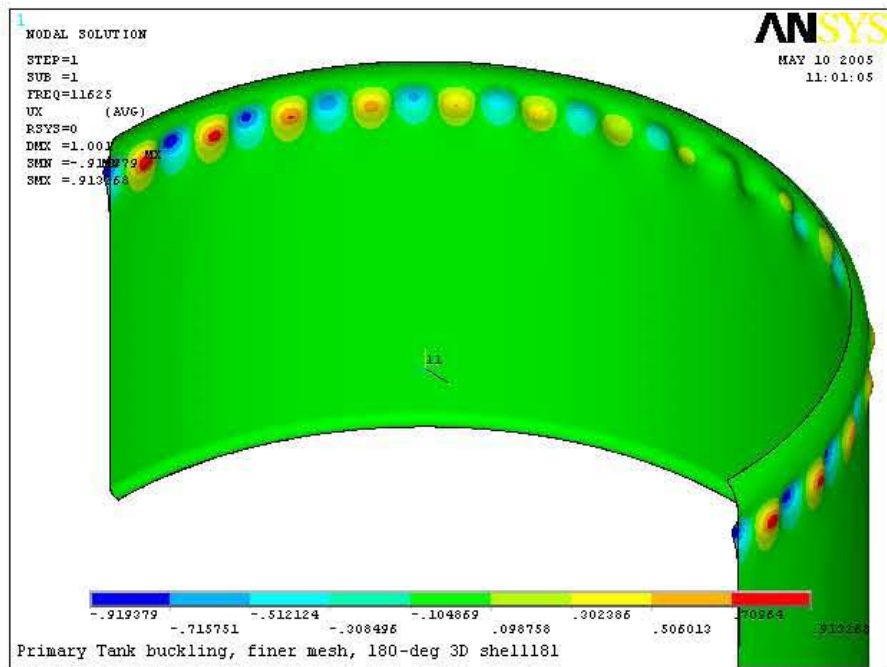
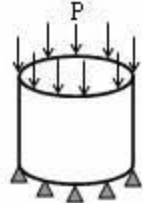
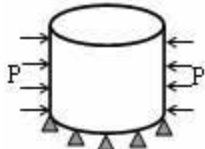
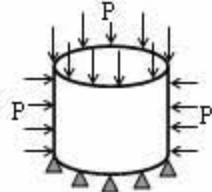
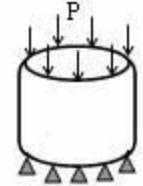
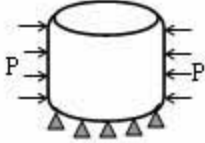
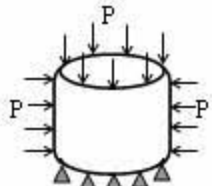


Figure 2-4. Predicted First Eigenvalue Buckling Mode for the AY Primary Tank Geometry with Fixed Displacements and Rotations at the Tangent Points of the Top and Bottom Knuckles

This comparison shows that using an average wall thickness and a buckling length from the waste level to the dome tangent point does not conservatively approximate the theoretical buckling load of the actual tank geometry. If one assumes that buckling is localized to the upper ring of the tank with the minimum wall thickness ($t_{av} = 0.315$ -inch, height = 78.75-inch), then the estimated critical buckling load is $1.82E7$ lb. This is still a factor of 1.82 greater than the critical buckling load predicted for the AY primary tank geometry. Therefore, the radiused shape of the upper knuckle significantly reduces the axial critical buckling load of the actual tank geometry.

External pressure boundary conditions were also applied to the above finite element model to predict the “harmonic” buckling mode. Symmetry boundary conditions were applied to the cut edges of the 180° model. The critical buckling loads predicted by ANSYS were compared against the theoretical buckling loads used in ASME code case N-284-1. The equation used in ASME code case N-284-1 is a simplification of the classical solution and it is independent of the number of lobes ‘n’ into which the cylinder collapses. A comparison with the classical solution showed that the simplified equation in N-284-1 is sufficiently accurate. Table 2-3 lists the predicted critical buckling load in the uniform cylindrical wall from the finite element model. The table shows that the critical buckling load predicted from the finite element model matches the theoretical value within 5%. Therefore, the ANSYS solution reproduces the theoretical buckling solution accurately, considering the fact that the theoretical solution involves trial and error substitutions for the number of lobes ‘n.’ Figure 2-5 shows the predicted buckling mode shape for the uniform cylinder loaded with external pressure.

Table 2-3. Summary of the Eigenvalue Buckling Comparisons of the Uniform Cylinder and the DST Primary Tank Geometry for Axial, Hoop, and Combined Axial and Hoop Loads

Cylinder Parameters	Diamond (Column) Buckling		Harmonic (External Pressure) Buckling		Combined	
Uniform Cylinder						
Thickness, in.	0.507		0.507		0.507	
Radius, in.	450		450		450	
Height, in.	460		460		460	
E, psi	29.5×10^6		29.5×10^6		29.5×10^6	
Boundary Conditions	End displacements fixed to remain circular		End displacements fixed to remain circular		End displacements fixed to remain circular	
Analysis	P_{cr} , lb	% of Theoretical P_{cr}	P_{cr} , psi	% of Theoretical P_{cr}	P_{cr} , psi	% of Theoretical P_{cr}
Theoretical (Timoshenko & Gere)	2.883E+07	--	1.50	--	1.46	--
ANSYS Eigenvalue Analysis	2.885E+07	100.09	1.42	95	1.42	97
DST 'AY' Cylinder						
Thickness, in.	DST wall thicknesses		DST wall thicknesses		DST wall thicknesses	
Radius, in.	450		450		450	
Height, in. (to the tangent point)	460		460		460	
E, psi	29.5×10^6		29.5×10^6		29.5×10^6	
Boundary Conditions	End displacements fixed to remain circular		End displacements fixed to remain circular		End displacements fixed to remain circular	
Analysis	P_{cr} , lb	% of Theoretical P_{cr} from Uniform Cylinder	P_{cr} , psi	% of Theoretical P_{cr} from Uniform Cylinder	P_{cr} , psi	% of Theoretical P_{cr} from Uniform Cylinder
ANSYS Eigenvalue Analysis	6.404E+06	22.21	1.154	76.93	1.154	79.04

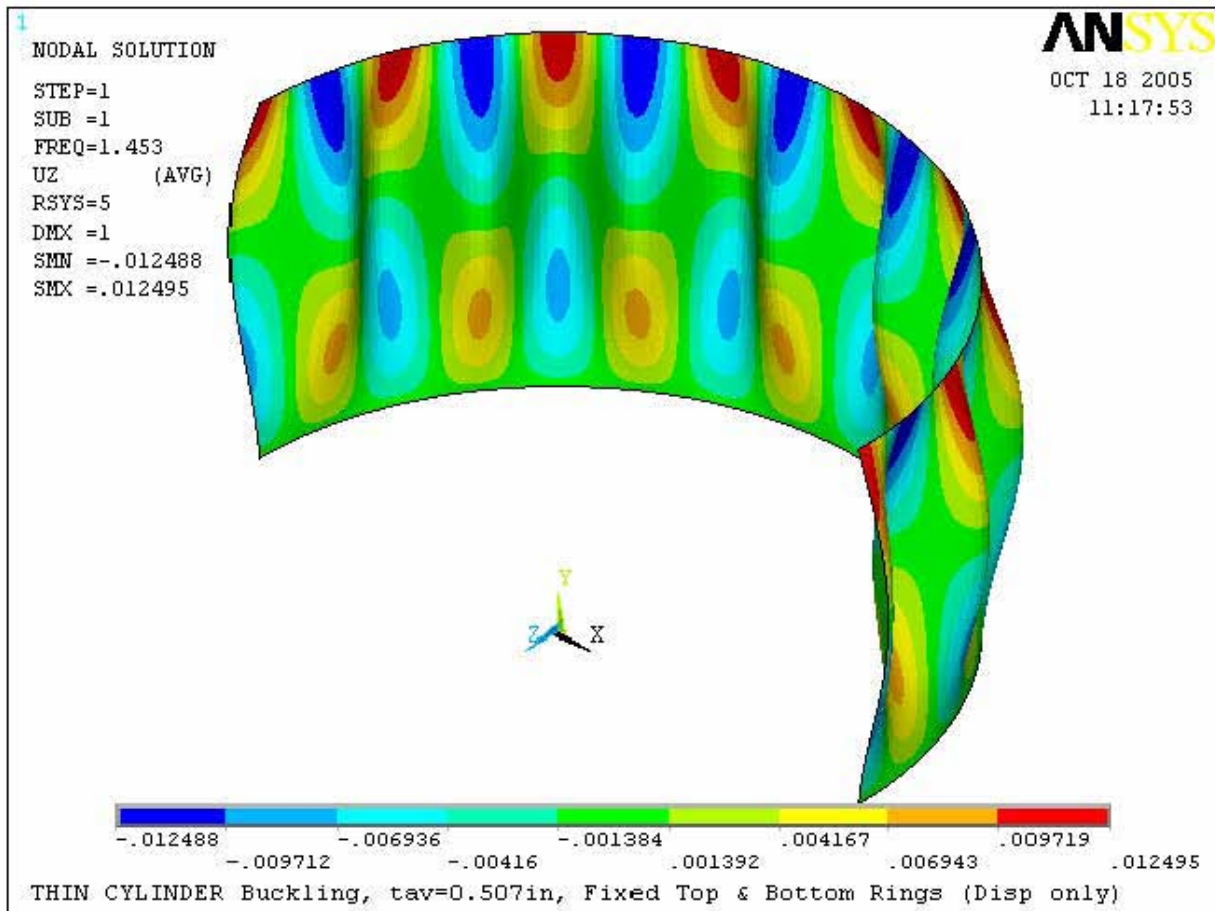


Figure 2-5. Predicted First Eigenvalue Buckling Mode for a Uniform Cylinder Loaded with External Pressure and Fixed Displacements (in the plane of the cylinder), Added at the Top and Bottom Edges of the Cylinder

The primary tank geometry and wall thickness variation of the AY design were again substituted into the model to compare the critical buckling load and the resulting buckling mode shape with that of the cylindrical approximation assumed in the ASME N-284-1 evaluation. Table 2-3 gives the eigenvalue buckling load for the AY tank geometry with the in-plane displacements of the cylindrical ends fixed (the same end-constraints assumed in the theoretical solution). The critical load for this case is only 76.93% of the theoretical buckling load from N-284-1. Figure 2-6 shows that the corresponding buckling mode shape is very similar to the uniform cylinder tank.

This comparison shows that using an average wall thickness and a buckling length from the waste level to the dome tangent point does not conservatively approximate the theoretical buckling load of the actual tank geometry even though they have similar mode shapes. Therefore, the gradation in wall thickness and the radiused shape of the upper knuckle reduces the critical buckling load of the actual tank geometry.

Combined external pressure and axial compression loads were also applied to the above finite element model to predict the combined buckling mode. This simulates the vacuum loading of a closed-ended cylinder where the axial stress is one-half the hoop stress. The critical buckling loads predicted by ANSYS were compared with the theoretical buckling loads predicted using the N-284-1 equations.

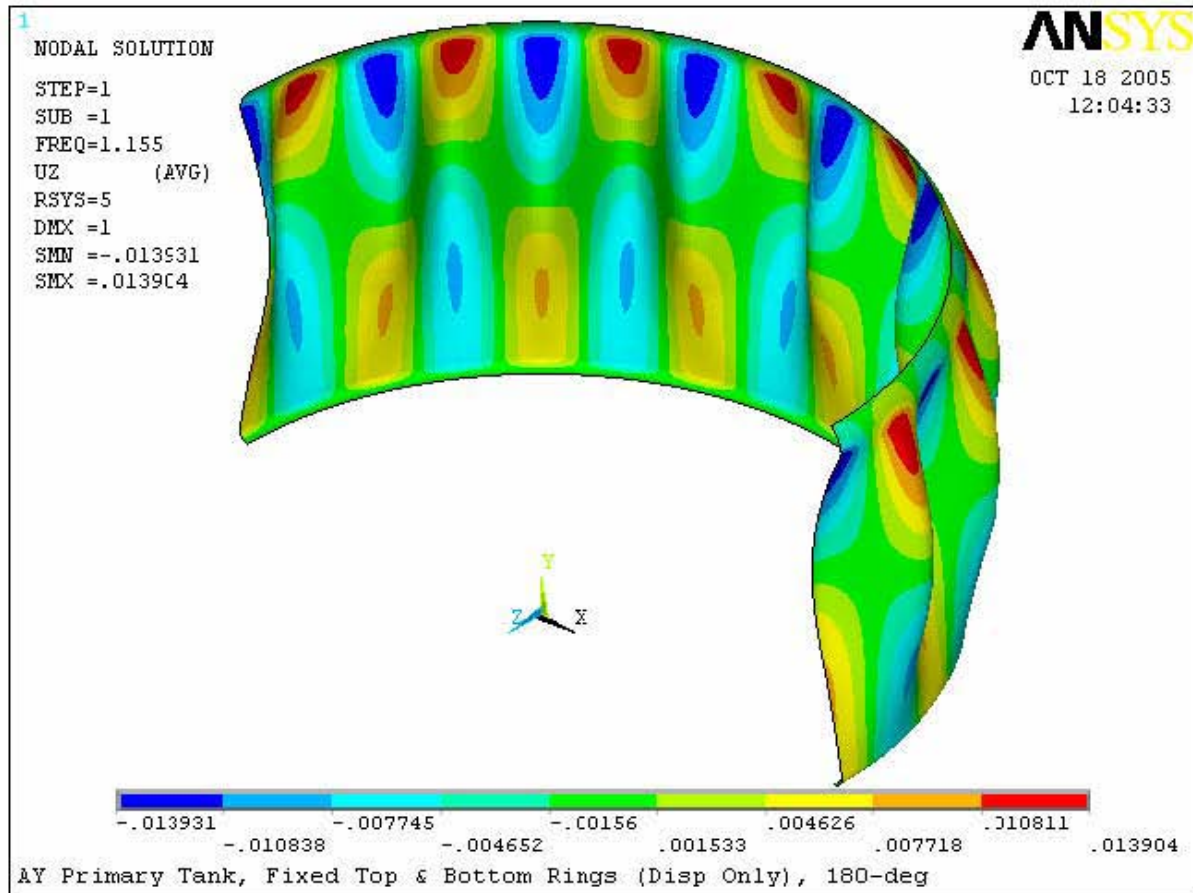


Figure 2-6. Predicted First Eigenvalue Buckling Mode for a DST Cylinder with External Pressure Loading, Plus Fixed Displacements (in the plane of the cylinder), Added at the Top and Bottom Edges of the Cylinder

Table 2-3 lists the predicted critical buckling load in the uniform cylindrical wall from the finite element model. The table shows that the critical buckling load predicted from the finite element model (with the end displacements fixed to remain circular) matches the theoretical value within 3%. Therefore, the ANSYS solution reproduces the theoretical buckling solution accurately. Figure 2-7 shows the predicted mode shape for ANSYS uniform cylinder buckling model case in Table 2-3.

The primary tank geometry and wall thicknesses of the AY design were substituted into the model to compare the critical buckling load and the resulting buckling mode shape with that of the cylindrical approximation assumed in the ASME N-284-1 evaluation. Table 2-3 shows that the eigenvalue buckling load for the AY tank geometry is 79% of the theoretical buckling load from N-284-1. Figure 2-8 shows that the corresponding buckling mode shape is again very similar to the uniform cylinder tank.

This comparison shows that using an average wall thickness and a buckling length from the waste level to the dome tangent point does not conservatively approximate the theoretical buckling load of the actual tank geometry but have the same mode shapes. Therefore, it is again shown that the gradation in wall thickness and the radiused shape of the upper knuckle tend to reduce the critical buckling load of the actual tank geometry.

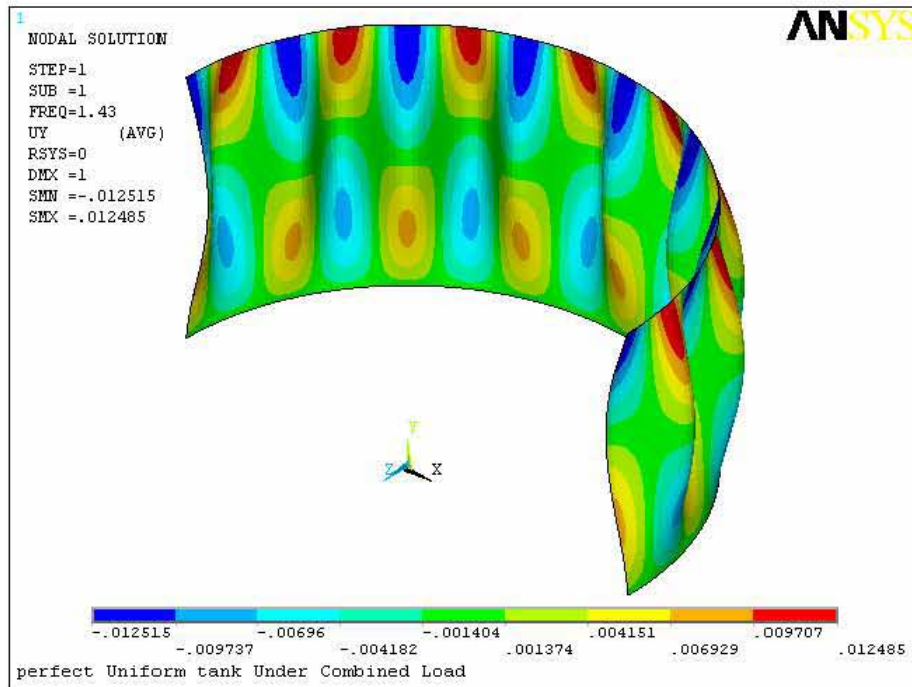


Figure 2-7. Predicted First Eigenvalue Buckling Mode for a Uniform Cylinder with Fixed Displacements (in the plane of the cylinder), Added at the Top and Bottom Edges of the Cylinder

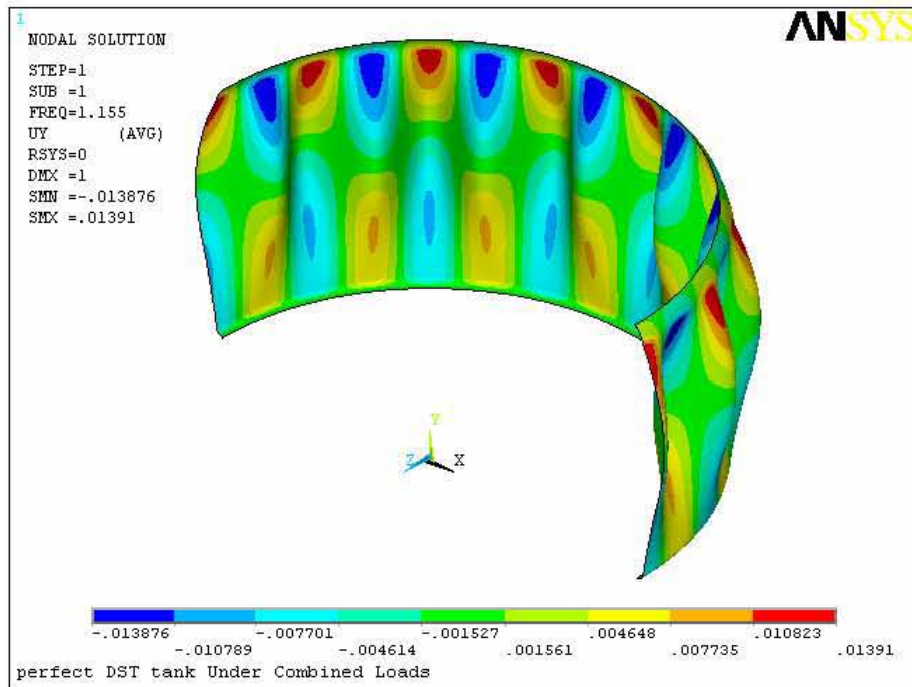


Figure 2-8. Predicted First Eigenvalue Buckling Mode for a DST Cylinder with Fixed Displacements (in the plane of the cylinder), Added at the Top and Bottom Edges of the Cylinder

In summary, the following observations were made from the above eigenvalue buckling solutions:

- Previous buckling analyses of the DSTs used the methodology in ASME Code Case N-284-1, which is based on the buckling of a constant thickness cylindrical shell with unsupported length, L . N-284-1 requires that the user estimate the length, L , as the distance “between lines of support with sufficient stiffness to act as bulk heads.” The DST primary tank cylindrical shell does not have constant wall thickness and it does not have clearly defined lines of support due to the varying wall thickness and the upper and lower knuckle geometries.
- The ANSYS finite element code is able to very accurately predict the theoretical buckling loads of a uniform cylinder under axial, hoop and combined loadings.
- Using an averaged wall thickness and a buckling length from the waste level to the dome tangent point does not conservatively approximate the theoretical buckling load of the actual tank geometry.
- The varying wall thickness and the radiused shape of the upper and lower knuckles significantly reduces the critical buckling load of the actual tank geometry (approximately 78% reduction in the column buckling load, 23% for harmonic buckling, and 21% for the combined loading case).
- The tank buckling loads deviate more from the N-284-1 solutions for column buckling (under pure axial compression) than they do for harmonic buckling (external pressure only) or buckling due to combined axial and hoop loads.

2.2 Sensitivity of Critical Buckling Loads to the Size and Number of Tank Imperfections

A study was also performed to determine the sensitivity of the buckling load to the size and number of geometric imperfections that act to initiate the buckling response. ASME code case N-284-1 uses geometric knockdown factors that are based on the allowable construction imperfection size given in ASME Section III NE-4220, whereas the tolerance on construction imperfections given in the DST tank construction specifications is somewhat different. Table 2-4 compares the NE-4220 dimensional tolerance with the maximum out of roundness allowed in the AY tank farm construction specifications, HWS-7789 (Hanford Engineering Services 1968).

Three different imperfection amplitudes ($1/10^{\text{th}}$, 1, and 10 times the specified imperfection depths) were modeled using ANSYS and are shown in Table 2-5 and Figures 2-9 and 2-10. For comparison purposes, the amplitude of two times the ASME imperfection (0.5 inch deep) is equal to the amplitude of the specified AY tank fabrication imperfection (1 inch deep) and is shown in Table 2-5.

The uniform cylinder and DST ‘AY’ tank models were analyzed for the different imperfection sizes, multiple numbers of imperfections and the three different loading cases listed in Table 2-3. Table 2-6 summarizes the variation in the buckling limits of axial compressive force and external pressure.

Table 2-4. Comparison of the Construction Imperfection Tolerances Specified in ASME NE-4220 and the AY Tank Construction Specifications

Requirement	ASME NE-4220 Fabrication Requirement	Typical Primary Tank Fabrication Specification
Maximum difference in cross-sectional diameter	Shall not exceed 1% of the nominal diameter	Shall not exceed 1% of the nominal diameter
Maximum deviation from true Theoretical form	Maximum plus-or-minus deviation from the true circular form shall not exceed the maximum permissible deviation obtained from Fig. NE-4221.1-1 (i.e., 0.5 in. when extrapolated for primary tank D/t) over an arc length equal to twice the arc length obtained from Fig. NE-4221.2-2 (i.e., 9.75 ft when extrapolated for primary tank D/t)	Maximum deviation from design curvature on 7 ft shall be 1 in. at center if less than design and at end if greater than design. Measurements shall be made at 3 ft vertical intervals. Circumference of the shell section at any horizontal plane shall not deviate from the theoretical by more than plus or minus 2 in. Top of shell shall be plumb within 2 in. of the bottom of the cylindrical section when measured from any point on the circumference. In any vertical plane cutting the cylindrical section the maximum deviation of the line of intersection from a true straight line shall not exceed ½ in. in any 5-ft length
AY/AZ primary tank geometric parameters L = 459 in. (between bottom knuckle and primary tank tangent line at weld to dome cap) D = 75 ft t = 0.508 in. (weighted average over length with corrosion allowance of 1 mil/yr for 50 yrs applied) L/D = 0.51 D/t = 1770		

Table 2-5. Matrix of Imperfection Sizes That were Simulated

ASME Specifications	<i>Imperfection Size</i>		
	(1/10) times ASME Specs	(2) times ASME Specs	(10) times ASME Specs
0.5 in. over 9.75 ft arc	0.05 in. over 9.75 ft arc	1 in. over 9.75 ft arc	5 in. over 9.75 ft arc
Tank Fabrication Specifications	(1/10) times Tank Fab Specs	-	(10) times Tank Fab Specs
1 in. over 7 ft arc	0.1 in. over 7 ft arc	-	10 in. over 7 ft arc

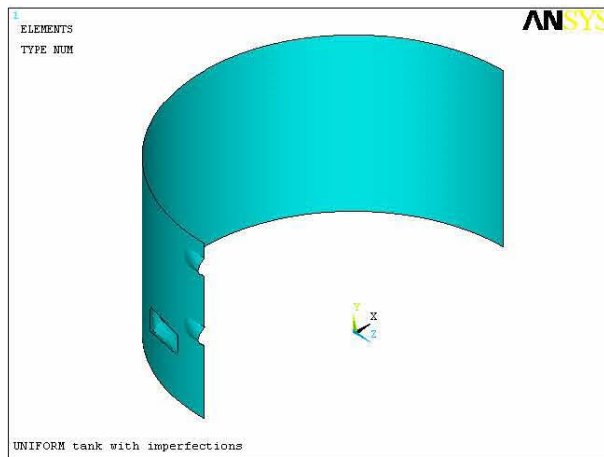


Figure 2-9. Uniform Cylinder with Imperfections

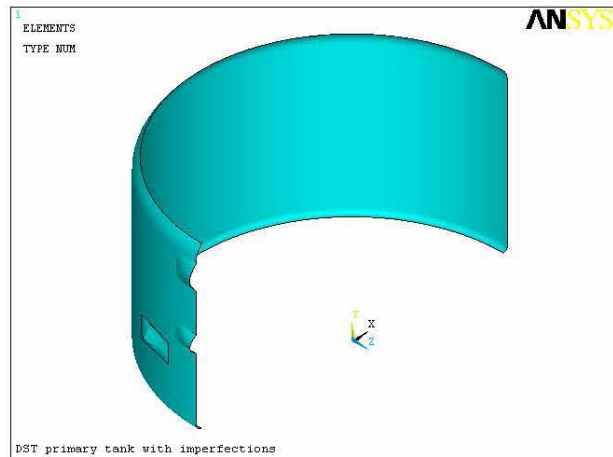


Figure 2-10. AY Tank with Imperfections
(The imperfection amplitudes are exaggerated in the plots to make them visible.)

The following observations were made from the imperfection sensitivity study:

- The buckling limit loads for axial, hoop, and combined loadings are insensitive to the number of imperfections.
- The axial limit load is sensitive to the amplitude of the imperfection, but the imperfection lengths from ASME NE-4220 and the AY specifications (9.75 and 7 feet, respectively) are similar and do not give different buckling limits. The 1-inch over 7-foot out-of-roundness from the AY construction standard gives a lower axial load limit than the 0.5-inch over 9.75-foot imperfection limit specified in NE-4220. Therefore, the limiting imperfection size from the AY construction specification will be used in predicting the buckling limits for the DST primary tanks.
- The limit pressure for both the pressure only and the combined loading (for a closed ended cylinder where the axial stress is $\frac{1}{2}$ the hoop stress) is not sensitive to the amplitude or number of imperfections. The limit pressure is 1.42 psi for the uniform cylinder and 1.14 psi for the AY tank geometry. The tank has a very large R/t ratio ($450/0.375 = 1,200$ inch in the 3/8-inch upper section of the tank wall) and any imperfection is enough to initiate buckling. The addition of a small amount of axial compression in the combined loading case is not enough to reduce the limiting external pressure load.
- Comparing the buckling limits for the AY tank geometry and the uniform cylindrical tank again shows that the AY tank geometry has significantly lower critical buckling loads than the uniform equivalent cylinder.

Table 2-6. Summary of the Critical Buckling Loads for the Sensitivity Study on the Number and Size of the Tank Imperfections

Uniform Cylinder		Cylinder with No Imperfection	Cylinder with one ASME *times imperfection				Cylinder with two ASME *times imperfection				Cylinder with four ASME *times imperfection			
			*(1/10)	*(1)	*(2)	*(10)	*(1/10)	*(1)	*(2)	*(10)	*(1/10)	*(1)	*(2)	*(10)
	Axial Load, lb/in.	10204	10196	8045	6279	3263	10190	8024	6378	3436	10188	7993	6328	3387
	Lateral Pressure, psi	1.419	1.419	1.418	1.417	1.424	1.419	1.418	1.417	1.426	1.419	1.417	1.416	1.429
	Combined, psi	1.419	1.419	1.418	1.417	1.424	1.419	1.418	1.417	1.426	1.418	1.417	1.416	1.428
			Cylinder with one Tank Fab *times imperfection				Cylinder with two Tank Fab *times imperfection				Cylinder with four Tank Fab *times imperfection			
			*(1/10)	-	*(1)	*(10)	*(1/10)	-	*(1)	*(10)	*(1/10)	-	*(1)	*(10)
	Axial Load, lb/in.		10119	-	6846	5188	10093	-	6941	5403	10081	-	6828	5354
DST 'AY' Cylinder	Lateral Pressure, psi		1.419	-	1.418	1.424	1.419	-	1.418	1.426	1.419	-	1.416	1.429
	Combined, psi		1.419	-	1.418	1.424	1.419	-	1.418	1.426	1.418	-	1.415	1.429
			Cylinder with one ASME *times imperfection				Cylinder with two ASME *times imperfection				Cylinder with four ASME *times imperfection			
			*(1/10)	*(1)	*(2)	*(10)	*(1/10)	*(1)	*(2)	*(10)	*(1/10)	*(1)	*(2)	*(10)
	Axial Load, lb/in.	2265	2265	2265	2265	1859	2265	2265	2265	1907	2265	2265	2265	1878
	Lateral Pressure, psi	1.154	1.154	1.152	1.145	1.152	1.154	1.151	1.136	1.157	1.154	1.147	1.129	1.159
	Combined, psi	1.154	1.154	1.152	1.145	1.151	1.154	1.151	1.135	1.157	1.154	1.146	1.129	1.159
			Cylinder with one Tank Fab *times imperfection				Cylinder with two Tank Fab *times imperfection				Cylinder with four Tank Fab *times imperfection			
			*(1/10)	-	*(1)	*(10)	*(1/10)	-	*(1)	*(10)	*(1/10)	-	*(1)	*(10)
	Axial Load, lb/in.		2265	-	2265	1791	2265	-	2265	1836	2265	-	2265	1829
	Lateral Pressure, psi		1.154	-	1.151	1.157	1.154	-	1.146	1.158	1.154	-	1.138	1.159
	Combined, psi		1.154	-	1.151	1.157	1.154	-	1.146	1.157	1.154	-	1.138	1.159

3.0 Buckling Evaluation Method for the DST Primary Tanks Based on Large Displacement Instability Analysis

Large displacement finite element analysis was used to predict the limiting vacuum load for the Hanford double-shell waste primary tanks under combined axial and vacuum loads. Figure 3-1 shows the model of the primary tank that was used in this analysis. The ANSYS model input files are listed in Appendix B. A downward deflection was applied to the dome of the tank (the area in contact with the concrete tank structure) to simulate the displacement controlled axial compression of the tank wall that occurs due to concrete thermal degradation and creep, plus the confined thermal expansion of the steel tank inside the concrete shell. The model includes a geometric imperfection to initiate the buckling instability under the radially symmetric vacuum load. The imperfection was sized to the maximum out-of-roundness (1-inch deviation in a 7-foot arc length) allowed in the AY tank farm construction specifications, HWS-7789 (Hanford Engineering Services 1968). Additional loads on the model include gravity and hydrostatic pressure of the waste at height, h , and specific gravity, SpG (see Figure 3-2).

The vacuum in the primary tank also increases the downward deflection of the concrete dome and tank walls, which increases the compression on the primary tank walls. Because the concrete tank structure is not included in the buckling model, this effect is not included in the current analysis. However, PNNL's previous work quantifying the effect of increased concentrated load on tank integrity (Rinker et al. 2005) provides information to estimate the increase in axial compression in the primary tank wall caused by the increased dome load due to vacuum. The area of the tank dome is about 637,000 inch². Therefore, the AP vacuum limit of 12 inch w.g. (0.43 psi) would increase the total load on the dome by 276 kip. Figure 3-3 shows axial (meridional) stresses in the nominal 1/2-inch wall section at several increased loads. (Note that the wall thickness in the model is 0.44 inches because of the 0.060 inch corrosion allowance). The figure shows that increasing the concentrated load by 400 kip increases the wall compression by less than 20 psi. The AP vacuum limit of 12 inch w.g. would increase the primary tank axial compression by less than 15 psi. This is a small effect compared to the total wall compression that is estimated to be on the order of 1,000 to 1,400 psi for the combined operating and seismic loads. Therefore, the increased downward deflection of the concrete dome due to tank vacuum is a minor effect in determining the vacuum limits for the tank.

The onset of the buckling instability was predicted by applying an increasing vacuum load on the inside surface of the tank while monitoring the maximum radial displacement of the tank wall as a function of the increasing vacuum load. The onset of instability is signaled by an increasing rate of radial deflection for a constant increment in the applied vacuum load. Figure 3-4 shows an example load deflection curve from one of the cases that was analyzed. Because vacuum is a primary load, the stresses are not self limiting and the model eventually fails to converge (numerically) as the physical load carrying capacity of the tank is reached. Figure 3-5 shows the distorted tank geometry at the final converged load step of the finite element analysis. However, using the final converged vacuum load as the buckling limit is not a reliable measure of the onset of instability because the final convergence is sensitive to non-physical factors including the load step size, the convergence tolerance, and the numerical precision of the computer. Therefore, the ASME code was reviewed to find an appropriate method for defining the limiting vacuum load.

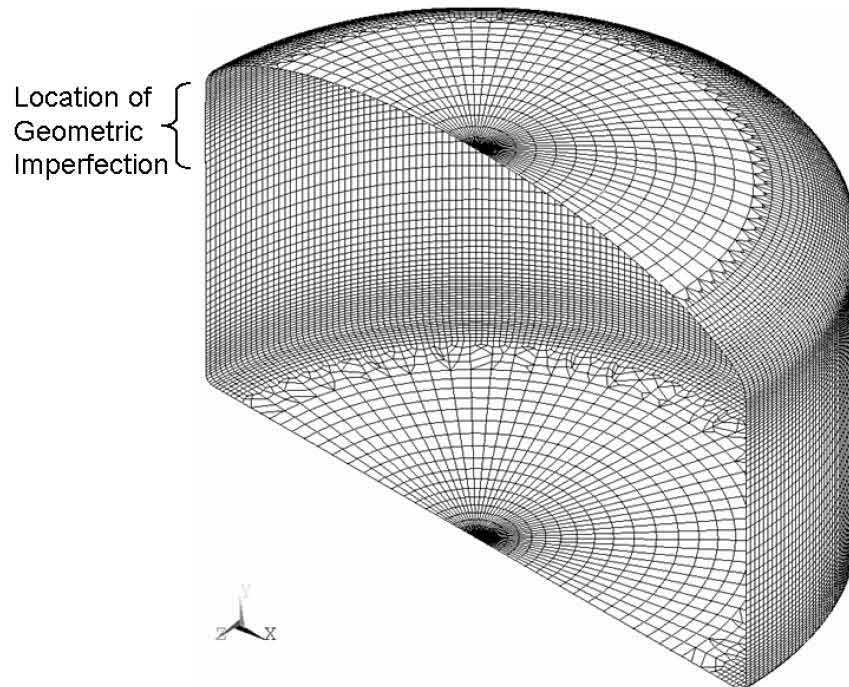


Figure 3-1. Double-Shell Primary Tank Model Used in the Large Deflection Buckling Analysis (The imperfection size was 1 inch out-of-roundness in a 7-foot circumferential arc.)

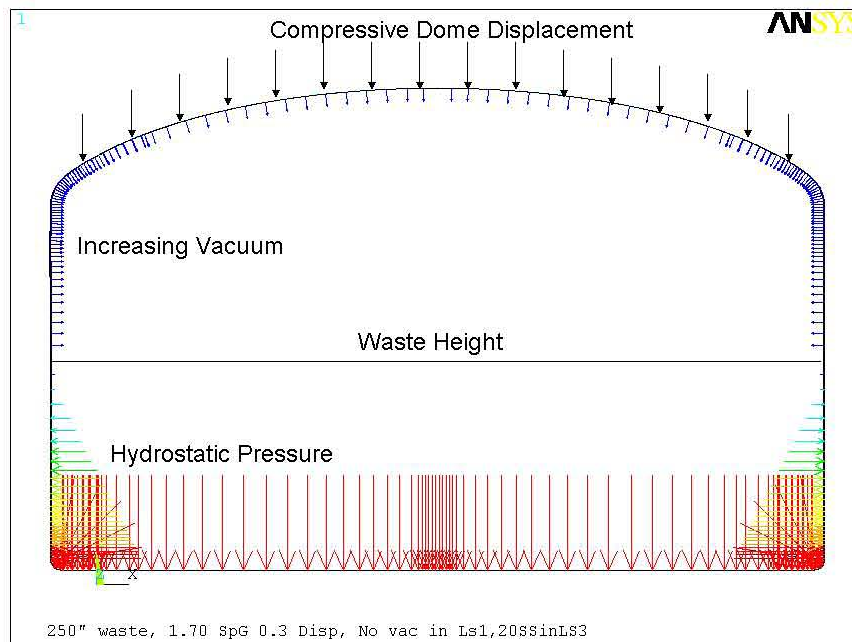


Figure 3-2. Loads Applied to the Large Deflection Buckling Model

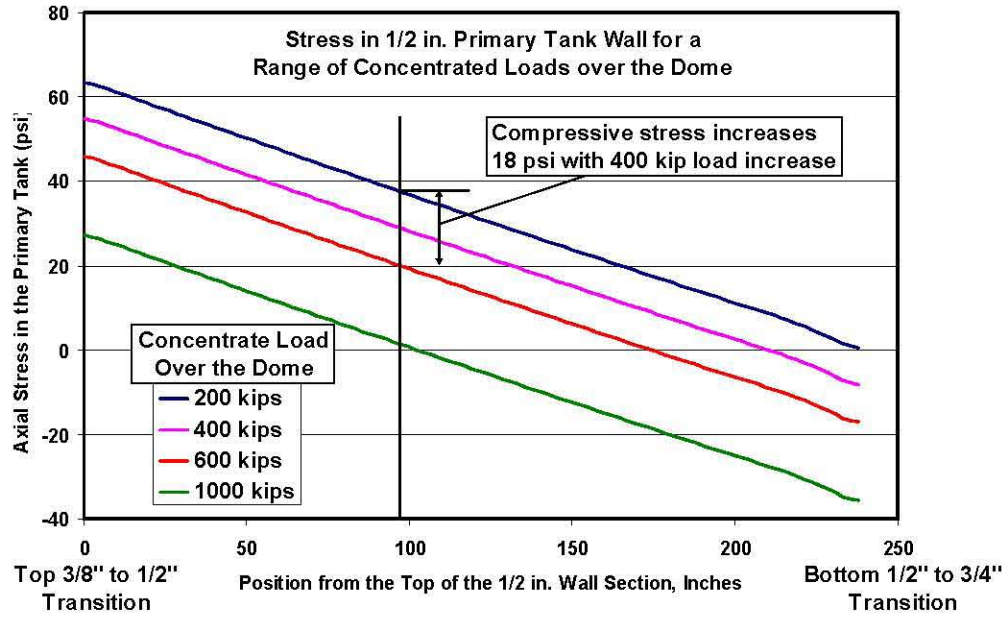


Figure 3-3. Effect of Increasing Dome Load on the Axial Stress in the AY Primary Tank

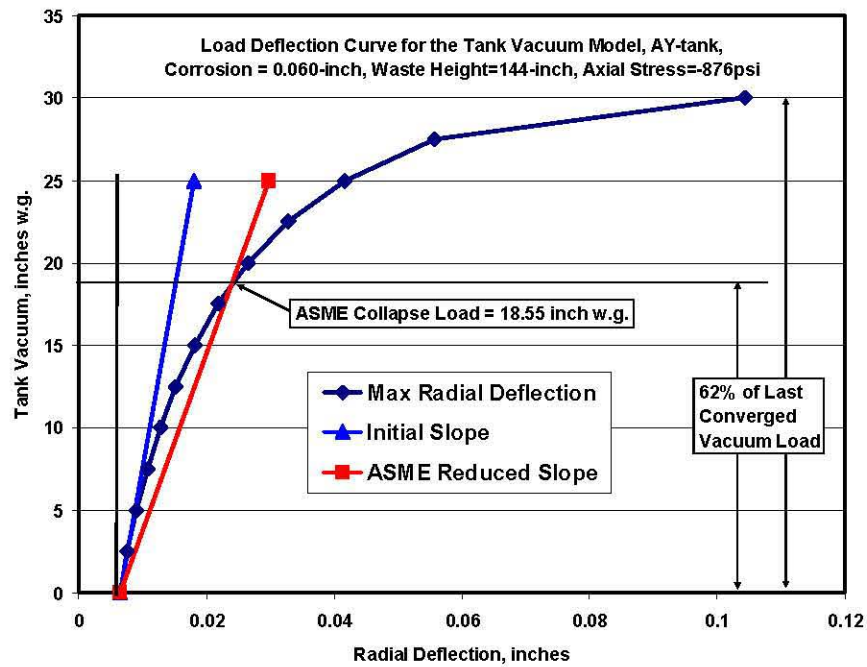


Figure 3-4. Load Deflection Curve for Increasing Vacuum Load Applied to the Large Displacement Tank Buckling Model (The results are for the AY tank model, with specific gravity = 1.7, waste height = 144 inches, and compressive dome displacement = 0.3 inches.)

The ASME Boiler and Pressure Vessel Code, Section III, NB-3213.25, provides guidance on establishing a reasonable collapse load for a structure undergoing controlled plastic deformation (ASME 2004a). Although we are evaluating an elastic buckling phenomenon (the buckling models predict that the tank membrane stresses are well below the elastic limit), the increasing rate of distortion in the tank wall (for a constant increasing vacuum load) represents a gradual decrease in structural stiffness that is similar to what occurs in a structure undergoing progressive plastic deformation. In the former case the stiffness reduction is due to the large deformations of the tank geometry that progressively decrease the load carrying capacity of the tank. In the later case it is due to plastic softening. The ASME code method establishes the collapse load by limiting the reduction in structural stiffness under increasing load.

NB-3213.25 Plastic Analysis — Collapse Load. *A plastic analysis may be used to determine the collapse load for a given combination of loads on a given structure. The following criterion for determination of the collapse load shall be used. A load–deflection or load–strain curve is plotted with load as the ordinate and deflection or strain as the abscissa. The angle that the linear part of the load–deflection or load–strain curve makes with the ordinate is called θ . A second straight line, hereafter called the collapse limit line, is drawn through the origin so that it makes an angle of $\tan^{-1}(2 \tan \theta)$ with the ordinate. The collapse load is the load at the intersection of the load–deflection or load–strain curve and the collapse limit line. If this method is used, particular care should be given to ensure that the strains or deflections that are used are indicative of the load carrying capacity of the structure.*

Figure 3-4 graphically illustrates the ASME code method based on the factor of two stiffness reduction. The radial displacement is offset from zero (at zero vacuum) because the initial loads (axial compression, hydrostatic pressure, and gravity) cause an initial radial deflection in the tank wall. The initial load/deflection slope was calculated and a second line was drawn at an angle with twice the tangent measured from the vertical axis. The vacuum limit was then calculated by interpolating to find the vacuum load where the second line crossed the load/deflection curve (Figure 3-4). In this case, the ASME collapse load is about 62% of the last converged vacuum load. This is typical of the other load cases that were run. Figure 3-5 shows the displaced shape of the tank model at the ASME collapse load. For the tank geometry, the ASME method results in a minor amount of tank distortion.

A matrix of tank models was run to develop equations for the tank vacuum limit as a function of waste height, specific gravity, wall thickness, and axial compressive load. Equations were developed for both the AY and AP primary tank designs. The AY equation also applies to the AZ, SY, AW, and AN primary tank designs because they have essentially the same geometry and wall thickness distributions. The different yield strengths of the different tank materials do not affect the predicted vacuum limits significantly because the membrane stresses are within the elastic range (the maximum membrane compression was about 2,500 psi in the 3/8-inch section of the AY tank wall). The AY and AP primary tank designs differ only by the wall thickness in the upper cylinder, where the AY tank is 3/8 inch thick and the AP tank is 1/2 inch thick. Table 3-1 lists the vacuum limits that were predicted for the load combinations that were analyzed for the AY tank design, and Table 3-2 lists similar results for the load combinations that were analyzed for the AP tank design. The approach used to curve fit these data for the AY tank design is described in detail below with the final results of the AP tank analysis following.

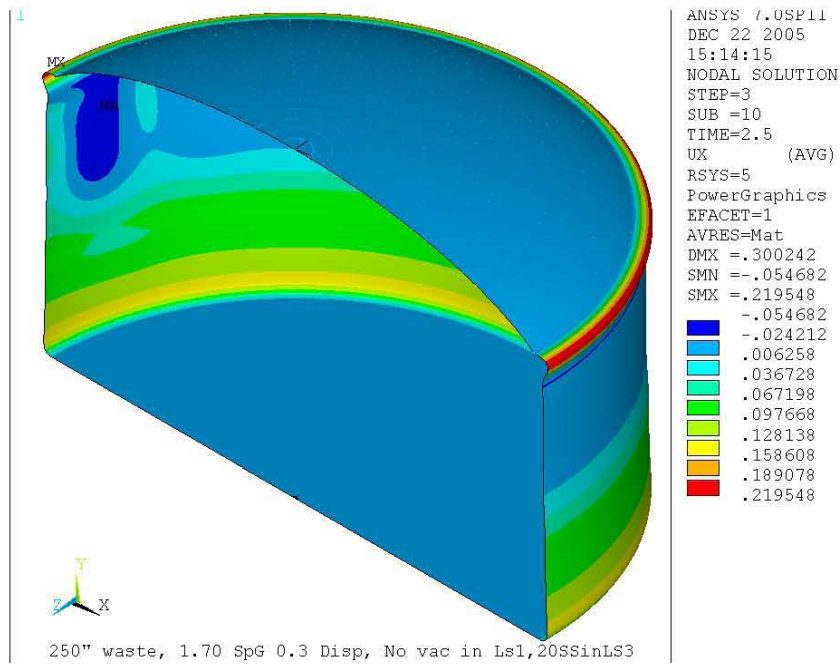


Figure 3-5. Displaced Shape of the AY Model at the Limit Vacuum Defined by the ASME Slope Reduction Method (The influence of the geometric imperfection is evident in the upper left of the plot. The results are for the AY tank model, with specific gravity = 1.7, waste height = 250 inches, and compressive dome displacement = 0.3 inches. The displacements are magnified 50 times so that they are visible.)

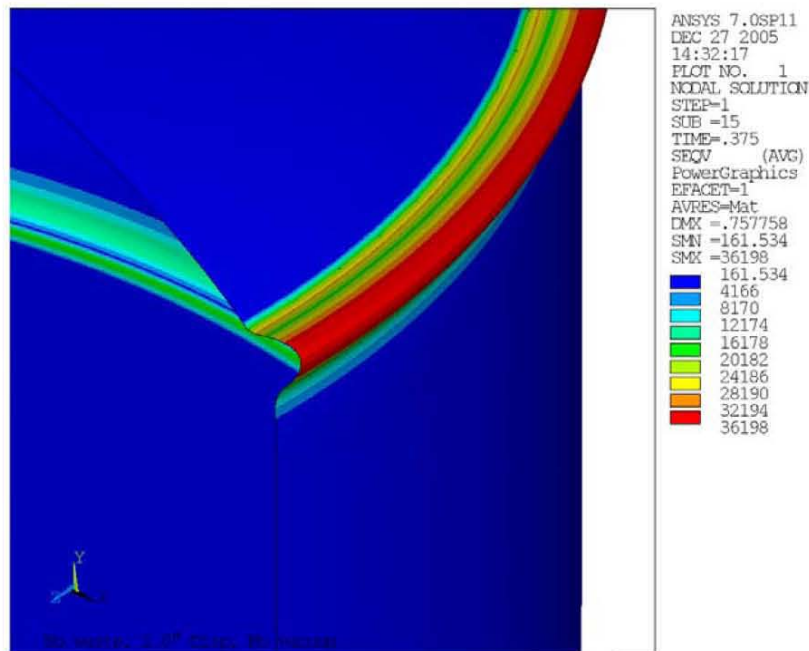


Figure 3-6. Contour Plot of the Maximum Surface Stress in the Upper Knuckle of the AY Tank (This large displacement elastic model shows that the surface stresses are above the 32 ksi yield strength. The displacements are magnified 50 times so that they are visible.)

Table 3-1. Large Deformation Tank Analyses for the AY Vacuum Limit Equations

	Dome Displ, inches =>	0.0"	0.2"	0.3"	0.4"	0.5"	0.6"	1.0"
	Equivalent Linear Elastic Axial Force, kip/inch =>	0.000	-0.290	-0.435	-0.580	-0.726	-0.871	-1.45103
AY Primary Tank, Corrosion = 0.060 inches, SpG = 1.7								
	Waste Height							
	inches	Primary Tank Vacuum Limits, Inches of Water						
	6	18.85	17.97	17.55	16.80	16.03	14.93	10.150
	25	18.86	17.98	17.56	16.82	16.03		
	50	18.91	18.02	17.59	16.88	16.08		
	75	19.02	18.11	17.67	17.00	16.19		
	100	19.29	18.32	17.85	17.28	16.42		
	144	20.19	19.12	18.55	17.96	17.26	16.30	
	200	22.83	21.62	20.95	20.28	19.36		
	250	27.23	25.71	24.97	23.93	22.90		
	300			32.10	30.85			
	350			50.50	56.21			
	400			94.59	87.43			
SpG Runs, Waste Height = 250-inches, 0.0 and 0.5 inch Tank Dome Displacement								
	SpG							
	1.0	25.74				21.59		
	1.5	26.85				22.64		
	1.7	27.23				22.90		
	2.0	27.67				23.26		
Wall Thickness Runs, Waste Height = 6-inches, 0.3 inch Dome Displacement								
Thickness,	Corrosion,							
inches	inches							
0.375	0.000			22.51				17.46
0.345	0.030			19.97				
0.315	0.060			17.55				
0.296	0.079			15.47				
0.278	0.098			13.54				

Additional models were run to determine a reasonable load limit for axial load alone. The compressive displacement of the tank dome was increased gradually until the maximum reaction load was reached and the load began to decrease. In this case, the finite element solution continues to converge beyond the peak load because the loading is fully displacement controlled. Figure 3-8 shows the load displacement curves for several cases with the AY and AP tank models. The load/displacement curves show that the maximum load is reached before the ASME factor of 2 slope reduction is achieved. Surface stress plots showed that the AY tank would yield in bending at the maximum compressive load (Figure 3-6). Therefore, the AY model was re-analyzed using the yield curves for A515-65 steel at temperatures of 100°F, 250°F, and 350°F (Figure 3-7). The model was also run with a yield strength of 35 ksi to represent the A516-65 steel used in the SY primary tank. The elastic response of the AY model is representative of the AN and AW tanks where higher strength material was used (see Table 3-3). Figure 3-8 shows that including plastic deformation reduces the maximum axial compression from 1,800 psi to 1,692 psi (for temperatures up to 100°F). Using the yield curve for the maximum AY operating temperature of 350°F further reduces the maximum axial compression to 1,500 psi in the 0.5 inch wall of the primary tank.

Table 3-2. Large Deformation Tank Analyses for the AP Vacuum Limit Equations

	Dome Displ, inches =>	0.0"	0.2"	0.3"	0.4"	0.5"	0.6"	1.0"
	Equivalent Linear Elastic Axial Force, kip/inch =>	0.000	-0.422	-0.634	-0.845	-1.056	-1.267	-2.112
AP Primary Tank, Corrosion = 0.060 inches, SpG = 1.7								
	Waste Height							
	inches	Primary Tank Vacuum Limits, Inches of Water						
	6	20.59	19.62	19.03	18.48	17.99	17.47	16.125
	25	20.60		19.03		18.00		
	50	20.64		19.08		18.02		
	75	20.74		19.19		18.17		
	100	20.96		19.45		18.32		
	144	21.79		20.25		19.07		
	200	24.43		22.68		21.36		
	250	28.77		26.65		25.25		
	300			35.08				
	350			68.51				
	400							
SpG Runs, Waste Height = 250-inches, 0.0 and 0.5 inch Tank Dome Displacement								
	SpG							
	1.0							
	1.5					24.97		
	1.7							
	2.0					25.62		
Wall Thickness Runs, Waste Height = 6-inches, 0.3 inch Dome Displacement								
Thickness, inches	Corrosion, inches							
0.5	0			24.36				21.68
0.47	0.03			21.62				
0.44	0.06			19.03				
0.421	0.079			17.60				
0.402	0.098			15.96				

The maximum surface stress in the AP model was 45.6 ksi, which is just above the yield strength of the AP A537 steel at room temperature ($S_y = 45$ ksi). Therefore, the elastic response is used for the AP tank.

When defining the limit load for axial compression it is important to recognize that the primary tank is fully confined within the concrete over-structure and it cannot collapse due to axial compression alone. Rather it will continue to deform stably under increasing compression beyond the maximum load. The stiffness reduces due to flexing (and plastic deformation in the case of the AY tank) of the upper knuckle, which acts to relieve the load and limit the contact force between the steel inner tank and the concrete over-structure. Figure 3-8 shows that this limits the compressive membrane stress in the 0.5 inch wall section to less than 2 ksi for the AY tank and less than 3 ksi for the AP tank. The maximum load is truly a maximum possible reaction force rather than a collapse load. In the case of tank AY (with a room temperature yield strength of 32 ksi) this includes a controlled amount of surface plasticity in the upper

Table 3-3. Yield Strength at Temperature for the Primary Tank Steels

Temperature, °F	Yield Strengths at Temperature, ksi			
	A515-65 (AY, AZ)	A516-65 (SY)	A537-Class 1 (AW, AN)	A537-Class 1 (AP Derated to Sy=45 ksi)
100	32	35	50	45
200	29.2	31.9	44.1	39.7
300	28.3	31	40.5	36.5
400	27.4	30	37.5	33.8
500	25.6	28.3	35.2	31.7

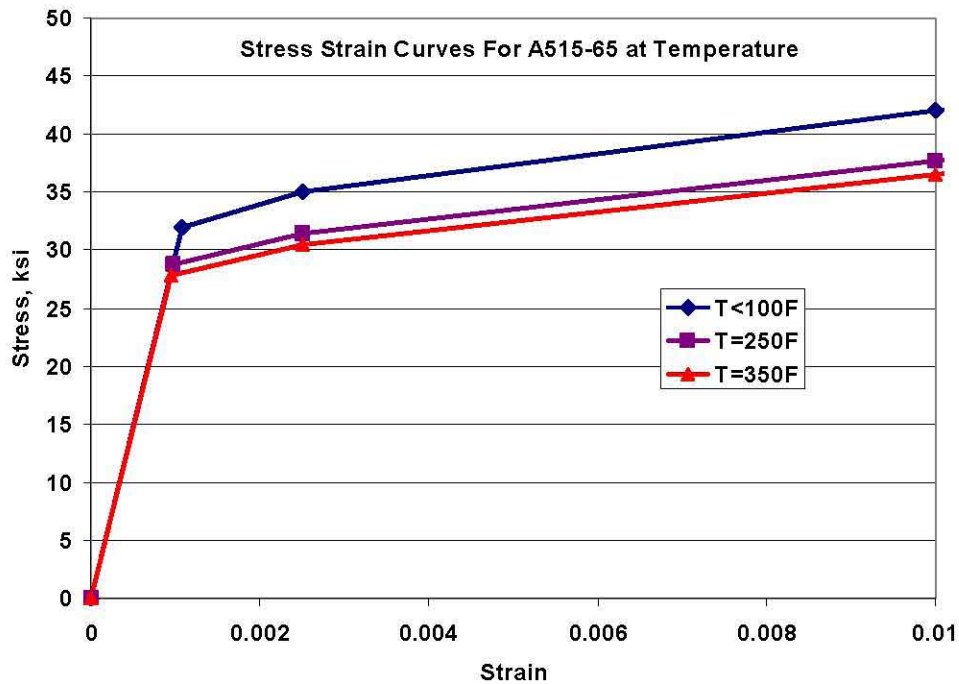


Figure 3-7. Stress Strain Curves for A515-65 Steel

knuckle region. Figure 3-9 shows the deformed shape of the AY primary tank at the maximum load for the elastic/plastic analysis at 350°F (dome deflection = 0.75 inch). Figure 3-10 shows a similar deformed shape at a dome deflection of 1.0 inch, well beyond the maximum load point. Even this rather severe loading condition does not result in gross distortions of the tank geometry. Therefore, the AMSE stiffness reduction method was used to define the allowable equivalent dome compressive displacement even though this is somewhat beyond the displacement that corresponds to the maximum load. This is justified because the axial deformation of the primary tank is fully displacement controlled and it is stable well beyond the maximum load.

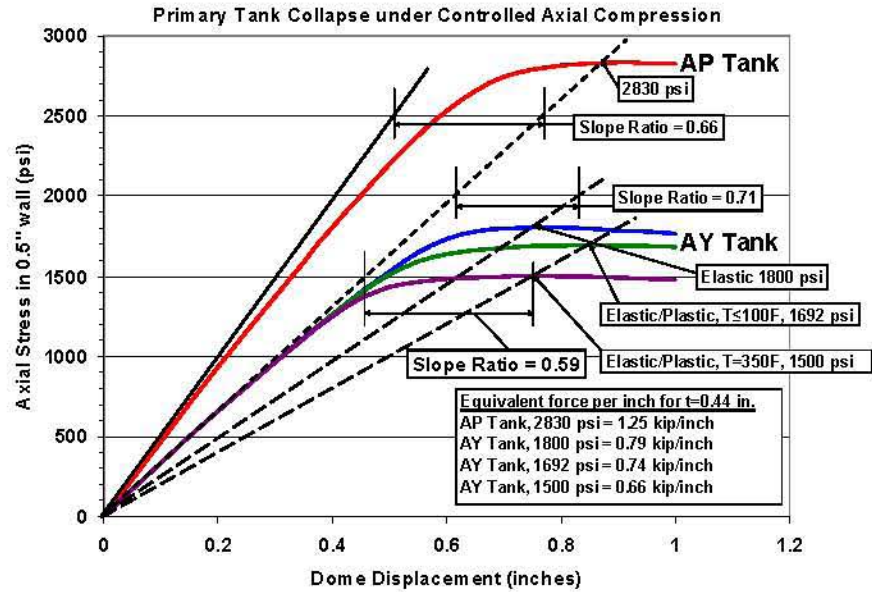


Figure 3-8. Load Deflection Curves of the AY and AP Primary Tanks Under Axial Compression Alone (These results are for a uniform corrosion allowance of 0.060 inches. Note that bending stresses in the upper knuckle of the elastic AY model exceeded the 32 ksi yield strength. The model was re-analyzed with elastic/plastic stress strain curves for A515 steel at $\leq 100^{\circ}\text{F}$ and 350°F .)

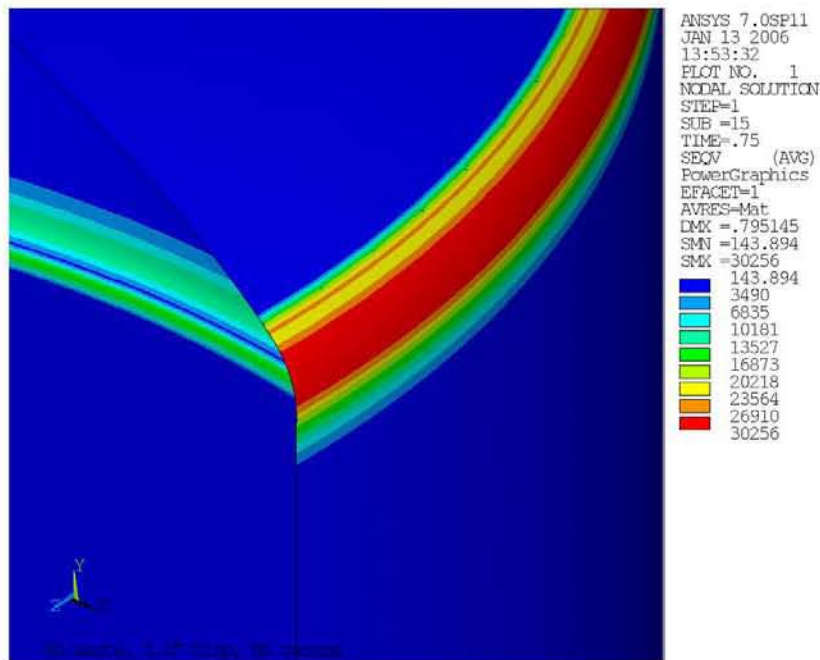


Figure 3-9. Surface Stress in the Upper Knuckle Region of the AY Tank at the Maximum Axial Compressive Load (dome deflection = 0.75 inch) (The yield curve corresponds to A515-65 steel at 350°F . The displaced shape is for a scale factor of 1.0.)

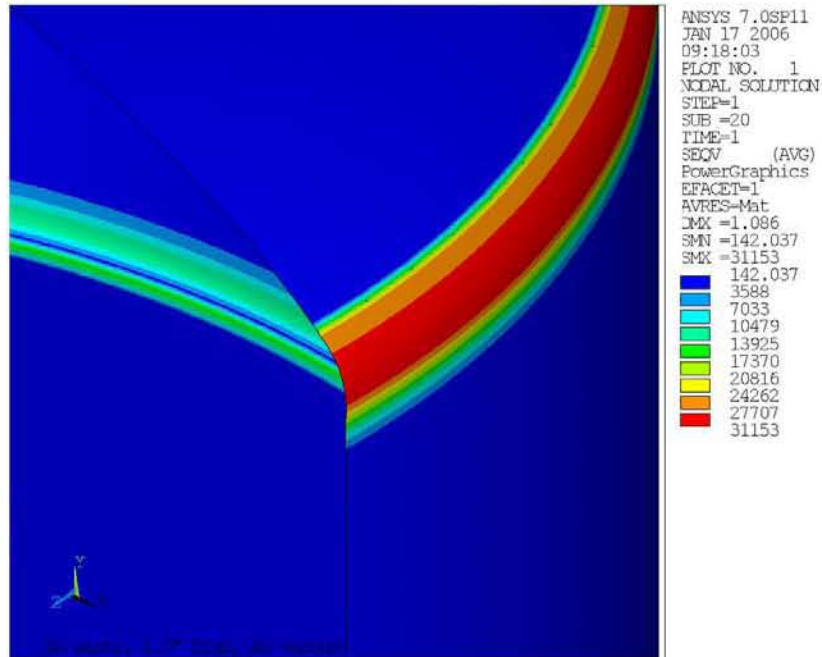


Figure 3-10. Surface Stress in the Upper Knuckle Region of the AY Tank at a Dome Deflection = 1.0 Inch (The yield curve corresponds to A515-65 steel at 350°F. The displaced shape is for a scale factor of 1.0.)

Figure 3-11 shows the ASME 50% stiffness slopes for the three corrosion allowances (0.000, 0.060, and 0.100 inch) that were modeled. Note that the assumed level of wall thinning significantly affects the stiffness of the tank. Figure 3-12 shows the family of nonlinear force/deflection curves for the AY tank geometry with 0.060 inch corrosion allowance and stress/strain curves corresponding to several different operating temperatures. The limiting equivalent dome deflections are defined where the ASME 50% slope intersects the load/deflection curve. Figure 3-13 shows the similar response of the AP tank. Figures 3-12 and 3-13 also define the equivalent linear elastic force, $F_e(\max)$, which would correspond to the limiting dome deflection if the tank deformed at the initial linear elastic stiffness. The equivalent linear elastic force is needed when correlating the applied axial force (the sum of the different axial load components) to the allowable vacuum. Finite element models were used to estimate the incremental axial force components due to individual loads such as concrete thermal degradation and creep, hydrostatically induce axial stress, surface loads, seismic loads, and differential thermal expansion. Each of these load components are relatively small and result in a linear response of the structure. However when combined, these loads can deform the tank into the nonlinear range. Therefore, the equivalent linear elastic force accounts for the sum of the force components and it corresponds to the sum of the linear dome deflections that the axial load components would apply to the tank. This assumes that the deformation of the primary tank is fully determined by the loads on the primary tank plus the deformations of the concrete over-structure. The equivalent linear elastic force is used in the curve fitting to correlate the axial compression in the tank with the allowable vacuum limit. It should be emphasized that the equivalent linear elastic force is not the maximum allowable force on the primary tank. It is simply defined to:

1. provide a limit on the sum of the axial load components that corresponds to the maximum tank deformation defined by the ASME stiffness reduction method, and
2. define the vacuum limit for the tanks as a function of the sum of the axial loads.

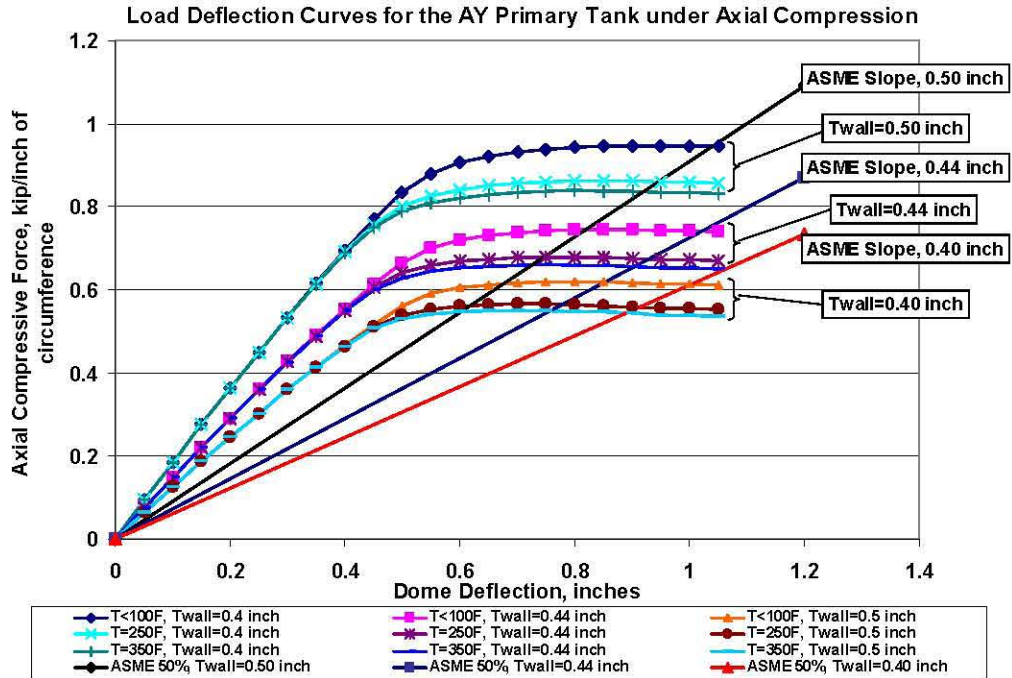


Figure 3-11. Load Deflection Curves for the AY Primary Tank Under Axial Compression for a Range of Yield Strengths and Wall Thicknesses (corrosion allowances) in the Nominal 0.5 Inch Wall Section

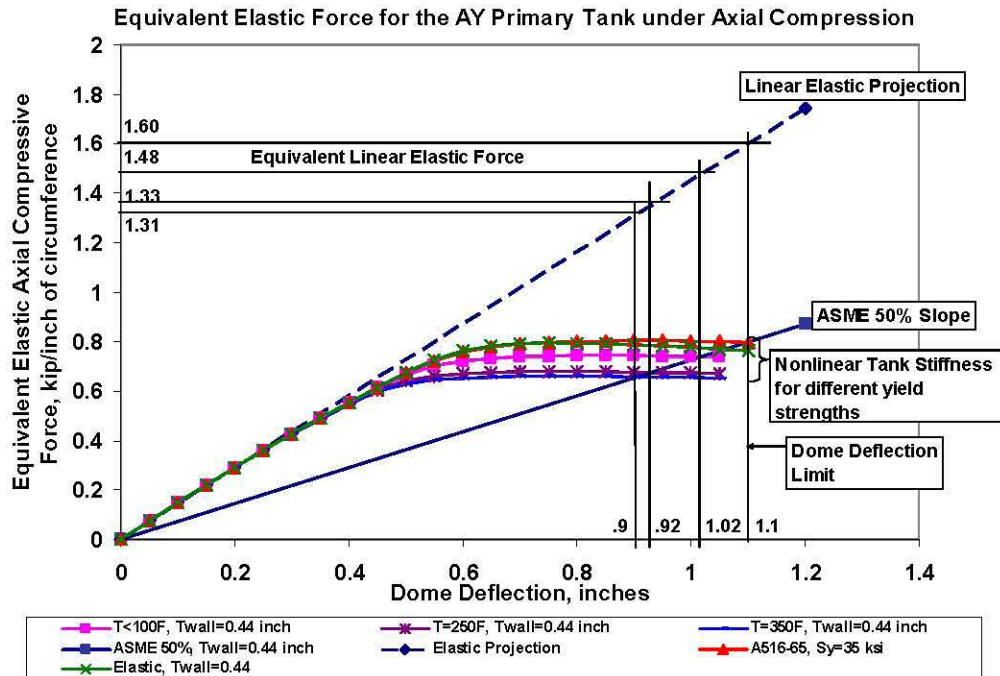


Figure 3-12. Nonlinear Load Deflection Curves for the AY Tank Plus the Linear Elastic Projected Stiffness, Showing the Definition of the Equivalent Linear Elastic Compressive Force

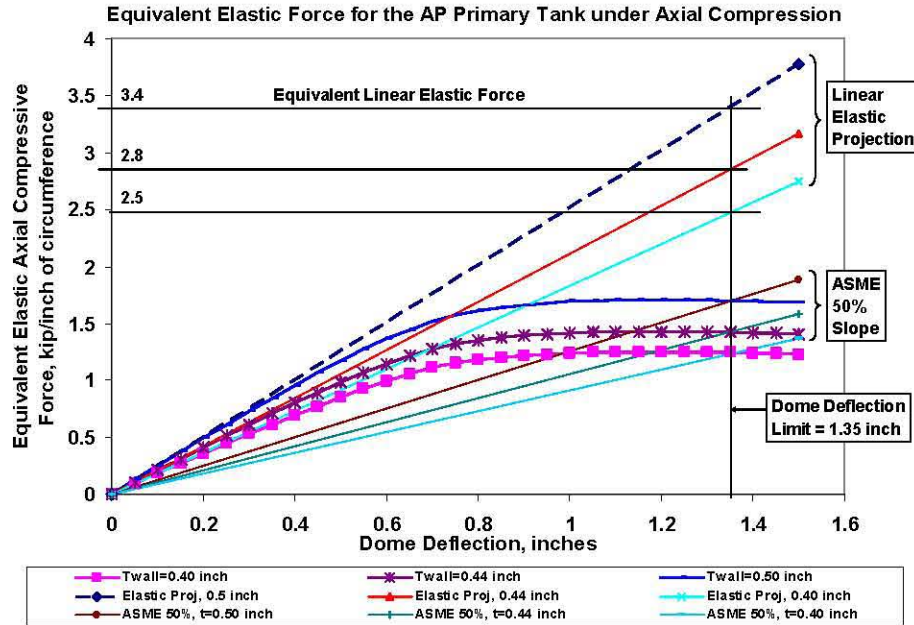


Figure 3-13. Nonlinear Load Deflection Curves for the AP Tank Plus the Linear Elastic Projected Stiffness, Showing the Definition of the Equivalent Linear Elastic Compressive Force

Tables 3-4 and 3-5 list the maximum axial force and its corresponding dome deflection plus the equivalent elastic force and its corresponding deflection for the AY and AP tanks, respectively. The tables show that the maximum axial force that the primary tank can support is roughly 50% of the equivalent linear elastic force. The maximum surface strains (in the haunch) are less than 0.5% for the limiting dome deflections in Tables 3-4 and 3-5.

Table 3-4. Summary of Maximum Dome Displacements and Maximum Equivalent Linear Elastic Compressive Forces for the AY Primary Tank

Temp.	Yield Stress	Dome Displacement at Max Force	Maximum Nonlinear Force	Dome Displacement Limit	Equiv. Elastic Force Limit
°F	ksi	inches	kip/inch	inches	kip/inch
Twall = 0.500 inches, Corrosion = 0.0 inch					
≤ 100	32.00	0.9	0.95	1.05	1.91
250	28.75	0.85	0.86	0.95	1.73
350	27.85	0.8	0.84	0.92	1.67
Twall = 0.440 inches, Corrosion = 0.060 inch					
Elastic	>36.6	0.75	0.79	1.06	1.54
A516-65	35.00	0.9	0.80	1.10	1.60
≤ 100	32.00	0.85	0.74	1.02	1.48
250	28.75	0.75	0.68	0.92	1.33
350	27.85	0.75	0.66	0.90	1.31
Twall = 0.400 inches, Corrosion = 0.100 inch					
≤ 100	32.00	0.8	0.62	1.00	1.22
250	28.75	0.7	0.57	0.91	1.11
350	27.85	0.7	0.55	0.89	1.09

Table 3-5. Summary of Maximum Dome Displacements and Maximum Equivalent Linear Elastic Compressive Forces for the AP Primary Tank

Wall Thickness	Corrosion	Dome Displacement at Max Force	Maximum Nonlinear Force	Dome Displacement Limit	Equiv. Elastic Force Limit
inches	inches	inches	kip/inch	inches	kip/inch
0.500	0.000	1.20	1.71	1.35	3.39
0.440	0.060	1.20	1.43	1.35	2.85
0.400	0.100	1.20	1.25	1.35	2.47

3.1 Vacuum Limit Equations for the AY Primary Tank

Figure 3-14 shows the AY vacuum limits that were calculated for waste heights from 0 to 300 inches and tank compressive displacements of 0 to 0.6 inches. The dome displacement of 0.6 inches gives compressive stresses in the AY and AP tanks that are above those predicted for the combined operating loads. These data points are for a corrosion allowance of 0.060 inch and a waste specific gravity of 1.7. The curve for axial compression of 0.3 inches give a similar initial stress to that predicted by the thermal and operating loads analysis (Rinker et al. 2004). These data points were curve fit and shifted upward to the vacuum limit for zero axial compression and zero waste height. (Note: The data points of the 0.3 inch axial compression were used for curve fitting because they give a slightly flatter curve with waste height and are thus slightly conservative compared to the data points for 0.0 inch axial compression). The predicted vacuum limit increases more rapidly at waste heights above 300 inches and, therefore, a second

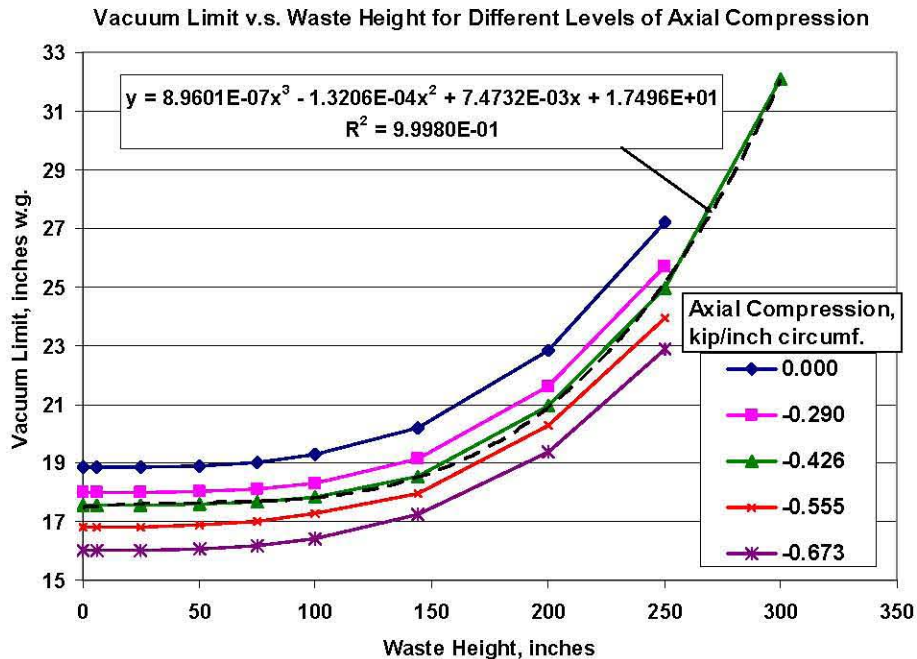


Figure 3-14. Calculated Vacuum Limit Versus Waste Heights for a Range of Axial Compressive Loads (These results are for the AY tank with waste SpG = 1.7 and corrosion allowance = 0.060 inch.)

linear projection was used to approximate the vacuum limits above 300 inches of waste. The resulting equations for limit vacuum in the AY tank with zero axial compression is:

$$\begin{aligned}
 P_{V(F_\phi=0)} &= 9.6251 \times 10^{-7} h^3 - 1.4185 \times 10^{-4} h^2 + 8.0271 \times 10^{-3} h + 18.855 \\
 &\text{for } 0 \leq h \leq 300 - \text{inches} \\
 P_{V(F_\phi=0)} &= 0.39530h - 84.104 \\
 &\text{for } 300 \leq h \leq 460 - \text{inches}
 \end{aligned} \tag{3.1}$$

Where h is the waste height in inches. The vacuum limit is expressed in inches of water gauge (inch w.g.).

The vacuum limits for a 6-inch waste depth and increasing compressive load were used to fit a scale factor to adjust the above curve for compressive load (Figure 3-15). The equivalent linear elastic force, F_ϕ , expressed in kip per inch of tank circumference, is used for the equation fitting because it is independent of the different thicknesses in the free-standing portion of the tank wall. The axial compressive force factor, $f(F_\phi)$ is

$$f(F_\phi) = -0.01437F_\phi^3 - 0.17908F_\phi^2 + 0.08798F_\phi + 0.9988 \tag{3.2}$$

Note that the equivalent linear elastic force, F_ϕ , is compressive and expressed as a negative quantity. This equation is valid for axial compressive forces up to the maximum equivalent linear elastic force, $F_\phi(\text{max})$, which was defined in the previous section.

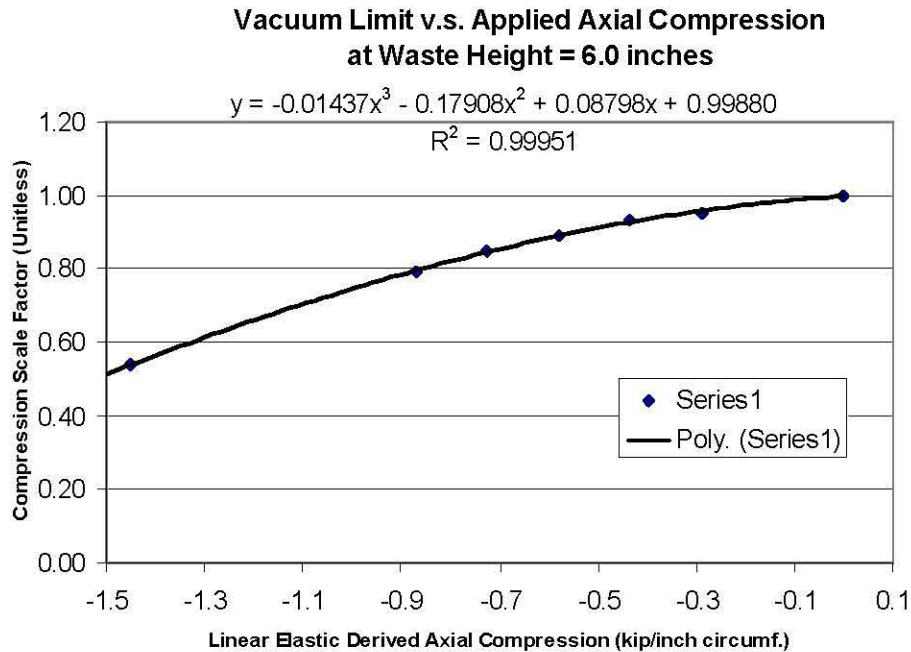


Figure 3-15. Axial Compression Scale Factor of Adjusting the Vacuum Limit for the AY Primary Tank

Tank models with corrosion allowances of 0.0 to nearly 0.1 inches were also run to determine the sensitivity of the vacuum limit to reductions in the wall thickness. Figure 3-16 shows the relationship of the limit vacuum ratio (normalized by the limit vacuum for a wall thickness reduction of 0.060 inch) for the range of wall thicknesses that were analyzed. The data in Figure 3-16 were curve fit to give the wall thickness factor, $g(t)$ as:

$$g(t) = 10.43255t^2 + 12.025t - 1.753 \quad (3.3)$$

Where t is the 0.375 inch wall thickness of the AY upper tank wall minus the corrosion allowance. The minimum wall thickness in the upper wall of the tank was used for the scaling because this is where the buckling deformation occurs. Equation 3.3 is valid for corrosion allowed from 0.0 to 0.1 inches.

The tank buckling model was also run with different specific gravities ranging from 1.0 to 2.0. Figure 3-17 shows the normalized vacuum limit as a function of specific gravity. These data were curve fit to give the specific gravity factor, $h(\text{SpG})$, as

$$h(\text{SpG}) = -0.0344(\text{SpG})^2 + 0.1758(\text{SpG}) + 0.801 \quad (3.4)$$

The specific gravity, SpG , is unitless. Equation 3.4 is valid for waste specific gravities from 1.0 to 2.0.

Finally, the vacuum limit, $P_v(F_\phi, t, \text{SpG}, h)$, can be calculated as the product of Equations 3.1 through 3.4.

$$P_v(F_\phi, t, \text{SpG}, h) = f(F_\phi)g(t)h(\text{SpG})P_{v(F_\phi=0)} \quad (3.5)$$

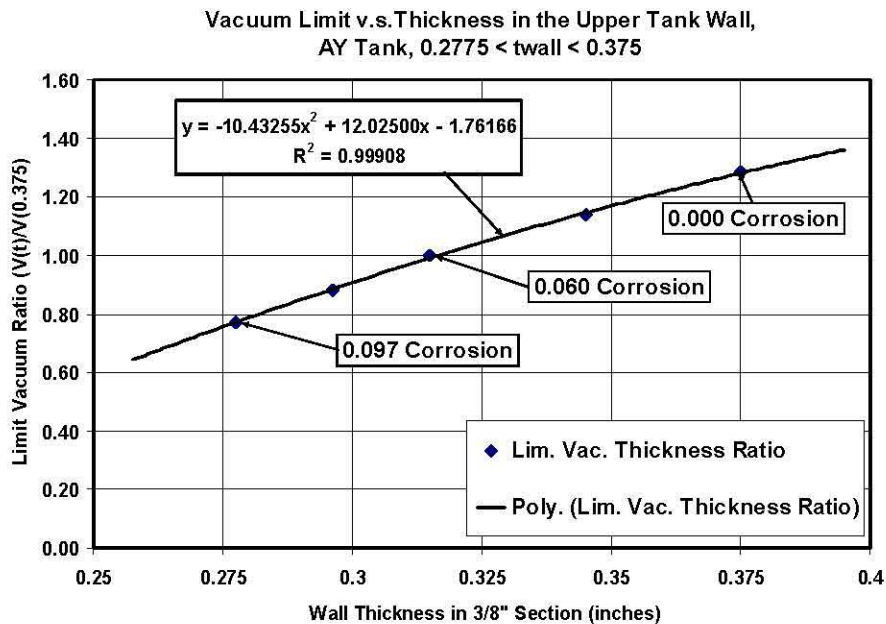


Figure 3-16. Wall Thickness Scale Factor for the AY Tank

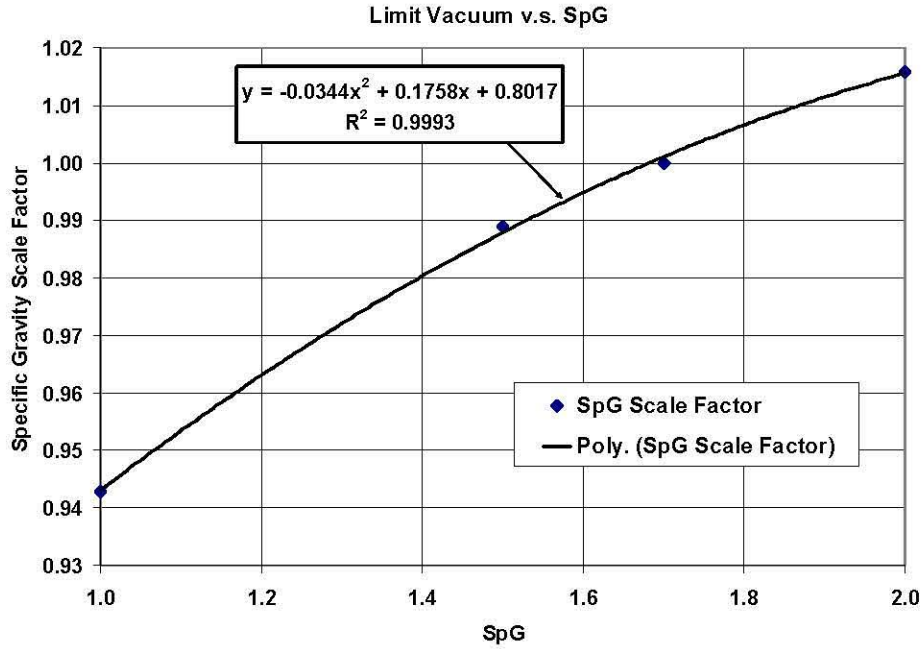


Figure 3-17. Specific Gravity Scale Factor for the AY Tank

The units for the vacuum limit are inches w.g. Figure 3-18 shows that the analytical equations fit the data in Table 3-1 quite well. A Microsoft Excel® spreadsheet (shown in Table 3-6 for the AY tank) was also constructed so that the vacuum limit can be easily calculated based on the parameters F_ϕ , t , SpG , and h .

Addition equations were fit to calculate the maximum equivalent linear elastic force, $F_\phi(\max)$, as a function of the wall thickness and the yield strength. Figure 3-19 shows that a linear relationship exists between the equivalent linear elastic force and the wall thickness for the AY tank. Figure 3-20 shows a similar trend for the AP tank geometry. For the AY tank the equation for the limiting equivalent linear elastic force, $F_\phi(\max)$, is:

$$F_\phi(\max) = \sigma_y(-0.21269t + 0.020025) \quad (3.6)$$

Where $F_\phi(\max)$ is in kip per inch of tank circumference, σ_y is the yield strength at temperature, and t is the 0.375 inch thickness of the upper AY tank wall minus the corrosion allowance.

Figure 3-21 shows the axial displacements of the AY tank are concentrated in the dome and upper knuckle of the tank. The deformed shape of the AP tank is similar. Since the deformation is confined in the upper knuckle at the thinnest wall section, the axial compressive load limit is not significantly influenced by the waste height.

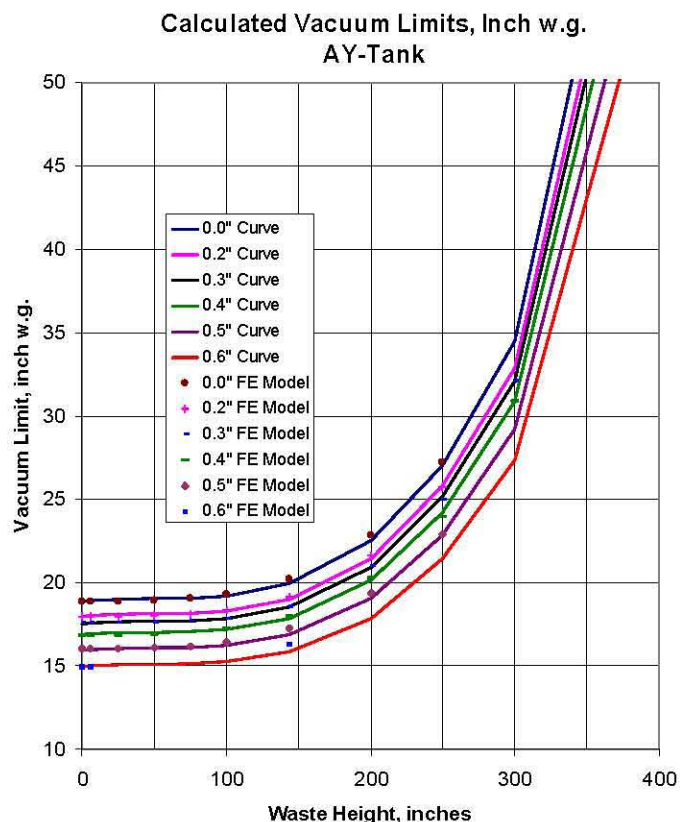


Figure 3-18. Comparison of the Analytical Equations for Vacuum Limit with the Discrete Values Predicted with Large Deformation Finite Element Analysis

Table 3-6. Excel® Spreadsheet for Calculating the Vacuum Limit of the AY Primary Tank

AY Vacuum Limits Calculated using the polynomial equations								
SpG =	1.7	h(SpG) =	1.000444					
Corrosion Allow=	0.06	g(t) =	0.999705226					
t(3/8) =	0.315	h(SpG) * g(t)	1.000149095					
Axl Stress, t=3/8"	psi	0	-317	-635	-952	-1270	-1587	-3175
		Equivalent Linear Elastic Axial Force (kip/in of circumference) ----->						
Lin. Axial Force, F(kip/in)		0.00	-0.10	-0.20	-0.30	-0.40	-0.50	-1.00
Force Factor, f(F) =		0.999	0.988	0.974	0.957	0.936	0.912	0.746
Waste Ht.								
inches		Limit Vacuums, inches w.g. ----->>>>						
1st equation	0	18.84	18.64	18.37	18.04	17.65	17.20	14.07
	6	18.88	18.68	18.41	18.08	17.69	17.23	14.10
	25	18.96	18.76	18.49	18.16	17.77	17.31	14.16
	50	19.00	18.80	18.53	18.20	17.80	17.35	14.19
	75	19.05	18.84	18.58	18.24	17.85	17.39	14.23
	100	19.18	18.98	18.71	18.37	17.97	17.51	14.33
	144	19.92	19.71	19.43	19.08	18.67	18.19	14.88
	200	22.46	22.23	21.91	21.52	21.05	20.51	16.78
	250	27.01	26.72	26.34	25.87	25.31	24.66	20.17
	300	34.45	34.08	33.60	33.00	32.28	31.45	25.73
2nd equation	300	34.45	34.09	33.60	33.00	32.28	31.45	25.73
	350	54.19	53.62	52.86	51.91	50.78	49.48	40.48
	400	73.94	73.16	72.11	70.82	69.28	67.50	55.23
	460	97.63	96.60	95.22	93.51	91.48	89.13	72.93

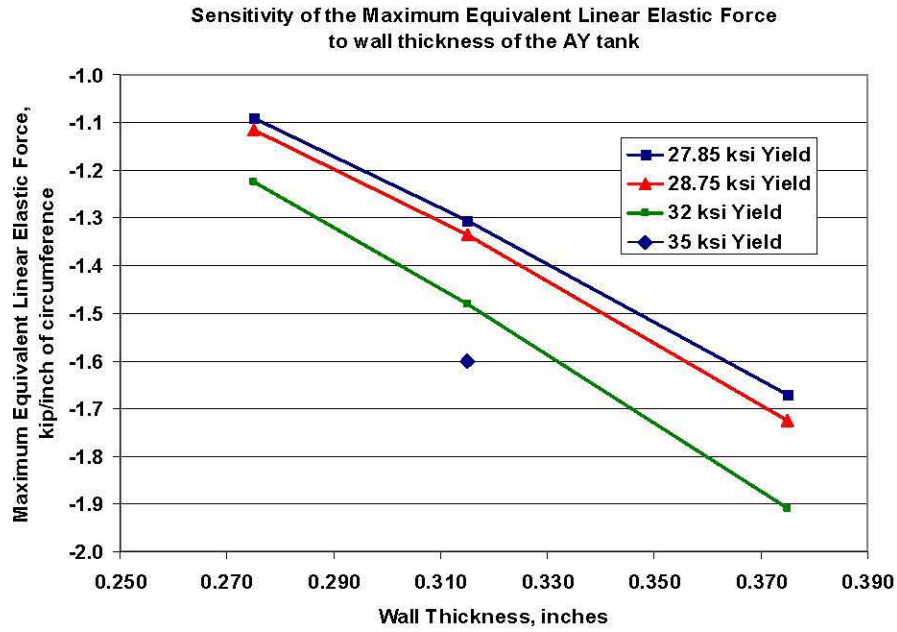


Figure 3-19. Effect of Wall Thickness and Yield Strength on the Axial Limit Load for the AY Primary Tank

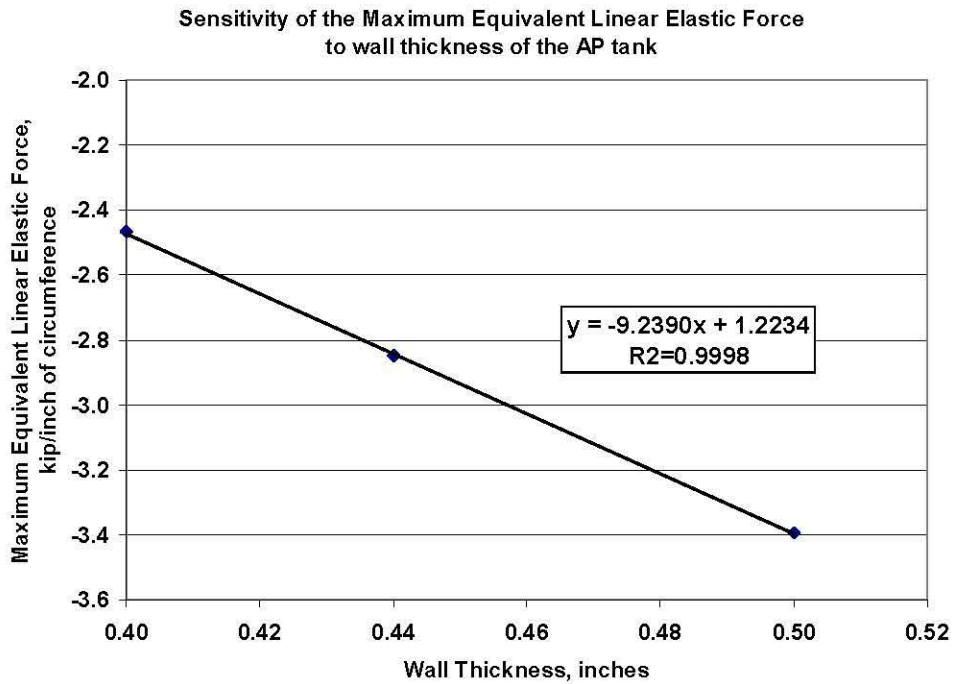


Figure 3-20. Effect of Wall Thickness on the Axial Limit Load for the AP Primary Tank

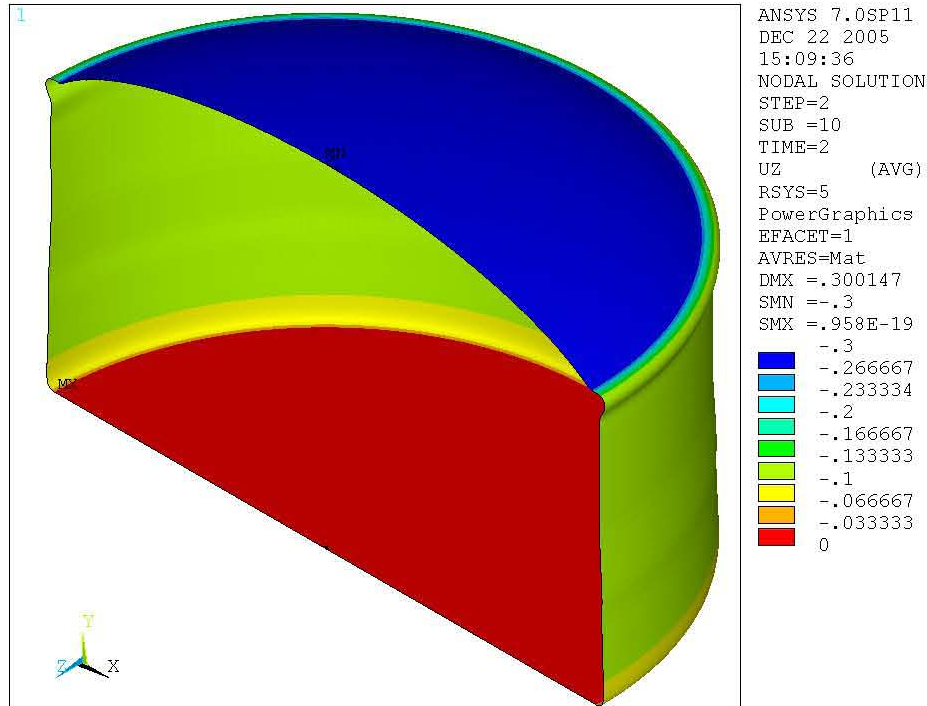


Figure 3-21. Typical Displacement Shape of the AY and AP Primary Tanks at the Axial Limit Load
(The displacements have been magnified 50 times in the plot.)

3.2 Vacuum Limit Equations for the AP Primary Tank

Equations for calculating the vacuum limit of the AP primary tank were fit using the model results listed in Table 3-2. The equations for limit vacuum in the AP tank with zero axial compression are:

$$\begin{aligned}
 P_{V(F_\phi=0)} &= 1.2233 \times 10^{-6} h^3 - 2.2759 \times 10^{-4} h^2 + 1.5927 \times 10^{-2} h + 20.5942 \\
 &\quad \text{for } 0 \leq h \leq 300 - \text{inches} \\
 P_{V(F_\phi=0)} &= 0.72364h - 179.172 \\
 &\quad \text{for } 300 \leq h \leq 460 - \text{inches}
 \end{aligned} \tag{3.7}$$

The axial compressive force factor, $f(F_\phi)$, is given by

$$f(F_\phi) = -0.01474F_\phi^3 - 0.02956F_\phi^2 + 0.10616F_\phi + 1.00025 \tag{3.8}$$

Where F_ϕ is the equivalent linear elastic compressive force in the tank wall in kip/inch of the circumference. Again, the compressive force is negative.

The wall thickness factor, $g(t)$ is given by

$$g(t) = 3.81011t^2 + 1.0394t - 0.1949 \tag{3.9}$$

Where t is the 0.5 inch thickness of the AP upper tank wall minus the corrosion allowance. Equation 3.9 is valid for corrosion allowance from 0.0 to 0.1 inches.

The specific gravity factor, $h(\text{SpG})$ is given by

$$h(\text{SpG}) = -0.0344(\text{SpG})^2 + 0.1758(\text{SpG}) + 0.801 \quad (3.10)$$

Equation 3.10 is valid for waste specific gravities from 1.0 to 2.0.

Finally, the vacuum limit, $P_v(F_\phi, t, \text{SpG}, h)$, is calculated as the product of Equations 3.7 through 3.10.

$$P_v(F_\phi, t, \text{SpG}) = f(F_\phi)g(t)h(\text{SpG})P_v(F_\phi = 0) \quad (3.11)$$

The units for the vacuum limit are again inches w.g. A Microsoft Excel® spreadsheet (shown in Table 3-7 for the AP tank) was constructed so that the vacuum limit can be easily calculated based on the parameters F_ϕ , t , SpG , and h .

From Figure 3-20, the equation for the maximum equivalent linear elastic force, $F_\phi(\text{max})$, for the AP primary tank is:

$$F_\phi(\text{max}) = -9.239t + 1.2234 \quad (3.12)$$

Where $F_\phi(\text{max})$ is in kip per inch of tank circumference and t is the 0.500 inch thickness of the AP upper tank wall minus the corrosion allowance.

Table 3-7. Excel® Spreadsheet for Calculating the Vacuum Limit of the AP Primary Tank

AP Vacuum Limits Calculated using the polynomial equations								
SpG =	1.7	$h(\text{SpG}) =$	1.000444					
Corrosion Allow=	0.06	$g(t) =$	1.000082096					
$t(0.5) =$	0.44	$h(\text{SpG}) * g(t)$	1.000526132					
Axl Stress, $t=1/2$	psi	-455	-909	-1364	-1818	-2273	-2727	-4773
Equivalent Linear Elastic Axial Force (kip/in of circumference) ----->								
Axial Force, $F(\text{kip/in})$		-0.200	-0.400	-0.600	-0.800	-1.000	-1.200	-2.100
Force Factor, $f(F) =$		0.980	0.956	0.931	0.906	0.882	0.858	0.786
Waste Ht.								
inches		Limit Vacuums, inches w.g. --->>>>						
1st equation	0	20.197	19.704	19.190	18.672	18.164	17.679	16.190
	6	20.283	19.787	19.272	18.752	18.241	17.755	16.259
	25	20.467	19.967	19.447	18.922	18.406	17.915	16.406
	50	20.570	20.067	19.545	19.017	18.499	18.006	16.489
	75	20.619	20.115	19.591	19.063	18.543	18.049	16.528
	100	20.727	20.220	19.694	19.162	18.640	18.143	16.614
	144	21.400	20.877	20.334	19.785	19.246	18.733	17.154
	200	23.991	23.404	22.795	22.180	21.575	21.000	19.231
	250	28.898	28.191	27.457	26.716	25.988	25.295	23.164
	300	37.187	36.278	35.334	34.380	33.443	32.551	29.809
2nd equation	300	37.189	36.280	35.335	34.381	33.445	32.553	29.810
	350	72.673	70.897	69.051	67.187	65.357	63.614	58.253
	400	108.158	105.515	102.767	99.992	97.269	94.675	86.697
	460	150.739	147.055	143.225	139.358	135.563	131.948	120.829

3.3 Comparison of Buckling Evaluations Using ASME N-284-1 and the DST Primary Tank Specific Method

Buckling evaluations were made for a DST primary tank using both the N-284-1 method and PNNL's tank-specific method described in Section 2.2. The AY tank was chosen with the conditions specified in Table 3-8. Three different cases were analyzed; two with different waste heights (6 inches and 144 inches) and the third with a waste height of 144 inches and the minimum wall thickness of the AY tank (0.375 inch minus the 0.060 inch corrosion allowance). The buckling length of the cylinder was assumed to be the vertical distance between the waste free surface and the tangent point between the upper knuckle and the dome. The wall thickness in cases 1 and 2 is the weighted average wall thickness over this length. Table 3-9 summarizes section properties and allowable stresses calculated using the N-284-1 methods. The allowable stresses from N-284-1 are defined as follows:

σ_{xa} = The allowable axial compressive stress, psi, for external radial pressure = 0.0

σ_{ra} = The allowable external radial pressure, psi, for axial stress = 0.0

σ_{ha} = The allowable hydrostatic external pressure, psi, where the axial stress, $\sigma_{axial} = 1/2 \sigma_{hoop}$ for a closed ended cylinder

Table 3-8. Buckling Evaluation Cases for Comparing the N-284-1 Method with the PNNL Large Displacement Buckling Evaluation Method

Case No.	R = tank radius, inches	h=waste height, inches	Length, L=460-h = distance from waste surface to dome tangent, inches	t = average wall thickness above the waste, inches	E=elastic modulus, psi
1	450	6	454	0.507	29.5E6
2	450	144	316	0.409	29.5E6
3	450	144	316	0.315	29.5E6

Table 3-9. ASME N-284-1 Calculated Section Properties and Allowable Stresses

Case No.	R/t	$M = \frac{L}{\sqrt{Rt}}$	σ_{xa} = allowable axial compressive stress, psi	σ_{ra} = allowable radial only compressive stress, psi	σ_{ha} = allowable hydrostatic compressive stress, psi ($\sigma_{axial}=1/2 \sigma_{hoop}$)
1	888	30.45	4028	808	794
2	1100	23.25	3250	860	840
2	1429	26.54	2590	750	730

Article 1713.1.1 of N-284-1 uses these three allowable loads to construct interaction diagrams for different combinations of axial compressive stress and external radial pressure. Figures 3-22 and 3-23 show interaction diagrams for the two different wastes with average wall thickness. Figure 3-24 shows similar results for the 144-inch waste height with the reduced wall thickness of the upper wall. In these plots the radial external pressure was converted to inches w.g. and the axial stress to kip/inch of tank circumference (by multiplying by the average wall thickness used in the N-284-1 calculations) for direct comparison with PNNL's large displacement buckling method.

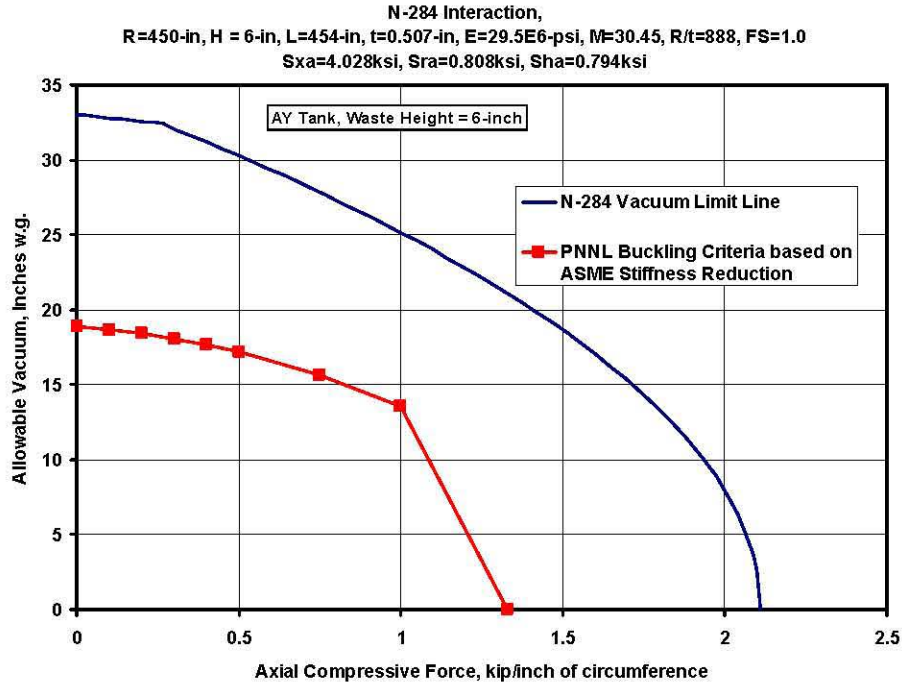


Figure 3-22. Comparison of the PNNL Large Displacement Buckling Evaluation Method with the ASME N-284-1 Method (The comparison is made for the AY tank with a waste height of 6 inches.)

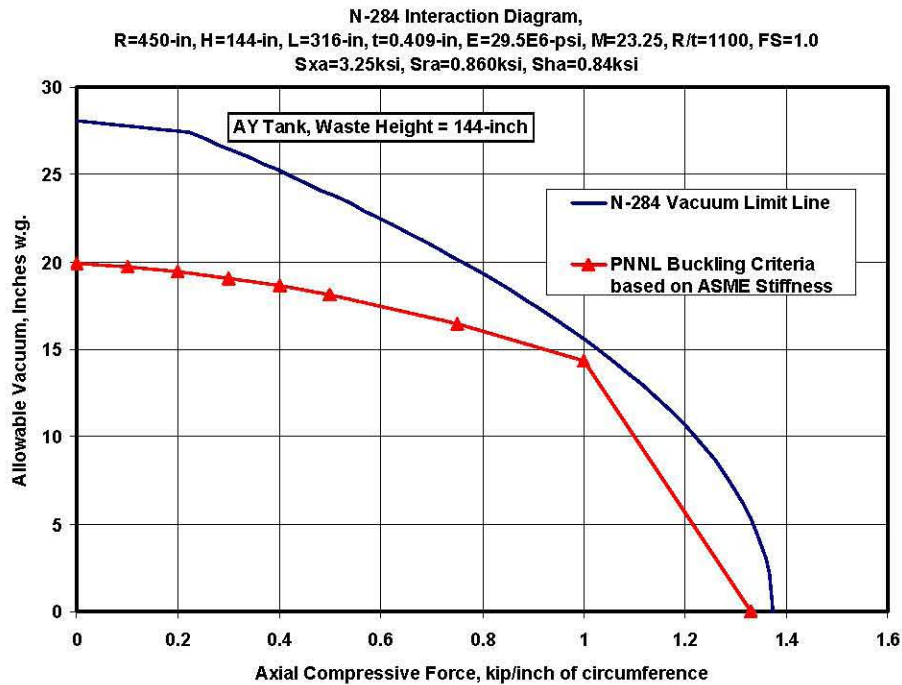


Figure 3-23. Comparison of the PNNL Large Displacement Buckling Evaluation Method with the ASME N-284-1 Method (The comparison is made for the AY tank with a waste height of 144 inches.)

Figures 3-22 and 3-23 show that the PNNL results give nearly the same limit curves for both the waste heights. The vacuum limit for the 6-inch waste height is slightly smaller than the vacuum limit for the 144 inch waste height. This is reasonable because the buckling deformation (the basis for the vacuum limits) primarily occurs in the upper section of the tank above the waste height. It is also reasonable for the vacuum limit to decrease slightly with reduced waste height because the tank wall is supported less at the lower waste height. However, Figures 3-22 and 3-23 show that the N-284-1 evaluation (based on the free height above the waste and the corresponding average wall thickness) predicts the opposite trend with a considerably higher vacuum limit for the lower waste height. The N-284-1 vacuum limit increases with decreasing waste height because it is a direct function of the thickness, and the average thickness increases as the waste height decreases. This is counter intuitive.

The third comparison case (Figure 3-24) shows the interaction diagram for the 144-inch waste height assuming that the average wall thickness is the minimum thickness of the upper section of the tank wall (0.315 inches). N-284-1 gives nearly the same vacuum limit as the PNNL method when using the minimum wall thickness. This is reasonable because the vacuum limit is proportional to the wall thickness and the finite element analysis has shown that the buckling deformation mode occurs primarily in the upper thin section of the tank wall. Although somewhat higher, the PNNL method gives a very comparable limit for the axial compression load. This is justifiable based on the detailed tank specific analysis that was performed and the understanding that the tank axial deformation is fully displacement controlled by the outer concrete structure.

In summary, the comparison cases presented here show that the PNNL tank-specific buckling method establishes buckling limits that are similar in magnitude to the limits calculated using the N-284-1 method. The PNNL method correctly accounts for the wall thickness effects and the confinement of the primary tank inside the concrete outer tank. These comparison cases support the validity of the buckling evaluation method developed by PNNL for the DST primary tanks.

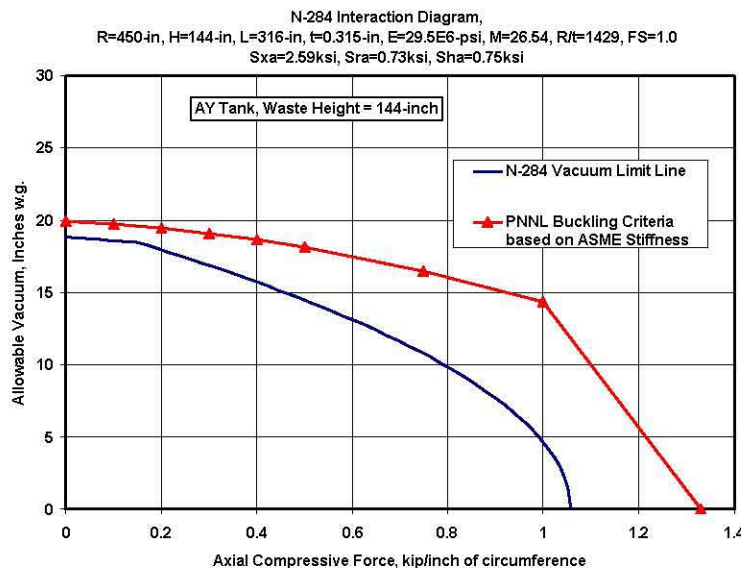


Figure 3-24. Comparison of the PNNL Large Displacement Buckling Evaluation Method with the ASME N-284-1 Method (The comparison is made for the AY tank with a waste height of 144 inches and an average wall thickness of 0.315 inches.)

4.0 ANSYS Thermal Model of the Double-Shell Waste Tanks

The Double-Shell Tank Thermal and Operating Loads Analysis (Rinker et al. 2004) used a TEMPEST thermal model to predict the temperature distributions for a single waste height and thermal transient. TEMPEST is a finite difference, thermal-hydraulics code developed at PNNL that has been used extensively for waste tank simulations (Antoniak and Recknagle 1995). The main benefit of using TEMPEST in the Thermal and Operating Loads Analysis was that an existing double-shell waste tank model was available. This model had been calibrated to match measured temperature distributions in the waste, and it could be easily modified to simulate the bounding waste tank geometry and the design basis waste temperature transient of the Thermal and Operating Loads Analysis.

However, the data mapping procedure used to transfer the TEMPEST temperature profiles to the ANSYS structural model made analyzing different waste heights and temperature transients difficult because of the different numerical grids that were used. Therefore, an ANSYS thermal model has been developed that is directly (node-to-node) compatible with the ANSYS DST structural model. This model supports the tank buckling analysis by allowing easy prediction of tank stresses due to different combinations of thermal and operating loads. This capability is required to calculate the allowable net vacuum loads as a function of the waste height and temperature. The ANSYS thermal model input files are listed in Appendix C.

4.1 Comparison of Previous Double-Shell Tank Thermal Models

The modeling features and methods used in previous waste tank thermal models were reviewed during the initial phase of the ANSYS thermal model development to ensure that the significant heat transfer mechanisms were accounted for in the ANSYS model. This section summarizes the main features of the TEMPEST model and other DST thermal models using the GOTH_SNF and P/THERMAL codes.

4.1.1 TEMPEST Model

The TEMPEST model by Antoniak and Recknagle (1995) includes conduction, radiation, and convection heat transfer effects on the transient tank temperatures. The model includes the following features:

- Convective (fully mixed) waste at a uniform temperature.
- Conduction from an upper non-convective waste layer to the convective waste below.
- Convection from the waste surface to the dome air, but no convection from the dome air to the dome.
- Convection from the tank wall to the annulus air, but no convection from the annulus air to the secondary tank wall.
- Radiation from the waste surface to the dome
- Radiation from the primary wall to the secondary wall.

The TEMPEST model configuration is shown in Figure 4-1.

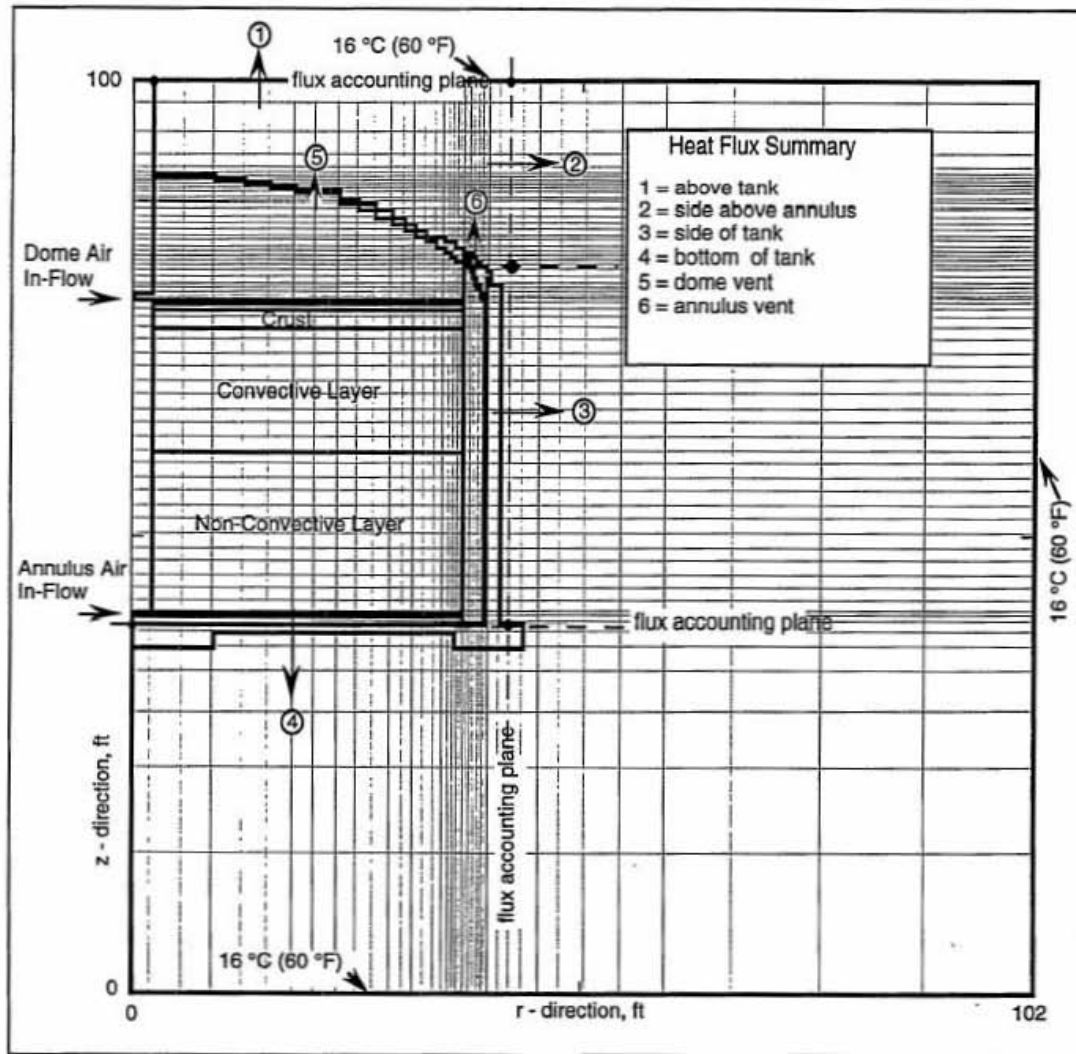
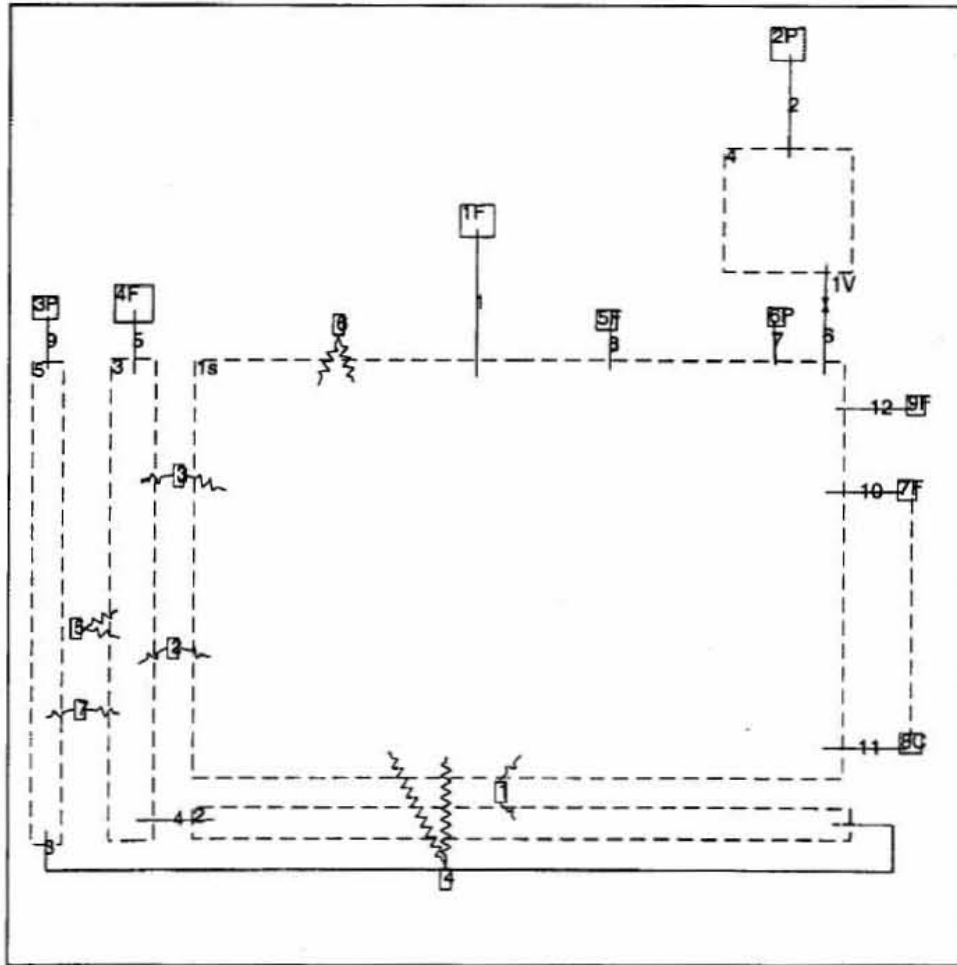


Figure 4-1. TEMPEST DST Model Configuration

4.1.2 GOTH_SNF Model

Crea, Sathyanarayana, and Ogden (2000) used the GOTH_SNF code to analyze the ability of the dome space and annulus ventilation systems to control the waste temperature during and following tank mixing. The GOTH model incorporates lumped-parameter and distributed parameter volumes, heat conductors, and flow and pressure boundary conditions to provide a one-dimensional model of tanks 241-AY-102 and 241-AZ-102. The GOTH_SNF model is shown in Figure 4-2, including the heat transfer volumes named below. Specific features of the model include:

- The tank volume is a distributed parameter volume with a 1-D (vertical) model of the waste, supernatant liquid, and the dome space (Vol. 1s in Figure 4-2).
- The waste is modeled with eight sub-volumes, the supernatant with multiple sub-volumes, and the dome with one sub-volume.
- Evaporation from the liquid is accounted for in the dome space.



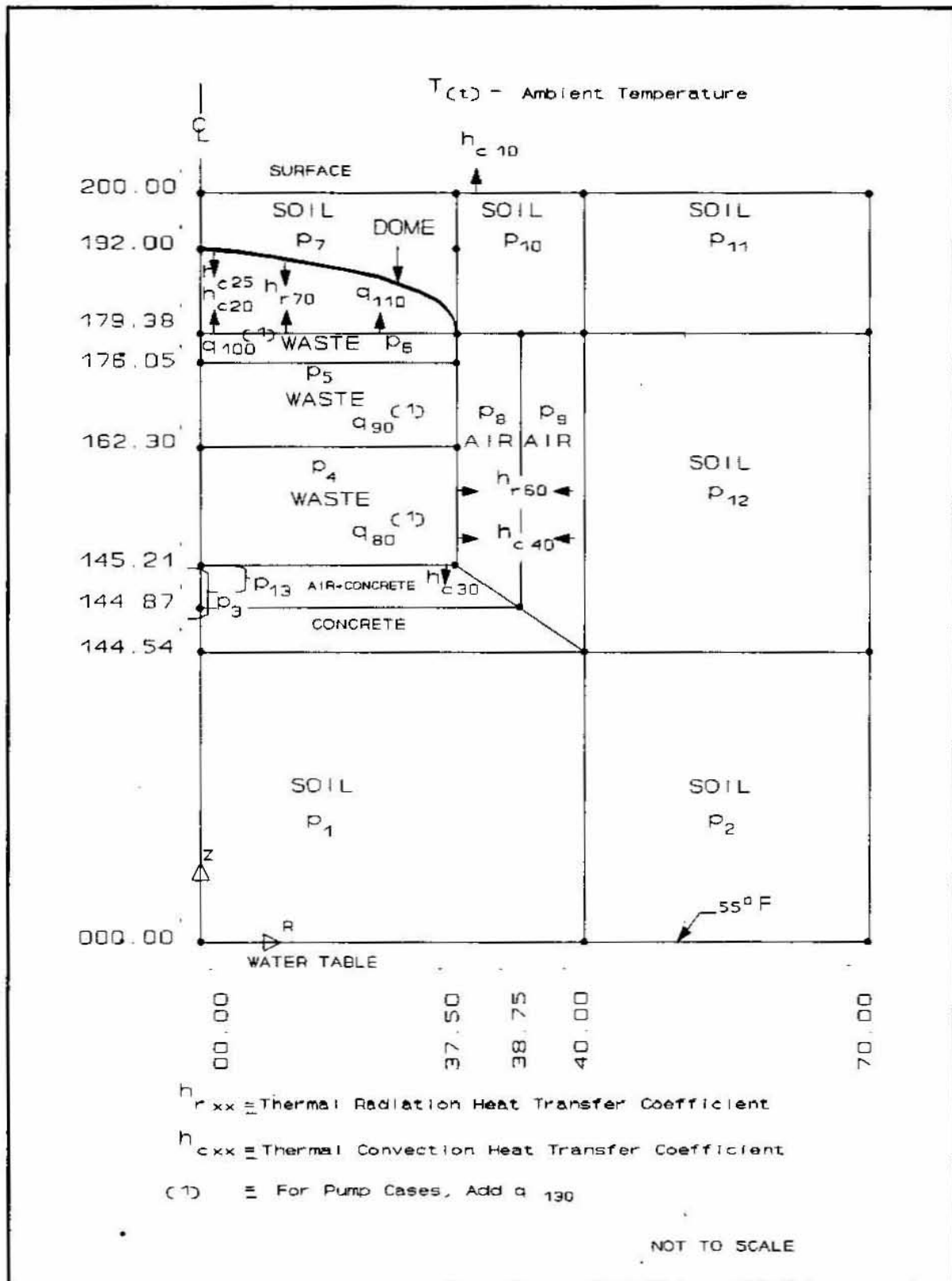


Figure 4-3. P/THERMAL DST Model Configuration

4.1.3 P/THERMAL Model

Beaver et al. (1993) describes a DST thermal model that was developed using the P/THERMAL code to predict the average waste temperatures in tank 241-SY-101 over the 13-year operating period of the tank. The model was also used to evaluate four different combinations of tank ventilation and mixer pump operations to arrest the continued cool down of the tank waste. A relatively simple 2-D axisymmetric model (Figure 4-3) was used with the following features:

- The steel walls of the tank and surrounding concrete structure were not modeled because 1) the wall thicknesses and associated temperature drops are small and 2) the controlling thermal resistances were determined to be in the waste, the air spaces, and the surrounding soil.
- The insulating concrete pad was modeled including the annulus ventilation flow channels.
- The annular air space between the primary and secondary tanks was modeled.
- The tank dome space was also modeled.
- The tank waste was treated as three separate layers each with differing thermal heat generation rates and material properties.
- The conductivity of the crust and non-convecting layers were varied with time to match the recorded temperature history for tank 241-SY-101.
- Heat flux between the primary and secondary tank walls was modeled as a combination of natural convection and thermal radiation.
- Heat loss through the bottom of the tank is modeled as conduction through the insulating concrete pad and convection to the air distribution slots.
- Heat loss from the surface of the waste includes convection, radiation (emissivity = 0.85), and evaporation.
- A progressive tank filling model was calibrated against measured temperatures between April 1977 and November 1980 to establish the baseline soil and waste temperatures and improve the accuracy of the temperature predictions in the later years of operation.

4.1.4 Summary of the Previous DST Thermal Models and the Objectives of the Buckling Analysis

Several similarities exist between the above thermal modeling studies even though different analysis methods were used.

- The objective of each study was to predict the temperature distribution in the waste rather than in the tank structure.

- The tank structure and the surrounding soil were included in the model to approximate the distribution of thermal mass and thermal resistance to better predict the waste temperature variation.
- The GOTH, SNF and P/Thermal models used a distributed heat flux in the waste whereas the TEMPEST model used a prescribed waste temperature history as the heat source.
- The waste was simulated in layers with different thermal and heat generation properties in order to better predict the measured temperature distributions.
- Many different assumptions were made regarding the input parameters and the relative importance of the competing heat transfer mechanisms, decay heat, conduction, convection, and radiation.
- Each study tuned the thermal properties to best match a set of measured temperatures in the waste column.

The major difference between these features and the thermal analysis supporting the DST structural analysis is the assumed heat source. The DST Thermal and Operating Loads Analysis is based on the operational temperature limits that are imposed on the tank structural. Therefore, specified waste temperature histories are applied as the heat source rather than a waste heat generation rate. This simulates an infinite heat source at a prescribed temperature, and it significantly affects the contribution of radiation and convection heat transfer on the tank temperatures compared to applying a waste heat generation rate. This effect is particularly significant in determining the steady state temperature of the tank dome, which approaches the temperature of the waste surface.

The TEMPEST model used in the Thermal and Operating Loads analysis included an upper non-convecting waste layer that effectively attenuated the waste surface temperature to give realistic steady state dome temperatures including the effect of radiant heat transfer. The thickness of this layer was adjusted to give the maximum dome surface temperature (235°F) from the ASA Phase III Structural Analysis (Rinker et al. 2004, Chapter 4 and Appendix A). However, using the estimated boiling temperature of the aqueous waste provides a much stronger physical basis for limiting the waste surface temperature. The high concentration of dissolved material in the supernate increases the boiling temperature from 212°F (boiling temperature of water) to upwards of 250°F depending on the specific waste chemistry of each tank. Operational experience at Hanford has shown that such temperatures are needed to achieve boiling in the evaporator units used to remove water and concentrate liquid wastes. In addition, calculations were performed by a Hanford chemist (D. Place) which estimated the boiling point of a saturated sodium nitrate solution to be 246°F (67.6% weight, or 12.2% molar concentration).

4.2 ANSYS Thermal Model

The ANSYS DST thermal model uses the boiling temperature as a rational limit on the waste surface temperature. The model applies different temperature histories to the bulk waste and surface waste throughout the thermal transient. Additional boundary conditions on the ANSYS thermal model include:

- Radiation from the waste surface to the dome.
- Convection to the dome for a prescribed film coefficient and conservatively assuming that the convective source is equal to the temperature of the waste surface.

- Radiation from the primary tank to the secondary tank.
- Convection from the annulus air to the primary and secondary tanks conservatively assuming the bulk temperature of the waste.

The ANSYS model does not include the air spaces (in the dome or annulus) in the finite element mesh. Therefore, convective heat transfer is included using a convective film coefficient and a convective source temperature. In addition, the thermal link elements used to simulate radiation (from the waste free surface to the dome and from the primary tank to the secondary tank) do not include convective heat transfer loads. However, since the temperatures of the radiating body and incident surfaces are nearly the same on the absolute temperature scale, the radiant heat transfer is for all purposes linear with the temperature difference and the convection can be lumped with the radiation term. Radiant heat transfer from a constant temperature source can be calculated as:

$$q_{\text{rad}} = \sigma \varepsilon (T_R^4 - T_S^4) \quad (4.1)$$

Where σ is the Stefan-Boltzmann constant ($2.86\text{E-}10 \text{ Btu/day-in}^2\text{-}^\circ\text{R}^4$), ε is the surface emissivity (0.7), T_R is the radiating source temperature, and T_S is the incident surface temperature. Note that absolute temperatures ($^\circ\text{R}$) must be used when calculating radiant heat transfer. When T_R and T_S are similar in absolute magnitude, Equation 4.1 can be accurately approximated as:

$$\begin{aligned} q_{\text{rad}} &= \sigma \varepsilon (4T_R^3)(T_R - T_S) = h_{\text{rad}}(T_R - T_S), \\ h_{\text{rad}} &= \sigma \varepsilon (4T_R^3) \end{aligned} \quad (4.2)$$

Assuming the maximum temperature difference corresponding to $T_R = 350^\circ\text{F}$ (810°R) and $T_S = 50^\circ\text{F}$ (510°R) gives only a 5% difference between Equations 4.1 and 4.2 ($T_R = 610^\circ\text{R}$ and $T_S = 510^\circ\text{R}$ gives only a 1% difference). Equation 4.2 was used to estimate the magnitude of the radiant heat transfer coefficient, h_{rad} , compared to the similar convective film coefficient, h_c . The surface emissivity, ε , was then scaled up in the ANSYS thermal model to account for both radiation and convection in the radiation term. This conservatively assumes that the convecting air temperature is equal to the radiating source temperature. In the tank analysis this means that the dome air is assumed to be equal to the waste surface temperature. In the annulus it means that the air temperature is equal to the primary tank wall temperatures. The primary wall temperature is equal to the bulk waste temperature at elevations below the free surface of the waste and it decreases toward the dome surface temperature at elevations above the waste.

Assuming $T_R = 250^\circ\text{F}$ (710°R) in the dome gives $h_{\text{rad}} = 0.286 \text{ Btu/day-in}^2\text{-}^\circ\text{R}$. The TEMPEST model used a convective coefficient, $h_c = 0.123 \text{ Btu/day-in}^2\text{-}^\circ\text{R}$, for natural convection in the dome. The convective coefficient is about 43% of the radiant heat transfer coefficient. Therefore, the emissivity was increased by a factor of 1.4 to include the effect of dome space natural convection in the radiant heat transfer analysis.

Similarly, assuming $T_R = 350^\circ\text{F}$ (810°R) in the annulus gives $h_{\text{rad}} = 0.425 \text{ Btu/day-in}^2\text{-}^\circ\text{R}$. The TEMPEST model used a convective coefficient, $h_c = 0.168 \text{ Btu/day-in}^2\text{-}^\circ\text{R}$, to represent forced convection in the annulus. This convective coefficient is about 40% of the radiant heat transfer coefficient. Therefore, the emissivity of the annulus surfaces was also increased by a factor of 1.4 to include the effect of forced convection in the annulus. Note that the adjusted emissivities should be recalculated for other temperature transients.

4.3 Comparison of the ANSYS and TEMPEST Results

The ANSYS temperature predictions were compared with the TEMPEST results from the DST Thermal and Operating Loads Analysis to confirm the accuracy of the ANSYS modeling approach and to quantify the differences in the temperature and resulting stress distributions. The thermal properties recommended by Rinker et al. (2004) were used in the previous TEMPEST model and also in the current ANSYS analysis.

Figure 4-4 shows the temperature transient that was applied to the bulk waste in contact with the primary tank wall. Figure 4-4 also shows that the waste surface temperature was defined to follow the bulk waste temperature until the limiting surface temperature of 222°F was reached. This temperature limit gave the same temperature of the dome center as did the TEMPEST model. Figure 4-5 shows a temperature contour plot of the TEMPEST results as they were mapped onto the ANSYS structural model in the Thermal and Operating Loads Analysis. This is the steady state temperature distribution for the design basis transient. Figure 4-6 shows the steady state temperature distribution predicted with the ANSYS model. Comparing Figures 4-5 and 4-6 shows that the temperature distributions are very similar. Figure 4-7 shows a larger view of the near field temperature zone around the tank. Figure 4-8 shows the temperature distribution that is predicted when the waste level is reduced to 144 inches.

Temperature path plots around the inside and outside surfaces of the concrete tank were also developed to provide a 1:1 comparison of the ANSYS and TEMPEST results. Figure 4-9 compares the TEMPEST and ANSYS temperature predictions along the inside surface of the concrete tank structure. The steady state condition at the maximum waste temperature of 350°F was again used for the comparison because this determines the maximum expected concrete degradation and creep. The ANSYS temperatures are slightly higher than the TEMPEST predictions everywhere except in the outer radius of the dome and haunch where they are about 20°F lower. The dome-to-haunch region is also where the mapping of the TEMPEST results onto the ANSYS mesh was more approximate. Figure 4-10 shows a similar plot of the outside surface temperatures. The ANSYS temperatures are again slightly higher than the TEMPEST values except at the very center of the dome.

Also of importance are the resulting meridional stresses in the primary tank wall because they determine the buckling response of the tank. In this case, the maximum stresses do not occur at the maximum steady state temperature condition, but rather during the increasing temperature part of the transient. In the buckling analysis in Rinker et al. (2004) the maximum compressive stresses in the tank occur in the analysis step designated H4 – just before the waste initially reaches the maximum temperature of 350°F. Figure 4-11 shows that the temperatures from the ANSYS model produce a meridional stress distribution in the tank wall that is only slightly higher (about 60 psi compression). This shows that the ANSYS thermal solution results in meridional stresses that are very close to those based on the TEMPEST thermal results.

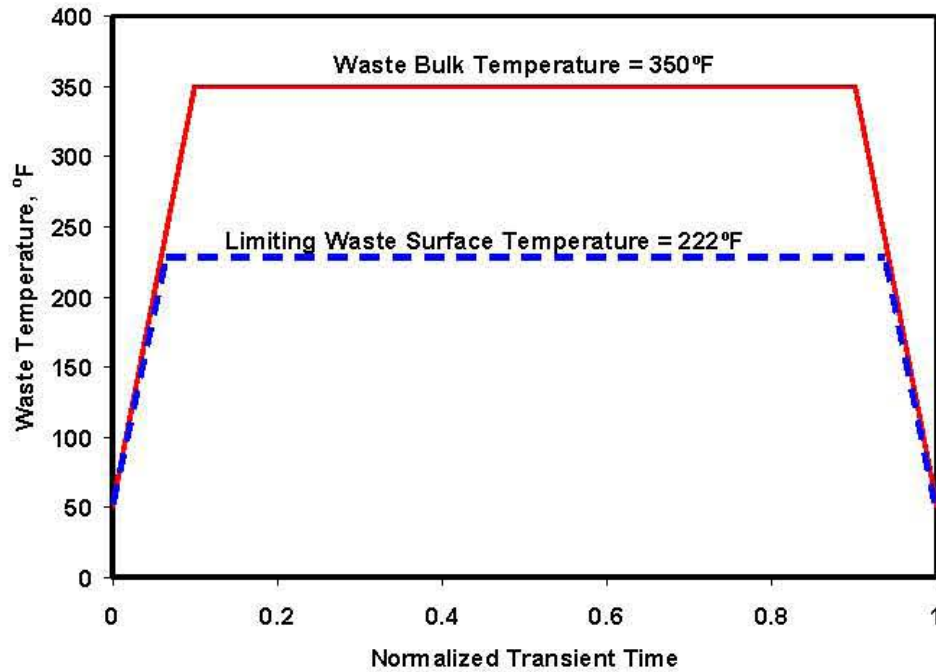


Figure 4-4. Example Waste Temperature Transient Showing the Limiting Waste Surface Temperature

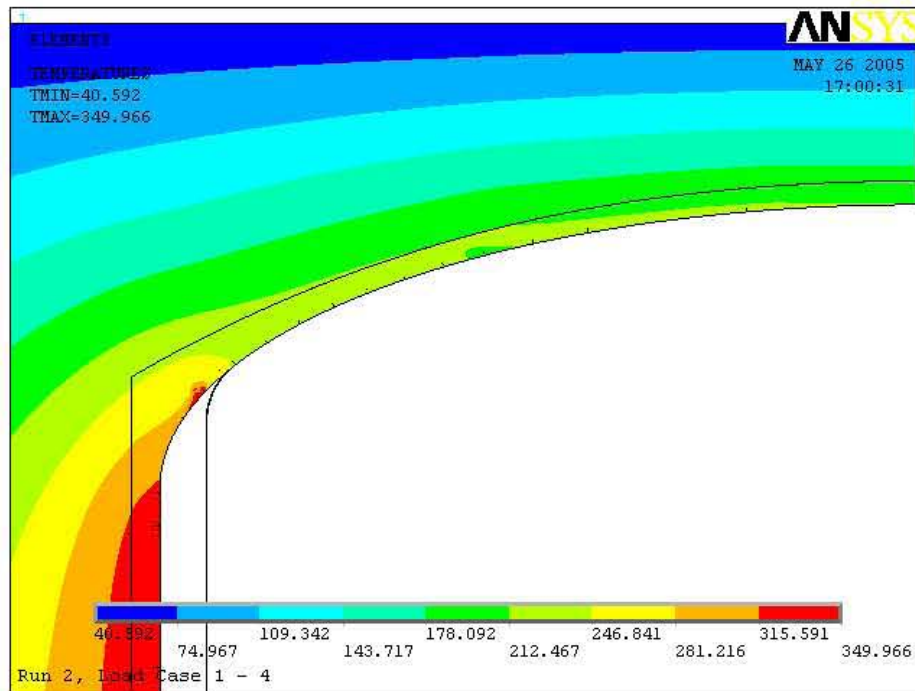


Figure 4-5. TEMPEST Temperatures Mapped onto the ANSYS DST Model (Steady State temperature solution, Waste Height = 422 inches, $T_{\text{waste}} = 350^{\circ}\text{F}$.)

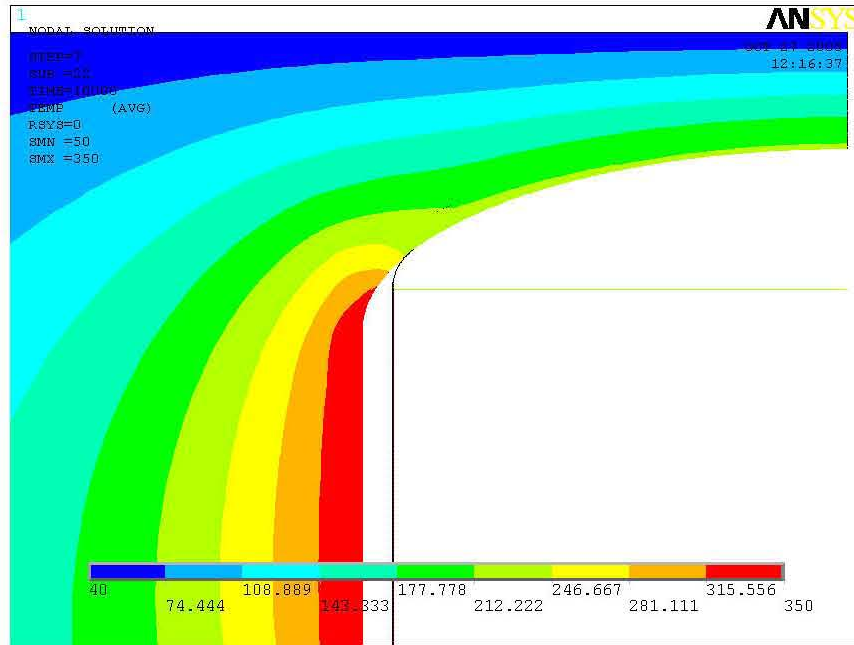


Figure 4-6. ANSYS Thermal Solution with Bulk Waste and Waste Surface Boundary Temperatures (Steady State temperature solution, Waste Height = 422 inches, $T_{\text{waste_bulk}} = 350^{\circ}\text{F}$, $T_{\text{waste_surface}} = 222^{\circ}\text{F}$. Maximum temperature of the dome surface = 217°F .)

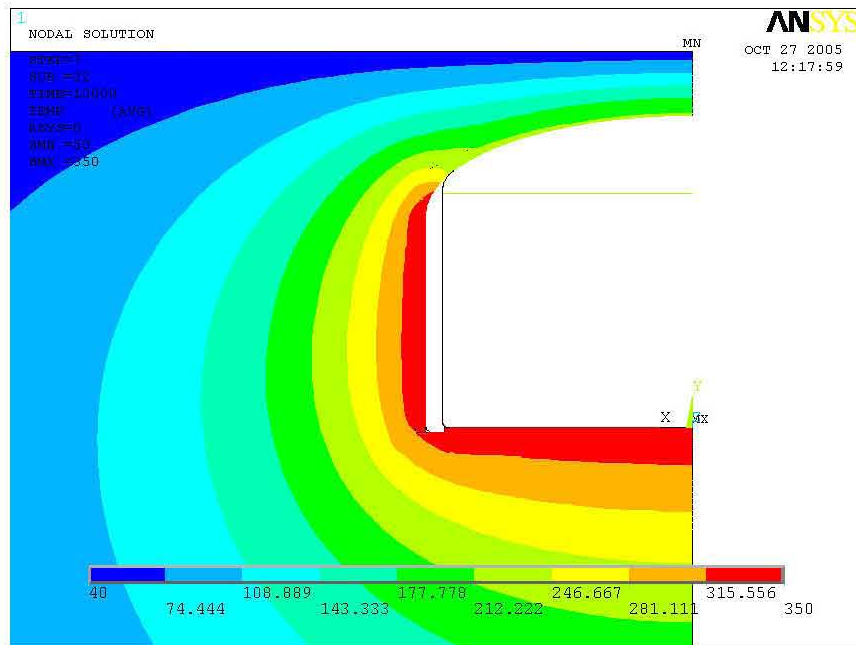


Figure 4-7. ANSYS Contour Plot Showing Temperatures Around and Beneath the Tank for a Waste Depth of 422 Inches (Bulk waste and waste surface boundary temperatures applied. Steady State, $T_{\text{waste_bulk}} = 350^{\circ}\text{F}$, $T_{\text{waste_surface}} = 222^{\circ}\text{F}$. Maximum temperature of the dome surface = 217°F .)

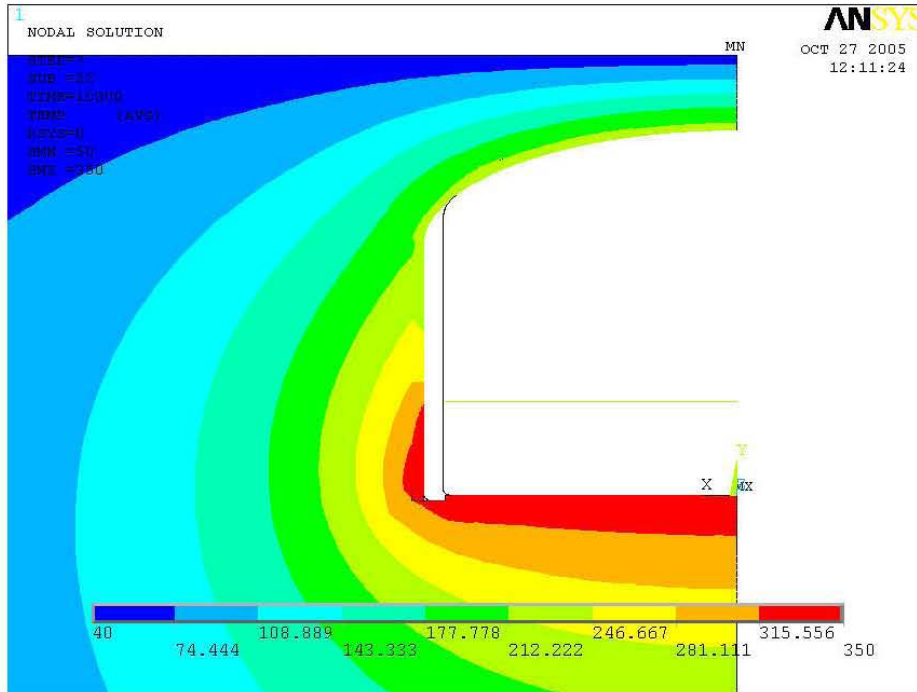


Figure 4-8. ANSYS Contour Plot Showing Temperatures Around and Beneath the Tank for a Waste Depth of 144 Inches (Bulk waste and waste surface boundary temperatures applied. Steady State, $T_{\text{waste_bulk}} = 350^{\circ}\text{F}$, $T_{\text{waste_surface}} = 222^{\circ}\text{F}$. Maximum temperature of the dome surface = 229°F .)

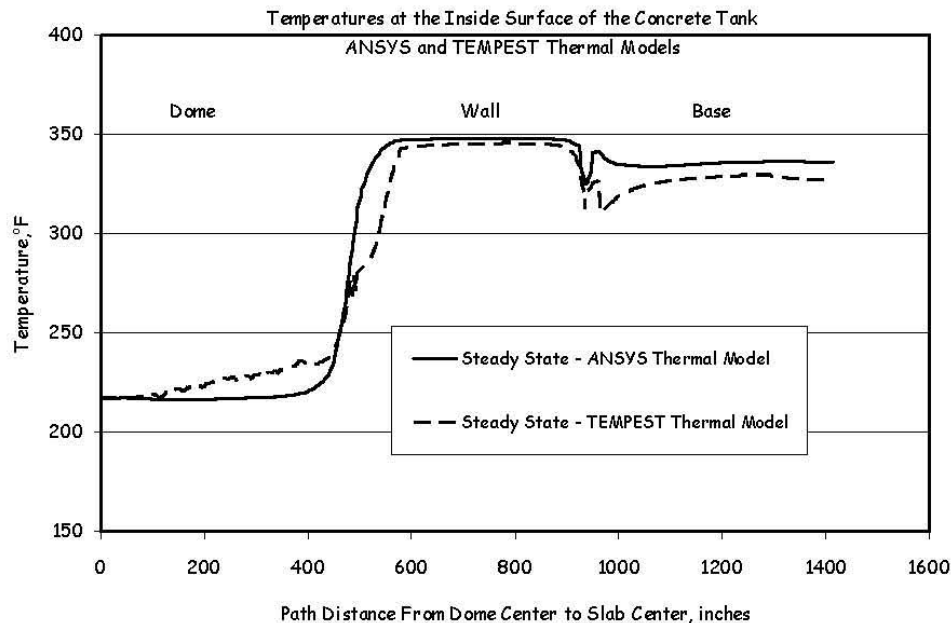


Figure 4-9. Comparison of the TEMPEST and ANSYS Temperature Predictions at the Inside Surface of the Concrete Tank (Steady State, $T_{\text{waste_bulk}} = 350^{\circ}\text{F}$, $T_{\text{waste_surface}} = 222^{\circ}\text{F}$. Temperature at the inside dome center = 244°F .)

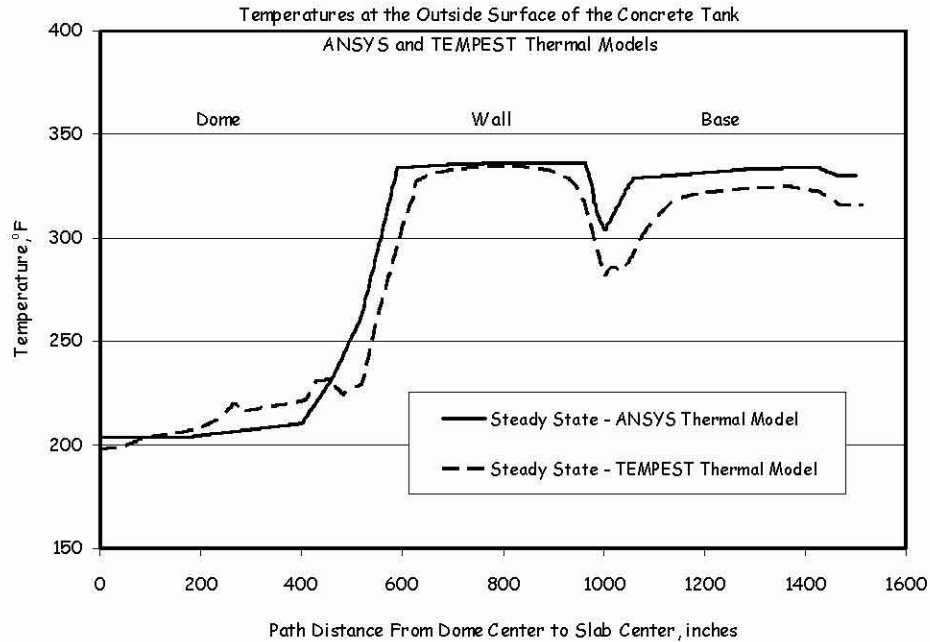


Figure 4-10. Comparison of the TEMPEST and ANSYS Temperature Predictions at the Outside Surface of the Concrete Tank (Steady State, $T_{\text{waste_bulk}} = 350^{\circ}\text{F}$, $T_{\text{waste_surface}} = 222^{\circ}\text{F}$. Temperature at the outside dome center = 244°F .)

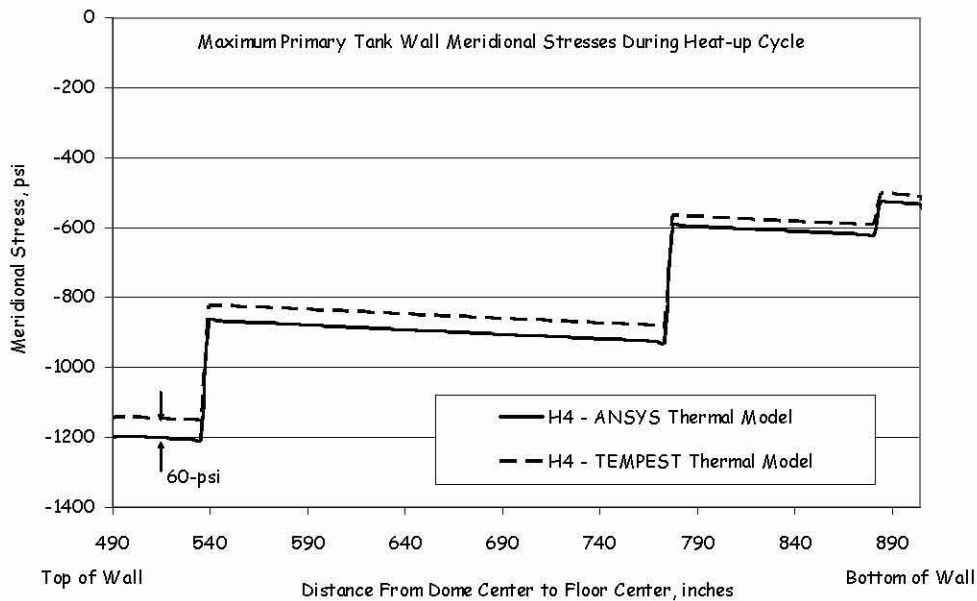


Figure 4-11. Comparison of Maximum Meridional Membrane Stresses During Heatup for the TEMPEST and ANSYS Temperature Distributions (Maximum stresses occur at heatup cycle H4.)

4.4 Calculated Boiling Temperatures for the Different Double-Shell Waste Tanks

The wastes in each of the double-shell tanks have different concentrations and chemistry that determine the boiling temperature of the mixture. Therefore, it is important to use an appropriate boiling temperature limit for each of the different tanks. Appendix B of Ogden et al. (2002) provides vapor pressure versus temperature data for the waste in each of the 28 tanks that can be used to estimate the saturation (boiling) temperature of each specific tank. The vapor pressure data were calculated using version 6.4 of the Environmental Simulation Program (ESP) based on the Best Basis Inventory of the waste constituents and concentration in each of the tanks. Table 4-1 provides an example of the calculated data for tank AY-101 (the data for all of the other tanks are listed in Ogden et al. (2002), Appendix B).

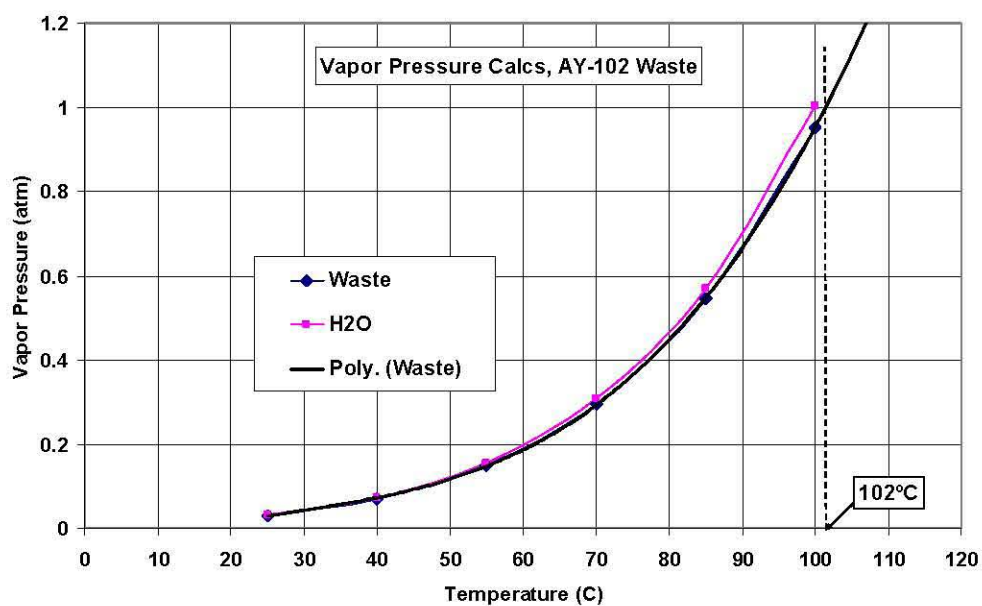
Table 4-1. Example Vapor Pressure Data from Ogden et al. (2002) for Tank AY-102

Tank AY-102				Major Solids (weight Fraction)
T deg-C	Waste Pvapor atm	H ₂ O Pvapor atm	Solid Density kg/L	
25	0.0301	0.0313	3.013	NALACO3OH2 (0.346), FEOOH (.339), ALOH3 (.171)
40	0.0699	0.0729	3.011	NALACO3OH2 (0.350), FEOOH (.338), ALOH3 (.162)
55	0.1489	0.1555	3.008	NALACO3OH2 (0.357), FEOOH (.337), ALOH3 (.153)
70	0.2943	0.3078	3.004	NALACO3OH2 (0.366), FEOOH (.337), ALOH3 (.143)
85	0.5449	0.5707	3.000	NALACO3OH2 (0.378), FEOOH (.339), ALOH3 (.131)
100	0.9535	1.0002	3.001	NALACO3OH2 (0.397), FEOOH (.340), ALOH3 (.111)

The boiling temperature was estimated as the temperature at which the vapor pressure is 1.00 atm. However, the vapor pressure calculations presented in Ogden et al. (2002) only go to 100°C where the waste vapor pressure is somewhat less than 1.00. Therefore, the data were curve fit and the curve was extrapolated to estimate the boiling temperature of the waste at atmospheric pressure. Figure 4-12 shows this procedure for the Tank AY-102 data, where the boiling temperature was estimated to be 102°C (216°F). This procedure was carried out for all 28 tanks, resulting in the estimated boiling temperatures listed in Table 4-2. Table 4-2 shows that the estimated boiling temperature of 216°F for AY-102 is higher than that of AY-101, and it is less than the limiting waste surface temperature (222°F) that was used to reproduce the TEMPEST results from the Thermal and Operating Loads analysis. The 222°F limiting waste surface temperature is recommended for the bounding waste tank calculations to be consistent with the previous work. Other analyses of specific tanks should use the values in Table 4-2.

Table 4-2. Estimated Boiling Temperature for the 28 Double-Shell Tanks

No	Tank	Boiling Temp, °F		No	Tank	Boiling Temp, °F
1	AN-101	225		15	AP-108	217
2	AN-102	230		16	AW-101	253
3	AN-103	234		17	AW-102	220
4	AN-104	229		18	AW-103	219
5	AN-105	244		19	AW-104	217
6	AN-106	235		20	AW-105	217
7	AN-107	230		21	AW-106	226
8	AP-101	226		22	AY-101	214
9	AP-102	223		23	AY-102	216
10	AP-103	212		24	AZ-101	221
11	AP-104	223		25	AZ-102	217
12	AP-105	226		26	SY-101	230
13	AP-106	216		27	SY-102	220
14	AP-107	213		28	SY-103	242

**Figure 4-12.** Vapor Pressure Data Used to Estimate the Boiling Temperature of Different Tank Wastes (The data for Tank AY-102 is shown.)

5.0 Influence Functions for Calculating the Applied Axial Force on the Primary Tank Wall

This chapter presents influence functions that were developed to estimate the applied axial force in the primary tank wall, which is required for evaluating buckling of the primary tank. The DST thermal model (Chapter 4) was run to provide temperature distributions in the steel and concrete tank and the surrounding soil for different combinations of waste height and temperature. The temperature distributions were then applied to the double-shell tank structural model to calculate the axial force due to differential thermal expansion. A matrix of different waste heights and temperatures was simulated that covers the tank operating limits on waste height and temperature. The axial forces for these discrete load combinations were then curve fit to allow estimating the thermal expansion force for intermediate waste heights and temperatures. The axial force contributions from other applied loads were also evaluated, giving the total axial force as the sum of the following loads:

- differential thermal expansion,
- gravity,
- surface loads,
- concrete thermal degradation and creep,
- seismic excitation, and
- effect of hydrostatic waste pressure on the confined axial force.

The baseline DST finite element model (Rinker et al. 2004) was used in the current study. (The input files for both the ANSYS thermal and structural models are listed in Appendix C.) Table 5-1 lists the loading conditions for this model. Two general classes of DST tanks were simulated: the AY tank and the AP tank. Although the baseline model was constructed using the specific dimensions of the AY tank, it also applies to the AZ, SY, AW, and AN primary tanks since they have similar geometry and wall thickness distributions. Table 1-1 shows that the AP primary tank wall is somewhat thicker than the others in the upper section of the tank. Because the scope of the current study did not allow for constructing specific models of each different tank design, the AP tank was approximated by substituting the AP wall thickness distribution into the baseline model. This approximation is reasonable because the primary tank is the focus of the buckling analysis and the significant influence of the massive concrete over-structure and the surrounding soil is to confine the vertical displacement of the primary tank dome. The axial stiffness of the AP primary tank is only about 1% of the axial stiffness of the concrete tank walls.

Table 5-1. Load Conditions for the Baseline DST Analysis

Design Load	Value	Notes
Design Life	> 50 years	A 60-year design life is used
Maximum Corrosion Rate	1 mil/yr	A total corrosion allowance of 0.060 inch is applied to the specified nominal thicknesses
Soil Cover	8.5 ft @ 125 lb/ft ³	Relative to dome apex
Concrete Density	145 lb/ft ³	Average including reinforcements
Surface Live Load	40 lb/ft ²	Uniform over the dome
	200,000 lb	Concentrated

5.1 Axial Compression in the Primary Tank Wall Due to Concrete Thermal Degradation and Creep

Analytical models that describe the creep compliance and modulus degradation with time and temperature are given in Rinker et al. (2004) for the concrete used in the double-shell waste tanks. The creep compliance, J , is modeled as a function of time and temperature as:

$$J(T, t) = \phi(T)C(t) \quad (5.1)$$

where $C(t)$ is the specific creep function versus time, and $\phi(T)$ adjusts the time dependency for temperature. A four-term exponential series describes the creep compliance as:

$$C(t) = 0.1936(1 - e^{-0.069t}) + 0.280(1 - e^{-0.0069t}) + 0.375(1 - e^{-0.00069t}) + 0.348(1 - e^{-0.000069t}) \quad (5.2)$$

where time, t , is in days and $C(t)$ is in units of 10^{-6} in/in per lbf/in². The temperature shift is given by:

$$\phi(T) = 226.09 - 0.00429T + 147.52T^{-0.367} - 309.26T^{-0.044} \quad (5.3)$$

where T is temperature in °F and $\phi(T)$ is a unitless scaling factor.

The elastic modulus is described by the following equation:

$$E = 5.3947 + 0.1233S - 0.006751T - 0.1786\ln(t+1)I + E_b \quad (5.4)$$

where: E = modulus of elasticity (10^6 psi)
 S = nominal 28-day compressive strength (ksi), (valid range is $3 \leq S \leq 4.5$)
 T = temperature (°F)
 t = time at constant temperature (days)
 I = 0 for $T \leq 200^\circ\text{F}$
 = $(T - 200)/50$ for $200^\circ\text{F} < T < 250^\circ\text{F}$
 = 1 for $T > 250^\circ\text{F}$
 E_b = uncertainty band width for modulus (10^6 psi)
 = 0.00 for best fit
 = ± 0.26 for 95% confidence band
 = ± 0.76 for 95/95% tolerance band

The equation for the modulus degradation with increasing temperature is:

$$F(T) = -0.39157\ln(T) + 2.80192 \quad (5.5)$$

The mean elastic modulus at $T=100^\circ\text{F}$ is used as the undegraded modulus, which is then scaled down for higher temperatures using the degradation factor, $F(T)$.

These models were used in spreadsheet calculations to estimate the compression in the primary tank due to creep and modulus degradation. The spreadsheet calculates the average compressive stress in the wall of the tank due to the weight of the tank walls, dome, overburden soil, and the surface loads. The tank

wall is then separated into sections above and below the waste surface. The creep and modulus degradation below the waste surface is calculated assuming that the concrete tank is at the maximum waste temperature. The similar quantities above the waste surface are calculated assuming that the concrete tank is at the maximum estimated waste surface temperature. The surface temperature is limited to the estimated boiling temperature of the supernate (222°F). The results of the ANSYS thermal models in Chapter 4 show that this is a reasonable approximation of the steady state temperature distribution in the concrete tank walls. The creep strains were calculated as the creep compliance times the applied stress. The strain due to modulus degradation was calculated as the applied stress divided by the undegraded modulus minus the stress divided by the degraded modulus. The foreshortening of the tank walls was then calculated as the individual strain components (for the creep and modulus reduction effects above and below the waste surface) times the height of the wall sections above and below the waste surface, respectively. Finally, the force in the tank wall was calculated using the tank axial stiffnesses that were calculated in Chapter 3 from the finite element models. Table 5-2 shows an example of the creep and thermal degradation calculations.

The axial compression due to concrete thermal degradation and creep is a function of each tank's operating history. Therefore, the available operating data were reviewed to define appropriate values of maximum waste height and temperature that bound the operating histories for each tank. Table 5-3 lists these tank-specific values along with the axial forces resulting from creep and thermal degradation (assuming a 60-year operating history and 0.060 inch corrosion). The forces due to modulus degradation are only 2% to 6% of the creep forces. The forces calculated for the AP tank are higher (for a specific temperature) because the axial stiffness of the AP primary tank is about 50% higher than the thinner AY tank. The values in Table 5-3 are of similar magnitude to previous results summarized in Table 3-12 of Rinker et al. (2004) from the Phase III analysis. The Phase III analysis showed the change in the primary tank axial stress with and without creep to be about 233 psi (233 psi times the average wall thickness of 0.5 inch = 0.117 kip/inch) for the AY primary tank design.

Table 5-2. Example Creep and Thermal Degradation Calculations

Creep and Thermal Degradation of Concrete							
Tank height			460	inches			
Concrete Tank Thickness =			18	inches			
Steel Modulus			2.80E+07	psi			
Load on Concrete Wall							
Soil			5613506				
Dome			980673				
1/2 Wall Weight			1113773				
Surface Load			208672				
Concentrated Load			200000				
Total Load			8116624	lb			
Wall Area			55305	inch^2			
Axial Stress in concrete			147	psi			
Max Waste Temp, F			250				
Waste surface Temp truncated to 222F			222				
Waste Height, inches			370				
Life, yrs			60	yrs			
James and Rashid Model		Above Waste	Below Waste				
Creep Compliance		Surface	Surface				
Temp, F		222	250				
Time		$X_i(T) =$	1.621	1.905			
days		Time Coeff	Crp Compl	Crp Compl			
		$C(t)$	(1E-6 in/in/psi)	(1E-6 in/in/psi)			
21900	1.1198	1.8148	2.1334				
Height of Tank Section		90	370				
Creep Strain, in/in		0.000266	0.000313				
Degraded Elastic Modulus v.s. temperature							
Specified Minimum Strength, ksi =		3	ksi				
Undegraded Mean Modulus =		5.0895	10^6 psi				
		Time	0	days			
Temp, F	Mean degrad Factors	Lower Bound E, (10^6psi)	Mean E, (10^6psi)	Upper Bound E, (10^6psi)			
222	0.686	2.733	3.493	4.253			
250	0.640	2.497	3.257	4.017			
		Above Waste	Below Waste				
Modulus Reduction		Surface	Surface				
Height of Tank Section		90	370				
Strain, at Low Temp Modulus		2.88E-05	2.88E-05				
Strain, at High Temp Modulus		4.20E-05	4.51E-05				
Increase in Strain		1.32E-05	1.62E-05				
Creep+Degrad Strain		2.80E-04	3.29E-04				
Tank Foreshortening		0.025156708	0.121851475	inch			
Tank Axial Stiffnesses from AY and AP Axial Compression Model							
		AY Stiffnesses		AP Stiffnesses			
Corrosion, inches ==>		0.000"	0.060"	0.100"	0.000"	0.060"	0.100"
Axl. Stiff, (kip/inch)/inch defl ==>		1.8175	1.45	1.2249	2.5758	2.14896	1.8844
Foreshortening		Axial Force	Axial Force	Axial Force	Axial Force	Axial Force	Axial Force
Above Waste	(inch)	(kip/inch)	(kip/inch)	(kip/inch)	(kip/inch)	(kip/inch)	(kip/inch)
Creep Force	0.024	0.044	0.035	0.029	0.062	0.052	0.045
Degrad Mod. Force	0.001	0.002	0.002	0.001	0.003	0.003	0.002
Below Waste							
Creep Force	0.116	0.211	0.168	0.142	0.298	0.249	0.218
Degrad Mod. Force	0.006	0.011	0.009	0.007	0.015	0.013	0.011
Total Creep+Degrad	0.147	-0.267	-0.213	-0.180	-0.379	-0.316	-0.277
Stress in 0.44 inch wall, psi		-607	-485	-409	-861	-718	-630

Table 5-3. Estimated Axial Force Due to Creep and Thermal Degradation of the Elastic Modulus for a Range of Tank Waste Temperatures and Waste Heights (The force calculations assume a 0.060 inch corrosion allowance and a 60-year operating history.)

Description	Temperature °F	Waste Height, Inches	Creep Axial Force (kip/in.)	Modulus Degradation Axial Force (kip/in.)
AY Bounding Analysis	350	422	-0.295	-0.018
AY Specified Limits	350	370	-0.280	-0.017
AY/AZ Operating History	250	422	-0.207	-0.011
SY/AW/AN Operating History	150	422	-0.092	-0.003
AP Operating History	120	422	-0.083	-0.002
AP Specified Limits	210	422	-0.243	-0.011

5.2 Differential Thermal Expansion Forces for Current Operating Conditions

Table 5-4 lists the differential thermal expansion forces for the matrix of operating conditions that were simulated for the AY primary tank geometry. Both the thermal expansion forces at the end of the heatup cycle and at the steady state temperature distribution are listed. The thermal expansion force at the end of heatup (see Figure 4-4) is generally larger than the steady state value and it is used to calculate the maximum operating force in the tank wall. This is also when the maximum thermal expansion stresses were observed in the thermal and operating loads analysis (Rinker et al. 2004). The steady state thermal expansion force is slightly lower (5% to 10%) and it is combined with the seismic force to calculate the total applied force during faulted or abnormal conditions. The differential thermal forces during heatup are plotted in Figure 5-1 along with curve fits of the form:

$$F_{\phi}(h, T) = a(T)h + b(T) \quad (5.6)$$

where

$$a(T) = -2.015 \times 10^{-9} T^2 - 1.852 \times 10^{-6} T + 8.513 \times 10^{-5} \quad (5.7)$$

$$b(T) = 1.189 \times 10^{-6} T^2 - 1.191 \times 10^{-3} T + 6.394 \times 10^{-2} \quad (5.8)$$

Equation 5.6 is also used for the AY steady state thermal expansion force, but the coefficients are

$$a(T) = -6.877 \times 10^{-9} T^2 + 6.773 \times 10^{-7} T - 2.927 \times 10^{-5} \quad (5.9)$$

$$b(T) = 2.359 \times 10^{-6} T^2 - 1.687 \times 10^{-3} T + 8.458 \times 10^{-2} \quad (5.10)$$

Figure 5-2 shows how the curve fits match the steady state forces from the finite element analysis. Table 5-5 lists the thermal expansion forces for the analyses of the AP primary tank. For the AP thermal expansion forces at the end of the heatup cycle, the temperature dependent coefficients, $a(T)$ and $b(T)$ are:

$$a(T) = 2.263 \times 10^{-8} T^2 - 8.946 \times 10^{-6} T + 3.908 \times 10^{-4} \quad (5.11)$$

$$b(T) = -8.896 \times 10^{-6} T^2 + 1.062 \times 10^{-3} T - 3.087 \times 10^{-2} \quad (5.12)$$

Table 5-4. Matrix of Waste Tank Models That were Analyzed to Estimate the Axial Thermal Expansion Forces for the AY Tank Design (The table lists the thermal expansion forces at the end of the heatup cycle and at the steady state temperature distribution.)

Waste Height, in.	Axial Thermal Expansion Force, kip/inch of circumference			
	Twaste = 50°F	Twaste = 150°F	Twaste = 250°F	Twaste = 350°F
Thermal expansion force at end of heatup cycle				
100	0	-0.093	-0.227	-0.281
200	0	-0.122	-0.278	-0.366
300	0	-0.147	-0.319	-0.447
370	0	-0.168	-0.355	-0.503
Steady state thermal expansion force				
100	0	-0.109	-0.234	-0.276
200	0	-0.117	-0.260	-0.339
300	0	-0.134	-0.284	-0.404
370	0	-0.140		-0.450

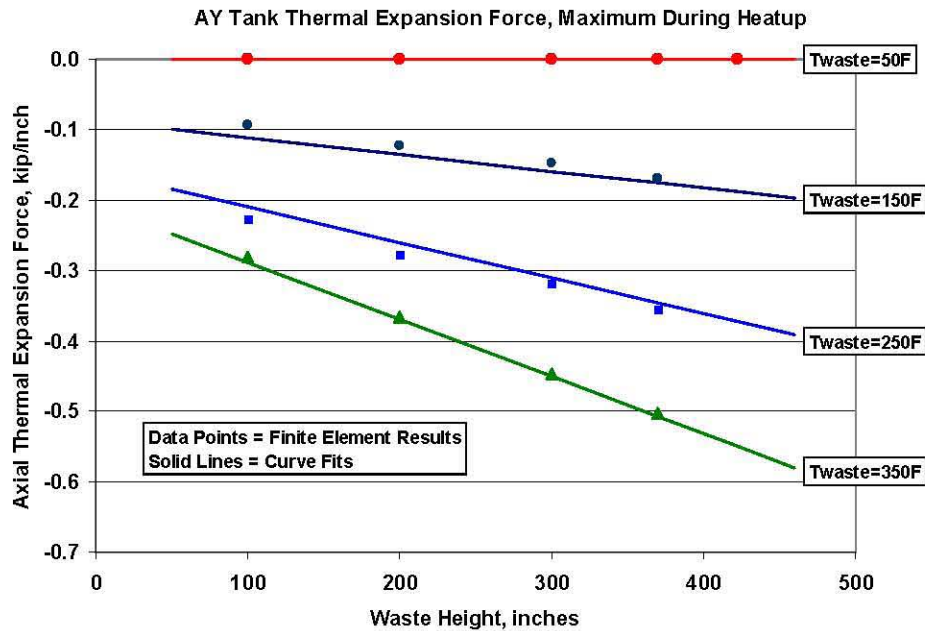


Figure 5-1. Relationship of Maximum Axial Thermal Expansion Force During the Heatup Cycle in the AY Primary Tank Wall for a Range of Waste Heights and Temperatures (The data points are the finite element results and the solid lines represent the curve fits of the data.)

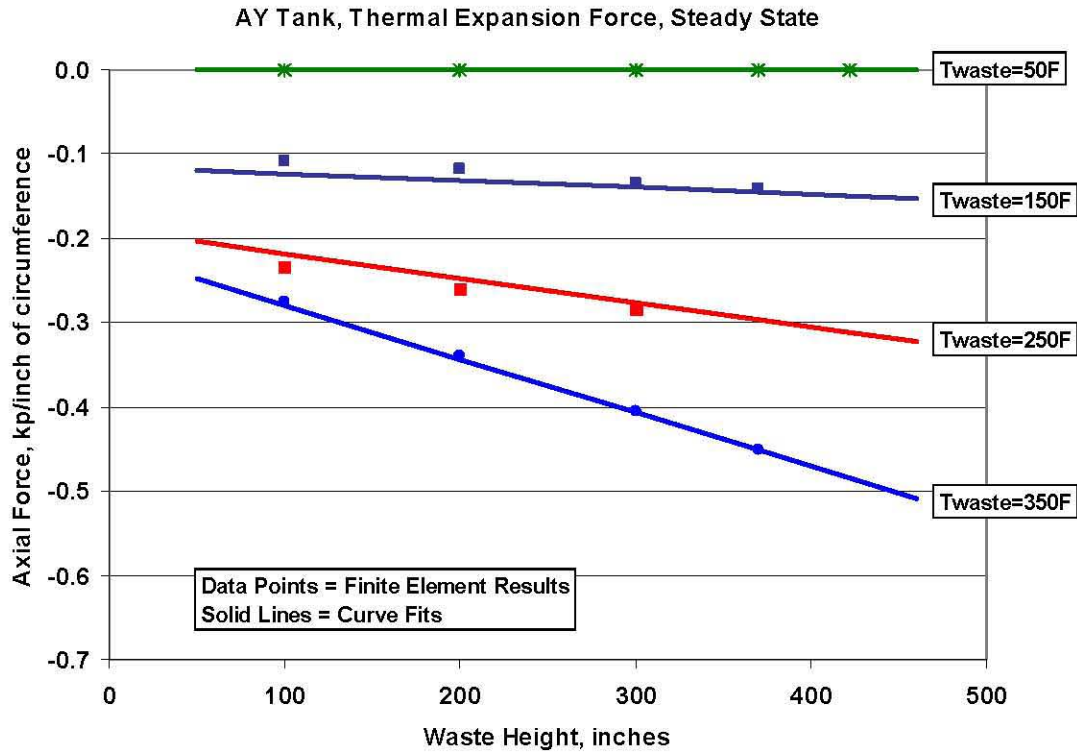


Figure 5-2. Relationship of the Steady State Axial Thermal Expansion Force in the AY Primary Tank Wall for a Range of Waste Heights and Temperatures (The data points are the finite element results and the solid lines represent the curve fits of the data.)

Table 5-5. Matrix of Waste Tank Models That were Analyzed to Estimate the Axial Thermal Expansion Forces for the AP Tank Design (The table lists the thermal expansion forces at the end of the heatup cycle and at the steady state temperature distribution.)

Waste Height, in.	Axial Thermal Expansion Force, kip/inch of circumference		
	Twaste = 50°F	Twaste = 150°F	Twaste = 250°F
Thermal expansion force at end of heatup cycle			
100	0	-0.067	-0.247
200	0	-0.103	-0.302
300	0	-0.138	-0.345
370	0	-0.164	-0.382
Steady state thermal expansion force			
100	0	-0.092	-0.264
200	0	-0.105	-0.283
300	0	-0.117	-0.298
370	0	-0.123	-0.313

At the steady state temperature distribution, the coefficients are:

$$a(T) = 5.172 \times 10^{-9} T^2 - 2.388 \times 10^{-6} T + 1.065 \times 10^{-4} \quad (5.13)$$

$$b(T) = -4.122 \times 10^{-6} T^2 - 4.832 \times 10^{-4} T + 3.447 \times 10^{-2} \quad (5.14)$$

Figures 5-3 and 5-4 show the axial forces and the curve fits for the AP thermal expansion at the end of the heatup cycle and at the steady state temperature distribution, respectively.

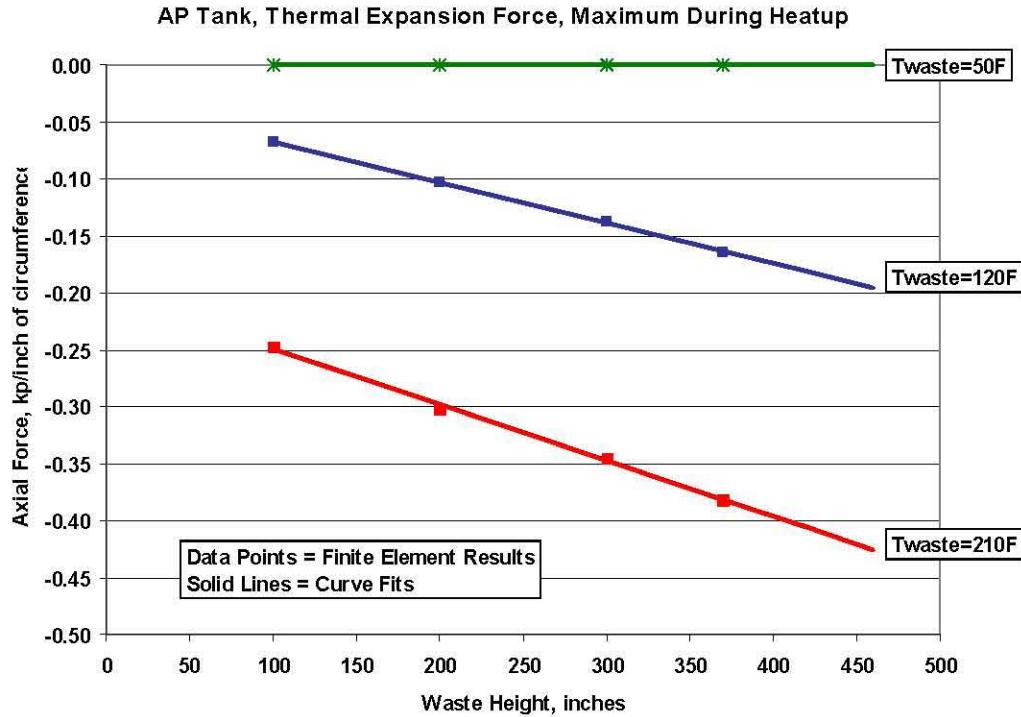


Figure 5-3. Relationship of the Maximum Axial Thermal Expansion Force During the Heatup Cycle in the AP Primary Tank Wall for a Range of Waste Heights and Temperatures (The data points are the finite element results and the solid lines represent the curve fits of the data.)

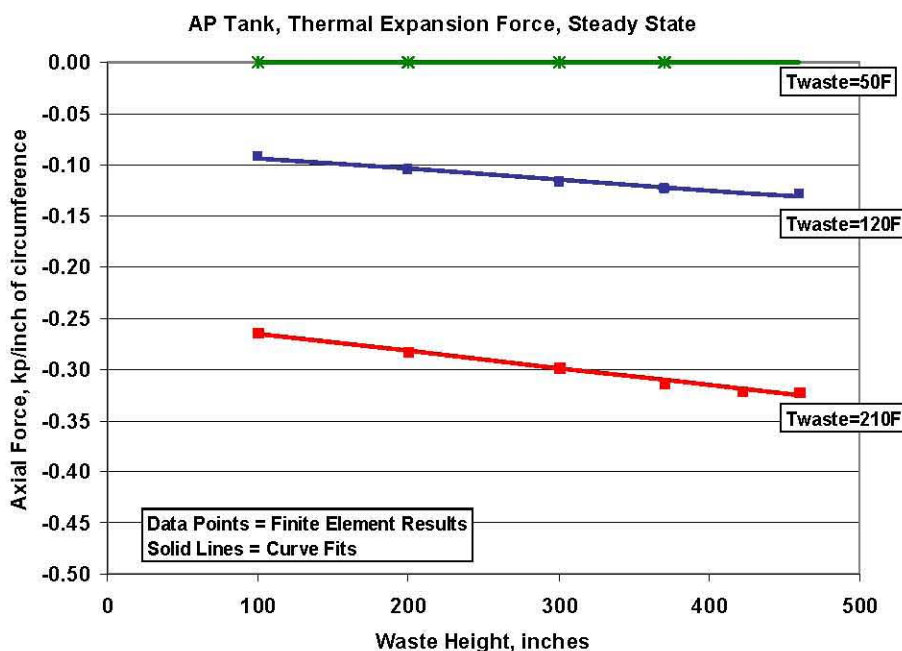


Figure 5-4. Relationship of the Steady State Axial Thermal Expansion Force in the AP Primary Tank Wall for a Range of Waste Heights and Temperatures (The data points are the finite element results and the solid lines represent the curve fits of the data.)

5.3 Axial Load Components Due to Gravity

The axial load component due to gravity considers the mass of the soil and the tank on loading the primary tank wall. Figures 5-5 and 5-6 show that the gravity component varies along the height of the tank. The values at 144 inches (the top of the 3/4-inch tank wall section) are used here as a reasonable average. For the soil depth and densities listed in Table 5-1, the gravity loads for the AY and AP tanks are estimated to be -0.135 kip/inch and -0.167 kip/inch, respectively. The gravity component is greater for the AP tank because it has a higher axial stiffness than the AY tank.

The gravity load components reported here are an output from detailed finite element analysis of the tank and the surrounding soil. If the reader wishes to consider other soil densities or cover depths it is recommended that this effect be considered by scaling the surface load effect to account for the difference compared to the assumed conditions in Table 5-1.

5.4 Axial Load Components Due to Surface Loads

Figures 5-5 and 5-6 show that the surface loads contribute almost no load to the primary tank wall (-0.010 and -0.005 kip/inch for the AY and AP tanks, respectively). This is consistent with the results of the concentrated load analysis (Rinker et al. 2005) and with the discussion of the vacuum load on axial compression presented in Chapter 3. Later sections will show that this is about 1 to 2% of the total axial load on the tank wall. The current calculations include the contribution of surface loads for completeness; however, it is undoubtedly smaller than the uncertainty in either the thermal expansion or seismic force components.

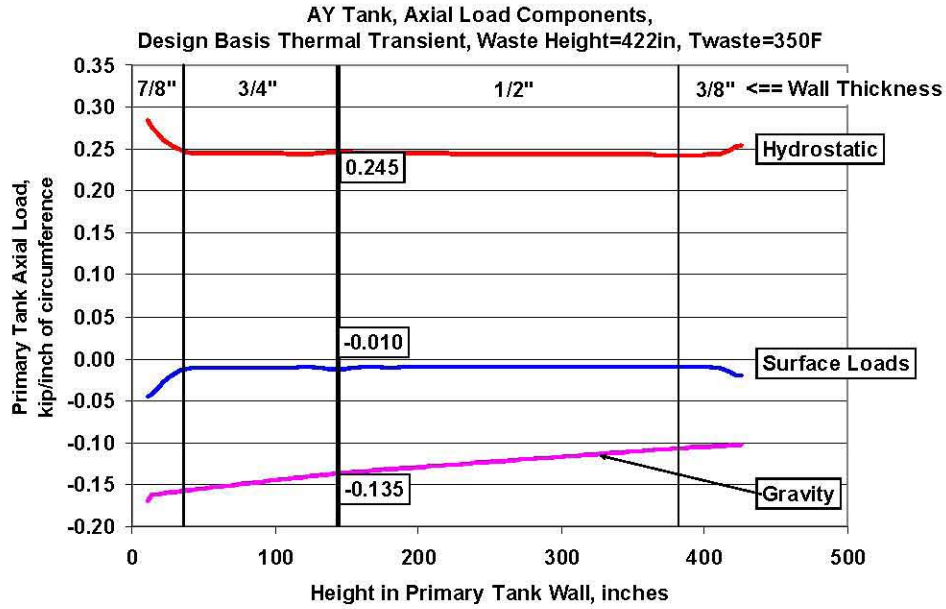


Figure 5-5. Comparison of the Axial Force Components in the AY Primary Tank Wall Due to the Different Tank Loads

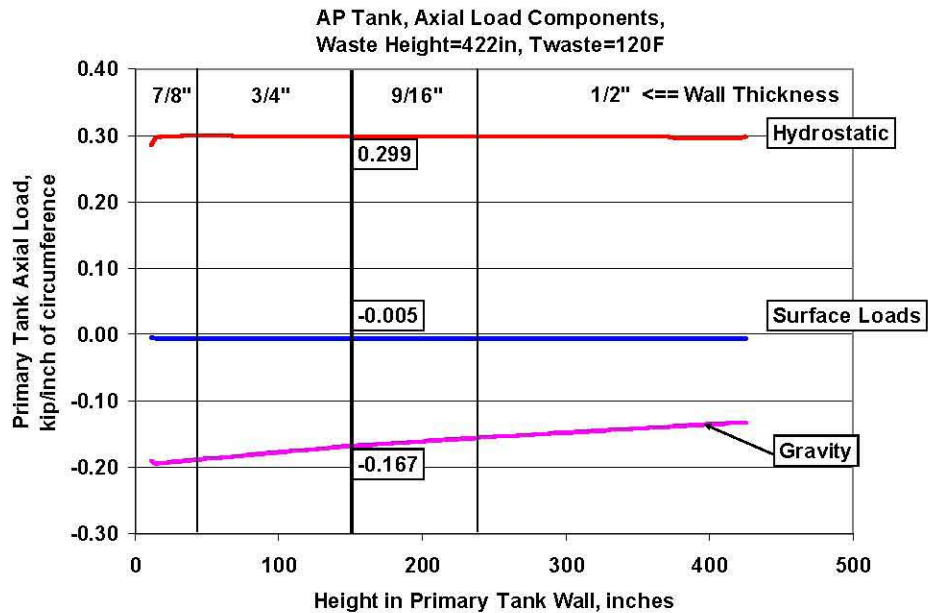


Figure 5-6. Comparison of the Axial Force Components in the AY Primary Tank Wall Due to the Different Tank Loads

5.5 Axial Load Component Due to Waste Hydrostatic Pressure

The waste hydrostatic pressure contributes a tensile axial force due the Poisson's effect from the tensile hoop stress. This effect was quantified using the model results considering different waste heights that were used to calculate the vacuum limits in Chapter 3. Figure 5-7 shows the relationship of axial force with increasing waste height for both the AY and AP tanks for a waste specific gravity of 1.7. The equation for the AY axial force due to hydrostatic waste pressure is:

$$F_{\text{waste}}(h) = 5.5322 \times 10^{-7} h^2 + 2.4877 \times 10^{-4} h - 2.1662 \times 10^{-3} \quad (5.15)$$

Where h is the waste height in inches and $F_{\text{waste}}(h)$ is the axial force in kip/inch. Note that $F_{\text{waste}}(h)$ is positive.

The equation for the axial force due to hydrostatic waste pressure in the AP tank is:

$$F_{\text{waste}}(h) = 7.2156 \times 10^{-7} h^2 + 3.3431 \times 10^{-4} h - 3.168 \times 10^{-3} \quad (5.16)$$

Both Equations 5.15 and 5.16 can be modified for different waste specific gravities by multiplying by the equation:

$$h(\text{SpG}) = 0.6072(\text{SpG}) - 0.0318 \quad (5.17)$$

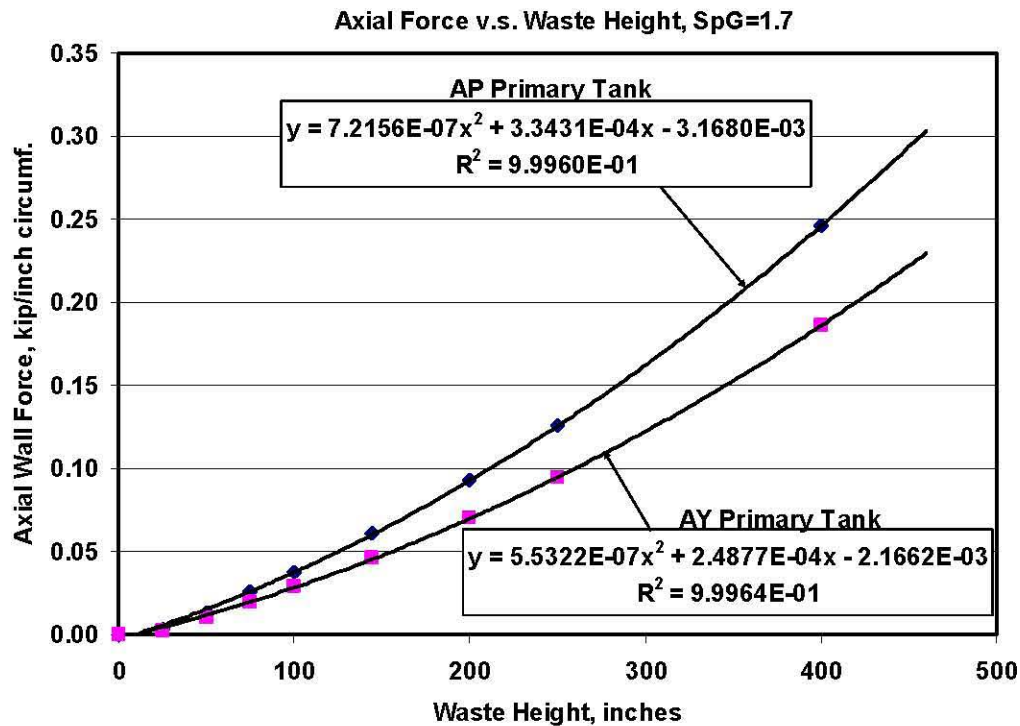


Figure 5-7. Axial Force in the Primary Tank Wall Due to Waste Hydrostatic Pressure

Figure 5-8 shows that this equation fits the AY axial force data for specific gravities from 1.0 to 2.0.

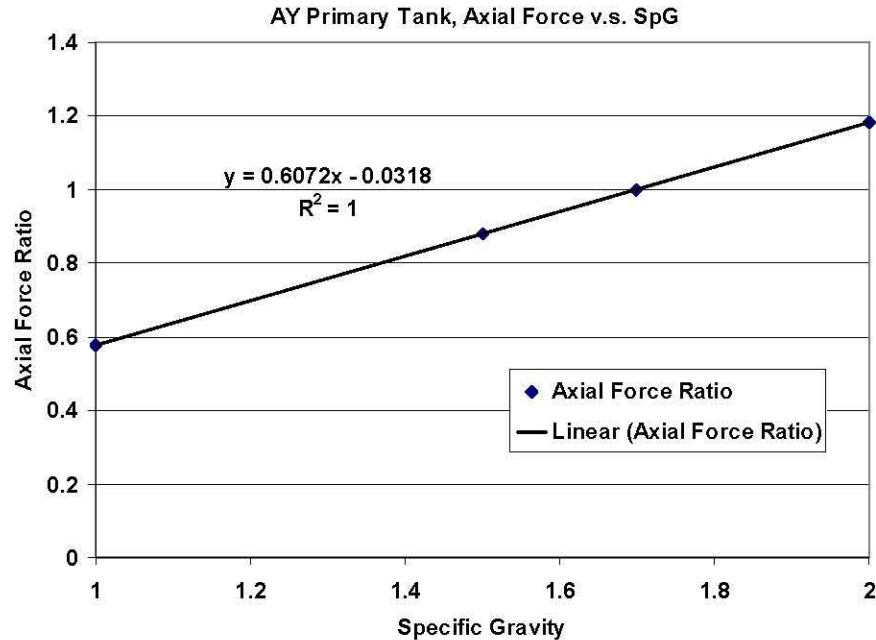


Figure 5-8. Effect of Specific Gravity on Axial Force in the AY Tank Wall

5.6 Axial Load Component Due to Seismic Excitation

Seismic motion will cause loads on the primary tank due to deformation of the concrete outer tank plus the impulsive load of the waste sloshing within the tank. The loads transmitted from the concrete tank will be directed axially to the primary tank wall, and they will be comprised of a rocking motion (positive on one side and negative on the other) plus a “breathing mode” that will exert uniform alternating tension and compression forces around the whole tank. The impulsive mode will primarily cause an increased hoop stress on one side of the tank and a reduced hoop stress on the other side. The seismic axial stress component is of interest to the buckling and J-bolt evaluations of the primary tank.

A seismic analysis of the AY tank has been performed by Carpenter et al. (2006). The maximum amplitudes of the axial and hoop membrane stresses were compiled at each meridional node location in the finite element model by scanning the stress at each band of nodes in the circumferential direction of the half-symmetry model. The scan was performed throughout the transient dynamic analysis, and the maximum and minimum values were recorded. The seismic analysis was performed for four combinations of soil and concrete stiffness properties:

1. Best Estimate Soil - Best Estimate Concrete (BES-BEC)
2. Best Estimate Soil - Fully Cracked Concrete (BES-FCC)
3. Lower Bound Soil - Best Estimate Concrete (LBS-BEC)
4. Upper Bound Soil - Best Estimate Concrete (UBS-BEC)

Figure 5-9 shows the distribution of meridional membrane stresses in the free-standing portion on the AY tank wall for the four combinations of soil and concrete properties. The maximum force is 0.627 kip/inch, but this occurs in the mid-section of the wall, not at the top of the wall where the buckle is

expected to occur. Therefore, the local maximum of 0.43 kip/inch at the transition between the free-standing tank wall and the dome was used as a more realistic approximation of the seismically induced compressive force. The seismic force for the AP tank was estimated by scaling the AY forces by the ratio of the AP/AY tank stiffnesses (a factor of 1.429), giving an axial seismic force of 0.614 kip/inch. Since the current evaluation considers the elastic buckling mode, no credit was taken for inelastic energy absorption (i.e., the F_u factor in IBC [2003]) reducing the seismic axial force.

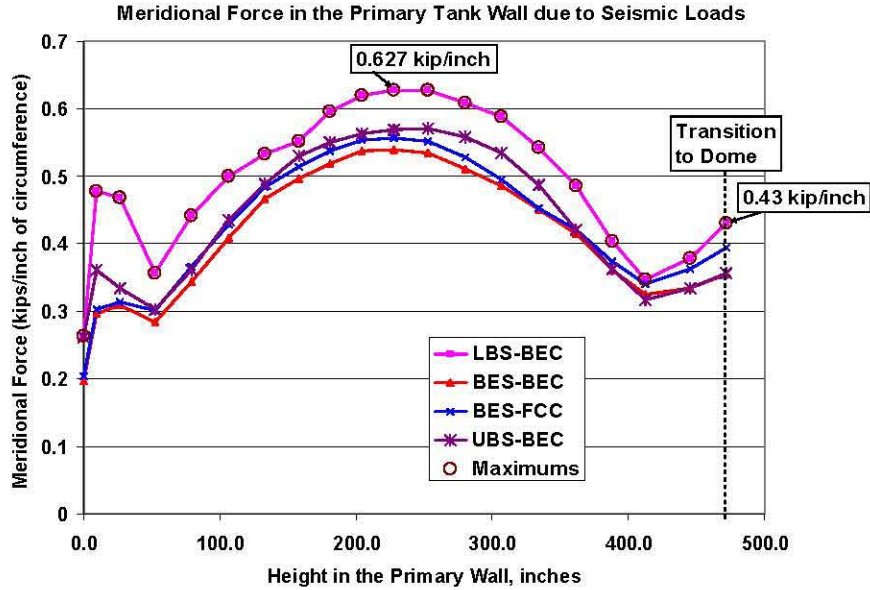


Figure 5-9. Meridional (axial) Membrane Stress in the AY Tank Wall for the Four Different Combinations of Soil and Concrete Properties

5.7 The Total Axial Force in the Primary Tank Wall

An Excel® spreadsheet was developed to calculate the total axial force in the primary tank wall based on the data and equations given in this chapter.

Assuming that the axial stress is primarily caused by the relative deformations of the primary tank and the outer concrete tank, then the axial stress for different corrosion allowances can be estimated by scaled by the ratio of the axial stiffnesses. As noted previously, this is a reasonable assumption because even the axial stiffness of the thicker AP tank is only about 1% of the axial stiffness of the concrete tank walls. Figure 5-10 shows this scaling method for the AY and AP tanks. The axial force scaling factor for the AY tank is:

$$k(c) = -4.093717c + 1.250545 \quad (5.18)$$

Where c is the corrosion allowance and $k(c)$ is the multiplication factor on the axial force. The similar equation for the AP tank is:

$$k(c) = -3.259365c + 1.193369 \quad (5.19)$$

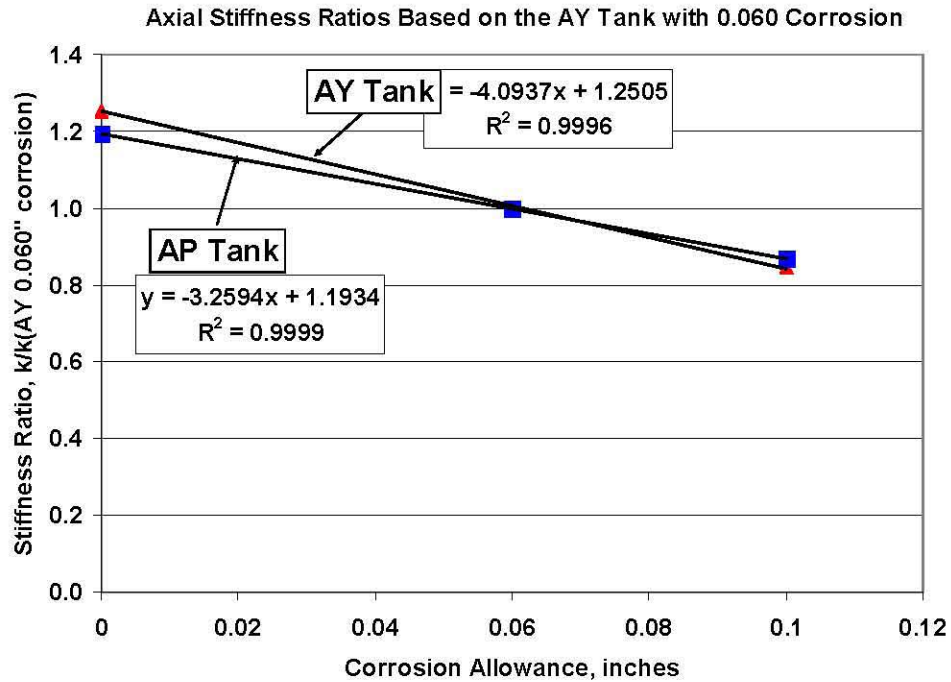


Figure 5-10. Stiffness Scale Factors to Estimate the Seismic Axial Force for the AY and AP Tanks with Different Corrosion Allowances

6.0 Evaluating the J-Bolt Anchors Under Axial Tank Compression, Vacuum, and Seismic Loads

The steel primary tank is anchored to the adjacent concrete using embedded J-bolts with a 2 feet x 2 feet spacing (Figure 2-1). The J-bolts were analyzed as part of the primary tank buckling evaluation. Buckling may occur in the primary tank due to compressive stresses in both the meridional and hoop directions. Meridional (axial) compression results from differential thermal expansion between the primary tank and the concrete over-structure plus creep-down of the concrete structure over time. Hoop compression results from net vacuum loads in the tank.

The finite element model used in Chapter 3 for predicting the tank vacuum limits was also used for the current J-bolt evaluation. A 3-D elastic beam element (BEAM4) was used to model the J-bolts. BEAM4 is a uniaxial element with tension, compression, torsion, and bending capabilities, and it has six degrees of freedom at each node. Figure 6-1 shows the model of the primary tank with the J-bolts. A downward deflection was applied to the J-bolts to simulate the displacement controlled axial compression of the tank wall that occurs due to concrete thermal degradation and creep, plus the confined thermal expansion of the steel tank inside the concrete shell. The model includes a geometric imperfection to initiate the buckling instability under the radially symmetric vacuum load. The onset of the buckling instability was predicted by applying an increasing vacuum load on the inside surface of the tank while monitoring the maximum radial displacement of the tank wall as a function of the increasing vacuum load. The J-bolt shear and normal forces were recorded throughout the application of the buckling loads.

6.1 J-Bolt Evaluation Criteria

The double-shell tank structural acceptance criteria document (Day 1995) requires that the J-bolts be evaluated using the methods found in ASME Section III, Division 2, Subsection CC-3730 (ASME 1992). The mechanical (non self-limiting) loads are evaluated against a force criterion. The allowable load criterion for either tension-only or shear-only loading (uncombined) is shown in Table 6-1. Table 6-2 shows the equations and logic that are used in CC-3730 to determine the yield force, F_y , and the ultimate force, F_u , for the J-bolts. For combined shear and tension forces, it has been shown that the following interaction equation provides a good fit for the force test data:

$$(P/F_{ap})^{5/3} + (S/F_{as})^{5/3} \leq 1 \quad (6.1)$$

where

- P = Applied tension load
- S = Applied shear load
- F_{ap} = Allowable for applied tension load
- F_{as} = Allowable for applied shear load.

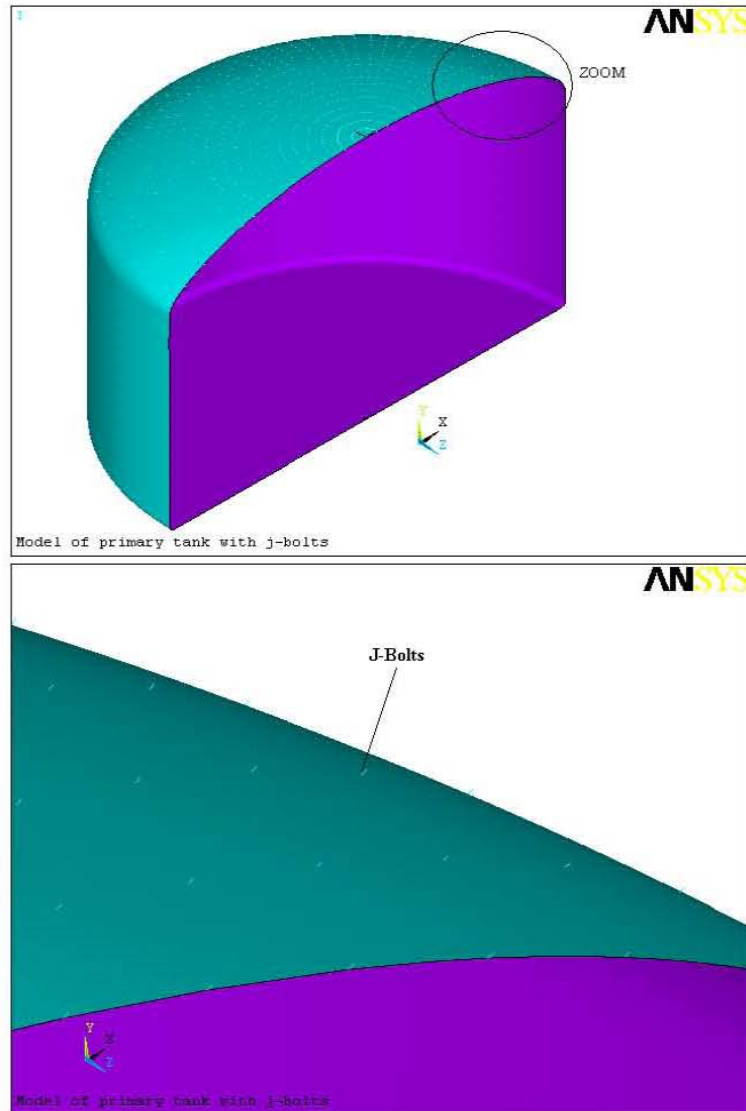


Figure 6-1. Buckling Model Showing the Location of the J-Bolts Attached to the Tank Dome

Table 6-1. J-Bolt Force Limits from ASME Section III, Division 2, Subsection CC-3730

Category	Force and Displacement Allowables	
	Mechanical Loads Lesser of:	Displacement Limited Loads
Normal, Extreme Environmental	$F_a = 0.67F_y$ $F_a = 0.33F_u$	$\delta_a = 0.25 \delta_u$
Abnormal	$F_a = 0.90F_y$ $F_a = 0.50F_u$	$\delta_a = 0.50 \delta_u$
F_a = Allowable force F_y = Force to reach J-bolt yield strength F_u = Force to reach J-bolt ultimate strength δ_a = Allowable displacement δ_u = Displacement at ultimate strength		

Table 6-2. F_y and F_u Relationships for J-Bolts

Nelson Anchor Type	F_y (lbf)		F_u (lbf)	
	Tension	Shear	Tension	Shear
J-bolt (or Bent Stud)	Lesser of: $A_s f_y$ $1/2 A_s f_u$	$A_s f_y$	$2/3 A_s f_u$	Lesser of: $0.9 A_s f_u$ $5.66 A_s f_c^{0.3} E_c^{0.44}$
A_s = Cross sectional area of the anchor shank (in.^2) f_y = Yield strength of the anchor material (lbf/in.^2) f_u = Tensile strength of the anchor material (lbf/in.^2) f_c = Compressive strength (lbf/in.^2) of concrete adjusted for temperature E_c = Concrete modulus of elasticity (lbf/in.^2) adjusted for temperature				

The yield strength, f_y , and ultimate strength, f_u , of the bolt and stud materials were conservatively taken as 36 ksi and 60 ksi, respectively. The full cross-sectional area of the 0.75-inch-diameter, internally threaded stud ($\pi d^2/4 = 0.442 \text{ in.}^2$) was used in the shear evaluation. This is justified because a J-bolt shear failure would likely occur at the interface between the concrete and the primary liner or due to concrete failure around the base of the stud. For axial loading, the diameter of the J-bolt shank (0.5 inches) is used to calculate the tensile area ($\pi d^2/4 = 0.196 \text{ in.}^2$). Table 6-3 lists the material data and the detailed calculations that were used to calculate the code based allowables. Table 6-4 summarizes the allowable J-bolt forces in tensile and shear for normal (operating) loads and abnormal (operating + seismic) loads for the combined and uncombined loading cases. The combined loading case allowables are used in Equation 6.1.

6.2 J-Bolt Force Evaluation

The previous buckling analyses performed in the thermal and operating loads analysis (Rinker et al. 2004) showed that an axial compressive stress of about 1 ksi (in the 0.44 inch wall thickness of the AY mid section) was typical of the tank loading conditions. This stress corresponds to nearly a 0.3 inch foreshortening of the tank wall, which was therefore used as a baseline condition for the J-bolt evaluation. From Table 2-1 it can be seen that the tank is more susceptible to buckling at low waste heights, so the J-bolts were first evaluated at a waste height of 25 inches and a tank wall foreshortening of 0.3 inches. Two alternate cases with no axial foreshortening and 25 inches and 400 inches of waste were also evaluated to investigate conditions where the J-bolts might be tension. This was done to address the concerns for J-bolt pullout failure that were raised by the EH-22 panel. Shear and normal forces are plotted in the following sections for a column of J-bolts oriented radially from the dome centerline to the haunch plus the J-bolts in the outer most circumferential row of anchors near the haunch.

Table 6-3. Calculation of the J-Bolt Allowables for Combined Loads and Tension and Shear Only Loads

J-Bolt Allowables for Combined Loading				J-Bolt Allowables for Tension/Shear only Loading			
$(P/F_{ap})^{5/3} + (S/F_{as})^{5/3} \leq 1$				$F_a = 0.67F_y$ $F_a = 0.33F_u$ $F_a =$ Allowable force $F_y =$ Force to reach anchor yield strength $F_u =$ Force to reach anchor ultimate strength			
P = Applied tension load S = Applied Shear load F_{ap} = Allowable for an applied Tension load F_{as} = Allowable for an applied Shear Load				Lesser of both values			
J-Bolt Steel Properties							
f_y	36000	Yield Strength, psi					
f_u	60000	Ultimate Strength, psi					
Concrete Properties, 3-ksi Hanford Mix							
f'_c	4860	Compressive Strength, psi, Mean value, 60 yrs at T=250F					
E	3.257E+06	Elastic Modulus, psi, Mean value, 60 yrs at 250F					
Shear and Tensile Areas							
A_s Tensile	0.196	Bolt Shank area, in ²					
A_s Shear	0.442	Stud Base area, in ²					
Shear F_y		Shear F_u					
$A_s f_y$	15904	$0.9A_s f_u$	23856	Steel Failure Limit			
		$5.66A_s f'_c{}^{0.3} E_c{}^{0.44}$	23424	Concrete Failure Limit			
Tensile F_y		Tensile F_u					
$A_s f_y$	7069	$2/3A_s f_u$	7854				
$1/2A_s f_u$	5890						
J-Bolt Allowables for Combined Loading				J-Bolt Allowables for Tension/Shear only Loading			
$(P/F_{ap})^{5/3} + (S/F_{as})^{5/3} \leq 1$							
(Unfactored Yield and Ultimate Limits)							
F_y		F_u		F_y		F_u	
Tension	Shear	Tension	Shear	Tension	Shear	Tension	Shear
5890	15904	7854	23424	5890	15904	7854	23424
(Normal Load Allowables)							
$0.67F_y$		$0.33F_u$		$0.67F_y$		$0.33F_u$	
Tension	Shear	Tension	Shear	Tension	Shear	Tension	Shear
3947	10656	2592	7730	3947	10656	2592	7730
$F_{ap} = 2592$		$F_{as} = 7730$		$F_a(tension) = 2592$		$F_a(shear) = 7730$	
(Abnormal Load Allowables)							
$0.9F_y$		$0.5F_u$		$0.9F_y$		$0.5F_u$	
Tension	Shear	Tension	Shear	Tension	Shear	Tension	Shear
5301	14314	3927	11712	5301	14314	3927	11712
$F_{ap} = 3927$		$F_{as} = 11712$		$F_a(tension) = 3927$		$F_a(shear) = 11712$	

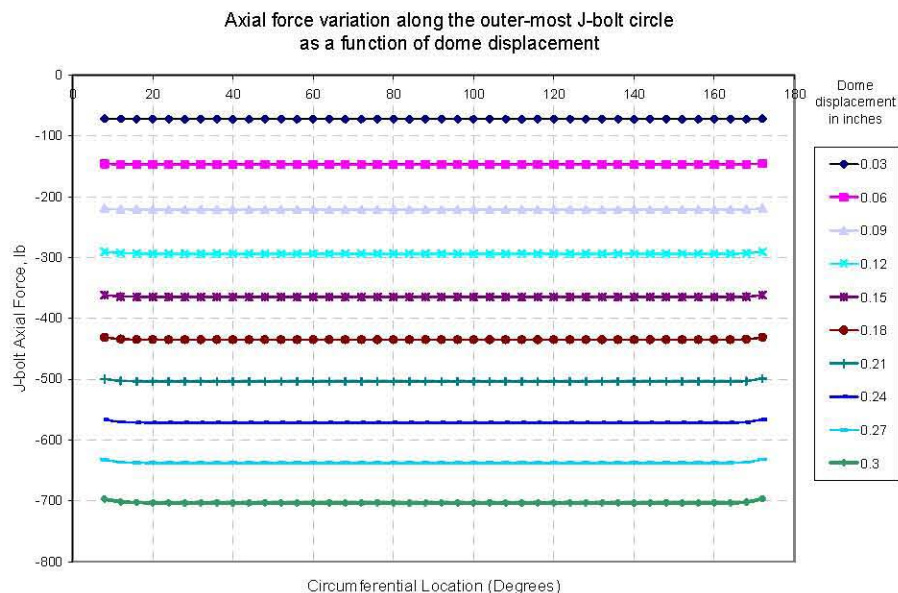
Table 6-4. Summary of Allowable J-Bolt Forces for Normal and Abnormal Loads

Tension Loading only or Shear Loading only		Combined Shear and Tension Loading	
Normal (Operating) Loads Allowables			
Allowable force for tension load, F_a (lb)	2592	Allowable for applied tension load, F_{ap} (lb)	2592
Allowable force for shear load, F_a (lb)	7730	Allowable for applied shear load, F_{as} (lb)	7730
Abnormal (Operating + Seismic) Loads Allowables			
Allowable force for tension load, F_a (lb)	3927	Allowable for applied tension load, F_{ap} (lb)	3927
Allowable force for shear load, F_a (lb)	11712	Allowable for applied shear load, F_{as} (lb)	11712

6.2.1 AY Tank with 0.3-Inch Wall Foreshortening and a 25-Inch Waste Height

Figure 6-2 shows the J-bolt axial force variation as a function of tank wall compression for the outermost circumferential row of J-bolts near the haunch. The axial J-bolt forces are compressive for axial tank compression and, therefore, the force would actually be distributed continuously over the interface between the concrete and the steel dome. Figure 6-3 shows the change in J-bolt shear forces as a function of increasing tank wall foreshortening. The maximum shear force at 0.3 inch axial compression is less than 4,000 lb compared to the shear limit of 7,730 lb. The axial forces and shear forces in the J-bolts increase linearly as the tank compression increases, but they are essentially uniform around the circumference of the tank. The tank wall compression was then fixed at 0.3 inches and the vacuum load was increased until the model failed to converge. Figures 6-4 and 6-5 show that the axial and shear forces do not change significantly when the vacuum is ramped from 0 inches to the maximum value.

Figures 6-6 and 6-7 show the J-bolt axial and shear force variation as a function of tank wall compression for one column of J-bolts from the dome centerline (J-bolt # 2) to the haunch (J-bolt # 20). Axial and shear forces in the J-bolts increase as the dome displacement increases; however, they do not change significantly when the vacuum is ramped from 0 inches to the maximum value.

**Figure 6-2.** Axial Force Variation Along the Outermost J-Bolt Circle for Increasing Tank Wall Foreshortening

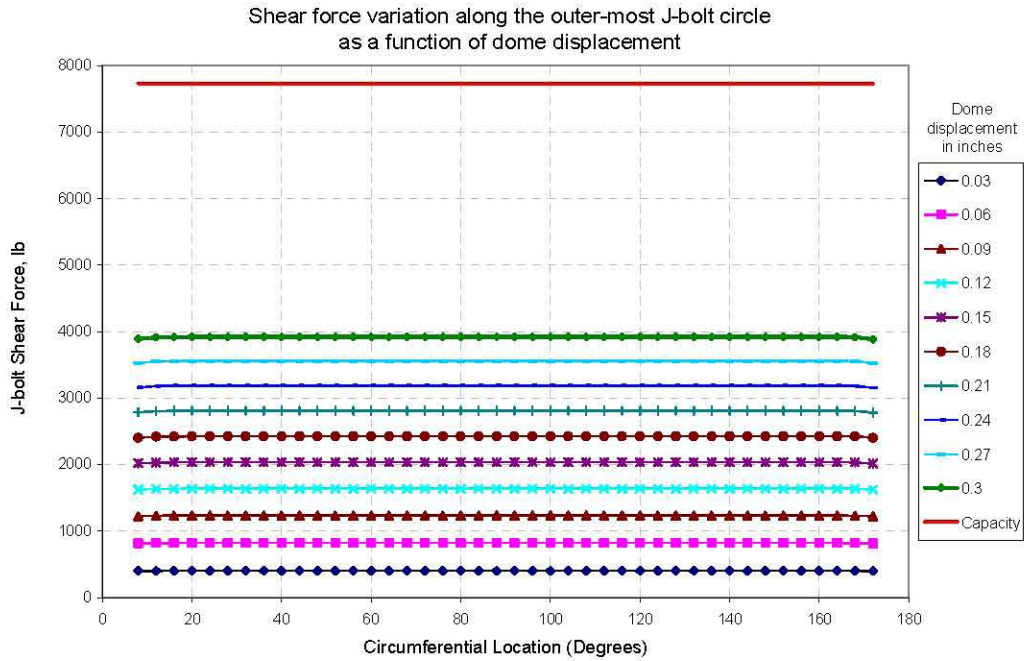


Figure 6-3. Shear Force Variation Along the Outermost J-Bolt Circle for Increasing Tank Wall Foreshortening

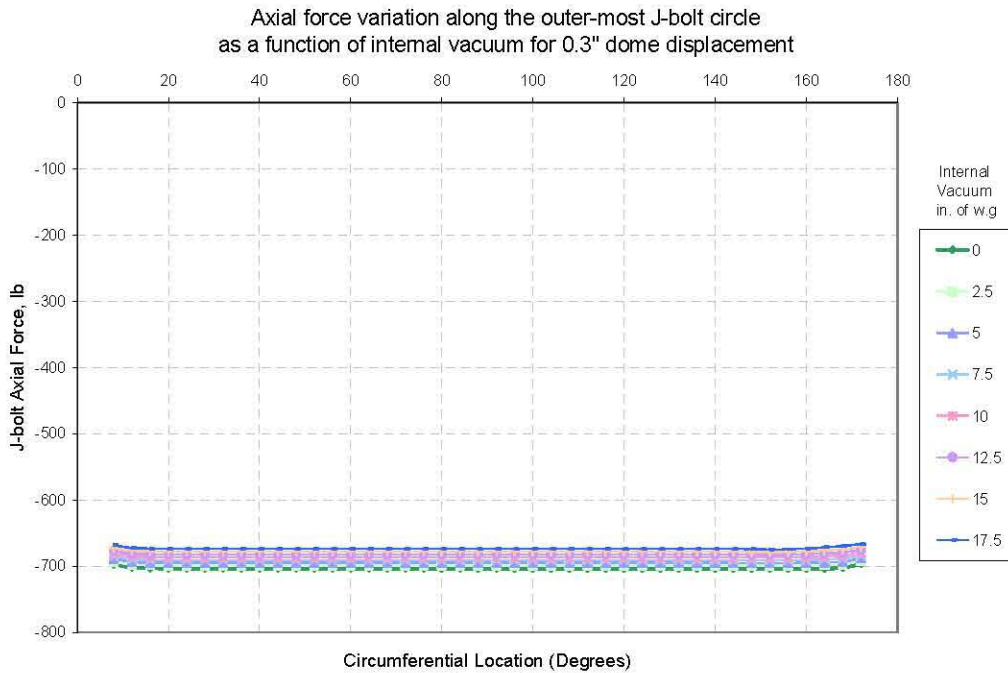


Figure 6-4. Axial Force Variation Along the Outermost J-Bolt Circle with Increasing Vacuum Load and a Constant Wall Foreshortening of 0.3 Inch (Note that the J-bolt axial force is nearly constant for increasing tank vacuum.)

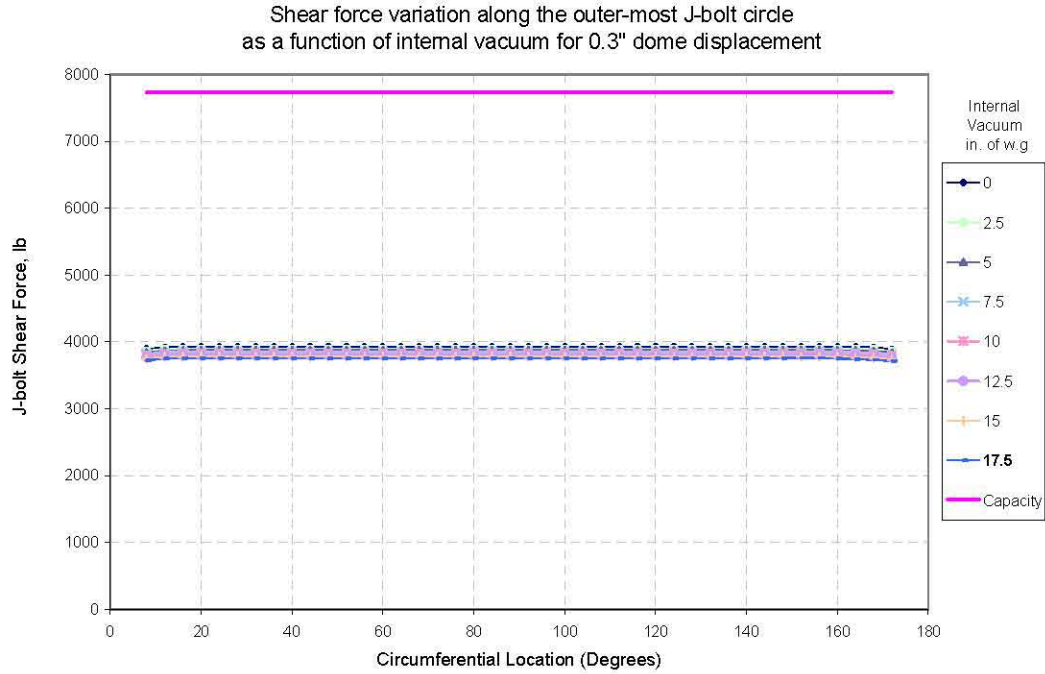


Figure 6-5. Shear Force Variation Along the Outer Ring of J-Bolts with Increasing Tank Vacuum and a Constant Wall Foreshortening of 0.3 Inch (The J-bolt shear force is nearly constant for increasing tank vacuum.)

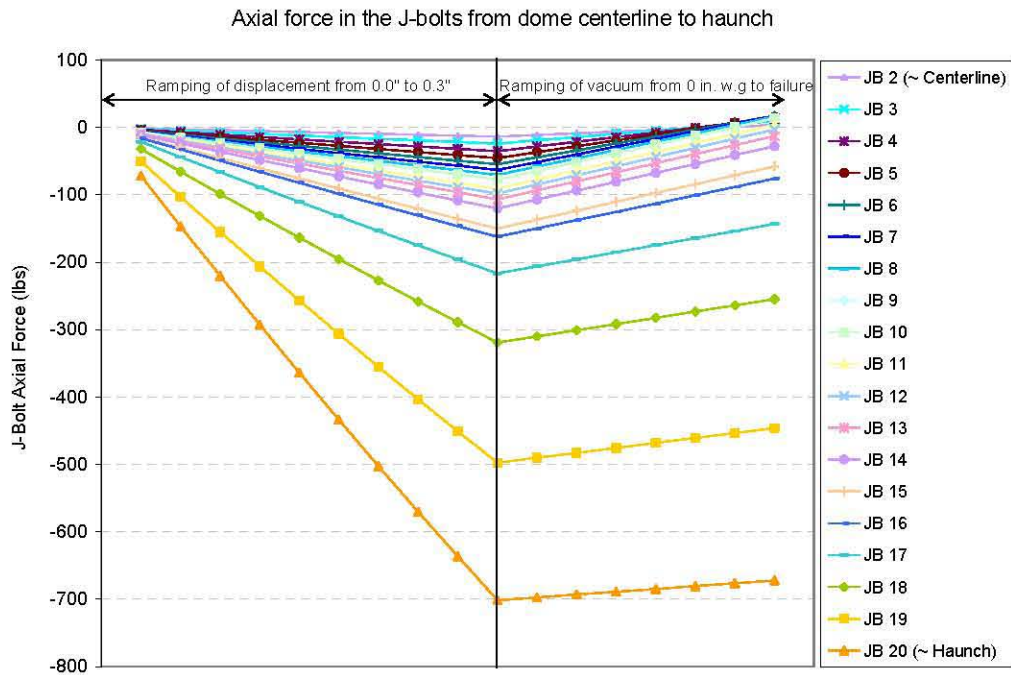


Figure 6-6. J-Bolt Axial Load Histories (for J-bolts from the dome centerline to the haunch) for Increasing Tank Wall Foreshortening Followed by Increasing Vacuum Load

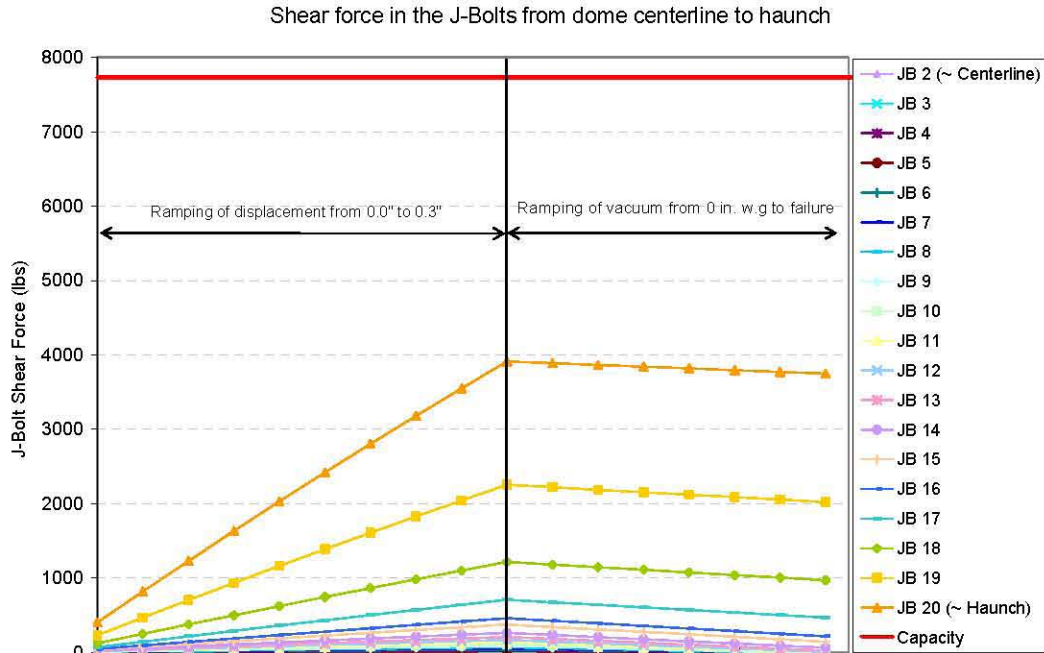


Figure 6-7. J-Bolt Shear Load Histories (for J-bolts from the dome centerline to the haunch) for Increasing Tank Wall Foreshortening Followed by Increasing Vacuum Load

6.2.2 AY Tank with No Tank Wall Foreshortening and 25 Inches of Waste

The second J-bolt evaluation considered the AY tank with zero axial compression and a low waste height of 25 inches. Figures 6-8 and 6-9 show the J-bolt axial and shear force variation as a function of increasing internal vacuum for the outermost row of J-bolts near the haunch. The axial and shear forces in the J-bolts increase as the internal vacuum increases, but they remain very small when the axial compression is zero. Note that the J-bolts are slightly in tension in this case and need to be evaluated for the combined loading condition. Figure 6-10 shows the evaluation for the combined loading case and all the values of $(P/F_{ap})^{5/3} + (S/F_{as})^{5/3}$ are less than 1% of the combined allowables. The axial and shear J-bolt forces show a wave pattern near the imperfection (at the circumferential location between 160 and 180 degrees) which is similar to the buckle pattern seen in Figure 2-5.

Figures 6-11 and 6-12 shows the axial and shear forces for the J-bolts from dome centerline (J-bolt # 2) to the haunch (J-bolt # 20). Axial forces and shear forces in the J-bolts increase as the internal vacuum increases. Figure 6-13 shows the evaluation for the combined loading case and all the values of $(P/F_{ap})^{5/3} + (S/F_{as})^{5/3}$ are less than 1.

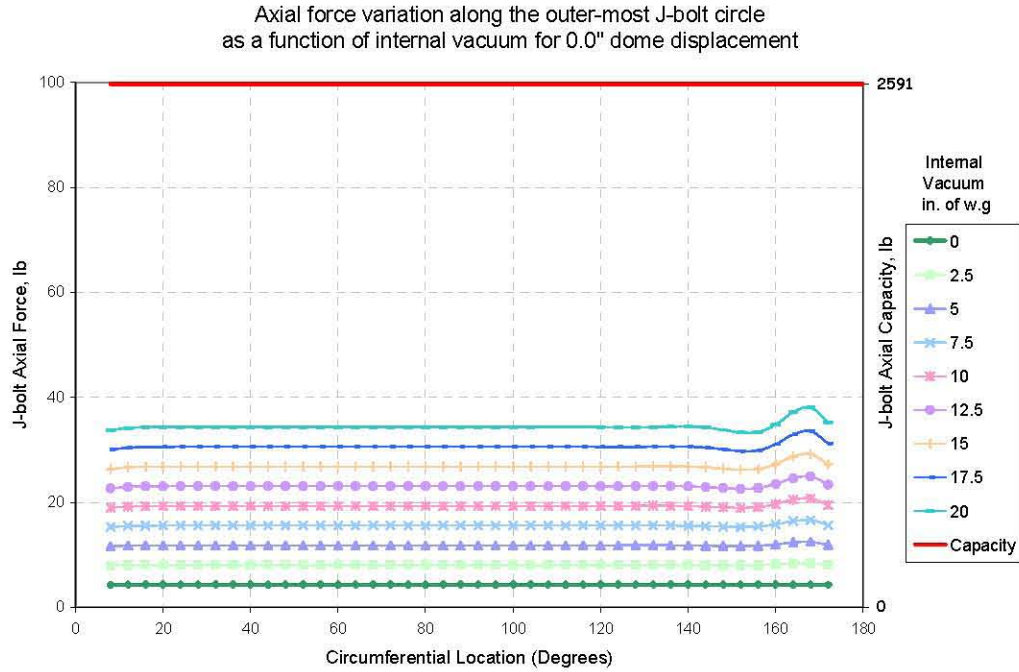


Figure 6-8. Axial Force Variation Along the Outermost J-Bolt Circle as a Function of Internal Vacuum for Zero Axial Foreshortening

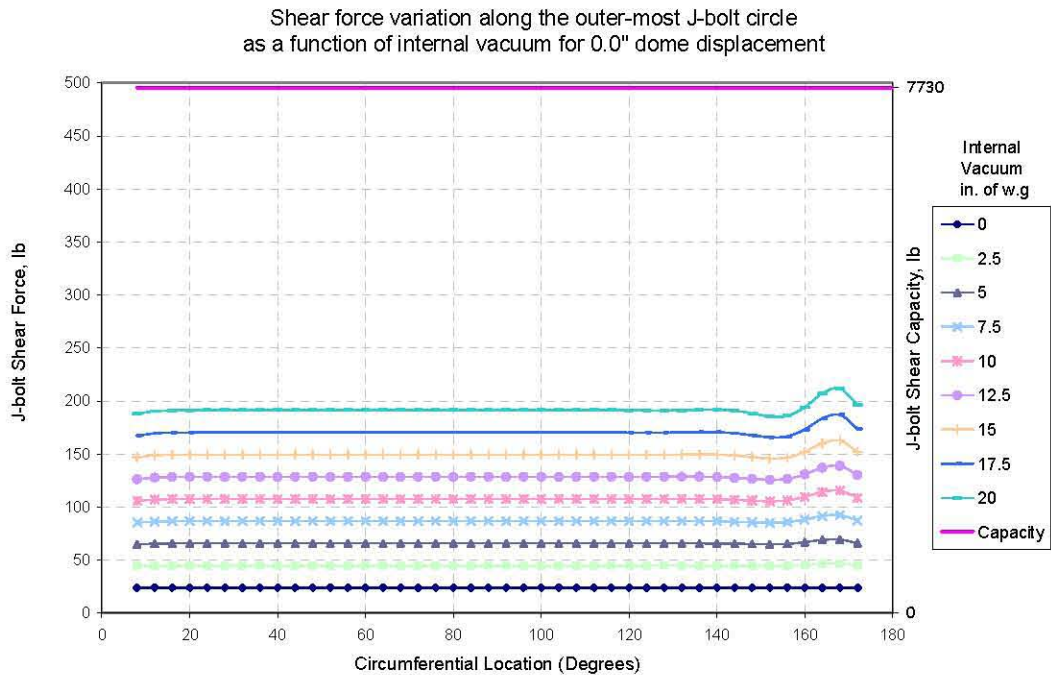


Figure 6-9. Shear Force Variation Along the Outermost J-Bolt Circle as a Function of Internal Vacuum for Zero Axial Foreshortening

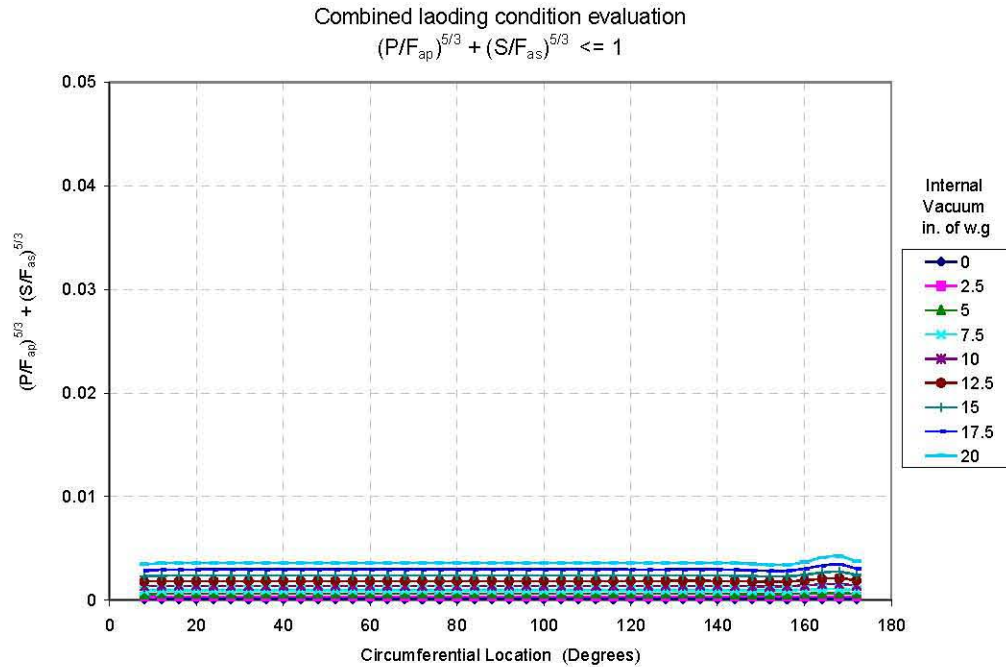


Figure 6-10. Combined Tensile and Shear J-Bolt Force Evaluation for the Case with Zero Axial Compression and Increasing Vacuum Load

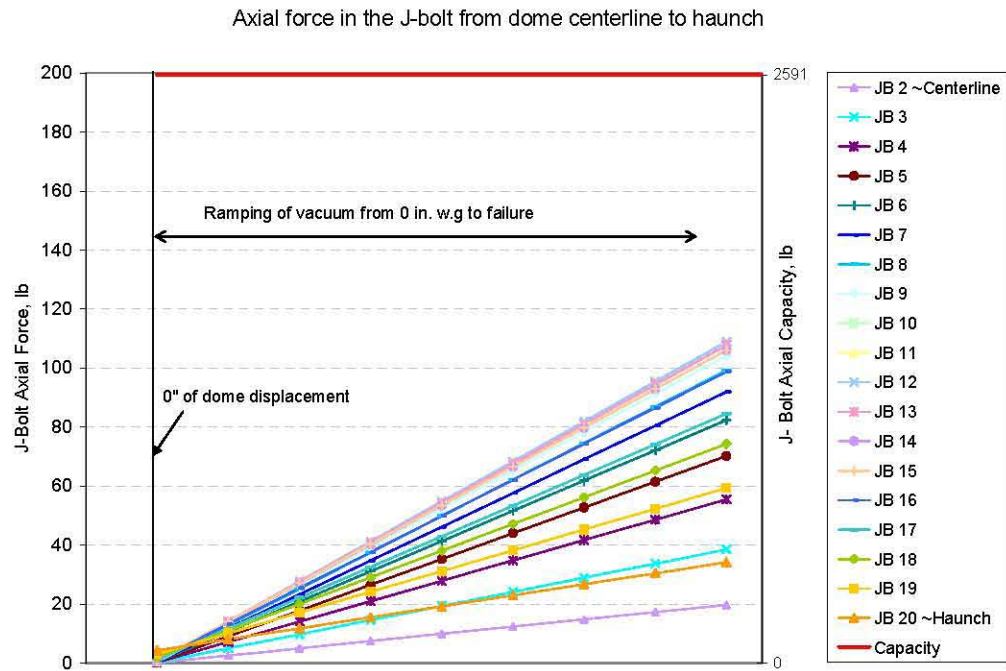


Figure 6-11. Axial Force Histories (for J-bolts from the dome centerline to the haunch) for Zero Axial Compression and Increasing Vacuum Load

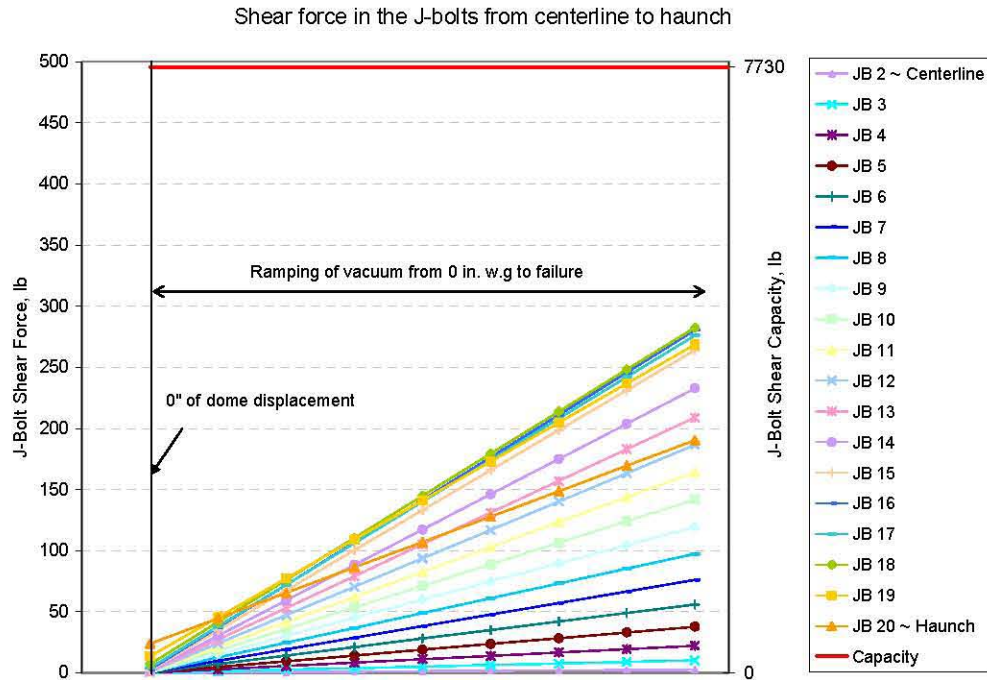


Figure 6-12. Shear Force Histories (for J-bolts from the dome centerline to the haunch) for Zero Axial Compression and Increasing Vacuum Load

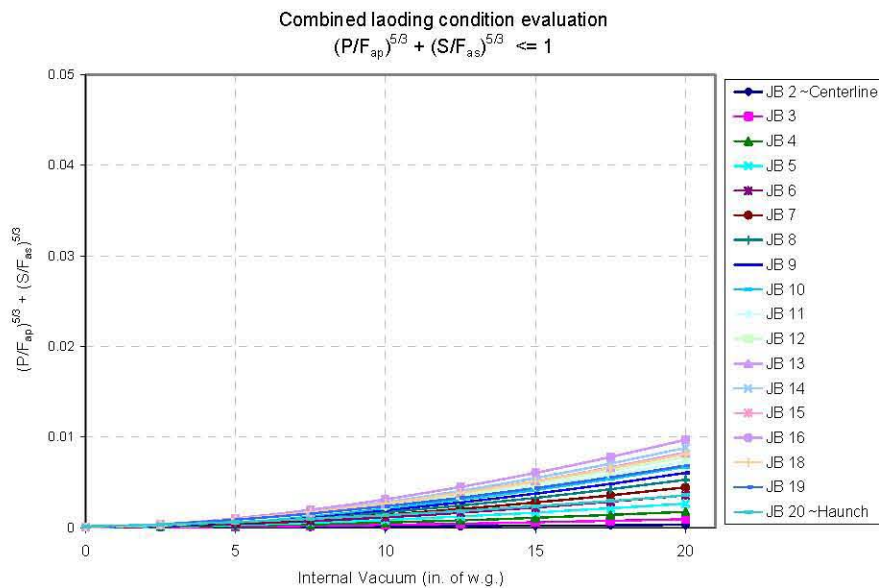


Figure 6-13. Combined Tensile and Shear J-Bolt Force Evaluation (for J-bolts from the dome centerline to the haunch) for the Case with Zero Axial Compression and Increasing Vacuum Load

6.2.3 AY Tank with No Tank Wall Compression and 400 Inches of Waste

The third J-bolt evaluation considered the AY tank with zero axial compression and a waste height of 400 inches. Figures 6-14 and 6-15 show the axial and shear forces for the J-bolts from dome centerline (J-bolt # 2) to the haunch (J-bolt # 20). Axial and shear forces in the J-bolts increase with increasing vacuum and waste height. However, they are still a small fraction of the tensile and shear allowables forces. Figure 6-16 shows the combined loading case where all the values of $(P/F_{ap})^{5/3} + (S/F_{as})^{5/3}$ are less than 20% of the combined allowables.

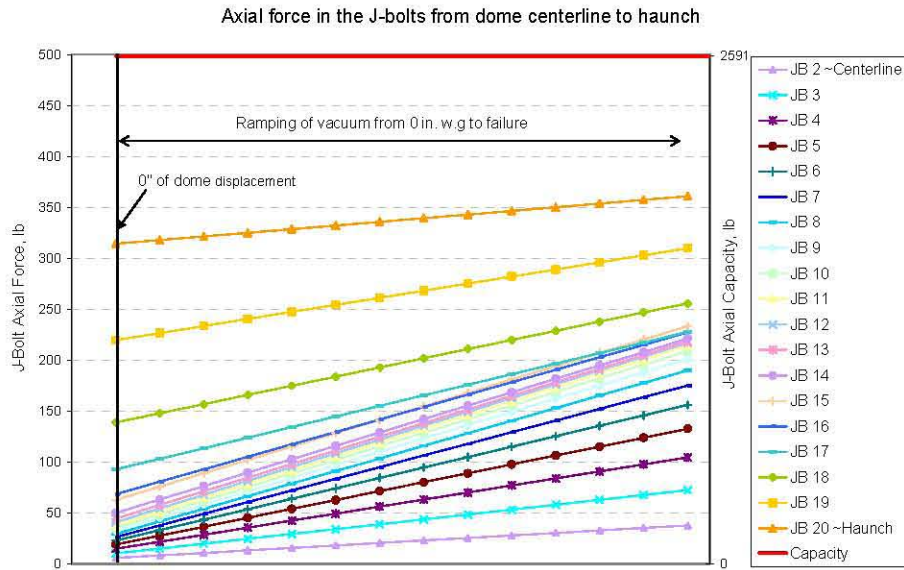


Figure 6-14. Axial Force Histories (for J-bolts from the dome centerline to the haunch) for Zero Axial Compression, 400-Inch Waste Height, and Increasing Vacuum Load

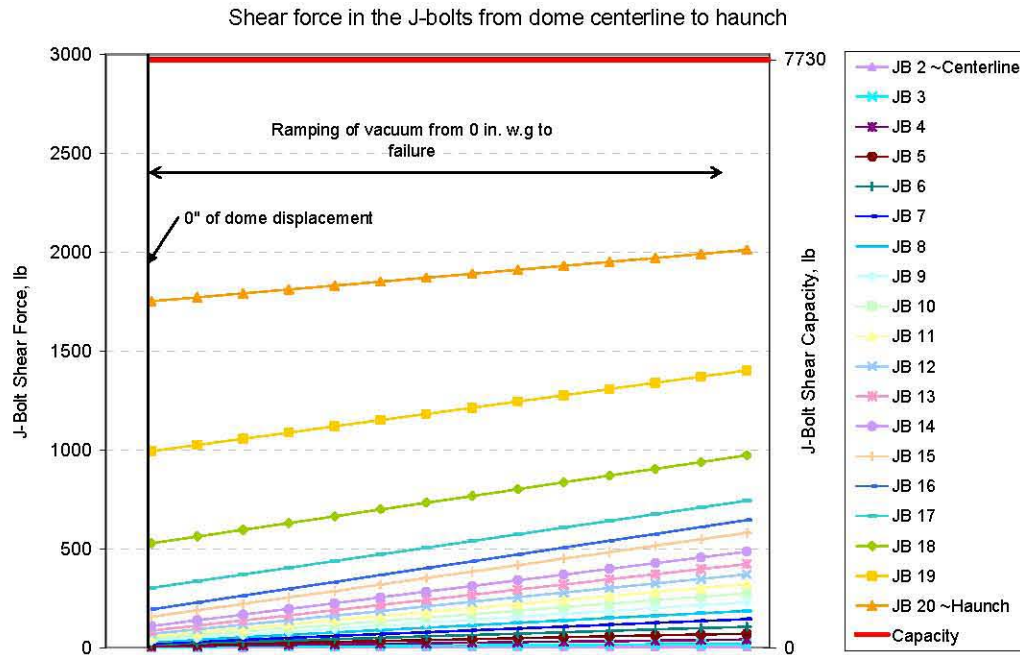


Figure 6-15. Shear Force Histories (for J-bolts from the dome centerline to the haunch) for Zero Axial Compression, 400-Inch Waste Height, and Increasing Vacuum Load

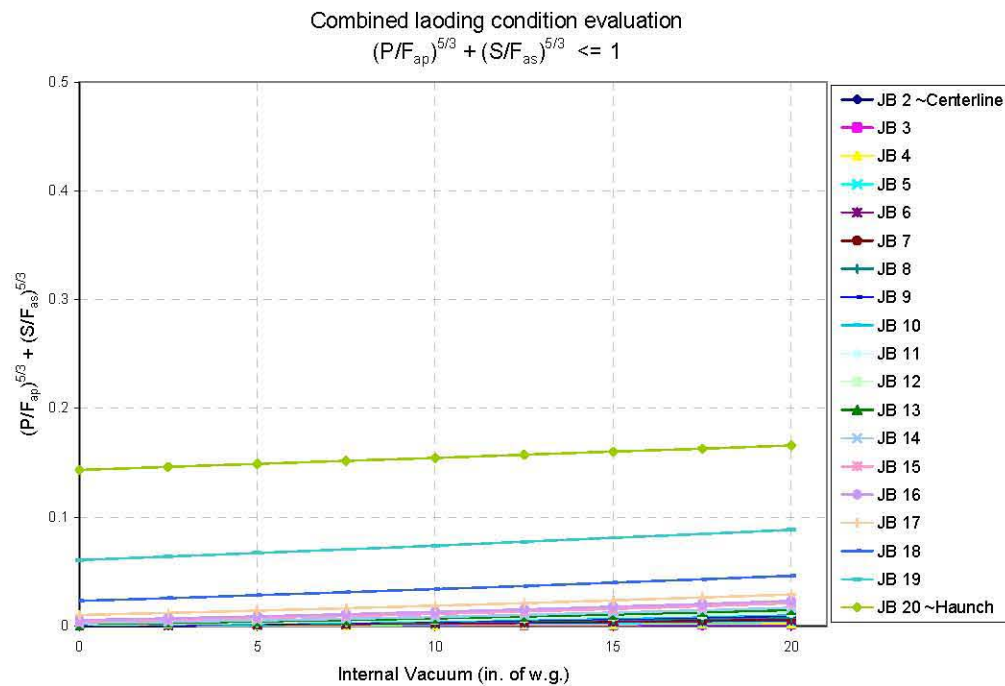


Figure 6-16. Combined Tensile and Shear J-Bolt Force Evaluation (for J-bolts from the dome centerline to the haunch) for the Case with Zero Axial Compression, 400-Inch Waste Height, and Increasing Vacuum Load

6.2.4 AP Tank with 0.3 Inches of Tank Wall Foreshortening and 25 Inches of Waste

Figures 6-17 and 6-18 show the J-bolt axial and shear force variation as a function of dome displacement for one column of J-bolts from dome centerline (J-bolt # 2) to the haunch (J-bolt # 20). Axial and shear forces in the J-bolts increase as the dome displacement increases. Axial and shear forces do not change significantly when the vacuum is ramped from 0 inches of water gauge to the maximum value.

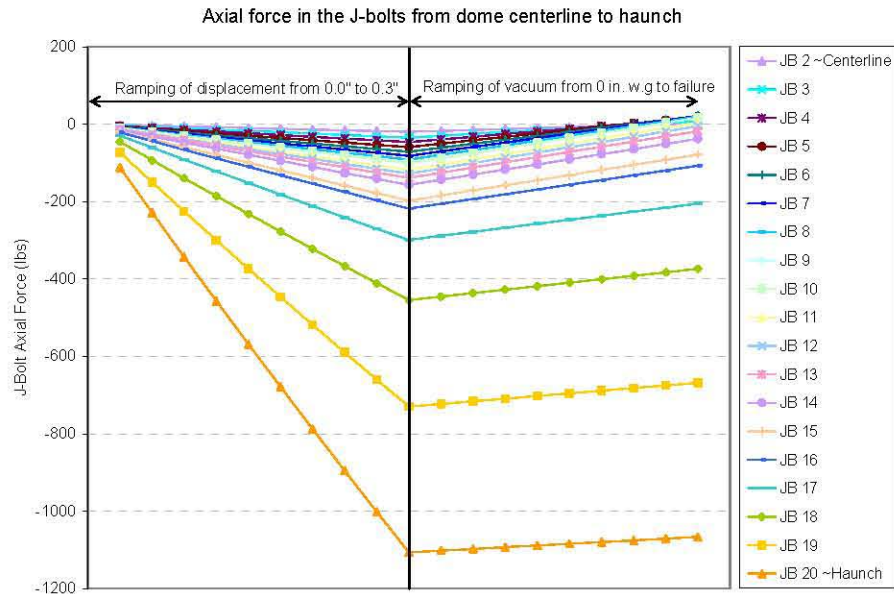


Figure 6-17. Axial Force Histories (for J-bolts from the dome centerline to the haunch) for the AP Tank with 0.3 Inch Axial Compression, 25-Inch Waste Height, and Increasing Vacuum Load



Figure 6-18. Shear Force Histories (for J-bolts from the dome centerline to the haunch) for the AP Tank with 0.3 Inch Axial Compression, 25-Inch Waste Height, and Increasing Vacuum Load

6.2.5 AP Tank with 0.0 Inches of Tank Wall Foreshortening and 25 Inches of Waste

Figures 6-19 and 6-20 show the axial and shear forces for the J-bolts from the dome centerline (J-bolt # 2) to the haunch (J-bolt # 20) for the AP tank with 25 inches of waste and zero axial compression.

Figure 6-21 shows the combined loading case values of $(P/F_{ap})^{5/3} + (S/F_{as})^{5/3}$ are less than 1% of the allowable combination.

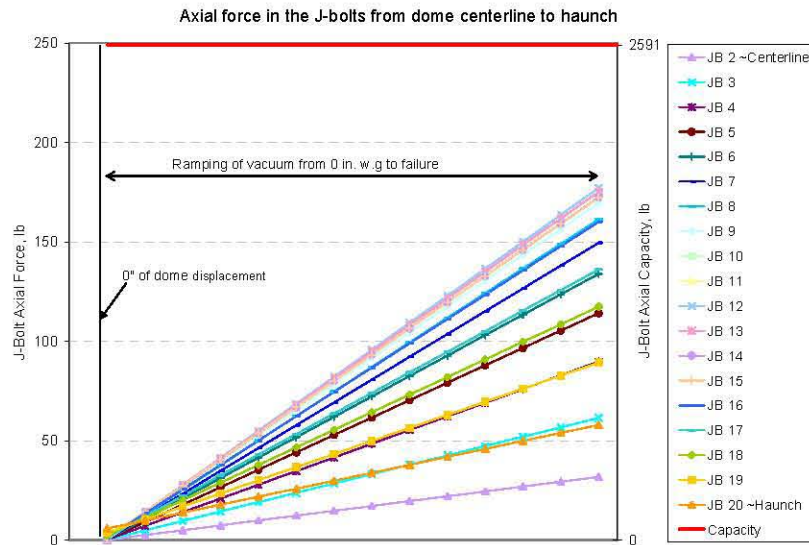


Figure 6-19. Axial Force Histories (for J-bolts from the dome centerline to the haunch) for the AP Tank with Zero Axial Compression, 25-Inch Waste Height, and Increasing Vacuum Load

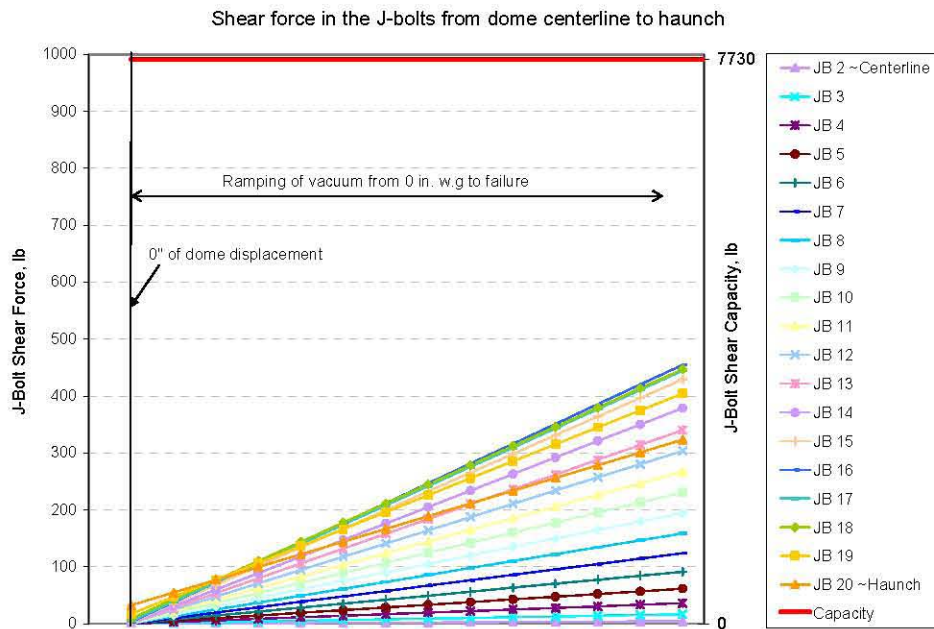


Figure 6-20. Shear Force Histories (for J-bolts from the dome centerline to the haunch) for the AP Tank with Zero Axial Compression, 25-Inch Waste Height, and Increasing Vacuum Load

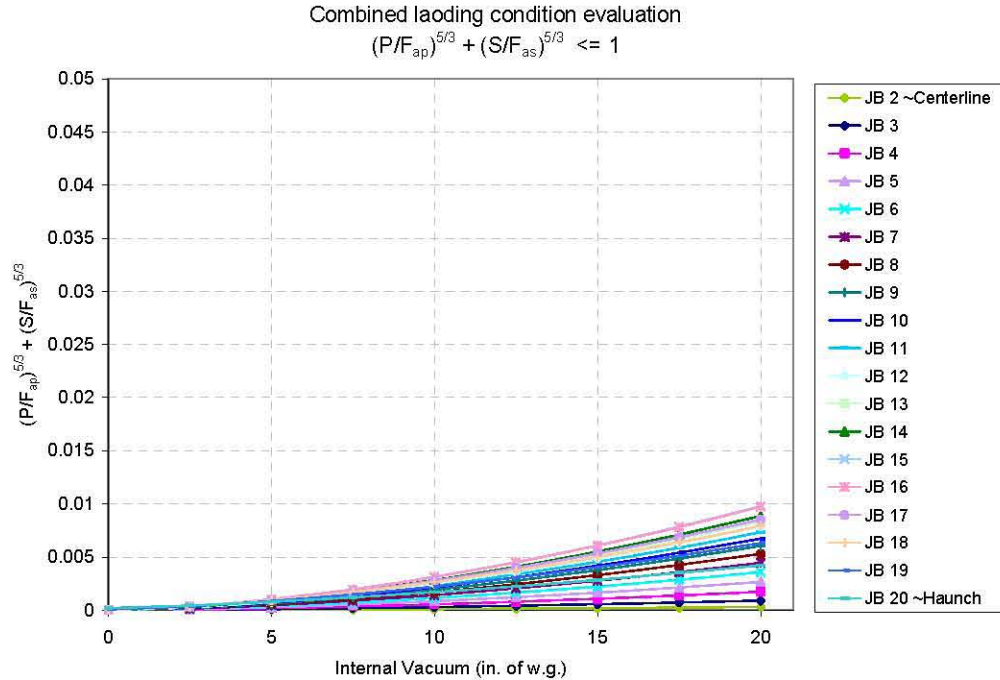


Figure 6-21. Combined Shear and Axial Forces (for J-bolts from the dome centerline to the haunch) for the AP Tank with Zero Axial Compression, 25-Inch Waste Height, and Increasing Vacuum Load

6.2.6 AP Tank with 0.0 Inches of Tank Wall Foreshortening and 400 Inches of Waste

Figures 6-22 and 6-23 show the J-bolt axial and shear force variation as a function of increasing internal vacuum for the outermost circumferential row of J-bolts near the haunch. The results are for the J-bolts from dome centerline (J-bolt # 2) to the haunch (J-bolt # 20). Axial and shear forces in the J-bolts increase as the internal vacuum increases. The zero vacuum represents the zero inches of dome displacement. Note that the J-bolts are slightly in tension in this case and need to be evaluated for the combined loading condition. Figure 6-24 shows the evaluation for the combined loading case and all the values of $(P/F_{ap})^{5/3} + (S/F_{as})^{5/3}$ are less than 1.

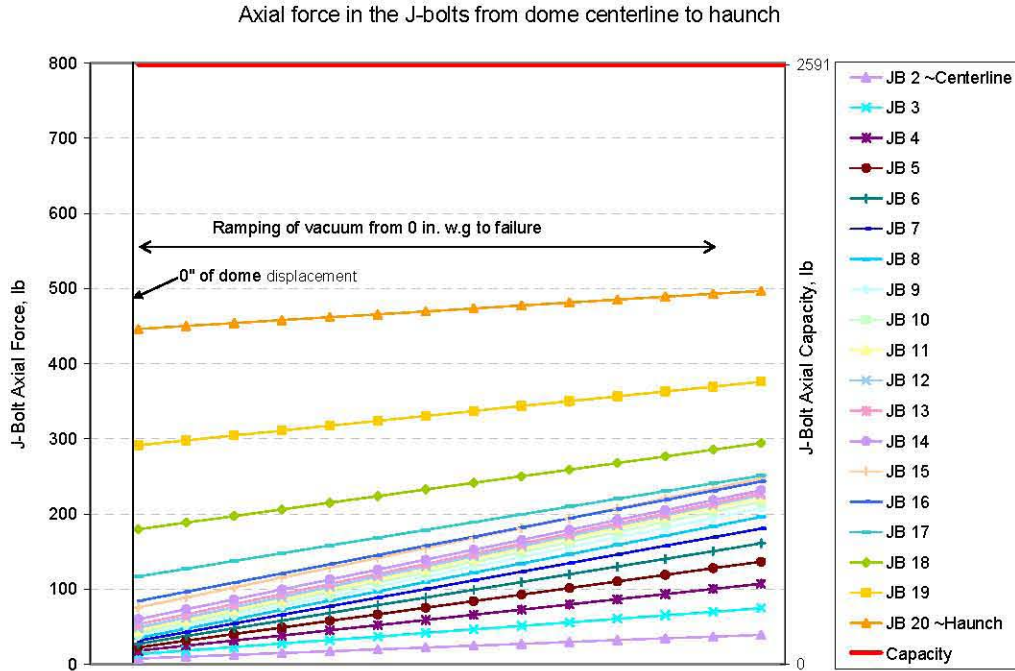


Figure 6-22. Axial Force Histories (for J-bolts from the dome centerline to the haunch) for the AP Tank with Zero Axial Compression, 400-Inch Waste Height, and Increasing Vacuum Load

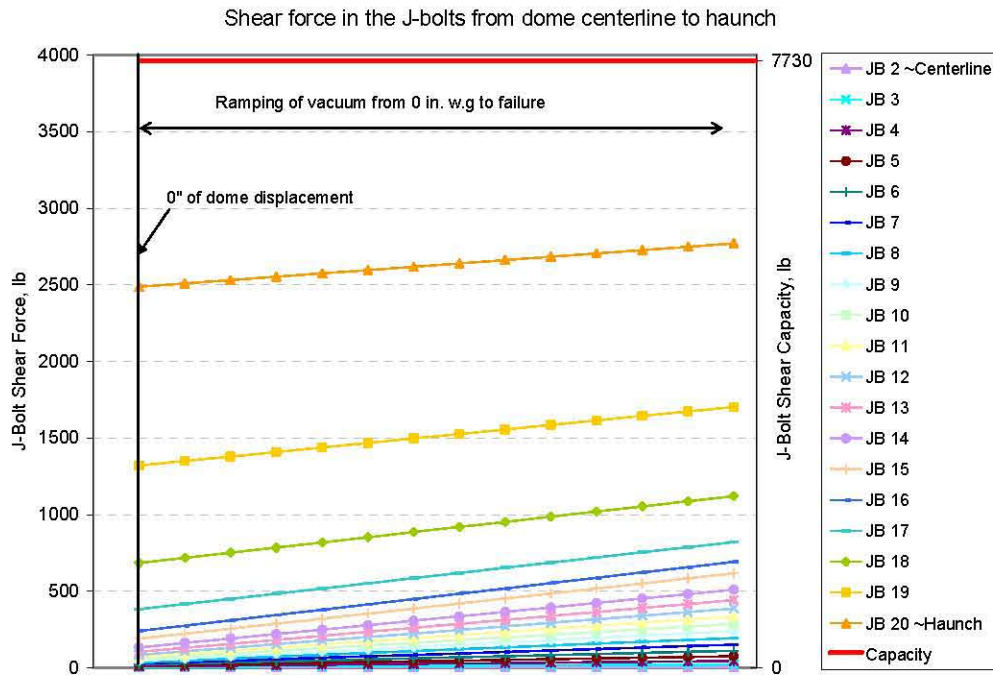


Figure 6-23. Shear Force Histories (for J-bolts from the dome centerline to the haunch) for the AP Tank with Zero Axial Compression, 400-Inch Waste Height, and Increasing Vacuum Load

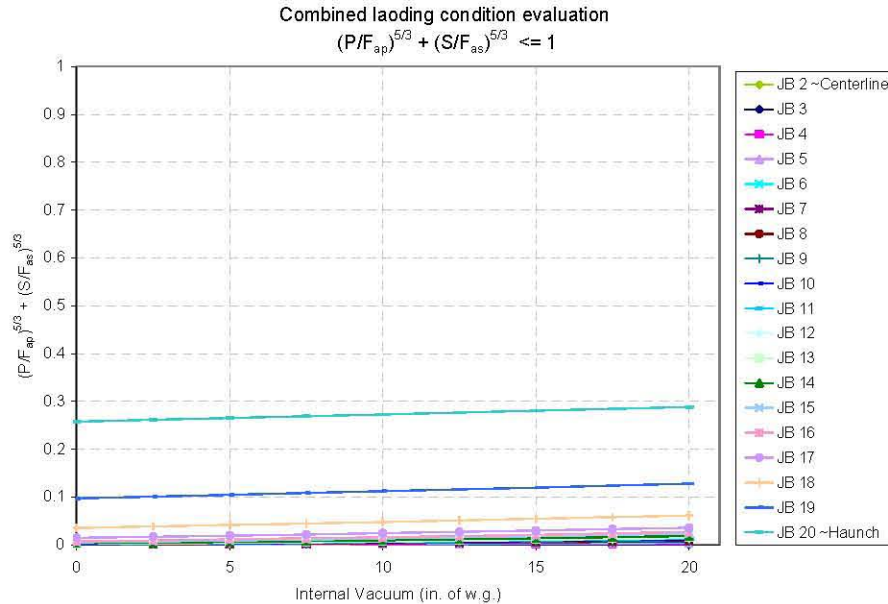


Figure 6-24. Combined Loads (for J-bolts from the dome centerline to the haunch) for the AP Tank with Zero Axial Compression, 400-Inch Waste Height, and Increasing Vacuum Load

6.3 Correlating J-Bolt Limit Loads with the Equivalent Linear Elastic Axial Force in the Primary Tank Wall

Figure 6-25 shows the distribution of shear and axial reaction forces in the J-bolt anchors from the center of the tank dome to the haunch. These forces are due to axial compressive loads in the tank wall. The maximum J-bolt force occurs at the outermost circle of the J-bolt, at the transition between the dome and the haunch. Since this force increases linearly with the axial compression in the tank wall, the results in Chapter 4 showing the axial force versus tank foreshortening can be rescaled to show the maximum J-bolt shear force (at the outermost bolt circle) as a function of the equivalent linear elastic force in the tank wall.

Additional shear force must be resisted by the J-bolts in a seismic event. Figure 6-26 shows the distribution of seismic induced shear force in the J-bolts from the center of the tank dome to the haunch. These are the maximum shear forces in the 1 and 2 directions (in the horizontal plane) that were predicted at each bolt throughout the time domain analysis performed by Carpenter et al. (2006). The maximum total shear was calculated as the square-root-sum-of-the-squares (SRSS) of the 1 and 2 shear components. The SRSS was done after sorting to find the maximum components, giving an additional level of conservatism. Figure 6-26 shows that the maximum shear force is 4.6 kip at the outermost J-bolt for the conditions of best-estimate soil and best-estimate concrete properties.

It should also be noted that the J-bolt shear force components in both Figures 6-25 and 6-26 are not reduced by frictional forces between the steel primary tank and the concrete dome. The shear forces due to axial tank compression (Figure 6-25) were calculated using a model that applied vertical compressive displacements directly to short beam elements at the J-bolt locations without including the concrete dome. The seismic model included the concrete dome and the steel-to-concrete interface, but the results in Figure 6-26 are for a coefficient of friction equal to zero.

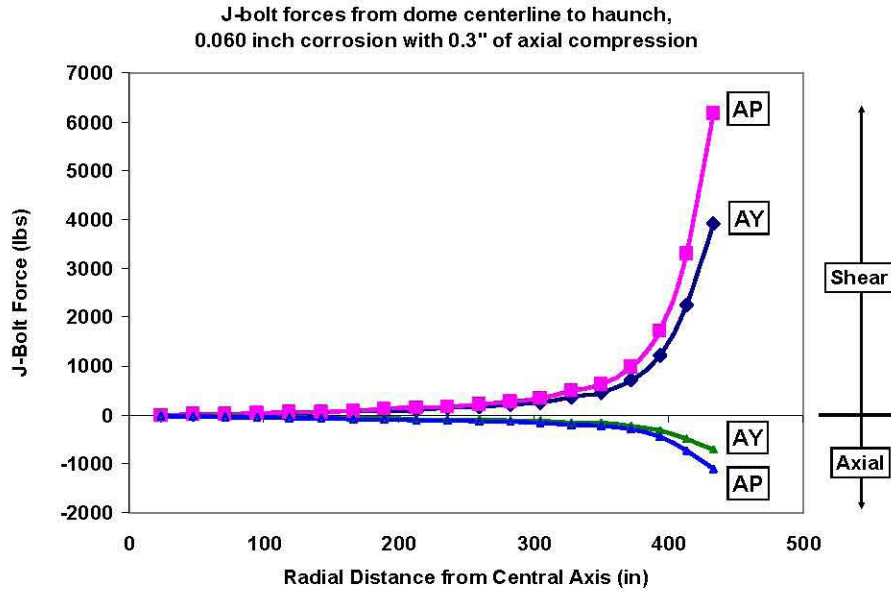


Figure 6-25. J-Bolt Shear and Axial Force Distributions for the AY and AP Tanks (The results are for a corrosion allowance of 0.060 inch and axial wall compression = 0.3 inch.)

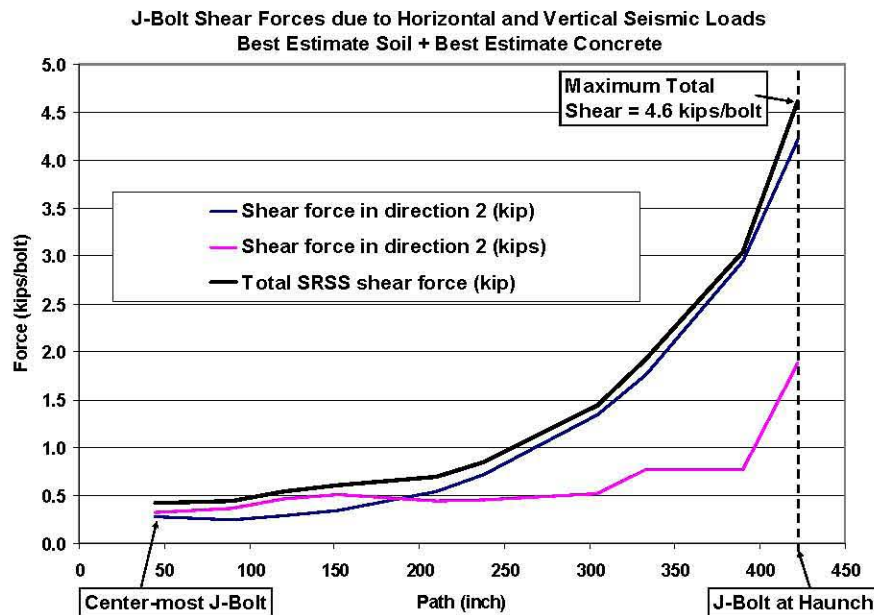


Figure 6-26. J-Bolt Shear Force Due to Horizontal and Vertical Seismic Loads

Figure 6-27 plots the shear force in the outermost J-bolt as a function of the applied axial compression in the tank wall. These results are for the AY tank with corrosion allowances of 0.00, 0.06, and 0.10 inches (wall thicknesses of 0.50, 0.44, and 0.40 inch, respectively). To include the seismic-induced shear force, the plot is offset (from zero force at zero axial compression) by the maximum axial shear force of 4.6 kip per bolt. The total elastically calculated seismic load is applied here with no credit taken for inelastic energy absorption (i.e., the F_u factor in IBC [2003]) reducing the seismic force on the J-bolts. Figure 6-27 also shows the abnormal loads limit from Table 6.4, plus an estimated “shear failure” limit line. The

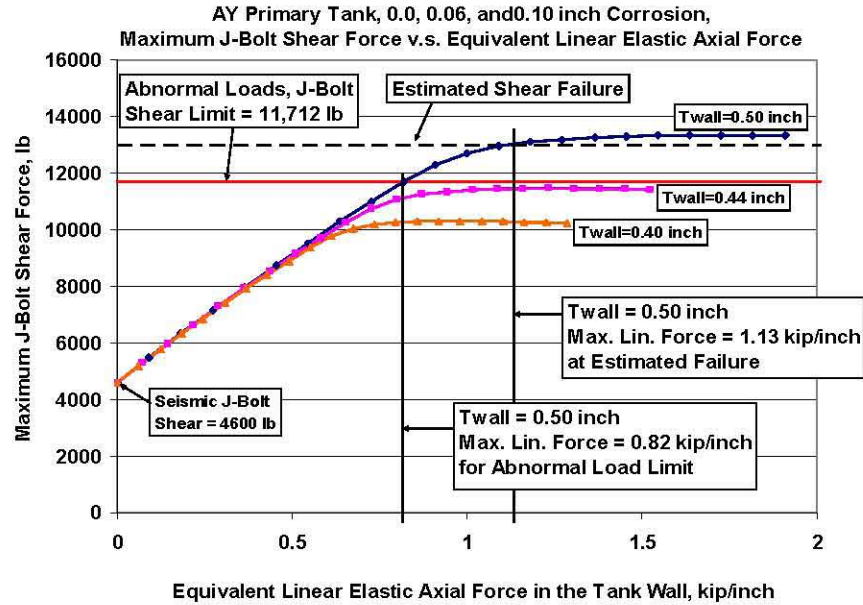


Figure 6-27. Maximum J-Bolt Force vs. the Equivalent Linear Elastic Axial Force for the AY Tank with Corrosion Allowances of 0.00, 0.06 and 0.10 Inches

shear force limit for abnormal loads is equal to 45% of the ultimate force (see Table 6-4). For brittle materials, a maximum shear (Tresca)-type failure would occur at about 50% of the tensile ultimate stress. Therefore, the shear failure limit was estimated by increasing the limit on abnormal loads by 11% (i.e., 50/45). Figure 6-27 shows that for corrosion allowances of 0.06 and 0.10 inch, the AY tank is flexible enough under axial load that it is not possible to achieve a compressive reaction force high enough to exceed the shear limit for abnormal loads. It should be noted here that the limit on shear reaction force is actually governed by concrete crushing around the anchor stud rather than shear overload through the metal stud itself (see Table 6-3). If no corrosion has occurred, then a maximum linear elastic axial force of 0.82 kip/inch corresponds to the shear limit for abnormal operating loads. Similarly, shear failure would be expected to occur at a linear elastic axial force of 1.13 kip/inch.

Figures 6-28 through 6-30 show similar plots for the AP tank with corrosion allowances of 0.00, 0.06, and 0.10 inch, respectively. However, the AP tank is stiffer than the AY tank and therefore the J-bolt shear versus equivalent axial load curves exceed the J-bolt force limits at somewhat lower values of equivalent linear elastic axial force.

The tank buckling evaluation in Chapter 7 includes calculations of the equivalent linear elastic force in the primary tank wall for the maximum operating conditions of each tank farm. Table 6-5 compares the total axial force due to operating loads with the maximum equivalent linear axial loads at the anchor shear limits shown in Figures 6-27 through 6-30. Note that the seismic-induced axial load is not included in the total operating load because the J-bolt shear force due to both horizontal and vertical seismic motion has already been accounted for in the seismic shear force offset. Table 6-5 shows that the only case where the shear reaction force is predicted to exceed the abnormal load limit is for the AY tank with no corrosion at a waste temperature of 350°F. In this case the applied load is 0.866 kip/inch compared to the abnormal loads limit of 0.82 kip/inch and the estimated shear failure limit of 1.13 kip/inch. The applied load exceeds the limit load by about 6% (demand/capacity ratio of 1.06), but it is about 29% below the

estimated failure load (demand/capacity ratio of 0.71). If the calculations are repeated for a maximum future waste temperature of 250°F, then the applied load is 0.665 kip/inch compared to the abnormal loads limit of 0.82 kip/inch, giving a demand/capacity ratio of 0.81.

In summary, the maximum J-bolt shear force due to operating loads plus horizontal and vertical seismic loads is calculated to be below the allowable shear force for abnormal loads for a conservative future waste temperature of 250°F. Therefore, it is not expected that the combined operating and seismic loads will jeopardize the structural integrity of any of the J-bolts.

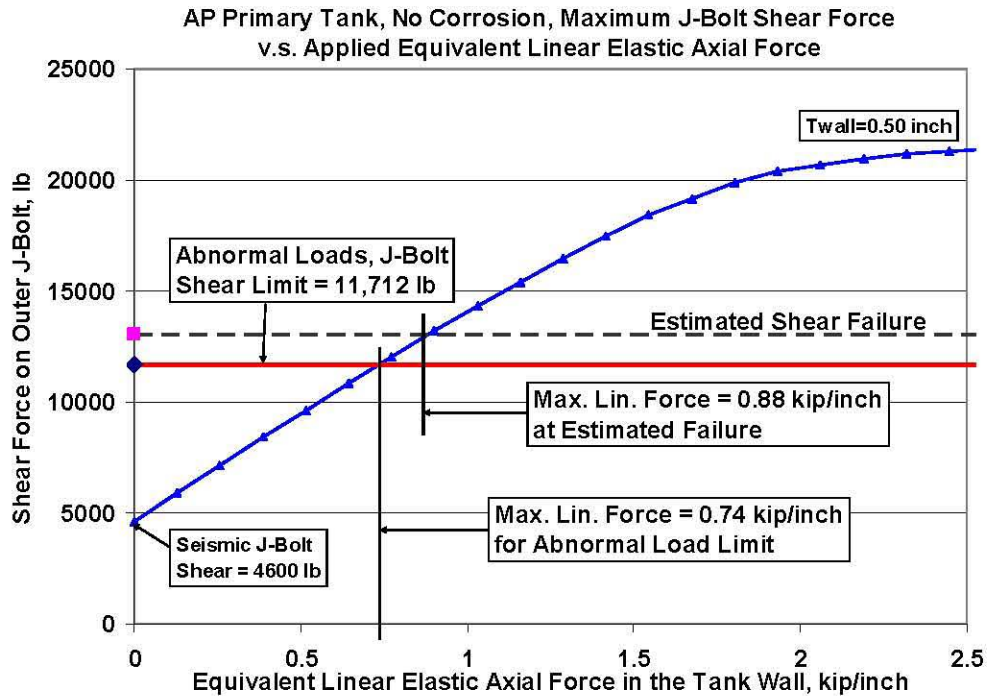


Figure 6-28. Maximum J-Bolt Force vs. the Equivalent Linear Elastic Axial Force for the AP Tank with a Corrosion Allowance of 0.000 Inches

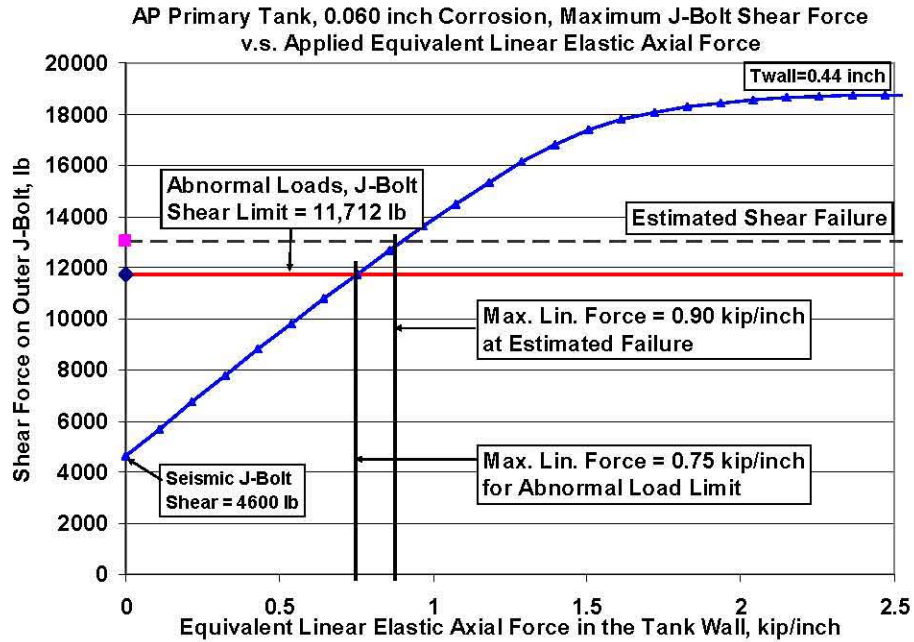


Figure 6-29. Maximum J-Bolt Force vs. the Equivalent Linear Elastic Axial Force for the AP Tank with a Corrosion Allowance of 0.060 Inches

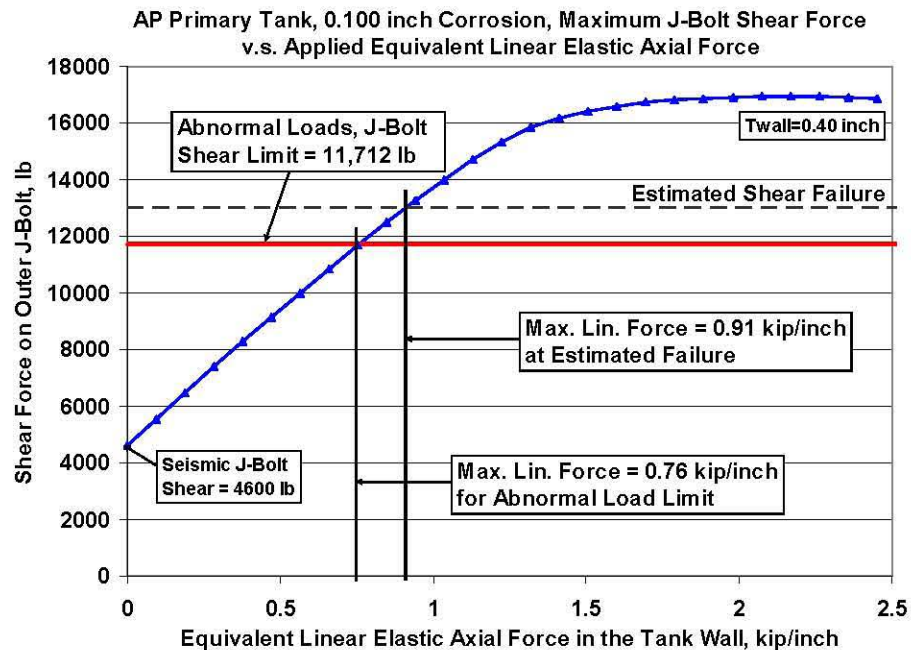


Figure 6-30. Maximum J-Bolt Force vs. the Equivalent Linear Elastic Axial Force for the AP Tank with a Corrosion Allowance of 0.100 Inches

Table 6-5. Summary of the Applied Equivalent Linear Axial Force and the Maximum Equivalent Linear Axial Forces (at the J-bolt shear limits) for the Buckling Evaluation of the Current Operating Limits (The force is in the tank wall and the units are kip/inch of circumference.)

		Demand	Capacity		111% of Capacity	
Tank	Corrosion, inch	Operating Axial Force, kip/inch	Maximum Axial Force at J-Bolt Abnormal Shear Limit, kip/inch	Demand/ Capacity Ratio Based on Abnormal Load Limit	Maximum Axial Force at J-Bolt Abnormal Shear Limit, kip/inch	Demand/ Capacity Ratio Based on Estimated Shear Failure
Maximum Waste Temperature = 350F						
Maximum of	0.000	0.866	0.82	1.06	1.13	0.77
AY,AZ,SY,AN,AW,	0.060	0.696	---	---	---	---
	0.100	0.583	---	---	---	---
Maximum Waste Temperature = 250F						
Maximum of	0.000	0.665	0.82	0.81	1.13	0.59
AY,AZ,SY,AN,AW,	0.060	0.534	---	---	---	---
	0.100	0.447	---	---	---	---
Maximum Waste Temperature = 210F						
AP	0.000	0.475	0.74	0.64	0.88	0.54
	0.060	0.397	0.75	0.53	0.90	0.44
	0.100	0.345	0.76	0.45	0.91	0.38
--- = The tank is not stiff enough for the reaction force to reach the anchor shear limit.						

6.4 Addressing the EH-22 Findings on the Potential for Progressive J-Bolt Failure and the Appropriate Safety Factors for Evaluating Local and Global Buckling

As described in Chapter 1, it was the opinion of the EH-22 review panel that non-conservative assumptions had been used in the previous primary tank buckling analysis. They also postulated that progressive J-bolt failure may occur which could cause local buckling (and local J-bolt failure) to progress to global buckling. The J-bolts or their attachments were identified as the unanalyzed weak link in the load path. Based on this postulated failure mode they suggested that the higher global buckling safety factors should have been used in the buckling evaluation. This section summarizes the predicted response of the J-bolts under the range of loading conditions that have currently been analyzed to determine:

- Can the EH-22 scenario develop if the vacuum is limited to -6.6 in. water gage by a relief valve?
- What is the appropriate factor of safety required to protect against buckling if the EH-22 scenario can develop?
- What is the appropriate factor of safety required to protect against buckling if the EH-22 scenario cannot develop?

6.4.1 Can the EH-22 Scenario Develop if the Vacuum is Limited to -6.6 Inch Water Gage by a Relief Valve?

The J-bolt analysis presented in Section 6.2 of this chapter and summarized in Section 6.3 shows that the EH-22 scenario cannot occur. The typical loading condition for the primary tanks includes axial compression in the wall of the primary tanks. Under these conditions, the finite element analysis predicts

that all the J-bolts, both at and away from the buckling instability (wrinkle), are in axial compression. Therefore, under typical conditions, J-bolt pullout cannot occur as was postulated by the EH-22 panel.

For the unlikely case of zero axial compression, the J-bolts are under a small amount of tension due to increasing vacuum and the Poisson's effect associated with the tensile hoop stress from the hydrostatic waste pressure. The combined shear and tensile loads are less than 30% of the combined allowables for all cases considered in this review. Therefore, even the low probability loading conditions result in small J-bolt tensile forces that are well below the allowable forces.

In addition, the finite element analyses in Chapter 3 that were used to establish the limiting vacuum and axial loads on the primary tank showed that the tank deformations are small at the unfactored limit loads and they increase stably at loads beyond these values. None of the analyses predicted that the tank dome would peel away from the concrete under increasing vacuum as was postulated by the EH-22 panel. This is true for vacuum loads up to and beyond the unfactored limits, which are at least a factor of 1.67 (i.e., the safety factor for global buckling with a service level C load) times the actual limits set on the tank vacuum. This is well below the gross tank wrinkling that would have to accompany the failure scenario postulated by the EH-22 panel.

The more probable failure mode would be shear of the outermost J-bolts. The maximum J-bolt shear and axial forces are observed in the outer ring of J-bolts near the haunch for both the AY and AP primary tanks. Section 6.3 concluded that the maximum J-bolt shear force due to operating loads plus horizontal and vertical seismic loads is below the allowable shear force for a conservatively high future waste temperature of 250°F. Therefore, it is not expected that the combined operating and seismic loads will jeopardize the structural integrity of any of the J-bolts.

Based on this review, J-bolt failure is not expected, and thus it is very unlikely that the EH-22 scenario could occur.

6.4.2 What is the Appropriate Factor of Safety Required to Protect Against Buckling if the EH-22 Scenario Can Develop?

Based on the buckling and J-bolt analyses presented in this report, it is very unlikely that the EH-22 scenario could occur.

6.4.3 What is the Appropriate Factor of Safety Required to Protect Against Buckling if the EH-22 Scenario Cannot Develop?

The buckling calculations will be conducted for four different service levels defined in Section III of the ASME Boiler and Pressure Vessel Code. Each service level has required factors of safety for local and global buckling:

	Factors of Safety	
	Local Buckling	Global Buckling
Level A = Normal operating conditions	2.0	2.4
Level B = Upset conditions	2.0	2.4
Level C = Emergency conditions	1.67	2.0
Level D = Faulted conditions	1.34	1.61

Attachment B of Julyk (2002) makes the argument that axial compression in the tank cylinder will be relieved by local bowing of the wall before the onset of general instability. This position is justified since the meridional (axial) compressive stresses are displacement-controlled as a result of differential thermal expansion and concrete creep-induced loads on the primary tank. The load deflection response of the large displacement finite element models used in the current buckling analysis confirm that the axial stress in the tank is self-limited by the deformation of the primary tank geometry (see Figures 3-12 and 3-13). This rationale leads to the following buckling criteria when combining the effects of axial and hoop loads on the allowable vacuum:

The allowable vacuum (net negative pressure) in the double-shell tanks is controlled by the minimum of two cases:

- A. Local Buckling (with *local* buckling safety factors imposed) evaluated considering the interaction of the net internal vacuum load (Δp) combined with the meridional compressive stress (σ_ϕ).
- B. General Instability (with *global* buckling safety factors imposed) evaluated considering the net internal vacuum load (Δp) acting alone. No interaction with the meridional compressive stress shall be considered ($\sigma_\phi = 0$).

These criteria were used by Julyk (2002) and they are also used in the current buckling evaluation. It is further assumed that the design basis loads used in the thermal and operating loads analysis conservatively represent Service Levels A, B, and C. This is consistent with the loading conditions assumed by Julyk (2002). Service Level D, however, requires that the incremental seismic stresses be added to the design basis stresses for evaluating the faulted condition.

Julyk (2002) states that activation of the tank relief valves at the limiting vacuum load should be classified as an ASME Service Level C (emergency) load condition. Service Level C loads are defined by the ASME Code, Section III, Division 1, NB-3113 (ASME 2004b) as:

“The total number of postulated occurrences for all specified service conditions for which Level C Limits are specified shall not cause more than 25 stress cycles having an S_a value greater than that for 10^6 cycles from the applicable fatigue design curves of Figures I-9.0.”

Evidence is provided below that the alternating stress associated with these vacuum cycles is well below the allowable, S_a , and also that the total number of vacuum cycles between normal operating vacuum and the limit vacuum are expected to be less than the maximum number of 25 cycles.

The AY primary tanks were constructed with A515 grade 60 steel, which has a minimum ultimate tensile strength, S_{ult} , of 60 ksi. The allowable alternating stress, S_a , at 10^6 cycles is 12,500 psi for carbon steels with $S_{ult} \leq 80$ ksi (ASME 2004c). The alternating stress due to tank vacuum is the hoop stress corresponding to the limiting vacuum load. The maximum alternating stresses for the different tank designs are:

AY, SY, AN, AY, AZ: Tank Radius = 450 inch, Pressure = -6 inch w.g. (-0.217 psi)
 Minimum Wall Thickness = $0.375 - 0.060 = 0.315$ inch
 Hoop Stress = $pr/t = (-0.217)(450)/0.315$ $S_a = 310$ psi

AP: Tank Radius = 450 inch, Pressure = -12 inch w.g. (-0.434 psi)
 Minimum Wall Thickness = $0.375 - 0.060 = 0.315$ inch
 Hoop Stress = $pr/t = (-0.434)(450)/0.315$ $S_a = 620$ psi

These alternating stresses are factors of 40 and 20 lower than the limiting value of 12,500 psi.

Tank farms operations staff recently reviewed all of the Occurrence Reports from 1990 to the present. This summary information will be released in the next revision of RPP-11413, *Technical Basis for the Ventilation Requirements Contained in Tank Farm Operating Specifications Documents*, authored by L. Payne. No incidents were found where the primary tank differential vacuum has exceeding the 6 inch w.g. maximum. There was a report of reaching a vacuum of 4 inch w.g. in the SY tank ventilation system, but the exhauster shut down on interlock. There was one incident in AW, but it was also limited to 4 inch w.g. or less. The incident that people remembered where a vacuum limit was exceeded was in the AN annulus system in 2005 (PER-2005-072). Note that this occurred in the annulus and not in the primary tank.

This review shows that there is no recorded evidence that the primary tank vacuum limits have ever been achieved during tank operation and even if they had the resulting cyclic stress would be insignificantly small. Therefore, it is very appropriate to define the occurrence of the maximum operating vacuum as an ASME Service Level C load condition.

7.0 Buckling Evaluation of the DST Primary Tanks

This chapter presents both elastic and plastic buckling analyses of the DST primary tanks. The elastic buckling evaluation presents a method for evaluating the allowable vacuum limit for each of the DST primary tanks. The method estimates the axial force in the primary tank wall using the equations in Chapter 5, and then uses this force to calculate the unfactored vacuum limit for elastic buckling based on the equations in Chapter 3. Once the unfactored axial force and vacuum limits are calculated, the safety factors for the ASME Section III service levels are applied to calculate the allowable tank vacuum limits. An independent review (Appendix B) was conducted to confirm the correct calculation of the axial tank force, the unfactored vacuum limit, and the application of the ASME safety factors. This chapter concludes with a plastic (elephant-foot) buckling evaluation of the tanks for the worst case loading conditions.

7.1 Elastic Buckling

An Excel™ spreadsheet was constructed using the equations of Chapters 3 and 5, and it applies the ASME Section III Service Level safety factors to calculate the vacuum allowables for the primary tanks. Tables 7-1 through 7-3 show an example of these calculations based on the AY tank geometry and operating conditions. Table 7-1 shows the input data to the spreadsheet (in light blue) and the calculated force components (in tan) plus the total axial force with and without the seismic axial force. Note that the thermal force during heatup is used to calculate the maximum operating force, but the steady state force is used when combining with the seismic load. This is to recognize the extremely low probability that the seismic force and the maximum transient thermal force would both occur at the same time. Table 7-1 also compares the total unfactored axial force with the limit value of the axial force. The hydrostatic force for the specified waste height is included in this comparison. Table 7-2 shows that the vacuum limits for three different axial forces (zero, total maximum operating force, and total steady state operating + seismic force) are used to calculate unfactored vacuum limits to evaluate the tank for local and global buckling. The hydrostatic force component for each increasing waste height is used in these calculations. Table 7-3 shows how these vacuum limits are reduced by the appropriate safety factors. The governing allowable vacuum limit listed in Table 7-3 is the minimum value of all the global and local buckling evaluations. This value assumes that the Service Level A&B safety factors apply to the limit vacuum load. However, justification for classifying the vacuum load as a Service Level C load has been provided in Section 6.4.3. Therefore, a second governing vacuum load is listed that considers the limit vacuum as a Service Level C load. The vacuum limit calculated based on Service Level C safety factors is used for comparison with the existing vacuum limits for the double shell tanks (see the last line of Table 7-3).

The spreadsheet contains individual worksheets for evaluating each of the DST primary tanks. Table 7-4 summarizes the allowable vacuum calculations that are based on the current operating limits for waste temperature, waste height, and waste specific gravity. A corrosion allowance of 0.060 inch was assumed in these calculations. Table 7-4 shows that the calculated allowable vacuum limits are greater than the current vacuum limits for all of the tanks except the AP tanks. The current AP vacuum allowable is 12-inch w.g. compared to the calculated allowable of 10.53-inch w.g. This limit vacuum is based on global buckling assuming a minimum waste height of 12 inches. The calculations show that although the AP tank is slightly thicker in the upper tank wall, this is not sufficient to double the vacuum limit

compared to the AY tank. The unfactored limit vacuum for the AY tank with 6 inches of waste is 18.98-inch w.g. compared to 21.07-inch w.g. for the AP tank with 12 inches of waste. Both tanks have a very large R/t ratio, which governs the vacuum limit for buckling.

Table 7-1. Calculation of Axial Applied Force for the AY Primary Tank

Allowable Vacuum for the AY Primary Tank					
Summation of Applied Axial Tank Force Components					
					Axial Force
					Component
		Temp, F	Waste Ht, in.	Time, yrs	kip/inch
History Effect					
	AY/AZ History	250	370	60	-0.213
		Temp	Waste Ht	SpG	
Current Operation					
		350	370	1.77	
Yield Strength at Temp, ksi =					
		27.85			
Corrosion Allowance, inches =					
		0.060			
Hydrostatic Axial Tension at operating waste height					
			SpG factor =	1.042944	0.173
(Hydrostatic tension is added later in the lim. vac. v.s. waste height calc)					
Max Operating Differential Thermal Exp. =					
			a(T) =	-8.099E-04	-0.507
			b(T) =	-2.073E-01	
Steady State Differential Thermal Exp. =					
			a(T) =	-6.346E-04	-0.451
			b(T) =	-2.166E-01	
(Combine with Seismic)					
Gravity =					
					-0.135
Surface Loads =					
					-0.010
Max. Seismic Axial Force =					
					-0.430
				Operating Force (Service Levels A, B, and C)	Operating + Seismic Force (Service Level
Total Axial Force in Empty Tank with 0.060 inch Corrosion				-0.865	-1.240
Corrosion Allowance, inches =		0.060	Corrosion Factor =	1.005	1.005
Total Axial Force - empty tank, kip/inch				-0.870	-1.246
Total Axial Force at Specified Waste Height, kip/inch				-0.696	-1.073
Calculate Axial Force Limit in Primary Tank Wall					
t_{min} =	0.315			F_φ(max) =	-1.308

Table 7-2. Calculation of Unfactored Vacuum Limit for the AY Primary Tank

Calculate the Vacuum limit based on the applied axial force above					
SpG =	1.77	h(SpG) =	1.00439424		
Corrosion Allow=	0.060	g(t) =	0.999705226		
t(3/8) =	0.315	h(SpG) * g(t)	1.004098171		
			Axial force for	Axial force for	Axial force for
			Global Buckling	Local Buckling	Local Buckling
			(Service Levels	(Service Levels	(Service Level D
			A, B, and C)	A, B, and C)	Oper + Seismic
Equiv.Axl Stress, t=3/8"	psi		0	-2761	-3956
		ForceFactor=>	1.00	0.80	0.64
		SpGFactor=>	1.042944	F(kip/in)	F(kip/in)
		Hydrostatic	0	-0.87	-1.25
	Waste Ht.	Force	Limit Vacuum	Limit Vacuum	Limit Vacuum
	inches	(kip/inch)	inch w.g.	inch w.g.	inch w.g.
1st equation	6	-0.001	18.98	15.10	12.12
	12	0.001	19.01	15.14	12.15
	25	0.005	19.06	15.21	12.22
	50	0.012	19.10	15.29	12.31
	75	0.021	19.14	15.39	12.41
	100	0.030	19.28	15.56	12.58
	144	0.047	20.03	16.29	13.23
	200	0.073	22.58	18.57	15.18
	250	0.099	27.15	22.56	18.57
	300	0.128	34.63	29.12	24.12
2nd equation	300	0.128	34.63	29.12	24.12
	370	0.174	62.41	53.40	44.70
	422	0.211	83.05	72.03	60.78
	460	0.240	98.13	85.97	72.99

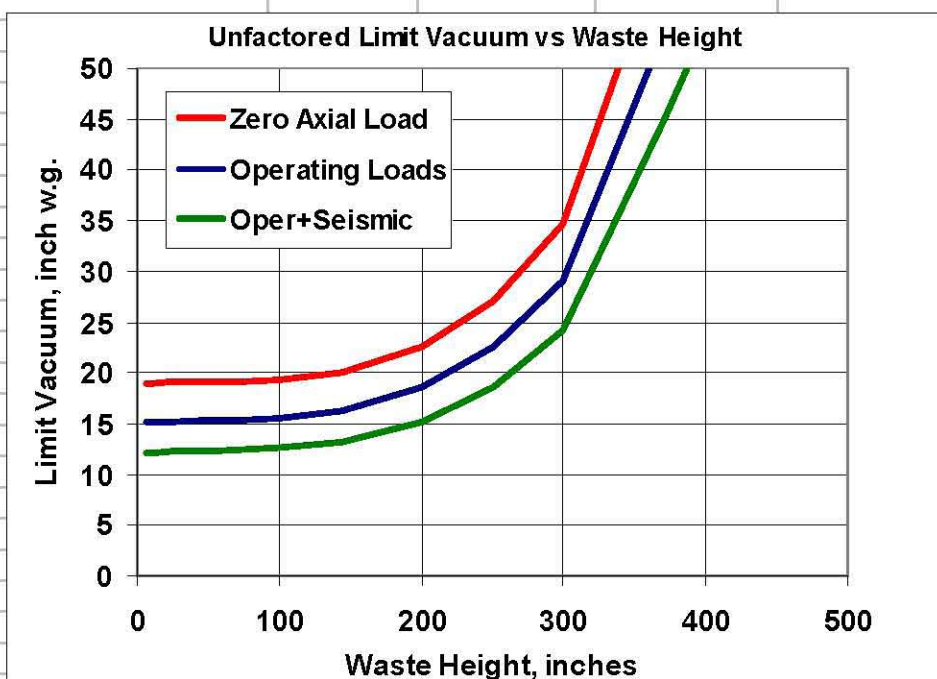


Table 7-3. Evaluation of the Allowable Vacuum Limit for the AY Tank Based on the ASME Section III Service Level Safety Factors

Calculate Allowable Vacuum with ASME Section III Service Level Safety Factors				
		Global Buckling (Service Levels A, B, and C)	Local Buckling (Service Levels A, B, and C)	Local Buckling Service Level D Oper + Seismic
Unfactored Limit Vacuum at 6 inch waste		18.98	15.10	12.12
	Safety Factor	Unfactored Vacuum	Allowable Vacuum	
Local Buckling				
Service Level A&B	2.00	15.10	7.55	
Service Level C	1.67	15.10	9.04	
Service Level D	1.34	12.12	9.04	
Global Buckling				
Service Level A&B	2.40	18.98	7.91	
Service Level C	2.00	18.98	9.49	
Governing Allowable Vacuum			7.55	inch w.g.
Governing when vacuum = Level C load			9.04	inch w.g.

The spreadsheet calculations were also performed for corrosion allowances ranging from 0.000 to 0.120 inch. Table 7-5 summarizes the calculated vacuum limits for these conditions, assuming that the limiting vacuum load is classified as a Service Level C Load. The upper half of Table 7-5 shows the results for the current temperature limits (350°F for all tanks except SY and AP). Scanning down the vacuum limits for all the tanks except AP shows that the vacuum limit first increases with increasing corrosion and then decreases for the highest corrosion allowances of 0.100, 0.110, and 0.120 inch. For each of these tanks the limit on local buckling governs and two competing wall thickness effects are at play. For a constant axial load the vacuum limit decreases with decreasing wall thickness; however, the axial load in the tank wall is also decreasing because the axial stiffness of the tank wall is lower for the thinner wall. The calculated vacuum limits for the AY, AZ, SY, AW, and AN tanks are above the current vacuum limit of 6 inch w.g. for all the cases. In comparison, the vacuum limits for the AP tank steadily decrease with decreasing wall thickness, because the global buckling criteria gives the limiting case (i.e., the axial force is not considered in the global buckling criteria). The calculated vacuum limit for the AP tank is above the current 12 inch w.g. limit for corrosion allowances of 0.000 to 0.025 inches. For corrosion greater than 0.025 inch, the calculated allowable vacuum is less than the current 12-inch w.g. limit.

Table 7-4. Summary of the DST Primary Tank Buckling Evaluations for the Specified Maximum Operating Conditions (corrosion allowance is 0.060 inches)

	DST Primary Tanks					
	AY	AZ	SY	AW	AN	AP
Approx. Operating History						
Temp, F	250	250	150	150	150	120
Hwaste, inch	370	370	422	422	422	422
Operating Limits						
Temp, F	350	350	250	350	350	210
Hwaste, inch	370	370	422	422	422	422
SpG	1.77	1.77	1.70	1.70	1.70	2.00
Corrosion Allowance, inch	0.060	0.060	0.060	0.060	0.060	0.060
Yield at Temp, ksi	27.85	27.85	31.45	39	39	39.7
Calculated Axial Forces						
Operating Axial Force, kip/inch	-0.696	-0.696	-0.413	-0.590	-0.590	-0.349
Oper+Seismic Force, kip/inch	-1.073	-1.073	-0.784	-0.958	-0.958	-0.875
Axial Force Limit, kip/inch	-1.308	-1.308	-1.477	-1.719	-1.719	-2.842
Calculated Allowable Vacuum Limits, inches w.g.						
Local Buckling						
Service Level A&B	7.55	7.55	8.32	7.78	7.78	9.70
Service Level C	9.04	9.04	9.96	9.32	9.32	11.62
Service Level D	9.04	9.04	10.60	9.56	9.56	13.48
Global Buckling						
Service Level A&B	7.91	7.91	7.88	7.88	7.88	8.78
Service Level C	9.49	9.49	9.45	9.45	9.45	10.53
Governing						
Allowable Vacuum, inch w.g.	7.55	7.55	7.88	7.78	7.78	8.78
Governing Allowable when vacuum = Level C load						
	9.04	9.04	9.45	9.32	9.32	10.53
Current Vacuum Limit, inches w.g.						
	6	6	6	6	6	12

Table 7-5. Summary of DST Primary Tank Buckling Evaluations for a Range of Corrosion Allowances and Operating Conditions

	Buckling Evaluation of the DST Primary Tanks					
	AY	AZ	SY	AW	AN	AP
Approx. Operating History						
Temp, F	250	250	150	150	150	120
Hwaste, Inch	370	370	422	422	422	422
Maximum Specified Operating Conditions						
Temp, F	350	350	250	350	350	210
Hwaste, Inch	370	370	422	422	422	422
SpG	1.77	1.77	1.70	1.70	1.70	2.00
Yield at Temp, ksi	27.85	27.85	31.45	39	39	39.7
Corrosion Allowance, Inch	0.000					
Level C Vacuum Limit, Inch w.g.	8.86	8.86	11.77	9.85	9.85	13.45
Corrosion Allowance, Inch	0.010					
Level C Vacuum Limit, Inch w.g.	9.04	9.04	11.70	9.94	9.94	12.95
Corrosion Allowance, Inch	0.025					
Level C Vacuum Limit, Inch w.g.	9.20	9.20	11.13	9.98	9.98	12.20
Corrosion Allowance, Inch	0.060					
Level C Vacuum Limit, Inch w.g.	9.04	9.04	9.45	9.32	9.32	10.53
Corrosion Allowance, Inch	0.100					
Level C Vacuum Limit, Inch w.g.	7.26	7.26	7.23	7.23	7.23	8.75
Corrosion Allowance, Inch	0.110					
Level C Vacuum Limit, Inch w.g.	6.65	6.65	6.63	6.63	6.63	8.32
Corrosion Allowance, Inch	0.120					
Level C Vacuum Limit, Inch w.g.	6.03	6.03	6.00	6.00	6.00	7.90
Maximum Expected Future Operating Conditions						
Temp, F	250	250	250	250	250	210
Hwaste, Inch	370	370	422	422	422	422
SpG	2.00	2.00	1.70	1.70	1.70	2.00
Yield at Temp, ksi	27.85	27.85	31.45	39.00	39.00	39.70
Corrosion Allowance, Inch	0.000					
Level C Vacuum Limit, Inch w.g.	10.69	10.69	11.77	11.77	11.77	13.45
Corrosion Allowance, Inch	0.010					
Level C Vacuum Limit, Inch w.g.	10.71	10.71	11.70	11.70	11.70	12.95
Corrosion Allowance, Inch	0.025					
Level C Vacuum Limit, Inch w.g.	10.65	10.65	11.13	11.13	11.13	12.20
Corrosion Allowance, Inch	0.060					
Level C Vacuum Limit, Inch w.g.	9.49	9.49	9.45	9.45	9.45	10.53
Corrosion Allowance, Inch	0.100					
Level C Vacuum Limit, Inch w.g.	7.26	7.26	7.23	7.23	7.23	8.75
Corrosion Allowance, Inch	0.110					
Level C Vacuum Limit, Inch w.g.	6.65	6.65	6.63	6.63	6.63	8.32
Corrosion Allowance, Inch	0.120					
Level C Vacuum Limit, Inch w.g.	6.03	6.03	6.00	6.00	6.00	7.90
Current Vacuum Limit, inches w.g.	6	6	6	6	6	12

However, limiting general corrosion in the AP tank evaluation to 0.025 inch over the remaining life of the tank is reasonable because a recent inspection has shown that the measured wall thickness of the AP tanks is generally greater than the nominal design thickness (Jensen 2005). Similar work measuring the wall thicknesses of all the other double-shell tanks has shown that little or no general wall thinning has occurred throughout the years of operation. For example, only three locations of very localized pitting corrosion (0.154 inch maximum depth over an area of 0.5 inch²) were found during the wall thickness assessment of tank AY-101 (Jensen 2003). In addition, the future operating temperature of the tanks is expected to be much lower than the current 350°F limit. Tests conducted on an aging waste tank (AZ-101) showed that the ventilation system maintained an average supernatant temperature of 190°F for a heat load of 4.7 mBTU/hr in the tank (Hoover 1990). This is about three times higher than the expected heat load in the future, based on extended operation of a pair of 300-HP mixer pumps in a single DST. The calculated heat load for the pair of mixer pumps is estimated to be 1.66 mBTU/hr (Keller 1997). The heat input from the tank radionuclide content in the future will be negligible compared to the mixer pump energy. Therefore, the waste temperature is not expected to exceed 200°F during future operations.

Other buckling cases were evaluated in Table 7-5 where the waste temperature limit for the AY, AZ, AW, and AN tanks was reduced to 250°F and the corrosion allowance was limited to 0.025 inch. The second half of Table 7-5 shows that the calculated allowable vacuums for these more reasonable operating conditions are greater than those for the more extreme combinations of design corrosion allowance and temperature.

Two additional cases are listed in Table 7-5 where the corrosion allowance was increased to the point where the calculated vacuum limit was nearly equal to the vacuum limit of 6.0 inch w.g. Table 7-5 estimates that the maximum allowable corrosion for the AY, AZ, SY, AW, and AN tanks is 0.120 inch. These calculated corrosion limits are the same for both the current waste temperature limit (350°F) and the estimated maximum future waste temperature (250°F) because global buckling governs and the difference in axial compressive stress is not considered in the calculation. Therefore, the minimum wall thickness for buckling in these tanks is estimated to be 0.255 inch in the thinnest upper section of the primary tank wall.

The spreadsheet described in this section provides a convenient tool for quickly calculating the applied loads, the vacuum and axial load limits, and the code-based allowable vacuum loads. The buckling evaluation method contained in this work uses curve fitting to condense many detailed analyses into a quick evaluation tool. As such, it includes necessary conservatism in the influence functions to ensure that the applied loads are not under-predicted or that the unfactored vacuum limit is not over-predicted for the range of input parameters that define the tanks. In addition, the ASME stiffness reduction method used to calculate the limiting vacuum and the axial loads is also judged to be conservative. The finite element results show that the unscaled tank deformations are barely visible on the tank geometry (see Figures 3-9 and 3-10) at the ASME limits for vacuum and axial loads. The models also predict that stable deformation will occur beyond these limits. Therefore, the buckling evaluation tool provides a conservative evaluation of the DST primary tanks. In cases where the calculated allowable vacuum is predicted to be below the current vacuum limit, then additional, more detailed analysis would be required to qualify the tank for the higher vacuum limit.

Based on the analysis contained in this report, the current limits on the maximum vacuum level of 6-inch w.g. for the AY, AZ, SY, AN, and AW tanks and 12-inch w.g. for the AP tanks are acceptable given the current lack of corrosion in the tanks and the expectation that the maximum waste temperature

will not exceed 250°F. These limits are predicated on maintaining the minimum allowable waste level at 6 inches for the AY, AZ, SY, AN, and AW tanks and 12 inches for the AP tanks to preclude bottom uplift from occurring.

7.2 Plastic Buckling

Since the ASME Code, Section III does not address the plastic elephant-foot mode of buckling, the DST structural acceptance criteria (Day et al. 1995) recommends using the compressive stress limit defined in the TSEP guidelines (Bandyopadhyay et al. 1995):

$$\sigma_{be} = \frac{0.6E_t}{R/t_{tw}} \left[1 - \left(\frac{p_{mx}R}{S_y t_{tw}} \right)^2 \right] \left[1 - \frac{1}{1.12 + k^{1.5}} \right] \left[\frac{k + (S_y/36)}{k + 1} \right] \quad (7.1)$$

where: $k = R/(400t_{tw})$

R = Primary tank mean radius

t_{tw} = Nominal tank wall thickness minus the corrosion allowance at the location of the cylindrical wall of interest.

S_y = Yield strength (ksi) of the material at the design temperature.

E_y = Elastic modulus of the primary tank material at the design temperature.

p_{mx} = Maximum net internal radial pressure coincident with the compressive stress at the location of the cylindrical wall of interest.

Under seismic loading

$$p_{mx} = p_{st} + p_h + 0.4p_v \quad (7.2)$$

where: p_{st} = Total static pressure equal to the sum of the vapor pressure and the hydrostatic pressure for the liquid waste at the location of interest.

p_h = Hydrodynamic pressure due to lateral seismic motion at the location of interest.

p_v = Hydrodynamic pressure due to vertical seismic motion at the location of interest.

Once σ_{be} is determined, the axial compressive membrane stress allowable can be calculated as:

$$\sigma_a = \frac{\sigma_{be}}{\text{Factor of Safety}} \quad (7.3)$$

Where the factors of safety are:

Service Level	Factor of Safety
A	2
B	2
C	5/3
D	4/3

Plastic elephant-foot buckling can only develop near the lower knuckle of the tank where large hoop stresses occur and hoop expansion is constrained by the base plate of the tank. Therefore, the hoop and

axial stresses near the base of the tank should be used in the elephant-foot buckling evaluation. The distributions of hoop stress from the combined seismic and deadweight analyses by Carpenter et al. (2006) are plotted in Figure 7-1. A local maximum hoop stress occurs at approximately 48 inches above the tank floor (22,889 psi). This occurs in the 0.75-inch-thick wall section about 2 feet above the tangent point between the lower knuckle and the vertical tank wall.

Equation 7-1 was recast using the maximum hoop stress directly

$$\sigma_{be} = \frac{0.6E_t}{R/t_{tw}} \left[1 - \left(\frac{\sigma_{hoop,max}}{S_y} \right)^2 \right] \left[1 - \frac{1}{1.12 + k^{1.5}} \right] \left[\frac{k + (S_y/36)}{k + 1} \right] \quad (7.4)$$

Table 7-6 summarizes the plastic buckling evaluation of the different double-shell tank designs. The applied axial compressive stress in the tank wall was conservatively assumed to be the maximum reaction force that can be supported by the primary tank. The load deflection curve in Figure 3-11 shows that the maximum reaction force for the uncorroded AY primary tank is 0.95 kip/inch of circumference. Similarly, Figure 3-13 shows that the maximum reaction force is 1.7 kip/inch for the uncorroded AP tank. The right-most column in Table 7-6 gives the demand/capacity ratio as the maximum applied axial compressive stress divided by the maximum axial stress at the onset of plastic-buckling. Table 7-6 shows that the maximum demand/capacity ratio of 0.34 occurs for the AY/AZ tanks. This means that the maximum axial reaction load that can be exerted by the primary tank is only 34% of the axial load required to initiate plastic buckling. Therefore, plastic buckling of the DST primary tanks is not a credible failure mode for the seismic loads considered here.

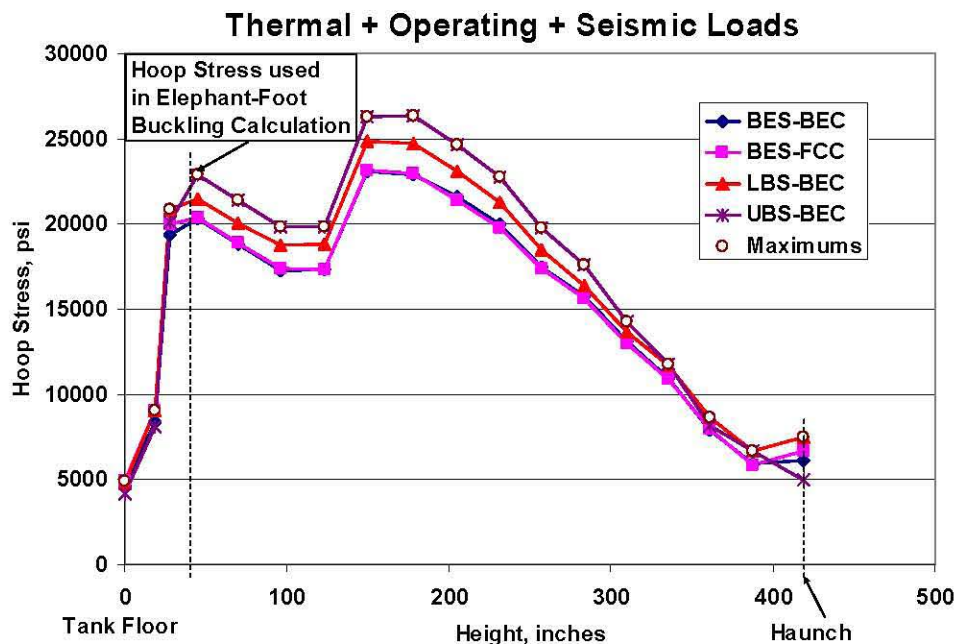


Figure 7-1. The Axial Distribution of Hoop Stress in the Primary Tank Wall Due to Thermal + Operating + Seismic Loads

Table 7-6. Reevaluation of Plastic Buckling for the DST Primary Tanks

AY / AZ Tanks									
Tank Radius	450	inch	Yield Strength		27850	psi			
Waste Height	370	inch	Corrosion Allowance		0.06	inch			
SpG	1.77		Max. Axial Force		0.95	kip/inch			
Temperature	350	F	Max. Seismic Hoop S		22889	psi			
Elastic Mod at Temp	2.85E+07	psi							
							Service		
							Level D		
							Safety	Smx =	
			Max.				Factor =	Max.	
		Nominal	Corroded	Seismic			1.33	Axial	
		Thickness	Thickness	Shoop	k =	σ_{be}	σ_a	Stress	Ratio
ELEM	Height, in.	Inch	Inch	psi	R/(400*t)	psi	psi	psi	Smx/ σ_a
1262	48.38	0.750	0.69	22889	1.63	5348	4011	1377	0.34
								Maximum Ratio, Smx/ σ_a =	0.34
AN / AW Tanks									
Tank Radius	450	inch	Yield Strength		39000	psi			
Waste Height	422	inch	Corrosion Allowance		0.06	inch			
SpG	1.70		Max. Axial Force		0.95	kip/inch			
Temperature	350	F	Max. Seismic Hoop S		22889	psi			
Elastic Mod at Temp	2.85E+07	psi							
							Service		
							Level D		
							Safety	Smx =	
			Max.				Factor =	Max.	
		Nominal	Corroded	Seismic			1.33	Axial	
		Thickness	Thickness	Shoop	k =	σ_{be}	σ_a	Stress	Ratio
ELEM	Height, in.	Inch	Inch	psi	R/(400*t)	psi	psi	psi	Smx/ σ_a
1262	48.38	0.750	0.69	22889	1.63	12195	9146	1377	0.15
								Maximum Ratio, Smx/ σ_a =	0.15
SY Tanks									
Tank Radius	450	inch	Yield Strength		30500	psi			
Waste Height	422	inch	Corrosion Allowance		0.060	inch			
SpG	1.70		Max. Axial Force		0.95	kip/inch			
Temperature	250	F	Max. Seismic Hoop S		22889	psi			
Elastic Mod at Temp	2.85E+07	psi							
							Service		
							Level D		
							Safety	Smx =	
			Max.				Factor =	Max.	
		Nominal	Corroded	Seismic			1.33	Axial	
		Thickness	Thickness	Shoop	k =	σ_{be}	σ_a	Stress	Ratio
ELEM	Height, in.	Inch	Inch	psi	R/(400*t)	psi	psi	psi	Smx/ σ_a
1262	48.38	0.750	0.69	22889	1.63	7419	5564	1377	0.25
								Maximum Ratio, Smx/ σ_a =	0.25
AP Tanks									
Tank Radius	450	inch	Yield Strength		39700	psi			
Waste Height	422	inch	Corrosion Allowance		0.06	inch			
SpG	1.70		Max. Axial Force		1.7	kip/inch			
Temperature	210	F	Max. Seismic Hoop S		22889	psi			
Elastic Mod at Temp	2.85E+07	psi							
							Service		
							Level D		
							Safety	Smx =	
			Max.				Factor =	Max.	
		Nominal	Corroded	Seismic			1.33	Axial	
		Thickness	Thickness	Shoop	k =	σ_{be}	σ_a	Stress	Ratio
ELEM	Height, in.	Inch	Inch	psi	R/(400*t)	psi	psi	psi	Smx/ σ_a
1262	48.38	0.750	0.69	22889	1.63	12508	9381	2464	0.26
								Maximum Ratio, Smx/ σ_a =	0.26

8.0 Summary and Conclusions

This report documents a detailed buckling evaluation of the primary tanks in the Hanford double-shell waste tanks, which is part of a comprehensive structural review for the Double-Shell Tank Integrity Project. This work also provides information on tank integrity that specifically responds to concerns raised by the Office of Environment, Safety, and Health (ES&H) Oversight (EH-22) during a review of work performed on the double-shell tank farms and the operation of the aging waste facility (AWF) primary tank ventilation system.

The current buckling review focuses on the following tasks:

- Evaluate the potential for progressive J-bolt failure and the appropriateness of the safety factors that were used for evaluating local and global buckling. The analysis will specifically answer the following questions:
 - Can the EH-22 scenario develop if the vacuum is limited to -6.6-inch water gage by a relief valve?
 - What is the appropriate factor of safety required to protect against buckling if the EH-22 scenario can develop?
 - What is the appropriate factor of safety required to protect against buckling if the EH-22 scenario cannot develop?
- Develop influence functions to estimate the axial stresses in the primary tanks for all reasonable combinations of tank loads, based on detailed finite element analysis. The analysis must account for the variation in design details and operating conditions between the different DSTs. The analysis must also address the imperfection sensitivity of the primary tank to buckling.
- Perform a detailed buckling analysis to determine the maximum allowable differential pressure for each of the DST primary tanks at the current specified limits on waste temperature, height, and specific gravity.

Previous buckling evaluations of the double-shell primary tanks used the analysis method in ASME Code Case N-284-1, which is based on the buckling of a constant thickness cylindrical shell with unsupported length, L . The cylindrical shell of the DST primary tanks does not have constant wall thickness and it does not have clearly defined lines of support due to the varying wall thickness and the upper and lower knuckle geometries.

The present buckling analysis used large displacement finite element analysis to predict the limiting vacuum load for the DST primary tanks under combined axial and vacuum loads. The analysis included tank models that were specific to the geometry and thickness distributions of the AY and the AP tanks. The AY results are also representative of the AZ, SY, AW, and AN tanks because they have very similar wall thickness distributions. The current buckling evaluation method uses the well established ASME NB-3213.25 stiffness reduction method to conservatively estimate the vacuum and axial load limits on the primary tank. Comparison with N-284-1 calculations showed that PNNL's large displacement method better accounts for the effect of the wall thickness variation on the limiting vacuum and axial loads. The

finite element analysis also predicts that the tank deformations are small at the limit loads and they increase stably at loads beyond the limit loads. A large matrix of analyses was run that covers the expected range of axial forces and vacuum loads on the primary tanks. Influence functions were fit to the limit load predictions to allow calculating the limiting vacuum and axial loads for all reasonable combinations of axial load, corrosion allowance, specific gravity, and waste height.

An ANSYS thermal model was developed that is directly node-to-node compatible with the ANSYS DST structural model. Previous thermal simulations for the thermal and operating loads analysis were performed using the TEMPEST finite difference code. A laborious data mapping step was required when transferring the TEMPEST thermal results to the ANSYS structural grid. The ANSYS thermal model supports the tank buckling analysis by allowing easy prediction of tank stresses due to different combinations of thermal and operating loads. This capability was required to calculate the allowable net vacuum loads as a function of the waste height and temperature. The ANSYS thermal model includes the effects of radiation and convection in the annulus and the dome space, and the thermal solution compared very closely with the previous TEMPEST thermal results. The two temperature solutions also give very similar stresses throughout the thermal transient.

Influence functions were also developed to estimate the applied axial force in the primary tank wall, which is required for evaluating buckling of the primary tank. The sequentially coupled ANSYS thermal and structural models were used to predict the axial thermal stresses in the wall of the primary tanks for a large matrix of waste height and temperature conditions. Analyses were conducted for both the AY and AP wall thickness distributions. The axial forces for the applied load components were curve fit to allow estimating the total equivalent linear elastic axial force as the sum of the following loads:

- Differential thermal expansion,
- Gravity,
- Surface loads,
- Concrete thermal degradation and creep,
- Seismic excitation, and
- Effect of hydrostatic waste pressure on the confined axial force.

The J-bolts that anchor the primary tank dome to the adjacent concrete dome were analyzed as part of the primary tank buckling evaluation. The finite element model used to predict the tank vacuum limits was also used for the J-bolt evaluation. Three-dimensional elastic beam elements were used to model the J-bolts. A downward deflection was applied to the J-bolts to simulate the displacement controlled axial compression of the tank wall that occurs due to concrete thermal degradation and creep plus confined thermal expansion. The J-bolt shear and normal forces were evaluated throughout the application of the buckling loads.

The J-bolts were evaluated to the methods of ASME Section III, Division 2, Subsection CC-3730, which covers the design of steel liners backed by concrete and their anchorage systems. The axial and shear forces at the J-bolt anchors increase linearly as the axial force in the tank wall increases. The J-bolt forces do not change significantly with the application of increased vacuum. The finite element analysis shows that increasing the vacuum to levels that exceed the current limits by a factor of at least 1.67 will not cause progressive tensile failure of the J-bolts as was postulated by the EH-22 panel. The typical operating load condition includes axial compression in the wall of the primary tanks. Under these conditions,

the finite element analysis shows that all the J-bolts are in compression whether they are at or away from the buckling instability (wrinkle). Therefore, under typical operating conditions J-bolt pullout cannot occur as was postulated by the EH-22 panel.

The maximum J-bolt shear and axial forces are observed in the outer ring of J-bolts near the haunch for both the AY and AP primary tanks (Figure 6-25).

For the unlikely case of zero axial compression, the J-bolts are under a small amount of tension due to increasing vacuum and the Poisson's effect associated with the tensile hoop stress from the hydrostatic waste pressure. The combined shear and axial loads are less than 30% of the allowable loads for all cases considered in this review.

The more probable failure mode is shear failure of the outermost J-bolts. Table 6-3 shows that concrete failure governs in estimating the limit load on the anchors in shear. Table 6-5 shows that the only case where the shear reaction force is predicted to exceed the J-bolt load limit is for the AY tank with no corrosion at a waste temperature of 350°F. In this case, the applied load exceeds the limit load by about 6%, but it is about 29% below the estimated failure load. However, the tank waste is not expected to exceed 200°F during future operations. If the calculations are repeated for a conservative maximum future temperature of 250°F, then the demand/capacity ratio is only 0.81. Therefore, it is not expected that the combined operating and seismic loads will jeopardize the structural integrity of any of the J-bolts. Since the J-bolts are not expected to fail, then it is unlikely that the EH-22 scenario could occur.

Both elastic and plastic buckling analyses were performed for the DST primary tanks. The elastic buckling evaluation provides a method for evaluating the allowable vacuum limits for the DST primary tanks. The current method follows the previous tank buckling evaluations; however, the N-284-1 calculations were replaced with the large displacement method that was developed in the current work. The method calculates the axial force on the primary tank wall and then uses this force to calculate the unfactored limits on vacuum and axial load. The safety factors for the ASME Section III service levels are applied to calculate the allowable tank vacuum limits. Each service level has required factors of safety for local and global buckling:

	Factors of Safety	
	Local Buckling	Global Buckling
Level A = Normal operating conditions	2.0	2.4
Level B = Upset conditions	2.0	2.4
Level C = Emergency conditions	1.67	2.0
Level D = Faulted conditions	1.34	1.61

An Excel™ spreadsheet was constructed to perform the above calculations and apply the safety factors. The spreadsheet was used to evaluate each of the DST primary tanks for their current operating conditions (waste temperature, height, and SpG) and corrosion allowances of 0.000, 0.060, and 0.100 inch. Table 7-4 shows that the calculated allowable vacuum limits for the conservative baseline assumption of 0.060 inch corrosion are greater than the current vacuum limits for all of the tanks except the AP tanks. The current AP vacuum allowable is 12-inch w.g. compared to the calculated allowable of 10.53-inch w.g. This vacuum limit is based on global buckling assuming a minimum waste height of 12 inches. The calculations show that although the AP tank is slightly thicker in the upper tank wall, this is not enough to double the vacuum limit compared to the other tanks.

Additional cases were analyzed with corrosion levels from 0.000 to 0.120 inches and a more realistic maximum future waste temperature of 250°F. The calculated allowable vacuum limits for the AY, AZ, SY, AW, and AN tanks are above the current vacuum limit of 6 inch w.g. for all the cases. The allowable vacuum limit for the AP tank is above the current 12 inch w.g. limit for corrosion allowances of 0.000 to 0.025 inches. Therefore, the minimum wall thickness for buckling in the AP tanks is estimated to be 0.475 inch in the upper section of the primary tank wall.

The corrosion allowance for the AY, AZ, SY, AW, and AN tanks was also increased to identify the maximum value where the calculated vacuum limit was nearly equal to the 6 inch w.g. vacuum limit. The maximum allowable corrosion for these tanks was estimated to be 0.120 inch. These calculated corrosion limits are the same for both the current waste temperature limit (350°F) and the lower maximum future waste temperature (250°F) because global buckling governs and the difference in axial compressive stress is not considered in the global buckling calculation. Therefore, the minimum wall thickness for buckling in these tanks is estimated to be 0.255 inch in the thinnest upper section of the primary tank wall.

The spreadsheet described in this section provides a convenient tool for quickly calculating the applied loads, the vacuum and axial load limits, and the code-based allowable vacuum loads. The buckling evaluation method contained in this work uses curve fitting to condense many detailed analyses into a quick evaluation tool. As such, it includes necessary conservatism in the influence functions to ensure that the applied loads are not under-predicted or that the unfactored vacuum limit is not over-predicted for the range of input parameters that define the tanks. In addition, the ASME stiffness reduction method used to calculate the limiting vacuum and the axial loads is also judged to be conservative. The finite element results show that the unscaled tank deformations are barely visible on the tank geometry (see Figures 3-9 and 3-10) at the ASME limits for vacuum and axial loads. The models also predict that stable deformation will occur beyond these limits. Therefore, the buckling evaluation tool provides a conservative evaluation of the DST primary tanks. In cases where the calculated allowable vacuum is predicted to be below the current vacuum limit then additional, more detailed analysis would be required to qualify the tank for the higher vacuum limit.

The tank farm occurrence reports from 1990 to the present were reviewed to identify the number of times that the vacuum limits have been challenged. This summary information will be released in the next revision of RPP-11413, *Technical Basis for the Ventilation Requirements Contained in Tank Farm Operating Specifications Documents*, authored by L. Payne. No incidents were found where the primary tank differential vacuum has exceeded the 6 inch w.g. maximum. There was a report of reaching a vacuum of 4 inch w.g. in the SY tank ventilation system, but the exhaustor shut down on interlock. There was one incident in AW, but it was also limited to 4 inch w.g. or less. The incident that people remembered where a vacuum limit was exceeded was in the AN annulus system in 2005 (PER-2005-072). Note that this occurred in the annulus and not in the primary tank.

Therefore, not only are the tanks able to withstand the expected loads without buckling, there are no recorded occurrences where the maximum vacuum has been achieved. There are also safety systems and operating procedures in place to ensure that the maximum vacuum loads are not achieved in future operations.

Based on the analysis contained in this report, the current limits on the maximum vacuum level of 6 inch w.g. for the AY, AZ, SY, AN, and AW tanks and 12 inch w.g. for the AP tanks are acceptable given the current lack of corrosion in the tanks and the expectation that the maximum waste temperature will not exceed 250°F. These limits are predicated on maintaining the minimum allowable waste level at 6 inches for the AY, AZ, SY, AN, and AW tanks and 12 inches for the AP tanks to preclude bottom uplift from occurring.

9.0 References

American Society of Mechanical Engineers. 1994. *Code Case N-530, Provisions for Establishing Allowable Axial Compressive Membrane Stresses in the Cylindrical Walls of 0-15 psi Storage Tanks, Classes 2 and 3, Section III, Division 1*. ASME Boiler and Pressure Vessel Code, American Society of Mechanical Engineers, New York, New York.

American Society of Mechanical Engineers. 1992. Section III, Division 2, Subsection CC, ASME Boiler and Pressure Vessel Code, American Society of Mechanical Engineers, New York.

American Society of Mechanical Engineers. 1995. Code Case N-284-1, 1995, Metal Containment Shell Buckling Design Method, Class MC, Section III, Division 1. ASME Boiler and Pressure Vessel Code, American Society of Mechanical Engineers, New York.

American Society of Mechanical Engineers. 2004a. Section III, Division 1, Subsection NB-3200 Design by Analysis, Article 3213.25 Plastic Analysis – Collapse Load. ASME Boiler and Pressure Vessel Code, American Society of Mechanical Engineers, New York.

American Society of Mechanical Engineers. 2004b. Section III, Division 1, Subsection NB-3113 Service Conditions. ASME Boiler and Pressure Vessel Code, American Society of Mechanical Engineers, New York.

American Society of Mechanical Engineers. 2004c. Section III, Division 1, Mandatory Appendix I, Design Stress Intensity Values, Allowable Stresses, Material Properties, and Design Fatigue Curves, Table I-9.1. ASME Boiler and Pressure Vessel Code, American Society of Mechanical Engineers, New York.

Antoniak ZI and KP Recknagle. 1995. *Thermal Modeling of Tanks 241-AW-101 and 241-AN104 with the TEMPEST Code*, PNL 10683, UC-510, Pacific Northwest Laboratory, Richland, Washington.

Bandyopadhyay K, A Cornell, C Costantino, R Kennedy, C Miller, and A Veletsos. 1995. *Seismic Design and Evaluation Guidelines for the Department of Energy High Level Waste Tanks and Appurtenances*. BNL 52361. Brookhaven National Laboratory. Associated Universities, Inc., Upton, New York.

Beaver TR, JG Fadeff, and TB McCall. 1993. *Thermal Analysis for Tank 241-SY-101*. WHC-SD-WM-ER-296, Rev. 0, Westinghouse Hanford Company, Richland, Washington.

Carpenter BG, C Hendrix, and FG Abatt. 2006. *Hanford Double Shell Tank Thermal and Seismic Project - ANSYS Seismic Analysis of Hanford Double Shell Primary Tank*. RPP-RPT-28966, Rev. 0. M&D Professional Services, Richland, Washington.

CH2M HILL. 2002. Contract No. DE-AC27-99RL14047 - Final Report of Focused Review of CH2M HILL Hanford Group, Inc. (CHG) Integrated Safety Management System (ISMS). 0204443/02-QAO-051. CHG Correspondence Control, CH2M HILL Hanford Group, Inc., Richland, Washington.

Crea BA, K Sathyanarayana, and D Ogden. 2000. *Parametric Analysis of Heat Removal from High-Level Waste Tanks*. RPP-5637, Revision 0, CH2M HILL Hanford Group, Richland, Washington.

Day JP, AD Dyrness, LJ Julyk, CJ Moore, WS Peterson, MA Scott, HP Shrivastava, JS Shulman, and TN Watts. 1995. *Structural Acceptance Criteria for the Evaluation of Existing Double-Shell Waste Storage Tanks Located at the Hanford Site, Richland, Washington*. WHC-SD-WM-DGS-003. Westinghouse Hanford Company, Richland, Washington.

Hoover DA. 1990. *Functional Design Criteria for the Tank Farm Ventilation Upgrade Project W-030*. SD-600-FDC-001, Rev. 3. Westinghouse Hanford Company. Richland, Washington.

Jensen CE. 2003. *Supplement 2 to Inspection Results for Double Shell Tank 241-AY-101 FY2003*. RPP-15763. CH2M HILL Hanford Group, Inc., Richland, Washington.

Jensen CE. 2005. *Ultrasonic Inspection Results for DST 241-AP-106 FY2005*. RPP-RPT-23205. CH2M HILL Hanford Group, Inc., Richland, Washington.

Julyk LJ. 1997. *Assessment of Project W-030 Relief Valve Pressure Setting on Internal Vacuum Specification Limits for AY and AZ Tank Farm Primary Tanks*. HNF-1838. CH2M HILL Hanford Group, Inc., Richland, Washington.

Julyk LJ and HH Ziada. 2002. *Assessment of Double-Shell Tank Internal Vacuum Specification Limits on Primary Tanks*. HNF-1838, Rev. 0-A. CH2M HILL Hanford Group, Inc., Richland, Washington.

Keller C. 1997. *Functional Design Criteria for the Tank Farm Ventilation Upgrade Project W-030*. HNF-SD-600-FDC-001, Rev. 4. Numatec Hanford Company, Richland, Washington.

Ogden DM, MJ Thurgood, WE Bryan, GP Duncan, and DH Shuford. 2002. *Engineering Evaluation of Double Shell Tank Vapor Space Condensation and Annulus Relative Humidity*. RPP-12422, Rev 0, CH2M HILL Hanford Group, Inc., Richland, Washington.

Rinker MW, JE Deibler, KI Johnson, SP Pilli, CE Guzman-Leong, and OD Mullen. 2004. *Hanford Double-Shell Tank Thermal and Seismic Project – Thermal and Operating Load Analysis*. RPP-RPT-23308, Rev. 0. Pacific Northwest National Laboratory, Richland, Washington.

Rinker MW, JE Deibler, KI Johnson, and SP Pilli. 2005. *Hanford Double-Shell Tank Thermal and Seismic Project – Increased Concentrated Load Analysis*. RPP-RPT-25608, Rev. 0. Pacific Northwest National Laboratory, Richland, Washington.

Appendix A

Seismic Model Primary Tank Knuckle Stress Evaluation

Appendix A

Seismic Model Primary Tank Knuckle Stress Evaluation

The detailed ANSYS® model used for the transient, seismic analyses (referred to as the ANSYS® detailed model) of the Hanford double-shell tanks (DSTs) is limited in model refinement at the knuckle of the primary tank. The 3-D slice model used in the TOLA evaluation (to be referred to as the TOLA model) has significantly more refinement in the primary tank knuckle. The TOLA model knuckle has 8 elements and the ANSYS® detailed model knuckle that has 2 elements. The TOLA model results will be combined with the ANSYS® detailed model seismic results to perform an ASME code evaluation. In order to ensure that the seismic portion of the combined primary tank stresses are adequate, the accuracy of the lower refinement ANSYS® detailed model must be evaluated.

The objective of this evaluation is to perform a study of mesh size sensitivity in the knuckle region of the primary tank. The results will be compared between the ANSYS® detailed model, the TOLA model and a simplified axisymmetric study model under hydrostatic loading. An evaluation will then be done to determine what factor(s), if any, need to be applied the seismic only primary tank hoop and meridional stresses.

A.1 Model

The DST Primary Tank has a 12-inch radius knuckle region that joins the tank cylindrical sidewalls to the tank bottom plates (Figure A-1). The bottom of the primary tank is supported below by insulating concrete. The insulating concrete extends past the bottom tangent of the knuckle, although the knuckle will not contact the insulating concrete outside of the tangent unless significant deflection occurs.

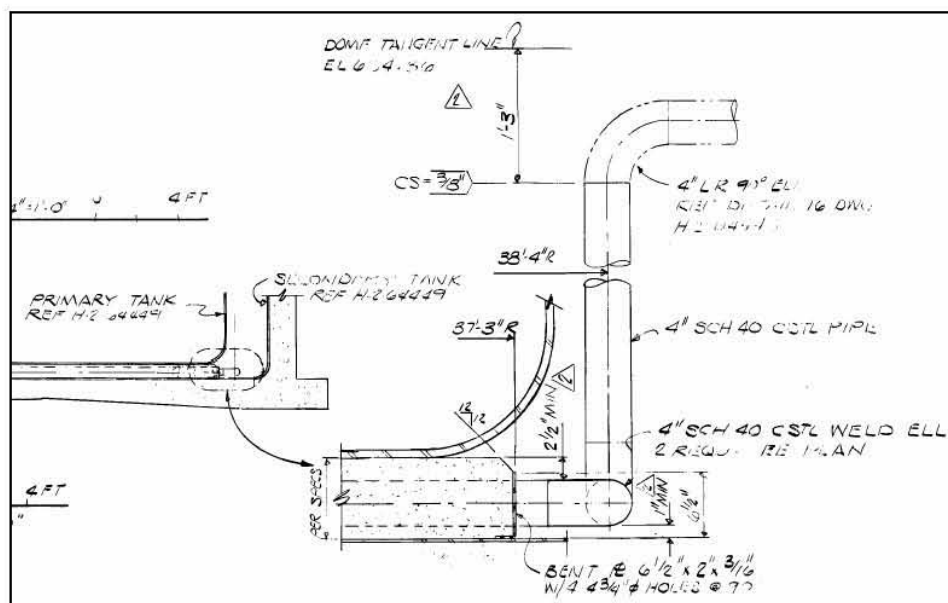


Figure A-1. Knuckle Detail from Drawing AY H-2-64307

The global ANSYS® detailed model approximates the knuckle curve using two elements as shown in Figure A-2. The TOLA model knuckle, shown in Figure A-3, uses 8 elements.

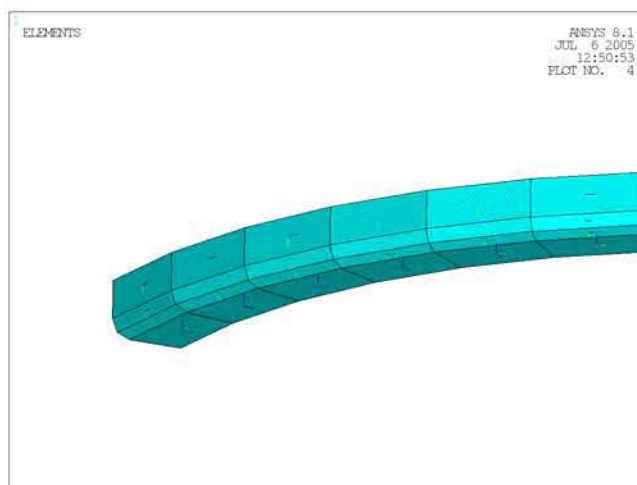


Figure A-2. Elements Used in Simplified Global Model – Detail Plot

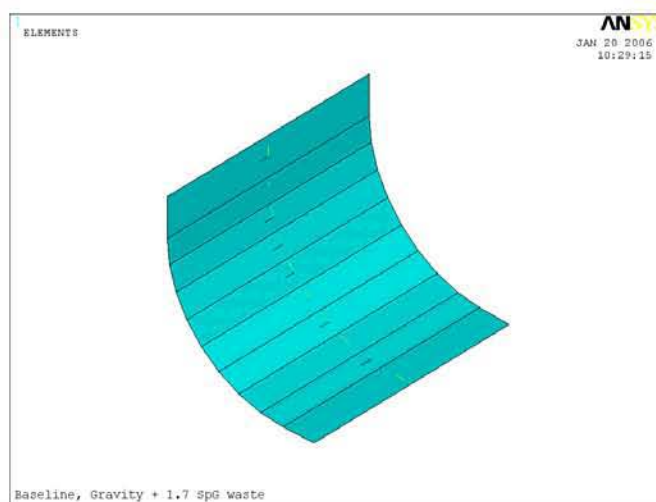


Figure A-3. Elements Used in TOLA Model – Detail Plot

The simplified axisymmetric study model includes the primary tank and a set of contact elements to simulate the interface between the primary tank and the insulating concrete. The primary tank is modeled, starting at the tangent point between the primary tank and the concrete tank, using axisymmetric shell elements, SHELL51. Duplicate nodes were created across the floor of the primary tank, and CONTAC52 elements were placed across the interface using a friction coefficient of 0.40. The duplicate nodes, representing the top surface of the insulating concrete, were then vertically constrained. The node at the tangent point is constrained horizontally and vertically representing the first j-bolt connection. Figure A-4 shows a full element plot of the simplified study model, Figure A-5 presents a detailed plot of the coarse mesh of the knuckle, and Figure A-6 presents the plot of the refined mesh.

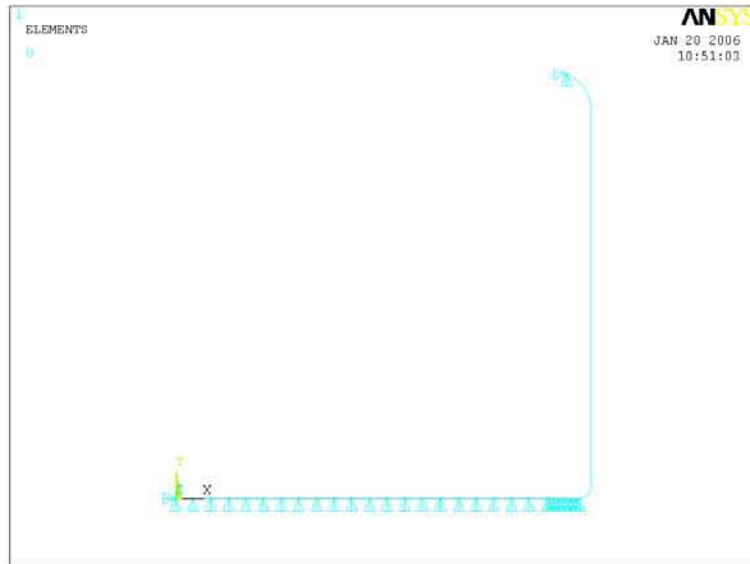


Figure A-4. Primary Tank Elements Used in Simplified Study Model

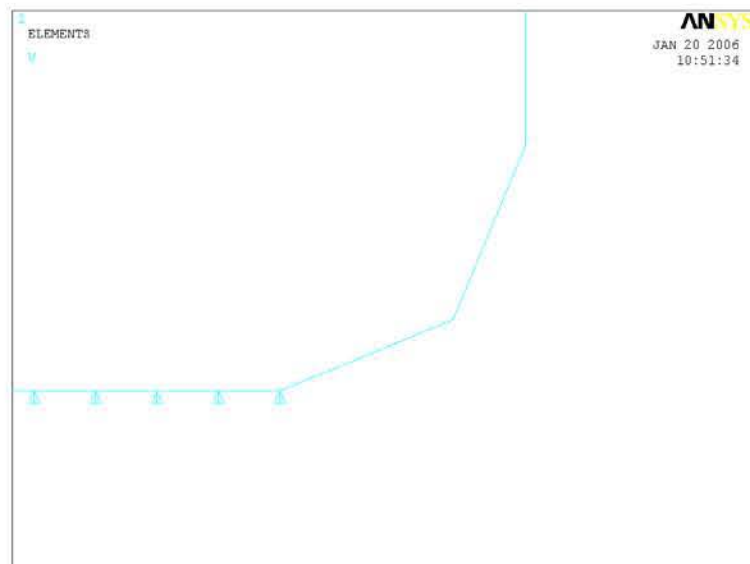


Figure A-5. Primary Tank Elements Used in Simplified Study Model - Detail Plot (coarse – 2 elements)

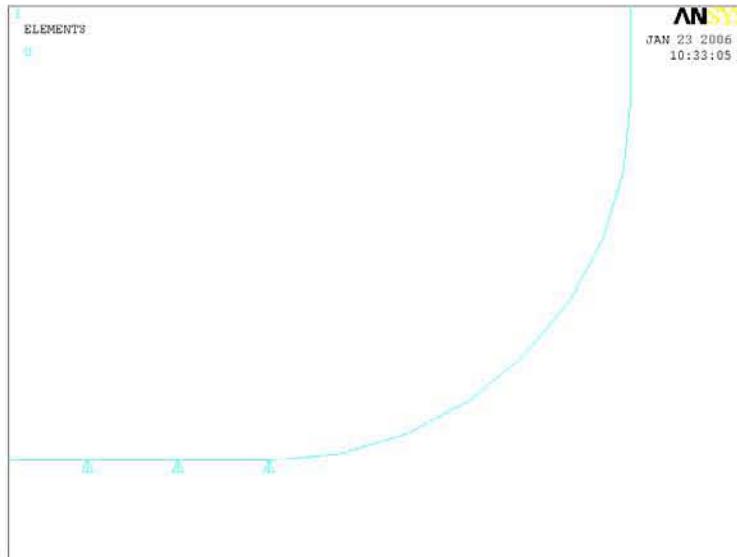


Figure A-6. Primary Tank Elements Used in Simplified Study Model – Detail Plot (refined – 8 elements)

A.2 Load Case

The TOLA model, the ANSYS® detailed model and the simplified study model were subjected to a hydrostatic load. The hydrostatic pressures were calculated based on AY tank waste depth of 422 inches and a specific gravity of 1.7. The ANSYS® detailed model results were obtained from ANSYS® Seismic Analysis of Hanford Double Shell Primary Tank (Carpenter et al. 2006) for best estimate soil and best estimate concrete. These results will be identified as AY-NL-BES-BEC Gravity Only in the results plots.

A.3 Results

The primary tank meridional and hoop stresses have been extracted and evaluated in the knuckle region. The primary tank stresses will be evaluated to verify that the simplified study model is providing similar results to the detailed TOLA model and ANSYS® detailed model when using the same mesh refinement. The results have been evaluated to determine the effect of mesh refinement on the meridional and hoop stresses. Lastly, the meridional and hoop stresses will also be evaluated to determine what factors need to be applied to the ANSYS® detailed model seismic results. Meridional and hoop stresses extracted from the simplified study model will be label SM and SH, respectively. The top, middle, and bottom shell surface from which the results are retrieved are identified by _T, _M, and _B, respectively.

A.3.1 Model Verifications

The meridional and hoop stresses for the simplified study model are compared to the TOLA model and the ANSYS® detailed model in Figures A-7 through A-12. The meridional stress comparisons show fairly good comparisons between the simplified and detailed models. The hoop stress comparisons between the models are very good. As a result of these comparisons, the simplified model is deemed to be acceptable for a mesh refinement study and providing meridional and hoop stress scaling factors.

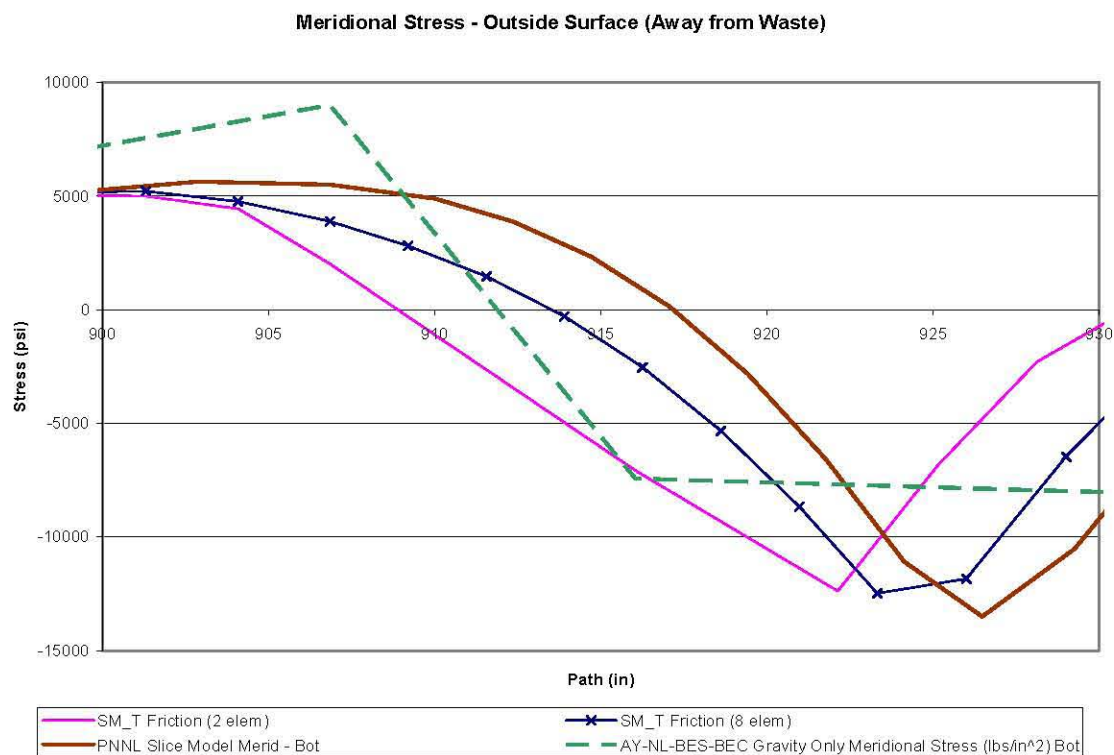


Figure A-7. Knuckle Meridional Stress – Outside Surface (Away from Waste)

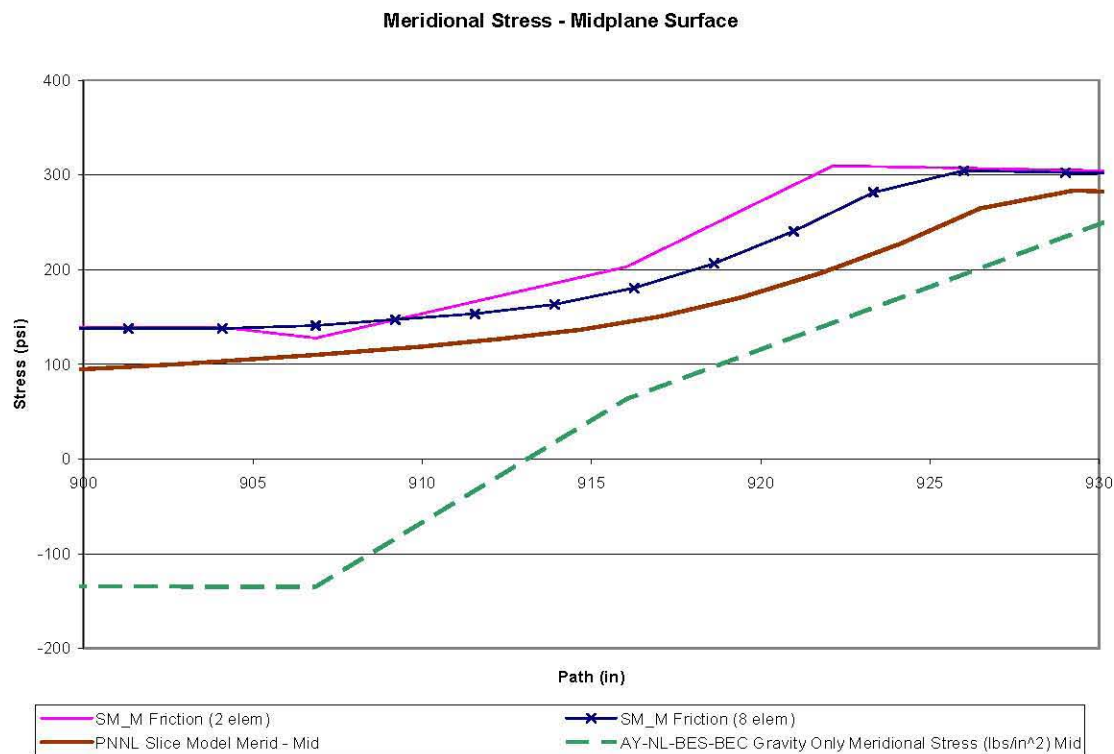


Figure A-8. Knuckle Meridional Stress – Mid-Plane Surface

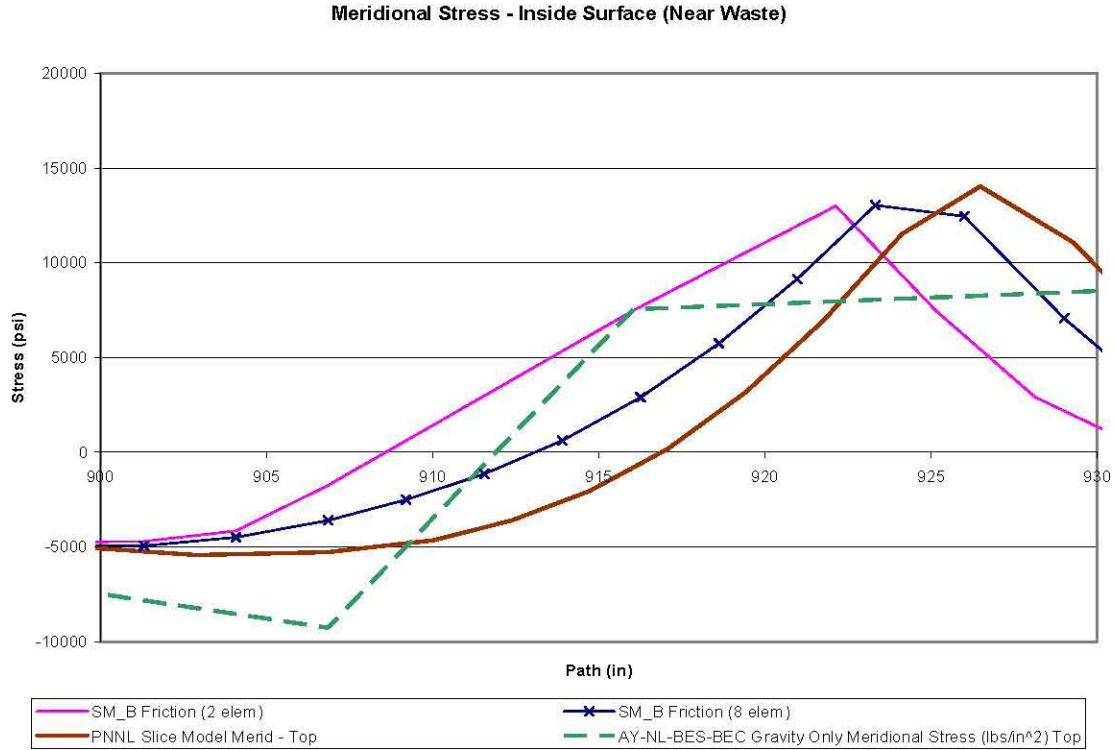


Figure A-9. Knuckle Meridional Stress – Inside Surface (Near Waste)

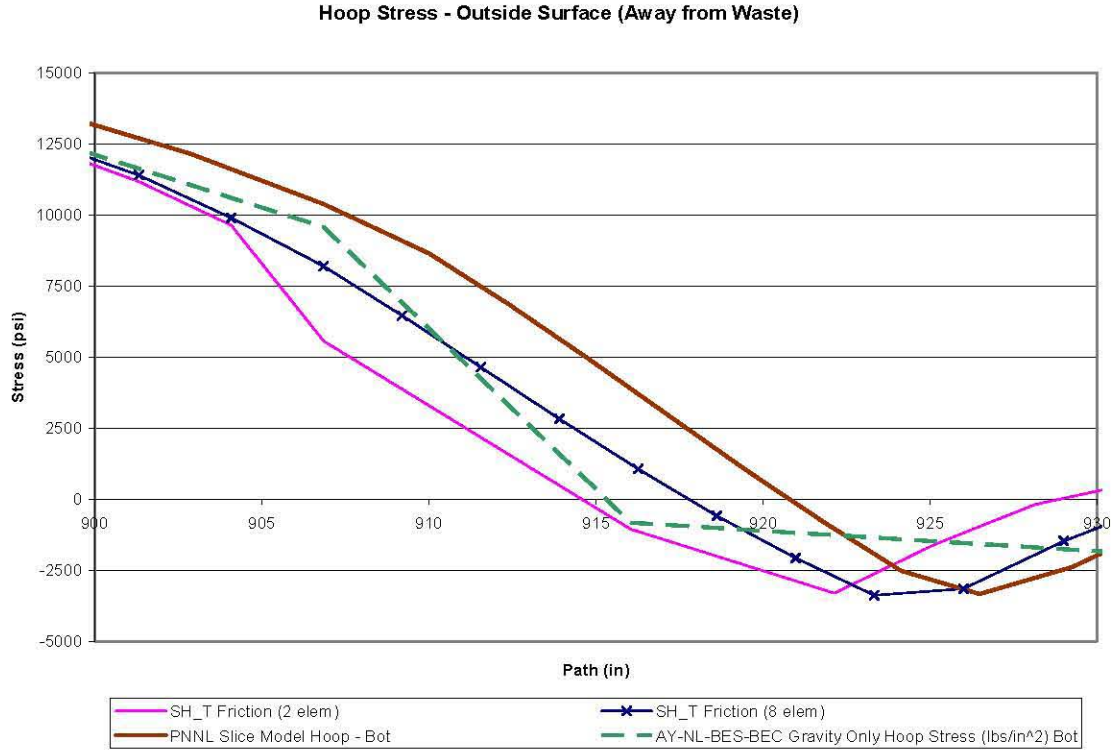


Figure A-10. Knuckle Hoop Stress – Outside Surface (Away from Waste)

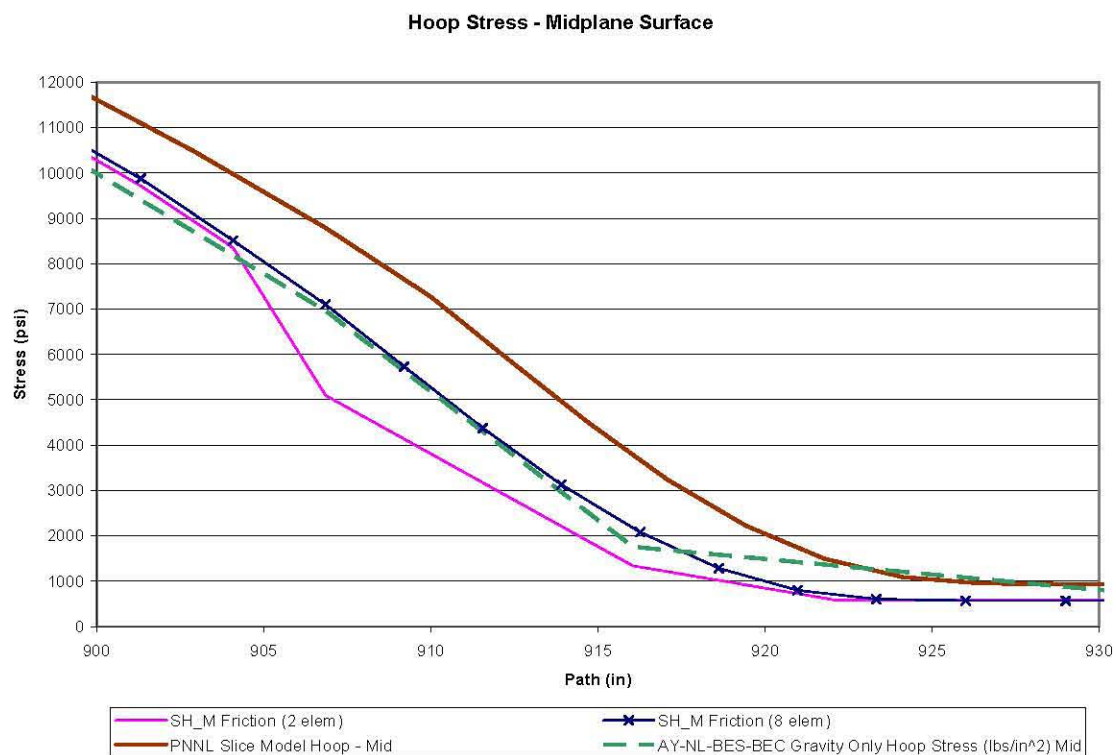


Figure A-11. Knuckle Hoop Stress – Mid-Plane Surface

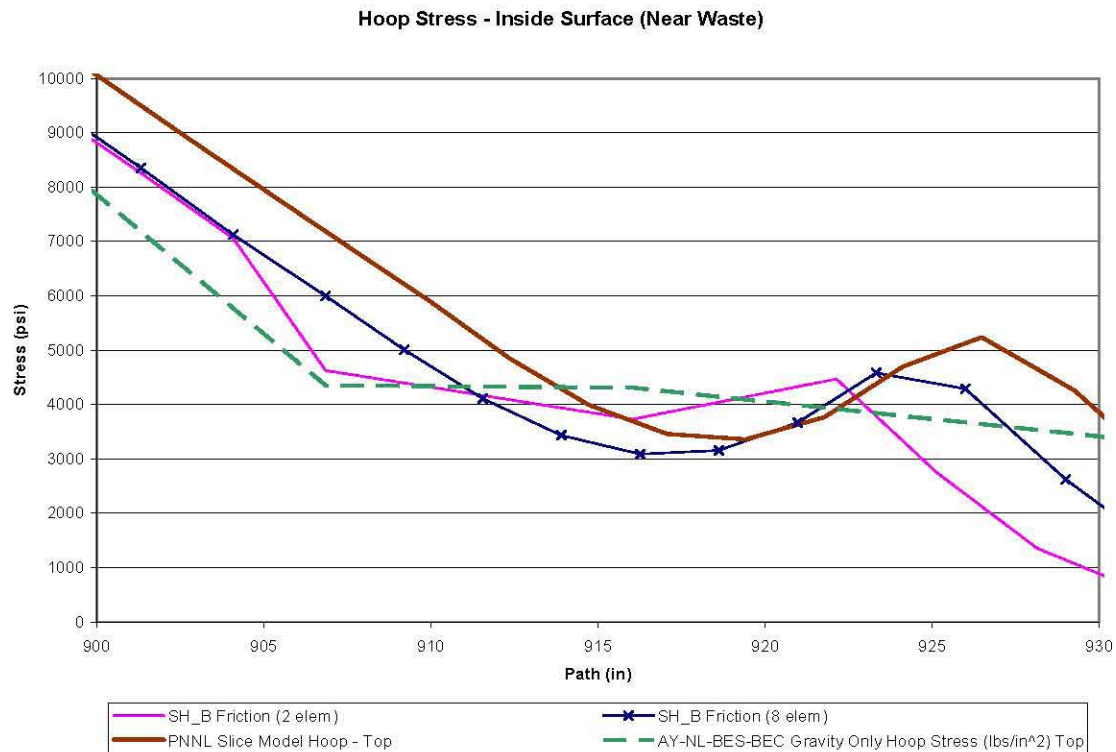


Figure A-12. Knuckle Hoop Stress – Inside Surface (Near Waste)

A.3.2 Model Mesh Refinement

The meridional and hoop stresses for the simplified study model with several mesh refinements are presented in Figures A-13 through A-18. The study model knuckle mesh refinement of 2 elements, 8 elements, and 16 elements. A mesh refinement of 2 elements represents the mesh resolution used in the ANSYS® detailed model and the refinement of 8 elements represents the TOLA model. An additional knuckle mesh refinement of 16 elements was done to verify that the 8-element refinement was adequate to accurately represent the meridional and hoop stresses present in the primary tank. As a result of this study, the mesh refinement of 8 elements in the primary tank knuckle is considered adequate.

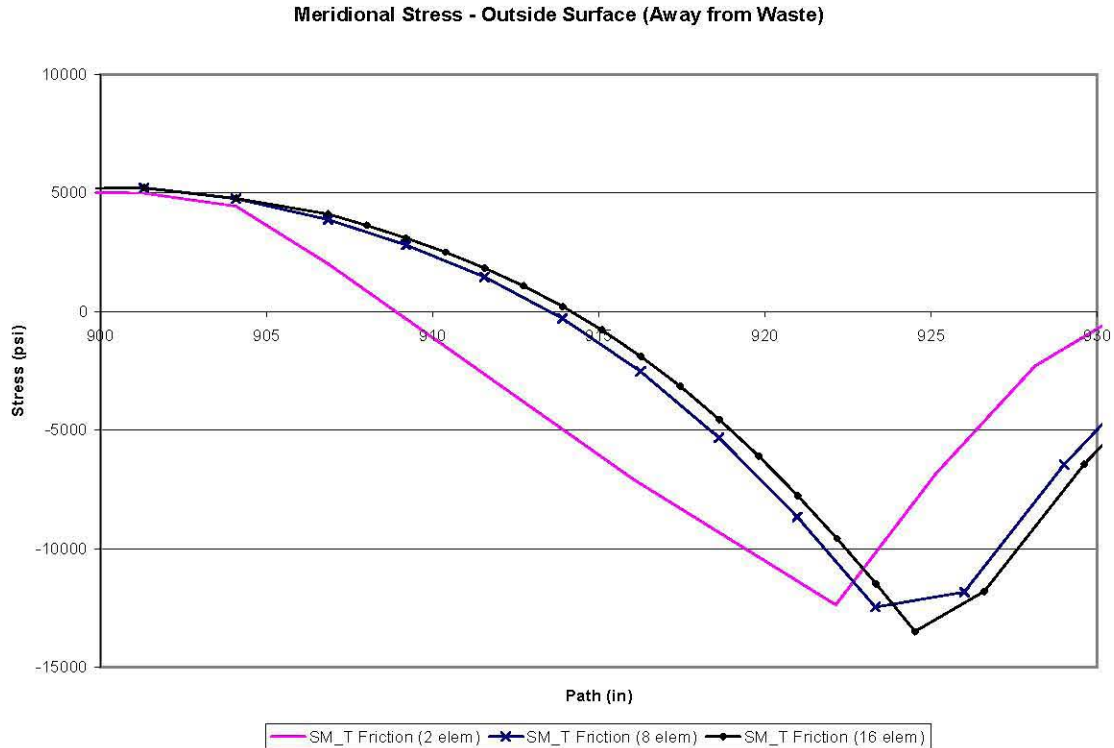


Figure A-13. Knuckle Meridional Stress Refined Mesh – Outside Surface (Away from Waste)

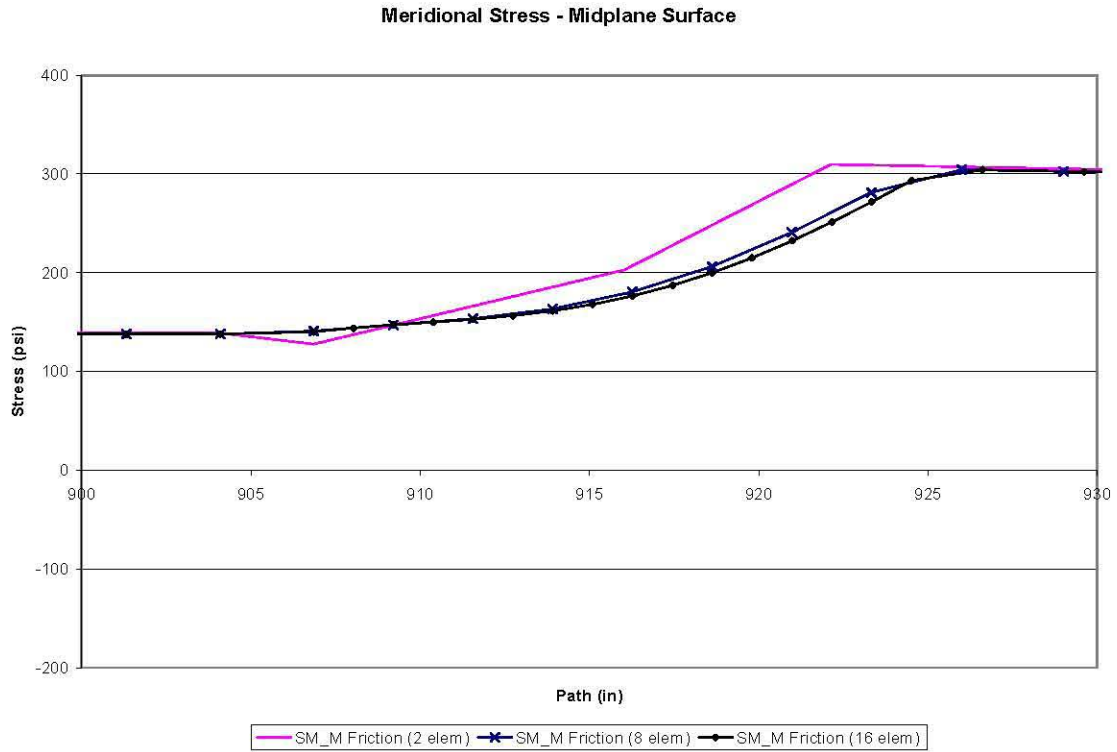


Figure A-14. Knuckle Meridional Stress Refined Mesh – Mid-Plane Surface

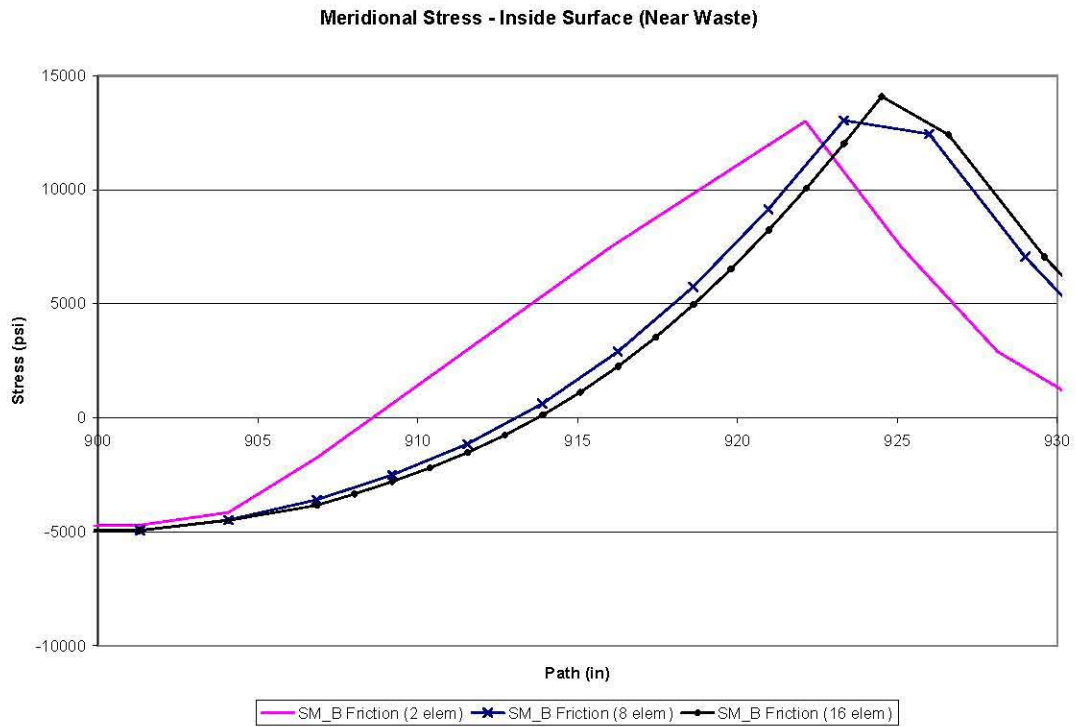


Figure A-15. Knuckle Meridional Stress Refined Mesh – Inside Surface (Near Waste)

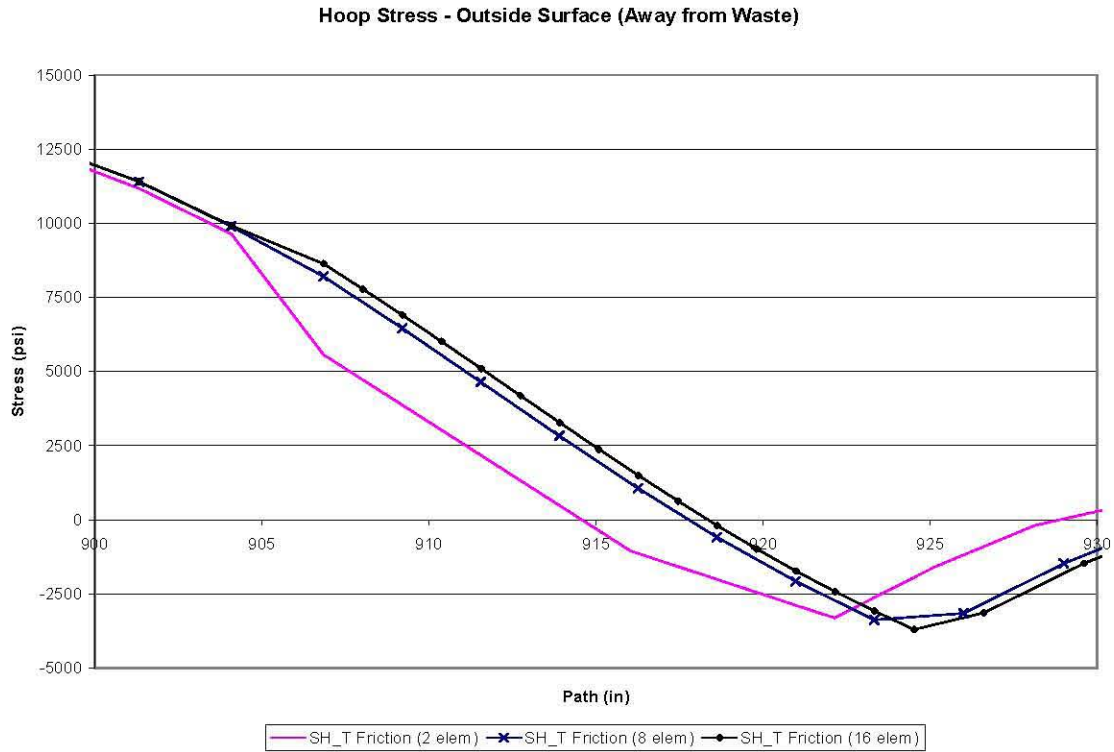


Figure A-16. Knuckle Hoop Stress Refined Mesh – Outside Surface (Away from Waste)

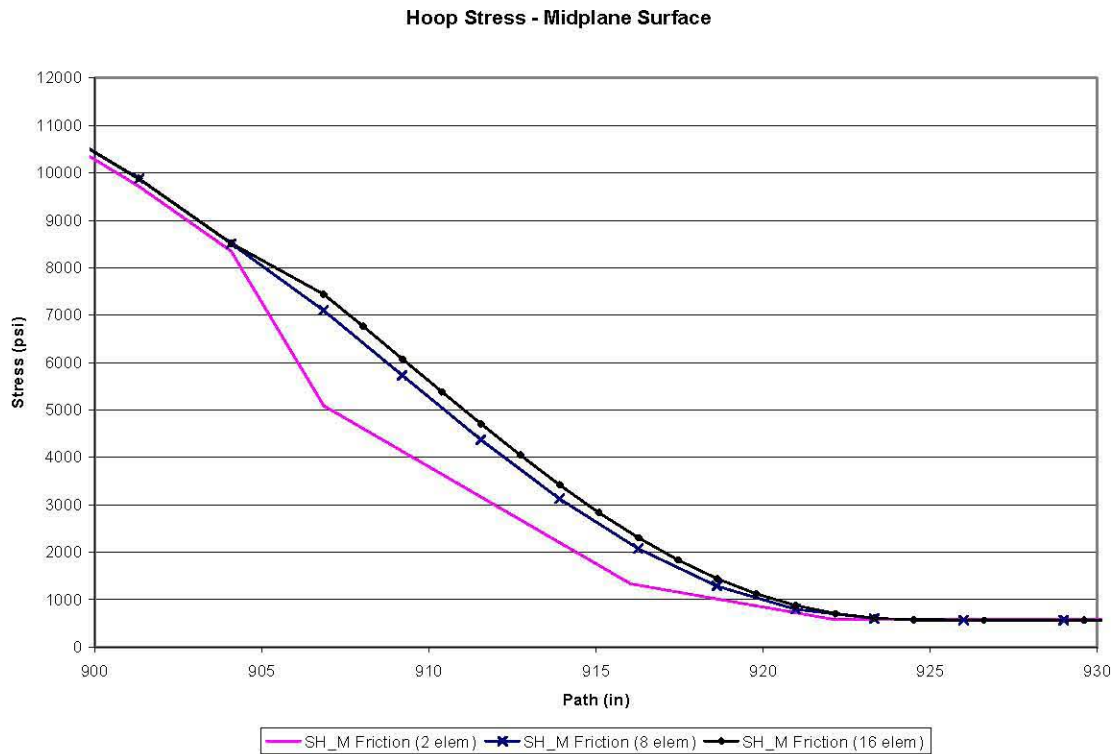


Figure A-17. Knuckle Hoop Stress Refined Mesh – Mid-Plane Surface

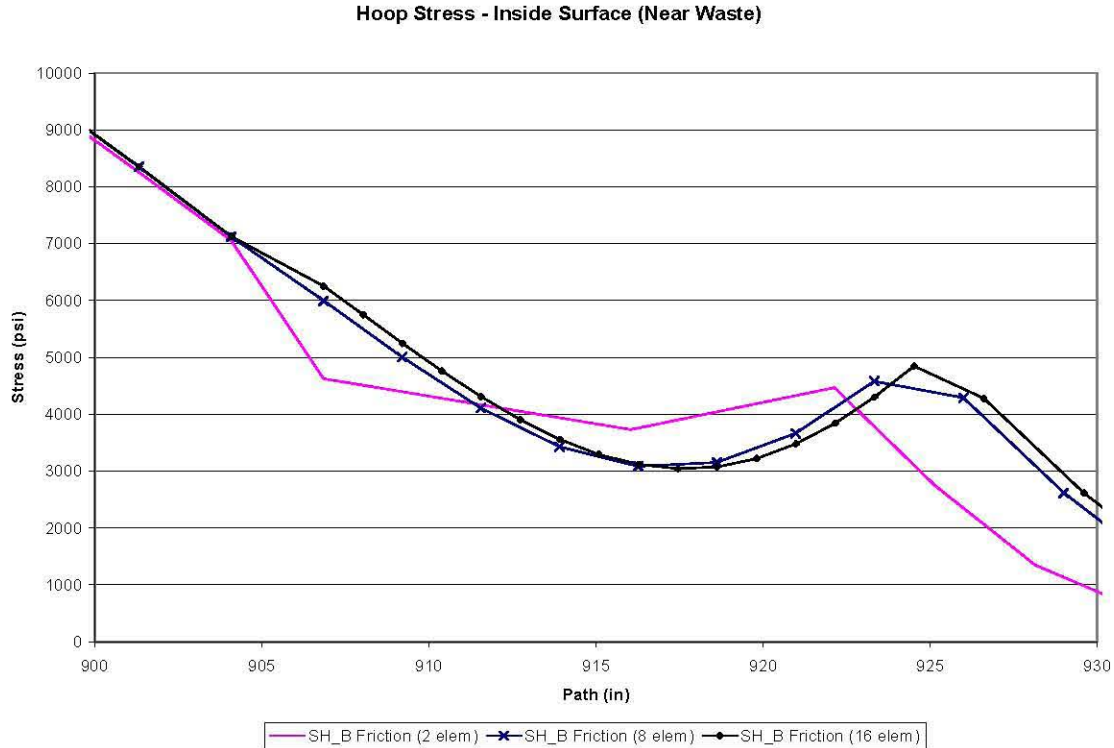


Figure A-18. Knuckle Hoop Stress Refined Mesh – Inside Surface (Near Waste)

A.3.3 Stress Factors

The meridional and hoop stresses extracted from the TOLA model and the ANSYS® detailed models have different mesh refinements in the primary tank knuckle. In order to make sure that conservative stresses are presented for the seismic analyses, a scaling factor needs to be determined to account for the lower mesh resolution in the ANSYS® detailed model. Comparing the absolute maximum meridional stress and absolute maximum hoops stresses from the two models, a factor can be determined for each component. For meridional stresses in the knuckle, the ratio of the maximum TOLA model to the ANSYS® detailed model, the correction factor is 1.96. The ratio of TOLA model to the ANSYS® detailed model hoop stresses produces a correction factor of 1.65. To ensure conservative analyses, the primary tank knuckle meridional and hoop stresses should both receive a stress factor of 2.0. The shear stresses in the primary tank knuckle are less than 10% of the maximum component stress, therefore it can be assumed that the meridional and hoop component stresses conservatively represent the maximum principal stress. Since the meridional and hoop stresses can be assumed to be representative of the principal stresses, a single stress factor of 2.0 can instead be placed on the stress intensity values obtained for the primary tank knuckle. The contributions of seismic stresses are relatively small in comparison to the operating loads and there is significant margin on the capacity of the primary tank; therefore, this method is considered acceptable.

A.4 Conclusion

Based on the evaluation of the TOLA model and the ANSYS® detailed model, the model refinement of 8 elements in the knuckle produces acceptable primary tank stress results. In addition, a single stress factor of 2.0 can be applied to the meridional and hoop stresses or the seismic-only stress intensity for the primary tank knuckle.

Appendix B

Description of ACI-349 Demand/Capacity Calculations

Appendix B

Description of ACI-349 Demand/Capacity Calculations

An EXCEL spreadsheet was used to calculate the ACI load-moment interaction diagrams for each of the 30 sections identified on the concrete tank. The diagrams are computed based on the concrete cross-section thickness, concrete strength, rebar placement and strength, and applied loads. The calculations follow the procedure defined in ACI-349 Chapter 10. Figures B-1 and B-2 describe the standard ACI calculations as implemented in the spreadsheet.

The spreadsheet includes tables with the following data necessary for reference during the calculations:

1. Section properties for all 30 sections.
2. Concrete strength as a function of temperature (Figure 2-6).
3. Average section temperatures from the thermal transient data.

The spreadsheet automatically refreshes the axial force, moment, and shear input data by reading the results file generated by the ANSYS ACI post-processing macro (see Appendix D). Table B-1 shows a typical results file from ANSYS. The load-moment interaction diagram for the meridional, circumferential and shear directions is generated. Figure B-3 shows a typical load-moment interaction diagram. This figure illustrates the change in demand with temperature at different thermal transient load steps. These plots also show the demand-to-capacity ratios for the meridional, circumferential and shear directions. Another macro automatically processes all 30 sections sequentially. A summary table is also produced for all the cross-sections at that load step.

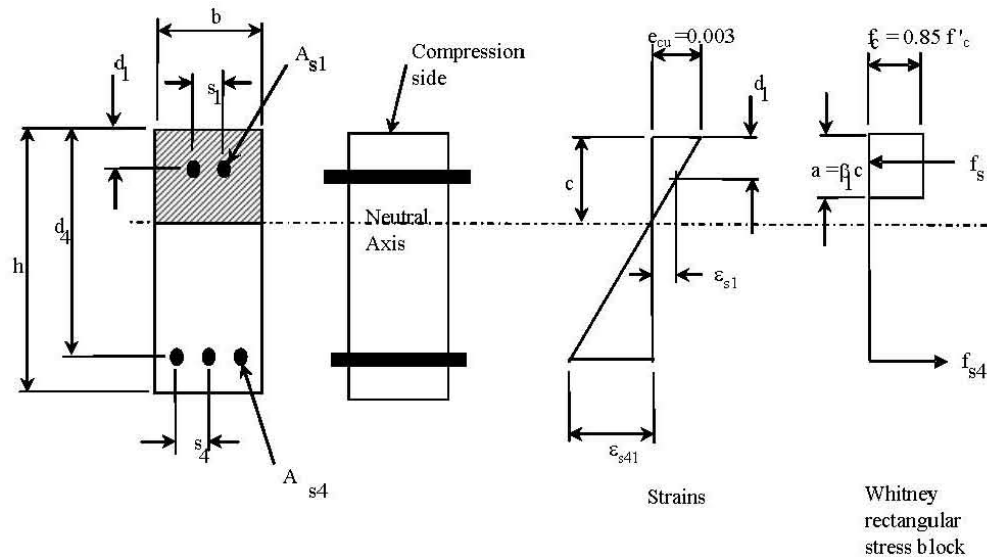


Figure B-1. ACI Nomenclature

RPP-RPT-28967, Rev. 1

Notation	Input	
Neutral axis relative to compression face = c		
Area of rebar at i th level	$A_{si} = (b/s_i) \pi (d_{bi}/2)^2$	s_i = bar spacing at i th rebar level
Center of A_{si} relative to compression face = d_i	d_{bi} = diameter of rebar at i th level relative to compression face	
Gross concrete area	$A_g = b \cdot h$	b = unit width (12 in.) of concrete section
Gross steel area	$A_{st} = \Sigma(A_{si})$	h = concrete section depth (thickness)
Centroid	$d_c = h/2$	
Plastic Centroid	$d_p = (0.85 f'_c A_g h/2 + f_y \Sigma(A_{si} d_i)) / (0.85 f'_c A_g + f_y A_{st})$	
Neutral axis relative to compression face = c		
Strain in A_{si}	$\epsilon_{si} = \epsilon_{cu} (c - d_i) / c$	(plane sections remain plane, positive for compression)
Stress in A_{si}	$f_{si} = \epsilon_{si} E_s$	$-f_y < F_{si} < f_y$ (elastic-perfectly plastic)
Concrete max compressive strain = $\epsilon_{cu} = 0.003$ (per ACI Code, Section 10.2.3)		
higher limiting strain values have been observed in members with significant moment gradient and in highly confined members		
	$\beta_1 = 0.85$	$f'_c < 4,000$ (per ACI Code)
	$= 0.85 - 0.05 (f'_c - 4,000) / 1,000$ not less than 0.65	
Depth of Whitney compression block	$a = \beta_1 c$ (equivalent rectangular concrete stress distribution)	
Compressive force in concrete	$C_c = 0.85 f'_c b a$	
Force in A_{si}	$F_{si} = f_{si} A_{si}$	$a < d_i$ (positive for compression)
	$= (f_{si} - 0.85 f'_c) A_{si}$	
Nominal axial load capacity	$P_n = C_c + \Sigma(F_{si})$	
Nominal moment capacity	$M_n = C_c (d_p - a/2) + \Sigma(F_{si} (d_p - d_i))$	
	$P_a = (0.10/0.70) f'_c A_g$	
Reduction factor on nominal capacity	$\phi = \max(0.70 + 0.20 (P_a - P_n) / P_a, 0.70)$	$P_n > 0$
	$= 0.9$	else
Neutral axis at balance point	$c_b = d_4 \epsilon_{cu} / (\epsilon_{cu} + \epsilon_y)$	
Max nominal compression load	$P_{nc} = 0.85 f'_c (A_g - A_{st}) + f_y A_{st}$	$\alpha \phi P_{nc}$ = code allowable for axial compression with nominal zero applied moment
Max nominal tension load	$P_{nt} = -f_y \Sigma A_{si} = -f_y A_{st}$	$\alpha = 0.8$ factor to account for small eccentricity of load on column

References:

- MacGregor, J. G., 1992, Reinforced Concrete: Mechanics and Design, 2nd edition, Prentice Hall, Englewood Cliffs, New Jersey.
- ACI 349-85, 1992, Code Requirements for Nuclear Safety Related Concrete Structures, ACI Manual of Concrete Practice, 1992, Part 4, American Concrete Institute, Detroit, Michigan.

Figure B-2. ACI Calculations

The demand-to-capacity ratio is defined as the ratio between the vector length from the origin to the force-moment pair to the vector length from the origin to the capacity curve assuming a constant ratio of force and moment (see Figure B-4). Caution should be exercised when interpreting this ratio as a margin of safety (or overload) as this assumes maintaining the same ratio of force to moment under changing loads. However, it does provide a convenient reference for evaluating the section capacity relative to the current demand.

The individual spreadsheets for each ACI evaluation and summary spreadsheets for the different load combinations for each of the analyses are available on the electronic media version of this report.

Table B-1. ANSYS Results File

Baseline, 5%K											
Year 61											
Steady-State											
40 psf uniform,100-ton concentrated, -20 in. annulus, -6 in. vapor space											
None											
Section	shear	F-merid	M-merid	F-hoop	M-hoop	Tmin	Tmax	Tave	xbar	ybar	sect thk
1	-0.5	-63.2	0.5	-61.3	0.5	149.2	177.2	164.8	31.6	568.4	14.99
2	-1	-63.4	0.8	-60.5	0.4	151.3	177.3	166.4	63.3	567.2	14.96
3	-1.5	-63.3	0.8	-58.1	-0.3	154.1	174.6	167.8	91.7	565.5	14.94
4	-1	-65.2	2.3	-56.9	1.5	152.9	175.9	167.3	122.6	562.8	14.92
5	0	-64.2	1.6	-53.8	1.3	152	173.6	166.4	153.4	559.4	14.95
6	0.6	-64.6	1.1	-48.9	0.7	151.6	172	165.2	185.7	554.9	15.04
7	0.9	-64.3	0.2	-47.5	0.1	152.4	172.4	165.6	213	550.2	15.01
8	-0.8	-57.8	-2	-40.4	-2.4	155.4	167.9	164.4	241	544.6	14.88
9	1.1	-55	0.3	-60.2	-2.5	158.7	165	164.1	272.6	537.1	14.72
10	0.3	-60	-1.9	-43.2	0.2	152.4	164.8	160.6	307.7	527.2	14.7
11	1.3	-59.9	-1.8	-47.7	0.1	151.3	165	161.1	318.2	523.9	14.76
12	1.7	-60.5	-1.3	-52.4	-0.5	150.7	165	162.4	338	517.2	15.03
13	2.1	-59.1	0.4	-43.9	3.1	145.4	164.6	157.6	358.2	509.6	15.59
14	2.6	-59.2	2.6	-44.7	5.2	142.4	165	158.2	372.5	503.8	16.27
15	3.1	-65.1	3.9	-10.8	3.1	139.4	164.2	155.5	394.4	494.2	17.82
16	5.3	-66.4	7.1	-3	1.8	138.6	163.3	152.7	405.5	488.8	18.92
17	7.8	-66.9	12.3	-1.2	3.5	137.9	167	153.4	416.6	483.3	20.31
18	11.6	-66	20.9	7.1	7.7	131	167.1	144.3	430.1	475.8	22.58
19	15	-67.4	20.7	-7.9	25.8	125.8	170	143.8	441.2	468.3	25.17
20	9.1	-36.9	-2.3	7.9	13.7	118	181.3	150	455.9	457.7	29.43
21	10.9	-44.1	8.9	4.7	28.5	115.2	203.9	158.9	474.1	444.4	37.15
22	7.5	-49.6	21.8	-1.5	16.7	147.2	209.8	180.4	484.6	421.6	29.71
23	2.1	-38.2	29.6	-13.2	4.8	177.8	217.8	199.3	487.6	404.8	22.52
24	5.3	-36	27.6	-27.3	3.9	201.1	233.7	219.2	488.2	393.5	19.07
25	-0.6	-37.4	25.2	-39.5	9	220.5	263.2	242.4	489	381.5	18
26	3.5	-41.8	22.5	-63.2	14	252.6	310.3	281.2	488.9	360.3	18
27	1.7	-26.8	8.6	-84.3	10.3	277.7	329.2	304.5	488.9	345.1	18
28	-0.6	-29.2	8.5	-82	8.8	280.1	330.2	306.3	488.9	333.6	18
29	-3.8	-30.9	7.7	-82.8	8.3	282.1	331	307.8	488.9	319.8	18
30	-1	-31.8	7.6	-80.8	7.3	283.5	331.6	308.8	488.9	304.6	18
31	-0.1	-31.8	7.9	-79.6	7.2	283.7	331.7	309	488.9	298.6	18
32	1.3	-29.2	9.9	-70.7	5.6	284.5	332.1	309.6	488.8	280.2	18
33	-6.2	-30.6	10.2	-77.8	8.9	285	332.4	310	488.9	258.9	18
34	-3.1	-31.3	8	-77.8	7.5	285.3	332.6	310.2	488.9	234.9	18
35	-5.3	-34.3	8.7	-80.4	7.6	285.4	332.8	310.4	488.9	211.3	18
36	-3.6	-34.4	9.7	-100.3	5.3	285.5	332.9	310.5	488.9	198.7	18
37	-5.1	-35.7	10	-90.5	1.7	285.6	333	310.6	488.8	184.8	18
38	-7.8	-41	12.9	-110.2	9.6	285.7	333.1	310.7	488.9	169.4	18
39	-6.3	-41.5	9.9	-112.8	6.4	285.7	333.2	310.7	488.9	150.7	18
40	-5.6	-42.1	9	-114.5	5.9	285.7	333.2	310.7	488.9	144.6	18
41	-8.8	-48.1	6.4	-123.2	4.1	285.5	333.3	310.7	488.9	118.7	18
42	-6.2	-47	1.1	-123.4	1.4	285.1	333.2	310.4	488.9	99.4	18
43	-9.8	-83.8	27.8	-145.4	10.4	284.1	333	309.8	488.9	78.4	18
44	-9.6	-90.1	19.5	-151.2	9.1	281.4	332.3	308	488.9	58.4	18
45	-11.6	-95.4	11.7	-155	8.3	275.1	330.1	303.4	488.9	37.9	18

Table B-1. (contd)

Section	shear	F-merid	M-merid	F-hoop	M-hoop	Tmin	Tmax	Tave	xbar	ybar	sect thk
46	-9	-95.2	6.7	-144	8.7	261	323.4	292.1	488.9	19.4	18
47	-9.9	-83.1	-6	-60.6	6	214.8	268.4	242	488.4	-5.8	18
48	-10.6	-42.5	4.9	-2.5	-0.8	134.3	164.4	149.2	515.6	-18.1	23.5
49	-22.7	-50	17.9	-7.3	-0.3	149.8	193.6	171.1	503.6	-17.5	23.5
50	1.8	-39.4	29	-16	-3	169.2	231.3	200	490.8	-19.3	22
51	11.1	-48.7	26.5	-39	-14.1	179.2	249.7	217.7	478.6	-19.3	22
52	3.6	-46.8	10.6	-21.8	-4.6	180.7	247	210	463.1	-19.3	22
53	-1.1	-45.2	10	-18.9	-2.1	185.8	241.1	213.6	441.1	-19.5	21.88
54	-1.5	-35.9	1.8	-10.4	-0.5	193.1	243.4	219.4	422.4	-18.1	19.55
55	-5.5	-34.2	5.1	-10.1	-0.1	205.8	244.4	225.6	391.1	-16.1	15.62
56	-4.8	-25.7	2.8	-10	0.1	218.2	244.6	230.5	360.3	-14.2	11.63
57	2.8	-21.4	1.9	-10.5	0	221.2	244.7	231.7	339.7	-13.5	10.5
58	3.2	-17.1	0.5	-10.2	0	221.3	244.7	231.8	279.6	-13.5	10.5
59	-3.9	-14.9	-0.8	-10.1	0.5	221.2	244.6	231.4	220.1	-13	10.5
60	-4.4	-13.3	0	-9.9	0	220.8	244.3	231.3	182.3	-13.5	10.5
61	-2.8	-11	0.1	-9.7	0	218.2	241.8	228.8	130.1	-13.5	10.5
62	5.6	-7.4	-0.4	-8.7	0	205.8	231.8	217.3	96.4	-13.5	10.5
63	1	-6.7	0.8	-9.4	0.3	182.2	223.9	200.6	55.8	-17	17.93

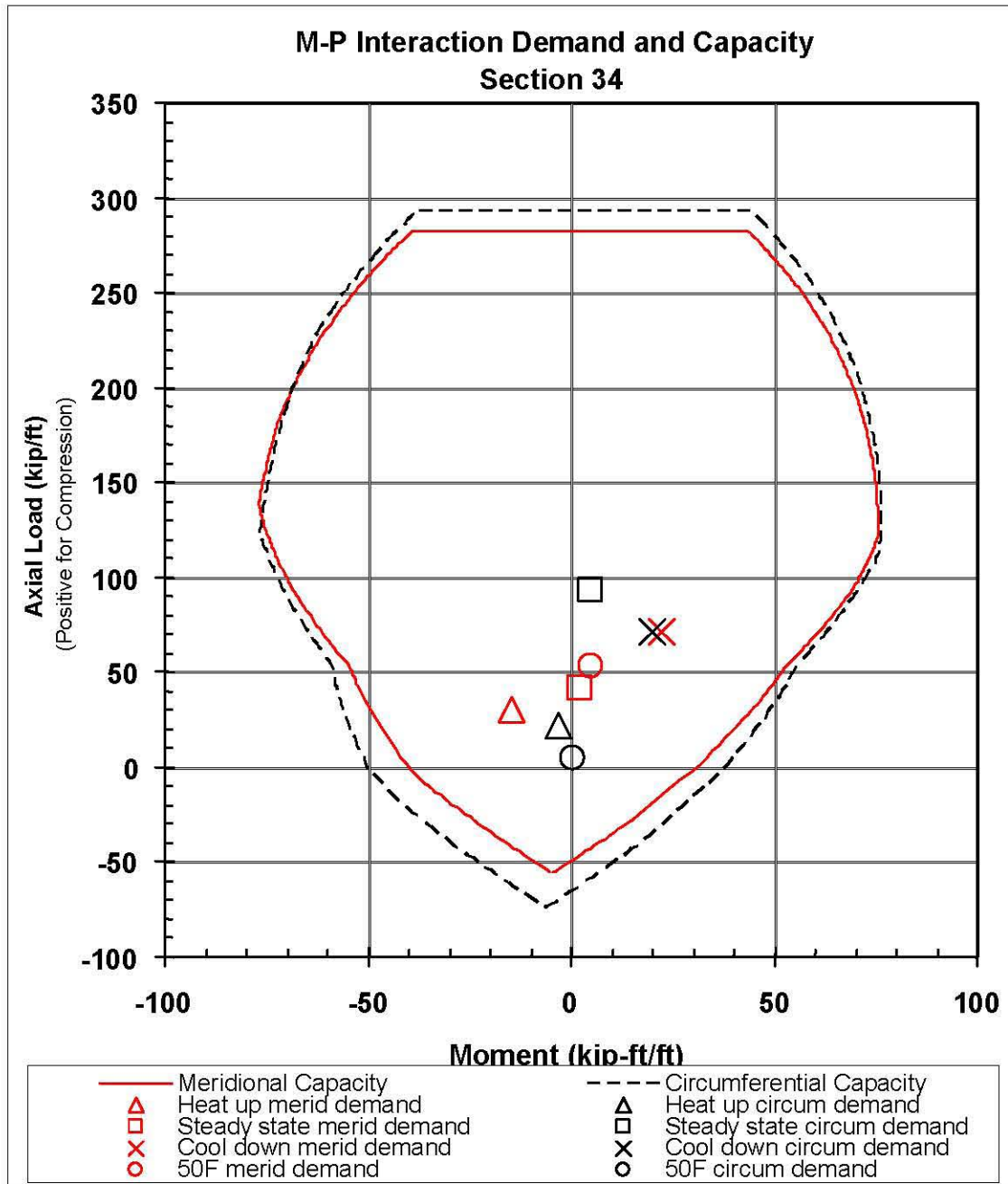


Figure B-3. Typical ACI Load-Moment Interaction Diagram

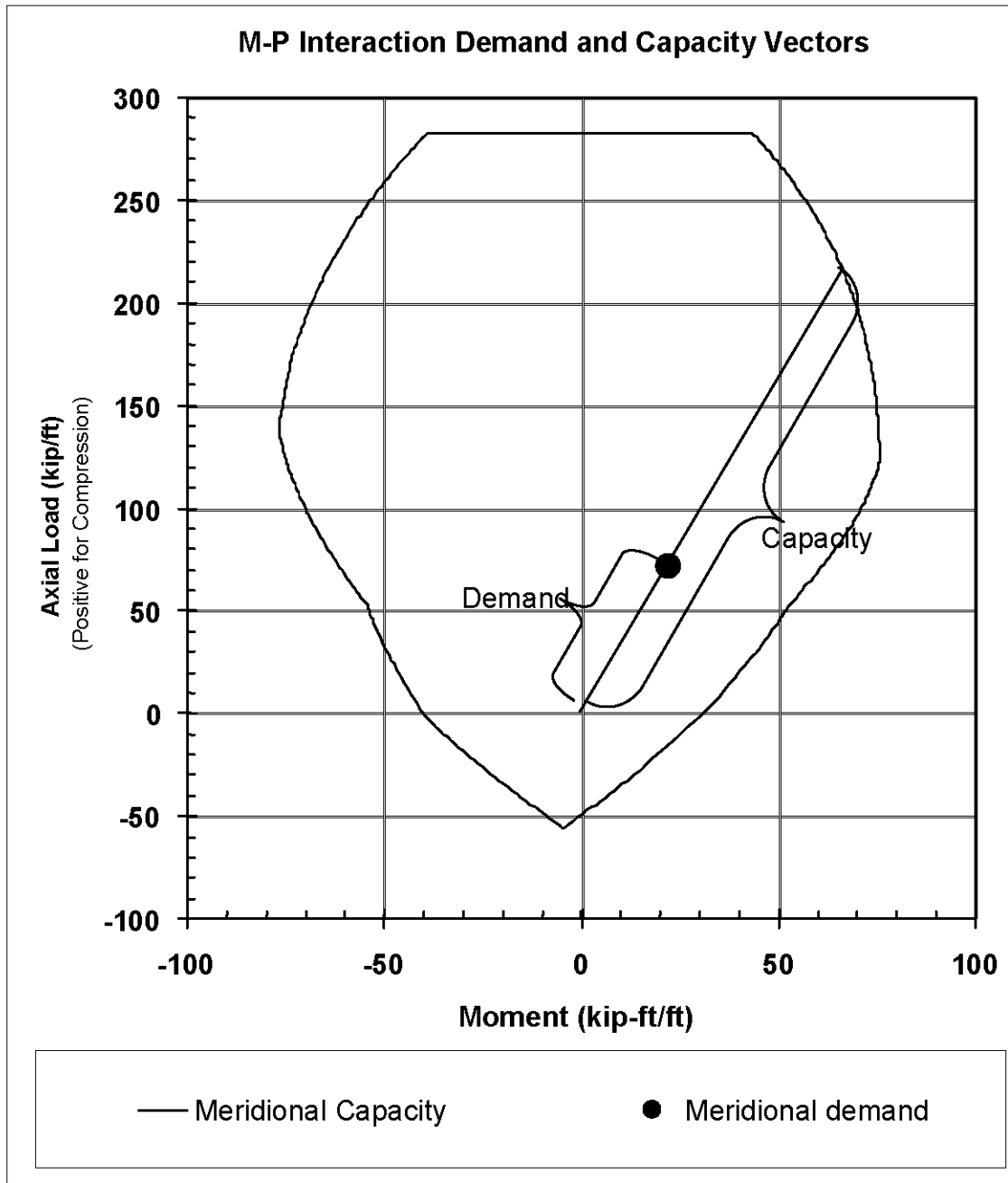


Figure B-4. ACI Demand/Capacity Ratio Definition

Appendix C

Software Acceptance

Appendix C

Software Acceptance

- 1) Project Title and Number: DST Thermal and Seismic Analyses 8971
- 2) Software Name and Version: ANSYS 7.0 (Rev. 11)
- 3) Computer and Property Number: Dell PWS 530 WD39892
- 4) Operating System: Windows XP Professional Version 2002 Service Pack 2
- 4) Scope of Testing: Software reinstallation (XP SP2)
- 5) Tests: Execute ANSYS Verification Testing Package
- 6) Discrepancies:
 - a) c0231. These differences are acceptable per the ANSYS Verification Package User's Guide – ANSYS Release 7.0 (AVPUG).
 - b) vm184. These differences occur at the 5th significant figure.
 - c) vm198. This difference is the reporting of the customer number for this installation.
 - d) vmc8. These differences are acceptable as noted in the output because of the difference in number of iterations and accuracy.
 - e) cyc-177s. This difference is acceptable due to the handling of the QAEND macro (see AVPUG).
 - f) cyc-178s. This difference is acceptable due to the handling of the QAEND macro (see AVPUG).
 - g) dds-13s. This test case requires the "Parallel Performance Module" which is not part of this software installation and is not required for the DST analyses.
 - h) dds-17s. This test case requires the "Parallel Performance Module" which is not part of this software installation and is not required for the DST analyses.
 - i) ev173-53s. This difference is acceptable due to the handling of the QAEND macro (see AVPUG).
 - j) ev175-20s. This difference is acceptable due to the handling of the QAEND macro (see AVPUG).
 - k) ev175-21s. This test case requires the "Parallel Performance Module" which is not part of this software installation and is not required for the DST analyses.
 - l) inrt-16s. This difference is acceptable due to the handling of the QAEND macro (see AVPUG).
 - m) sx120-1s. This test case requires the "Frequency Sweep Module" which is not part of this software installation and is not required for the DST analyses.
- 7) Finding: This installation of ANSYS is acceptable

Certified by:

JE Deibler John E Deibler 2/24/05
Code Custodian

Reviewed by:

KI Johnson Kenneth I Johnson 4/16/05
Lead Engineer

12/1 0/2002 Page 1 of 1 Addendum to ANSYS Verification Testing Package User's Guide -ANSYS Release 7.0

Notes for test case cO231

Test case cO231 may show considerable differences for the Phase Angle value that is part of the Post1 Nodal Degree of Freedom Listing (PRNS command) output. Any such differences do not indicate a problem with this test case's results and should be considered acceptable. The output items of significance for this test case are the UZ values in the Post1 Nodal Degree of Freedom Listing. Machine precision differences in the form of small numerical differences that are trivial with respect to the test's output items of significance may also show for this test case in the compare output for this test. Please see **Verifying ANSYS and Evaluating COMPARE Differences** in Chapter 2 of the *ANSYS Verification Testing Package User's Guide* for more information on evaluating COMPARE differences. The following is an example of acceptable COMPARE differences for test case cO231:

COMPARE DIFFERENCE FOUND AT G= NODAL RESULTS ARE FOR CYCLIC SECTOR T= NODAL RESULTS ARE FOR CYCLIC SECTOR

COMPARE DIFFERENCE FOUND AT G= VALUE -9.8117 -3.7700 22. T= VALUE -9.8119 -3.7693 22.

COMPARE DIFFERENCE FOUND AT G= NODAL RESULTS ARE FOR CYCLIC SECTOR T= NODAL RESULTS ARE FOR CYCLIC SECTOR

COMPARE DIFFERENCE FOUND AT G= VALUE -9.7579 -3.9649 22. T= VALUE -9.7581 -3.9643 22.

COMPARE DIFFERENCE FOUND AT G= NODAL RESULTS ARE FOR CYCLIC SECTOR T= NODAL RESULTS ARE FOR CYCLIC SECTOR

COMPARE DIFFERENCE FOUND AT G= 8 0.53291 0.39425 10 T= 8 0.53293 0.39419 10

COMPARE DIFFERENCE FOUND AT G= 10 0.52495 0.39568 9. T= 10 0.52497 0.39562 9.

COMPARE DIFFERENCE FOUND AT NG= 259 NT= 259 G= 12 0.50433 0.40282 8.6482 8.6722 T= 12 0.50435 0.40276 8.6471 8.6711

COMPARE DIFFERENCE FOUND AT NG= 260 NT= 260 G= 14 0.48186 0.41201 7.8710 7.8965 T= 14 0.48188 0.41196 7.8700 7.8955

COMPARE DIFFERENCE FOUND AT NG= 261 NT= 261 G= 16 0.45505 0.42478 7.0719 7.0992 T= 16 0.45507 0.42473 7.0710 7.0983

COMPARE DIFFERENCE FOUND AT NG= 262 NT= 262 G= 18 0.42339 0.44092 6.2424 6.2723 T= 18 0.42341 0.44086 6.2417 6.2715

COMPARE DIFFERENCE FOUND AT NG= 263 NT= 263 G= 20 0.38501 0.46124 5.3732 5.4067 T= 20 0.38502 0.46118 5.3726 5.4061

COMPARE DIFFERENCE FOUND AT NG= 267 NT= 267 G= VALUE -9.6034 -3.9649 18.806 21.413 T= VALUE -9.6036 -3.9643 18.805 21.412

NG= 271 NT= 271 22.469 24.766 22.469 24.766

NG= 192 NT= 192 1 -PHASE ANGLE = 1- PHASE ANGLE =

NG= 213 NT= 213 469 24.766 469 24.766

NG= 219 NT= 219 2- PHASE ANGLE = 2- PHASE ANGLE =

NG= 240 NT= 240 440 24.710 440 24.710

NG= 246 NT= 246 3- PHASE ANGLE = 3- PHASE ANGLE =

NG= 257 NT= 257 161 10.183 160 10.181

NG= 4080 4068

258 NT= 258 9.4309 9.4297

COMPARE DIFFERENCE FOUND AT G= VALUE -9.8117 -3.9649 T= VALUE -9.8119 -3.9643

30.580 306.570

30.580 306.570

30.580 306.570

Notes for Test Case vrn212

Test case vm212 may produce an expected compare difference due to an inconsequential warning message that appears in the ANSYS, Inc. supplied output file that may not appear in the output file generated by your system for this test case. This compare difference should be considered acceptable. The following is an example of this compare difference.

```
COMPARE DIFFERENCE FOUND AT          NG= 445 NT= 436
G= NUMBER OF WARNING MESSAGES ENCOUNTERED= 1
T= NUMBER OF WARNING MESSAGES ENCOUNTERED= 0
```

Notes for Test Cases cyc-177s, cyc-178s, ev-173-53s, ev-175-20s, inrt-16s, and inrt-9s

Test cases cyc-177s, cyc-178s, ev-173-53s, ev-175-20s, inrt-16s, and inrt-9s may produce expected compare differences due to the use of a macro named qaend. The method that is used in the verification procedure (runqa) to handle this macro may cause one or more comparison differences. Any such compare differences are inconsequential and should be considered acceptable. The following is an example of such a compare difference.

```
EXTRA DATA SKIPPED ON TEST FILE          NG= 1033 NT= 1030
T= USE COMMAND MACRO qaend
T= ARGS= 137.00
END OF SKIPPED DATA                     NG= 1033 NT= 1033
```

Notes for test Cases dds-13s, dds-17s, and ev175-21 s

The test cases dds-13s, dds-17s, and ev175-21 s will run to completion only if the "Parallel Performance for ANSYS" product (DDS and AMG solvers) is included in your ANSYS installation.

c0211r2	7020021010	70SP20030909	0	0	605	605	81%	02/12/2005	11:02 INTEL_NT
INTEL_NT	QA70-1	COMPARE_REL	3.8	UP20020121	WINDOWS				
c0212	7020021010	70SP20030909	0	0	223	223	45%	02/12/2005	11:02 INTEL_NT
INTEL_NT	QA70-1	COMPARE_REL	3.8	UP20020121	WINDOWS				
c0213	7020021010	70SP20030909	0	0	197	197	41%	02/12/2005	11:02 INTEL_NT
INTEL_NT	QA70-1	COMPARE_REL	3.8	UP20020121	WINDOWS				
c0214	7020021010	70SP20030909	0	0	409	409	67%	02/12/2005	11:02 INTEL_NT
INTEL_NT	QA70-1	COMPARE_REL	3.8	UP20020121	WINDOWS				
c0215	7020021010	70SP20030909	0	0	648	648	81%	02/12/2005	11:02 INTEL_NT
INTEL_NT	QA70-1	COMPARE_REL	3.8	UP20020121	WINDOWS				
c0216	7020021010	70SP20030909	0	0	510	510	74%	02/12/2005	11:02 INTEL_NT
INTEL_NT	QA70-1	COMPARE_REL	3.8	UP20020121	WINDOWS				
c0217	7020021010	70SP20030909	0	0	332	332	66%	02/12/2005	11:02 INTEL_NT
INTEL_NT	QA70-1	COMPARE_REL	3.8	UP20020121	WINDOWS				
c0218	7020021010	70SP20030909	0	0	1627	1627	93%	02/12/2005	11:02 INTEL_NT
INTEL_NT	QA70-1	COMPARE_REL	3.8	UP20020121	WINDOWS				
c0219	7020021010	70SP20030909	0	0	2732	2732	95%	02/12/2005	11:03 INTEL_NT
INTEL_NT	QA70-1	COMPARE_REL	3.8	UP20020121	WINDOWS				
c0220	7020021010	70SP20030909	0	0	494	494	76%	02/12/2005	11:03 INTEL_NT
INTEL_NT	QA70-1	COMPARE_REL	3.8	UP20020121	WINDOWS				
c0221	7020021010	70SP20030909	0	0	1265	1265	90%	02/12/2005	11:03 INTEL_NT
INTEL_NT	QA70-1	COMPARE_REL	3.8	UP20020121	WINDOWS				
c0222	7020021010	70SP20030909	0	0	1543	1543	92%	02/12/2005	11:03 INTEL_NT
INTEL_NT	QA70-1	COMPARE_REL	3.8	UP20020121	WINDOWS				
c0223	7020021010	70SP20030909	0	0	362	362	66%	02/12/2005	11:03 INTEL_NT
INTEL_NT	QA70-1	COMPARE_REL	3.8	UP20020121	WINDOWS				
c0224	7020021010	70SP20030909	0	0	307	307	59%	02/12/2005	11:04 INTEL_NT
INTEL_NT	QA70-1	COMPARE_REL	3.8	UP20020121	WINDOWS				
c0225	7020021010	70SP20030909	0	0	420	420	70%	02/12/2005	11:04 INTEL_NT
INTEL_NT	QA70-1	COMPARE_REL	3.8	UP20020121	WINDOWS				
c0226	7020021010	70SP20030909	0	0	521	521	74%	02/12/2005	11:04 INTEL_NT
INTEL_NT	QA70-1	COMPARE_REL	3.8	UP20020121	WINDOWS				
c0227	7020021010	70SP20030909	0	0	380	380	65%	02/12/2005	11:04 INTEL_NT
INTEL_NT	QA70-1	COMPARE_REL	3.8	UP20020121	WINDOWS				
c0227a	7020021010	70SP20030909	0	0	380	380	65%	02/12/2005	11:04 INTEL_NT
INTEL_NT	QA70-1	COMPARE_REL	3.8	UP20020121	WINDOWS				
c0228	7020021010	70SP20030909	0	0	236	236	50%	02/12/2005	11:04 INTEL_NT
INTEL_NT	QA70-1	COMPARE_REL	3.8	UP20020121	WINDOWS				
c0229	7020021010	70SP20030909	0	0	715	715	81%	02/12/2005	11:04 INTEL_NT
INTEL_NT	QA70-1	COMPARE_REL	3.8	UP20020121	WINDOWS				
c0230	7020021010	70SP20030909	0	0	2513	2513	94%	02/12/2005	11:04 INTEL_NT
INTEL_NT	QA70-1	COMPARE_REL	3.8	UP20020121	WINDOWS				
c0231	7020021010	70SP20030909	3	0	304	304	61%	02/12/2005	11:05 INTEL_NT
INTEL_NT	QA70-1	COMPARE_REL	3.8	UP20020121	WINDOWS				

c0232	7020021010	70SP20030909	0	0	517	517	79%	02/12/2005	11:06	INTEL_NT
INTEL_NT	QA70-1	COMPARE_REL	3.8	UP20020121	WINDOWS					
c0233	7020021010	70SP20030909	0	0	542	542	75%	02/12/2005	11:06	INTEL_NT
INTEL_NT	QA70-1	COMPARE_REL	3.8	UP20020121	WINDOWS					
c0234	7020021010	70SP20030909	0	0	420	420	68%	02/12/2005	11:06	INTEL_NT
INTEL_NT	QA70-1	COMPARE_REL	3.8	UP20020121	WINDOWS					
vm1	7020021010	70SP20030909	0	0	474	474	72%	02/12/2005	11:06	INTEL_NT
INTEL_NT	QA70-1	COMPARE_REL	3.8	UP20020121	WINDOWS					
vm2	7020021010	70SP20030909	0	0	667	667	81%	02/12/2005	11:06	INTEL_NT
INTEL_NT	QA70-1	COMPARE_REL	3.8	UP20020121	WINDOWS					
vm3	7020021010	70SP20030909	0	0	499	499	73%	02/12/2005	11:06	INTEL_NT
INTEL_NT	QA70-1	COMPARE_REL	3.8	UP20020121	WINDOWS					
vm4	7020021010	70SP20030909	0	0	434	434	69%	02/12/2005	11:06	INTEL_NT
INTEL_NT	QA70-1	COMPARE_REL	3.8	UP20020121	WINDOWS					
vm5	7020021010	70SP20030909	0	0	884	884	85%	02/12/2005	11:06	INTEL_NT
INTEL_NT	QA70-1	COMPARE_REL	3.8	UP20020121	WINDOWS					
vm6	7020021010	70SP20030909	0	0	854	854	83%	02/12/2005	11:06	INTEL_NT
INTEL_NT	QA70-1	COMPARE_REL	3.8	UP20020121	WINDOWS					
vm7	7020021010	70SP20030909	0	0	2176	2176	93%	02/12/2005	11:06	INTEL_NT
INTEL_NT	QA70-1	COMPARE_REL	3.8	UP20020121	WINDOWS					
vm8	7020021010	70SP20030909	0	0	346	346	64%	02/12/2005	11:06	INTEL_NT
INTEL_NT	QA70-1	COMPARE_REL	3.8	UP20020121	WINDOWS					
vm9	7020021010	70SP20030909	0	0	851	851	85%	02/12/2005	11:06	INTEL_NT
INTEL_NT	QA70-1	COMPARE_REL	3.8	UP20020121	WINDOWS					
vm10	7020021010	70SP20030909	0	0	437	437	69%	02/12/2005	11:06	INTEL_NT
INTEL_NT	QA70-1	COMPARE_REL	3.8	UP20020121	WINDOWS					
vm11	7020021010	70SP20030909	0	0	885	885	85%	02/12/2005	11:06	INTEL_NT
INTEL_NT	QA70-1	COMPARE_REL	3.8	UP20020121	WINDOWS					
vm12	7020021010	70SP20030909	0	0	444	444	70%	02/12/2005	11:06	INTEL_NT
INTEL_NT	QA70-1	COMPARE_REL	3.8	UP20020121	WINDOWS					
vm13	7020021010	70SP20030909	0	0	464	464	71%	02/12/2005	11:06	INTEL_NT
INTEL_NT	QA70-1	COMPARE_REL	3.8	UP20020121	WINDOWS					
vm14	7020021010	70SP20030909	0	0	537	537	76%	02/12/2005	11:06	INTEL_NT
INTEL_NT	QA70-1	COMPARE_REL	3.8	UP20020121	WINDOWS					
vm15	7020021010	70SP20030909	0	0	1356	1356	91%	02/12/2005	11:07	INTEL_NT
INTEL_NT	QA70-1	COMPARE_REL	3.8	UP20020121	WINDOWS					
vm16	7020021010	70SP20030909	0	0	740	740	82%	02/12/2005	11:07	INTEL_NT
INTEL_NT	QA70-1	COMPARE_REL	3.8	UP20020121	WINDOWS					
vm17	7020021010	70SP20030909	0	0	546	546	76%	02/12/2005	11:07	INTEL_NT
INTEL_NT	QA70-1	COMPARE_REL	3.8	UP20020121	WINDOWS					
vm18	7020021010	70SP20030909	0	0	450	450	71%	02/12/2005	11:07	INTEL_NT
INTEL_NT	QA70-1	COMPARE_REL	3.8	UP20020121	WINDOWS					
vm19	7020021010	70SP20030909	0	0	725	725	80%	02/12/2005	11:07	INTEL_NT
INTEL_NT	QA70-1	COMPARE_REL	3.8	UP20020121	WINDOWS					

vm20	7020021010	70SP20030909	0	0	449	449	70%	02/12/2005	11:07	INTEL_NT
INTEL_NT	QA70-1	COMPARE_REL	3.8	UP20020121	WINDOWS					
vm21	7020021010	70SP20030909	0	0	805	805	82%	02/12/2005	11:07	INTEL_NT
INTEL_NT	QA70-1	COMPARE_REL	3.8	UP20020121	WINDOWS					
vm22	7020021010	70SP20030909	0	0	398	398	66%	02/12/2005	11:07	INTEL_NT
INTEL_NT	QA70-1	COMPARE_REL	3.8	UP20020121	WINDOWS					
vm23	7020021010	70SP20030909	0	0	1043	1043	88%	02/12/2005	11:07	INTEL_NT
INTEL_NT	QA70-1	COMPARE_REL	3.8	UP20020121	WINDOWS					
vm24	7020021010	70SP20030909	0	0	766	766	82%	02/12/2005	11:07	INTEL_NT
INTEL_NT	QA70-1	COMPARE_REL	3.8	UP20020121	WINDOWS					
vm25	7020021010	70SP20030909	0	0	2350	2350	95%	02/12/2005	11:07	INTEL_NT
INTEL_NT	QA70-1	COMPARE_REL	3.8	UP20020121	WINDOWS					
vm26	7020021010	70SP20030909	0	0	1829	1829	89%	02/12/2005	11:08	INTEL_NT
INTEL_NT	QA70-1	COMPARE_REL	3.8	UP20020121	WINDOWS					
vm27	7020021010	70SP20030909	0	0	910	910	85%	02/12/2005	11:08	INTEL_NT
INTEL_NT	QA70-1	COMPARE_REL	3.8	UP20020121	WINDOWS					
vm28	7020021010	70SP20030909	0	0	418	418	70%	02/12/2005	11:08	INTEL_NT
INTEL_NT	QA70-1	COMPARE_REL	3.8	UP20020121	WINDOWS					
vm29	7020021010	70SP20030909	0	0	683	683	80%	02/12/2005	11:08	INTEL_NT
INTEL_NT	QA70-1	COMPARE_REL	3.8	UP20020121	WINDOWS					
vm30	7020021010	70SP20030909	0	0	449	449	70%	02/12/2005	11:08	INTEL_NT
INTEL_NT	QA70-1	COMPARE_REL	3.8	UP20020121	WINDOWS					
vm31	7020021010	70SP20030909	0	0	551	551	76%	02/12/2005	11:08	INTEL_NT
INTEL_NT	QA70-1	COMPARE_REL	3.8	UP20020121	WINDOWS					
vm32	7020021010	70SP20030909	0	0	881	881	84%	02/12/2005	11:08	INTEL_NT
INTEL_NT	QA70-1	COMPARE_REL	3.8	UP20020121	WINDOWS					
vm33	7020021010	70SP20030909	0	0	902	902	85%	02/12/2005	11:08	INTEL_NT
INTEL_NT	QA70-1	COMPARE_REL	3.8	UP20020121	WINDOWS					
vm34	7020021010	70SP20030909	0	0	1380	1380	90%	02/12/2005	11:08	INTEL_NT
INTEL_NT	QA70-1	COMPARE_REL	3.8	UP20020121	WINDOWS					
vm35	7020021010	70SP20030909	0	0	594	594	77%	02/12/2005	11:08	INTEL_NT
INTEL_NT	QA70-1	COMPARE_REL	3.8	UP20020121	WINDOWS					
vm36	7020021010	70SP20030909	0	0	1086	1086	88%	02/12/2005	11:08	INTEL_NT
INTEL_NT	QA70-1	COMPARE_REL	3.8	UP20020121	WINDOWS					
vm37	7020021010	70SP20030909	0	0	690	690	81%	02/12/2005	11:08	INTEL_NT
INTEL_NT	QA70-1	COMPARE_REL	3.8	UP20020121	WINDOWS					
vm38	7020021010	70SP20030909	0	0	1667	1667	92%	02/12/2005	11:08	INTEL_NT
INTEL_NT	QA70-1	COMPARE_REL	3.8	UP20020121	WINDOWS					
vm39	7020021010	70SP20030909	0	0	819	819	84%	02/12/2005	11:09	INTEL_NT
INTEL_NT	QA70-1	COMPARE_REL	3.8	UP20020121	WINDOWS					
vm40	7020021010	70SP20030909	0	0	876	876	86%	02/12/2005	11:09	INTEL_NT
INTEL_NT	QA70-1	COMPARE_REL	3.8	UP20020121	WINDOWS					
vm41	7020021010	70SP20030909	0	0	829	829	83%	02/12/2005	11:09	INTEL_NT
INTEL_NT	QA70-1	COMPARE_REL	3.8	UP20020121	WINDOWS					

vm42	7020021010	70SP20030909	0	0	607	607	77%	02/12/2005	11:09	INTEL_NT
INTEL_NT	QA70-1	COMPARE_REL	3.8	UP20020121	WINDOWS					
vm43	7020021010	70SP20030909	0	0	860	860	85%	02/12/2005	11:09	INTEL_NT
INTEL_NT	QA70-1	COMPARE_REL	3.8	UP20020121	WINDOWS					
vm44	7020021010	70SP20030909	0	0	1198	1198	90%	02/12/2005	11:09	INTEL_NT
INTEL_NT	QA70-1	COMPARE_REL	3.8	UP20020121	WINDOWS					
vm45	7020021010	70SP20030909	0	0	416	416	67%	02/12/2005	11:09	INTEL_NT
INTEL_NT	QA70-1	COMPARE_REL	3.8	UP20020121	WINDOWS					
vm46	7020021010	70SP20030909	0	0	794	794	82%	02/12/2005	11:09	INTEL_NT
INTEL_NT	QA70-1	COMPARE_REL	3.8	UP20020121	WINDOWS					
vm47	7020021010	70SP20030909	0	0	416	416	67%	02/12/2005	11:09	INTEL_NT
INTEL_NT	QA70-1	COMPARE_REL	3.8	UP20020121	WINDOWS					
vm48	7020021010	70SP20030909	0	0	421	421	68%	02/12/2005	11:09	INTEL_NT
INTEL_NT	QA70-1	COMPARE_REL	3.8	UP20020121	WINDOWS					
vm49	7020021010	70SP20030909	0	0	700	700	80%	02/12/2005	11:09	INTEL_NT
INTEL_NT	QA70-1	COMPARE_REL	3.8	UP20020121	WINDOWS					
vm50	7020021010	70SP20030909	0	0	500	500	72%	02/12/2005	11:09	INTEL_NT
INTEL_NT	QA70-1	COMPARE_REL	3.8	UP20020121	WINDOWS					
vm51	7020021010	70SP20030909	0	0	531	531	77%	02/12/2005	11:10	INTEL_NT
INTEL_NT	QA70-1	COMPARE_REL	3.8	UP20020121	WINDOWS					
vm52	7020021010	70SP20030909	0	0	520	520	74%	02/12/2005	11:10	INTEL_NT
INTEL_NT	QA70-1	COMPARE_REL	3.8	UP20020121	WINDOWS					
vm53	7020021010	70SP20030909	0	0	789	789	82%	02/12/2005	11:10	INTEL_NT
INTEL_NT	QA70-1	COMPARE_REL	3.8	UP20020121	WINDOWS					
vm54	7020021010	70SP20030909	0	0	564	564	75%	02/12/2005	11:10	INTEL_NT
INTEL_NT	QA70-1	COMPARE_REL	3.8	UP20020121	WINDOWS					
vm55	7020021010	70SP20030909	0	0	995	995	87%	02/12/2005	11:10	INTEL_NT
INTEL_NT	QA70-1	COMPARE_REL	3.8	UP20020121	WINDOWS					
vm56	7020021010	70SP20030909	0	0	1577	1577	91%	02/12/2005	11:10	INTEL_NT
INTEL_NT	QA70-1	COMPARE_REL	3.8	UP20020121	WINDOWS					
vm57	7020021010	70SP20030909	0	0	737	737	81%	02/12/2005	11:10	INTEL_NT
INTEL_NT	QA70-1	COMPARE_REL	3.8	UP20020121	WINDOWS					
vm58	7020021010	70SP20030909	0	0	580	580	76%	02/12/2005	11:10	INTEL_NT
INTEL_NT	QA70-1	COMPARE_REL	3.8	UP20020121	WINDOWS					
vm59	7020021010	70SP20030909	0	0	833	833	84%	02/12/2005	11:10	INTEL_NT
INTEL_NT	QA70-1	COMPARE_REL	3.8	UP20020121	WINDOWS					
vm60	7020021010	70SP20030909	0	0	537	537	72%	02/12/2005	11:10	INTEL_NT
INTEL_NT	QA70-1	COMPARE_REL	3.8	UP20020121	WINDOWS					
vm61	7020021010	70SP20030909	0	0	402	402	66%	02/12/2005	11:10	INTEL_NT
INTEL_NT	QA70-1	COMPARE_REL	3.8	UP20020121	WINDOWS					
vm62	7020021010	70SP20030909	0	0	755	755	82%	02/12/2005	11:10	INTEL_NT
INTEL_NT	QA70-1	COMPARE_REL	3.8	UP20020121	WINDOWS					
vm63	7020021010	70SP20030909	0	0	1280	1280	89%	02/12/2005	11:10	INTEL_NT
INTEL_NT	QA70-1	COMPARE_REL	3.8	UP20020121	WINDOWS					

vm64	7020021010	70SP20030909	0	0	510	510	74%	02/12/2005	11:10	INTEL_NT
INTEL_NT	QA70-1	COMPARE_REL	3.8	UP20020121	WINDOWS					
vm65	7020021010	70SP20030909	0	0	3323	3323	96%	02/12/2005	11:11	INTEL_NT
INTEL_NT	QA70-1	COMPARE_REL	3.8	UP20020121	WINDOWS					
vm66	7020021010	70SP20030909	0	0	516	516	74%	02/12/2005	11:11	INTEL_NT
INTEL_NT	QA70-1	COMPARE_REL	3.8	UP20020121	WINDOWS					
vm67	7020021010	70SP20030909	0	0	591	591	76%	02/12/2005	11:11	INTEL_NT
INTEL_NT	QA70-1	COMPARE_REL	3.8	UP20020121	WINDOWS					
vm68	7020021010	70SP20030909	0	0	739	739	80%	02/12/2005	11:11	INTEL_NT
INTEL_NT	QA70-1	COMPARE_REL	3.8	UP20020121	WINDOWS					
vm69	7020021010	70SP20030909	0	0	553	553	75%	02/12/2005	11:11	INTEL_NT
INTEL_NT	QA70-1	COMPARE_REL	3.8	UP20020121	WINDOWS					
vm70	7020021010	70SP20030909	0	0	940	940	86%	02/12/2005	11:11	INTEL_NT
INTEL_NT	QA70-1	COMPARE_REL	3.8	UP20020121	WINDOWS					
vm71	7020021010	70SP20030909	0	0	1307	1307	87%	02/12/2005	11:11	INTEL_NT
INTEL_NT	QA70-1	COMPARE_REL	3.8	UP20020121	WINDOWS					
vm72	7020021010	70SP20030909	0	0	2161	2161	90%	02/12/2005	11:11	INTEL_NT
INTEL_NT	QA70-1	COMPARE_REL	3.8	UP20020121	WINDOWS					
vm73	7020021010	70SP20030909	0	0	4189	4189	97%	02/12/2005	11:12	INTEL_NT
INTEL_NT	QA70-1	COMPARE_REL	3.8	UP20020121	WINDOWS					
vm74	7020021010	70SP20030909	0	0	855	855	81%	02/12/2005	11:12	INTEL_NT
INTEL_NT	QA70-1	COMPARE_REL	3.8	UP20020121	WINDOWS					
vm75	7020021010	70SP20030909	0	0	1129	1129	84%	02/12/2005	11:12	INTEL_NT
INTEL_NT	QA70-1	COMPARE_REL	3.8	UP20020121	WINDOWS					
vm76	7020021010	70SP20030909	0	0	1187	1187	89%	02/12/2005	11:12	INTEL_NT
INTEL_NT	QA70-1	COMPARE_REL	3.8	UP20020121	WINDOWS					
vm77	7020021010	70SP20030909	0	0	876	876	82%	02/12/2005	11:12	INTEL_NT
INTEL_NT	QA70-1	COMPARE_REL	3.8	UP20020121	WINDOWS					
vm78	7020021010	70SP20030909	0	0	872	872	86%	02/12/2005	11:12	INTEL_NT
INTEL_NT	QA70-1	COMPARE_REL	3.8	UP20020121	WINDOWS					
vm79	7020021010	70SP20030909	0	0	954	954	83%	02/12/2005	11:12	INTEL_NT
INTEL_NT	QA70-1	COMPARE_REL	3.8	UP20020121	WINDOWS					
vm80	7020021010	70SP20030909	0	0	2205	2205	92%	02/12/2005	11:12	INTEL_NT
INTEL_NT	QA70-1	COMPARE_REL	3.8	UP20020121	WINDOWS					
vm81	7020021010	70SP20030909	0	0	2015	2015	93%	02/12/2005	11:13	INTEL_NT
INTEL_NT	QA70-1	COMPARE_REL	3.8	UP20020121	WINDOWS					
vm82	7020021010	70SP20030909	0	0	2144	2144	94%	02/12/2005	11:13	INTEL_NT
INTEL_NT	QA70-1	COMPARE_REL	3.8	UP20020121	WINDOWS					
vm83	7020021010	70SP20030909	0	0	2191	2191	94%	02/12/2005	11:13	INTEL_NT
INTEL_NT	QA70-1	COMPARE_REL	3.8	UP20020121	WINDOWS					
vm84	7020021010	70SP20030909	0	0	821	821	82%	02/12/2005	11:13	INTEL_NT
INTEL_NT	QA70-1	COMPARE_REL	3.8	UP20020121	WINDOWS					
vm85	7020021010	70SP20030909	0	0	858	858	84%	02/12/2005	11:13	INTEL_NT
INTEL_NT	QA70-1	COMPARE_REL	3.8	UP20020121	WINDOWS					

vm86	7020021010	70SP20030909	0	0	428	428	68%	02/12/2005	11:13	INTEL_NT
INTEL_NT	QA70-1	COMPARE_REL	3.8	UP20020121	WINDOWS					
vm87	7020021010	70SP20030909	0	0	434	434	69%	02/12/2005	11:13	INTEL_NT
INTEL_NT	QA70-1	COMPARE_REL	3.8	UP20020121	WINDOWS					
vm88	7020021010	70SP20030909	0	0	450	450	70%	02/12/2005	11:14	INTEL_NT
INTEL_NT	QA70-1	COMPARE_REL	3.8	UP20020121	WINDOWS					
vm89	7020021010	70SP20030909	0	0	480	480	72%	02/12/2005	11:14	INTEL_NT
INTEL_NT	QA70-1	COMPARE_REL	3.8	UP20020121	WINDOWS					
vm90	7020021010	70SP20030909	0	0	761	761	82%	02/12/2005	11:14	INTEL_NT
INTEL_NT	QA70-1	COMPARE_REL	3.8	UP20020121	WINDOWS					
vm91	7020021010	70SP20030909	0	0	2102	2102	94%	02/12/2005	11:14	INTEL_NT
INTEL_NT	QA70-1	COMPARE_REL	3.8	UP20020121	WINDOWS					
vm92	7020021010	70SP20030909	0	0	501	501	73%	02/12/2005	11:14	INTEL_NT
INTEL_NT	QA70-1	COMPARE_REL	3.8	UP20020121	WINDOWS					
vm93	7020021010	70SP20030909	0	0	436	436	69%	02/12/2005	11:14	INTEL_NT
INTEL_NT	QA70-1	COMPARE_REL	3.8	UP20020121	WINDOWS					
vm94	7020021010	70SP20030909	0	0	508	508	73%	02/12/2005	11:14	INTEL_NT
INTEL_NT	QA70-1	COMPARE_REL	3.8	UP20020121	WINDOWS					
vm95	7020021010	70SP20030909	0	0	1044	1044	86%	02/12/2005	11:14	INTEL_NT
INTEL_NT	QA70-1	COMPARE_REL	3.8	UP20020121	WINDOWS					
vm96	7020021010	70SP20030909	0	0	633	633	78%	02/12/2005	11:14	INTEL_NT
INTEL_NT	QA70-1	COMPARE_REL	3.8	UP20020121	WINDOWS					
vm97	7020021010	70SP20030909	0	0	809	809	83%	02/12/2005	11:14	INTEL_NT
INTEL_NT	QA70-1	COMPARE_REL	3.8	UP20020121	WINDOWS					
vm98	7020021010	70SP20030909	0	0	703	703	80%	02/12/2005	11:14	INTEL_NT
INTEL_NT	QA70-1	COMPARE_REL	3.8	UP20020121	WINDOWS					
vm99	7020021010	70SP20030909	0	0	482	482	72%	02/12/2005	11:14	INTEL_NT
INTEL_NT	QA70-1	COMPARE_REL	3.8	UP20020121	WINDOWS					
vm100	7020021010	70SP20030909	0	0	642	642	79%	02/12/2005	11:14	INTEL_NT
INTEL_NT	QA70-1	COMPARE_REL	3.8	UP20020121	WINDOWS					
vm101	7020021010	70SP20030909	0	0	720	720	81%	02/12/2005	11:14	INTEL_NT
INTEL_NT	QA70-1	COMPARE_REL	3.8	UP20020121	WINDOWS					
vm102	7020021010	70SP20030909	0	0	761	761	82%	02/12/2005	11:15	INTEL_NT
INTEL_NT	QA70-1	COMPARE_REL	3.8	UP20020121	WINDOWS					
vm103	7020021010	70SP20030909	0	0	782	782	84%	02/12/2005	11:15	INTEL_NT
INTEL_NT	QA70-1	COMPARE_REL	3.8	UP20020121	WINDOWS					
vm104	7020021010	70SP20030909	0	0	1822	1822	93%	02/12/2005	11:15	INTEL_NT
INTEL_NT	QA70-1	COMPARE_REL	3.8	UP20020121	WINDOWS					
vm105	7020021010	70SP20030909	0	0	589	589	77%	02/12/2005	11:15	INTEL_NT
INTEL_NT	QA70-1	COMPARE_REL	3.8	UP20020121	WINDOWS					
vm106	7020021010	70SP20030909	0	0	432	432	69%	02/12/2005	11:15	INTEL_NT
INTEL_NT	QA70-1	COMPARE_REL	3.8	UP20020121	WINDOWS					
vm107	7020021010	70SP20030909	0	0	476	476	72%	02/12/2005	11:15	INTEL_NT
INTEL_NT	QA70-1	COMPARE_REL	3.8	UP20020121	WINDOWS					

vm108	7020021010	70SP20030909	0	0	437	437	69%	02/12/2005	11:15	INTEL_NT
INTEL_NT	QA70-1	COMPARE_REL	3.8	UP20020121	WINDOWS					
vm109	7020021010	70SP20030909	0	0	1025	1025	87%	02/12/2005	11:15	INTEL_NT
INTEL_NT	QA70-1	COMPARE_REL	3.8	UP20020121	WINDOWS					
vm110	7020021010	70SP20030909	0	0	743	743	82%	02/12/2005	11:15	INTEL_NT
INTEL_NT	QA70-1	COMPARE_REL	3.8	UP20020121	WINDOWS					
vm111	7020021010	70SP20030909	0	0	3511	3511	96%	02/12/2005	11:16	INTEL_NT
INTEL_NT	QA70-1	COMPARE_REL	3.8	UP20020121	WINDOWS					
vm112	7020021010	70SP20030909	0	0	726	726	81%	02/12/2005	11:16	INTEL_NT
INTEL_NT	QA70-1	COMPARE_REL	3.8	UP20020121	WINDOWS					
vm113	7020021010	70SP20030909	0	0	732	732	82%	02/12/2005	11:17	INTEL_NT
INTEL_NT	QA70-1	COMPARE_REL	3.8	UP20020121	WINDOWS					
vm114	7020021010	70SP20030909	0	0	693	693	80%	02/12/2005	11:17	INTEL_NT
INTEL_NT	QA70-1	COMPARE_REL	3.8	UP20020121	WINDOWS					
vm115	7020021010	70SP20030909	0	0	604	604	78%	02/12/2005	11:17	INTEL_NT
INTEL_NT	QA70-1	COMPARE_REL	3.8	UP20020121	WINDOWS					
vm116	7020021010	70SP20030909	0	0	830	830	84%	02/12/2005	11:17	INTEL_NT
INTEL_NT	QA70-1	COMPARE_REL	3.8	UP20020121	WINDOWS					
vm117	7020021010	70SP20030909	0	0	1048	1048	86%	02/12/2005	11:17	INTEL_NT
INTEL_NT	QA70-1	COMPARE_REL	3.8	UP20020121	WINDOWS					
vm118	7020021010	70SP20030909	0	0	918	918	85%	02/12/2005	11:17	INTEL_NT
INTEL_NT	QA70-1	COMPARE_REL	3.8	UP20020121	WINDOWS					
vm119	7020021010	70SP20030909	0	0	1225	1225	89%	02/12/2005	11:17	INTEL_NT
INTEL_NT	QA70-1	COMPARE_REL	3.8	UP20020121	WINDOWS					
vm120	7020021010	70SP20030909	0	0	485	485	72%	02/12/2005	11:17	INTEL_NT
INTEL_NT	QA70-1	COMPARE_REL	3.8	UP20020121	WINDOWS					
vm121	7020021010	70SP20030909	0	0	811	811	83%	02/12/2005	11:18	INTEL_NT
INTEL_NT	QA70-1	COMPARE_REL	3.8	UP20020121	WINDOWS					
vm122	7020021010	70SP20030909	0	0	422	422	68%	02/12/2005	11:18	INTEL_NT
INTEL_NT	QA70-1	COMPARE_REL	3.8	UP20020121	WINDOWS					
vm123	7020021010	70SP20030909	0	0	467	467	71%	02/12/2005	11:18	INTEL_NT
INTEL_NT	QA70-1	COMPARE_REL	3.8	UP20020121	WINDOWS					
vm124	7020021010	70SP20030909	0	0	591	591	77%	02/12/2005	11:18	INTEL_NT
INTEL_NT	QA70-1	COMPARE_REL	3.8	UP20020121	WINDOWS					
vm125	7020021010	70SP20030909	0	0	762	762	82%	02/12/2005	11:18	INTEL_NT
INTEL_NT	QA70-1	COMPARE_REL	3.8	UP20020121	WINDOWS					
vm126	7020021010	70SP20030909	0	0	661	661	80%	02/12/2005	11:18	INTEL_NT
INTEL_NT	QA70-1	COMPARE_REL	3.8	UP20020121	WINDOWS					
vm127	7020021010	70SP20030909	0	0	625	625	79%	02/12/2005	11:18	INTEL_NT
INTEL_NT	QA70-1	COMPARE_REL	3.8	UP20020121	WINDOWS					
vm128	7020021010	70SP20030909	0	0	815	815	83%	02/12/2005	11:18	INTEL_NT
INTEL_NT	QA70-1	COMPARE_REL	3.8	UP20020121	WINDOWS					
vm129	7020021010	70SP20030909	0	0	373	373	66%	02/12/2005	11:18	INTEL_NT
INTEL_NT	QA70-1	COMPARE_REL	3.8	UP20020121	WINDOWS					

vm130	7020021010	70SP20030909	0	0	553	553	78%	02/12/2005	11:18	INTEL_NT
INTEL_NT	QA70-1	COMPARE_REL	3.8	UP20020121	WINDOWS					
vm131	7020021010	70SP20030909	0	0	448	448	70%	02/12/2005	11:18	INTEL_NT
INTEL_NT	QA70-1	COMPARE_REL	3.8	UP20020121	WINDOWS					
vm132	7020021010	70SP20030909	0	0	1827	1827	93%	02/12/2005	11:18	INTEL_NT
INTEL_NT	QA70-1	COMPARE_REL	3.8	UP20020121	WINDOWS					
vm133	7020021010	70SP20030909	0	0	1701	1701	92%	02/12/2005	11:18	INTEL_NT
INTEL_NT	QA70-1	COMPARE_REL	3.8	UP20020121	WINDOWS					
vm134	7020021010	70SP20030909	0	0	1808	1808	93%	02/12/2005	11:19	INTEL_NT
INTEL_NT	QA70-1	COMPARE_REL	3.8	UP20020121	WINDOWS					
vm135	7020021010	70SP20030909	0	0	561	561	77%	02/12/2005	11:19	INTEL_NT
INTEL_NT	QA70-1	COMPARE_REL	3.8	UP20020121	WINDOWS					
vm136	7020021010	70SP20030909	0	0	1909	1909	93%	02/12/2005	11:19	INTEL_NT
INTEL_NT	QA70-1	COMPARE_REL	3.8	UP20020121	WINDOWS					
vm137	7020021010	70SP20030909	0	0	1395	1395	91%	02/12/2005	11:19	INTEL_NT
INTEL_NT	QA70-1	COMPARE_REL	3.8	UP20020121	WINDOWS					
vm138	7020021010	70SP20030909	0	0	528	528	75%	02/12/2005	11:19	INTEL_NT
INTEL_NT	QA70-1	COMPARE_REL	3.8	UP20020121	WINDOWS					
vm139	7020021010	70SP20030909	0	0	1132	1132	88%	02/12/2005	11:19	INTEL_NT
INTEL_NT	QA70-1	COMPARE_REL	3.8	UP20020121	WINDOWS					
vm140	7020021010	70SP20030909	0	0	1184	1184	89%	02/12/2005	11:19	INTEL_NT
INTEL_NT	QA70-1	COMPARE_REL	3.8	UP20020121	WINDOWS					
vm141	7020021010	70SP20030909	0	0	2040	2040	93%	02/12/2005	11:19	INTEL_NT
INTEL_NT	QA70-1	COMPARE_REL	3.8	UP20020121	WINDOWS					
vm142	7020021010	70SP20030909	0	0	879	879	85%	02/12/2005	11:19	INTEL_NT
INTEL_NT	QA70-1	COMPARE_REL	3.8	UP20020121	WINDOWS					
vm143	7020021010	70SP20030909	0	0	1672	1672	91%	02/12/2005	11:20	INTEL_NT
INTEL_NT	QA70-1	COMPARE_REL	3.8	UP20020121	WINDOWS					
vm144	7020021010	70SP20030909	0	0	2164	2164	94%	02/12/2005	11:20	INTEL_NT
INTEL_NT	QA70-1	COMPARE_REL	3.8	UP20020121	WINDOWS					
vm145	7020021010	70SP20030909	0	0	532	532	75%	02/12/2005	11:20	INTEL_NT
INTEL_NT	QA70-1	COMPARE_REL	3.8	UP20020121	WINDOWS					
vm146	7020021010	70SP20030909	0	0	883	883	86%	02/12/2005	11:20	INTEL_NT
INTEL_NT	QA70-1	COMPARE_REL	3.8	UP20020121	WINDOWS					
vm147	7020021010	70SP20030909	0	0	588	588	77%	02/12/2005	11:20	INTEL_NT
INTEL_NT	QA70-1	COMPARE_REL	3.8	UP20020121	WINDOWS					
vm148	7020021010	70SP20030909	0	0	588	588	78%	02/12/2005	11:20	INTEL_NT
INTEL_NT	QA70-1	COMPARE_REL	3.8	UP20020121	WINDOWS					
vm149	7020021010	70SP20030909	0	0	520	520	74%	02/12/2005	11:20	INTEL_NT
INTEL_NT	QA70-1	COMPARE_REL	3.8	UP20020121	WINDOWS					
vm150	7020021010	70SP20030909	0	0	657	657	79%	02/12/2005	11:20	INTEL_NT
INTEL_NT	QA70-1	COMPARE_REL	3.8	UP20020121	WINDOWS					
vm151	7020021010	70SP20030909	0	0	1058	1058	87%	02/12/2005	11:20	INTEL_NT
INTEL_NT	QA70-1	COMPARE_REL	3.8	UP20020121	WINDOWS					

vm152	7020021010	70SP20030909	0	0	1211	1211	88%	02/12/2005	11:20	INTEL_NT
INTEL_NT	QA70-1	COMPARE_REL	3.8		UP20020121	WINDOWS				
vm153	7020021010	70SP20030909	0	0	507	507	74%	02/12/2005	11:20	INTEL_NT
INTEL_NT	QA70-1	COMPARE_REL	3.8		UP20020121	WINDOWS				
vm154	7020021010	70SP20030909	0	0	814	814	82%	02/12/2005	11:20	INTEL_NT
INTEL_NT	QA70-1	COMPARE_REL	3.8		UP20020121	WINDOWS				
vm155	7020021010	70SP20030909	0	0	1255	1255	89%	02/12/2005	11:24	INTEL_NT
INTEL_NT	QA70-1	COMPARE_REL	3.8		UP20020121	WINDOWS				
vm156	7020021010	70SP20030909	0	0	2047	2047	94%	02/12/2005	11:24	INTEL_NT
INTEL_NT	QA70-1	COMPARE_REL	3.8		UP20020121	WINDOWS				
vm157	7020021010	70SP20030909	0	0	952	952	85%	02/12/2005	11:24	INTEL_NT
INTEL_NT	QA70-1	COMPARE_REL	3.8		UP20020121	WINDOWS				
vm158	7020021010	70SP20030909	0	0	955	955	87%	02/12/2005	11:25	INTEL_NT
INTEL_NT	QA70-1	COMPARE_REL	3.8		UP20020121	WINDOWS				
vm159	7020021010	70SP20030909	0	0	1524	1524	91%	02/12/2005	11:25	INTEL_NT
INTEL_NT	QA70-1	COMPARE_REL	3.8		UP20020121	WINDOWS				
vm160	7020021010	70SP20030909	0	0	600	600	78%	02/12/2005	11:25	INTEL_NT
INTEL_NT	QA70-1	COMPARE_REL	3.8		UP20020121	WINDOWS				
vm161	7020021010	70SP20030909	0	0	539	539	75%	02/12/2005	11:25	INTEL_NT
INTEL_NT	QA70-1	COMPARE_REL	3.8		UP20020121	WINDOWS				
vm162	7020021010	70SP20030909	0	0	548	548	76%	02/12/2005	11:25	INTEL_NT
INTEL_NT	QA70-1	COMPARE_REL	3.8		UP20020121	WINDOWS				
vm163	7020021010	70SP20030909	0	0	563	563	76%	02/12/2005	11:25	INTEL_NT
INTEL_NT	QA70-1	COMPARE_REL	3.8		UP20020121	WINDOWS				
vm164	7020021010	70SP20030909	0	0	556	556	76%	02/12/2005	11:25	INTEL_NT
INTEL_NT	QA70-1	COMPARE_REL	3.8		UP20020121	WINDOWS				
vm165	7020021010	70SP20030909	0	0	703	703	80%	02/12/2005	11:25	INTEL_NT
INTEL_NT	QA70-1	COMPARE_REL	3.8		UP20020121	WINDOWS				
vm166	7020021010	70SP20030909	0	0	700	700	80%	02/12/2005	11:25	INTEL_NT
INTEL_NT	QA70-1	COMPARE_REL	3.8		UP20020121	WINDOWS				
vm167	7020021010	70SP20030909	0	0	1138	1138	88%	02/12/2005	11:25	INTEL_NT
INTEL_NT	QA70-1	COMPARE_REL	3.8		UP20020121	WINDOWS				
vm168	7020021010	70SP20030909	0	0	687	687	81%	02/12/2005	11:25	INTEL_NT
INTEL_NT	QA70-1	COMPARE_REL	3.8		UP20020121	WINDOWS				
vm169	7020021010	70SP20030909	0	0	777	777	82%	02/12/2005	11:25	INTEL_NT
INTEL_NT	QA70-1	COMPARE_REL	3.8		UP20020121	WINDOWS				
vm170	7020021010	70SP20030909	0	0	436	436	69%	02/12/2005	11:25	INTEL_NT
INTEL_NT	QA70-1	COMPARE_REL	3.8		UP20020121	WINDOWS				
vm171	7020021010	70SP20030909	0	0	759	759	82%	02/12/2005	11:25	INTEL_NT
INTEL_NT	QA70-1	COMPARE_REL	3.8		UP20020121	WINDOWS				
vm172	7020021010	70SP20030909	0	0	1528	1528	90%	02/12/2005	11:25	INTEL_NT
INTEL_NT	QA70-1	COMPARE_REL	3.8		UP20020121	WINDOWS				
vm173	7020021010	70SP20030909	0	0	545	545	75%	02/12/2005	11:26	INTEL_NT
INTEL_NT	QA70-1	COMPARE_REL	3.8		UP20020121	WINDOWS				

vm174	7020021010	70SP20030909	0	0	602	602	77%	02/12/2005	11:26	INTEL_NT
INTEL_NT	QA70-1	COMPARE_REL	3.8	UP20020121	WINDOWS					
vm175	7020021010	70SP20030909	0	0	855	855	84%	02/12/2005	11:26	INTEL_NT
INTEL_NT	QA70-1	COMPARE_REL	3.8	UP20020121	WINDOWS					
vm176	7020021010	70SP20030909	0	0	999	999	86%	02/12/2005	11:26	INTEL_NT
INTEL_NT	QA70-1	COMPARE_REL	3.8	UP20020121	WINDOWS					
vm177	7020021010	70SP20030909	0	0	1127	1127	87%	02/12/2005	11:26	INTEL_NT
INTEL_NT	QA70-1	COMPARE_REL	3.8	UP20020121	WINDOWS					
vm178	7020021010	70SP20030909	0	0	679	679	80%	02/12/2005	11:26	INTEL_NT
INTEL_NT	QA70-1	COMPARE_REL	3.8	UP20020121	WINDOWS					
vm179	7020021010	70SP20030909	0	0	768	768	82%	02/12/2005	11:27	INTEL_NT
INTEL_NT	QA70-1	COMPARE_REL	3.8	UP20020121	WINDOWS					
vm180	7020021010	70SP20030909	0	0	651	651	79%	02/12/2005	11:27	INTEL_NT
INTEL_NT	QA70-1	COMPARE_REL	3.8	UP20020121	WINDOWS					
vm181	7020021010	70SP20030909	0	0	484	484	71%	02/12/2005	11:27	INTEL_NT
INTEL_NT	QA70-1	COMPARE_REL	3.8	UP20020121	WINDOWS					
vm182	7020021010	70SP20030909	0	0	973	973	87%	02/12/2005	11:27	INTEL_NT
INTEL_NT	QA70-1	COMPARE_REL	3.8	UP20020121	WINDOWS					
vm183	7020021010	70SP20030909	0	0	722	722	81%	02/12/2005	11:27	INTEL_NT
INTEL_NT	QA70-1	COMPARE_REL	3.8	UP20020121	WINDOWS					
vm184	7020021010	70SP20030909	1	5	3162	3162	95%	02/12/2005	11:27	INTEL_NT
INTEL_NT	QA70-1	COMPARE_REL	3.8	UP20020121	WINDOWS					
vm185	7020021010	70SP20030909	0	0	738	738	81%	02/12/2005	11:27	INTEL_NT
INTEL_NT	QA70-1	COMPARE_REL	3.8	UP20020121	WINDOWS					
vm186	7020021010	70SP20030909	0	0	1392	1392	91%	02/12/2005	11:27	INTEL_NT
INTEL_NT	QA70-1	COMPARE_REL	3.8	UP20020121	WINDOWS					
vm187	7020021010	70SP20030909	0	0	1489	1489	90%	02/12/2005	11:28	INTEL_NT
INTEL_NT	QA70-1	COMPARE_REL	3.8	UP20020121	WINDOWS					
vm188	7020021010	70SP20030909	0	0	658	658	79%	02/12/2005	11:28	INTEL_NT
INTEL_NT	QA70-1	COMPARE_REL	3.8	UP20020121	WINDOWS					
vm189	7020021010	70SP20030909	0	0	1067	1067	87%	02/12/2005	11:28	INTEL_NT
INTEL_NT	QA70-1	COMPARE_REL	3.8	UP20020121	WINDOWS					
vm190	7020021010	70SP20030909	0	0	715	715	81%	02/12/2005	11:28	INTEL_NT
INTEL_NT	QA70-1	COMPARE_REL	3.8	UP20020121	WINDOWS					
vm191	7020021010	70SP20030909	0	0	3075	3075	95%	02/12/2005	11:28	INTEL_NT
INTEL_NT	QA70-1	COMPARE_REL	3.8	UP20020121	WINDOWS					
vm192	7020021010	70SP20030909	0	0	645	645	80%	02/12/2005	11:28	INTEL_NT
INTEL_NT	QA70-1	COMPARE_REL	3.8	UP20020121	WINDOWS					
vm193	7020021010	70SP20030909	0	0	411	411	68%	02/12/2005	11:28	INTEL_NT
INTEL_NT	QA70-1	COMPARE_REL	3.8	UP20020121	WINDOWS					
vm194	7020021010	70SP20030909	0	0	821	821	83%	02/12/2005	11:29	INTEL_NT
INTEL_NT	QA70-1	COMPARE_REL	3.8	UP20020121	WINDOWS					
vm195	7020021010	70SP20030909	0	0	824	824	84%	02/12/2005	11:29	INTEL_NT
INTEL_NT	QA70-1	COMPARE_REL	3.8	UP20020121	WINDOWS					

vm196	7020021010	70SP20030909	0	0	505	505	73%	02/12/2005	11:29	INTEL_NT
INTEL_NT	QA70-1	COMPARE_REL	3.8	UP20020121	WINDOWS					
vm197	7020021010	70SP20030909	0	0	509	509	74%	02/12/2005	11:29	INTEL_NT
INTEL_NT	QA70-1	COMPARE_REL	3.8	UP20020121	WINDOWS					
vm198	7020021010	70SP20030909	2	0	1208	1208	88%	02/12/2005	11:29	INTEL_NT
INTEL_NT	QA70-1	COMPARE_REL	3.8	UP20020121	WINDOWS					
vm199	7020021010	70SP20030909	0	0	835	835	84%	02/12/2005	11:30	INTEL_NT
INTEL_NT	QA70-1	COMPARE_REL	3.8	UP20020121	WINDOWS					
vm200	7020021010	70SP20030909	0	0	1258	1258	89%	02/12/2005	11:32	INTEL_NT
INTEL_NT	QA70-1	COMPARE_REL	3.8	UP20020121	WINDOWS					
vm201	7020021010	70SP20030909	0	0	3072	3072	95%	02/12/2005	11:32	INTEL_NT
INTEL_NT	QA70-1	COMPARE_REL	3.8	UP20020121	WINDOWS					
vm202	7020021010	70SP20030909	0	0	604	604	77%	02/12/2005	11:32	INTEL_NT
INTEL_NT	QA70-1	COMPARE_REL	3.8	UP20020121	WINDOWS					
vm203	7020021010	70SP20030909	0	0	1020	1020	87%	02/12/2005	11:32	INTEL_NT
INTEL_NT	QA70-1	COMPARE_REL	3.8	UP20020121	WINDOWS					
vm204	7020021010	70SP20030909	0	0	621	621	79%	02/12/2005	11:33	INTEL_NT
INTEL_NT	QA70-1	COMPARE_REL	3.8	UP20020121	WINDOWS					
vm205	7020021010	70SP20030909	0	0	652	652	79%	02/12/2005	11:33	INTEL_NT
INTEL_NT	QA70-1	COMPARE_REL	3.8	UP20020121	WINDOWS					
vm206	7020021010	70SP20030909	0	0	903	903	84%	02/12/2005	11:33	INTEL_NT
INTEL_NT	QA70-1	COMPARE_REL	3.8	UP20020121	WINDOWS					
vm207	7020021010	70SP20030909	0	0	1079	1079	87%	02/12/2005	11:33	INTEL_NT
INTEL_NT	QA70-1	COMPARE_REL	3.8	UP20020121	WINDOWS					
vm208	7020021010	70SP20030909	0	0	701	701	82%	02/12/2005	11:33	INTEL_NT
INTEL_NT	QA70-1	COMPARE_REL	3.8	UP20020121	WINDOWS					
vm209	7020021010	70SP20030909	0	0	3159	3159	96%	02/12/2005	11:34	INTEL_NT
INTEL_NT	QA70-1	COMPARE_REL	3.8	UP20020121	WINDOWS					
vm210	7020021010	70SP20030909	0	0	1426	1426	90%	02/12/2005	11:35	INTEL_NT
INTEL_NT	QA70-1	COMPARE_REL	3.8	UP20020121	WINDOWS					
vm211	7020021010	70SP20030909	0	0	2658	2658	94%	02/12/2005	11:36	INTEL_NT
INTEL_NT	QA70-1	COMPARE_REL	3.8	UP20020121	WINDOWS					
vm212	7020021010	70SP20030909	0	0	1041	1041	86%	02/12/2005	11:36	INTEL_NT
INTEL_NT	QA70-1	COMPARE_REL	3.8	UP20020121	WINDOWS					
vm213	7020021010	70SP20030909	0	0	687	687	80%	02/12/2005	11:36	INTEL_NT
INTEL_NT	QA70-1	COMPARE_REL	3.8	UP20020121	WINDOWS					
vm214	7020021010	70SP20030909	0	0	557	557	76%	02/12/2005	11:36	INTEL_NT
INTEL_NT	QA70-1	COMPARE_REL	3.8	UP20020121	WINDOWS					
vm215	7020021010	70SP20030909	0	0	637	637	80%	02/12/2005	11:36	INTEL_NT
INTEL_NT	QA70-1	COMPARE_REL	3.8	UP20020121	WINDOWS					
vm216	7020021010	70SP20030909	0	0	1111	1111	87%	02/12/2005	11:37	INTEL_NT
INTEL_NT	QA70-1	COMPARE_REL	3.8	UP20020121	WINDOWS					
vm217	7020021010	70SP20030909	0	0	873	873	84%	02/12/2005	11:37	INTEL_NT
INTEL_NT	QA70-1	COMPARE_REL	3.8	UP20020121	WINDOWS					

vm218	7020021010	70SP20030909	0	0	744	744	82%	02/12/2005	11:37	INTEL_NT
INTEL_NT	QA70-1	COMPARE_REL	3.8	UP20020121	WINDOWS					
vm219	7020021010	70SP20030909	0	0	698	698	81%	02/12/2005	11:38	INTEL_NT
INTEL_NT	QA70-1	COMPARE_REL	3.8	UP20020121	WINDOWS					
vm220	7020021010	70SP20030909	0	0	477	477	75%	02/12/2005	11:38	INTEL_NT
INTEL_NT	QA70-1	COMPARE_REL	3.8	UP20020121	WINDOWS					
vm221	7020021010	70SP20030909	0	0	605	605	80%	02/12/2005	11:39	INTEL_NT
INTEL_NT	QA70-1	COMPARE_REL	3.8	UP20020121	WINDOWS					
vm222	7020021010	70SP20030909	0	0	1536	1536	91%	02/12/2005	11:39	INTEL_NT
INTEL_NT	QA70-1	COMPARE_REL	3.8	UP20020121	WINDOWS					
vm223	7020021010	70SP20030909	0	0	484	484	74%	02/12/2005	11:39	INTEL_NT
INTEL_NT	QA70-1	COMPARE_REL	3.8	UP20020121	WINDOWS					
vm224	7020021010	70SP20030909	0	0	577	577	79%	02/12/2005	11:39	INTEL_NT
INTEL_NT	QA70-1	COMPARE_REL	3.8	UP20020121	WINDOWS					
vm225	7020021010	70SP20030909	0	0	496	496	73%	02/12/2005	11:39	INTEL_NT
INTEL_NT	QA70-1	COMPARE_REL	3.8	UP20020121	WINDOWS					
vm226	7020021010	70SP20030909	0	0	1622	1622	91%	02/12/2005	11:42	INTEL_NT
INTEL_NT	QA70-1	COMPARE_REL	3.8	UP20020121	WINDOWS					
vm227	7020021010	70SP20030909	0	0	957	957	87%	02/12/2005	11:42	INTEL_NT
INTEL_NT	QA70-1	COMPARE_REL	3.8	UP20020121	WINDOWS					
vm228	7020021010	70SP20030909	0	0	5849	5849	98%	02/12/2005	11:42	INTEL_NT
INTEL_NT	QA70-1	COMPARE_REL	3.8	UP20020121	WINDOWS					
vm229	7020021010	70SP20030909	0	0	3944	3944	97%	02/12/2005	11:43	INTEL_NT
INTEL_NT	QA70-1	COMPARE_REL	3.8	UP20020121	WINDOWS					
vm230	7020021010	70SP20030909	0	0	26798	26798	99%	02/12/2005	12:03	INTEL_NT
INTEL_NT	QA70-1	COMPARE_REL	3.8	UP20020121	WINDOWS					
vm231	7020021010	70SP20030909	0	0	528	528	76%	02/12/2005	12:03	INTEL_NT
INTEL_NT	QA70-1	COMPARE_REL	3.8	UP20020121	WINDOWS					
vm232	7020021010	70SP20030909	0	0	14057	14057	98%	02/12/2005	12:10	INTEL_NT
INTEL_NT	QA70-1	COMPARE_REL	3.8	UP20020121	WINDOWS					
vm233	7020021010	70SP20030909	0	0	583	583	80%	02/12/2005	12:12	INTEL_NT
INTEL_NT	QA70-1	COMPARE_REL	3.8	UP20020121	WINDOWS					
vm234	7020021010	70SP20030909	0	0	1468	1468	92%	02/12/2005	12:17	INTEL_NT
INTEL_NT	QA70-1	COMPARE_REL	3.8	UP20020121	WINDOWS					
vm235	7020021010	70SP20030909	0	0	769	769	81%	02/12/2005	12:17	INTEL_NT
INTEL_NT	QA70-1	COMPARE_REL	3.8	UP20020121	WINDOWS					
vm236	7020021010	70SP20030909	0	0	1760	1760	92%	02/12/2005	12:18	INTEL_NT
INTEL_NT	QA70-1	COMPARE_REL	3.8	UP20020121	WINDOWS					
vmc1	7020021010	70SP20030909	0	0	643	643	81%	02/12/2005	12:19	INTEL_NT
INTEL_NT	QA70-1	COMPARE_REL	3.8	UP20020121	WINDOWS					
vmc2	7020021010	70SP20030909	0	0	1692	1692	90%	02/12/2005	12:19	INTEL_NT
INTEL_NT	QA70-1	COMPARE_REL	3.8	UP20020121	WINDOWS					
vmc3	7020021010	70SP20030909	0	0	426	426	72%	02/12/2005	12:20	INTEL_NT
INTEL_NT	QA70-1	COMPARE_REL	3.8	UP20020121	WINDOWS					

vmc4	7020021010	70SP20030909	0	0	773	773	85%	02/12/2005	12:20	INTEL_NT
INTEL_NT	QA70-1	COMPARE_REL	3.8	UP20020121	WINDOWS					
vmc5	7020021010	70SP20030909	0	0	513	513	78%	02/12/2005	12:21	INTEL_NT
INTEL_NT	QA70-1	COMPARE_REL	3.8	UP20020121	WINDOWS					
vmc6	7020021010	70SP20030909	0	0	433	433	74%	02/12/2005	12:22	INTEL_NT
INTEL_NT	QA70-1	COMPARE_REL	3.8	UP20020121	WINDOWS					
vmc7	7020021010	70SP20030909	0	0	337	337	67%	02/12/2005	12:22	INTEL_NT
INTEL_NT	QA70-1	COMPARE_REL	3.8	UP20020121	WINDOWS					
vmc8	7020021010	70SP20030909	2	0	1894	1894	92%	02/12/2005	12:56	INTEL_NT
INTEL_NT	QA70-1	COMPARE_REL	3.8	UP20020121	WINDOWS					
vmd1	7020021010	70SP20030909	0	0	816	816	86%	02/12/2005	12:57	INTEL_NT
INTEL_NT	QA70-1	COMPARE_REL	3.8	UP20020121	WINDOWS					
vmd2	7020021010	70SP20030909	0	0	337	337	67%	02/12/2005	12:57	INTEL_NT
INTEL_NT	QA70-1	COMPARE_REL	3.8	UP20020121	WINDOWS					
vmd3	7020021010	70SP20030909	0	0	608	608	82%	02/12/2005	12:59	INTEL_NT
INTEL_NT	QA70-1	COMPARE_REL	3.8	UP20020121	WINDOWS					
cyc-177s	7020021010	70SP20030909	1	0	1219	1222	91%	02/12/2005	13:01	INTEL_NT
INTEL_NT	QA70-1	COMPARE_REL	3.8	UP20020121	WINDOWS					
cyc-178s	7020021010	70SP20030909	1	0	1219	1222	91%	02/12/2005	13:04	INTEL_NT
INTEL_NT	QA70-1	COMPARE_REL	3.8	UP20020121	WINDOWS					
dds-13s	7020021010	NO_UPDATE	-88	0	402	146	49%	02/12/2005	13:04	INTEL_NT
NOT_AVAILABLE	QA70-1	COMPARE_REL	3.8	UP20020121	WINDOWS					
dds-17s	7020021010	NO_UPDATE	-88	0	746	146	67%	02/12/2005	13:04	INTEL_NT
NOT_AVAILABLE	QA70-1	COMPARE_REL	3.8	UP20020121	WINDOWS					
esp-112s	7020021010	70SP20030909	0	0	279	279	58%	02/12/2005	13:04	INTEL_NT
INTEL_NT	QA70-1	COMPARE_REL	3.8	UP20020121	WINDOWS					
esp-124s	7020021010	70SP20030909	0	0	392	392	66%	02/12/2005	13:04	INTEL_NT
INTEL_NT	QA70-1	COMPARE_REL	3.8	UP20020121	WINDOWS					
esp-127s	7020021010	70SP20030909	0	0	527	527	75%	02/12/2005	13:04	INTEL_NT
INTEL_NT	QA70-1	COMPARE_REL	3.8	UP20020121	WINDOWS					
ess-26s	7020021010	70SP20030909	0	0	1846	1846	92%	02/12/2005	13:04	INTEL_NT
INTEL_NT	QA70-1	COMPARE_REL	3.8	UP20020121	WINDOWS					
ess-97s	7020021010	70SP20030909	0	0	1378	1378	90%	02/12/2005	13:04	INTEL_NT
INTEL_NT	QA70-1	COMPARE_REL	3.8	UP20020121	WINDOWS					
ev117-106s	7020021010	70SP20030909	0	0	1333	1333	91%	02/12/2005	13:04	INTEL_NT
INTEL_NT	QA70-1	COMPARE_REL	3.8	UP20020121	WINDOWS					
ev119-35s	7020021010	70SP20030909	0	0	506	506	74%	02/12/2005	13:04	INTEL_NT
INTEL_NT	QA70-1	COMPARE_REL	3.8	UP20020121	WINDOWS					
ev120-85s	7020021010	70SP20030909	0	0	411	411	71%	02/12/2005	13:04	INTEL_NT
INTEL_NT	QA70-1	COMPARE_REL	3.8	UP20020121	WINDOWS					
ev141-208s	7020021010	70SP20030909	0	0	341	341	66%	02/12/2005	13:04	INTEL_NT
INTEL_NT	QA70-1	COMPARE_REL	3.8	UP20020121	WINDOWS					
ev144-13s	7020021010	70SP20030909	0	8	8804	8804	98%	02/12/2005	13:07	INTEL_NT
INTEL_NT	QA70-1	COMPARE_REL	3.8	UP20020121	WINDOWS					

ev144-23s	7020021010	70SP20030909	0	0	1740	1740	92%	02/12/2005	13:10	INTEL_NT
INTEL_NT	QA70-1	COMPARE_REL	3.8	UP20020121	WINDOWS					
ev154-23s	7020021010	70SP20030909	0	0	1259	1259	89%	02/12/2005	13:10	INTEL_NT
INTEL_NT	QA70-1	COMPARE_REL	3.8	UP20020121	WINDOWS					
ev154-25s	7020021010	70SP20030909	0	0	587	587	76%	02/12/2005	13:10	INTEL_NT
INTEL_NT	QA70-1	COMPARE_REL	3.8	UP20020121	WINDOWS					
ev171-57s	7020021010	70SP20030909	0	0	542	542	79%	02/12/2005	13:10	INTEL_NT
INTEL_NT	QA70-1	COMPARE_REL	3.8	UP20020121	WINDOWS					
ev173-53s	7020021010	70SP20030909	1	0	1426	1429	92%	02/12/2005	13:11	INTEL_NT
INTEL_NT	QA70-1	COMPARE_REL	3.8	UP20020121	WINDOWS					
ev174-46s	7020021010	70SP20030909	0	0	562	562	80%	02/12/2005	13:11	INTEL_NT
INTEL_NT	QA70-1	COMPARE_REL	3.8	UP20020121	WINDOWS					
ev175-20s	7020021010	70SP20030909	1	0	538	541	79%	02/12/2005	13:11	INTEL_NT
INTEL_NT	QA70-1	COMPARE_REL	3.8	UP20020121	WINDOWS					
ev175-21s	7020021010	NO_UPDATE	-88	0	566	146	64%	02/12/2005	13:11	INTEL_NT
NOT AVAILABLE	QA70-1	COMPARE_REL	3.8	UP20020121	WINDOWS					
ev175-38s	7020021010	70SP20030909	0	0	808	808	85%	02/12/2005	13:11	INTEL_NT
INTEL_NT	QA70-1	COMPARE_REL	3.8	UP20020121	WINDOWS					
ev182-zbdpg11s	7020021010	70SP20030909	0	0	660	660	83%	02/12/2005	13:11	INTEL_NT
INTEL_NT	QA70-1	COMPARE_REL	3.8	UP20020121	WINDOWS					
ev183-zdpl20s	7020021010	70SP20030909	0	0	577	577	80%	02/12/2005	13:11	INTEL_NT
INTEL_NT	QA70-1	COMPARE_REL	3.8	UP20020121	WINDOWS					
ev184-02s	7020021010	70SP20030909	0	0	267	267	56%	02/12/2005	13:12	INTEL_NT
INTEL_NT	QA70-1	COMPARE_REL	3.8	UP20020121	WINDOWS					
ev184-07s	7020021010	70SP20030909	0	0	661	661	80%	02/12/2005	13:12	INTEL_NT
INTEL_NT	QA70-1	COMPARE_REL	3.8	UP20020121	WINDOWS					
ev35-23s	7020021010	70SP20030909	0	0	293	293	61%	02/12/2005	13:12	INTEL_NT
INTEL_NT	QA70-1	COMPARE_REL	3.8	UP20020121	WINDOWS					
ev95-45s	7020021010	70SP20030909	0	0	892	892	85%	02/12/2005	13:12	INTEL_NT
INTEL_NT	QA70-1	COMPARE_REL	3.8	UP20020121	WINDOWS					
ev97-73s	7020021010	70SP20030909	0	0	621	621	82%	02/12/2005	13:12	INTEL_NT
INTEL_NT	QA70-1	COMPARE_REL	3.8	UP20020121	WINDOWS					
f1o-136s	7020021010	70SP20030909	0	0	419	419	73%	02/12/2005	13:12	INTEL_NT
INTEL_NT	QA70-1	COMPARE_REL	3.8	UP20020121	WINDOWS					
f1o-138s	7020021010	70SP20030909	0	0	352	352	68%	02/12/2005	13:13	INTEL_NT
INTEL_NT	QA70-1	COMPARE_REL	3.8	UP20020121	WINDOWS					
inrt-16s	7020021010	70SP20030909	1	0	484	486	77%	02/12/2005	13:13	INTEL_NT
INTEL_NT	QA70-1	COMPARE_REL	3.8	UP20020121	WINDOWS					
inrt-9s	7020021010	70SP20030909	0	0	421	421	73%	02/12/2005	13:13	INTEL_NT
INTEL_NT	QA70-1	COMPARE_REL	3.8	UP20020121	WINDOWS					
mvhy-bk501	7020021010	70SP20030909	0	0	536	536	78%	02/12/2005	13:13	INTEL_NT
INTEL_NT	QA70-1	COMPARE_REL	3.8	UP20020121	WINDOWS					
mvhy-gt202	7020021010	70SP20030909	0	0	780	780	84%	02/12/2005	13:14	INTEL_NT
INTEL_NT	QA70-1	COMPARE_REL	3.8	UP20020121	WINDOWS					

mvve-cr003	7020021010	70SP20030909	0	0	328	328	65%	02/12/2005	13:15	INTEL_NT
INTEL_NT	QA70-1	COMPARE_REL	3.8	UP20020121	WINDOWS					
mvve-cr804	7020021010	70SP20030909	0	0	329	329	65%	02/12/2005	13:16	INTEL_NT
INTEL_NT	QA70-1	COMPARE_REL	3.8	UP20020121	WINDOWS					
se-1s	7020021010	70SP20030909	0	0	400	400	72%	02/12/2005	13:16	INTEL_NT
INTEL_NT	QA70-1	COMPARE_REL	3.8	UP20020121	WINDOWS					
se-20s	7020021010	70SP20030909	0	0	879	879	85%	02/12/2005	13:16	INTEL_NT
INTEL_NT	QA70-1	COMPARE_REL	3.8	UP20020121	WINDOWS					
sx120-1s	7020021010	NO_UPDATE	-88	0	248	146	30%	02/12/2005	13:16	INTEL_NT
NOT_AVAILABLE	QA70-1	COMPARE_REL	3.8	UP20020121	WINDOWS					
tbc-155s	7020021010	70SP20030909	0	0	351	351	64%	02/12/2005	13:16	INTEL_NT
INTEL_NT	QA70-1	COMPARE_REL	3.8	UP20020121	WINDOWS					

RPP-RPT-28967, Rev. 1

1

```
00000000          VERSION=INTEL NT          RELEASE= 7.0          UP20021010

EXPECTED COMPARE DIFFERENCE FOUND AT  NG=  113 NT=  113
G= 00000000          VERSION=INTEL NT          RELEASE= 7.0          UP20021010
T= 00292062          VERSION=INTEL NT          RELEASE= 7.0SP11 UP20030909
```

```
EXPECTED COMPARE DIFFERENCE FOUND AT  NG=  114 NT=  114
G= CURRENT JOBNAME=c0231  10:37:04  OCT 15, 2002 CP=          0.219
T= CURRENT JOBNAME=c0231  11:04:48  FEB 12, 2005 CP=          0.156
```

```
0 /verify,c0231
```

```
0 /title, c0231 (fsk) Unmatched nodes mapping
```

```
COMPARE DIFFERENCE FOUND AT          NG=  192 NT=  192
G= NODAL RESULTS ARE FOR CYCLIC SECTOR  1 - PHASE ANGLE =          30.580
T= NODAL RESULTS ARE FOR CYCLIC SECTOR  1 - PHASE ANGLE =          237.330
```

```
COMPARE DIFFERENCE FOUND AT          NG=  219 NT=  219
G= NODAL RESULTS ARE FOR CYCLIC SECTOR  2 - PHASE ANGLE =          30.580
T= NODAL RESULTS ARE FOR CYCLIC SECTOR  2 - PHASE ANGLE =          237.330
```

```
COMPARE DIFFERENCE FOUND AT          NG=  246 NT=  246
G= NODAL RESULTS ARE FOR CYCLIC SECTOR  3 - PHASE ANGLE =          30.580
T= NODAL RESULTS ARE FOR CYCLIC SECTOR  3 - PHASE ANGLE =          237.330
```

```
BOTTOM OF GOOD FILE REACHED AT LINE    289
G= |                                ANSYS RUN COMPLETED
```

```
~~~~~
NOTE- NONSTANDARD COMPARE - DIFOPT NAME QA70-1  HAS BEEN USED
NUMBER OF LINES SKIPPED IN GOOD FILE(BLANK LINES EXCLUDED) -      0
NUMBER OF LINES SKIPPED IN TEST FILE(BLANK LINES EXCLUDED) -      0
NUMBER OF LINES ON GOOD FILE WITH STRINGS CONDENSED OUT    -      0
NUMBER OF LINES ON TEST FILE WITH STRINGS CONDENSED OUT    -      0
~~~~~
```

```
*****
COMPARE ERRORS =          3          *
*****
```

=====

===

```
PROBLEM: c0231          COMPARE OPTIONS  COMPARE_REL 3.8 UP20020121
WINDOWS
```

```
ALMOST ZERO (GOOD)    = 1.0000E-006          KROUND (DROP LAST DIGIT)=  1
```

RPP-RPT-28967, Rev. 1

ALMOST ZERO (TEST)	= 1.0000E-006	KABSPR (0=SUMMARY 1=ALL)=	1
ABSOLUTE VALUE TOL	= 1.0000E-010	KSKIP(SKIP=ERR 0=Y, 1=N)=	0
FRACTIONAL DIFFERENCE=	1.0000E-004	MAXERR (STOP WHEN ERRS)=	100
ABSOLUTE DIFFERENCE	= 1.0000E-006	MAXBUF (# LINES TO SCAN)=	6
		KNOWN (# OF KNOWN ERRS)=	0
		GREAD, TREAD =	1, 1

=====

===

LINES ON GOOD FILE =	304
LINES ON TEST FILE =	304

RPP-RPT-28967, Rev. 1

1

00000000 VERSION=INTEL NT RELEASE= 7.0 UP20021010

EXPECTED COMPARE DIFFERENCE FOUND AT NG= 113 NT= 113
G= 00000000 VERSION=INTEL NT RELEASE= 7.0 UP20021010
T= 00292062 VERSION=INTEL NT RELEASE= 7.0SP11 UP20030909

EXPECTED COMPARE DIFFERENCE FOUND AT NG= 114 NT= 114
G= CURRENT JOBNAME=vm184 20:46:18 OCT 15, 2002 CP= 0.250
T= CURRENT JOBNAME=vm184 11:27:32 FEB 12, 2005 CP= 0.297

0 /VERIFY,VM184

0 /TITLE, VM184, STRAIGHT CANTILEVER BEAM

0 /stitle,1,Reason COMPARE differences are acceptable:

0 /stitle,2, mesher accuracy - element number on warning;
near-zero values

0 /TITLE, VM184, STRAIGHT CANTILEVER BEAM

NOW COMPARING LINES FROM ***** ANSYS ANALYSIS DEFINITION (PREP7)

NOW COMPARING LINES FROM ***** ANSYS RESULTS INTERPRETATION (POST1)

ABSOLUTE VALUE DIFFERENCE FOUND AT NG= 926 NT= 926
G= VALUE -0.24849E-01 0.98917 -0.43496E-05 0.98948
T= VALUE -0.24849E-01 0.98917 0.43497E-05 0.98948

ABSOLUTE VALUE DIFFERENCE FOUND AT NG= 982 NT= 982
G= VALUE -0.53544E-02-0.26671E-05 0.42554 0.42557
T= VALUE -0.53544E-02 0.26671E-05 0.42554 0.42557

ABSOLUTE VALUE DIFFERENCE FOUND AT NG= 1011 NT= 1011
G= VALUE -0.12394E-01-0.61739E-05 0.98504 0.98511
T= VALUE -0.12394E-01 0.61739E-05 0.98504 0.98511

NOW COMPARING LINES FROM ***** ANSYS ANALYSIS DEFINITION (PREP7)

NOW COMPARING LINES FROM ***** ANSYS RESULTS INTERPRETATION (POST1)

COMPARE DIFFERENCE FOUND AT NG= 1580 NT= 1580
G= VALUE 0.24811E-01 0.98813 -0.43696E-05 0.98844
T= VALUE 0.24811E-01 0.98813 0.43701E-05 0.98844

RPP-RPT-28967, Rev. 1

ABSOLUTE VALUE DIFFERENCE FOUND AT NG= 1639 NT= 1639
G= VALUE -0.53533E-02-0.30755E-05 0.42553 0.42556
T= VALUE -0.53533E-02 0.30756E-05 0.42553 0.42556

ABSOLUTE VALUE DIFFERENCE FOUND AT NG= 1673 NT= 1673
G= VALUE -0.12392E-01-0.71193E-05 0.98502 0.98510
T= VALUE -0.12392E-01 0.71194E-05 0.98502 0.98510

NOW COMPARING LINES FROM ***** ANSYS ANALYSIS DEFINITION (PREP7)

NOW COMPARING LINES FROM ***** ANSYS RESULTS INTERPRETATION (POST1)

NOW COMPARING LINES FROM ***** ANSYS ANALYSIS DEFINITION (PREP7)

NOW COMPARING LINES FROM ***** ANSYS RESULTS INTERPRETATION (POST1)

BOTTOM OF GOOD FILE REACHED AT LINE 3147
G= | ANSYS RUN COMPLETED
|

~~~~~  
NOTE- NONSTANDARD COMPARE - DIFOPT NAME QA70-1 HAS BEEN USED  
NUMBER OF LINES SKIPPED IN GOOD FILE(BLANK LINES EXCLUDED) - 0  
NUMBER OF LINES SKIPPED IN TEST FILE(BLANK LINES EXCLUDED) - 0  
NUMBER OF LINES ON GOOD FILE WITH STRINGS CONDENSED OUT - 0  
NUMBER OF LINES ON TEST FILE WITH STRINGS CONDENSED OUT - 0  
~~~~~

COMPARE ERRORS = 1 *

WARNING - 5 ABSOLUTE VALUE DIFFERENCE(S) FOUND.

NOTE - 1 summary line(s) contained absolute value differences.

=====
===

RPP-RPT-28967, Rev. 1

PROBLEM: vm184
WINDOWS

COMPARE OPTIONS COMPARE_REL 3.8 UP20020121

ALMOST ZERO (GOOD) = 1.0000E-006
ALMOST ZERO (TEST) = 1.0000E-006
ABSOLUTE VALUE TOL = 1.0000E-010
FRACTIONAL DIFFERENCE= 1.0000E-004
ABSOLUTE DIFFERENCE = 1.0000E-006

KROUND (DROP LAST DIGIT)= 1
KABSPR (0=SUMMARY 1=ALL)= 1
KSKIP(SKIP=ERR 0=Y, 1=N)= 0
MAXERR (STOP WHEN ERRS)= 100
MAXBUF (# LINES TO SCAN)= 6
KNOWN (# OF KNOWN ERRS)= 0
GREAD, TREAD = 1, 1

=====
===

Lines on GOOD file = 3162
Lines on TEST file = 3162

RPP-RPT-28967, Rev. 1

1

00000000 VERSION=INTEL NT RELEASE= 7.0 UP20021010

EXPECTED COMPARE DIFFERENCE FOUND AT NG= 113 NT= 113
G= 00000000 VERSION=INTEL NT RELEASE= 7.0 UP20021010
T= 00292062 VERSION=INTEL NT RELEASE= 7.0SP11 UP20030909

EXPECTED COMPARE DIFFERENCE FOUND AT NG= 114 NT= 114
G= CURRENT JOBNAME=vm198 20:50:49 OCT 15, 2002 CP= 0.266
T= CURRENT JOBNAME=vm198 11:29:13 FEB 12, 2005 CP= 0.172

0 /VERIFY,VM198

0 /TITLE, VM198, LARGE STRAIN IN-PLANE TORSION TEST (%EL%)

NOW COMPARING LINES FROM ***** ANSYS ANALYSIS DEFINITION (PREP7)

NOW COMPARING LINES FROM ***** ANSYS RESULTS INTERPRETATION (POST1)

NOW COMPARING LINES FROM ***** TIME-HISTORY POSTPROCESSOR (POST26)

NOW COMPARING LINES FROM ***** ANSYS ANALYSIS DEFINITION (PREP7)

COMPARE DIFFERENCE FOUND AT NG= 618 NT= 618
G= RELEASE 0.0 UPDATE 0 CUSTOMER 00000000
T= RELEASE 0.0 UPDATE 0 CUSTOMER 00292062

NOW COMPARING LINES FROM ***** ANSYS RESULTS INTERPRETATION (POST1)

NOW COMPARING LINES FROM ***** TIME-HISTORY POSTPROCESSOR (POST26)

NOW COMPARING LINES FROM ***** ANSYS ANALYSIS DEFINITION (PREP7)

COMPARE DIFFERENCE FOUND AT NG= 907 NT= 907
G= RELEASE 0.0 UPDATE 0 CUSTOMER 00000000
T= RELEASE 0.0 UPDATE 0 CUSTOMER 00292062

NOW COMPARING LINES FROM ***** ANSYS RESULTS INTERPRETATION (POST1)

RPP-RPT-28967, Rev. 1

NOW COMPARING LINES FROM ***** TIME-HISTORY POSTPROCESSOR (POST26)

BOTTOM OF GOOD FILE REACHED AT LINE 1193
G= | ANSYS RUN COMPLETED
|

~~~~~  
NOTE- NONSTANDARD COMPARE - DIFOPT NAME QA70-1 HAS BEEN USED  
NUMBER OF LINES SKIPPED IN GOOD FILE (BLANK LINES EXCLUDED) - 2  
NUMBER OF LINES SKIPPED IN TEST FILE (BLANK LINES EXCLUDED) - 2  
NUMBER OF LINES ON GOOD FILE WITH STRINGS CONDENSED OUT - 0  
NUMBER OF LINES ON TEST FILE WITH STRINGS CONDENSED OUT - 0  
~~~~~

COMPARE ERRORS = 2 *

=====

PROBLEM: vm198	COMPARE OPTIONS	COMPARE_REL 3.8 UP20020121
----------------	-----------------	----------------------------

WINDOWS

ALMOST ZERO (GOOD)	= 1.0000E-006	KROUND (DROP LAST DIGIT)= 1
ALMOST ZERO (TEST)	= 1.0000E-006	KABSPR (0=SUMMARY 1=ALL)= 1
ABSOLUTE VALUE TOL	= 1.0000E-010	KSKIP (SKIP=ERR 0=Y, 1=N)= 0
FRACTIONAL DIFFERENCE	= 1.0000E-004	MAXERR (STOP WHEN ERRS)= 100
ABSOLUTE DIFFERENCE	= 1.0000E-006	MAXBUF (# LINES TO SCAN)= 6
		KNOWN (# OF KNOWN ERRS)= 0
		GREAD, TREAD = 1, 1

=====

=====
LINES ON GOOD FILE = 1208
LINES ON TEST FILE = 1208

RPP-RPT-28967, Rev. 1

1

00000000 VERSION=INTEL NT RELEASE= 7.0 UP20021010

EXPECTED COMPARE DIFFERENCE FOUND AT NG= 113 NT= 113
G= 00000000 VERSION=INTEL NT RELEASE= 7.0 UP20021010
T= 00292062 VERSION=INTEL NT RELEASE= 7.0SP11 UP20030909

EXPECTED COMPARE DIFFERENCE FOUND AT NG= 114 NT= 114
G= CURRENT JOBNAME=vmc8 21:52:06 OCT 15, 2002 CP= 0.219
T= CURRENT JOBNAME=vmc8 12:22:49 FEB 12, 2005 CP= 0.188

0 /VERIFY,VMC8

0 /TITLE, VMC8, ALUMINUM BAR IMPACTING A RIGID BOUNDARY

0 /stitle,1,Reason COMPARE differences are acceptable:

0 /stitle,2, number of iterations, accuracy

0 /title, VMC8, ALUMINUM BAR IMPACTING A RIGID BOUNDARY -
PLANE2

0 /title, VMC8, ALUMINUM BAR IMPACTING A RIGID BOUNDARY -
PLANE42

0 /title, VMC8, ALUMINUM BAR IMPACTING A RIGID BOUNDARY -
PLANE82

0 /title, VMC8, ALUMINUM BAR IMPACTING A RIGID BOUNDARY -
VISCO106

0 /title, VMC8, ALUMINUM BAR IMPACTING A RIGID BOUNDARY -
SOLID45

0 /title, VMC8, ALUMINUM BAR IMPACTING A RIGID BOUNDARY -
SOLID95

0 /title, VMC8, ALUMINUM BAR IMPACTING A RIGID BOUNDARY -
VISCO107

0 /TITLE, VMC8, ALUMINUM BAR IMPACTING A RIGID BOUNDARY

NOW COMPARING LINES FROM ***** ANSYS ANALYSIS DEFINITION (PREP7)

NOW COMPARING LINES FROM ***** ANSYS RESULTS INTERPRETATION (POST1)

COMPARE DIFFERENCE FOUND AT NG= 880 NT= 880
G= SET COMMAND GOT LOAD STEP= 2 SUBSTEP= 320 CUMULATIVE ITERATION=
3255

RPP-RPT-28967, Rev. 1

```
T= SET COMMAND GOT LOAD STEP=      2  SUBSTEP=    320  CUMULATIVE ITERATION=
3240

NOW COMPARING LINES FROM          ***** TIME-HISTORY POSTPROCESSOR (POST26)
*****

NOW COMPARING LINES FROM          ***** ANSYS ANALYSIS DEFINITION (PREP7)
*****

NOW COMPARING LINES FROM          ***** ANSYS RESULTS INTERPRETATION (POST1)
*****

NOW COMPARING LINES FROM          ***** TIME-HISTORY POSTPROCESSOR (POST26)
*****

NOW COMPARING LINES FROM          ***** ANSYS ANALYSIS DEFINITION (PREP7)
*****

NOW COMPARING LINES FROM          ***** ANSYS RESULTS INTERPRETATION (POST1)
*****

NOW COMPARING LINES FROM          ***** TIME-HISTORY POSTPROCESSOR (POST26)
*****

COMPARE DIFFERENCE FOUND AT          NG= 1227 NT= 1227
G=   3 ESOL      1 EPPL EQV  EPPLEQV  0.7401E-16  0.000      3.410
0.000
T=   3 ESOL      1 EPPL EQV  EPPLEQV  0.2694E-35  0.000      3.422
0.000

NOW COMPARING LINES FROM          ***** ANSYS ANALYSIS DEFINITION (PREP7)
*****

NOW COMPARING LINES FROM          ***** ANSYS RESULTS INTERPRETATION (POST1)
*****

NOW COMPARING LINES FROM          ***** TIME-HISTORY POSTPROCESSOR (POST26)
*****

NOW COMPARING LINES FROM          ***** ANSYS ANALYSIS DEFINITION (PREP7)
*****

NOW COMPARING LINES FROM          ***** ANSYS RESULTS INTERPRETATION (POST1)
*****
```

RPP-RPT-28967, Rev. 1

```
NOW COMPARING LINES FROM          ***** TIME-HISTORY POSTPROCESSOR (POST26)
*****

NOW COMPARING LINES FROM          ***** ANSYS ANALYSIS DEFINITION (PREP7)
*****

NOW COMPARING LINES FROM          ***** ANSYS RESULTS INTERPRETATION (POST1)
*****

NOW COMPARING LINES FROM          ***** TIME-HISTORY POSTPROCESSOR (POST26)
*****

BOTTOM OF GOOD FILE REACHED AT LINE   1879
G= |                                ANSYS RUN COMPLETED
|
```

```
~~~~~
NOTE- NONSTANDARD COMPARE - DIFOPT NAME QA70-1 HAS BEEN USED
NUMBER OF LINES SKIPPED IN GOOD FILE(BLANK LINES EXCLUDED) -      0
NUMBER OF LINES SKIPPED IN TEST FILE(BLANK LINES EXCLUDED) -      0
NUMBER OF LINES ON GOOD FILE WITH STRINGS CONDENSED OUT    -      0
NUMBER OF LINES ON TEST FILE WITH STRINGS CONDENSED OUT    -      0
~~~~~
```

```
*****
COMPARE ERRORS =          2          *
*****
```

```
=====
===
PROBLEM: vmc8          COMPARE OPTIONS  COMPARE_REL 3.8 UP20020121
WINDOWS
```

```
ALMOST ZERO (GOOD)    = 1.0000E-006          KROUND (DROP LAST DIGIT)= 1
ALMOST ZERO (TEST)    = 1.0000E-006          KABSPR (0=SUMMARY 1=ALL)= 1
ABSOLUTE VALUE TOL    = 1.0000E-010          KSKIP(SKIP=ERR 0=Y, 1=N)= 0
FRACTIONAL DIFFERENCE= 1.0000E-004          MAXERR (STOP WHEN ERRS )= 100
ABSOLUTE DIFFERENCE   = 1.0000E-006          MAXBUF (# LINES TO SCAN)= 6
                                          KNOWN (# OF KNOWN ERRS)= 0
                                          GREAD, TREAD = 1, 1
```

```
=====
===
LINES ON GOOD FILE =      1894
LINES ON TEST FILE =      1894
```

```
*****
```

RPP-RPT-28967, Rev. 1

1

```
00000000          VERSION=INTEL NT          RELEASE= 7.0          UP20021010

EXPECTED COMPARE DIFFERENCE FOUND AT  NG=  113 NT=  113
G= 00000000          VERSION=INTEL NT          RELEASE= 7.0          UP20021010
T= 00292062          VERSION=INTEL NT          RELEASE= 7.0SP11 UP20030909
```

```
EXPECTED COMPARE DIFFERENCE FOUND AT  NG=  114 NT=  114
G= CURRENT JOBNAME=cyc-177s  11:45:34  OCT 15, 2002 CP=          0.219
T= CURRENT JOBNAME=cyc-177s  12:59:19  FEB 12, 2005 CP=          0.266
```

```
0  /verify,cyc-177s

0  /TITLE, ceb,cyc-177s, Test cyc symm Buckling element 42

0  /title,1,Full Results to Sector Results!

0  /stitle,Reason Compare differences are acceptable:
```

```
EXTRA DATA SKIPPED ON TEST FILE          NG= 1202 NT= 1194
T= USE COMMAND MACRO QAEND
T= ARGS= 289.00
END OF SKIPPED DATA                      NG= 1202 NT= 1199
```

```
BOTTOM OF GOOD FILE REACHED AT LINE 1204
G= |                                ANSYS RUN COMPLETED
|
```

```
~~~~~
NOTE- NONSTANDARD COMPARE - DIFOPT NAME QA70-1 HAS BEEN USED
NUMBER OF LINES SKIPPED IN GOOD FILE(BLANK LINES EXCLUDED) - 2
NUMBER OF LINES SKIPPED IN TEST FILE(BLANK LINES EXCLUDED) - 2
NUMBER OF LINES ON GOOD FILE WITH STRINGS CONDENSED OUT - 0
NUMBER OF LINES ON TEST FILE WITH STRINGS CONDENSED OUT - 0
~~~~~
```

```
*****
COMPARE ERRORS = 1 *
*****
```

=====

```
===
PROBLEM: cyc-177s          COMPARE OPTIONS  COMPARE_REL 3.8 UP20020121
WINDOWS

ALMOST ZERO (GOOD)      = 1.0000E-006          KROUND (DROP LAST DIGIT)= 1
ALMOST ZERO (TEST)      = 1.0000E-006          KABSPR (0=SUMMARY 1=ALL)= 1
ABSOLUTE VALUE TOL      = 1.0000E-010          KSKIP(SKIP=ERR 0=Y, 1=N)= 0
FRACTIONAL DIFFERENCE= 1.0000E-004          MAXERR (STOP WHEN ERRS )= 100
```

RPP-RPT-28967, Rev. 1

ABSOLUTE DIFFERENCE = 1.0000E-006

MAXBUF (# LINES TO SCAN)= 6

KNOWN (# OF KNOWN ERRS)= 0

GREAD, TREAD = 1, 1

=====
===

LINES ON GOOD FILE = 1219

LINES ON TEST FILE = 1222

1

```

00000000          VERSION=INTEL NT          RELEASE= 7.0          UP20021010

EXPECTED COMPARE DIFFERENCE FOUND AT  NG=  113 NT=  113
G= 00000000          VERSION=INTEL NT          RELEASE= 7.0          UP20021010
T= 00292062          VERSION=INTEL NT          RELEASE= 7.0SP11 UP20030909

```

```

EXPECTED COMPARE DIFFERENCE FOUND AT  NG=  114 NT=  114
G= CURRENT JOBNAME=cyc-178s  11:48:41  OCT 15, 2002 CP=          0.250
T= CURRENT JOBNAME=cyc-178s  13:01:42  FEB 12, 2005 CP=          0.234

```

```

0  /verify,cyc-178s

0  /TITLE, ceb,cyc-178s, Test cyc symm Buckling element 182

0  /title,1,Full Results to Sector Results!

0  /stitle,Reason Compare differences are acceptable:

```

```

EXTRA DATA SKIPPED ON TEST FILE          NG= 1202 NT= 1194
T= USE COMMAND MACRO QAEND
T= ARGS= 289.00
END OF SKIPPED DATA                      NG= 1202 NT= 1199

```

```

BOTTOM OF GOOD FILE REACHED AT LINE 1204
G= |                                ANSYS RUN COMPLETED
|

```

```

~~~~~
NOTE- NONSTANDARD COMPARE - DIFOPT NAME QA70-1 HAS BEEN USED
NUMBER OF LINES SKIPPED IN GOOD FILE(BLANK LINES EXCLUDED) -      2
NUMBER OF LINES SKIPPED IN TEST FILE(BLANK LINES EXCLUDED) -      2
NUMBER OF LINES ON GOOD FILE WITH STRINGS CONDENSED OUT      -      0
NUMBER OF LINES ON TEST FILE WITH STRINGS CONDENSED OUT      -      0
~~~~~

```

```

*****
COMPARE ERRORS =          1          *
*****

```

=====

===

```

PROBLEM: cyc-178s          COMPARE OPTIONS  COMPARE_REL 3.8 UP20020121
WINDOWS

```

```

ALMOST ZERO (GOOD)      = 1.0000E-006          KROUND (DROP LAST DIGIT)= 1
ALMOST ZERO (TEST)      = 1.0000E-006          KABSPR (0=SUMMARY 1=ALL)= 1
ABSOLUTE VALUE TOL      = 1.0000E-010          KSKIP(SKIP=ERR 0=Y, 1=N)= 0
FRACTIONAL DIFFERENCE= 1.0000E-004          MAXERR (STOP WHEN ERRS )= 100

```

RPP-RPT-28967, Rev. 1

ABSOLUTE DIFFERENCE = 1.0000E-006

MAXBUF (# LINES TO SCAN)= 6

KNOWN (# OF KNOWN ERRS)= 0

GREAD, TREAD = 1, 1

=====
===

LINES ON GOOD FILE = 1219

LINES ON TEST FILE = 1222

1

```
*****
```

```
*** ERROR -- (VERSION=) was not found anywhere in the "TEST" file.
***
*** Comparison was supposed to start at this string, specified in CMPOPT.
***
```

```
~~~~~
NOTE- NONSTANDARD COMPARE - DIFOPT NAME QA70-1 HAS BEEN USED
NUMBER OF LINES SKIPPED IN GOOD FILE(BLANK LINES EXCLUDED) -      0
NUMBER OF LINES SKIPPED IN TEST FILE(BLANK LINES EXCLUDED) -      0
NUMBER OF LINES ON GOOD FILE WITH STRINGS CONDENSED OUT -      0
NUMBER OF LINES ON TEST FILE WITH STRINGS CONDENSED OUT -      0
~~~~~
```

```
*****
COMPARE ERRORS =      -88                      *
*****
```

```
=====
===
```

```
PROBLEM: dds-13s          COMPARE OPTIONS  COMPARE_REL 3.8 UP20020121
WINDOWS
```

ALMOST ZERO (GOOD)	= 1.0000E-006	KROUND (DROP LAST DIGIT)=	1
ALMOST ZERO (TEST)	= 1.0000E-006	KABSPR (0=SUMMARY 1=ALL)=	1
ABSOLUTE VALUE TOL	= 1.0000E-010	KSKIP(SKIP=ERR 0=Y, 1=N)=	0
FRACTIONAL DIFFERENCE	= 1.0000E-004	MAXERR (STOP WHEN ERRS)=	100
ABSOLUTE DIFFERENCE	= 1.0000E-006	MAXBUF (# LINES TO SCAN)=	6
		KNOWN (# OF KNOWN ERRS)=	0
		GREAD, TREAD =	1, 1

```
=====
===
```

```

LINES ON GOOD FILE =      402
LINES ON TEST FILE =      146
```

```
*****
```

1

*** ERROR -- (VERSION=) was not found anywhere in the "TEST" file.

 *** Comparison was supposed to start at this string, specified in CMPOPT.

~~~~~  
 NOTE- NONSTANDARD COMPARE - DIFOPT NAME QA70-1 HAS BEEN USED  
 NUMBER OF LINES SKIPPED IN GOOD FILE(BLANK LINES EXCLUDED) - 0  
 NUMBER OF LINES SKIPPED IN TEST FILE(BLANK LINES EXCLUDED) - 0  
 NUMBER OF LINES ON GOOD FILE WITH STRINGS CONDENSED OUT - 0  
 NUMBER OF LINES ON TEST FILE WITH STRINGS CONDENSED OUT - 0  
 ~~~~~

 COMPARE ERRORS = -88 *

=====

===
 PROBLEM: dds-17s COMPARE OPTIONS COMPARE_REL 3.8 UP20020121
 WINDOWS

ALMOST ZERO (GOOD)	= 1.0000E-006	KROUND (DROP LAST DIGIT)=	1
ALMOST ZERO (TEST)	= 1.0000E-006	KABSPR (0=SUMMARY 1=ALL)=	1
ABSOLUTE VALUE TOL	= 1.0000E-010	KSKIP(SKIP=ERR 0=Y, 1=N)=	0
FRACTIONAL DIFFERENCE=	1.0000E-004	MAXERR (STOP WHEN ERRS)=	100
ABSOLUTE DIFFERENCE	= 1.0000E-006	MAXBUF (# LINES TO SCAN)=	6
		KNOWN (# OF KNOWN ERRS)=	0
		GREAD, TREAD =	1, 1

=====

===
 LINES ON GOOD FILE = 746
 LINES ON TEST FILE = 146

1

00000000 VERSION=INTEL NT RELEASE= 7.0 UP20021010

EXPECTED COMPARE DIFFERENCE FOUND AT NG= 113 NT= 113
 G= 00000000 VERSION=INTEL NT RELEASE= 7.0 UP20021010
 T= 00292062 VERSION=INTEL NT RELEASE= 7.0SP11 UP20030909

EXPECTED COMPARE DIFFERENCE FOUND AT NG= 114 NT= 114
 G= CURRENT JOBNAME=ev173-53s 14:02:31 OCT 15, 2002 CP= 0.234
 T= CURRENT JOBNAME=ev173-53s 13:10:45 FEB 12, 2005 CP= 0.172

0 /verify,ev173-53s

0 /title,ev173-53s,mfquresh,Test to verify PSOVLE,ELFORM for
 171-175 (3D) with PENE

EXTRA DATA SKIPPED ON TEST FILE NG= 1409 NT= 1401
 T= USE COMMAND MACRO QAEND
 T= ARGS= 20.000
 END OF SKIPPED DATA NG= 1409 NT= 1406

BOTTOM OF GOOD FILE REACHED AT LINE 1411
 G= | ANSYS RUN COMPLETED

~~~~~  
 NOTE- NONSTANDARD COMPARE - DIFOPT NAME QA70-1 HAS BEEN USED  
 NUMBER OF LINES SKIPPED IN GOOD FILE(BLANK LINES EXCLUDED) - 2  
 NUMBER OF LINES SKIPPED IN TEST FILE(BLANK LINES EXCLUDED) - 2  
 NUMBER OF LINES ON GOOD FILE WITH STRINGS CONDENSED OUT - 0  
 NUMBER OF LINES ON TEST FILE WITH STRINGS CONDENSED OUT - 0  
 ~~~~~

 COMPARE ERRORS = 1 *

=====

===
 PROBLEM: ev173-53s COMPARE OPTIONS COMPARE_REL 3.8 UP20020121
 WINDOWS

ALMOST ZERO (GOOD) = 1.0000E-006	KROUND (DROP LAST DIGIT)= 1
ALMOST ZERO (TEST) = 1.0000E-006	KABSPR (0=SUMMARY 1=ALL)= 1
ABSOLUTE VALUE TOL = 1.0000E-010	KSKIP(SKIP=ERR 0=Y, 1=N)= 0
FRACTIONAL DIFFERENCE= 1.0000E-004	MAXERR (STOP WHEN ERRS)= 100
ABSOLUTE DIFFERENCE = 1.0000E-006	MAXBUF (# LINES TO SCAN)= 6
	KNOWN (# OF KNOWN ERRS)= 0
	GREAD, TREAD = 1, 1

=====

====

LINES ON GOOD FILE =	1426
LINES ON TEST FILE =	1429

RPP-RPT-28967, Rev. 1

1

00000000 VERSION=INTEL NT RELEASE= 7.0 UP20021010

EXPECTED COMPARE DIFFERENCE FOUND AT NG= 113 NT= 113
G= 00000000 VERSION=INTEL NT RELEASE= 7.0 UP20021010
T= 00292062 VERSION=INTEL NT RELEASE= 7.0SP11 UP20030909

EXPECTED COMPARE DIFFERENCE FOUND AT NG= 114 NT= 114
G= CURRENT JOBNAME=ev175-20s 14:22:03 OCT 15, 2002 CP= 0.250
T= CURRENT JOBNAME=ev175-20s 13:11:18 FEB 12, 2005 CP= 0.156

0 /verify,ev175-20s

0 /title,ev175-20s,mfq, Check real constant FKN and FTOLN and
KEYOPT(2)=0,1

NOW COMPARING LINES FROM ***** ANSYS ANALYSIS DEFINITION (PREP7)

EXTRA DATA SKIPPED ON TEST FILE NG= 521 NT= 513
T= USE COMMAND MACRO QAEND
T= ARGS= 3.0000
END OF SKIPPED DATA NG= 521 NT= 518

BOTTOM OF GOOD FILE REACHED AT LINE 523
G= | ANSYS RUN COMPLETED
|

~~~~~  
NOTE- NONSTANDARD COMPARE - DIFOPT NAME QA70-1 HAS BEEN USED  
NUMBER OF LINES SKIPPED IN GOOD FILE(BLANK LINES EXCLUDED) - 2  
NUMBER OF LINES SKIPPED IN TEST FILE(BLANK LINES EXCLUDED) - 2  
NUMBER OF LINES ON GOOD FILE WITH STRINGS CONDENSED OUT - 0  
NUMBER OF LINES ON TEST FILE WITH STRINGS CONDENSED OUT - 0  
~~~~~

COMPARE ERRORS = 1 *

=====

===

PROBLEM: ev175-20s COMPARE OPTIONS COMPARE_REL 3.8 UP20020121
WINDOWS

ALMOST ZERO (GOOD)	= 1.0000E-006	KROUND (DROP LAST DIGIT)=	1
ALMOST ZERO (TEST)	= 1.0000E-006	KABSPR (0=SUMMARY 1=ALL)=	1
ABSOLUTE VALUE TOL	= 1.0000E-010	KSKIP(SKIP=ERR 0=Y, 1=N)=	0

RPP-RPT-28967, Rev. 1

FRACTIONAL DIFFERENCE= 1.0000E-004
ABSOLUTE DIFFERENCE = 1.0000E-006

MAXERR (STOP WHEN ERRS)= 100
MAXBUF (# LINES TO SCAN)= 6
KNOWN (# OF KNOWN ERRS)= 0
GREAD, TREAD = 1, 1

=====
===

LINES ON GOOD FILE = 538
LINES ON TEST FILE = 541

1

*** ERROR -- (VERSION=) was not found anywhere in the "TEST" file.

 *** Comparison was supposed to start at this string, specified in CMPOPT.

~~~~~  
 NOTE- NONSTANDARD COMPARE - DIFOPT NAME QA70-1 HAS BEEN USED  
 NUMBER OF LINES SKIPPED IN GOOD FILE(BLANK LINES EXCLUDED) - 0  
 NUMBER OF LINES SKIPPED IN TEST FILE(BLANK LINES EXCLUDED) - 0  
 NUMBER OF LINES ON GOOD FILE WITH STRINGS CONDENSED OUT - 0  
 NUMBER OF LINES ON TEST FILE WITH STRINGS CONDENSED OUT - 0  
 ~~~~~

 COMPARE ERRORS = -88 *

=====

===
 PROBLEM: ev175-21s COMPARE OPTIONS COMPARE_REL 3.8 UP20020121
 WINDOWS

ALMOST ZERO (GOOD)	= 1.0000E-006	KROUND (DROP LAST DIGIT)=	1
ALMOST ZERO (TEST)	= 1.0000E-006	KABSPR (0=SUMMARY 1=ALL)=	1
ABSOLUTE VALUE TOL	= 1.0000E-010	KSKIP(SKIP=ERR 0=Y, 1=N)=	0
FRACTIONAL DIFFERENCE=	1.0000E-004	MAXERR (STOP WHEN ERRS)=	100
ABSOLUTE DIFFERENCE	= 1.0000E-006	MAXBUF (# LINES TO SCAN)=	6
		KNOWN (# OF KNOWN ERRS)=	0
		GREAD, TREAD =	1, 1

=====

===
 LINES ON GOOD FILE = 566
 LINES ON TEST FILE = 146

1

00000000 VERSION=INTEL NT RELEASE= 7.0 UP20021010

EXPECTED COMPARE DIFFERENCE FOUND AT NG= 113 NT= 113
 G= 00000000 VERSION=INTEL NT RELEASE= 7.0 UP20021010
 T= 00292062 VERSION=INTEL NT RELEASE= 7.0SP11 UP20030909

EXPECTED COMPARE DIFFERENCE FOUND AT NG= 114 NT= 114
 G= CURRENT JOBNAME=inrt-16s 16:14:59 OCT 15, 2002 CP= 0.219
 T= CURRENT JOBNAME=inrt-16s 13:13:40 FEB 12, 2005 CP= 0.188

0 /VERIFY, INRT-16S

0 /TITLE, INRT-16S, ceb, component omega loading and layer
 elements

0 /TITLE, INRT-16S, BENDING OF A COMPOSITE BEAM

EXTRA DATA SKIPPED ON TEST FILE NG= 462 NT= 459
 T= USE COMMAND MACRO QAEND
 END OF SKIPPED DATA NG= 462 NT= 463

BOTTOM OF GOOD FILE REACHED AT LINE 469
 G= | ANSYS RUN COMPLETED

~~~~~  
 NOTE- NONSTANDARD COMPARE - DIFOPT NAME QA70-1    HAS BEEN USED  
 NUMBER OF LINES SKIPPED IN GOOD FILE(BLANK LINES EXCLUDED) -    1  
 NUMBER OF LINES SKIPPED IN TEST FILE(BLANK LINES EXCLUDED) -    1  
 NUMBER OF LINES ON GOOD FILE WITH STRINGS CONDENSED OUT    -    0  
 NUMBER OF LINES ON TEST FILE WITH STRINGS CONDENSED OUT    -    0  
 ~~~~~

 COMPARE ERRORS = 1 *

=====

===
 PROBLEM: inrt-16s COMPARE OPTIONS COMPARE_REL 3.8 UP20020121
 WINDOWS

ALMOST ZERO (GOOD)	= 1.0000E-006	KROUND (DROP LAST DIGIT)=	1
ALMOST ZERO (TEST)	= 1.0000E-006	KABSPR (0=SUMMARY 1=ALL)=	1
ABSOLUTE VALUE TOL	= 1.0000E-010	KSKIP(SKIP=ERR 0=Y, 1=N)=	0
FRACTIONAL DIFFERENCE=	1.0000E-004	MAXERR (STOP WHEN ERRS)=	100
ABSOLUTE DIFFERENCE	= 1.0000E-006	MAXBUF (# LINES TO SCAN)=	6
		KNOWN (# OF KNOWN ERRS)=	0

GREAD, TREAD = 1, 1

=====

====

 LINES ON GOOD FILE = 484
 LINES ON TEST FILE = 486

1

```
*****
```

```
*** ERROR -- (VERSION=) was not found anywhere in the "TEST" file.
***
*** Comparison was supposed to start at this string, specified in CMPOPT.
***
```

```
~~~~~
NOTE- NONSTANDARD COMPARE - DIFOPT NAME QA70-1 HAS BEEN USED
NUMBER OF LINES SKIPPED IN GOOD FILE(BLANK LINES EXCLUDED) -      0
NUMBER OF LINES SKIPPED IN TEST FILE(BLANK LINES EXCLUDED) -      0
NUMBER OF LINES ON GOOD FILE WITH STRINGS CONDENSED OUT -      0
NUMBER OF LINES ON TEST FILE WITH STRINGS CONDENSED OUT -      0
~~~~~
```

```
*****
COMPARE ERRORS =      -88      *
*****
```

```
=====
===
```

```
PROBLEM:  sx120-1s      COMPARE OPTIONS  COMPARE_REL 3.8 UP20020121
WINDOWS
```

ALMOST ZERO (GOOD)	= 1.0000E-006	KROUND (DROP LAST DIGIT)=	1
ALMOST ZERO (TEST)	= 1.0000E-006	KABSPR (0=SUMMARY 1=ALL)=	1
ABSOLUTE VALUE TOL	= 1.0000E-010	KSKIP(SKIP=ERR 0=Y, 1=N)=	0
FRACTIONAL DIFFERENCE=	1.0000E-004	MAXERR (STOP WHEN ERRS)=	100
ABSOLUTE DIFFERENCE	= 1.0000E-006	MAXBUF (# LINES TO SCAN)=	6
		KNOWN (# OF KNOWN ERRS)=	0
		GREAD, TREAD =	1, 1

```
=====
===
```

```
LINES ON GOOD FILE =      248
LINES ON TEST FILE =      146
```

```
*****
```

Software Acceptance

- 1) Project Title and Number: DST Thermal and Seismic Analyses 48971
- 2) Software Name and Version: ANSYS 7.0 (Rev. 11)
- 3) Computer and Property Number: Dell DHM WD44879
- 4) Operating System: Windows XP Professional Version 2002 Service Pack 2
- 4) Scope of Testing: Software reinstallation (XP SP2)
- 5) Tests: Execute ANSYS Verification Testing Package
- 6) Discrepancies:
 - n) c0231. These differences are acceptable per the ANSYS Verification Package User's Guide – ANSYS Release 7.0 (AVPUG).
 - o) vm184. These differences occur at the 5th significant figure.
 - p) vm198. This difference is the reporting of the customer number for this installation.
 - q) vmc8. These differences are acceptable as noted in the output because of the difference in number of iterations and accuracy.
 - r) cyc-177s. This difference is acceptable due to the handling of the QAEND macro (see AVPUG).
 - s) cyc-178s. This difference is acceptable due to the handling of the QAEND macro (see AVPUG).
 - t) dds-13s. This test case requires the "Parallel Performance Module" which is not part of this software installation and is not required for the DST analyses.
 - u) dds-17s. This test case requires the "Parallel Performance Module" which is not part of this software installation and is not required for the DST analyses.
 - v) ev173-53s. This difference is acceptable due to the handling of the QAEND macro (see AVPUG).
 - w) ev175-20s. This difference is acceptable due to the handling of the QAEND macro (see AVPUG).
 - x) ev175-21s. This test case requires the "Parallel Performance Module" which is not part of this software installation and is not required for the DST analyses.
 - y) inrt-16s. This difference is acceptable due to the handling of the QAEND macro (see AVPUG).
 - z) sx120-1s. This test case requires the "Frequency Sweep Module" which is not part of this software installation and is not required for the DST analyses.
- 7) Finding: This installation of ANSYS is acceptable

Certified by:

JE Deibler John E Deibler 2/24/05
Code Custodian

Reviewed by:

KI Johnson Kenneth I Johnson 4/16/05
Lead Engineer

Notes for test case cO231

Test case cO231 may show considerable differences for the Phase Angle value that is part of the Post1 Nodal Degree of Freedom Listing (PRNS command) output. Any such differences do not indicate a problem with this test case's results and should be considered acceptable. The output items of significance for this test case are the UZ values in the Post1 Nodal Degree of Freedom Listing. Machine precision differences in the form of small numerical differences that are trivial with respect to the test's output items of significance may also show for this test case in the compare output for this test. Please see **Verifying ANSYS and Evaluating COMPARE Differences** in Chapter 2 of the *ANSYS Verification Testing Package User's Guide* for more information on evaluating COMPARE differences. The following is an example of acceptable COMPARE differences for test case cO231:

COMPARE DIFFERENCE FOUND AT G= NODAL RESULTS ARE FOR CYCLIC SECTOR T= NODAL RESULTS ARE FOR CYCLIC SECTOR

COMPARE DIFFERENCE FOUND AT G= VALUE -9.8117 -3.7700 22. T= VALUE -9.8119 -3.7693 22.

COMPARE DIFFERENCE FOUND AT G= NODAL RESULTS ARE FOR CYCLIC SECTOR T= NODAL RESULTS ARE FOR CYCLIC SECTOR

COMPARE DIFFERENCE FOUND AT G= VALUE -9.7579 -3.9649 22. T= VALUE -9.7581 -3.9643 22.

COMPARE DIFFERENCE FOUND AT G= NODAL RESULTS ARE FOR CYCLIC SECTOR T= NODAL RESULTS ARE FOR CYCLIC SECTOR

COMPARE DIFFERENCE FOUWAT ---c;;;i';; G= 8 0.53291 0.39425 io T= 8 0.53293 p.39419 10

COMPARE DIFFERENCE FOUND AT G= 10 0.52495 0.39568 9. T= 10 0.52497 0.39562 9.

COMPARE DIFFERENCE FOUND AT NG= 259 NT= 259 G= 12 0.50433 0.40282 8.6482 8.6722 T= 12 0.50435 0.40276 8.6471 8.6711

COMPARE DIFFERENCE FOUND AT NG= 260 NT= 260 G= 14 0.48186 0.41201 7.8710 7.8965 T= 14 0.48188 0.41196 7.8700 7.8955

COMPARE DIFFERENCE FOUND AT NG= 261 NT= 261 G= 16 0.45505 0.42478 7.0719 7.0992 T= 16 0.45507 0.42473 7.0710 7.0983

COMPARE DIFFERENCE FOUND AT NG= 262 NT= 262 G= 18 0.42339 0.44092 6.2424 6.2723 T= 18 0.42341 0.44086 6.2417 6.2715

COMPARE DIFFERENCE FOUND AT NG= 263 NT= 263 G= 20 0.38501 0.46124 5.3732 5.4067 T= 20 0.38502 0.46118 5.3726 5.4061

COMPARE DIFFERENCE FOUND AT NG= 267 NT= 267 G= VALUE -9.6034 -3.9649 18.806 21.413 T= VALUE -9.6036 -3.9643 18.805 21.412

NG= 271 NT= 271 22.469 24.766 22.469 24.766

NG= 192 NT= 192 1 -PHASE ANGLE = 1- PHASE ANGLE =

NG= 213 NT= 213 469 24.766 469 24.766

NG= 219 NT= 219 2- PHASE ANGLE = 2- PHASE ANGLE =

NG= 240 NT= 240 440 24.710 440 24.710

NG= 246 NT= 246 3- PHASE ANGLE = 3- PHASE ANGLE =

NG= 257 m--257 .161 10.183 .160 10.181

NG= 4080 4068

258 NT= 258 9.4309 9.4297

COMPARE DIFFERENCE FOUND AT G= VALUE -9.8117 -3.9649 T= VALUE -9.8119 -3.9643

30.580 306.570

30.580 306.570

30.580 306.570

Notes for Test Case vrn212

Test case vm212 may produce an expected compare difference due to an inconsequential warning message that appears in the ANSYS, Inc. supplied output file that may not appear in the output file generated by your system for this test case. This compare difference should be considered acceptable. The following is an example of this compare difference.

```
COMPARE DIFFERENCE FOUND AT          NG= 445 NT= 436
G= NUMBER OF WARNING MESSAGES ENCOUNTERED= 1
T= NUMBER OF WARNING MESSAGES ENCOUNTERED= 0
```

Notes for Test Cases cyc-177s, cyc-178s, ev-173-53s, ev-175-20s, inrt-16s, and inrt-9s

Test cases cyc-177s, cyc-178s, ev-173-53s, ev-175-20s, inrt-16s, and inrt-9s may produce expected compare differences due to the use of a macro named qaend. The method that is used in the verification procedure (runqa) to handle this macro may cause one or more comparison differences. Any such compare differences are inconsequential and should be considered acceptable. The following is an example of such a compare difference.

```
EXTRA DATA SKIPPED ON TEST FILE          NG= 1033 NT= 1030
T= USE COMMAND MACRO qaend
T= ARGS= 137.00
END OF SKIPPED DATA                     NG= 1033 NT= 1033
```

Notes for test Cases dds-13s, dds-17s, and ev175-21 s

The test cases dds-13s, dds-17s, and ev175-21 s will run to completion only if the "Parallel Performance for ANSYS" product (DDS and AMG solvers) is included in your ANSYS installation.

c0211r2	7020021010	70SP20030909	0	0	605	605	81%	02/12/2005	21:31	INTEL_NT
INTEL_NT	QA70-1	COMPARE_REL	3.8	UP20020121	WINDOWS					
c0212	7020021010	70SP20030909	0	0	223	223	45%	02/12/2005	21:31	INTEL_NT
INTEL_NT	QA70-1	COMPARE_REL	3.8	UP20020121	WINDOWS					
c0213	7020021010	70SP20030909	0	0	197	197	41%	02/12/2005	21:31	INTEL_NT
INTEL_NT	QA70-1	COMPARE_REL	3.8	UP20020121	WINDOWS					
c0214	7020021010	70SP20030909	0	0	409	409	67%	02/12/2005	21:31	INTEL_NT
INTEL_NT	QA70-1	COMPARE_REL	3.8	UP20020121	WINDOWS					
c0215	7020021010	70SP20030909	0	0	648	648	81%	02/12/2005	21:31	INTEL_NT
INTEL_NT	QA70-1	COMPARE_REL	3.8	UP20020121	WINDOWS					
c0216	7020021010	70SP20030909	0	0	510	510	74%	02/12/2005	21:31	INTEL_NT
INTEL_NT	QA70-1	COMPARE_REL	3.8	UP20020121	WINDOWS					
c0217	7020021010	70SP20030909	0	0	332	332	66%	02/12/2005	21:31	INTEL_NT
INTEL_NT	QA70-1	COMPARE_REL	3.8	UP20020121	WINDOWS					
c0218	7020021010	70SP20030909	0	0	1627	1627	93%	02/12/2005	21:31	INTEL_NT
INTEL_NT	QA70-1	COMPARE_REL	3.8	UP20020121	WINDOWS					
c0219	7020021010	70SP20030909	0	0	2732	2732	95%	02/12/2005	21:31	INTEL_NT
INTEL_NT	QA70-1	COMPARE_REL	3.8	UP20020121	WINDOWS					
c0220	7020021010	70SP20030909	0	0	494	494	76%	02/12/2005	21:31	INTEL_NT
INTEL_NT	QA70-1	COMPARE_REL	3.8	UP20020121	WINDOWS					
c0221	7020021010	70SP20030909	0	0	1265	1265	90%	02/12/2005	21:31	INTEL_NT
INTEL_NT	QA70-1	COMPARE_REL	3.8	UP20020121	WINDOWS					
c0222	7020021010	70SP20030909	0	0	1543	1543	92%	02/12/2005	21:32	INTEL_NT
INTEL_NT	QA70-1	COMPARE_REL	3.8	UP20020121	WINDOWS					
c0223	7020021010	70SP20030909	0	0	362	362	66%	02/12/2005	21:32	INTEL_NT
INTEL_NT	QA70-1	COMPARE_REL	3.8	UP20020121	WINDOWS					
c0224	7020021010	70SP20030909	0	0	307	307	59%	02/12/2005	21:32	INTEL_NT
INTEL_NT	QA70-1	COMPARE_REL	3.8	UP20020121	WINDOWS					
c0225	7020021010	70SP20030909	0	0	420	420	70%	02/12/2005	21:32	INTEL_NT
INTEL_NT	QA70-1	COMPARE_REL	3.8	UP20020121	WINDOWS					
c0226	7020021010	70SP20030909	0	0	521	521	74%	02/12/2005	21:32	INTEL_NT
INTEL_NT	QA70-1	COMPARE_REL	3.8	UP20020121	WINDOWS					
c0227	7020021010	70SP20030909	0	0	380	380	65%	02/12/2005	21:32	INTEL_NT
INTEL_NT	QA70-1	COMPARE_REL	3.8	UP20020121	WINDOWS					
c0227a	7020021010	70SP20030909	0	0	380	380	65%	02/12/2005	21:32	INTEL_NT
INTEL_NT	QA70-1	COMPARE_REL	3.8	UP20020121	WINDOWS					
c0228	7020021010	70SP20030909	0	0	236	236	50%	02/12/2005	21:32	INTEL_NT
INTEL_NT	QA70-1	COMPARE_REL	3.8	UP20020121	WINDOWS					
c0229	7020021010	70SP20030909	0	0	715	715	81%	02/12/2005	21:32	INTEL_NT
INTEL_NT	QA70-1	COMPARE_REL	3.8	UP20020121	WINDOWS					
c0230	7020021010	70SP20030909	0	0	2513	2513	94%	02/12/2005	21:33	INTEL_NT
INTEL_NT	QA70-1	COMPARE_REL	3.8	UP20020121	WINDOWS					
c0231	7020021010	70SP20030909	3	0	304	304	61%	02/12/2005	21:33	INTEL_NT
INTEL_NT	QA70-1	COMPARE_REL	3.8	UP20020121	WINDOWS					

c0232	7020021010	70SP20030909	0	0	517	517	79%	02/12/2005	21:33	INTEL_NT
INTEL_NT	QA70-1	COMPARE_REL	3.8	UP20020121	WINDOWS					
c0233	7020021010	70SP20030909	0	0	542	542	75%	02/12/2005	21:33	INTEL_NT
INTEL_NT	QA70-1	COMPARE_REL	3.8	UP20020121	WINDOWS					
c0234	7020021010	70SP20030909	0	0	420	420	68%	02/12/2005	21:33	INTEL_NT
INTEL_NT	QA70-1	COMPARE_REL	3.8	UP20020121	WINDOWS					
vm1	7020021010	70SP20030909	0	0	474	474	72%	02/12/2005	21:33	INTEL_NT
INTEL_NT	QA70-1	COMPARE_REL	3.8	UP20020121	WINDOWS					
vm2	7020021010	70SP20030909	0	0	667	667	81%	02/12/2005	21:33	INTEL_NT
INTEL_NT	QA70-1	COMPARE_REL	3.8	UP20020121	WINDOWS					
vm3	7020021010	70SP20030909	0	0	499	499	73%	02/12/2005	21:33	INTEL_NT
INTEL_NT	QA70-1	COMPARE_REL	3.8	UP20020121	WINDOWS					
vm4	7020021010	70SP20030909	0	0	434	434	69%	02/12/2005	21:33	INTEL_NT
INTEL_NT	QA70-1	COMPARE_REL	3.8	UP20020121	WINDOWS					
vm5	7020021010	70SP20030909	0	0	884	884	85%	02/12/2005	21:33	INTEL_NT
INTEL_NT	QA70-1	COMPARE_REL	3.8	UP20020121	WINDOWS					
vm6	7020021010	70SP20030909	0	0	854	854	83%	02/12/2005	21:34	INTEL_NT
INTEL_NT	QA70-1	COMPARE_REL	3.8	UP20020121	WINDOWS					
vm7	7020021010	70SP20030909	0	0	2176	2176	93%	02/12/2005	21:34	INTEL_NT
INTEL_NT	QA70-1	COMPARE_REL	3.8	UP20020121	WINDOWS					
vm8	7020021010	70SP20030909	0	0	346	346	64%	02/12/2005	21:34	INTEL_NT
INTEL_NT	QA70-1	COMPARE_REL	3.8	UP20020121	WINDOWS					
vm9	7020021010	70SP20030909	0	0	851	851	85%	02/12/2005	21:34	INTEL_NT
INTEL_NT	QA70-1	COMPARE_REL	3.8	UP20020121	WINDOWS					
vm10	7020021010	70SP20030909	0	0	437	437	69%	02/12/2005	21:34	INTEL_NT
INTEL_NT	QA70-1	COMPARE_REL	3.8	UP20020121	WINDOWS					
vm11	7020021010	70SP20030909	0	0	885	885	85%	02/12/2005	21:34	INTEL_NT
INTEL_NT	QA70-1	COMPARE_REL	3.8	UP20020121	WINDOWS					
vm12	7020021010	70SP20030909	0	0	444	444	70%	02/12/2005	21:34	INTEL_NT
INTEL_NT	QA70-1	COMPARE_REL	3.8	UP20020121	WINDOWS					
vm13	7020021010	70SP20030909	0	0	464	464	71%	02/12/2005	21:34	INTEL_NT
INTEL_NT	QA70-1	COMPARE_REL	3.8	UP20020121	WINDOWS					
vm14	7020021010	70SP20030909	0	0	537	537	76%	02/12/2005	21:34	INTEL_NT
INTEL_NT	QA70-1	COMPARE_REL	3.8	UP20020121	WINDOWS					
vm15	7020021010	70SP20030909	0	0	1356	1356	91%	02/12/2005	21:34	INTEL_NT
INTEL_NT	QA70-1	COMPARE_REL	3.8	UP20020121	WINDOWS					
vm16	7020021010	70SP20030909	0	0	740	740	82%	02/12/2005	21:34	INTEL_NT
INTEL_NT	QA70-1	COMPARE_REL	3.8	UP20020121	WINDOWS					
vm17	7020021010	70SP20030909	0	0	546	546	76%	02/12/2005	21:34	INTEL_NT
INTEL_NT	QA70-1	COMPARE_REL	3.8	UP20020121	WINDOWS					
vm18	7020021010	70SP20030909	0	0	450	450	71%	02/12/2005	21:34	INTEL_NT
INTEL_NT	QA70-1	COMPARE_REL	3.8	UP20020121	WINDOWS					
vm19	7020021010	70SP20030909	0	0	725	725	80%	02/12/2005	21:34	INTEL_NT
INTEL_NT	QA70-1	COMPARE_REL	3.8	UP20020121	WINDOWS					

vm20	7020021010	70SP20030909	0	0	449	449	70%	02/12/2005	21:34	INTEL_NT
INTEL_NT	QA70-1	COMPARE_REL	3.8	UP20020121	WINDOWS					
vm21	7020021010	70SP20030909	0	0	805	805	82%	02/12/2005	21:34	INTEL_NT
INTEL_NT	QA70-1	COMPARE_REL	3.8	UP20020121	WINDOWS					
vm22	7020021010	70SP20030909	0	0	398	398	66%	02/12/2005	21:34	INTEL_NT
INTEL_NT	QA70-1	COMPARE_REL	3.8	UP20020121	WINDOWS					
vm23	7020021010	70SP20030909	0	0	1043	1043	88%	02/12/2005	21:34	INTEL_NT
INTEL_NT	QA70-1	COMPARE_REL	3.8	UP20020121	WINDOWS					
vm24	7020021010	70SP20030909	0	0	766	766	82%	02/12/2005	21:34	INTEL_NT
INTEL_NT	QA70-1	COMPARE_REL	3.8	UP20020121	WINDOWS					
vm25	7020021010	70SP20030909	0	0	2350	2350	95%	02/12/2005	21:34	INTEL_NT
INTEL_NT	QA70-1	COMPARE_REL	3.8	UP20020121	WINDOWS					
vm26	7020021010	70SP20030909	0	0	1829	1829	89%	02/12/2005	21:35	INTEL_NT
INTEL_NT	QA70-1	COMPARE_REL	3.8	UP20020121	WINDOWS					
vm27	7020021010	70SP20030909	0	0	910	910	85%	02/12/2005	21:35	INTEL_NT
INTEL_NT	QA70-1	COMPARE_REL	3.8	UP20020121	WINDOWS					
vm28	7020021010	70SP20030909	0	0	418	418	70%	02/12/2005	21:35	INTEL_NT
INTEL_NT	QA70-1	COMPARE_REL	3.8	UP20020121	WINDOWS					
vm29	7020021010	70SP20030909	0	0	683	683	80%	02/12/2005	21:35	INTEL_NT
INTEL_NT	QA70-1	COMPARE_REL	3.8	UP20020121	WINDOWS					
vm30	7020021010	70SP20030909	0	0	449	449	70%	02/12/2005	21:35	INTEL_NT
INTEL_NT	QA70-1	COMPARE_REL	3.8	UP20020121	WINDOWS					
vm31	7020021010	70SP20030909	0	0	551	551	76%	02/12/2005	21:35	INTEL_NT
INTEL_NT	QA70-1	COMPARE_REL	3.8	UP20020121	WINDOWS					
vm32	7020021010	70SP20030909	0	0	881	881	84%	02/12/2005	21:35	INTEL_NT
INTEL_NT	QA70-1	COMPARE_REL	3.8	UP20020121	WINDOWS					
vm33	7020021010	70SP20030909	0	0	902	902	85%	02/12/2005	21:35	INTEL_NT
INTEL_NT	QA70-1	COMPARE_REL	3.8	UP20020121	WINDOWS					
vm34	7020021010	70SP20030909	0	0	1380	1380	90%	02/12/2005	21:35	INTEL_NT
INTEL_NT	QA70-1	COMPARE_REL	3.8	UP20020121	WINDOWS					
vm35	7020021010	70SP20030909	0	0	594	594	77%	02/12/2005	21:35	INTEL_NT
INTEL_NT	QA70-1	COMPARE_REL	3.8	UP20020121	WINDOWS					
vm36	7020021010	70SP20030909	0	0	1086	1086	88%	02/12/2005	21:35	INTEL_NT
INTEL_NT	QA70-1	COMPARE_REL	3.8	UP20020121	WINDOWS					
vm37	7020021010	70SP20030909	0	0	690	690	81%	02/12/2005	21:35	INTEL_NT
INTEL_NT	QA70-1	COMPARE_REL	3.8	UP20020121	WINDOWS					
vm38	7020021010	70SP20030909	0	0	1667	1667	92%	02/12/2005	21:35	INTEL_NT
INTEL_NT	QA70-1	COMPARE_REL	3.8	UP20020121	WINDOWS					
vm39	7020021010	70SP20030909	0	0	819	819	84%	02/12/2005	21:35	INTEL_NT
INTEL_NT	QA70-1	COMPARE_REL	3.8	UP20020121	WINDOWS					
vm40	7020021010	70SP20030909	0	0	876	876	86%	02/12/2005	21:35	INTEL_NT
INTEL_NT	QA70-1	COMPARE_REL	3.8	UP20020121	WINDOWS					
vm41	7020021010	70SP20030909	0	0	829	829	83%	02/12/2005	21:35	INTEL_NT
INTEL_NT	QA70-1	COMPARE_REL	3.8	UP20020121	WINDOWS					

vm42	7020021010	70SP20030909	0	0	607	607	77%	02/12/2005	21:35	INTEL_NT
INTEL_NT	QA70-1	COMPARE_REL	3.8	UP20020121	WINDOWS					
vm43	7020021010	70SP20030909	0	0	860	860	85%	02/12/2005	21:36	INTEL_NT
INTEL_NT	QA70-1	COMPARE_REL	3.8	UP20020121	WINDOWS					
vm44	7020021010	70SP20030909	0	0	1198	1198	90%	02/12/2005	21:36	INTEL_NT
INTEL_NT	QA70-1	COMPARE_REL	3.8	UP20020121	WINDOWS					
vm45	7020021010	70SP20030909	0	0	416	416	67%	02/12/2005	21:36	INTEL_NT
INTEL_NT	QA70-1	COMPARE_REL	3.8	UP20020121	WINDOWS					
vm46	7020021010	70SP20030909	0	0	794	794	82%	02/12/2005	21:36	INTEL_NT
INTEL_NT	QA70-1	COMPARE_REL	3.8	UP20020121	WINDOWS					
vm47	7020021010	70SP20030909	0	0	416	416	67%	02/12/2005	21:36	INTEL_NT
INTEL_NT	QA70-1	COMPARE_REL	3.8	UP20020121	WINDOWS					
vm48	7020021010	70SP20030909	0	0	421	421	68%	02/12/2005	21:36	INTEL_NT
INTEL_NT	QA70-1	COMPARE_REL	3.8	UP20020121	WINDOWS					
vm49	7020021010	70SP20030909	0	0	700	700	80%	02/12/2005	21:36	INTEL_NT
INTEL_NT	QA70-1	COMPARE_REL	3.8	UP20020121	WINDOWS					
vm50	7020021010	70SP20030909	0	0	500	500	72%	02/12/2005	21:36	INTEL_NT
INTEL_NT	QA70-1	COMPARE_REL	3.8	UP20020121	WINDOWS					
vm51	7020021010	70SP20030909	0	0	531	531	77%	02/12/2005	21:36	INTEL_NT
INTEL_NT	QA70-1	COMPARE_REL	3.8	UP20020121	WINDOWS					
vm52	7020021010	70SP20030909	0	0	520	520	74%	02/12/2005	21:36	INTEL_NT
INTEL_NT	QA70-1	COMPARE_REL	3.8	UP20020121	WINDOWS					
vm53	7020021010	70SP20030909	0	0	789	789	82%	02/12/2005	21:36	INTEL_NT
INTEL_NT	QA70-1	COMPARE_REL	3.8	UP20020121	WINDOWS					
vm54	7020021010	70SP20030909	0	0	564	564	75%	02/12/2005	21:36	INTEL_NT
INTEL_NT	QA70-1	COMPARE_REL	3.8	UP20020121	WINDOWS					
vm55	7020021010	70SP20030909	0	0	995	995	87%	02/12/2005	21:36	INTEL_NT
INTEL_NT	QA70-1	COMPARE_REL	3.8	UP20020121	WINDOWS					
vm56	7020021010	70SP20030909	0	0	1577	1577	91%	02/12/2005	21:36	INTEL_NT
INTEL_NT	QA70-1	COMPARE_REL	3.8	UP20020121	WINDOWS					
vm57	7020021010	70SP20030909	0	0	737	737	81%	02/12/2005	21:37	INTEL_NT
INTEL_NT	QA70-1	COMPARE_REL	3.8	UP20020121	WINDOWS					
vm58	7020021010	70SP20030909	0	0	580	580	76%	02/12/2005	21:37	INTEL_NT
INTEL_NT	QA70-1	COMPARE_REL	3.8	UP20020121	WINDOWS					
vm59	7020021010	70SP20030909	0	0	833	833	84%	02/12/2005	21:37	INTEL_NT
INTEL_NT	QA70-1	COMPARE_REL	3.8	UP20020121	WINDOWS					
vm60	7020021010	70SP20030909	0	0	537	537	72%	02/12/2005	21:37	INTEL_NT
INTEL_NT	QA70-1	COMPARE_REL	3.8	UP20020121	WINDOWS					
vm61	7020021010	70SP20030909	0	0	402	402	66%	02/12/2005	21:37	INTEL_NT
INTEL_NT	QA70-1	COMPARE_REL	3.8	UP20020121	WINDOWS					
vm62	7020021010	70SP20030909	0	0	755	755	82%	02/12/2005	21:37	INTEL_NT
INTEL_NT	QA70-1	COMPARE_REL	3.8	UP20020121	WINDOWS					
vm63	7020021010	70SP20030909	0	0	1280	1280	89%	02/12/2005	21:37	INTEL_NT
INTEL_NT	QA70-1	COMPARE_REL	3.8	UP20020121	WINDOWS					

vm64	7020021010	70SP20030909	0	0	510	510	74%	02/12/2005	21:37	INTEL_NT
INTEL_NT	QA70-1	COMPARE_REL	3.8	UP20020121	WINDOWS					
vm65	7020021010	70SP20030909	0	0	3323	3323	96%	02/12/2005	21:37	INTEL_NT
INTEL_NT	QA70-1	COMPARE_REL	3.8	UP20020121	WINDOWS					
vm66	7020021010	70SP20030909	0	0	516	516	74%	02/12/2005	21:37	INTEL_NT
INTEL_NT	QA70-1	COMPARE_REL	3.8	UP20020121	WINDOWS					
vm67	7020021010	70SP20030909	0	0	591	591	76%	02/12/2005	21:37	INTEL_NT
INTEL_NT	QA70-1	COMPARE_REL	3.8	UP20020121	WINDOWS					
vm68	7020021010	70SP20030909	0	0	739	739	80%	02/12/2005	21:37	INTEL_NT
INTEL_NT	QA70-1	COMPARE_REL	3.8	UP20020121	WINDOWS					
vm69	7020021010	70SP20030909	0	0	553	553	75%	02/12/2005	21:37	INTEL_NT
INTEL_NT	QA70-1	COMPARE_REL	3.8	UP20020121	WINDOWS					
vm70	7020021010	70SP20030909	0	0	940	940	86%	02/12/2005	21:37	INTEL_NT
INTEL_NT	QA70-1	COMPARE_REL	3.8	UP20020121	WINDOWS					
vm71	7020021010	70SP20030909	0	0	1307	1307	87%	02/12/2005	21:37	INTEL_NT
INTEL_NT	QA70-1	COMPARE_REL	3.8	UP20020121	WINDOWS					
vm72	7020021010	70SP20030909	0	0	2161	2161	90%	02/12/2005	21:37	INTEL_NT
INTEL_NT	QA70-1	COMPARE_REL	3.8	UP20020121	WINDOWS					
vm73	7020021010	70SP20030909	0	0	4189	4189	97%	02/12/2005	21:38	INTEL_NT
INTEL_NT	QA70-1	COMPARE_REL	3.8	UP20020121	WINDOWS					
vm74	7020021010	70SP20030909	0	0	855	855	81%	02/12/2005	21:38	INTEL_NT
INTEL_NT	QA70-1	COMPARE_REL	3.8	UP20020121	WINDOWS					
vm75	7020021010	70SP20030909	0	0	1129	1129	84%	02/12/2005	21:38	INTEL_NT
INTEL_NT	QA70-1	COMPARE_REL	3.8	UP20020121	WINDOWS					
vm76	7020021010	70SP20030909	0	0	1187	1187	89%	02/12/2005	21:38	INTEL_NT
INTEL_NT	QA70-1	COMPARE_REL	3.8	UP20020121	WINDOWS					
vm77	7020021010	70SP20030909	0	0	876	876	82%	02/12/2005	21:38	INTEL_NT
INTEL_NT	QA70-1	COMPARE_REL	3.8	UP20020121	WINDOWS					
vm78	7020021010	70SP20030909	0	0	872	872	86%	02/12/2005	21:38	INTEL_NT
INTEL_NT	QA70-1	COMPARE_REL	3.8	UP20020121	WINDOWS					
vm79	7020021010	70SP20030909	0	0	954	954	83%	02/12/2005	21:38	INTEL_NT
INTEL_NT	QA70-1	COMPARE_REL	3.8	UP20020121	WINDOWS					
vm80	7020021010	70SP20030909	0	0	2205	2205	92%	02/12/2005	21:38	INTEL_NT
INTEL_NT	QA70-1	COMPARE_REL	3.8	UP20020121	WINDOWS					
vm81	7020021010	70SP20030909	0	0	2015	2015	93%	02/12/2005	21:38	INTEL_NT
INTEL_NT	QA70-1	COMPARE_REL	3.8	UP20020121	WINDOWS					
vm82	7020021010	70SP20030909	0	0	2144	2144	94%	02/12/2005	21:38	INTEL_NT
INTEL_NT	QA70-1	COMPARE_REL	3.8	UP20020121	WINDOWS					
vm83	7020021010	70SP20030909	0	0	2191	2191	94%	02/12/2005	21:38	INTEL_NT
INTEL_NT	QA70-1	COMPARE_REL	3.8	UP20020121	WINDOWS					
vm84	7020021010	70SP20030909	0	0	821	821	82%	02/12/2005	21:38	INTEL_NT
INTEL_NT	QA70-1	COMPARE_REL	3.8	UP20020121	WINDOWS					
vm85	7020021010	70SP20030909	0	0	858	858	84%	02/12/2005	21:38	INTEL_NT
INTEL_NT	QA70-1	COMPARE_REL	3.8	UP20020121	WINDOWS					

vm86	7020021010	70SP20030909	0	0	428	428	68%	02/12/2005	21:39	INTEL_NT
INTEL_NT	QA70-1	COMPARE_REL	3.8	UP20020121	WINDOWS					
vm87	7020021010	70SP20030909	0	0	434	434	69%	02/12/2005	21:39	INTEL_NT
INTEL_NT	QA70-1	COMPARE_REL	3.8	UP20020121	WINDOWS					
vm88	7020021010	70SP20030909	0	0	450	450	70%	02/12/2005	21:39	INTEL_NT
INTEL_NT	QA70-1	COMPARE_REL	3.8	UP20020121	WINDOWS					
vm89	7020021010	70SP20030909	0	0	480	480	72%	02/12/2005	21:39	INTEL_NT
INTEL_NT	QA70-1	COMPARE_REL	3.8	UP20020121	WINDOWS					
vm90	7020021010	70SP20030909	0	0	761	761	82%	02/12/2005	21:39	INTEL_NT
INTEL_NT	QA70-1	COMPARE_REL	3.8	UP20020121	WINDOWS					
vm91	7020021010	70SP20030909	0	0	2102	2102	94%	02/12/2005	21:39	INTEL_NT
INTEL_NT	QA70-1	COMPARE_REL	3.8	UP20020121	WINDOWS					
vm92	7020021010	70SP20030909	0	0	501	501	73%	02/12/2005	21:39	INTEL_NT
INTEL_NT	QA70-1	COMPARE_REL	3.8	UP20020121	WINDOWS					
vm93	7020021010	70SP20030909	0	0	436	436	69%	02/12/2005	21:39	INTEL_NT
INTEL_NT	QA70-1	COMPARE_REL	3.8	UP20020121	WINDOWS					
vm94	7020021010	70SP20030909	0	0	508	508	73%	02/12/2005	21:39	INTEL_NT
INTEL_NT	QA70-1	COMPARE_REL	3.8	UP20020121	WINDOWS					
vm95	7020021010	70SP20030909	0	0	1044	1044	86%	02/12/2005	21:39	INTEL_NT
INTEL_NT	QA70-1	COMPARE_REL	3.8	UP20020121	WINDOWS					
vm96	7020021010	70SP20030909	0	0	633	633	78%	02/12/2005	21:39	INTEL_NT
INTEL_NT	QA70-1	COMPARE_REL	3.8	UP20020121	WINDOWS					
vm97	7020021010	70SP20030909	0	0	809	809	83%	02/12/2005	21:39	INTEL_NT
INTEL_NT	QA70-1	COMPARE_REL	3.8	UP20020121	WINDOWS					
vm98	7020021010	70SP20030909	0	0	703	703	80%	02/12/2005	21:39	INTEL_NT
INTEL_NT	QA70-1	COMPARE_REL	3.8	UP20020121	WINDOWS					
vm99	7020021010	70SP20030909	0	0	482	482	72%	02/12/2005	21:39	INTEL_NT
INTEL_NT	QA70-1	COMPARE_REL	3.8	UP20020121	WINDOWS					
vm100	7020021010	70SP20030909	0	0	642	642	79%	02/12/2005	21:39	INTEL_NT
INTEL_NT	QA70-1	COMPARE_REL	3.8	UP20020121	WINDOWS					
vm101	7020021010	70SP20030909	0	0	720	720	81%	02/12/2005	21:39	INTEL_NT
INTEL_NT	QA70-1	COMPARE_REL	3.8	UP20020121	WINDOWS					
vm102	7020021010	70SP20030909	0	0	761	761	82%	02/12/2005	21:39	INTEL_NT
INTEL_NT	QA70-1	COMPARE_REL	3.8	UP20020121	WINDOWS					
vm103	7020021010	70SP20030909	0	0	782	782	84%	02/12/2005	21:39	INTEL_NT
INTEL_NT	QA70-1	COMPARE_REL	3.8	UP20020121	WINDOWS					
vm104	7020021010	70SP20030909	0	0	1822	1822	93%	02/12/2005	21:40	INTEL_NT
INTEL_NT	QA70-1	COMPARE_REL	3.8	UP20020121	WINDOWS					
vm105	7020021010	70SP20030909	0	0	589	589	77%	02/12/2005	21:40	INTEL_NT
INTEL_NT	QA70-1	COMPARE_REL	3.8	UP20020121	WINDOWS					
vm106	7020021010	70SP20030909	0	0	432	432	69%	02/12/2005	21:40	INTEL_NT
INTEL_NT	QA70-1	COMPARE_REL	3.8	UP20020121	WINDOWS					
vm107	7020021010	70SP20030909	0	0	476	476	72%	02/12/2005	21:40	INTEL_NT
INTEL_NT	QA70-1	COMPARE_REL	3.8	UP20020121	WINDOWS					

vm108	7020021010	70SP20030909	0	0	437	437	69%	02/12/2005	21:40	INTEL_NT
INTEL_NT	QA70-1	COMPARE_REL	3.8	UP20020121	WINDOWS					
vm109	7020021010	70SP20030909	0	0	1025	1025	87%	02/12/2005	21:40	INTEL_NT
INTEL_NT	QA70-1	COMPARE_REL	3.8	UP20020121	WINDOWS					
vm110	7020021010	70SP20030909	0	0	743	743	82%	02/12/2005	21:40	INTEL_NT
INTEL_NT	QA70-1	COMPARE_REL	3.8	UP20020121	WINDOWS					
vm111	7020021010	70SP20030909	0	0	3511	3511	96%	02/12/2005	21:41	INTEL_NT
INTEL_NT	QA70-1	COMPARE_REL	3.8	UP20020121	WINDOWS					
vm112	7020021010	70SP20030909	0	0	726	726	81%	02/12/2005	21:41	INTEL_NT
INTEL_NT	QA70-1	COMPARE_REL	3.8	UP20020121	WINDOWS					
vm113	7020021010	70SP20030909	0	0	732	732	82%	02/12/2005	21:41	INTEL_NT
INTEL_NT	QA70-1	COMPARE_REL	3.8	UP20020121	WINDOWS					
vm114	7020021010	70SP20030909	0	0	693	693	80%	02/12/2005	21:41	INTEL_NT
INTEL_NT	QA70-1	COMPARE_REL	3.8	UP20020121	WINDOWS					
vm115	7020021010	70SP20030909	0	0	604	604	78%	02/12/2005	21:41	INTEL_NT
INTEL_NT	QA70-1	COMPARE_REL	3.8	UP20020121	WINDOWS					
vm116	7020021010	70SP20030909	0	0	830	830	84%	02/12/2005	21:41	INTEL_NT
INTEL_NT	QA70-1	COMPARE_REL	3.8	UP20020121	WINDOWS					
vm117	7020021010	70SP20030909	0	0	1048	1048	86%	02/12/2005	21:41	INTEL_NT
INTEL_NT	QA70-1	COMPARE_REL	3.8	UP20020121	WINDOWS					
vm118	7020021010	70SP20030909	0	0	918	918	85%	02/12/2005	21:41	INTEL_NT
INTEL_NT	QA70-1	COMPARE_REL	3.8	UP20020121	WINDOWS					
vm119	7020021010	70SP20030909	0	0	1225	1225	89%	02/12/2005	21:41	INTEL_NT
INTEL_NT	QA70-1	COMPARE_REL	3.8	UP20020121	WINDOWS					
vm120	7020021010	70SP20030909	0	0	485	485	72%	02/12/2005	21:41	INTEL_NT
INTEL_NT	QA70-1	COMPARE_REL	3.8	UP20020121	WINDOWS					
vm121	7020021010	70SP20030909	0	0	811	811	83%	02/12/2005	21:42	INTEL_NT
INTEL_NT	QA70-1	COMPARE_REL	3.8	UP20020121	WINDOWS					
vm122	7020021010	70SP20030909	0	0	422	422	68%	02/12/2005	21:42	INTEL_NT
INTEL_NT	QA70-1	COMPARE_REL	3.8	UP20020121	WINDOWS					
vm123	7020021010	70SP20030909	0	0	467	467	71%	02/12/2005	21:42	INTEL_NT
INTEL_NT	QA70-1	COMPARE_REL	3.8	UP20020121	WINDOWS					
vm124	7020021010	70SP20030909	0	0	591	591	77%	02/12/2005	21:42	INTEL_NT
INTEL_NT	QA70-1	COMPARE_REL	3.8	UP20020121	WINDOWS					
vm125	7020021010	70SP20030909	0	0	762	762	82%	02/12/2005	21:42	INTEL_NT
INTEL_NT	QA70-1	COMPARE_REL	3.8	UP20020121	WINDOWS					
vm126	7020021010	70SP20030909	0	0	661	661	80%	02/12/2005	21:42	INTEL_NT
INTEL_NT	QA70-1	COMPARE_REL	3.8	UP20020121	WINDOWS					
vm127	7020021010	70SP20030909	0	0	625	625	79%	02/12/2005	21:42	INTEL_NT
INTEL_NT	QA70-1	COMPARE_REL	3.8	UP20020121	WINDOWS					
vm128	7020021010	70SP20030909	0	0	815	815	83%	02/12/2005	21:42	INTEL_NT
INTEL_NT	QA70-1	COMPARE_REL	3.8	UP20020121	WINDOWS					
vm129	7020021010	70SP20030909	0	0	373	373	66%	02/12/2005	21:42	INTEL_NT
INTEL_NT	QA70-1	COMPARE_REL	3.8	UP20020121	WINDOWS					

vm130	7020021010	70SP20030909	0	0	553	553	78%	02/12/2005	21:42	INTEL_NT
INTEL_NT	QA70-1	COMPARE_REL	3.8	UP20020121	WINDOWS					
vm131	7020021010	70SP20030909	0	0	448	448	70%	02/12/2005	21:42	INTEL_NT
INTEL_NT	QA70-1	COMPARE_REL	3.8	UP20020121	WINDOWS					
vm132	7020021010	70SP20030909	0	0	1827	1827	93%	02/12/2005	21:42	INTEL_NT
INTEL_NT	QA70-1	COMPARE_REL	3.8	UP20020121	WINDOWS					
vm133	7020021010	70SP20030909	0	0	1701	1701	92%	02/12/2005	21:42	INTEL_NT
INTEL_NT	QA70-1	COMPARE_REL	3.8	UP20020121	WINDOWS					
vm134	7020021010	70SP20030909	0	0	1808	1808	93%	02/12/2005	21:42	INTEL_NT
INTEL_NT	QA70-1	COMPARE_REL	3.8	UP20020121	WINDOWS					
vm135	7020021010	70SP20030909	0	0	561	561	77%	02/12/2005	21:42	INTEL_NT
INTEL_NT	QA70-1	COMPARE_REL	3.8	UP20020121	WINDOWS					
vm136	7020021010	70SP20030909	0	0	1909	1909	93%	02/12/2005	21:43	INTEL_NT
INTEL_NT	QA70-1	COMPARE_REL	3.8	UP20020121	WINDOWS					
vm137	7020021010	70SP20030909	0	0	1395	1395	91%	02/12/2005	21:43	INTEL_NT
INTEL_NT	QA70-1	COMPARE_REL	3.8	UP20020121	WINDOWS					
vm138	7020021010	70SP20030909	0	0	528	528	75%	02/12/2005	21:43	INTEL_NT
INTEL_NT	QA70-1	COMPARE_REL	3.8	UP20020121	WINDOWS					
vm139	7020021010	70SP20030909	0	0	1132	1132	88%	02/12/2005	21:43	INTEL_NT
INTEL_NT	QA70-1	COMPARE_REL	3.8	UP20020121	WINDOWS					
vm140	7020021010	70SP20030909	0	0	1184	1184	89%	02/12/2005	21:43	INTEL_NT
INTEL_NT	QA70-1	COMPARE_REL	3.8	UP20020121	WINDOWS					
vm141	7020021010	70SP20030909	0	0	2040	2040	93%	02/12/2005	21:43	INTEL_NT
INTEL_NT	QA70-1	COMPARE_REL	3.8	UP20020121	WINDOWS					
vm142	7020021010	70SP20030909	0	0	879	879	85%	02/12/2005	21:43	INTEL_NT
INTEL_NT	QA70-1	COMPARE_REL	3.8	UP20020121	WINDOWS					
vm143	7020021010	70SP20030909	0	0	1672	1672	91%	02/12/2005	21:43	INTEL_NT
INTEL_NT	QA70-1	COMPARE_REL	3.8	UP20020121	WINDOWS					
vm144	7020021010	70SP20030909	0	0	2164	2164	94%	02/12/2005	21:43	INTEL_NT
INTEL_NT	QA70-1	COMPARE_REL	3.8	UP20020121	WINDOWS					
vm145	7020021010	70SP20030909	0	0	532	532	75%	02/12/2005	21:43	INTEL_NT
INTEL_NT	QA70-1	COMPARE_REL	3.8	UP20020121	WINDOWS					
vm146	7020021010	70SP20030909	0	0	883	883	86%	02/12/2005	21:43	INTEL_NT
INTEL_NT	QA70-1	COMPARE_REL	3.8	UP20020121	WINDOWS					
vm147	7020021010	70SP20030909	0	0	588	588	77%	02/12/2005	21:43	INTEL_NT
INTEL_NT	QA70-1	COMPARE_REL	3.8	UP20020121	WINDOWS					
vm148	7020021010	70SP20030909	0	0	588	588	78%	02/12/2005	21:43	INTEL_NT
INTEL_NT	QA70-1	COMPARE_REL	3.8	UP20020121	WINDOWS					
vm149	7020021010	70SP20030909	0	0	520	520	74%	02/12/2005	21:43	INTEL_NT
INTEL_NT	QA70-1	COMPARE_REL	3.8	UP20020121	WINDOWS					
vm150	7020021010	70SP20030909	0	0	657	657	79%	02/12/2005	21:43	INTEL_NT
INTEL_NT	QA70-1	COMPARE_REL	3.8	UP20020121	WINDOWS					
vm151	7020021010	70SP20030909	0	0	1058	1058	87%	02/12/2005	21:43	INTEL_NT
INTEL_NT	QA70-1	COMPARE_REL	3.8	UP20020121	WINDOWS					

vm152	7020021010	70SP20030909	0	0	1211	1211	88%	02/12/2005	21:43	INTEL_NT
INTEL_NT	QA70-1	COMPARE_REL	3.8		UP20020121	WINDOWS				
vm153	7020021010	70SP20030909	0	0	507	507	74%	02/12/2005	21:44	INTEL_NT
INTEL_NT	QA70-1	COMPARE_REL	3.8		UP20020121	WINDOWS				
vm154	7020021010	70SP20030909	0	0	814	814	82%	02/12/2005	21:44	INTEL_NT
INTEL_NT	QA70-1	COMPARE_REL	3.8		UP20020121	WINDOWS				
vm155	7020021010	70SP20030909	0	0	1255	1255	89%	02/12/2005	21:46	INTEL_NT
INTEL_NT	QA70-1	COMPARE_REL	3.8		UP20020121	WINDOWS				
vm156	7020021010	70SP20030909	0	0	2047	2047	94%	02/12/2005	21:46	INTEL_NT
INTEL_NT	QA70-1	COMPARE_REL	3.8		UP20020121	WINDOWS				
vm157	7020021010	70SP20030909	0	0	952	952	85%	02/12/2005	21:46	INTEL_NT
INTEL_NT	QA70-1	COMPARE_REL	3.8		UP20020121	WINDOWS				
vm158	7020021010	70SP20030909	0	0	955	955	87%	02/12/2005	21:47	INTEL_NT
INTEL_NT	QA70-1	COMPARE_REL	3.8		UP20020121	WINDOWS				
vm159	7020021010	70SP20030909	0	0	1524	1524	91%	02/12/2005	21:47	INTEL_NT
INTEL_NT	QA70-1	COMPARE_REL	3.8		UP20020121	WINDOWS				
vm160	7020021010	70SP20030909	0	0	600	600	78%	02/12/2005	21:47	INTEL_NT
INTEL_NT	QA70-1	COMPARE_REL	3.8		UP20020121	WINDOWS				
vm161	7020021010	70SP20030909	0	0	539	539	75%	02/12/2005	21:47	INTEL_NT
INTEL_NT	QA70-1	COMPARE_REL	3.8		UP20020121	WINDOWS				
vm162	7020021010	70SP20030909	0	0	548	548	76%	02/12/2005	21:47	INTEL_NT
INTEL_NT	QA70-1	COMPARE_REL	3.8		UP20020121	WINDOWS				
vm163	7020021010	70SP20030909	0	0	563	563	76%	02/12/2005	21:47	INTEL_NT
INTEL_NT	QA70-1	COMPARE_REL	3.8		UP20020121	WINDOWS				
vm164	7020021010	70SP20030909	0	0	556	556	76%	02/12/2005	21:47	INTEL_NT
INTEL_NT	QA70-1	COMPARE_REL	3.8		UP20020121	WINDOWS				
vm165	7020021010	70SP20030909	0	0	703	703	80%	02/12/2005	21:47	INTEL_NT
INTEL_NT	QA70-1	COMPARE_REL	3.8		UP20020121	WINDOWS				
vm166	7020021010	70SP20030909	0	0	700	700	80%	02/12/2005	21:47	INTEL_NT
INTEL_NT	QA70-1	COMPARE_REL	3.8		UP20020121	WINDOWS				
vm167	7020021010	70SP20030909	0	0	1138	1138	88%	02/12/2005	21:47	INTEL_NT
INTEL_NT	QA70-1	COMPARE_REL	3.8		UP20020121	WINDOWS				
vm168	7020021010	70SP20030909	0	0	687	687	81%	02/12/2005	21:47	INTEL_NT
INTEL_NT	QA70-1	COMPARE_REL	3.8		UP20020121	WINDOWS				
vm169	7020021010	70SP20030909	0	0	777	777	82%	02/12/2005	21:47	INTEL_NT
INTEL_NT	QA70-1	COMPARE_REL	3.8		UP20020121	WINDOWS				
vm170	7020021010	70SP20030909	0	0	436	436	69%	02/12/2005	21:47	INTEL_NT
INTEL_NT	QA70-1	COMPARE_REL	3.8		UP20020121	WINDOWS				
vm171	7020021010	70SP20030909	0	0	759	759	82%	02/12/2005	21:47	INTEL_NT
INTEL_NT	QA70-1	COMPARE_REL	3.8		UP20020121	WINDOWS				
vm172	7020021010	70SP20030909	0	0	1528	1528	90%	02/12/2005	21:47	INTEL_NT
INTEL_NT	QA70-1	COMPARE_REL	3.8		UP20020121	WINDOWS				
vm173	7020021010	70SP20030909	0	0	545	545	75%	02/12/2005	21:47	INTEL_NT
INTEL_NT	QA70-1	COMPARE_REL	3.8		UP20020121	WINDOWS				

vm174	7020021010	70SP20030909	0	0	602	602	77%	02/12/2005	21:47	INTEL_NT
INTEL_NT	QA70-1	COMPARE_REL	3.8	UP20020121	WINDOWS					
vm175	7020021010	70SP20030909	0	0	855	855	84%	02/12/2005	21:47	INTEL_NT
INTEL_NT	QA70-1	COMPARE_REL	3.8	UP20020121	WINDOWS					
vm176	7020021010	70SP20030909	0	0	999	999	86%	02/12/2005	21:47	INTEL_NT
INTEL_NT	QA70-1	COMPARE_REL	3.8	UP20020121	WINDOWS					
vm177	7020021010	70SP20030909	0	0	1127	1127	87%	02/12/2005	21:48	INTEL_NT
INTEL_NT	QA70-1	COMPARE_REL	3.8	UP20020121	WINDOWS					
vm178	7020021010	70SP20030909	0	0	679	679	80%	02/12/2005	21:48	INTEL_NT
INTEL_NT	QA70-1	COMPARE_REL	3.8	UP20020121	WINDOWS					
vm179	7020021010	70SP20030909	0	0	768	768	82%	02/12/2005	21:48	INTEL_NT
INTEL_NT	QA70-1	COMPARE_REL	3.8	UP20020121	WINDOWS					
vm180	7020021010	70SP20030909	0	0	651	651	79%	02/12/2005	21:48	INTEL_NT
INTEL_NT	QA70-1	COMPARE_REL	3.8	UP20020121	WINDOWS					
vm181	7020021010	70SP20030909	0	0	484	484	71%	02/12/2005	21:48	INTEL_NT
INTEL_NT	QA70-1	COMPARE_REL	3.8	UP20020121	WINDOWS					
vm182	7020021010	70SP20030909	0	0	973	973	87%	02/12/2005	21:48	INTEL_NT
INTEL_NT	QA70-1	COMPARE_REL	3.8	UP20020121	WINDOWS					
vm183	7020021010	70SP20030909	0	0	722	722	81%	02/12/2005	21:48	INTEL_NT
INTEL_NT	QA70-1	COMPARE_REL	3.8	UP20020121	WINDOWS					
vm184	7020021010	70SP20030909	1	5	3162	3162	95%	02/12/2005	21:48	INTEL_NT
INTEL_NT	QA70-1	COMPARE_REL	3.8	UP20020121	WINDOWS					
vm185	7020021010	70SP20030909	0	0	738	738	81%	02/12/2005	21:48	INTEL_NT
INTEL_NT	QA70-1	COMPARE_REL	3.8	UP20020121	WINDOWS					
vm186	7020021010	70SP20030909	0	0	1392	1392	91%	02/12/2005	21:49	INTEL_NT
INTEL_NT	QA70-1	COMPARE_REL	3.8	UP20020121	WINDOWS					
vm187	7020021010	70SP20030909	0	0	1489	1489	90%	02/12/2005	21:49	INTEL_NT
INTEL_NT	QA70-1	COMPARE_REL	3.8	UP20020121	WINDOWS					
vm188	7020021010	70SP20030909	0	0	658	658	79%	02/12/2005	21:49	INTEL_NT
INTEL_NT	QA70-1	COMPARE_REL	3.8	UP20020121	WINDOWS					
vm189	7020021010	70SP20030909	0	0	1067	1067	87%	02/12/2005	21:49	INTEL_NT
INTEL_NT	QA70-1	COMPARE_REL	3.8	UP20020121	WINDOWS					
vm190	7020021010	70SP20030909	0	0	715	715	81%	02/12/2005	21:49	INTEL_NT
INTEL_NT	QA70-1	COMPARE_REL	3.8	UP20020121	WINDOWS					
vm191	7020021010	70SP20030909	0	0	3075	3075	95%	02/12/2005	21:49	INTEL_NT
INTEL_NT	QA70-1	COMPARE_REL	3.8	UP20020121	WINDOWS					
vm192	7020021010	70SP20030909	0	0	645	645	80%	02/12/2005	21:49	INTEL_NT
INTEL_NT	QA70-1	COMPARE_REL	3.8	UP20020121	WINDOWS					
vm193	7020021010	70SP20030909	0	0	411	411	68%	02/12/2005	21:49	INTEL_NT
INTEL_NT	QA70-1	COMPARE_REL	3.8	UP20020121	WINDOWS					
vm194	7020021010	70SP20030909	0	0	821	821	83%	02/12/2005	21:49	INTEL_NT
INTEL_NT	QA70-1	COMPARE_REL	3.8	UP20020121	WINDOWS					
vm195	7020021010	70SP20030909	0	0	824	824	84%	02/12/2005	21:49	INTEL_NT
INTEL_NT	QA70-1	COMPARE_REL	3.8	UP20020121	WINDOWS					

vm196	7020021010	70SP20030909	0	0	505	505	73%	02/12/2005	21:49	INTEL_NT
INTEL_NT	QA70-1	COMPARE_REL	3.8	UP20020121	WINDOWS					
vm197	7020021010	70SP20030909	0	0	509	509	74%	02/12/2005	21:49	INTEL_NT
INTEL_NT	QA70-1	COMPARE_REL	3.8	UP20020121	WINDOWS					
vm198	7020021010	70SP20030909	2	0	1208	1208	88%	02/12/2005	21:50	INTEL_NT
INTEL_NT	QA70-1	COMPARE_REL	3.8	UP20020121	WINDOWS					
vm199	7020021010	70SP20030909	0	0	835	835	84%	02/12/2005	21:50	INTEL_NT
INTEL_NT	QA70-1	COMPARE_REL	3.8	UP20020121	WINDOWS					
vm200	7020021010	70SP20030909	0	0	1258	1258	89%	02/12/2005	21:51	INTEL_NT
INTEL_NT	QA70-1	COMPARE_REL	3.8	UP20020121	WINDOWS					
vm201	7020021010	70SP20030909	0	0	3072	3072	95%	02/12/2005	21:51	INTEL_NT
INTEL_NT	QA70-1	COMPARE_REL	3.8	UP20020121	WINDOWS					
vm202	7020021010	70SP20030909	0	0	604	604	77%	02/12/2005	21:52	INTEL_NT
INTEL_NT	QA70-1	COMPARE_REL	3.8	UP20020121	WINDOWS					
vm203	7020021010	70SP20030909	0	0	1020	1020	87%	02/12/2005	21:52	INTEL_NT
INTEL_NT	QA70-1	COMPARE_REL	3.8	UP20020121	WINDOWS					
vm204	7020021010	70SP20030909	0	0	621	621	79%	02/12/2005	21:52	INTEL_NT
INTEL_NT	QA70-1	COMPARE_REL	3.8	UP20020121	WINDOWS					
vm205	7020021010	70SP20030909	0	0	652	652	79%	02/12/2005	21:52	INTEL_NT
INTEL_NT	QA70-1	COMPARE_REL	3.8	UP20020121	WINDOWS					
vm206	7020021010	70SP20030909	0	0	903	903	84%	02/12/2005	21:52	INTEL_NT
INTEL_NT	QA70-1	COMPARE_REL	3.8	UP20020121	WINDOWS					
vm207	7020021010	70SP20030909	0	0	1079	1079	87%	02/12/2005	21:52	INTEL_NT
INTEL_NT	QA70-1	COMPARE_REL	3.8	UP20020121	WINDOWS					
vm208	7020021010	70SP20030909	0	0	701	701	82%	02/12/2005	21:52	INTEL_NT
INTEL_NT	QA70-1	COMPARE_REL	3.8	UP20020121	WINDOWS					
vm209	7020021010	70SP20030909	0	0	3159	3159	96%	02/12/2005	21:53	INTEL_NT
INTEL_NT	QA70-1	COMPARE_REL	3.8	UP20020121	WINDOWS					
vm210	7020021010	70SP20030909	0	0	1426	1426	90%	02/12/2005	21:53	INTEL_NT
INTEL_NT	QA70-1	COMPARE_REL	3.8	UP20020121	WINDOWS					
vm211	7020021010	70SP20030909	0	0	2658	2658	94%	02/12/2005	21:55	INTEL_NT
INTEL_NT	QA70-1	COMPARE_REL	3.8	UP20020121	WINDOWS					
vm212	7020021010	70SP20030909	0	0	1041	1041	86%	02/12/2005	21:55	INTEL_NT
INTEL_NT	QA70-1	COMPARE_REL	3.8	UP20020121	WINDOWS					
vm213	7020021010	70SP20030909	0	0	687	687	80%	02/12/2005	21:55	INTEL_NT
INTEL_NT	QA70-1	COMPARE_REL	3.8	UP20020121	WINDOWS					
vm214	7020021010	70SP20030909	0	0	557	557	76%	02/12/2005	21:55	INTEL_NT
INTEL_NT	QA70-1	COMPARE_REL	3.8	UP20020121	WINDOWS					
vm215	7020021010	70SP20030909	0	0	637	637	80%	02/12/2005	21:55	INTEL_NT
INTEL_NT	QA70-1	COMPARE_REL	3.8	UP20020121	WINDOWS					
vm216	7020021010	70SP20030909	0	0	1111	1111	87%	02/12/2005	21:55	INTEL_NT
INTEL_NT	QA70-1	COMPARE_REL	3.8	UP20020121	WINDOWS					
vm217	7020021010	70SP20030909	0	0	873	873	84%	02/12/2005	21:56	INTEL_NT
INTEL_NT	QA70-1	COMPARE_REL	3.8	UP20020121	WINDOWS					

vm218	7020021010	70SP20030909	0	0	744	744	82%	02/12/2005	21:56	INTEL_NT
INTEL_NT	QA70-1	COMPARE_REL	3.8	UP20020121	WINDOWS					
vm219	7020021010	70SP20030909	0	0	698	698	81%	02/12/2005	21:56	INTEL_NT
INTEL_NT	QA70-1	COMPARE_REL	3.8	UP20020121	WINDOWS					
vm220	7020021010	70SP20030909	0	0	477	477	75%	02/12/2005	21:57	INTEL_NT
INTEL_NT	QA70-1	COMPARE_REL	3.8	UP20020121	WINDOWS					
vm221	7020021010	70SP20030909	0	0	605	605	80%	02/12/2005	21:57	INTEL_NT
INTEL_NT	QA70-1	COMPARE_REL	3.8	UP20020121	WINDOWS					
vm222	7020021010	70SP20030909	0	0	1536	1536	91%	02/12/2005	21:57	INTEL_NT
INTEL_NT	QA70-1	COMPARE_REL	3.8	UP20020121	WINDOWS					
vm223	7020021010	70SP20030909	0	0	484	484	74%	02/12/2005	21:57	INTEL_NT
INTEL_NT	QA70-1	COMPARE_REL	3.8	UP20020121	WINDOWS					
vm224	7020021010	70SP20030909	0	0	577	577	79%	02/12/2005	21:57	INTEL_NT
INTEL_NT	QA70-1	COMPARE_REL	3.8	UP20020121	WINDOWS					
vm225	7020021010	70SP20030909	0	0	496	496	73%	02/12/2005	21:57	INTEL_NT
INTEL_NT	QA70-1	COMPARE_REL	3.8	UP20020121	WINDOWS					
vm226	7020021010	70SP20030909	0	0	1622	1622	91%	02/12/2005	21:58	INTEL_NT
INTEL_NT	QA70-1	COMPARE_REL	3.8	UP20020121	WINDOWS					
vm227	7020021010	70SP20030909	0	0	957	957	87%	02/12/2005	21:58	INTEL_NT
INTEL_NT	QA70-1	COMPARE_REL	3.8	UP20020121	WINDOWS					
vm228	7020021010	70SP20030909	0	0	5849	5849	98%	02/12/2005	21:58	INTEL_NT
INTEL_NT	QA70-1	COMPARE_REL	3.8	UP20020121	WINDOWS					
vm229	7020021010	70SP20030909	0	0	3944	3944	97%	02/12/2005	21:59	INTEL_NT
INTEL_NT	QA70-1	COMPARE_REL	3.8	UP20020121	WINDOWS					
vm230	7020021010	70SP20030909	0	0	26798	26798	99%	02/12/2005	22:37	INTEL_NT
INTEL_NT	QA70-1	COMPARE_REL	3.8	UP20020121	WINDOWS					
vm231	7020021010	70SP20030909	0	0	528	528	76%	02/12/2005	22:37	INTEL_NT
INTEL_NT	QA70-1	COMPARE_REL	3.8	UP20020121	WINDOWS					
vm232	7020021010	70SP20030909	0	0	14057	14057	98%	02/12/2005	22:43	INTEL_NT
INTEL_NT	QA70-1	COMPARE_REL	3.8	UP20020121	WINDOWS					
vm233	7020021010	70SP20030909	0	0	583	583	80%	02/12/2005	22:44	INTEL_NT
INTEL_NT	QA70-1	COMPARE_REL	3.8	UP20020121	WINDOWS					
vm234	7020021010	70SP20030909	0	0	1468	1468	92%	02/12/2005	22:47	INTEL_NT
INTEL_NT	QA70-1	COMPARE_REL	3.8	UP20020121	WINDOWS					
vm235	7020021010	70SP20030909	0	0	769	769	81%	02/12/2005	22:47	INTEL_NT
INTEL_NT	QA70-1	COMPARE_REL	3.8	UP20020121	WINDOWS					
vm236	7020021010	70SP20030909	0	0	1760	1760	92%	02/12/2005	22:47	INTEL_NT
INTEL_NT	QA70-1	COMPARE_REL	3.8	UP20020121	WINDOWS					
vmc1	7020021010	70SP20030909	0	0	643	643	81%	02/12/2005	22:48	INTEL_NT
INTEL_NT	QA70-1	COMPARE_REL	3.8	UP20020121	WINDOWS					
vmc2	7020021010	70SP20030909	0	0	1692	1692	90%	02/12/2005	22:49	INTEL_NT
INTEL_NT	QA70-1	COMPARE_REL	3.8	UP20020121	WINDOWS					
vmc3	7020021010	70SP20030909	0	0	426	426	72%	02/12/2005	22:49	INTEL_NT
INTEL_NT	QA70-1	COMPARE_REL	3.8	UP20020121	WINDOWS					

vmc4	7020021010	70SP20030909	0	0	773	773	85%	02/12/2005	22:49	INTEL_NT
INTEL_NT	QA70-1	COMPARE_REL	3.8		UP20020121	WINDOWS				
vmc5	7020021010	70SP20030909	0	0	513	513	78%	02/12/2005	22:50	INTEL_NT
INTEL_NT	QA70-1	COMPARE_REL	3.8		UP20020121	WINDOWS				
vmc6	7020021010	70SP20030909	0	0	433	433	74%	02/12/2005	22:51	INTEL_NT
INTEL_NT	QA70-1	COMPARE_REL	3.8		UP20020121	WINDOWS				
vmc7	7020021010	70SP20030909	0	0	337	337	67%	02/12/2005	22:51	INTEL_NT
INTEL_NT	QA70-1	COMPARE_REL	3.8		UP20020121	WINDOWS				
vmc8	7020021010	70SP20030909	2	0	1894	1894	92%	02/12/2005	23:09	INTEL_NT
INTEL_NT	QA70-1	COMPARE_REL	3.8		UP20020121	WINDOWS				
vmd1	7020021010	70SP20030909	0	0	816	816	86%	02/12/2005	23:09	INTEL_NT
INTEL_NT	QA70-1	COMPARE_REL	3.8		UP20020121	WINDOWS				
vmd2	7020021010	70SP20030909	0	0	337	337	67%	02/12/2005	23:09	INTEL_NT
INTEL_NT	QA70-1	COMPARE_REL	3.8		UP20020121	WINDOWS				
vmd3	7020021010	70SP20030909	0	0	608	608	82%	02/12/2005	23:11	INTEL_NT
INTEL_NT	QA70-1	COMPARE_REL	3.8		UP20020121	WINDOWS				
cyc-177s	7020021010	70SP20030909	1	0	1219	1222	91%	02/12/2005	23:13	INTEL_NT
INTEL_NT	QA70-1	COMPARE_REL	3.8		UP20020121	WINDOWS				
cyc-178s	7020021010	70SP20030909	1	0	1219	1222	91%	02/12/2005	23:14	INTEL_NT
INTEL_NT	QA70-1	COMPARE_REL	3.8		UP20020121	WINDOWS				
dds-13s	7020021010	NO_UPDATE	-88	0	402	146	49%	02/12/2005	23:14	INTEL_NT
NOT_AVAILABLE	QA70-1	COMPARE_REL	3.8		UP20020121	WINDOWS				
dds-17s	7020021010	NO_UPDATE	-88	0	746	146	67%	02/12/2005	23:14	INTEL_NT
NOT_AVAILABLE	QA70-1	COMPARE_REL	3.8		UP20020121	WINDOWS				
esp-112s	7020021010	70SP20030909	0	0	279	279	58%	02/12/2005	23:15	INTEL_NT
INTEL_NT	QA70-1	COMPARE_REL	3.8		UP20020121	WINDOWS				
esp-124s	7020021010	70SP20030909	0	0	392	392	66%	02/12/2005	23:15	INTEL_NT
INTEL_NT	QA70-1	COMPARE_REL	3.8		UP20020121	WINDOWS				
esp-127s	7020021010	70SP20030909	0	0	527	527	75%	02/12/2005	23:15	INTEL_NT
INTEL_NT	QA70-1	COMPARE_REL	3.8		UP20020121	WINDOWS				
ess-26s	7020021010	70SP20030909	0	0	1846	1846	92%	02/12/2005	23:15	INTEL_NT
INTEL_NT	QA70-1	COMPARE_REL	3.8		UP20020121	WINDOWS				
ess-97s	7020021010	70SP20030909	0	0	1378	1378	90%	02/12/2005	23:15	INTEL_NT
INTEL_NT	QA70-1	COMPARE_REL	3.8		UP20020121	WINDOWS				
ev117-106s	7020021010	70SP20030909	0	0	1333	1333	91%	02/12/2005	23:15	INTEL_NT
INTEL_NT	QA70-1	COMPARE_REL	3.8		UP20020121	WINDOWS				
ev119-35s	7020021010	70SP20030909	0	0	506	506	74%	02/12/2005	23:15	INTEL_NT
INTEL_NT	QA70-1	COMPARE_REL	3.8		UP20020121	WINDOWS				
ev120-85s	7020021010	70SP20030909	0	0	411	411	71%	02/12/2005	23:15	INTEL_NT
INTEL_NT	QA70-1	COMPARE_REL	3.8		UP20020121	WINDOWS				
ev141-208s	7020021010	70SP20030909	0	0	341	341	66%	02/12/2005	23:15	INTEL_NT
INTEL_NT	QA70-1	COMPARE_REL	3.8		UP20020121	WINDOWS				
ev144-13s	7020021010	70SP20030909	0	8	8804	8804	98%	02/12/2005	23:17	INTEL_NT
INTEL_NT	QA70-1	COMPARE_REL	3.8		UP20020121	WINDOWS				

ev144-23s	7020021010	70SP20030909	0	0	1740	1740	92%	02/12/2005	23:20	INTEL_NT
INTEL_NT	QA70-1	COMPARE_REL	3.8		UP20020121	WINDOWS				
ev154-23s	7020021010	70SP20030909	0	0	1259	1259	89%	02/12/2005	23:20	INTEL_NT
INTEL_NT	QA70-1	COMPARE_REL	3.8		UP20020121	WINDOWS				
ev154-25s	7020021010	70SP20030909	0	0	587	587	76%	02/12/2005	23:20	INTEL_NT
INTEL_NT	QA70-1	COMPARE_REL	3.8		UP20020121	WINDOWS				
ev171-57s	7020021010	70SP20030909	0	0	542	542	79%	02/12/2005	23:20	INTEL_NT
INTEL_NT	QA70-1	COMPARE_REL	3.8		UP20020121	WINDOWS				
ev173-53s	7020021010	70SP20030909	1	0	1426	1429	92%	02/12/2005	23:20	INTEL_NT
INTEL_NT	QA70-1	COMPARE_REL	3.8		UP20020121	WINDOWS				
ev174-46s	7020021010	70SP20030909	0	0	562	562	80%	02/12/2005	23:20	INTEL_NT
INTEL_NT	QA70-1	COMPARE_REL	3.8		UP20020121	WINDOWS				
ev175-20s	7020021010	70SP20030909	1	0	538	541	79%	02/12/2005	23:20	INTEL_NT
INTEL_NT	QA70-1	COMPARE_REL	3.8		UP20020121	WINDOWS				
ev175-21s	7020021010	NO_UPDATE	-88	0	566	146	64%	02/12/2005	23:20	INTEL_NT
NOT AVAILABLE	QA70-1	COMPARE_REL	3.8		UP20020121	WINDOWS				
ev175-38s	7020021010	70SP20030909	0	0	808	808	85%	02/12/2005	23:21	INTEL_NT
INTEL_NT	QA70-1	COMPARE_REL	3.8		UP20020121	WINDOWS				
ev182-zbdpg11s	7020021010	70SP20030909	0	0	660	660	83%	02/12/2005	23:21	INTEL_NT
INTEL_NT	QA70-1	COMPARE_REL	3.8		UP20020121	WINDOWS				
ev183-zdpl20s	7020021010	70SP20030909	0	0	577	577	80%	02/12/2005	23:21	INTEL_NT
INTEL_NT	QA70-1	COMPARE_REL	3.8		UP20020121	WINDOWS				
ev184-02s	7020021010	70SP20030909	0	0	267	267	56%	02/12/2005	23:21	INTEL_NT
INTEL_NT	QA70-1	COMPARE_REL	3.8		UP20020121	WINDOWS				
ev184-07s	7020021010	70SP20030909	0	0	661	661	80%	02/12/2005	23:21	INTEL_NT
INTEL_NT	QA70-1	COMPARE_REL	3.8		UP20020121	WINDOWS				
ev35-23s	7020021010	70SP20030909	0	0	293	293	61%	02/12/2005	23:21	INTEL_NT
INTEL_NT	QA70-1	COMPARE_REL	3.8		UP20020121	WINDOWS				
ev95-45s	7020021010	70SP20030909	0	0	892	892	85%	02/12/2005	23:21	INTEL_NT
INTEL_NT	QA70-1	COMPARE_REL	3.8		UP20020121	WINDOWS				
ev97-73s	7020021010	70SP20030909	0	0	621	621	82%	02/12/2005	23:21	INTEL_NT
INTEL_NT	QA70-1	COMPARE_REL	3.8		UP20020121	WINDOWS				
f1o-136s	7020021010	70SP20030909	0	0	419	419	73%	02/12/2005	23:22	INTEL_NT
INTEL_NT	QA70-1	COMPARE_REL	3.8		UP20020121	WINDOWS				
f1o-138s	7020021010	70SP20030909	0	0	352	352	68%	02/12/2005	23:22	INTEL_NT
INTEL_NT	QA70-1	COMPARE_REL	3.8		UP20020121	WINDOWS				
inrt-16s	7020021010	70SP20030909	1	0	484	486	77%	02/12/2005	23:22	INTEL_NT
INTEL_NT	QA70-1	COMPARE_REL	3.8		UP20020121	WINDOWS				
inrt-9s	7020021010	70SP20030909	0	0	421	421	73%	02/12/2005	23:22	INTEL_NT
INTEL_NT	QA70-1	COMPARE_REL	3.8		UP20020121	WINDOWS				
mvhy-bk501	7020021010	70SP20030909	0	0	536	536	78%	02/12/2005	23:23	INTEL_NT
INTEL_NT	QA70-1	COMPARE_REL	3.8		UP20020121	WINDOWS				
mvhy-gt202	7020021010	70SP20030909	0	0	780	780	84%	02/12/2005	23:23	INTEL_NT
INTEL_NT	QA70-1	COMPARE_REL	3.8		UP20020121	WINDOWS				

mvve-cr003	7020021010	70SP20030909	0	0	328	328	65%	02/12/2005	23:24	INTEL_NT
INTEL_NT	QA70-1	COMPARE_REL	3.8	UP20020121	WINDOWS					
mvve-cr804	7020021010	70SP20030909	0	0	329	329	65%	02/12/2005	23:24	INTEL_NT
INTEL_NT	QA70-1	COMPARE_REL	3.8	UP20020121	WINDOWS					
se-1s	7020021010	70SP20030909	0	0	400	400	72%	02/12/2005	23:24	INTEL_NT
INTEL_NT	QA70-1	COMPARE_REL	3.8	UP20020121	WINDOWS					
se-20s	7020021010	70SP20030909	0	0	879	879	85%	02/12/2005	23:24	INTEL_NT
INTEL_NT	QA70-1	COMPARE_REL	3.8	UP20020121	WINDOWS					
sx120-1s	7020021010	NO_UPDATE	-88	0	248	146	30%	02/12/2005	23:24	INTEL_NT
NOT_AVAILABLE	QA70-1	COMPARE_REL	3.8	UP20020121	WINDOWS					
tbc-155s	7020021010	70SP20030909	0	0	351	351	64%	02/12/2005	23:24	INTEL_NT
INTEL_NT	QA70-1	COMPARE_REL	3.8	UP20020121	WINDOWS					

RPP-RPT-28967, Rev. 1

1

```
00000000          VERSION=INTEL NT          RELEASE= 7.0          UP20021010

EXPECTED COMPARE DIFFERENCE FOUND AT  NG= 113 NT= 113
G= 00000000          VERSION=INTEL NT          RELEASE= 7.0          UP20021010
T= 00292062          VERSION=INTEL NT          RELEASE= 7.0SP11 UP20030909
```

```
EXPECTED COMPARE DIFFERENCE FOUND AT  NG= 114 NT= 114
G= CURRENT JOBNAME=c0231 10:37:04 OCT 15, 2002 CP= 0.219
T= CURRENT JOBNAME=c0231 21:33:01 FEB 12, 2005 CP= 0.094
```

0 /verify,c0231

0 /title, c0231 (fsk) Unmatched nodes mapping

```
COMPARE DIFFERENCE FOUND AT          NG= 192 NT= 192
G= NODAL RESULTS ARE FOR CYCLIC SECTOR 1 - PHASE ANGLE = 30.580
T= NODAL RESULTS ARE FOR CYCLIC SECTOR 1 - PHASE ANGLE = 237.330
```

```
COMPARE DIFFERENCE FOUND AT          NG= 219 NT= 219
G= NODAL RESULTS ARE FOR CYCLIC SECTOR 2 - PHASE ANGLE = 30.580
T= NODAL RESULTS ARE FOR CYCLIC SECTOR 2 - PHASE ANGLE = 237.330
```

```
COMPARE DIFFERENCE FOUND AT          NG= 246 NT= 246
G= NODAL RESULTS ARE FOR CYCLIC SECTOR 3 - PHASE ANGLE = 30.580
T= NODAL RESULTS ARE FOR CYCLIC SECTOR 3 - PHASE ANGLE = 237.330
```

```
BOTTOM OF GOOD FILE REACHED AT LINE 289
G= |
|
```

```
~~~~~
NOTE- NONSTANDARD COMPARE - DIFOPT NAME QA70-1 HAS BEEN USED
NUMBER OF LINES SKIPPED IN GOOD FILE(BLANK LINES EXCLUDED) - 0
NUMBER OF LINES SKIPPED IN TEST FILE(BLANK LINES EXCLUDED) - 0
NUMBER OF LINES ON GOOD FILE WITH STRINGS CONDENSED OUT - 0
NUMBER OF LINES ON TEST FILE WITH STRINGS CONDENSED OUT - 0
~~~~~
```

```
*****
COMPARE ERRORS = 3
*****
```

```
=====
===
PROBLEM: c0231          COMPARE OPTIONS COMPARE_REL 3.8 UP20020121
WINDOWS
```

```
ALMOST ZERO (GOOD) = 1.0000E-006          KROUND (DROP LAST DIGIT)= 1
```

RPP-RPT-28967, Rev. 1

ALMOST ZERO (TEST)	= 1.0000E-006	KABSPR (0=SUMMARY 1=ALL)=	1
ABSOLUTE VALUE TOL	= 1.0000E-010	KSKIP(SKIP=ERR 0=Y, 1=N)=	0
FRACTIONAL DIFFERENCE=	1.0000E-004	MAXERR (STOP WHEN ERRS)=	100
ABSOLUTE DIFFERENCE	= 1.0000E-006	MAXBUF (# LINES TO SCAN)=	6
		KNOWN (# OF KNOWN ERRS)=	0
		GREAD, TREAD =	1, 1

=====
===

LINES ON GOOD FILE =	304
LINES ON TEST FILE =	304

RPP-RPT-28967, Rev. 1

1

00000000 VERSION=INTEL NT RELEASE= 7.0 UP20021010

EXPECTED COMPARE DIFFERENCE FOUND AT NG= 113 NT= 113
G= 00000000 VERSION=INTEL NT RELEASE= 7.0 UP20021010
T= 00292062 VERSION=INTEL NT RELEASE= 7.0SP11 UP20030909

EXPECTED COMPARE DIFFERENCE FOUND AT NG= 114 NT= 114
G= CURRENT JOBNAME=vm184 20:46:18 OCT 15, 2002 CP= 0.250
T= CURRENT JOBNAME=vm184 21:48:44 FEB 12, 2005 CP= 0.109

0 /VERIFY,VM184

0 /TITLE, VM184, STRAIGHT CANTILEVER BEAM

0 /stitle,1,Reason COMPARE differences are acceptable:

0 /stitle,2, mesher accuracy - element number on warning;
near-zero values

0 /TITLE, VM184, STRAIGHT CANTILEVER BEAM

NOW COMPARING LINES FROM ***** ANSYS ANALYSIS DEFINITION (PREP7)

NOW COMPARING LINES FROM ***** ANSYS RESULTS INTERPRETATION (POST1)

ABSOLUTE VALUE DIFFERENCE FOUND AT NG= 926 NT= 926
G= VALUE -0.24849E-01 0.98917 -0.43496E-05 0.98948
T= VALUE -0.24849E-01 0.98917 0.43497E-05 0.98948

ABSOLUTE VALUE DIFFERENCE FOUND AT NG= 982 NT= 982
G= VALUE -0.53544E-02-0.26671E-05 0.42554 0.42557
T= VALUE -0.53544E-02 0.26671E-05 0.42554 0.42557

ABSOLUTE VALUE DIFFERENCE FOUND AT NG= 1011 NT= 1011
G= VALUE -0.12394E-01-0.61739E-05 0.98504 0.98511
T= VALUE -0.12394E-01 0.61739E-05 0.98504 0.98511

NOW COMPARING LINES FROM ***** ANSYS ANALYSIS DEFINITION (PREP7)

NOW COMPARING LINES FROM ***** ANSYS RESULTS INTERPRETATION (POST1)

COMPARE DIFFERENCE FOUND AT NG= 1580 NT= 1580
G= VALUE 0.24811E-01 0.98813 -0.43696E-05 0.98844
T= VALUE 0.24811E-01 0.98813 0.43701E-05 0.98844

RPP-RPT-28967, Rev. 1

ABSOLUTE VALUE DIFFERENCE FOUND AT NG= 1639 NT= 1639
G= VALUE -0.53533E-02-0.30755E-05 0.42553 0.42556
T= VALUE -0.53533E-02 0.30756E-05 0.42553 0.42556

ABSOLUTE VALUE DIFFERENCE FOUND AT NG= 1673 NT= 1673
G= VALUE -0.12392E-01-0.71193E-05 0.98502 0.98510
T= VALUE -0.12392E-01 0.71194E-05 0.98502 0.98510

NOW COMPARING LINES FROM ***** ANSYS ANALYSIS DEFINITION (PREP7)

NOW COMPARING LINES FROM ***** ANSYS RESULTS INTERPRETATION (POST1)

NOW COMPARING LINES FROM ***** ANSYS ANALYSIS DEFINITION (PREP7)

NOW COMPARING LINES FROM ***** ANSYS RESULTS INTERPRETATION (POST1)

BOTTOM OF GOOD FILE REACHED AT LINE 3147
G= | ANSYS RUN COMPLETED
|

~~~~~  
NOTE- NONSTANDARD COMPARE - DIFOPT NAME QA70-1 HAS BEEN USED  
NUMBER OF LINES SKIPPED IN GOOD FILE(BLANK LINES EXCLUDED) - 0  
NUMBER OF LINES SKIPPED IN TEST FILE(BLANK LINES EXCLUDED) - 0  
NUMBER OF LINES ON GOOD FILE WITH STRINGS CONDENSED OUT - 0  
NUMBER OF LINES ON TEST FILE WITH STRINGS CONDENSED OUT - 0  
~~~~~

COMPARE ERRORS = 1 *

WARNING - 5 ABSOLUTE VALUE DIFFERENCE(S) FOUND.

NOTE - 1 summary line(s) contained absolute value differences.

=====
===

RPP-RPT-28967, Rev. 1

PROBLEM: vm184
WINDOWS

COMPARE OPTIONS COMPARE_REL 3.8 UP20020121

ALMOST ZERO (GOOD) = 1.0000E-006
ALMOST ZERO (TEST) = 1.0000E-006
ABSOLUTE VALUE TOL = 1.0000E-010
FRACTIONAL DIFFERENCE= 1.0000E-004
ABSOLUTE DIFFERENCE = 1.0000E-006

KROUND (DROP LAST DIGIT)= 1
KABSPR (0=SUMMARY 1=ALL)= 1
KSKIP(SKIP=ERR 0=Y, 1=N)= 0
MAXERR (STOP WHEN ERRS)= 100
MAXBUF (# LINES TO SCAN)= 6
KNOWN (# OF KNOWN ERRS)= 0
GREAD, TREAD = 1, 1

=====
===

Lines on GOOD file = 3162
Lines on TEST file = 3162

RPP-RPT-28967, Rev. 1

1

00000000 VERSION=INTEL NT RELEASE= 7.0 UP20021010

EXPECTED COMPARE DIFFERENCE FOUND AT NG= 113 NT= 113
G= 00000000 VERSION=INTEL NT RELEASE= 7.0 UP20021010
T= 00292062 VERSION=INTEL NT RELEASE= 7.0SP11 UP20030909

EXPECTED COMPARE DIFFERENCE FOUND AT NG= 114 NT= 114
G= CURRENT JOBNAME=vm198 20:50:49 OCT 15, 2002 CP= 0.266
T= CURRENT JOBNAME=vm198 21:49:55 FEB 12, 2005 CP= 0.094

0 /VERIFY,VM198

0 /TITLE, VM198, LARGE STRAIN IN-PLANE TORSION TEST (%EL%)

NOW COMPARING LINES FROM ***** ANSYS ANALYSIS DEFINITION (PREP7)

NOW COMPARING LINES FROM ***** ANSYS RESULTS INTERPRETATION (POST1)

NOW COMPARING LINES FROM ***** TIME-HISTORY POSTPROCESSOR (POST26)

NOW COMPARING LINES FROM ***** ANSYS ANALYSIS DEFINITION (PREP7)

COMPARE DIFFERENCE FOUND AT NG= 618 NT= 618
G= RELEASE 0.0 UPDATE 0 CUSTOMER 00000000
T= RELEASE 0.0 UPDATE 0 CUSTOMER 00292062

NOW COMPARING LINES FROM ***** ANSYS RESULTS INTERPRETATION (POST1)

NOW COMPARING LINES FROM ***** TIME-HISTORY POSTPROCESSOR (POST26)

NOW COMPARING LINES FROM ***** ANSYS ANALYSIS DEFINITION (PREP7)

COMPARE DIFFERENCE FOUND AT NG= 907 NT= 907
G= RELEASE 0.0 UPDATE 0 CUSTOMER 00000000
T= RELEASE 0.0 UPDATE 0 CUSTOMER 00292062

NOW COMPARING LINES FROM ***** ANSYS RESULTS INTERPRETATION (POST1)

RPP-RPT-28967, Rev. 1

NOW COMPARING LINES FROM ***** TIME-HISTORY POSTPROCESSOR (POST26)

BOTTOM OF GOOD FILE REACHED AT LINE 1193
G= | ANSYS RUN COMPLETED
|

~~~~~  
NOTE- NONSTANDARD COMPARE - DIFOPT NAME QA70-1 HAS BEEN USED  
NUMBER OF LINES SKIPPED IN GOOD FILE (BLANK LINES EXCLUDED) - 2  
NUMBER OF LINES SKIPPED IN TEST FILE (BLANK LINES EXCLUDED) - 2  
NUMBER OF LINES ON GOOD FILE WITH STRINGS CONDENSED OUT - 0  
NUMBER OF LINES ON TEST FILE WITH STRINGS CONDENSED OUT - 0  
~~~~~

COMPARE ERRORS = 2 *

=====

PROBLEM: vm198	COMPARE OPTIONS	COMPARE_REL 3.8 UP20020121
----------------	-----------------	----------------------------

WINDOWS

ALMOST ZERO (GOOD)	= 1.0000E-006	KROUND (DROP LAST DIGIT)= 1
ALMOST ZERO (TEST)	= 1.0000E-006	KABSPR (0=SUMMARY 1=ALL)= 1
ABSOLUTE VALUE TOL	= 1.0000E-010	KSKIP (SKIP=ERR 0=Y, 1=N)= 0
FRACTIONAL DIFFERENCE	= 1.0000E-004	MAXERR (STOP WHEN ERRS)= 100
ABSOLUTE DIFFERENCE	= 1.0000E-006	MAXBUF (# LINES TO SCAN)= 6
		KNOWN (# OF KNOWN ERRS)= 0
		GREAD, TREAD = 1, 1

=====

=====
LINES ON GOOD FILE = 1208
LINES ON TEST FILE = 1208

RPP-RPT-28967, Rev. 1

1

```

00000000          VERSION=INTEL NT          RELEASE= 7.0          UP20021010

EXPECTED COMPARE DIFFERENCE FOUND AT  NG=  113 NT=  113
G= 00000000          VERSION=INTEL NT          RELEASE= 7.0          UP20021010
T= 00292062          VERSION=INTEL NT          RELEASE= 7.0SP11 UP20030909

EXPECTED COMPARE DIFFERENCE FOUND AT  NG=  114 NT=  114
G= CURRENT JOBNAME=vmc8  21:52:06  OCT 15, 2002 CP=          0.219
T= CURRENT JOBNAME=vmc8  22:51:25  FEB 12, 2005 CP=          0.125

0  /VERIFY,VMC8

0  /TITLE, VMC8, ALUMINUM BAR IMPACTING A RIGID BOUNDARY

0  /stitle,1,Reason COMPARE differences are acceptable:

0  /stitle,2,  number of iterations, accuracy

0  /title, VMC8, ALUMINUM BAR IMPACTING A RIGID BOUNDARY -
PLANE2

0  /title, VMC8, ALUMINUM BAR IMPACTING A RIGID BOUNDARY -
PLANE42

0  /title, VMC8, ALUMINUM BAR IMPACTING A RIGID BOUNDARY -
PLANE82

0  /title, VMC8, ALUMINUM BAR IMPACTING A RIGID BOUNDARY -
VISCO106

0  /title, VMC8, ALUMINUM BAR IMPACTING A RIGID BOUNDARY -
SOLID45

0  /title, VMC8, ALUMINUM BAR IMPACTING A RIGID BOUNDARY -
SOLID95

0  /title, VMC8, ALUMINUM BAR IMPACTING A RIGID BOUNDARY -
VISCO107

0  /TITLE, VMC8, ALUMINUM BAR IMPACTING A RIGID BOUNDARY

```

```

NOW COMPARING LINES FROM          ***** ANSYS ANALYSIS DEFINITION (PREP7)
*****

```

```

NOW COMPARING LINES FROM          ***** ANSYS RESULTS INTERPRETATION (POST1)
*****

```

```

COMPARE DIFFERENCE FOUND AT          NG=  880 NT=  880
G= SET COMMAND GOT LOAD STEP= 2  SUBSTEP=  320  CUMULATIVE ITERATION=
3255

```

RPP-RPT-28967, Rev. 1

```
T= SET COMMAND GOT LOAD STEP=      2  SUBSTEP=    320  CUMULATIVE ITERATION=
3240

NOW COMPARING LINES FROM          ***** TIME-HISTORY POSTPROCESSOR (POST26)
*****

NOW COMPARING LINES FROM          ***** ANSYS ANALYSIS DEFINITION (PREP7)
*****

NOW COMPARING LINES FROM          ***** ANSYS RESULTS INTERPRETATION (POST1)
*****

NOW COMPARING LINES FROM          ***** TIME-HISTORY POSTPROCESSOR (POST26)
*****

NOW COMPARING LINES FROM          ***** ANSYS ANALYSIS DEFINITION (PREP7)
*****

NOW COMPARING LINES FROM          ***** ANSYS RESULTS INTERPRETATION (POST1)
*****

NOW COMPARING LINES FROM          ***** TIME-HISTORY POSTPROCESSOR (POST26)
*****

COMPARE DIFFERENCE FOUND AT          NG= 1227 NT= 1227
G=   3 ESOL      1 EPPL EQV  EPPLEQV  0.7401E-16  0.000      3.410
0.000
T=   3 ESOL      1 EPPL EQV  EPPLEQV  0.2694E-35  0.000      3.422
0.000

NOW COMPARING LINES FROM          ***** ANSYS ANALYSIS DEFINITION (PREP7)
*****

NOW COMPARING LINES FROM          ***** ANSYS RESULTS INTERPRETATION (POST1)
*****

NOW COMPARING LINES FROM          ***** TIME-HISTORY POSTPROCESSOR (POST26)
*****

NOW COMPARING LINES FROM          ***** ANSYS ANALYSIS DEFINITION (PREP7)
*****

NOW COMPARING LINES FROM          ***** ANSYS RESULTS INTERPRETATION (POST1)
*****
```

RPP-RPT-28967, Rev. 1

```
NOW COMPARING LINES FROM          ***** TIME-HISTORY POSTPROCESSOR (POST26)
*****

NOW COMPARING LINES FROM          ***** ANSYS ANALYSIS DEFINITION (PREP7)
*****

NOW COMPARING LINES FROM          ***** ANSYS RESULTS INTERPRETATION (POST1)
*****

NOW COMPARING LINES FROM          ***** TIME-HISTORY POSTPROCESSOR (POST26)
*****

BOTTOM OF GOOD FILE REACHED AT LINE    1879
G= |                                ANSYS RUN COMPLETED
|
```

```
~~~~~
NOTE- NONSTANDARD COMPARE - DIFOPT NAME QA70-1  HAS BEEN USED
NUMBER OF LINES SKIPPED IN GOOD FILE(BLANK LINES EXCLUDED) -      0
NUMBER OF LINES SKIPPED IN TEST FILE(BLANK LINES EXCLUDED) -      0
NUMBER OF LINES ON GOOD FILE WITH STRINGS CONDENSED OUT    -      0
NUMBER OF LINES ON TEST FILE WITH STRINGS CONDENSED OUT    -      0
~~~~~
```

```
*****
COMPARE ERRORS =          2          *
*****
```

```
=====
===
PROBLEM: vmc8          COMPARE OPTIONS  COMPARE_REL 3.8 UP20020121
WINDOWS
```

```
ALMOST ZERO (GOOD)    = 1.0000E-006          KROUND (DROP LAST DIGIT)=    1
ALMOST ZERO (TEST)    = 1.0000E-006          KABSPR (0=SUMMARY 1=ALL)=    1
ABSOLUTE VALUE TOL    = 1.0000E-010          KSKIP(SKIP=ERR 0=Y, 1=N)=    0
FRACTIONAL DIFFERENCE= 1.0000E-004          MAXERR (STOP WHEN ERRS )= 100
ABSOLUTE DIFFERENCE   = 1.0000E-006          MAXBUF (# LINES TO SCAN)=    6
                                   KNOWN  (# OF KNOWN ERRS)=    0
                                   GREAD, TREAD =    1,    1
```

```
=====
===
LINES ON GOOD FILE =    1894
LINES ON TEST FILE =    1894
```

```
*****
```

1

```

00000000          VERSION=INTEL NT          RELEASE= 7.0          UP20021010

EXPECTED COMPARE DIFFERENCE FOUND AT  NG=  113 NT=  113
G= 00000000          VERSION=INTEL NT          RELEASE= 7.0          UP20021010
T= 00292062          VERSION=INTEL NT          RELEASE= 7.0SP11 UP20030909

```

```

EXPECTED COMPARE DIFFERENCE FOUND AT  NG=  114 NT=  114
G= CURRENT JOBNAME=cyc-177s  11:45:34  OCT 15, 2002 CP=          0.219
T= CURRENT JOBNAME=cyc-177s  23:11:09  FEB 12, 2005 CP=          0.109

```

```

0  /verify,cyc-177s

```

```

0  /TITLE, ceb,cyc-177s, Test cyc symm Buckling element 42

```

```

0  /title,1,Full Results to Sector Results!

```

```

0  /stitle,Reason Compare differences are acceptable:

```

```

EXTRA DATA SKIPPED ON TEST FILE          NG= 1202 NT= 1194
T= USE COMMAND MACRO QAEND
T= ARGS= 289.00
END OF SKIPPED DATA                      NG= 1202 NT= 1199

```

```

BOTTOM OF GOOD FILE REACHED AT LINE 1204
G= |                                ANSYS RUN COMPLETED
|

```

```

~~~~~
NOTE- NONSTANDARD COMPARE - DIFOPT NAME QA70-1 HAS BEEN USED

```

```

NUMBER OF LINES SKIPPED IN GOOD FILE(BLANK LINES EXCLUDED) -      2
NUMBER OF LINES SKIPPED IN TEST FILE(BLANK LINES EXCLUDED) -      2
NUMBER OF LINES ON GOOD FILE WITH STRINGS CONDENSED OUT      -      0
NUMBER OF LINES ON TEST FILE WITH STRINGS CONDENSED OUT      -      0
~~~~~

```

```

*****
COMPARE ERRORS =          1          *
*****

```

```

=====
===

```

```

PROBLEM: cyc-177s          COMPARE OPTIONS  COMPARE_REL 3.8 UP20020121
WINDOWS

```

```

ALMOST ZERO (GOOD)      = 1.0000E-006          KROUND (DROP LAST DIGIT)= 1
ALMOST ZERO (TEST)      = 1.0000E-006          KABSPR (0=SUMMARY 1=ALL)= 1
ABSOLUTE VALUE TOL      = 1.0000E-010          KSKIP(SKIP=ERR 0=Y, 1=N)= 0
FRACTIONAL DIFFERENCE= 1.0000E-004          MAXERR (STOP WHEN ERRS )= 100

```

RPP-RPT-28967, Rev. 1

ABSOLUTE DIFFERENCE = 1.0000E-006

MAXBUF (# LINES TO SCAN)= 6

KNOWN (# OF KNOWN ERRS)= 0

GREAD, TREAD = 1, 1

=====
===

LINES ON GOOD FILE = 1219

LINES ON TEST FILE = 1222

1

```

00000000          VERSION=INTEL NT          RELEASE= 7.0          UP20021010

EXPECTED COMPARE DIFFERENCE FOUND AT  NG=  113 NT=  113
G= 00000000          VERSION=INTEL NT          RELEASE= 7.0          UP20021010
T= 00292062          VERSION=INTEL NT          RELEASE= 7.0SP11 UP20030909

```

```

EXPECTED COMPARE DIFFERENCE FOUND AT  NG=  114 NT=  114
G= CURRENT JOBNAME=cyc-178s  11:48:41  OCT 15, 2002 CP=          0.250
T= CURRENT JOBNAME=cyc-178s  23:13:04  FEB 12, 2005 CP=          0.125

```

```

0  /verify,cyc-178s

0  /TITLE, ceb,cyc-178s, Test cyc symm Buckling element 182

0  /title,1,Full Results to Sector Results!

0  /stitle,Reason Compare differences are acceptable:

```

```

EXTRA DATA SKIPPED ON TEST FILE          NG= 1202 NT= 1194
T= USE COMMAND MACRO QAEND
T= ARGS= 289.00
END OF SKIPPED DATA                      NG= 1202 NT= 1199

```

```

BOTTOM OF GOOD FILE REACHED AT LINE 1204
G= |                                ANSYS RUN COMPLETED
|

```

```

~~~~~
NOTE- NONSTANDARD COMPARE - DIFOPT NAME QA70-1 HAS BEEN USED
NUMBER OF LINES SKIPPED IN GOOD FILE(BLANK LINES EXCLUDED) -      2
NUMBER OF LINES SKIPPED IN TEST FILE(BLANK LINES EXCLUDED) -      2
NUMBER OF LINES ON GOOD FILE WITH STRINGS CONDENSED OUT      -      0
NUMBER OF LINES ON TEST FILE WITH STRINGS CONDENSED OUT      -      0
~~~~~

```

```

*****
COMPARE ERRORS =          1          *
*****

```

=====

===

```

PROBLEM: cyc-178s          COMPARE OPTIONS  COMPARE_REL 3.8 UP20020121
WINDOWS

```

```

ALMOST ZERO (GOOD)      = 1.0000E-006          KROUND (DROP LAST DIGIT)= 1
ALMOST ZERO (TEST)      = 1.0000E-006          KABSPR (0=SUMMARY 1=ALL)= 1
ABSOLUTE VALUE TOL      = 1.0000E-010          KSKIP(SKIP=ERR 0=Y, 1=N)= 0
FRACTIONAL DIFFERENCE= 1.0000E-004          MAXERR (STOP WHEN ERRS )= 100

```

RPP-RPT-28967, Rev. 1

ABSOLUTE DIFFERENCE = 1.0000E-006

MAXBUF (# LINES TO SCAN)= 6

KNOWN (# OF KNOWN ERRS)= 0

GREAD, TREAD = 1, 1

=====
===

LINES ON GOOD FILE = 1219

LINES ON TEST FILE = 1222

1

```
*****
```

```
*** ERROR -- (VERSION=) was not found anywhere in the "TEST" file.
***
*** Comparison was supposed to start at this string, specified in CMPOPT.
***
```

```
~~~~~
NOTE- NONSTANDARD COMPARE - DIFOPT NAME QA70-1 HAS BEEN USED
NUMBER OF LINES SKIPPED IN GOOD FILE(BLANK LINES EXCLUDED) -      0
NUMBER OF LINES SKIPPED IN TEST FILE(BLANK LINES EXCLUDED) -      0
NUMBER OF LINES ON GOOD FILE WITH STRINGS CONDENSED OUT -      0
NUMBER OF LINES ON TEST FILE WITH STRINGS CONDENSED OUT -      0
~~~~~
```

```
*****
COMPARE ERRORS =      -88                      *
*****
```

```
=====
===
```

```
PROBLEM: dds-13s          COMPARE OPTIONS  COMPARE_REL 3.8 UP20020121
WINDOWS
```

ALMOST ZERO (GOOD)	= 1.0000E-006	KROUND (DROP LAST DIGIT)=	1
ALMOST ZERO (TEST)	= 1.0000E-006	KABSPR (0=SUMMARY 1=ALL)=	1
ABSOLUTE VALUE TOL	= 1.0000E-010	KSKIP(SKIP=ERR 0=Y, 1=N)=	0
FRACTIONAL DIFFERENCE=	1.0000E-004	MAXERR (STOP WHEN ERRS)=	100
ABSOLUTE DIFFERENCE	= 1.0000E-006	MAXBUF (# LINES TO SCAN)=	6
		KNOWN (# OF KNOWN ERRS)=	0
		GREAD, TREAD =	1, 1

```
=====
===
```

```

LINES ON GOOD FILE =      402
LINES ON TEST FILE =      146
```

```
*****
```

1

*** ERROR -- (VERSION=) was not found anywhere in the "TEST" file.

 *** Comparison was supposed to start at this string, specified in CMPOPT.

~~~~~  
 NOTE- NONSTANDARD COMPARE - DIFOPT NAME QA70-1 HAS BEEN USED  
 NUMBER OF LINES SKIPPED IN GOOD FILE(BLANK LINES EXCLUDED) - 0  
 NUMBER OF LINES SKIPPED IN TEST FILE(BLANK LINES EXCLUDED) - 0  
 NUMBER OF LINES ON GOOD FILE WITH STRINGS CONDENSED OUT - 0  
 NUMBER OF LINES ON TEST FILE WITH STRINGS CONDENSED OUT - 0  
 ~~~~~

 COMPARE ERRORS = -88 *

=====

===
 PROBLEM: dds-17s COMPARE OPTIONS COMPARE_REL 3.8 UP20020121
 WINDOWS

ALMOST ZERO (GOOD)	= 1.0000E-006	KROUND (DROP LAST DIGIT)=	1
ALMOST ZERO (TEST)	= 1.0000E-006	KABSPR (0=SUMMARY 1=ALL)=	1
ABSOLUTE VALUE TOL	= 1.0000E-010	KSKIP(SKIP=ERR 0=Y, 1=N)=	0
FRACTIONAL DIFFERENCE=	1.0000E-004	MAXERR (STOP WHEN ERRS)=	100
ABSOLUTE DIFFERENCE	= 1.0000E-006	MAXBUF (# LINES TO SCAN)=	6
		KNOWN (# OF KNOWN ERRS)=	0
		GREAD, TREAD =	1, 1

=====

===
 LINES ON GOOD FILE = 746
 LINES ON TEST FILE = 146

1

```

00000000          VERSION=INTEL NT          RELEASE= 7.0          UP20021010

EXPECTED COMPARE DIFFERENCE FOUND AT  NG= 113 NT= 113
G= 00000000          VERSION=INTEL NT          RELEASE= 7.0          UP20021010
T= 00292062          VERSION=INTEL NT          RELEASE= 7.0SP11 UP20030909

```

```

EXPECTED COMPARE DIFFERENCE FOUND AT  NG= 114 NT= 114
G= CURRENT JOBNAME=ev173-53s  14:02:31  OCT 15, 2002 CP=          0.234
T= CURRENT JOBNAME=ev173-53s  23:20:30  FEB 12, 2005 CP=          0.094

```

```

0 /verify,ev173-53s

```

```

0 /title,ev173-53s,mfquresh,Test to verify PSOVLE,ELFORM for
171-175 (3D) with PENE

```

```

EXTRA DATA SKIPPED ON TEST FILE          NG= 1409 NT= 1401
T= USE COMMAND MACRO QAEND
T= ARGS= 20.000
END OF SKIPPED DATA                      NG= 1409 NT= 1406

```

```

BOTTOM OF GOOD FILE REACHED AT LINE 1411
G= |                                ANSYS RUN COMPLETED
|

```

```

~~~~~
NOTE- NONSTANDARD COMPARE - DIFOPT NAME QA70-1 HAS BEEN USED

```

```

NUMBER OF LINES SKIPPED IN GOOD FILE(BLANK LINES EXCLUDED) - 2
NUMBER OF LINES SKIPPED IN TEST FILE(BLANK LINES EXCLUDED) - 2
NUMBER OF LINES ON GOOD FILE WITH STRINGS CONDENSED OUT - 0
NUMBER OF LINES ON TEST FILE WITH STRINGS CONDENSED OUT - 0
~~~~~

```

```

*****
COMPARE ERRORS = 1 *
*****

```

```

=====
===

```

```

PROBLEM: ev173-53s          COMPARE OPTIONS  COMPARE_REL 3.8 UP20020121
WINDOWS

```

```

ALMOST ZERO (GOOD)    = 1.0000E-006          KROUND (DROP LAST DIGIT)= 1
ALMOST ZERO (TEST)    = 1.0000E-006          KABSPR (0=SUMMARY 1=ALL)= 1
ABSOLUTE VALUE TOL    = 1.0000E-010          KSKIP(SKIP=ERR 0=Y, 1=N)= 0
FRACTIONAL DIFFERENCE= 1.0000E-004          MAXERR (STOP WHEN ERRS )= 100
ABSOLUTE DIFFERENCE   = 1.0000E-006          MAXBUF (# LINES TO SCAN)= 6
                                          KNOWN (# OF KNOWN ERRS)= 0
                                          GREAD, TREAD = 1, 1

```

=====

====

LINE	ON	GOOD	FILE	=	1426
LINE	ON	TEST	FILE	=	1429

RPP-RPT-28967, Rev. 1

1

00000000 VERSION=INTEL NT RELEASE= 7.0 UP20021010

EXPECTED COMPARE DIFFERENCE FOUND AT NG= 113 NT= 113
G= 00000000 VERSION=INTEL NT RELEASE= 7.0 UP20021010
T= 00292062 VERSION=INTEL NT RELEASE= 7.0SP11 UP20030909

EXPECTED COMPARE DIFFERENCE FOUND AT NG= 114 NT= 114
G= CURRENT JOBNAME=ev175-20s 14:22:03 OCT 15, 2002 CP= 0.250
T= CURRENT JOBNAME=ev175-20s 23:20:55 FEB 12, 2005 CP= 0.094

0 /verify, ev175-20s

0 /title, ev175-20s, mfg, Check real constant FKN and FTOLN and
KEYOPT(2)=0,1

NOW COMPARING LINES FROM ***** ANSYS ANALYSIS DEFINITION (PREP7)

EXTRA DATA SKIPPED ON TEST FILE NG= 521 NT= 513
T= USE COMMAND MACRO QAEND
T= ARGS= 3.0000
END OF SKIPPED DATA NG= 521 NT= 518

BOTTOM OF GOOD FILE REACHED AT LINE 523
G= | ANSYS RUN COMPLETED
|

~~~~~  
NOTE- NONSTANDARD COMPARE - DIFOPT NAME QA70-1    HAS BEEN USED  
NUMBER OF LINES SKIPPED IN GOOD FILE (BLANK LINES EXCLUDED) -    2  
NUMBER OF LINES SKIPPED IN TEST FILE (BLANK LINES EXCLUDED) -    2  
NUMBER OF LINES ON GOOD FILE WITH STRINGS CONDENSED OUT    -    0  
NUMBER OF LINES ON TEST FILE WITH STRINGS CONDENSED OUT    -    0  
~~~~~

COMPARE ERRORS = 1 *

=====

====
PROBLEM: ev175-20s COMPARE OPTIONS COMPARE_REL 3.8 UP20020121
WINDOWS

ALMOST ZERO (GOOD)	= 1.0000E-006	KROUND (DROP LAST DIGIT)=	1
ALMOST ZERO (TEST)	= 1.0000E-006	KABSPR (0=SUMMARY 1=ALL)=	1
ABSOLUTE VALUE TOL	= 1.0000E-010	KSKIP (SKIP=ERR 0=Y, 1=N)=	0

RPP-RPT-28967, Rev. 1

FRACTIONAL DIFFERENCE= 1.0000E-004
ABSOLUTE DIFFERENCE = 1.0000E-006

MAXERR (STOP WHEN ERRS)= 100
MAXBUF (# LINES TO SCAN)= 6
KNOWN (# OF KNOWN ERRS)= 0
GREAD, TREAD = 1, 1

=====
===

LINES ON GOOD FILE = 538
LINES ON TEST FILE = 541

1

*** ERROR -- (VERSION=) was not found anywhere in the "TEST" file.

 *** Comparison was supposed to start at this string, specified in CMPOPT.

~~~~~  
 NOTE- NONSTANDARD COMPARE - DIFOPT NAME QA70-1 HAS BEEN USED  
 NUMBER OF LINES SKIPPED IN GOOD FILE(BLANK LINES EXCLUDED) - 0  
 NUMBER OF LINES SKIPPED IN TEST FILE(BLANK LINES EXCLUDED) - 0  
 NUMBER OF LINES ON GOOD FILE WITH STRINGS CONDENSED OUT - 0  
 NUMBER OF LINES ON TEST FILE WITH STRINGS CONDENSED OUT - 0  
 ~~~~~

 COMPARE ERRORS = -88 *

=====

===
 PROBLEM: ev175-21s COMPARE OPTIONS COMPARE_REL 3.8 UP20020121
 WINDOWS

ALMOST ZERO (GOOD)	= 1.0000E-006	KROUND (DROP LAST DIGIT)=	1
ALMOST ZERO (TEST)	= 1.0000E-006	KABSPR (0=SUMMARY 1=ALL)=	1
ABSOLUTE VALUE TOL	= 1.0000E-010	KSKIP(SKIP=ERR 0=Y, 1=N)=	0
FRACTIONAL DIFFERENCE=	1.0000E-004	MAXERR (STOP WHEN ERRS)=	100
ABSOLUTE DIFFERENCE	= 1.0000E-006	MAXBUF (# LINES TO SCAN)=	6
		KNOWN (# OF KNOWN ERRS)=	0
		GREAD, TREAD =	1, 1

=====

===
 LINES ON GOOD FILE = 566
 LINES ON TEST FILE = 146

1

00000000 VERSION=INTEL NT RELEASE= 7.0 UP20021010

EXPECTED COMPARE DIFFERENCE FOUND AT NG= 113 NT= 113
 G= 00000000 VERSION=INTEL NT RELEASE= 7.0 UP20021010
 T= 00292062 VERSION=INTEL NT RELEASE= 7.0SP11 UP20030909

EXPECTED COMPARE DIFFERENCE FOUND AT NG= 114 NT= 114
 G= CURRENT JOBNAME=inrt-16s 16:14:59 OCT 15, 2002 CP= 0.219
 T= CURRENT JOBNAME=inrt-16s 23:22:50 FEB 12, 2005 CP= 0.109

0 /VERIFY, INRT-16S

0 /TITLE, INRT-16S, ceb, component omega loading and layer
 elements

0 /TITLE, INRT-16S, BENDING OF A COMPOSITE BEAM

EXTRA DATA SKIPPED ON TEST FILE NG= 462 NT= 459
 T= USE COMMAND MACRO QAEND
 END OF SKIPPED DATA NG= 462 NT= 463

BOTTOM OF GOOD FILE REACHED AT LINE 469
 G= | ANSYS RUN COMPLETED

~~~~~  
 NOTE- NONSTANDARD COMPARE - DIFOPT NAME QA70-1    HAS BEEN USED  
 NUMBER OF LINES SKIPPED IN GOOD FILE(BLANK LINES EXCLUDED) -    1  
 NUMBER OF LINES SKIPPED IN TEST FILE(BLANK LINES EXCLUDED) -    1  
 NUMBER OF LINES ON GOOD FILE WITH STRINGS CONDENSED OUT    -    0  
 NUMBER OF LINES ON TEST FILE WITH STRINGS CONDENSED OUT    -    0  
 ~~~~~

 COMPARE ERRORS = 1 *

1

```
*****
```

```
*** ERROR -- (VERSION=) was not found anywhere in the "TEST" file.
***
*** Comparison was supposed to start at this string, specified in CMPOPT.
***
```

```
~~~~~
NOTE- NONSTANDARD COMPARE - DIFOPT NAME QA70-1 HAS BEEN USED
NUMBER OF LINES SKIPPED IN GOOD FILE(BLANK LINES EXCLUDED) -      0
NUMBER OF LINES SKIPPED IN TEST FILE(BLANK LINES EXCLUDED) -      0
NUMBER OF LINES ON GOOD FILE WITH STRINGS CONDENSED OUT -      0
NUMBER OF LINES ON TEST FILE WITH STRINGS CONDENSED OUT -      0
~~~~~
```

```
*****
COMPARE ERRORS =      -88      *
*****
```

```
=====
===
```

```
PROBLEM:  sx120-1s          COMPARE OPTIONS  COMPARE_REL 3.8 UP20020121
WINDOWS
```

ALMOST ZERO (GOOD)	= 1.0000E-006	KROUND (DROP LAST DIGIT)=	1
ALMOST ZERO (TEST)	= 1.0000E-006	KABSPR (0=SUMMARY 1=ALL)=	1
ABSOLUTE VALUE TOL	= 1.0000E-010	KSKIP(SKIP=ERR 0=Y, 1=N)=	0
FRACTIONAL DIFFERENCE=	1.0000E-004	MAXERR (STOP WHEN ERRS)=	100
ABSOLUTE DIFFERENCE	= 1.0000E-006	MAXBUF (# LINES TO SCAN)=	6
		KNOWN (# OF KNOWN ERRS)=	0
		GREAD, TREAD =	1, 1

```
=====
===
```

```

LINES ON GOOD FILE =      248
LINES ON TEST FILE =      146
```

```
*****
```

Software Acceptance

- 1) Project Title and Number: DST Thermal and Seismic Analyses 48971
- 2) Software Name and Version: ANSYS 7.0 (Rev. 11)
- 3) Computer and Property Number: Generic PC WD44903
- 4) Operating System: Windows XP Professional Version 2002 Service Pack 2
- 4) Scope of Testing: Hardware replacement and Software reinstallation (XP SP2)
- 5) Tests: Execute ANSYS Verification Testing Package
- 6) Discrepancies:

- aa) c0231. These differences are acceptable per the ANSYS Verification Package User's Guide – ANSYS Release 7.0 (AVPUG).
- bb) vm33. These differences are acceptable due to the unused degree of freedom (see AVPUG).
- cc) vm176. These differences are acceptable due to the unused degree of freedom (see AVPUG).
- dd) vm184. These differences occur at the 5th significant figure.
- ee) vm198. This difference is the reporting of the customer number for this installation.
- ff) vmc8. These differences are acceptable as noted in the output because of the difference in number of iterations and accuracy.
- gg) cyc-177s. This difference is acceptable due to the handling of the QAEND macro (see AVPUG).
- hh) cyc-178s. This difference is acceptable due to the handling of the QAEND macro (see AVPUG).
- ii) dds-13s. This test case requires the "Parallel Performance Module" which is not part of this software installation and is not required for the DST analyses.
- jj) dds-17s. This test case requires the "Parallel Performance Module" which is not part of this software installation and is not required for the DST analyses.
- kk) ev173-53s. This difference is acceptable due to the handling of the QAEND macro (see AVPUG).
- ll) ev175-20s. This difference is acceptable due to the handling of the QAEND macro (see AVPUG).
- mm) ev175-21s. This test case requires the "Parallel Performance Module" which is not part of this software installation and is not required for the DST analyses.
- nn) inrt-16s. This difference is acceptable due to the handling of the QAEND macro (see AVPUG).

- 7) Finding: This installation of ANSYS is acceptable

Certified by:

JE Deibler

Code Custodian

John E Deibler 11/11/05

Reviewed by:

SP Pilli

Staff Engineer

Siva prasad P 02/03/06

12/1 0/2002 Page 1 of 1 Addendum to ANSYS Verification Testing Package User's Guide -ANSYS Release 7.0

Notes for test case cO231

Test case cO231 may show considerable differences for the Phase Angle value that is part of the Post1 Nodal Degree of Freedom Listing (PRNS command) output. Any such differences do not indicate a problem with this test case's results and should be considered acceptable. The output items of significance for this test case are the UZ values in the Post1 Nodal Degree of Freedom Listing. Machine precision differences in the form of small numerical differences that are trivial with respect to the test's output items of significance may also show for this test case in the compare output for this test. Please see **Verifying ANSYS and Evaluating COMPARE Differences** in Chapter 2 of the *ANSYS Verification Testing Package User's Guide* for more information on evaluating COMPARE differences. The following is an example of acceptable COMPARE differences for test case cO231:

COMPARE DIFFERENCE FOUND AT G= NODAL RESULTS ARE FOR CYCLIC SECTOR T= NODAL RESULTS ARE FOR CYCLIC SECTOR

COMPARE DIFFERENCE FOUND AT G= VALUE -9.8117 -3.7700 22. T= VALUE -9.8119 -3.7693 22.

COMPARE DIFFERENCE FOUND AT G= NODAL RESULTS ARE FOR CYCLIC SECTOR T= NODAL RESULTS ARE FOR CYCLIC SECTOR

COMPARE DIFFERENCE FOUND AT G= VALUE -9.7579 -3.9649 22. T= VALUE -9.7581 -3.9643 22.

COMPARE DIFFERENCE FOUND AT G= NODAL RESULTS ARE FOR CYCLIC SECTOR T= NODAL RESULTS ARE FOR CYCLIC SECTOR

COMPARE DIFFERENCE FOUND AT G= 8 0.53291 0.39425 10 T= 8 0.53293 0.39419 10

COMPARE DIFFERENCE FOUND AT G= 10 0.52495 0.39568 9. T= 10 0.52497 0.39562 9.

COMPARE DIFFERENCE FOUND AT NG= 259 NT= 259 G= 12 0.50433 0.40282 8.6482 8.6722 T= 12 0.50435 0.40276 8.6471 8.6711

COMPARE DIFFERENCE FOUND AT NG= 260 NT= 260 G= 14 0.48186 0.41201 7.8710 7.8965 T= 14 0.48188 0.41196 7.8700 7.8955

COMPARE DIFFERENCE FOUND AT NG= 261 NT= 261 G= 16 0.45505 0.42478 7.0719 7.0992 T= 16 0.45507 0.42473 7.0710 7.0983

COMPARE DIFFERENCE FOUND AT NG= 262 NT= 262 G= 18 0.42339 0.44092 6.2424 6.2723 T= 18 0.42341 0.44086 6.2417 6.2715

COMPARE DIFFERENCE FOUND AT NG= 263 NT= 263 G= 20 0.38501 0.46124 5.3732 5.4067 T= 20 0.38502 0.46118 5.3726 5.4061

COMPARE DIFFERENCE FOUND AT NG= 267 NT= 267 G= VALUE -9.6034 -3.9649 18.806 21.413 T= VALUE -9.6036 -3.9643 18.805 21.412

NG= 271 NT= 271 22.469 24.766 22.469 24.766

NG= 192 NT= 192 1 -PHASE ANGLE = 1- PHASE ANGLE =

NG= 213 NT= 213 469 24.766 469 24.766

NG= 219 NT= 219 2- PHASE ANGLE = 2- PHASE ANGLE =

NG= 240 NT= 240 440 24.710 440 24.710

NG= 246 NT= 246 3- PHASE ANGLE = 3- PHASE ANGLE =

NG= 257 NT= 257 161 10.183 160 10.181

NG= 4080 4068

258 NT= 258 9.4309 9.4297

COMPARE DIFFERENCE FOUND AT G= VALUE -9.8117 -3.9649 T= VALUE -9.8119 -3.9643

30.580 306.570

30.580 306.570

30.580 306.570

Notes for Test Case vm33 and vm176

Test case vm33 and vm176 will produce a number of expected compare differences due to product restrictions in the PLANE13 element's functionality. The expected compare differences are the result of the MAG degree of freedom being absent in the test case's output when it is run with the ANSYS/ Mechanical product. Since the MAG degree of freedom is unused in these test cases, these compare differences should be considered acceptable.

3-1 ANSYS Verification Testing Package User's Guide . ANSYS Release 7.0. 001767. @ SAS If,' Inc.

Notes for Test Case vrn212

Test case vm212 may produce an expected compare difference due to an inconsequential warning message that appears in the ANSYS, Inc. supplied output file that may not appear in the output file generated by your system for this test case. This compare difference should be considered acceptable. The following is an example of this compare difference.

```
COMPARE DIFFERENCE FOUND AT          NG= 445 NT= 436
G= NUMBER OF WARNING MESSAGES ENCOUNTERED= 1
T= NUMBER OF WARNING MESSAGES ENCOUNTERED= 0
```

Notes for Test Cases cyc-177s, cyc-178s, ev-173-53s, ev-175-20s, inrt-16s, and inrt-9s

Test cases cyc-177s, cyc-178s, ev-173-53s, ev-175-20s, inrt-16s, and inrt-9s may produce expected compare differences due to the use of a macro named qaend. The method that is used in the verification procedure (runqa) to handle this macro may cause one or more comparison differences. Any such compare differences are inconsequential and should be considered acceptable. The following is an example of such a compare difference.

```
EXTRA DATA SKIPPED ON TEST FILE          NG= 1033 NT= 1030
T= USE COMMAND MACRO qaend
T= ARGS= 137.00
END OF SKIPPED DATA                     NG= 1033 NT= 1033
```

Notes for test Cases dds-13s, dds-17s, and ev175-21 s

The test cases dds-13s, dds-17s, and ev175-21 s will run to completion only if the "Parallel Performance for ANSYS" product (DDS and AMG solvers) is included in your ANSYS installation.

3-6 ANSYS Verification Testing Package User's Guide . ANSYS Release 7.0. 001767. @ SAS If,' Inc.

c0211r2	7020021010	70SP20030909	0	0	605	605	81%	11/10/2005	17:25 INTEL_NT
INTEL_NT	QA70-1	COMPARE_REL	3.8	UP20020121	WINDOWS				
c0212	7020021010	70SP20030909	0	0	223	223	45%	11/10/2005	17:26 INTEL_NT
INTEL_NT	QA70-1	COMPARE_REL	3.8	UP20020121	WINDOWS				
c0213	7020021010	70SP20030909	0	0	197	197	41%	11/10/2005	17:26 INTEL_NT
INTEL_NT	QA70-1	COMPARE_REL	3.8	UP20020121	WINDOWS				
c0214	7020021010	70SP20030909	0	0	409	409	67%	11/10/2005	17:26 INTEL_NT
INTEL_NT	QA70-1	COMPARE_REL	3.8	UP20020121	WINDOWS				
c0215	7020021010	70SP20030909	0	0	648	648	81%	11/10/2005	17:26 INTEL_NT
INTEL_NT	QA70-1	COMPARE_REL	3.8	UP20020121	WINDOWS				
c0216	7020021010	70SP20030909	0	0	510	510	74%	11/10/2005	17:26 INTEL_NT
INTEL_NT	QA70-1	COMPARE_REL	3.8	UP20020121	WINDOWS				
c0218	7020021010	70SP20030909	0	0	1627	1627	93%	11/10/2005	17:26 INTEL_NT
INTEL_NT	QA70-1	COMPARE_REL	3.8	UP20020121	WINDOWS				
c0219	7020021010	70SP20030909	0	0	2732	2732	95%	11/10/2005	17:26 INTEL_NT
INTEL_NT	QA70-1	COMPARE_REL	3.8	UP20020121	WINDOWS				
c0220	7020021010	70SP20030909	0	0	494	494	76%	11/10/2005	17:26 INTEL_NT
INTEL_NT	QA70-1	COMPARE_REL	3.8	UP20020121	WINDOWS				
c0221	7020021010	70SP20030909	0	0	1265	1265	90%	11/10/2005	17:26 INTEL_NT
INTEL_NT	QA70-1	COMPARE_REL	3.8	UP20020121	WINDOWS				
c0222	7020021010	70SP20030909	0	0	1543	1543	92%	11/10/2005	17:27 INTEL_NT
INTEL_NT	QA70-1	COMPARE_REL	3.8	UP20020121	WINDOWS				
c0223	7020021010	70SP20030909	0	0	362	362	66%	11/10/2005	17:27 INTEL_NT
INTEL_NT	QA70-1	COMPARE_REL	3.8	UP20020121	WINDOWS				
c0224	7020021010	70SP20030909	0	0	307	307	59%	11/10/2005	17:27 INTEL_NT
INTEL_NT	QA70-1	COMPARE_REL	3.8	UP20020121	WINDOWS				
c0225	7020021010	70SP20030909	0	0	420	420	70%	11/10/2005	17:27 INTEL_NT
INTEL_NT	QA70-1	COMPARE_REL	3.8	UP20020121	WINDOWS				
c0226	7020021010	70SP20030909	0	0	521	521	74%	11/10/2005	17:27 INTEL_NT
INTEL_NT	QA70-1	COMPARE_REL	3.8	UP20020121	WINDOWS				
c0227	7020021010	70SP20030909	0	0	380	380	65%	11/10/2005	17:28 INTEL_NT
INTEL_NT	QA70-1	COMPARE_REL	3.8	UP20020121	WINDOWS				
c0227a	7020021010	70SP20030909	0	0	380	380	65%	11/10/2005	17:28 INTEL_NT
INTEL_NT	QA70-1	COMPARE_REL	3.8	UP20020121	WINDOWS				
c0228	7020021010	70SP20030909	0	0	236	236	50%	11/10/2005	17:28 INTEL_NT
INTEL_NT	QA70-1	COMPARE_REL	3.8	UP20020121	WINDOWS				
c0229	7020021010	70SP20030909	0	0	715	715	81%	11/10/2005	17:28 INTEL_NT
INTEL_NT	QA70-1	COMPARE_REL	3.8	UP20020121	WINDOWS				
c0230	7020021010	70SP20030909	0	0	2513	2513	94%	11/10/2005	17:28 INTEL_NT
INTEL_NT	QA70-1	COMPARE_REL	3.8	UP20020121	WINDOWS				
c0231	7020021010	70SP20030909	3	0	304	304	61%	11/10/2005	17:28 INTEL_NT
INTEL_NT	QA70-1	COMPARE_REL	3.8	UP20020121	WINDOWS				
c0232	7020021010	70SP20030909	0	0	517	517	79%	11/10/2005	17:29 INTEL_NT
INTEL_NT	QA70-1	COMPARE_REL	3.8	UP20020121	WINDOWS				

c0233	7020021010	70SP20030909	0	0	542	542	75%	11/10/2005	17:29	INTEL_NT
INTEL_NT	QA70-1	COMPARE_REL	3.8	UP20020121	WINDOWS					
c0234	7020021010	70SP20030909	0	0	420	420	68%	11/10/2005	17:29	INTEL_NT
INTEL_NT	QA70-1	COMPARE_REL	3.8	UP20020121	WINDOWS					
vm1	7020021010	70SP20030909	0	0	474	474	72%	11/10/2005	17:29	INTEL_NT
INTEL_NT	QA70-1	COMPARE_REL	3.8	UP20020121	WINDOWS					
vm2	7020021010	70SP20030909	0	0	667	667	81%	11/10/2005	17:29	INTEL_NT
INTEL_NT	QA70-1	COMPARE_REL	3.8	UP20020121	WINDOWS					
vm3	7020021010	70SP20030909	0	0	499	499	73%	11/10/2005	17:29	INTEL_NT
INTEL_NT	QA70-1	COMPARE_REL	3.8	UP20020121	WINDOWS					
vm4	7020021010	70SP20030909	0	0	434	434	69%	11/10/2005	17:29	INTEL_NT
INTEL_NT	QA70-1	COMPARE_REL	3.8	UP20020121	WINDOWS					
vm5	7020021010	70SP20030909	0	0	884	884	85%	11/10/2005	17:29	INTEL_NT
INTEL_NT	QA70-1	COMPARE_REL	3.8	UP20020121	WINDOWS					
vm6	7020021010	70SP20030909	0	0	854	854	83%	11/10/2005	17:29	INTEL_NT
INTEL_NT	QA70-1	COMPARE_REL	3.8	UP20020121	WINDOWS					
vm7	7020021010	70SP20030909	0	0	2176	2176	93%	11/10/2005	17:29	INTEL_NT
INTEL_NT	QA70-1	COMPARE_REL	3.8	UP20020121	WINDOWS					
vm8	7020021010	70SP20030909	0	0	346	346	64%	11/10/2005	17:29	INTEL_NT
INTEL_NT	QA70-1	COMPARE_REL	3.8	UP20020121	WINDOWS					
vm9	7020021010	70SP20030909	0	0	851	851	85%	11/10/2005	17:29	INTEL_NT
INTEL_NT	QA70-1	COMPARE_REL	3.8	UP20020121	WINDOWS					
vm10	7020021010	70SP20030909	0	0	437	437	69%	11/10/2005	17:29	INTEL_NT
INTEL_NT	QA70-1	COMPARE_REL	3.8	UP20020121	WINDOWS					
vm11	7020021010	70SP20030909	0	0	885	885	85%	11/10/2005	17:30	INTEL_NT
INTEL_NT	QA70-1	COMPARE_REL	3.8	UP20020121	WINDOWS					
vm12	7020021010	70SP20030909	0	0	444	444	70%	11/10/2005	17:30	INTEL_NT
INTEL_NT	QA70-1	COMPARE_REL	3.8	UP20020121	WINDOWS					
vm13	7020021010	70SP20030909	0	0	464	464	71%	11/10/2005	17:30	INTEL_NT
INTEL_NT	QA70-1	COMPARE_REL	3.8	UP20020121	WINDOWS					
vm14	7020021010	70SP20030909	0	0	537	537	76%	11/10/2005	17:30	INTEL_NT
INTEL_NT	QA70-1	COMPARE_REL	3.8	UP20020121	WINDOWS					
vm15	7020021010	70SP20030909	0	0	1356	1356	91%	11/10/2005	17:30	INTEL_NT
INTEL_NT	QA70-1	COMPARE_REL	3.8	UP20020121	WINDOWS					
vm16	7020021010	70SP20030909	0	0	740	740	82%	11/10/2005	17:30	INTEL_NT
INTEL_NT	QA70-1	COMPARE_REL	3.8	UP20020121	WINDOWS					
vm17	7020021010	70SP20030909	0	0	546	546	76%	11/10/2005	17:30	INTEL_NT
INTEL_NT	QA70-1	COMPARE_REL	3.8	UP20020121	WINDOWS					
vm18	7020021010	70SP20030909	0	0	450	450	71%	11/10/2005	17:30	INTEL_NT
INTEL_NT	QA70-1	COMPARE_REL	3.8	UP20020121	WINDOWS					
vm19	7020021010	70SP20030909	0	0	725	725	80%	11/10/2005	17:30	INTEL_NT
INTEL_NT	QA70-1	COMPARE_REL	3.8	UP20020121	WINDOWS					
vm20	7020021010	70SP20030909	0	0	449	449	70%	11/10/2005	17:30	INTEL_NT
INTEL_NT	QA70-1	COMPARE_REL	3.8	UP20020121	WINDOWS					

vm21	7020021010	70SP20030909	0	0	805	805	82%	11/10/2005	17:30	INTEL_NT
INTEL_NT	QA70-1	COMPARE_REL	3.8	UP20020121	WINDOWS					
vm22	7020021010	70SP20030909	0	0	398	398	66%	11/10/2005	17:30	INTEL_NT
INTEL_NT	QA70-1	COMPARE_REL	3.8	UP20020121	WINDOWS					
vm23	7020021010	70SP20030909	0	0	1043	1043	88%	11/10/2005	17:30	INTEL_NT
INTEL_NT	QA70-1	COMPARE_REL	3.8	UP20020121	WINDOWS					
vm24	7020021010	70SP20030909	0	0	766	766	82%	11/10/2005	17:31	INTEL_NT
INTEL_NT	QA70-1	COMPARE_REL	3.8	UP20020121	WINDOWS					
vm25	7020021010	70SP20030909	0	0	2350	2350	95%	11/10/2005	17:31	INTEL_NT
INTEL_NT	QA70-1	COMPARE_REL	3.8	UP20020121	WINDOWS					
vm26	7020021010	70SP20030909	0	0	1829	1829	89%	11/10/2005	17:31	INTEL_NT
INTEL_NT	QA70-1	COMPARE_REL	3.8	UP20020121	WINDOWS					
vm27	7020021010	70SP20030909	0	0	910	910	85%	11/10/2005	17:31	INTEL_NT
INTEL_NT	QA70-1	COMPARE_REL	3.8	UP20020121	WINDOWS					
vm28	7020021010	70SP20030909	0	0	418	418	70%	11/10/2005	17:31	INTEL_NT
INTEL_NT	QA70-1	COMPARE_REL	3.8	UP20020121	WINDOWS					
vm29	7020021010	70SP20030909	0	0	683	683	80%	11/10/2005	17:31	INTEL_NT
INTEL_NT	QA70-1	COMPARE_REL	3.8	UP20020121	WINDOWS					
vm30	7020021010	70SP20030909	0	0	449	449	70%	11/10/2005	17:31	INTEL_NT
INTEL_NT	QA70-1	COMPARE_REL	3.8	UP20020121	WINDOWS					
vm31	7020021010	70SP20030909	0	0	551	551	76%	11/10/2005	17:31	INTEL_NT
INTEL_NT	QA70-1	COMPARE_REL	3.8	UP20020121	WINDOWS					
vm32	7020021010	70SP20030909	0	0	881	881	84%	11/10/2005	17:31	INTEL_NT
INTEL_NT	QA70-1	COMPARE_REL	3.8	UP20020121	WINDOWS					
vm33	7020021010	70SP20030909	6	0	902	896	85%	11/10/2005	17:31	INTEL_NT
INTEL_NT	QA70-1	COMPARE_REL	3.8	UP20020121	WINDOWS					
vm34	7020021010	70SP20030909	0	0	1380	1380	90%	11/10/2005	17:31	INTEL_NT
INTEL_NT	QA70-1	COMPARE_REL	3.8	UP20020121	WINDOWS					
vm35	7020021010	70SP20030909	0	0	594	594	77%	11/10/2005	17:32	INTEL_NT
INTEL_NT	QA70-1	COMPARE_REL	3.8	UP20020121	WINDOWS					
vm36	7020021010	70SP20030909	0	0	1086	1086	88%	11/10/2005	17:32	INTEL_NT
INTEL_NT	QA70-1	COMPARE_REL	3.8	UP20020121	WINDOWS					
vm37	7020021010	70SP20030909	0	0	690	690	81%	11/10/2005	17:32	INTEL_NT
INTEL_NT	QA70-1	COMPARE_REL	3.8	UP20020121	WINDOWS					
vm38	7020021010	70SP20030909	0	0	1667	1667	92%	11/10/2005	17:32	INTEL_NT
INTEL_NT	QA70-1	COMPARE_REL	3.8	UP20020121	WINDOWS					
vm39	7020021010	70SP20030909	0	0	819	819	84%	11/10/2005	17:32	INTEL_NT
INTEL_NT	QA70-1	COMPARE_REL	3.8	UP20020121	WINDOWS					
vm40	7020021010	70SP20030909	0	0	876	876	86%	11/10/2005	17:32	INTEL_NT
INTEL_NT	QA70-1	COMPARE_REL	3.8	UP20020121	WINDOWS					
vm41	7020021010	70SP20030909	0	0	829	829	83%	11/10/2005	17:32	INTEL_NT
INTEL_NT	QA70-1	COMPARE_REL	3.8	UP20020121	WINDOWS					
vm42	7020021010	70SP20030909	0	0	607	607	77%	11/10/2005	17:32	INTEL_NT
INTEL_NT	QA70-1	COMPARE_REL	3.8	UP20020121	WINDOWS					

vm43	7020021010	70SP20030909	0	0	860	860	85%	11/10/2005	17:32	INTEL_NT
INTEL_NT	QA70-1	COMPARE_REL	3.8	UP20020121	WINDOWS					
vm44	7020021010	70SP20030909	0	0	1198	1198	90%	11/10/2005	17:32	INTEL_NT
INTEL_NT	QA70-1	COMPARE_REL	3.8	UP20020121	WINDOWS					
vm45	7020021010	70SP20030909	0	0	416	416	67%	11/10/2005	17:32	INTEL_NT
INTEL_NT	QA70-1	COMPARE_REL	3.8	UP20020121	WINDOWS					
vm47	7020021010	70SP20030909	0	0	416	416	67%	11/10/2005	17:32	INTEL_NT
INTEL_NT	QA70-1	COMPARE_REL	3.8	UP20020121	WINDOWS					
vm48	7020021010	70SP20030909	0	0	421	421	68%	11/10/2005	17:32	INTEL_NT
INTEL_NT	QA70-1	COMPARE_REL	3.8	UP20020121	WINDOWS					
vm50	7020021010	70SP20030909	0	0	500	500	72%	11/10/2005	17:32	INTEL_NT
INTEL_NT	QA70-1	COMPARE_REL	3.8	UP20020121	WINDOWS					
vm52	7020021010	70SP20030909	0	0	520	520	74%	11/10/2005	17:33	INTEL_NT
INTEL_NT	QA70-1	COMPARE_REL	3.8	UP20020121	WINDOWS					
vm53	7020021010	70SP20030909	0	0	789	789	82%	11/10/2005	17:33	INTEL_NT
INTEL_NT	QA70-1	COMPARE_REL	3.8	UP20020121	WINDOWS					
vm54	7020021010	70SP20030909	0	0	564	564	75%	11/10/2005	17:33	INTEL_NT
INTEL_NT	QA70-1	COMPARE_REL	3.8	UP20020121	WINDOWS					
vm55	7020021010	70SP20030909	0	0	995	995	87%	11/10/2005	17:33	INTEL_NT
INTEL_NT	QA70-1	COMPARE_REL	3.8	UP20020121	WINDOWS					
vm56	7020021010	70SP20030909	0	0	1577	1577	91%	11/10/2005	17:33	INTEL_NT
INTEL_NT	QA70-1	COMPARE_REL	3.8	UP20020121	WINDOWS					
vm57	7020021010	70SP20030909	0	0	737	737	81%	11/10/2005	17:33	INTEL_NT
INTEL_NT	QA70-1	COMPARE_REL	3.8	UP20020121	WINDOWS					
vm58	7020021010	70SP20030909	0	0	580	580	76%	11/10/2005	17:33	INTEL_NT
INTEL_NT	QA70-1	COMPARE_REL	3.8	UP20020121	WINDOWS					
vm59	7020021010	70SP20030909	0	0	833	833	84%	11/10/2005	17:33	INTEL_NT
INTEL_NT	QA70-1	COMPARE_REL	3.8	UP20020121	WINDOWS					
vm60	7020021010	70SP20030909	0	0	537	537	72%	11/10/2005	17:33	INTEL_NT
INTEL_NT	QA70-1	COMPARE_REL	3.8	UP20020121	WINDOWS					
vm61	7020021010	70SP20030909	0	0	402	402	66%	11/10/2005	17:33	INTEL_NT
INTEL_NT	QA70-1	COMPARE_REL	3.8	UP20020121	WINDOWS					
vm62	7020021010	70SP20030909	0	0	755	755	82%	11/10/2005	17:33	INTEL_NT
INTEL_NT	QA70-1	COMPARE_REL	3.8	UP20020121	WINDOWS					
vm63	7020021010	70SP20030909	0	0	1280	1280	89%	11/10/2005	17:34	INTEL_NT
INTEL_NT	QA70-1	COMPARE_REL	3.8	UP20020121	WINDOWS					
vm64	7020021010	70SP20030909	0	0	510	510	74%	11/10/2005	17:34	INTEL_NT
INTEL_NT	QA70-1	COMPARE_REL	3.8	UP20020121	WINDOWS					
vm65	7020021010	70SP20030909	0	0	3323	3323	96%	11/10/2005	17:34	INTEL_NT
INTEL_NT	QA70-1	COMPARE_REL	3.8	UP20020121	WINDOWS					
vm66	7020021010	70SP20030909	0	0	516	516	74%	11/10/2005	17:34	INTEL_NT
INTEL_NT	QA70-1	COMPARE_REL	3.8	UP20020121	WINDOWS					
vm67	7020021010	70SP20030909	0	0	591	591	76%	11/10/2005	17:34	INTEL_NT
INTEL_NT	QA70-1	COMPARE_REL	3.8	UP20020121	WINDOWS					

vm68	7020021010	70SP20030909	0	0	739	739	80%	11/10/2005	17:34	INTEL_NT
INTEL_NT	QA70-1	COMPARE_REL	3.8	UP20020121	WINDOWS					
vm69	7020021010	70SP20030909	0	0	553	553	75%	11/10/2005	17:34	INTEL_NT
INTEL_NT	QA70-1	COMPARE_REL	3.8	UP20020121	WINDOWS					
vm70	7020021010	70SP20030909	0	0	940	940	86%	11/10/2005	17:34	INTEL_NT
INTEL_NT	QA70-1	COMPARE_REL	3.8	UP20020121	WINDOWS					
vm71	7020021010	70SP20030909	0	0	1307	1307	87%	11/10/2005	17:34	INTEL_NT
INTEL_NT	QA70-1	COMPARE_REL	3.8	UP20020121	WINDOWS					
vm72	7020021010	70SP20030909	0	0	2161	2161	90%	11/10/2005	17:34	INTEL_NT
INTEL_NT	QA70-1	COMPARE_REL	3.8	UP20020121	WINDOWS					
vm73	7020021010	70SP20030909	0	0	4189	4189	97%	11/10/2005	17:35	INTEL_NT
INTEL_NT	QA70-1	COMPARE_REL	3.8	UP20020121	WINDOWS					
vm74	7020021010	70SP20030909	0	0	855	855	81%	11/10/2005	17:35	INTEL_NT
INTEL_NT	QA70-1	COMPARE_REL	3.8	UP20020121	WINDOWS					
vm75	7020021010	70SP20030909	0	0	1129	1129	84%	11/10/2005	17:35	INTEL_NT
INTEL_NT	QA70-1	COMPARE_REL	3.8	UP20020121	WINDOWS					
vm76	7020021010	70SP20030909	0	0	1187	1187	89%	11/10/2005	17:35	INTEL_NT
INTEL_NT	QA70-1	COMPARE_REL	3.8	UP20020121	WINDOWS					
vm77	7020021010	70SP20030909	0	0	876	876	82%	11/10/2005	17:35	INTEL_NT
INTEL_NT	QA70-1	COMPARE_REL	3.8	UP20020121	WINDOWS					
vm78	7020021010	70SP20030909	0	0	872	872	86%	11/10/2005	17:35	INTEL_NT
INTEL_NT	QA70-1	COMPARE_REL	3.8	UP20020121	WINDOWS					
vm79	7020021010	70SP20030909	0	0	954	954	83%	11/10/2005	17:35	INTEL_NT
INTEL_NT	QA70-1	COMPARE_REL	3.8	UP20020121	WINDOWS					
vm80	7020021010	70SP20030909	0	0	2205	2205	92%	11/10/2005	17:35	INTEL_NT
INTEL_NT	QA70-1	COMPARE_REL	3.8	UP20020121	WINDOWS					
vm81	7020021010	70SP20030909	0	0	2015	2015	93%	11/10/2005	17:35	INTEL_NT
INTEL_NT	QA70-1	COMPARE_REL	3.8	UP20020121	WINDOWS					
vm82	7020021010	70SP20030909	0	0	2144	2144	94%	11/10/2005	17:35	INTEL_NT
INTEL_NT	QA70-1	COMPARE_REL	3.8	UP20020121	WINDOWS					
vm83	7020021010	70SP20030909	0	0	2191	2191	94%	11/10/2005	17:35	INTEL_NT
INTEL_NT	QA70-1	COMPARE_REL	3.8	UP20020121	WINDOWS					
vm84	7020021010	70SP20030909	0	0	821	821	82%	11/10/2005	17:35	INTEL_NT
INTEL_NT	QA70-1	COMPARE_REL	3.8	UP20020121	WINDOWS					
vm85	7020021010	70SP20030909	0	0	858	858	84%	11/10/2005	17:36	INTEL_NT
INTEL_NT	QA70-1	COMPARE_REL	3.8	UP20020121	WINDOWS					
vm86	7020021010	70SP20030909	0	0	428	428	68%	11/10/2005	17:36	INTEL_NT
INTEL_NT	QA70-1	COMPARE_REL	3.8	UP20020121	WINDOWS					
vm87	7020021010	70SP20030909	0	0	434	434	69%	11/10/2005	17:36	INTEL_NT
INTEL_NT	QA70-1	COMPARE_REL	3.8	UP20020121	WINDOWS					
vm88	7020021010	70SP20030909	0	0	450	450	70%	11/10/2005	17:36	INTEL_NT
INTEL_NT	QA70-1	COMPARE_REL	3.8	UP20020121	WINDOWS					
vm89	7020021010	70SP20030909	0	0	480	480	72%	11/10/2005	17:36	INTEL_NT
INTEL_NT	QA70-1	COMPARE_REL	3.8	UP20020121	WINDOWS					

vm90	7020021010	70SP20030909	0	0	761	761	82%	11/10/2005	17:36	INTEL_NT
INTEL_NT	QA70-1	COMPARE_REL	3.8	UP20020121	WINDOWS					
vm91	7020021010	70SP20030909	0	0	2102	2102	94%	11/10/2005	17:36	INTEL_NT
INTEL_NT	QA70-1	COMPARE_REL	3.8	UP20020121	WINDOWS					
vm92	7020021010	70SP20030909	0	0	501	501	73%	11/10/2005	17:36	INTEL_NT
INTEL_NT	QA70-1	COMPARE_REL	3.8	UP20020121	WINDOWS					
vm93	7020021010	70SP20030909	0	0	436	436	69%	11/10/2005	17:36	INTEL_NT
INTEL_NT	QA70-1	COMPARE_REL	3.8	UP20020121	WINDOWS					
vm94	7020021010	70SP20030909	0	0	508	508	73%	11/10/2005	17:36	INTEL_NT
INTEL_NT	QA70-1	COMPARE_REL	3.8	UP20020121	WINDOWS					
vm95	7020021010	70SP20030909	0	0	1044	1044	86%	11/10/2005	17:36	INTEL_NT
INTEL_NT	QA70-1	COMPARE_REL	3.8	UP20020121	WINDOWS					
vm96	7020021010	70SP20030909	0	0	633	633	78%	11/10/2005	17:36	INTEL_NT
INTEL_NT	QA70-1	COMPARE_REL	3.8	UP20020121	WINDOWS					
vm97	7020021010	70SP20030909	0	0	809	809	83%	11/10/2005	17:36	INTEL_NT
INTEL_NT	QA70-1	COMPARE_REL	3.8	UP20020121	WINDOWS					
vm98	7020021010	70SP20030909	0	0	703	703	80%	11/10/2005	17:37	INTEL_NT
INTEL_NT	QA70-1	COMPARE_REL	3.8	UP20020121	WINDOWS					
vm99	7020021010	70SP20030909	0	0	482	482	72%	11/10/2005	17:37	INTEL_NT
INTEL_NT	QA70-1	COMPARE_REL	3.8	UP20020121	WINDOWS					
vm100	7020021010	70SP20030909	0	0	642	642	79%	11/10/2005	17:37	INTEL_NT
INTEL_NT	QA70-1	COMPARE_REL	3.8	UP20020121	WINDOWS					
vm101	7020021010	70SP20030909	0	0	720	720	81%	11/10/2005	17:37	INTEL_NT
INTEL_NT	QA70-1	COMPARE_REL	3.8	UP20020121	WINDOWS					
vm102	7020021010	70SP20030909	0	0	761	761	82%	11/10/2005	17:37	INTEL_NT
INTEL_NT	QA70-1	COMPARE_REL	3.8	UP20020121	WINDOWS					
vm103	7020021010	70SP20030909	0	0	782	782	84%	11/10/2005	17:37	INTEL_NT
INTEL_NT	QA70-1	COMPARE_REL	3.8	UP20020121	WINDOWS					
vm104	7020021010	70SP20030909	0	0	1822	1822	93%	11/10/2005	17:37	INTEL_NT
INTEL_NT	QA70-1	COMPARE_REL	3.8	UP20020121	WINDOWS					
vm105	7020021010	70SP20030909	0	0	589	589	77%	11/10/2005	17:37	INTEL_NT
INTEL_NT	QA70-1	COMPARE_REL	3.8	UP20020121	WINDOWS					
vm106	7020021010	70SP20030909	0	0	432	432	69%	11/10/2005	17:37	INTEL_NT
INTEL_NT	QA70-1	COMPARE_REL	3.8	UP20020121	WINDOWS					
vm107	7020021010	70SP20030909	0	0	476	476	72%	11/10/2005	17:37	INTEL_NT
INTEL_NT	QA70-1	COMPARE_REL	3.8	UP20020121	WINDOWS					
vm108	7020021010	70SP20030909	0	0	437	437	69%	11/10/2005	17:37	INTEL_NT
INTEL_NT	QA70-1	COMPARE_REL	3.8	UP20020121	WINDOWS					
vm109	7020021010	70SP20030909	0	0	1025	1025	87%	11/10/2005	17:37	INTEL_NT
INTEL_NT	QA70-1	COMPARE_REL	3.8	UP20020121	WINDOWS					
vm110	7020021010	70SP20030909	0	0	743	743	82%	11/10/2005	17:38	INTEL_NT
INTEL_NT	QA70-1	COMPARE_REL	3.8	UP20020121	WINDOWS					
vm111	7020021010	70SP20030909	0	0	3511	3511	96%	11/10/2005	17:38	INTEL_NT
INTEL_NT	QA70-1	COMPARE_REL	3.8	UP20020121	WINDOWS					

vm112	7020021010	70SP20030909	0	0	726	726	81%	11/10/2005	17:38	INTEL_NT
INTEL_NT	QA70-1	COMPARE_REL	3.8	UP20020121	WINDOWS					
vm113	7020021010	70SP20030909	0	0	732	732	82%	11/10/2005	17:38	INTEL_NT
INTEL_NT	QA70-1	COMPARE_REL	3.8	UP20020121	WINDOWS					
vm114	7020021010	70SP20030909	0	0	693	693	80%	11/10/2005	17:38	INTEL_NT
INTEL_NT	QA70-1	COMPARE_REL	3.8	UP20020121	WINDOWS					
vm115	7020021010	70SP20030909	0	0	604	604	78%	11/10/2005	17:38	INTEL_NT
INTEL_NT	QA70-1	COMPARE_REL	3.8	UP20020121	WINDOWS					
vm116	7020021010	70SP20030909	0	0	830	830	84%	11/10/2005	17:38	INTEL_NT
INTEL_NT	QA70-1	COMPARE_REL	3.8	UP20020121	WINDOWS					
vm118	7020021010	70SP20030909	0	0	918	918	85%	11/10/2005	17:38	INTEL_NT
INTEL_NT	QA70-1	COMPARE_REL	3.8	UP20020121	WINDOWS					
vm119	7020021010	70SP20030909	0	0	1225	1225	89%	11/10/2005	17:38	INTEL_NT
INTEL_NT	QA70-1	COMPARE_REL	3.8	UP20020121	WINDOWS					
vm122	7020021010	70SP20030909	0	0	422	422	68%	11/10/2005	17:38	INTEL_NT
INTEL_NT	QA70-1	COMPARE_REL	3.8	UP20020121	WINDOWS					
vm123	7020021010	70SP20030909	0	0	467	467	71%	11/10/2005	17:38	INTEL_NT
INTEL_NT	QA70-1	COMPARE_REL	3.8	UP20020121	WINDOWS					
vm124	7020021010	70SP20030909	0	0	591	591	77%	11/10/2005	17:39	INTEL_NT
INTEL_NT	QA70-1	COMPARE_REL	3.8	UP20020121	WINDOWS					
vm125	7020021010	70SP20030909	0	0	762	762	82%	11/10/2005	17:39	INTEL_NT
INTEL_NT	QA70-1	COMPARE_REL	3.8	UP20020121	WINDOWS					
vm126	7020021010	70SP20030909	0	0	661	661	80%	11/10/2005	17:39	INTEL_NT
INTEL_NT	QA70-1	COMPARE_REL	3.8	UP20020121	WINDOWS					
vm127	7020021010	70SP20030909	0	0	625	625	79%	11/10/2005	17:39	INTEL_NT
INTEL_NT	QA70-1	COMPARE_REL	3.8	UP20020121	WINDOWS					
vm128	7020021010	70SP20030909	0	0	815	815	83%	11/10/2005	17:39	INTEL_NT
INTEL_NT	QA70-1	COMPARE_REL	3.8	UP20020121	WINDOWS					
vm129	7020021010	70SP20030909	0	0	373	373	66%	11/10/2005	17:39	INTEL_NT
INTEL_NT	QA70-1	COMPARE_REL	3.8	UP20020121	WINDOWS					
vm130	7020021010	70SP20030909	0	0	553	553	78%	11/10/2005	17:39	INTEL_NT
INTEL_NT	QA70-1	COMPARE_REL	3.8	UP20020121	WINDOWS					
vm131	7020021010	70SP20030909	0	0	448	448	70%	11/10/2005	17:39	INTEL_NT
INTEL_NT	QA70-1	COMPARE_REL	3.8	UP20020121	WINDOWS					
vm132	7020021010	70SP20030909	0	0	1827	1827	93%	11/10/2005	17:39	INTEL_NT
INTEL_NT	QA70-1	COMPARE_REL	3.8	UP20020121	WINDOWS					
vm133	7020021010	70SP20030909	0	0	1701	1701	92%	11/10/2005	17:39	INTEL_NT
INTEL_NT	QA70-1	COMPARE_REL	3.8	UP20020121	WINDOWS					
vm134	7020021010	70SP20030909	0	0	1808	1808	93%	11/10/2005	17:39	INTEL_NT
INTEL_NT	QA70-1	COMPARE_REL	3.8	UP20020121	WINDOWS					
vm135	7020021010	70SP20030909	0	0	561	561	77%	11/10/2005	17:39	INTEL_NT
INTEL_NT	QA70-1	COMPARE_REL	3.8	UP20020121	WINDOWS					
vm136	7020021010	70SP20030909	0	0	1909	1909	93%	11/10/2005	17:40	INTEL_NT
INTEL_NT	QA70-1	COMPARE_REL	3.8	UP20020121	WINDOWS					

vm137	7020021010	70SP20030909	0	0	1395	1395	91%	11/10/2005	17:40	INTEL_NT
INTEL_NT	QA70-1	COMPARE_REL	3.8	UP20020121	WINDOWS					
vm138	7020021010	70SP20030909	0	0	528	528	75%	11/10/2005	17:40	INTEL_NT
INTEL_NT	QA70-1	COMPARE_REL	3.8	UP20020121	WINDOWS					
vm139	7020021010	70SP20030909	0	0	1132	1132	88%	11/10/2005	17:40	INTEL_NT
INTEL_NT	QA70-1	COMPARE_REL	3.8	UP20020121	WINDOWS					
vm140	7020021010	70SP20030909	0	0	1184	1184	89%	11/10/2005	17:40	INTEL_NT
INTEL_NT	QA70-1	COMPARE_REL	3.8	UP20020121	WINDOWS					
vm141	7020021010	70SP20030909	0	0	2040	2040	93%	11/10/2005	17:40	INTEL_NT
INTEL_NT	QA70-1	COMPARE_REL	3.8	UP20020121	WINDOWS					
vm142	7020021010	70SP20030909	0	0	879	879	85%	11/10/2005	17:40	INTEL_NT
INTEL_NT	QA70-1	COMPARE_REL	3.8	UP20020121	WINDOWS					
vm143	7020021010	70SP20030909	0	0	1672	1672	91%	11/10/2005	17:40	INTEL_NT
INTEL_NT	QA70-1	COMPARE_REL	3.8	UP20020121	WINDOWS					
vm144	7020021010	70SP20030909	0	0	2164	2164	94%	11/10/2005	17:40	INTEL_NT
INTEL_NT	QA70-1	COMPARE_REL	3.8	UP20020121	WINDOWS					
vm145	7020021010	70SP20030909	0	0	532	532	75%	11/10/2005	17:40	INTEL_NT
INTEL_NT	QA70-1	COMPARE_REL	3.8	UP20020121	WINDOWS					
vm146	7020021010	70SP20030909	0	0	883	883	86%	11/10/2005	17:40	INTEL_NT
INTEL_NT	QA70-1	COMPARE_REL	3.8	UP20020121	WINDOWS					
vm147	7020021010	70SP20030909	0	0	588	588	77%	11/10/2005	17:40	INTEL_NT
INTEL_NT	QA70-1	COMPARE_REL	3.8	UP20020121	WINDOWS					
vm148	7020021010	70SP20030909	0	0	588	588	78%	11/10/2005	17:41	INTEL_NT
INTEL_NT	QA70-1	COMPARE_REL	3.8	UP20020121	WINDOWS					
vm149	7020021010	70SP20030909	0	0	520	520	74%	11/10/2005	17:41	INTEL_NT
INTEL_NT	QA70-1	COMPARE_REL	3.8	UP20020121	WINDOWS					
vm150	7020021010	70SP20030909	0	0	657	657	79%	11/10/2005	17:41	INTEL_NT
INTEL_NT	QA70-1	COMPARE_REL	3.8	UP20020121	WINDOWS					
vm151	7020021010	70SP20030909	0	0	1058	1058	87%	11/10/2005	17:41	INTEL_NT
INTEL_NT	QA70-1	COMPARE_REL	3.8	UP20020121	WINDOWS					
vm152	7020021010	70SP20030909	0	0	1211	1211	88%	11/10/2005	17:41	INTEL_NT
INTEL_NT	QA70-1	COMPARE_REL	3.8	UP20020121	WINDOWS					
vm153	7020021010	70SP20030909	0	0	507	507	74%	11/10/2005	17:41	INTEL_NT
INTEL_NT	QA70-1	COMPARE_REL	3.8	UP20020121	WINDOWS					
vm154	7020021010	70SP20030909	0	0	814	814	82%	11/10/2005	17:41	INTEL_NT
INTEL_NT	QA70-1	COMPARE_REL	3.8	UP20020121	WINDOWS					
vm155	7020021010	70SP20030909	0	0	1255	1255	89%	11/10/2005	17:42	INTEL_NT
INTEL_NT	QA70-1	COMPARE_REL	3.8	UP20020121	WINDOWS					
vm156	7020021010	70SP20030909	0	0	2047	2047	94%	11/10/2005	17:42	INTEL_NT
INTEL_NT	QA70-1	COMPARE_REL	3.8	UP20020121	WINDOWS					
vm157	7020021010	70SP20030909	0	0	952	952	85%	11/10/2005	17:42	INTEL_NT
INTEL_NT	QA70-1	COMPARE_REL	3.8	UP20020121	WINDOWS					
vm158	7020021010	70SP20030909	0	0	955	955	87%	11/10/2005	17:42	INTEL_NT
INTEL_NT	QA70-1	COMPARE_REL	3.8	UP20020121	WINDOWS					

vm159	7020021010	70SP20030909	0	0	1524	1524	91%	11/10/2005	17:42	INTEL_NT
INTEL_NT	QA70-1	COMPARE_REL	3.8		UP20020121	WINDOWS				
vm160	7020021010	70SP20030909	0	0	600	600	78%	11/10/2005	17:42	INTEL_NT
INTEL_NT	QA70-1	COMPARE_REL	3.8		UP20020121	WINDOWS				
vm161	7020021010	70SP20030909	0	0	539	539	75%	11/10/2005	17:42	INTEL_NT
INTEL_NT	QA70-1	COMPARE_REL	3.8		UP20020121	WINDOWS				
vm162	7020021010	70SP20030909	0	0	548	548	76%	11/10/2005	17:43	INTEL_NT
INTEL_NT	QA70-1	COMPARE_REL	3.8		UP20020121	WINDOWS				
vm163	7020021010	70SP20030909	0	0	563	563	76%	11/10/2005	17:43	INTEL_NT
INTEL_NT	QA70-1	COMPARE_REL	3.8		UP20020121	WINDOWS				
vm164	7020021010	70SP20030909	0	0	556	556	76%	11/10/2005	17:43	INTEL_NT
INTEL_NT	QA70-1	COMPARE_REL	3.8		UP20020121	WINDOWS				
vm170	7020021010	70SP20030909	0	0	436	436	69%	11/10/2005	17:43	INTEL_NT
INTEL_NT	QA70-1	COMPARE_REL	3.8		UP20020121	WINDOWS				
vm171	7020021010	70SP20030909	0	0	759	759	82%	11/10/2005	17:43	INTEL_NT
INTEL_NT	QA70-1	COMPARE_REL	3.8		UP20020121	WINDOWS				
vm173	7020021010	70SP20030909	0	0	545	545	75%	11/10/2005	17:43	INTEL_NT
INTEL_NT	QA70-1	COMPARE_REL	3.8		UP20020121	WINDOWS				
vm174	7020021010	70SP20030909	0	0	602	602	77%	11/10/2005	17:43	INTEL_NT
INTEL_NT	QA70-1	COMPARE_REL	3.8		UP20020121	WINDOWS				
vm175	7020021010	70SP20030909	0	0	855	855	84%	11/10/2005	17:43	INTEL_NT
INTEL_NT	QA70-1	COMPARE_REL	3.8		UP20020121	WINDOWS				
vm176	7020021010	70SP20030909	22	0	999	970	86%	11/10/2005	17:43	INTEL_NT
INTEL_NT	QA70-1	COMPARE_REL	3.8		UP20020121	WINDOWS				
vm177	7020021010	70SP20030909	0	0	1127	1127	87%	11/10/2005	17:43	INTEL_NT
INTEL_NT	QA70-1	COMPARE_REL	3.8		UP20020121	WINDOWS				
vm179	7020021010	70SP20030909	0	0	768	768	82%	11/10/2005	17:44	INTEL_NT
INTEL_NT	QA70-1	COMPARE_REL	3.8		UP20020121	WINDOWS				
vm180	7020021010	70SP20030909	0	0	651	651	79%	11/10/2005	17:44	INTEL_NT
INTEL_NT	QA70-1	COMPARE_REL	3.8		UP20020121	WINDOWS				
vm181	7020021010	70SP20030909	0	0	484	484	71%	11/10/2005	17:44	INTEL_NT
INTEL_NT	QA70-1	COMPARE_REL	3.8		UP20020121	WINDOWS				
vm182	7020021010	70SP20030909	0	0	973	973	87%	11/10/2005	17:44	INTEL_NT
INTEL_NT	QA70-1	COMPARE_REL	3.8		UP20020121	WINDOWS				
vm183	7020021010	70SP20030909	0	0	722	722	81%	11/10/2005	17:44	INTEL_NT
INTEL_NT	QA70-1	COMPARE_REL	3.8		UP20020121	WINDOWS				
vm184	7020021010	70SP20030909	1	5	3162	3162	95%	11/10/2005	17:44	INTEL_NT
INTEL_NT	QA70-1	COMPARE_REL	3.8		UP20020121	WINDOWS				
vm187	7020021010	70SP20030909	0	0	1489	1489	90%	11/10/2005	17:44	INTEL_NT
INTEL_NT	QA70-1	COMPARE_REL	3.8		UP20020121	WINDOWS				
vm191	7020021010	70SP20030909	0	0	3075	3075	95%	11/10/2005	17:44	INTEL_NT
INTEL_NT	QA70-1	COMPARE_REL	3.8		UP20020121	WINDOWS				
vm192	7020021010	70SP20030909	0	0	645	645	80%	11/10/2005	17:44	INTEL_NT
INTEL_NT	QA70-1	COMPARE_REL	3.8		UP20020121	WINDOWS				

vm193	7020021010	70SP20030909	0	0	411	411	68%	11/10/2005	17:45	INTEL_NT
INTEL_NT	QA70-1	COMPARE_REL	3.8		UP20020121	WINDOWS				
vm194	7020021010	70SP20030909	0	0	821	821	83%	11/10/2005	17:45	INTEL_NT
INTEL_NT	QA70-1	COMPARE_REL	3.8		UP20020121	WINDOWS				
vm195	7020021010	70SP20030909	0	0	824	824	84%	11/10/2005	17:45	INTEL_NT
INTEL_NT	QA70-1	COMPARE_REL	3.8		UP20020121	WINDOWS				
vm196	7020021010	70SP20030909	0	0	505	505	73%	11/10/2005	17:45	INTEL_NT
INTEL_NT	QA70-1	COMPARE_REL	3.8		UP20020121	WINDOWS				
vm197	7020021010	70SP20030909	0	0	509	509	74%	11/10/2005	17:45	INTEL_NT
INTEL_NT	QA70-1	COMPARE_REL	3.8		UP20020121	WINDOWS				
vm198	7020021010	70SP20030909	2	0	1208	1208	88%	11/10/2005	17:45	INTEL_NT
INTEL_NT	QA70-1	COMPARE_REL	3.8		UP20020121	WINDOWS				
vm199	7020021010	70SP20030909	0	0	835	835	84%	11/10/2005	17:45	INTEL_NT
INTEL_NT	QA70-1	COMPARE_REL	3.8		UP20020121	WINDOWS				
vm200	7020021010	70SP20030909	0	0	1258	1258	89%	11/10/2005	17:47	INTEL_NT
INTEL_NT	QA70-1	COMPARE_REL	3.8		UP20020121	WINDOWS				
vm201	7020021010	70SP20030909	0	0	3072	3072	95%	11/10/2005	17:47	INTEL_NT
INTEL_NT	QA70-1	COMPARE_REL	3.8		UP20020121	WINDOWS				
vm202	7020021010	70SP20030909	0	0	604	604	77%	11/10/2005	17:47	INTEL_NT
INTEL_NT	QA70-1	COMPARE_REL	3.8		UP20020121	WINDOWS				
vm203	7020021010	70SP20030909	0	0	1020	1020	87%	11/10/2005	17:47	INTEL_NT
INTEL_NT	QA70-1	COMPARE_REL	3.8		UP20020121	WINDOWS				
vm204	7020021010	70SP20030909	0	0	621	621	79%	11/10/2005	17:47	INTEL_NT
INTEL_NT	QA70-1	COMPARE_REL	3.8		UP20020121	WINDOWS				
vm205	7020021010	70SP20030909	0	0	652	652	79%	11/10/2005	17:47	INTEL_NT
INTEL_NT	QA70-1	COMPARE_REL	3.8		UP20020121	WINDOWS				
vm210	7020021010	70SP20030909	0	0	1426	1426	90%	11/10/2005	17:47	INTEL_NT
INTEL_NT	QA70-1	COMPARE_REL	3.8		UP20020121	WINDOWS				
vm211	7020021010	70SP20030909	0	0	2658	2658	94%	11/10/2005	17:48	INTEL_NT
INTEL_NT	QA70-1	COMPARE_REL	3.8		UP20020121	WINDOWS				
vm215	7020021010	70SP20030909	0	0	637	637	80%	11/10/2005	17:48	INTEL_NT
INTEL_NT	QA70-1	COMPARE_REL	3.8		UP20020121	WINDOWS				
vm216	7020021010	70SP20030909	0	0	1111	1111	87%	11/10/2005	17:49	INTEL_NT
INTEL_NT	QA70-1	COMPARE_REL	3.8		UP20020121	WINDOWS				
vm217	7020021010	70SP20030909	0	0	873	873	84%	11/10/2005	17:49	INTEL_NT
INTEL_NT	QA70-1	COMPARE_REL	3.8		UP20020121	WINDOWS				
vm218	7020021010	70SP20030909	0	0	744	744	82%	11/10/2005	17:49	INTEL_NT
INTEL_NT	QA70-1	COMPARE_REL	3.8		UP20020121	WINDOWS				
vm222	7020021010	70SP20030909	0	0	1536	1536	91%	11/10/2005	17:49	INTEL_NT
INTEL_NT	QA70-1	COMPARE_REL	3.8		UP20020121	WINDOWS				
vm224	7020021010	70SP20030909	0	0	577	577	79%	11/10/2005	17:49	INTEL_NT
INTEL_NT	QA70-1	COMPARE_REL	3.8		UP20020121	WINDOWS				
vm225	7020021010	70SP20030909	0	0	496	496	73%	11/10/2005	17:49	INTEL_NT
INTEL_NT	QA70-1	COMPARE_REL	3.8		UP20020121	WINDOWS				

vm227	7020021010	70SP20030909	0	0	957	957	87%	11/10/2005	17:49	INTEL_NT
INTEL_NT	QA70-1	COMPARE_REL	3.8	UP20020121	WINDOWS					
vm228	7020021010	70SP20030909	0	0	5849	5849	98%	11/10/2005	17:50	INTEL_NT
INTEL_NT	QA70-1	COMPARE_REL	3.8	UP20020121	WINDOWS					
vm229	7020021010	70SP20030909	0	0	3944	3944	97%	11/10/2005	17:53	INTEL_NT
INTEL_NT	QA70-1	COMPARE_REL	3.8	UP20020121	WINDOWS					
vm230	7020021010	70SP20030909	0	0	26798	26798	99%	11/10/2005	17:54	INTEL_NT
INTEL_NT	QA70-1	COMPARE_REL	3.8	UP20020121	WINDOWS					
vm231	7020021010	70SP20030909	0	0	528	528	76%	11/10/2005	17:54	INTEL_NT
INTEL_NT	QA70-1	COMPARE_REL	3.8	UP20020121	WINDOWS					
vm232	7020021010	70SP20030909	0	0	14057	14057	98%	11/10/2005	17:56	INTEL_NT
INTEL_NT	QA70-1	COMPARE_REL	3.8	UP20020121	WINDOWS					
vm234	7020021010	70SP20030909	0	0	1468	1468	92%	11/10/2005	17:57	INTEL_NT
INTEL_NT	QA70-1	COMPARE_REL	3.8	UP20020121	WINDOWS					
vmc1	7020021010	70SP20030909	0	0	643	643	81%	11/10/2005	17:58	INTEL_NT
INTEL_NT	QA70-1	COMPARE_REL	3.8	UP20020121	WINDOWS					
vmc2	7020021010	70SP20030909	0	0	1692	1692	90%	11/10/2005	17:58	INTEL_NT
INTEL_NT	QA70-1	COMPARE_REL	3.8	UP20020121	WINDOWS					
vmc3	7020021010	70SP20030909	0	0	426	426	72%	11/10/2005	17:58	INTEL_NT
INTEL_NT	QA70-1	COMPARE_REL	3.8	UP20020121	WINDOWS					
vmc4	7020021010	70SP20030909	0	0	773	773	85%	11/10/2005	17:58	INTEL_NT
INTEL_NT	QA70-1	COMPARE_REL	3.8	UP20020121	WINDOWS					
vmc5	7020021010	70SP20030909	0	0	513	513	78%	11/10/2005	17:59	INTEL_NT
INTEL_NT	QA70-1	COMPARE_REL	3.8	UP20020121	WINDOWS					
vmc6	7020021010	70SP20030909	0	0	433	433	74%	11/10/2005	17:59	INTEL_NT
INTEL_NT	QA70-1	COMPARE_REL	3.8	UP20020121	WINDOWS					
vmc7	7020021010	70SP20030909	0	0	337	337	67%	11/10/2005	17:59	INTEL_NT
INTEL_NT	QA70-1	COMPARE_REL	3.8	UP20020121	WINDOWS					
vmc8	7020021010	70SP20030909	2	0	1894	1894	92%	11/10/2005	18:28	INTEL_NT
INTEL_NT	QA70-1	COMPARE_REL	3.8	UP20020121	WINDOWS					
vmd1	7020021010	70SP20030909	0	0	816	816	86%	11/10/2005	18:28	INTEL_NT
INTEL_NT	QA70-1	COMPARE_REL	3.8	UP20020121	WINDOWS					
vmd2	7020021010	70SP20030909	0	0	337	337	67%	11/10/2005	18:28	INTEL_NT
INTEL_NT	QA70-1	COMPARE_REL	3.8	UP20020121	WINDOWS					
vmd3	7020021010	70SP20030909	0	0	608	608	82%	11/10/2005	18:28	INTEL_NT
INTEL_NT	QA70-1	COMPARE_REL	3.8	UP20020121	WINDOWS					
cyc-177s	7020021010	70SP20030909	1	0	1219	1222	91%	11/10/2005	18:29	INTEL_NT
INTEL_NT	QA70-1	COMPARE_REL	3.8	UP20020121	WINDOWS					
cyc-178s	7020021010	70SP20030909	1	0	1219	1222	91%	11/10/2005	18:30	INTEL_NT
INTEL_NT	QA70-1	COMPARE_REL	3.8	UP20020121	WINDOWS					
dds-13s	7020021010	NO_UPDATE	-88	0	402	146	49%	11/10/2005	18:30	INTEL_NT
NOT_AVAILABLE	QA70-1	COMPARE_REL	3.8	UP20020121	WINDOWS					
dds-17s	7020021010	NO_UPDATE	-88	0	746	146	67%	11/10/2005	18:30	INTEL_NT
NOT_AVAILABLE	QA70-1	COMPARE_REL	3.8	UP20020121	WINDOWS					

esp-112s	7020021010	70SP20030909	0	0	279	279	58%	11/10/2005	18:30	INTEL_NT
INTEL_NT	QA70-1	COMPARE_REL	3.8		UP20020121	WINDOWS				
esp-124s	7020021010	70SP20030909	0	0	392	392	66%	11/10/2005	18:30	INTEL_NT
INTEL_NT	QA70-1	COMPARE_REL	3.8		UP20020121	WINDOWS				
esp-127s	7020021010	70SP20030909	0	0	527	527	75%	11/10/2005	18:30	INTEL_NT
INTEL_NT	QA70-1	COMPARE_REL	3.8		UP20020121	WINDOWS				
ess-26s	7020021010	70SP20030909	0	0	1846	1846	92%	11/10/2005	18:30	INTEL_NT
INTEL_NT	QA70-1	COMPARE_REL	3.8		UP20020121	WINDOWS				
ess-97s	7020021010	70SP20030909	0	0	1378	1378	90%	11/10/2005	18:30	INTEL_NT
INTEL_NT	QA70-1	COMPARE_REL	3.8		UP20020121	WINDOWS				
ev154-23s	7020021010	70SP20030909	0	0	1259	1259	89%	11/10/2005	18:30	INTEL_NT
INTEL_NT	QA70-1	COMPARE_REL	3.8		UP20020121	WINDOWS				
ev154-25s	7020021010	70SP20030909	0	0	587	587	76%	11/10/2005	18:31	INTEL_NT
INTEL_NT	QA70-1	COMPARE_REL	3.8		UP20020121	WINDOWS				
ev171-57s	7020021010	70SP20030909	0	0	542	542	79%	11/10/2005	18:31	INTEL_NT
INTEL_NT	QA70-1	COMPARE_REL	3.8		UP20020121	WINDOWS				
ev173-53s	7020021010	70SP20030909	1	0	1426	1429	92%	11/10/2005	18:31	INTEL_NT
INTEL_NT	QA70-1	COMPARE_REL	3.8		UP20020121	WINDOWS				
ev175-20s	7020021010	70SP20030909	1	0	538	541	79%	11/10/2005	18:31	INTEL_NT
INTEL_NT	QA70-1	COMPARE_REL	3.8		UP20020121	WINDOWS				
ev175-21s	7020021010	NO_UPDATE	-88	0	566	146	64%	11/10/2005	18:31	INTEL_NT
NOT AVAILABLE	QA70-1	COMPARE_REL	3.8		UP20020121	WINDOWS				
ev175-38s	7020021010	70SP20030909	0	0	808	808	85%	11/10/2005	18:31	INTEL_NT
INTEL_NT	QA70-1	COMPARE_REL	3.8		UP20020121	WINDOWS				
ev182-zbdpg11s	7020021010	70SP20030909	0	0	660	660	83%	11/10/2005	18:31	INTEL_NT
INTEL_NT	QA70-1	COMPARE_REL	3.8		UP20020121	WINDOWS				
ev183-zdpl20s	7020021010	70SP20030909	0	0	577	577	80%	11/10/2005	18:32	INTEL_NT
INTEL_NT	QA70-1	COMPARE_REL	3.8		UP20020121	WINDOWS				
ev184-02s	7020021010	70SP20030909	0	0	267	267	56%	11/10/2005	18:32	INTEL_NT
INTEL_NT	QA70-1	COMPARE_REL	3.8		UP20020121	WINDOWS				
ev184-07s	7020021010	70SP20030909	0	0	661	661	80%	11/10/2005	18:32	INTEL_NT
INTEL_NT	QA70-1	COMPARE_REL	3.8		UP20020121	WINDOWS				
ev35-23s	7020021010	70SP20030909	0	0	293	293	61%	11/10/2005	18:32	INTEL_NT
INTEL_NT	QA70-1	COMPARE_REL	3.8		UP20020121	WINDOWS				
ev95-45s	7020021010	70SP20030909	0	0	892	892	85%	11/10/2005	18:32	INTEL_NT
INTEL_NT	QA70-1	COMPARE_REL	3.8		UP20020121	WINDOWS				
inrt-16s	7020021010	70SP20030909	1	0	484	486	77%	11/10/2005	18:32	INTEL_NT
INTEL_NT	QA70-1	COMPARE_REL	3.8		UP20020121	WINDOWS				
inrt-9s	7020021010	70SP20030909	0	0	421	421	73%	11/10/2005	18:32	INTEL_NT
INTEL_NT	QA70-1	COMPARE_REL	3.8		UP20020121	WINDOWS				
mvhy-bk501	7020021010	70SP20030909	0	0	536	536	78%	11/10/2005	18:32	INTEL_NT
INTEL_NT	QA70-1	COMPARE_REL	3.8		UP20020121	WINDOWS				
mvhy-gt202	7020021010	70SP20030909	0	0	780	780	84%	11/10/2005	18:32	INTEL_NT
INTEL_NT	QA70-1	COMPARE_REL	3.8		UP20020121	WINDOWS				

mvve-cr003	7020021010	70SP20030909	0	0	328	328	65%	11/10/2005	18:33	INTEL_NT
INTEL_NT	QA70-1	COMPARE_REL	3.8	UP20020121	WINDOWS					
mvve-cr804	7020021010	70SP20030909	0	0	329	329	65%	11/10/2005	18:33	INTEL_NT
INTEL_NT	QA70-1	COMPARE_REL	3.8	UP20020121	WINDOWS					
se-1s	7020021010	70SP20030909	0	0	400	400	72%	11/10/2005	18:33	INTEL_NT
INTEL_NT	QA70-1	COMPARE_REL	3.8	UP20020121	WINDOWS					
se-20s	7020021010	70SP20030909	0	0	879	879	85%	11/10/2005	18:33	INTEL_NT
INTEL_NT	QA70-1	COMPARE_REL	3.8	UP20020121	WINDOWS					

1

00000000 VERSION=INTEL NT RELEASE= 7.0 UP20021010

EXPECTED COMPARE DIFFERENCE FOUND AT NG= 113 NT= 113

G= 00000000 VERSION=INTEL NT RELEASE= 7.0 UP20021010

T= 00292062 VERSION=INTEL NT RELEASE= 7.0SP11 UP20030909

EXPECTED COMPARE DIFFERENCE FOUND AT NG= 114 NT= 114

G= CURRENT JOBNAME=c0231 10:37:04 OCT 15, 2002 CP= 0.219

T= CURRENT JOBNAME=c0231 17:28:23 NOV 10, 2005 CP= 0.375

0 /verify,c0231

0 /title, c0231 (fsk) Unmatched nodes mapping

COMPARE DIFFERENCE FOUND AT NG= 192 NT= 192

G= NODAL RESULTS ARE FOR CYCLIC SECTOR 1 - PHASE ANGLE = 30.580

T= NODAL RESULTS ARE FOR CYCLIC SECTOR 1 - PHASE ANGLE = 237.330

COMPARE DIFFERENCE FOUND AT NG= 219 NT= 219

G= NODAL RESULTS ARE FOR CYCLIC SECTOR 2 - PHASE ANGLE = 30.580

T= NODAL RESULTS ARE FOR CYCLIC SECTOR 2 - PHASE ANGLE = 237.330

COMPARE DIFFERENCE FOUND AT NG= 246 NT= 246

G= NODAL RESULTS ARE FOR CYCLIC SECTOR 3 - PHASE ANGLE = 30.580

T= NODAL RESULTS ARE FOR CYCLIC SECTOR 3 - PHASE ANGLE = 237.330

BOTTOM OF GOOD FILE REACHED AT LINE 289

G= | ANSYS RUN COMPLETED |

```

~~~~~
NOTE- NONSTANDARD COMPARE - DIFOPT NAME QA70-1 HAS BEEN USED
NUMBER OF LINES SKIPPED IN GOOD FILE(BLANK LINES EXCLUDED) - 0
NUMBER OF LINES SKIPPED IN TEST FILE(BLANK LINES EXCLUDED) - 0
NUMBER OF LINES ON GOOD FILE WITH STRINGS CONDENSED OUT - 0
NUMBER OF LINES ON TEST FILE WITH STRINGS CONDENSED OUT - 0
~~~~~

```

```

*****
COMPARE ERRORS = 3 *
*****

```

```

=====
PROBLEM: c0231            COMPARE OPTIONS    COMPARE_REL 3.8 UP20020121    WINDOWS

```

```

ALMOST ZERO (GOOD)    = 1.0000E-006            KROUND (DROP LAST DIGIT)= 1
ALMOST ZERO (TEST)    = 1.0000E-006            KABSPR (0=SUMMARY 1=ALL)= 1
ABSOLUTE VALUE TOL    = 1.0000E-010           KSKIP(SKIP=ERR 0=Y, 1=N)= 0
FRACTIONAL DIFFERENCE= 1.0000E-004           MAXERR (STOP WHEN ERRS )= 100
ABSOLUTE DIFFERENCE   = 1.0000E-006           MAXBUF (# LINES TO SCAN)= 6
                                              KNOWN (# OF KNOWN ERRS)= 0

```

GREAD, TREAD = 1, 1

=====

LINES ON GOOD FILE = 304

LINES ON TEST FILE = 304

RPP-RPT-28967, Rev. 1

1

[illegible]

```

00000000          VERSION=INTEL NT          RELEASE= 7.0          UP20021010
EXPECTED COMPARE DIFFERENCE FOUND AT    NG= 113 NT= 113
G= 00000000          VERSION=INTEL NT          RELEASE= 7.0          UP20021010
T= 00292062          VERSION=INTEL NT          RELEASE= 7.0SP11 UP20030909

EXPECTED COMPARE DIFFERENCE FOUND AT    NG= 114 NT= 114
G= CURRENT JOBNAME=vm33 20:03:05 OCT 15, 2002 CP=          0.219
T= CURRENT JOBNAME=vm33 17:31:47 NOV 10, 2005 CP=          0.375

```

```
0  /VERIFY,VM33
```

0 /TITLE, VM33, TRANSIENT THERMAL STRESS IN A CYLINDER

NOW COMPARING LINES FROM ***** ANSYS ANALYSIS DEFINITION (PREP7) *****

COMPARE DIFFERENCE FOUND AT						NG=	236	NT=	236		
G=	CURRENT	NODAL	DOF	SET	IS	UX	UY	UZ	TEMP	VOLT	MAG
T=	CURRENT	NODAL	DOF	SET	IS	UX	UY	UZ	TEMP	VOLT	

COMPARE DIFFERENCE FOUND AT				NG=	419	NT=	419
G=	DEGREES OF FREEDOM.	UX	UY	UZ	TEMP	VOLT MAG
T=	DEGREES OF FREEDOM.	UX	UY	UZ	TEMP	VOLT

```
EXTRA DATA SKIPPED ON GOOD FILE          NG=  422 NT=  425  
G=    ELECTRO-MAGNETIC UNITS. . . . . MKS  
G=      MUZERO . . . . . 0.12566E-05  
END OF SKIPPED DATA                     NG=  424 NT=  425
```

```

EXTRA DATA SKIPPED ON GOOD FILE          NG=  427 NT=  428
G= Element 1 references undefined MURX or BH table for material 1.
G= *** WARNING ***                        CP=      0.000    TIME= 00:00:00
END OF SKIPPED DATA                      NG=  430 NT=  428

```

```

EXTRA DATA SKIPPED ON GOOD FILE          NG=  453 NT=  449
G=      MAGNETIC DOFS. . . . . ON
END OF SKIPPED DATA                     NG=  454 NT=  449

```

```

NOW COMPARING LINES FROM          ***** ANSYS RESULTS INTERPRETATION (POST1)
*****

```

```

NOW COMPARING LINES FROM          ***** TIME-HISTORY POSTPROCESSOR (POST26)
*****

```

```
COMPARE DIFFERENCE FOUND AT          NG= 881 NT= 875
G= NUMBER OF WARNING MESSAGES ENCOUNTERED= 4
T= NUMBER OF WARNING MESSAGES ENCOUNTERED= 3
```

```

BOTTOM OF GOOD FILE REACHED AT LINE      887
G= |                                     ANSYS RUN COMPLETED

```

```

~~~~~
NOTE- NONSTANDARD COMPARE - DIFOPT NAME QA70-1 HAS BEEN USED
NUMBER OF LINES SKIPPED IN GOOD FILE(BLANK LINES EXCLUDED) - 0
NUMBER OF LINES SKIPPED IN TEST FILE(BLANK LINES EXCLUDED) - 0
NUMBER OF LINES ON GOOD FILE WITH STRINGS CONDENSED OUT - 0
NUMBER OF LINES ON TEST FILE WITH STRINGS CONDENSED OUT - 0
~~~~~

```

```

*****
COMPARE ERRORS = 6 *
*****

```

```

=====
PROBLEM: vm33          COMPARE OPTIONS  COMPARE_REL 3.8 UP20020121  WINDOWS

ALMOST ZERO (GOOD)    = 1.0000E-006          KROUND (DROP LAST DIGIT)= 1
ALMOST ZERO (TEST)    = 1.0000E-006          KABSPR (0=SUMMARY 1=ALL)= 1
ABSOLUTE VALUE TOL    = 1.0000E-010          KSKIP(SKIP=ERR 0=Y, 1=N)= 0
FRACTIONAL DIFFERENCE= 1.0000E-004          MAXERR (STOP WHEN ERRS )= 100
ABSOLUTE DIFFERENCE   = 1.0000E-006          MAXBUF (# LINES TO SCAN)= 6
                                          KNOWN (# OF KNOWN ERRS)= 0
                                          GREAD, TREAD = 1, 1
=====

```

```

LINES ON GOOD FILE = 902
LINES ON TEST FILE = 896

```

```

*****

```

1

00000000 VERSION=INTEL NT RELEASE= 7.0 UP20021010

EXPECTED COMPARE DIFFERENCE FOUND AT NG= 113 NT= 113
 G= 00000000 VERSION=INTEL NT RELEASE= 7.0 UP20021010
 T= 00292062 VERSION=INTEL NT RELEASE= 7.0SP11 UP20030909

EXPECTED COMPARE DIFFERENCE FOUND AT NG= 114 NT= 114
 G= CURRENT JOBNAME=vm176 20:43:52 OCT 15, 2002 CP= 0.234
 T= CURRENT JOBNAME=vm176 17:43:39 NOV 10, 2005 CP= 0.375

0 /VERIFY,VM176

0 /TITLE, VM176, FREQUENCY RESPONSE OF ELECTRICAL INPUT
 ADMITTANCE FOR A

NOW COMPARING LINES FROM ***** ANSYS ANALYSIS DEFINITION (PREP7) *****

COMPARE DIFFERENCE FOUND AT NG= 276 NT= 276
 G= CURRENT NODAL DOF SET IS UX UY UZ TEMP VOLT MAG
 T= CURRENT NODAL DOF SET IS UX UY UZ TEMP VOLT

COMPARE DIFFERENCE FOUND AT NG= 617 NT= 617
 G= DEGREES OF FREEDOM. UX UY UZ TEMP VOLT MAG
 T= DEGREES OF FREEDOM. UX UY UZ TEMP VOLT

EXTRA DATA SKIPPED ON GOOD FILE NG= 623 NT= 627
 G= ELECTRO-MAGNETIC UNITS.MKS
 G= MUZERO 0.12566E-05
 END OF SKIPPED DATA NG= 626 NT= 627

COMPARE DIFFERENCE FOUND AT NG= 627 NT= 625
 G= Element 1 references undefined MURX or BH table for material 3.
 T= Element 1 references undefined KXX for material 3.

EXTRA DATA SKIPPED ON GOOD FILE NG= 630 NT= 630
 G= Element 1 references undefined KXX for material 3.
 G= *** WARNING *** CP= 0.000 TIME= 00:00:00
 END OF SKIPPED DATA NG= 633 NT= 630

COMPARE DIFFERENCE FOUND AT NG= 638 NT= 633
 G= Element 11 references undefined MURX or BH table for material 4.
 T= Element 11 references undefined KXX for material 4.

COMPARE DIFFERENCE FOUND AT NG= 641 NT= 636
 G= Element 11 references undefined KXX for material 4.
 T= Element 11 references undefined RSVX or PERX for material 4.

COMPARE DIFFERENCE FOUND AT NG= 644 NT= 639
 G= Element 11 references undefined RSVX or PERX for material 4.
 T= Element 16 references undefined KXX for material 2.

EXTRA DATA SKIPPED ON GOOD FILE NG= 647 NT= 648

RPP-RPT-28967, Rev. 1

G= Element 16 references undefined MURX or BH table for material 2.
G= *** WARNING *** CP= 0.000 TIME= 00:00:00
G= Element 16 references undefined KXX for material 2.
G= *** WARNING *** CP= 0.000 TIME= 00:00:00
END OF SKIPPED DATA NG= 653 NT= 648

COMPARE DIFFERENCE FOUND AT NG= 731 NT= 720
G= Element 1 references undefined MURX or BH table for material 3.
T= Element 1 references undefined KXX for material 3.

EXTRA DATA SKIPPED ON GOOD FILE NG= 734 NT= 725
G= Element 1 references undefined KXX for material 3.
G= *** WARNING *** CP= 0.000 TIME= 00:00:00
END OF SKIPPED DATA NG= 737 NT= 725

COMPARE DIFFERENCE FOUND AT NG= 742 NT= 728
G= Element 11 references undefined MURX or BH table for material 4.
T= Element 11 references undefined KXX for material 4.

COMPARE DIFFERENCE FOUND AT NG= 745 NT= 731
G= Element 11 references undefined KXX for material 4.
T= Element 11 references undefined RSVX or PERX for material 4.

COMPARE DIFFERENCE FOUND AT NG= 748 NT= 734
G= Element 11 references undefined RSVX or PERX for material 4.
T= Element 16 references undefined KXX for material 2.

EXTRA DATA SKIPPED ON GOOD FILE NG= 751 NT= 742
G= Element 16 references undefined MURX or BH table for material 2.
G= *** WARNING *** CP= 0.000 TIME= 00:00:00
G= Element 16 references undefined KXX for material 2.
G= *** WARNING *** CP= 0.000 TIME= 00:00:00
END OF SKIPPED DATA NG= 757 NT= 742

COMPARE DIFFERENCE FOUND AT NG= 784 NT= 764
G= Element 1 references undefined MURX or BH table for material 3.
T= Element 1 references undefined KXX for material 3.

EXTRA DATA SKIPPED ON GOOD FILE NG= 787 NT= 769
G= Element 1 references undefined KXX for material 3.
G= *** WARNING *** CP= 0.000 TIME= 00:00:00
END OF SKIPPED DATA NG= 790 NT= 769

COMPARE DIFFERENCE FOUND AT NG= 795 NT= 772
G= Element 11 references undefined MURX or BH table for material 4.
T= Element 11 references undefined KXX for material 4.

COMPARE DIFFERENCE FOUND AT NG= 798 NT= 775
G= Element 11 references undefined KXX for material 4.
T= Element 11 references undefined RSVX or PERX for material 4.

COMPARE DIFFERENCE FOUND AT NG= 801 NT= 778
G= Element 11 references undefined RSVX or PERX for material 4.
T= Element 16 references undefined KXX for material 2.

EXTRA DATA SKIPPED ON GOOD FILE NG= 804 NT= 786
G= Element 16 references undefined MURX or BH table for material 2.

RPP-RPT-28967, Rev. 1

```
G= *** WARNING ***                      CP=      0.000    TIME= 00:00:00
G= Element 16 references undefined KXX for material 2.
G= *** WARNING ***                      CP=      0.000    TIME= 00:00:00
END OF SKIPPED DATA                    NG=   810 NT=   786
```

```
NOW COMPARING LINES FROM                ***** TIME-HISTORY POSTPROCESSOR (POST26)
*****
```

```
COMPARE DIFFERENCE FOUND AT            NG=   978 NT=   949
G= NUMBER OF WARNING MESSAGES ENCOUNTERED=      32
T= NUMBER OF WARNING MESSAGES ENCOUNTERED=      23
```

```
BOTTOM OF GOOD FILE REACHED AT LINE    984
G= |                                ANSYS RUN COMPLETED |
```

```
~~~~~
NOTE- NONSTANDARD COMPARE - DIFOPT NAME QA70-1  HAS BEEN USED
NUMBER OF LINES SKIPPED IN GOOD FILE(BLANK LINES EXCLUDED) -      0
NUMBER OF LINES SKIPPED IN TEST FILE(BLANK LINES EXCLUDED) -      0
NUMBER OF LINES ON GOOD FILE WITH STRINGS CONDENSED OUT    -      0
NUMBER OF LINES ON TEST FILE WITH STRINGS CONDENSED OUT    -      0
~~~~~
```

```
*****
COMPARE ERRORS =      22      *
*****
```

```
=====
PROBLEM: vm176                COMPARE OPTIONS  COMPARE_REL 3.8 UP20020121  WINDOWS

ALMOST ZERO (GOOD)    = 1.0000E-006                KROUND (DROP LAST DIGIT)=    1
ALMOST ZERO (TEST)    = 1.0000E-006                KABSPR (0=SUMMARY 1=ALL)=    1
ABSOLUTE VALUE TOL    = 1.0000E-010                KSKIP(SKIP=ERR 0=Y, 1=N)=    0
FRACTIONAL DIFFERENCE= 1.0000E-004                MAXERR (STOP WHEN ERRS )= 100
ABSOLUTE DIFFERENCE   = 1.0000E-006                MAXBUF (# LINES TO SCAN)=    6
                                                KNOWN  (# OF KNOWN ERRS)=    0
                                                GREAD, TREAD =    1,    1
=====
```

```
LINES ON GOOD FILE =      999
LINES ON TEST FILE =      970
```

```
*****
```


1

00000000 VERSION=INTEL NT RELEASE= 7.0 UP20021010

EXPECTED COMPARE DIFFERENCE FOUND AT NG= 113 NT= 113
 G= 00000000 VERSION=INTEL NT RELEASE= 7.0 UP20021010
 T= 00292062 VERSION=INTEL NT RELEASE= 7.0SP11 UP20030909

EXPECTED COMPARE DIFFERENCE FOUND AT NG= 114 NT= 114
 G= CURRENT JOBNAME=vm184 20:46:18 OCT 15, 2002 CP= 0.250
 T= CURRENT JOBNAME=vm184 17:44:26 NOV 10, 2005 CP= 0.375

0 /VERIFY,VM184

0 /TITLE, VM184, STRAIGHT CANTILEVER BEAM

0 /stitle,1,Reason COMPARE differences are acceptable:

0 /stitle,2, mesher accuracy - element number on warning; near-
 zero values

0 /TITLE, VM184, STRAIGHT CANTILEVER BEAM

NOW COMPARING LINES FROM ***** ANSYS ANALYSIS DEFINITION (PREP7) *****

NOW COMPARING LINES FROM ***** ANSYS RESULTS INTERPRETATION (POST1)

ABSOLUTE VALUE DIFFERENCE FOUND AT NG= 926 NT= 926
 G= VALUE -0.24849E-01 0.98917 -0.43496E-05 0.98948
 T= VALUE -0.24849E-01 0.98917 0.43497E-05 0.98948

ABSOLUTE VALUE DIFFERENCE FOUND AT NG= 982 NT= 982
 G= VALUE -0.53544E-02-0.26671E-05 0.42554 0.42557
 T= VALUE -0.53544E-02 0.26671E-05 0.42554 0.42557

ABSOLUTE VALUE DIFFERENCE FOUND AT NG= 1011 NT= 1011
 G= VALUE -0.12394E-01-0.61739E-05 0.98504 0.98511
 T= VALUE -0.12394E-01 0.61739E-05 0.98504 0.98511

NOW COMPARING LINES FROM ***** ANSYS ANALYSIS DEFINITION (PREP7) *****

NOW COMPARING LINES FROM ***** ANSYS RESULTS INTERPRETATION (POST1)

COMPARE DIFFERENCE FOUND AT NG= 1580 NT= 1580
 G= VALUE 0.24811E-01 0.98813 -0.43696E-05 0.98844
 T= VALUE 0.24811E-01 0.98813 0.43701E-05 0.98844

ABSOLUTE VALUE DIFFERENCE FOUND AT NG= 1639 NT= 1639
 G= VALUE -0.53533E-02-0.30755E-05 0.42553 0.42556

RPP-RPT-28967, Rev. 1

T= VALUE -0.53533E-02 0.30756E-05 0.42553 0.42556

ABSOLUTE VALUE DIFFERENCE FOUND AT NG= 1673 NT= 1673

G= VALUE -0.12392E-01-0.71193E-05 0.98502 0.98510

T= VALUE -0.12392E-01 0.71194E-05 0.98502 0.98510

NOW COMPARING LINES FROM ***** ANSYS ANALYSIS DEFINITION (PREP7) *****

NOW COMPARING LINES FROM ***** ANSYS RESULTS INTERPRETATION (POST1)

NOW COMPARING LINES FROM ***** ANSYS ANALYSIS DEFINITION (PREP7) *****

NOW COMPARING LINES FROM ***** ANSYS RESULTS INTERPRETATION (POST1)

BOTTOM OF GOOD FILE REACHED AT LINE 3147
G= | ANSYS RUN COMPLETED |

~~~~~  
NOTE- NONSTANDARD COMPARE - DIFOPT NAME QA70-1 HAS BEEN USED  
NUMBER OF LINES SKIPPED IN GOOD FILE(BLANK LINES EXCLUDED) - 0  
NUMBER OF LINES SKIPPED IN TEST FILE(BLANK LINES EXCLUDED) - 0  
NUMBER OF LINES ON GOOD FILE WITH STRINGS CONDENSED OUT - 0  
NUMBER OF LINES ON TEST FILE WITH STRINGS CONDENSED OUT - 0  
~~~~~

COMPARE ERRORS = 1 *

WARNING - 5 ABSOLUTE VALUE DIFFERENCE(S) FOUND.

NOTE - 1 summary line(s) contained absolute value differences.

=====

PROBLEM: vm184	COMPARE OPTIONS	COMPARE_REL 3.8 UP20020121	WINDOWS
ALMOST ZERO (GOOD)	= 1.0000E-006	KROUND (DROP LAST DIGIT)=	1
ALMOST ZERO (TEST)	= 1.0000E-006	KABSPR (0=SUMMARY 1=ALL)=	1
ABSOLUTE VALUE TOL	= 1.0000E-010	KSKIP(SKIP=ERR 0=Y, 1=N)=	0
FRACTIONAL DIFFERENCE=	1.0000E-004	MAXERR (STOP WHEN ERRS)=	100
ABSOLUTE DIFFERENCE	= 1.0000E-006	MAXBUF (# LINES TO SCAN)=	6
		KNOWN (# OF KNOWN ERRS)=	0

GREAD, TREAD = 1, 1

=====

LINES ON GOOD FILE = 3162

LINES ON TEST FILE = 3162

RPP-RPT-28967, Rev. 1

1

```

*****

00000000          VERSION=INTEL NT          RELEASE= 7.0          UP20021010

EXPECTED COMPARE DIFFERENCE FOUND AT  NG=  113 NT=  113
G= 00000000          VERSION=INTEL NT          RELEASE= 7.0          UP20021010
T= 00292062          VERSION=INTEL NT          RELEASE= 7.0SP11 UP20030909

EXPECTED COMPARE DIFFERENCE FOUND AT  NG=  114 NT=  114
G= CURRENT JOBNAME=vm198  20:50:49  OCT 15, 2002 CP=          0.266
T= CURRENT JOBNAME=vm198  17:45:25  NOV 10, 2005 CP=          0.344

      0  /VERIFY,VM198

      0  /TITLE, VM198, LARGE STRAIN IN-PLANE TORSION TEST (%EL%)

NOW COMPARING LINES FROM          ***** ANSYS ANALYSIS DEFINITION (PREP7) *****

NOW COMPARING LINES FROM          ***** ANSYS RESULTS INTERPRETATION (POST1)
*****

NOW COMPARING LINES FROM          ***** TIME-HISTORY POSTPROCESSOR (POST26)
*****

NOW COMPARING LINES FROM          ***** ANSYS ANALYSIS DEFINITION (PREP7) *****

COMPARE DIFFERENCE FOUND AT          NG=  618 NT=  618
G= RELEASE  0.0          UPDATE          0  CUSTOMER  00000000
T= RELEASE  0.0          UPDATE          0  CUSTOMER  00292062

NOW COMPARING LINES FROM          ***** ANSYS RESULTS INTERPRETATION (POST1)
*****

NOW COMPARING LINES FROM          ***** TIME-HISTORY POSTPROCESSOR (POST26)
*****

NOW COMPARING LINES FROM          ***** ANSYS ANALYSIS DEFINITION (PREP7) *****

COMPARE DIFFERENCE FOUND AT          NG=  907 NT=  907
G= RELEASE  0.0          UPDATE          0  CUSTOMER  00000000
T= RELEASE  0.0          UPDATE          0  CUSTOMER  00292062

NOW COMPARING LINES FROM          ***** ANSYS RESULTS INTERPRETATION (POST1)
*****

NOW COMPARING LINES FROM          ***** TIME-HISTORY POSTPROCESSOR (POST26)
*****

```

RPP-RPT-28967, Rev. 1

BOTTOM OF GOOD FILE REACHED AT LINE 1193
G= | ANSYS RUN COMPLETED |

~~~~~  
NOTE- NONSTANDARD COMPARE - DIFOPT NAME QA70-1 HAS BEEN USED  
NUMBER OF LINES SKIPPED IN GOOD FILE(BLANK LINES EXCLUDED) - 2  
NUMBER OF LINES SKIPPED IN TEST FILE(BLANK LINES EXCLUDED) - 2  
NUMBER OF LINES ON GOOD FILE WITH STRINGS CONDENSED OUT - 0  
NUMBER OF LINES ON TEST FILE WITH STRINGS CONDENSED OUT - 0  
~~~~~

COMPARE ERRORS = 2 *

=====

PROBLEM: vm198	COMPARE OPTIONS	COMPARE_REL 3.8 UP20020121	WINDOWS
----------------	-----------------	----------------------------	---------

ALMOST ZERO (GOOD)	= 1.0000E-006	KROUND (DROP LAST DIGIT)=	1
ALMOST ZERO (TEST)	= 1.0000E-006	KABSPR (0=SUMMARY 1=ALL)=	1
ABSOLUTE VALUE TOL	= 1.0000E-010	KSKIP(SKIP=ERR 0=Y, 1=N)=	0
FRACTIONAL DIFFERENCE=	1.0000E-004	MAXERR (STOP WHEN ERRS)=	100
ABSOLUTE DIFFERENCE	= 1.0000E-006	MAXBUF (# LINES TO SCAN)=	6
		KNOWN (# OF KNOWN ERRS)=	0
		GREAD, TREAD =	1, 1

=====

=====

LINE	ON GOOD FILE	=	1208
LINE	ON TEST FILE	=	1208

1

00000000 VERSION=INTEL NT RELEASE= 7.0 UP20021010

EXPECTED COMPARE DIFFERENCE FOUND AT NG= 113 NT= 113
 G= 00000000 VERSION=INTEL NT RELEASE= 7.0 UP20021010
 T= 00292062 VERSION=INTEL NT RELEASE= 7.0SP11 UP20030909

EXPECTED COMPARE DIFFERENCE FOUND AT NG= 114 NT= 114
 G= CURRENT JOBNAME=vmc8 21:52:06 OCT 15, 2002 CP= 0.219
 T= CURRENT JOBNAME=vmc8 17:59:57 NOV 10, 2005 CP= 0.375

0 /VERIFY,VMC8

0 /TITLE, VMC8, ALUMINUM BAR IMPACTING A RIGID BOUNDARY

0 /stitle,1,Reason COMPARE differences are acceptable:

0 /stitle,2, number of iterations, accuracy

PLANE2

0 /title, VMC8, ALUMINUM BAR IMPACTING A RIGID BOUNDARY -

PLANE42

0 /title, VMC8, ALUMINUM BAR IMPACTING A RIGID BOUNDARY -

PLANE82

0 /title, VMC8, ALUMINUM BAR IMPACTING A RIGID BOUNDARY -

VISCO106

0 /title, VMC8, ALUMINUM BAR IMPACTING A RIGID BOUNDARY -

SOLID45

0 /title, VMC8, ALUMINUM BAR IMPACTING A RIGID BOUNDARY -

SOLID95

0 /title, VMC8, ALUMINUM BAR IMPACTING A RIGID BOUNDARY -

VISCO107

0 /title, VMC8, ALUMINUM BAR IMPACTING A RIGID BOUNDARY -

0 /TITLE, VMC8, ALUMINUM BAR IMPACTING A RIGID BOUNDARY

NOW COMPARING LINES FROM ***** ANSYS ANALYSIS DEFINITION (PREP7) *****

NOW COMPARING LINES FROM ***** ANSYS RESULTS INTERPRETATION (POST1)

COMPARE DIFFERENCE FOUND AT NG= 880 NT= 880
 G= SET COMMAND GOT LOAD STEP= 2 SUBSTEP= 320 CUMULATIVE ITERATION= 3255
 T= SET COMMAND GOT LOAD STEP= 2 SUBSTEP= 320 CUMULATIVE ITERATION= 3240

NOW COMPARING LINES FROM

***** TIME-HISTORY POSTPROCESSOR (POST26)

NOW COMPARING LINES FROM

***** ANSYS ANALYSIS DEFINITION (PREP7) *****

NOW COMPARING LINES FROM

***** ANSYS RESULTS INTERPRETATION (POST1)

NOW COMPARING LINES FROM

***** TIME-HISTORY POSTPROCESSOR (POST26)

NOW COMPARING LINES FROM

***** ANSYS ANALYSIS DEFINITION (PREP7) *****

NOW COMPARING LINES FROM

***** ANSYS RESULTS INTERPRETATION (POST1)

NOW COMPARING LINES FROM

***** TIME-HISTORY POSTPROCESSOR (POST26)

COMPARE DIFFERENCE FOUND AT

NG= 1227 NT= 1227

G=	3 ESOL	1 EPPL EQV	EPPLEQV	0.7401E-16	0.000	3.410	0.000
T=	3 ESOL	1 EPPL EQV	EPPLEQV	0.2694E-35	0.000	3.422	0.000

NOW COMPARING LINES FROM

***** ANSYS ANALYSIS DEFINITION (PREP7) *****

NOW COMPARING LINES FROM

***** ANSYS RESULTS INTERPRETATION (POST1)

NOW COMPARING LINES FROM

***** TIME-HISTORY POSTPROCESSOR (POST26)

NOW COMPARING LINES FROM

***** ANSYS ANALYSIS DEFINITION (PREP7) *****

NOW COMPARING LINES FROM

***** ANSYS RESULTS INTERPRETATION (POST1)

NOW COMPARING LINES FROM

***** TIME-HISTORY POSTPROCESSOR (POST26)

NOW COMPARING LINES FROM

***** ANSYS ANALYSIS DEFINITION (PREP7) *****

NOW COMPARING LINES FROM

***** ANSYS RESULTS INTERPRETATION (POST1)

RPP-RPT-28967, Rev. 1

NOW COMPARING LINES FROM ***** TIME-HISTORY POSTPROCESSOR (POST26)

BOTTOM OF GOOD FILE REACHED AT LINE 1879
 G= | ANSYS RUN COMPLETED |

~~~~~  
 NOTE- NONSTANDARD COMPARE - DIFOPT NAME QA70-1 HAS BEEN USED  
 NUMBER OF LINES SKIPPED IN GOOD FILE (BLANK LINES EXCLUDED) - 0  
 NUMBER OF LINES SKIPPED IN TEST FILE (BLANK LINES EXCLUDED) - 0  
 NUMBER OF LINES ON GOOD FILE WITH STRINGS CONDENSED OUT - 0  
 NUMBER OF LINES ON TEST FILE WITH STRINGS CONDENSED OUT - 0  
 ~~~~~

 COMPARE ERRORS = 2 *

=====

PROBLEM: vmc8	COMPARE OPTIONS	COMPARE_REL 3.8 UP20020121	WINDOWS
ALMOST ZERO (GOOD) = 1.0000E-006	KROUND (DROP LAST DIGIT)=	1	
ALMOST ZERO (TEST) = 1.0000E-006	KABSPR (0=SUMMARY 1=ALL)=	1	
ABSOLUTE VALUE TOL = 1.0000E-010	KSKIP (SKIP=ERR 0=Y, 1=N)=	0	
FRACTIONAL DIFFERENCE= 1.0000E-004	MAXERR (STOP WHEN ERRS)=	100	
ABSOLUTE DIFFERENCE = 1.0000E-006	MAXBUF (# LINES TO SCAN)=	6	
	KNOWN (# OF KNOWN ERRS)=	0	
	GREAD, TREAD =	1, 1	

=====

LINES ON GOOD FILE = 1894
 LINES ON TEST FILE = 1894

1

```

00000000          VERSION=INTEL NT          RELEASE= 7.0          UP20021010

EXPECTED COMPARE DIFFERENCE FOUND AT  NG=  113 NT=  113
G= 00000000          VERSION=INTEL NT          RELEASE= 7.0          UP20021010
T= 00292062          VERSION=INTEL NT          RELEASE= 7.0SP11 UP20030909

EXPECTED COMPARE DIFFERENCE FOUND AT  NG=  114 NT=  114
G= CURRENT JOBNAME=cyc-177s  11:45:34  OCT 15, 2002 CP=          0.219
T= CURRENT JOBNAME=cyc-177s  18:28:58  NOV 10, 2005 CP=          0.359

```

```

0  /verify,cyc-177s

0  /TITLE, ceb,cyc-177s, Test cyc symm Buckling element 42

0  /title,1,Full Results to Sector Results!

0  /stitle,Reason Compare differences are acceptable:

```

```

EXTRA DATA SKIPPED ON TEST FILE          NG= 1202 NT= 1194
T= USE COMMAND MACRO QAEND
T= ARGS= 289.00
END OF SKIPPED DATA                      NG= 1202 NT= 1199

```

```

BOTTOM OF GOOD FILE REACHED AT LINE 1204
G= |                                ANSYS RUN COMPLETED                                |

```

```

~~~~~
NOTE- NONSTANDARD COMPARE - DIFOPT NAME QA70-1 HAS BEEN USED
NUMBER OF LINES SKIPPED IN GOOD FILE(BLANK LINES EXCLUDED) - 2
NUMBER OF LINES SKIPPED IN TEST FILE(BLANK LINES EXCLUDED) - 2
NUMBER OF LINES ON GOOD FILE WITH STRINGS CONDENSED OUT - 0
NUMBER OF LINES ON TEST FILE WITH STRINGS CONDENSED OUT - 0
~~~~~

```

```

*****
COMPARE ERRORS = 1 *
*****

```

```

=====
PROBLEM: cyc-177s          COMPARE OPTIONS  COMPARE_REL 3.8 UP20020121  WINDOWS

ALMOST ZERO (GOOD)   = 1.0000E-006          KROUND (DROP LAST DIGIT)= 1
ALMOST ZERO (TEST)   = 1.0000E-006          KABSPR (0=SUMMARY 1=ALL)= 1
ABSOLUTE VALUE TOL    = 1.0000E-010          KSKIP(SKIP=ERR 0=Y, 1=N)= 0
FRACTIONAL DIFFERENCE= 1.0000E-004          MAXERR (STOP WHEN ERRS )= 100
ABSOLUTE DIFFERENCE  = 1.0000E-006          MAXBUF (# LINES TO SCAN)= 6
                                          KNOWN (# OF KNOWN ERRS)= 0
                                          GREAD, TREAD = 1, 1
=====

```

RPP-RPT-28967, Rev. 1

LINEs ON GOOD FILE = 1219
LINEs ON TEST FILE = 1222

1

```

00000000          VERSION=INTEL NT          RELEASE= 7.0          UP20021010

EXPECTED COMPARE DIFFERENCE FOUND AT  NG=  113 NT=  113
G= 00000000          VERSION=INTEL NT          RELEASE= 7.0          UP20021010
T= 00292062          VERSION=INTEL NT          RELEASE= 7.0SP11 UP20030909

EXPECTED COMPARE DIFFERENCE FOUND AT  NG=  114 NT=  114
G= CURRENT JOBNAME=cyc-178s  11:48:41  OCT 15, 2002 CP=          0.250
T= CURRENT JOBNAME=cyc-178s  18:29:39  NOV 10, 2005 CP=          0.359

```

```

0  /verify,cyc-178s

0  /TITLE, ceb,cyc-178s, Test cyc symm Buckling element 182

0  /title,1,Full Results to Sector Results!

0  /stitle,Reason Compare differences are acceptable:

```

```

EXTRA DATA SKIPPED ON TEST FILE          NG= 1202 NT= 1194
T= USE COMMAND MACRO QAEND
T= ARGS= 289.00
END OF SKIPPED DATA                      NG= 1202 NT= 1199

```

```

BOTTOM OF GOOD FILE REACHED AT LINE 1204
G= |                                ANSYS RUN COMPLETED                                |

```

```

~~~~~
NOTE- NONSTANDARD COMPARE - DIFOPT NAME QA70-1 HAS BEEN USED
NUMBER OF LINES SKIPPED IN GOOD FILE(BLANK LINES EXCLUDED) - 2
NUMBER OF LINES SKIPPED IN TEST FILE(BLANK LINES EXCLUDED) - 2
NUMBER OF LINES ON GOOD FILE WITH STRINGS CONDENSED OUT - 0
NUMBER OF LINES ON TEST FILE WITH STRINGS CONDENSED OUT - 0
~~~~~

```

```

*****
COMPARE ERRORS = 1 *
*****

```

```

=====
PROBLEM: cyc-178s          COMPARE OPTIONS  COMPARE_REL 3.8 UP20020121  WINDOWS

ALMOST ZERO (GOOD)   = 1.0000E-006          KROUND (DROP LAST DIGIT)= 1
ALMOST ZERO (TEST)   = 1.0000E-006          KABSPR (0=SUMMARY 1=ALL)= 1
ABSOLUTE VALUE TOL    = 1.0000E-010         KSKIP(SKIP=ERR 0=Y, 1=N)= 0
FRACTIONAL DIFFERENCE= 1.0000E-004         MAXERR (STOP WHEN ERRS )= 100
ABSOLUTE DIFFERENCE  = 1.0000E-006         MAXBUF (# LINES TO SCAN)= 6
                                          KNOWN (# OF KNOWN ERRS)= 0
                                          GREAD, TREAD = 1, 1
=====

```

RPP-RPT-28967, Rev. 1

LINES ON GOOD FILE = 1219
LINES ON TEST FILE = 1222

1

*** ERROR -- (VERSION=) was not found anywhere in the "TEST" file. ***

*** Comparison was supposed to start at this string, specified in CMPOPT. ***

~~~~~

NOTE- NONSTANDARD COMPARE - DIFOPT NAME QA70-1 HAS BEEN USED  
 NUMBER OF LINES SKIPPED IN GOOD FILE(BLANK LINES EXCLUDED) - 0  
 NUMBER OF LINES SKIPPED IN TEST FILE(BLANK LINES EXCLUDED) - 0  
 NUMBER OF LINES ON GOOD FILE WITH STRINGS CONDENSED OUT - 0  
 NUMBER OF LINES ON TEST FILE WITH STRINGS CONDENSED OUT - 0

~~~~~

COMPARE ERRORS = -88 *

=====

PROBLEM: dds-13s	COMPARE OPTIONS	COMPARE_REL 3.8 UP20020121	WINDOWS
ALMOST ZERO (GOOD) = 1.0000E-006		KROUND (DROP LAST DIGIT)= 1	
ALMOST ZERO (TEST) = 1.0000E-006		KABSPR (0=SUMMARY 1=ALL)= 1	
ABSOLUTE VALUE TOL = 1.0000E-010		KSKIP(SKIP=ERR 0=Y, 1=N)= 0	
FRACTIONAL DIFFERENCE= 1.0000E-004		MAXERR (STOP WHEN ERRS)= 100	
ABSOLUTE DIFFERENCE = 1.0000E-006		MAXBUF (# LINES TO SCAN)= 6	
		KNOWN (# OF KNOWN ERRS)= 0	
		GREAD, TREAD = 1, 1	

=====

LINES ON GOOD FILE = 402
 LINES ON TEST FILE = 146

1

*** ERROR -- (VERSION=) was not found anywhere in the "TEST" file. ***

*** Comparison was supposed to start at this string, specified in CMPOPT. ***

~~~~~

NOTE- NONSTANDARD COMPARE - DIFOPT NAME QA70-1 HAS BEEN USED  
 NUMBER OF LINES SKIPPED IN GOOD FILE(BLANK LINES EXCLUDED) - 0  
 NUMBER OF LINES SKIPPED IN TEST FILE(BLANK LINES EXCLUDED) - 0  
 NUMBER OF LINES ON GOOD FILE WITH STRINGS CONDENSED OUT - 0  
 NUMBER OF LINES ON TEST FILE WITH STRINGS CONDENSED OUT - 0

~~~~~

COMPARE ERRORS = -88 *

=====

PROBLEM: dds-17s	COMPARE OPTIONS	COMPARE_REL 3.8 UP20020121	WINDOWS
ALMOST ZERO (GOOD)	= 1.0000E-006	KROUND (DROP LAST DIGIT)=	1
ALMOST ZERO (TEST)	= 1.0000E-006	KABSPR (0=SUMMARY 1=ALL)=	1
ABSOLUTE VALUE TOL	= 1.0000E-010	KSKIP(SKIP=ERR 0=Y, 1=N)=	0
FRACTIONAL DIFFERENCE=	1.0000E-004	MAXERR (STOP WHEN ERRS)=	100
ABSOLUTE DIFFERENCE	= 1.0000E-006	MAXBUF (# LINES TO SCAN)=	6
		KNOWN (# OF KNOWN ERRS)=	0
		GREAD, TREAD =	1, 1

=====

LINES ON GOOD FILE = 746
 LINES ON TEST FILE = 146

1

00000000 VERSION=INTEL NT RELEASE= 7.0 UP20021010

EXPECTED COMPARE DIFFERENCE FOUND AT NG= 113 NT= 113
 G= 00000000 VERSION=INTEL NT RELEASE= 7.0 UP20021010
 T= 00292062 VERSION=INTEL NT RELEASE= 7.0SP11 UP20030909

EXPECTED COMPARE DIFFERENCE FOUND AT NG= 114 NT= 114
 G= CURRENT JOBNAME=ev173-53s 14:02:31 OCT 15, 2002 CP= 0.234
 T= CURRENT JOBNAME=ev173-53s 18:31:16 NOV 10, 2005 CP= 0.406

0 /verify,ev173-53s

0 /title,ev173-53s,mfquresh,Test to verify PSOVLE,ELFORM for 171-
 175 (3D) with PENE

EXTRA DATA SKIPPED ON TEST FILE NG= 1409 NT= 1401
 T= USE COMMAND MACRO QAEND
 T= ARGS= 20.000
 END OF SKIPPED DATA NG= 1409 NT= 1406

BOTTOM OF GOOD FILE REACHED AT LINE 1411
 G= | ANSYS RUN COMPLETED

~~~~~

NOTE- NONSTANDARD COMPARE - DIFOPT NAME QA70-1    HAS BEEN USED  
 NUMBER OF LINES SKIPPED IN GOOD FILE(BLANK LINES EXCLUDED) -        2  
 NUMBER OF LINES SKIPPED IN TEST FILE(BLANK LINES EXCLUDED) -        2  
 NUMBER OF LINES ON GOOD FILE WITH STRINGS CONDENSED OUT        -        0  
 NUMBER OF LINES ON TEST FILE WITH STRINGS CONDENSED OUT        -        0

~~~~~

 COMPARE ERRORS = 1 *

=====

PROBLEM: ev173-53s COMPARE OPTIONS COMPARE_REL 3.8 UP20020121 WINDOWS

ALMOST ZERO (GOOD)	= 1.0000E-006	KROUND (DROP LAST DIGIT)=	1
ALMOST ZERO (TEST)	= 1.0000E-006	KABSPR (0=SUMMARY 1=ALL)=	1
ABSOLUTE VALUE TOL	= 1.0000E-010	KSKIP(SKIP=ERR 0=Y, 1=N)=	0
FRACTIONAL DIFFERENCE	= 1.0000E-004	MAXERR (STOP WHEN ERRS)=	100
ABSOLUTE DIFFERENCE	= 1.0000E-006	MAXBUF (# LINES TO SCAN)=	6
		KNOWN (# OF KNOWN ERRS)=	0
		GREAD, TREAD =	1, 1

=====

Lines ON GOOD FILE = 1426
 Lines ON TEST FILE = 1429

1

00000000 VERSION=INTEL NT RELEASE= 7.0 UP20021010

EXPECTED COMPARE DIFFERENCE FOUND AT NG= 113 NT= 113
 G= 00000000 VERSION=INTEL NT RELEASE= 7.0 UP20021010
 T= 00292062 VERSION=INTEL NT RELEASE= 7.0SP11 UP20030909

EXPECTED COMPARE DIFFERENCE FOUND AT NG= 114 NT= 114
 G= CURRENT JOBNAME=ev175-20s 14:22:03 OCT 15, 2002 CP= 0.250
 T= CURRENT JOBNAME=ev175-20s 18:31:34 NOV 10, 2005 CP= 0.328

0 /verify,ev175-20s

0 /title,ev175-20s,mfq, Check real constant FKN and FTOLN and
 KEYOPT(2)=0,1

NOW COMPARING LINES FROM ***** ANSYS ANALYSIS DEFINITION (PREP7) *****

EXTRA DATA SKIPPED ON TEST FILE NG= 521 NT= 513
 T= USE COMMAND MACRO QAEND
 T= ARGS= 3.0000
 END OF SKIPPED DATA NG= 521 NT= 518

BOTTOM OF GOOD FILE REACHED AT LINE 523
 G= | ANSYS RUN COMPLETED |

~~~~~  
 NOTE- NONSTANDARD COMPARE - DIFOPT NAME QA70-1 HAS BEEN USED  
 NUMBER OF LINES SKIPPED IN GOOD FILE(BLANK LINES EXCLUDED) -    2  
 NUMBER OF LINES SKIPPED IN TEST FILE(BLANK LINES EXCLUDED) -    2  
 NUMBER OF LINES ON GOOD FILE WITH STRINGS CONDENSED OUT    -    0  
 NUMBER OF LINES ON TEST FILE WITH STRINGS CONDENSED OUT    -    0  
 ~~~~~

 COMPARE ERRORS = 1 *

```
=====
PROBLEM: ev175-20s            COMPARE OPTIONS    COMPARE_REL 3.8 UP20020121    WINDOWS

ALMOST ZERO (GOOD)    = 1.0000E-006            KROUND (DROP LAST DIGIT)=    1
ALMOST ZERO (TEST)    = 1.0000E-006            KABSPR (0=SUMMARY 1=ALL)=    1
ABSOLUTE VALUE TOL    = 1.0000E-010           KSKIP(SKIP=ERR 0=Y, 1=N)=    0
FRACTIONAL DIFFERENCE= 1.0000E-004           MAXERR (STOP WHEN ERRS )= 100
ABSOLUTE DIFFERENCE   = 1.0000E-006           MAXBUF (# LINES TO SCAN)=    6
                                             KNOWN (# OF KNOWN ERRS)=    0
                                             GREAD, TREAD =    1,    1
=====
```


RPP-RPT-28967, Rev. 1

LINEs ON GOOD FILE = 538
LINEs ON TEST FILE = 541

1

*** ERROR -- (VERSION=) was not found anywhere in the "TEST" file. ***

*** Comparison was supposed to start at this string, specified in CMPOPT. ***

~~~~~

NOTE- NONSTANDARD COMPARE - DIFOPT NAME QA70-1 HAS BEEN USED  
 NUMBER OF LINES SKIPPED IN GOOD FILE(BLANK LINES EXCLUDED) - 0  
 NUMBER OF LINES SKIPPED IN TEST FILE(BLANK LINES EXCLUDED) - 0  
 NUMBER OF LINES ON GOOD FILE WITH STRINGS CONDENSED OUT - 0  
 NUMBER OF LINES ON TEST FILE WITH STRINGS CONDENSED OUT - 0

~~~~~

COMPARE ERRORS = -88 *

=====

PROBLEM: ev175-21s	COMPARE OPTIONS	COMPARE_REL 3.8 UP20020121	WINDOWS
ALMOST ZERO (GOOD) = 1.0000E-006	KROUND (DROP LAST DIGIT)=	1	
ALMOST ZERO (TEST) = 1.0000E-006	KABSPR (0=SUMMARY 1=ALL)=	1	
ABSOLUTE VALUE TOL = 1.0000E-010	KSKIP(SKIP=ERR 0=Y, 1=N)=	0	
FRACTIONAL DIFFERENCE= 1.0000E-004	MAXERR (STOP WHEN ERRS)=	100	
ABSOLUTE DIFFERENCE = 1.0000E-006	MAXBUF (# LINES TO SCAN)=	6	
	KNOWN (# OF KNOWN ERRS)=	0	
	GREAD, TREAD =	1, 1	

=====

LINES ON GOOD FILE = 566
 LINES ON TEST FILE = 146

1

00000000 VERSION=INTEL NT RELEASE= 7.0 UP20021010

EXPECTED COMPARE DIFFERENCE FOUND AT NG= 113 NT= 113
 G= 00000000 VERSION=INTEL NT RELEASE= 7.0 UP20021010
 T= 00292062 VERSION=INTEL NT RELEASE= 7.0SP11 UP20030909

EXPECTED COMPARE DIFFERENCE FOUND AT NG= 114 NT= 114
 G= CURRENT JOBNAME=inrt-16s 16:14:59 OCT 15, 2002 CP= 0.219
 T= CURRENT JOBNAME=inrt-16s 18:32:29 NOV 10, 2005 CP= 0.391

0 /VERIFY,INRT-16S

0 /TITLE, INRT-16S, ceb, component omega loading and layer
 elements

0 /TITLE, INRT-16S, BENDING OF A COMPOSITE BEAM

EXTRA DATA SKIPPED ON TEST FILE NG= 462 NT= 459
 T= USE COMMAND MACRO QAEND
 END OF SKIPPED DATA NG= 462 NT= 463

BOTTOM OF GOOD FILE REACHED AT LINE 469
 G= | ANSYS RUN COMPLETED |

~~~~~  
 NOTE- NONSTANDARD COMPARE - DIFOPT NAME QA70-1    HAS BEEN USED  
 NUMBER OF LINES SKIPPED IN GOOD FILE(BLANK LINES EXCLUDED) -    1  
 NUMBER OF LINES SKIPPED IN TEST FILE(BLANK LINES EXCLUDED) -    1  
 NUMBER OF LINES ON GOOD FILE WITH STRINGS CONDENSED OUT    -    0  
 NUMBER OF LINES ON TEST FILE WITH STRINGS CONDENSED OUT    -    0  
 ~~~~~

 COMPARE ERRORS = 1 *

=====

PROBLEM: inrt-16s	COMPARE OPTIONS	COMPARE_REL 3.8	UP20020121	WINDOWS
ALMOST ZERO (GOOD)	= 1.0000E-006	KROUND (DROP LAST DIGIT)=	1	
ALMOST ZERO (TEST)	= 1.0000E-006	KABSPR (0=SUMMARY 1=ALL)=	1	
ABSOLUTE VALUE TOL	= 1.0000E-010	KSKIP(SKIP=ERR 0=Y, 1=N)=	0	
FRACTIONAL DIFFERENCE	= 1.0000E-004	MAXERR (STOP WHEN ERRS)=	100	
ABSOLUTE DIFFERENCE	= 1.0000E-006	MAXBUF (# LINES TO SCAN)=	6	
		KNOWN (# OF KNOWN ERRS)=	0	
		GREAD, TREAD =	1, 1	

=====

Lines ON GOOD FILE = 484
 Lines ON TEST FILE = 486

Appendix D

Reviewer Comments and Discussion

Appendix D

Reviewer Comments and Discussion

An independent review of the Double Shell Tanks (DST) Thermal and Operating Load (TOLA) and Seismic analyses was conducted by Dr. Robert P. Kennedy of RPK Structural Mechanics Consulting and Dr. Anestis S. Veletsos of Rice University. Their comments are reported below. Comment responses regarding the buckling analysis are found in the Executive Summary and Sections 5.6, 6.3, 6.4.1, 6.4.3, 7.1, 7.2, and 8.0 of the main report.

Reviewer Comments

Additional Comments and Recommendations Concerning Seismic Evaluation of Hanford Double-Shell Tanks

by

R.P. Kennedy and A.S. Veletsos

May 2006

1. Introduction

Our initial comments and recommendations regarding the seismic evaluation of the Hanford Double-Shell Tanks (DSTs) were presented in Ref. 1 based on our review of the studies reported through July 2005.

Our present input refers to the additional studies conducted since then, and it is based on:

- Our review of Refs. 2 through 7; and
- The presentations and ensuing discussions at the Review Meeting of March 20 and 21, 2006, in which we participated to provide an independent oversight and comment on the adequacy and completeness of the approach being used.

Our views and recommendations are presented under the following six topic headings.

2. Use of ANSYS for Soil-Structure Interaction Analyses

The methodology used to evaluate the soil-structure interaction (SSI) effects for the DSTs is described in Ref. 2. It involves the use of the ANSYS computer program in which the analysis is implemented directly in the time domain. Unlike the more commonly used SASSI program which is limited to the analysis of linear, elastic systems, the ANSYS program can also be used to assess the effects of nonlinear, hysteretic actions.

Reference 2 presents the results of a number of comparative analyses implemented using both ANSYS and SASSI. The results obtained by the two approaches are in quite good agreement for system frequencies less than about 10 Hz, but for the higher frequencies, the ANSYS predictions are generally higher than the SASSI. In as much as the natural frequencies of the tank-liquid systems that contribute materially to the desired responses are less than 10 Hz, however, the conservative bias of the ANSYS results is of no practical consequence.

We, therefore, concur with the appropriateness and reliability of the ANSYS program to evaluate the SSI effects of the DSTs, and of the methodology described in Ref. 3. However, we do not concur that it was necessary to have performed the Ref. 3 analyses using ANSYS, but do respect an analyst's preference for and right to use any acceptable approach to a desired end.

The rationale for using ANSYS was to make it possible to account for the effects of potential sliding at the interface of the concrete vault and surrounding soil, and more importantly, the interface of the base of the primary tank and the insulating concrete basemat. Since these effects – as might have been

anticipated by simple, exploratory analyses – did not prove to be of practical importance, the SSI analyses could have been performed using the SASSI or some other linear program.

Specifically, starting with a simplified, single-degree-of-freedom idealization of the waste-containing tank, the response of the tank-vault-soil system could have been evaluated using the SASSI program. The resulting response history of the concrete vault could then have been used as input to a refined model of the waste-containing tank, and its response determined either by ANSYS, making due provision for localized nonlinear actions, or by the DYTRAN program.

In the methodology described in Ref. 3, the waste-containing tank, concrete vault, and surrounding soil were analyzed as a single interacting system using the ANSYS program. As noted in Section 6 of Ref. 1, this one-step approach leads to a highly complex model that imposes practical limits to the degree of refinement with which critical regions of the system may be modeled. We believe that the two-step approach referred to above – even when implemented exclusively with ANSYS – would have been preferable, as it would have permitted the use of more refined but simpler subsystems which might have led to improved solutions in regions of rapid pressure variation or high stress concentration.

Incidentally, it is not clear why, in the simplified analysis described in Section 7 of Ref. 2, the simple-mass-spring systems used to model the waste-containing tank were attached to the concrete vault at 5 feet from its top. Considering that the tank is supported laterally at both the top and base of the concrete vault, the approximating system should have been similarly supported at the two levels. The appropriate approach is comparable to the one used in Section 8.1.1 of the same reference to evaluate the fluid-structure interaction effects.

3. Fluid-Structure Interaction Analyses of Primary Tanks

References 4 and 5 present the results of fluid-structure interaction (FSI) analyses for the primary tank using the ANSYS and Dytran program, respectively. Solutions for waste heights of both 424 or 422 inches and 460 inches are presented. The results of the two approaches for each of the two waste levels considered are discussed separately in the following subsections.

3.1 ANSYS Results for 424-inch Waste Level. With the exception noted in the following, the solutions for both the rigid and flexible tanks reported in Ref. 4 are in reasonable agreement with the corresponding theoretical solutions. The exception refers mainly to the surface sloshing action of the waste. The ANSYS model severely underpredicts this action; it leads to a maximum slosh-height of only 8 inches, while the corresponding theoretical value is 23.7 inches. This underprediction also adversely affects the accuracy of the hydrodynamic pressures in a shallow region around the top of the primary tank, as these effects are dominated by the sloshing action of the waste.

There are also differences between the theoretical and ANSYS solutions of the impulsive components of response, but these are generally limited to about 13 percent, the ANSYS results being consistently higher than the theoretical.

It is extremely important in our view to understand the reasons for these differences, especially the severe underprediction of the surface slosh-height. Parts of these differences may well be due to differences in the damping values used in the two approaches.

Considering first the impulsive effects, it should be noted that the theoretical solutions for the horizontally excited flexible tank presented in Appendix B of Ref. 4 are for a fundamental impulsive modal damping of 4 percent critical. By contrast, the corresponding damping determined from the decay rate of the free vibrational phase of the impulsive response of the ANSYS solution shown in Fig. 5-3 of Ref. 4 is 2.7 percent critical. The larger damping in the theoretical solution will naturally reduce the response, but the reduction may partly be offset by differences in the natural frequencies of the models used in the two solutions.

Whereas the fundamental natural frequency of the impulsive mode in the theoretical solution presented in Appendix B of Ref. 4 is 7.0 Hz, that of the ANSYS model was determined to be about 7.5 Hz. The response spectrum in Fig. 2-22 of Ref. 4 shows that the spectral pseudo-acceleration and hence the system response at 7.0 Hz is indeed higher than at 7.5 Hz. As a result, the effect of the difference in frequencies is opposite to that of the difference in damping, and the combined effect is expected to be a reduced level of impulsive response and improved agreement between the theoretical predictions and those arrived at by the ANSYS program.

Regarding the convective components of response, it should be noted that whereas the theoretical solution in Appendix B of Ref. 4 is based on a damping value of 0.5 percent critical for the fundamental convective mode, the corresponding damping determined from the free vibrational phase of the response of the ANSYS model in Fig. 5-2 of Ref. 4 is 17 percent of critical. The severe underprediction of the slosh height in the ANSYS solution is clearly due, at least in part, to the higher damping of the ANSYS model.

An additional factor that may contribute to the underestimation of the sloshing action may be the extent to which the waste in ANSYS is modeled as an incompressible, practically inviscid liquid. Additional studies are needed to determine whether the ANSYS code can indeed accurately predict the convective, sloshing action of the waste.

To address this issue, it is recommended that the ANSYS analysis for the horizontally excited flexible tank with the 424-inch waste height be repeated using the following values for the coefficients α and β in the expression for the Rayleigh-form of damping.

$$\alpha = 0.00930 \quad \text{and} \quad \beta = 0.00169$$

These values correspond to a damping of 0.5 percent critical for the fundamental convective mode of 0.184 Hz, and of 4.0 percent critical for the fundamental impulsive mode of 7.5 Hz. The resulting solution should, of course, be compared with the corresponding theoretical solution.

It would also be desirable to assess the sensitivity of the ANSYS solutions to the approximations involved in the modeling of the waste as an incompressible, inviscid liquid. The relevant analyses should preferably be implemented for a flexible tank with an open top and a waste level of 424 inches.

Despite the fact that the ANSYS model for the tank considered in Ref. 4 does not adequately predict the slosh-height of the contained waste, it does predict reasonably the total hydrodynamic reactions and associated wall pressures, except, of course, for the pressures on a small segment of the tank wall around the waste surface that are dominated by the sloshing action. Shown in Table 1-2 and Fig. 5-11 of Ref. 4,

the ANSYS results are overpredicted by less than 15 percent compared to their theoretical counterparts, the degree of overprediction being almost identical to that of the impulsive component of response referred to earlier.

For the tank with the 424-in waste height considered in this section, there is no indication from any of the solutions obtained that the sloshing waste will interact with the concrete dome at the top. It is relevant to note in this regard that the radial distribution of the maximum vertical surface displacements of the oscillating waste in the solution presented in Fig. 5-19 of Ref. 4 is in good agreement with the theoretical distribution for a tank with an open top. This is, of course, not true of the comparable solution shown in Fig. 4-18 of the same reference for a tank with the 460-in waste height.

In summary, the approach used in Ref. 4 to evaluate the seismic response of the primary tank with the 424-inch waste height is acceptable in our view. However, we still feel the need for the recommended additional studies to determine the reason or reasons for the severe overestimation of the surface sloshing action in the ANSYS solution.

3.2 Dytran Results for 422-inch Waste Level. For the indicated waste height, the results of the Dytran analyses for both rigid and flexible tanks are generally in very good agreement with the corresponding theoretical solutions, and better than those obtained with the ANSYS program. Satisfactory agreement was achieved for the fundamental natural frequencies of both the impulsive and convective modes, the maximum slosh-height, the total hydrodynamic reaction, as well as the magnitude and distribution of the associated wall pressures. The best agreement was achieved for Case 2c damping, which corresponds to a damping coefficient $\alpha = 2$ and a damping factor of 1 percent critical for the fundamental convective mode.

Apart from demonstrating the accuracy of the Dytran results for the conditions considered, the information presented also demonstrates the advantage of our preferred two-step approach that permits the use of different means for analyzing the components of the complex system involved in the present study.

3.3 Results for 460-inch Waste Level. If the waste in the tanks is raised to the 460-inch level, the concern is that the roof will partially suppress the surface sloshing action, reducing the portion of the waste mass that acts convectively and increasing the portion that acts impulsively. Considering that the natural frequencies of the impulsive modes are normally much higher than of the convective, the net effect of this constraining action would be an increase in the maximum values of the total hydrodynamic wall pressures and associated reactions over the values computed for the same tanks with an open top.

The portion of the waste mass being transformed from convective to impulsive, and the resulting increase in the overall response, clearly depend on the area of the roof being impacted by the sloshing waste. This area, in turn, depends on the available clearance between the waste surface and the roof. For a tank with a rigid, horizontal roof located immediately over the waste surface, the entire mass of the waste would respond in the impulsive mode, and the maximum values of the resulting hydrodynamic wall pressures and reactions would be significantly larger than those for an open-top tank.

Both the ANSYS and Dytran solutions for the maximum hydrodynamic pressures and reactions presented in Refs. 4 and 5 for the domed-tank with the 460-inch waste height are similar to the corresponding theoretical solutions obtained for a tank with an open top. If correct, these results would indicate that, for

the waste level considered, the dome does not materially constrain the sloshing action of the waste, and that either program may also be used to evaluate the response of the tank with the 460-inch waste level. At this time, however, we are not convinced of the validity of this conclusion.

As already noted in Subsection 3.1, the ANSYS model does not accurately predict the surface sloshing action of the waste for an open-top tank. As a result, it is unlikely that it would accurately predict the constraining effect of the dome. It may be possible, however, to correct this deficiency by modifying the α and β parameters in the expression for the Rayleigh-form of damping, as suggested in Subsection 3.1. If this adjustment does lead to an acceptable solution for the tank with the 424-inch waste level, our confidence in the appropriateness of the ANSYS model for the FSI analysis of the tank with the 460-inch waste height will improve significantly.

Although of high accuracy for the tank with the 422-inch waste height, the results of the Dytran analyses for the 460-inch height also are suspect. In the solution displayed in Fig. 6-25 of Ref. 5, the waste around the tank periphery prior to the seismic excitation appears to have risen about 8 to 10 inches under gravity load. This obvious deficiency must be corrected before one can have confidence in the Dytran results. We suspect that a more refined mesh may be required to adequately model the waste in regions of potential interaction with the dome.

In summary, we feel that the effects of waste-roof interaction need to be further studied. In addition to the analyses with the indicated adjustments referred to above, it is recommended that

- Solutions be obtained for a flexible tank with a rigid, horizontal roof located at different distances above the waste surface; and that
- These solutions, along with those for the tank with the spherical dome, be compared with the predictions of the simple, approximate procedures described in Appendix D of Ref. 8 and in Ref. 9.

4. Forces Resisted by J-Bolts

The axial and shearing forces induced by the gravity and seismic loads at the interface of the concrete- and underlying steel-domes are resisted mainly by the interconnecting J-bolts. Both sets of forces, as shown in Figs. 6-36 and 6-41 of Ref. 3, are largest along the outermost ring of bolts. The maximum values of the tensile forces, T_b , and of the corresponding shearing forces, V_b , were determined to be

$$T_b = 2.61 \text{ kips/bolt} \quad \text{and} \quad V_b = 4.54 \text{ kips/bolt}$$

for the 'Upper Bound Soil – Best Estimate Concrete' case, and

$$T_b = 2.35 \text{ kips/bolt} \quad \text{and} \quad V_b = 5.40 \text{ kips/bolt}$$

for the 'Best Estimate Soil – Fully Cracked Concrete' case. These values are lower than the Abnormal (operating plus seismic) Load Allowables of

$$T_{bA} = 3.93 \text{ kips/bolt} \quad \text{and} \quad V_{bA} = 11.71 \text{ kips/bolt}$$

presented in Table 6-4 of Ref. 7.

Neither of us is familiar with the basis of the acceptance criteria for the reported allowables. Furthermore, we do not have sufficient information regarding the Nelson Internally Threaded Studs used to

attach the J-bolts to the steel tank so that we may assess the appropriateness of the indicated allowables. However, we do question the accuracy of the reported demands.

The maximum forces in the bolts were computed on the assumption that the shear at the interface of the concrete and steel domes is resisted partly by friction, and a value of 0.4 was used for the coefficient of friction which is, of course, appropriate only for a non-sliding surface.

While we do agree that the frictional resistance at the interface of the two domes should not be ignored, considering that the seismic action is likely to induce at least some slippage at this interface, we feel that a lower value for the coefficient of friction than the one used would be more appropriate.

To gain some insight into the sensitivity of the results to the uncertainties involved in this issue, it is recommended that the analysis for the 'Best Estimate Soil – Fully Cracked Concrete' case, which leads to the maximum shear for the outermost ring of bolts, be repeated using the zero and 0.2 values for the coefficient of friction. In our judgment, the use of the sliding friction coefficient of 0.2 would be appropriate for the final solution.

In the J-bolt evaluation presented in Chapter 6 of Ref. 7, it appears that the shear forces considered were only those induced by the axial force in the wall of the primary tank. The analysis does not appear to have provided for the effect of the horizontal hydrodynamic reaction at the top of the primary tank, which is expected to be the dominant contributor to the shear forces in the outermost ring of J-bolts. Unless we have misinterpreted the reported solutions, this deficiency must be corrected.

5. Buckling Evaluations

Reference 7 presents the results of a series of evaluations for the buckling of the primary tanks due to the axial forces induced by static and seismic effects, concrete creep, differential thermal expansion, and internal vacuum. Because of our lack of detailed familiarity with several of the analyses presented, and the fact that some of the reported results are not described in sufficient detail for an independent check, we comment on only a few of the issues addressed in this reference.

5.1 Local Bowing and Global Buckling. We concur that, as indicated in Fig. 3-5 of Ref. 7, the upper knuckle region of the tank is the critical region for the development of localized, radial bowing in the tank wall due to the combined effects of axial forces and internal vacuum. We further concur with the adequacy of the ASME reduced stiffness approach for determining the critical or limiting levels of these effects.

In evaluating the contribution of the seismic effects, however, it should be kept in mind that the axial force in the tank wall is not uniformly distributed over its height. It is unduly conservative, therefore, to use the maximum value of the axial force, which for the top-supported tank considered occurs near midheight, in evaluating the bowing action near the upper knuckle. Instead, the value in the region of the upper knuckle should be used.

As indicated in Figs. 3-11 through 3-13 of Ref. 7, global buckling of the primary tank cannot be induced by differential axial deformation between the tank and concrete vault. The compressive axial forces due to such deformation are self-limiting as a result of the local bowing action referred to above.

Furthermore, as long as the J-bolts interconnecting the steel and concrete domes do not fail, the tank can displace axially only by an amount equal to the axial displacement of the concrete vault.

5.2 Elephant-Foot Buckling. Plastic elephant-foot buckling can occur only near the lower knuckle of the tank where, in addition to the compressive axial stresses, the circumferential tensile stresses are large and radial expansion is constrained by the base plate. This is the only location for which such buckling needs to be checked. The appropriate axial force for this evaluation is, of course, the force near the lower knuckle. As indicated in connection with the estimation of the bowing action in the upper knuckle region, it is unduly conservative to use the maximum value of the axial force which, for the top-supported tanks considered, occurs near midheight. Conversely, the seismically induced hoop stresses should not be reduced by the inelastic factor $F_\mu = 1.67$, because the hoop stresses continue to be in their elastic range at the onset of elephant-foot buckling.

We concur that elephant-foot buckling is not an issue for the tanks of interest. As long as the J-bolts interconnecting the steel and concrete domes do not fail and the tank is supported both laterally and vertically at the top and bottom, any localized bowing that may develop will relieve the axial force in the tank wall, and will prevent the bowing action from progressing to severe buckling.

The compressive axial force for the onset of elephant-foot buckling in Ref. 7 was determined by application of Eq. 7-1 in that reference, which is effectively an approximate, empirical equation. This force could also in that reference, have been determined by the method used to evaluate the localized bowing in the upper knuckle region. A relatively simple model, involving only the lower segment of the tank along with the appropriate conditions of support along its upper boundary, could have been used for this purpose.

6. A Concluding Comment

In the seismic analyses of the Hanford DSTs conducted so far — as in all previous analyses of waste-containing tanks that we are aware of — the waste was effectively modeled as a homogeneous, incompressible, practically inviscid liquid. As already noted in our earlier review (Ref. 1), there are fundamental uncertainties in this idealization, and it would be highly desirable to assess their effect on critical tank responses.

To this end, it was recommended that the ANSYS program be used to evaluate the response of a representative tank with the waste modeled more realistically as a deformable medium of low shearing resistance and finite energy dissipating capacity, and that a range of likely values be used for the latter properties. We conclude by repeating this recommendation, as the hydrodynamic effects for a tank storing a solid-like material may be materially larger than for a liquid-containing tank.

References

1. Kennedy, R.P. and A.S. Veletsos, *Comments and Recommendations Concerning Seismic Evaluation of Hanford Double-Shell Tanks*, Sept. 2005

2. Rinker, M.W., F.G. Abatt, B.G. Carpenter and C.A. Hendrix, *Hanford Double-Shell Tank Thermal and Seismic Project—Establishment of Methodology for Time Domain Soil-Structure Interaction Analysis of a Hanford Double-Shell Tank*, RPP-RPT-28964, Rev. 0, Pacific Northwest National Laboratory, Jan. 2006
3. Carpenter, B.G., C. Hendrix and F.G. Abatt, *ANSYS Seismic Analysis of Hanford Double-Shell Primary Tank*, M&D-2008-004-CALC-001, Rev. 0A, Draft, M&D Professional Services, Inc., Jan 2006
4. Rinker, M.W., B.G. Carpenter and F. G. Abatt, *Hanford Thermal and Seismic Project – ANSYS Benchmark Analysis of Seismically Induced Fluid-Structure Interaction in a Hanford Double-Shell Primary Tank*, RPP-RPT-28965, Rev. 0, Pacific Northwest National Laboratory, Jan 2006
5. Rinker, M.W. and F.G. Abatt, *Hanford Thermal and Seismic Project—Dytran Analysis of Seismically Induced Fluid-Structure Interaction on a Hanford Double-Shell Primary Tank*, RPP-RPT-28963, Rev. 0, Pacific Northwest National Laboratory, Jan. 2006
6. Rinker, M.W., et al., *Hanford Double-Shell Tank Thermal and Seismic Project—Summary of Combined Thermal and Operating Loads with Seismic Analysis*, RPP-RPT-xxxxx, Rev. 0, Jan. 2006
7. Johnson, K.I., et al., *Hanford Double-Shell Tank Thermal and Seismic Project—Buckling Evaluation Methods and Results for the Primary Tanks*, prepared for CH2M Hill Hanford Group, Feb. 2006
8. Bandyopadhyay, K. et al., *Seismic Design and Evaluation Guidelines for the Department of Energy High-Level Waste Storage Tanks and Appurtenances*, BNL 52361, Brookhaven National Laboratory, Upton, N.Y., Oct. 1995
9. Malhotra, P.K., *Sloshing Loads in Liquid-Storage Tanks with Insufficient Freeboard*, *Earthquake Spectra*, Vol. 23, No. 4, pp. 1185-1192, Nov. 2005.

Appendix E

Independent Confirmation of PNNL's Use of N-284-1 Safety Factors in Computing the Double Shell Primary Tank Allowable Vacuum Level Governed by Buckling

Appendix E

Independent Confirmation of PNNL's Use of N-284-1 Safety Factors in Computing the Double Shell Primary Tank Allowable Vacuum Level Governed by Buckling

This appendix contains an independent review (conducted in October 2006) of the methods used to calculate the buckling loads on the double-shell waste primary tanks. The review specifically confirms the correct calculation of the axial tank force, the unfactored vacuum limit at incipient buckling, and the application of the safety factors for the ASME Service Levels A, B, C, and D.

**Independent Confirmation of PNNL's
Use of N-284-1 Safety Factors in Computing the
Double Shell Primary Tank Allowable Vacuum
Level Governed by Buckling**

R.P. Kennedy
October 14, 2006

Review Performed

I have independently checked the vacuum load capacity calculations presented in Tables 7-1 through 7-3 of Ref. 1* for the AY tank with 6-inch waste depth, and similar tables provided to me by PNNL for the AP tank with 12-inch waste depth. These are the minimum waste depths considered and thus control the reported vacuum load capacity of the AY and AP tanks. Furthermore, I confirmed that the use of zero waste depth would have resulted in negligible reduction in the reported vacuum load capacity.

I have confirmed that the unfactored limit vacuum reported in Table 7-2 and 7-3 of Ref. 1 for the AY tank with 6-inch waste depth and on similar tables for the AP tank with 12-inch waste depth have been computed in accordance with the vacuum capacity equations in Sections 3.1 and 3.2 of Ref. 1. Therefore, these reported unfactored limit vacuums satisfy the nonlinear limit deformation approach of ASME and represent conservative estimates of the vacuum capacity of these tanks.

Next the safety factors shown in Table 7-3 of Ref. 1 have been applied to these unfactored limit vacuums to obtain the allowable vacuums for both local and global buckling. These safety factors have been defined in accordance with Section 1400 of ASME Code Case N-284-1 for Service Levels A, B, C, and D for both Local and Global buckling. The required 20% increase in the safety factors for Global buckling has been properly included.

The Governing Allowable Vacuum Levels reported in Table 7-4 of Ref. 1 have been computed using the appropriate safety factors defined in accordance with Section 1400 of ASME Code Case N-284-1.

The Governing Allowable Vacuum Levels are reported separately for when Operating Conditions are assigned to Service Level A & B versus being assigned to Service Level C. Since I don't know how often these vacuum limits are approached during the service life, I have no comment on whether Operating Conditions should be assigned to Service Level A & B or to Service level C.

The case where Seismic Loads are included are assigned to Service Level D. However, since these tanks cannot be taken out of service after a seismic event, it is debatable whether the Seismic Load case should be assigned to Service Level C or D. If the Seismic Load case had been assigned to Service Level C, the Governing Allowable Vacuum for the AY tanks would have been reduced to 6.15-inch w.g. No reduction would occur for the Governing Allowable Vacuum for the AP tanks.

* Ref. 1: Johnson, K.I., et. al., *Hanford Double-Shell Tank Thermal and Seismic Project-Buckling Evaluation Methods and Results for the Primary Tanks*, PNNL, Feb. 2006

Conclusions

The Safety factors have been appropriately defined in accordance with Section 1400 of ASME Code Case N-284-1 for the various Service Levels. The Allowable Vacuum Limits have been appropriately determined for the assigned Service Levels. It is open to some debate as to what is the appropriate Service Level that should be assigned to the various Load Cases. This assignment of Service Levels will affect the reported Governing Allowable Vacuum. It is outside of my review to review the assigned Service Levels. However, the reported Governing Allowable Vacuums have been correctly determined for the assigned Service Levels.

Appendix F

Buckling Resistance of the DST Primary Tanks Under Internal Vacuum When in the Full Condition

Appendix F

Buckling Resistance of the DST Primary Tanks Under Internal Vacuum When in the Full Condition

This appendix summarizes buckling evaluations from the body of this report (RPP-28967, Rev. 1) that address the resistance of the Hanford double-shell tank (DST) primary tanks to buckling when in the full condition. These results were compiled in response to a question by CH2M HILL staff regarding the potential for primary tank buckling to occur when the tank is full and being drawn down during waste treatment efforts.

Section F.1 presents the background justification for using the ASME Code Case N-284-1 method for evaluating buckling of the primary tanks under combined axial compression and internal vacuum loads. Section 1 also presents information that was used to justify classifying the limit vacuum load as an ASME Service Level C emergency load condition for DST operations.

Section F.2 presents the results of the buckling analysis for a range of waste heights from the minimum allowable waste height to the full tank condition. The increased waste height acts to stabilize the primary tank wall against buckling. The results in Section F.3 show that the vacuum limits of the full tanks are more than a factor of two times the vacuum limits at the minimum waste height.

Section F.3 presents a J-bolt analysis that considered the case of a full tank with zero applied axial compression in the tank wall. This case is judged to be conservative because differential thermal expansion and concrete creep-down tend to apply compression on the tank wall. These results show that the combined loading case (J-bolt tension plus shear) is less than 20% of the combined allowables for vacuum loads up to 20-inch water gage (w.g.). Therefore, the J-bolt forces are predicted to be well below the allowable value for vacuum loads that are more than 3 times the current vacuum limit of 6-inch w.g.

The conclusion from this review is that the buckling resistance of the DST primary tanks increases significantly with increased waste height and that the J-bolts are equally able to withstand the increased vacuum load.

F.1 Justification for Using the ASME Code Case N-284-1 Method for Evaluating DST Primary Tank Buckling

Buckling of the primary tank is of concern because of compressive stresses that occur in both the meridional and hoop directions. Meridional (axial) compression results from differential thermal expansion between the primary tank and the concrete over-structure, plus creep-down of the concrete structure over time. Hoop compression results from net vacuum loads in the tank. These loading conditions (displacement controlled in the meridional direction and load controlled in the hoop direction) are unique compared to the vacuum-induced stresses in typical free-standing storage tanks, and are a direct result of the unique design of the underground double-shell waste storage tanks.

The buckling evaluation method defined in Code Case N-284-1, *Metal Containment Shell Buckling Design Methods*, of the American Society of Mechanical Engineers (ASME) Boiler and Pressure Vessel Code, Section III, Division 1 (ASME 1995) has been used in previous evaluations of the DST primary tanks because it considers the interaction of independent levels of compressive stress in both the meridional and hoop directions. By comparison, the ASME Code Case N-530 method (ASME 1994) that is described in the Brookhaven report, BNL 52361 (Bandyopadhyay et al. 1995), only addresses buckling of thin-walled tanks loaded with hoop tension. The N-530 method is not applicable to tanks subjected to vacuum loads.

The N-284-1 method provides an acceptance criteria with respect to buckling instability for defining the allowable loads for a given tank design. The method is based on theoretical critical buckling loads (hoop and axial limit stresses) that are adjusted by knockdown factors to account for geometric imperfections, the height of the tank, the radius-to-thickness ratio, and material plasticity. The intent of these calculations is to accurately estimate the actual bifurcation buckling load for a specific tank geometry. These loads are then reduced by safety factors (specified for four different service levels) to set the allowable combination of axial compressive load and tank vacuum. The bifurcation buckling solutions and knockdown factors used in N-284-1 are for simplified geometries that are intended to conservatively apply to typical storage tank geometries. This section reviews the analytical basis for N-284-1 and compares the solutions with finite element models that include the specific geometric features of the DST primary tanks.

Although the DST designs vary somewhat between tank farms, the primary tanks typically consist of a 75-ft-diameter by 34-ft-high cylindrical portion that is connected to a flat bottom through a 1-ft-radius lower knuckle (Figure F-1). The wall thickness of the tank cylinder is graduated to counteract the hydrostatic stress of the contained waste (see Table F-1). The tanks are capped by a shallow spherical dome that transitions to the cylindrical section through a radiused upper knuckle. The dome is attached to the concrete over-structures with J-bolts that are imbedded in the concrete. The total height of the tank is approximately 46.8 feet.

The formulas presented in Section 1710 of ASME Code Case N-284-1 are based on the buckling of a constant thickness cylindrical shell with an unsupported length, L . The length, L , is defined between “lines of support that provide sufficient stiffness to act as bulkheads.” In previous analyses, L has been defined as the vertical distance from the waste-free surface to the tangent point between the upper knuckle and the dome. The wall thickness used in the N-284-1 equations was then calculated as the weighted

average over this length. However, the primary tank cylindrical shell does not have a constant wall thickness and it does not have clearly defined lines of support due to the upper and lower knuckles.

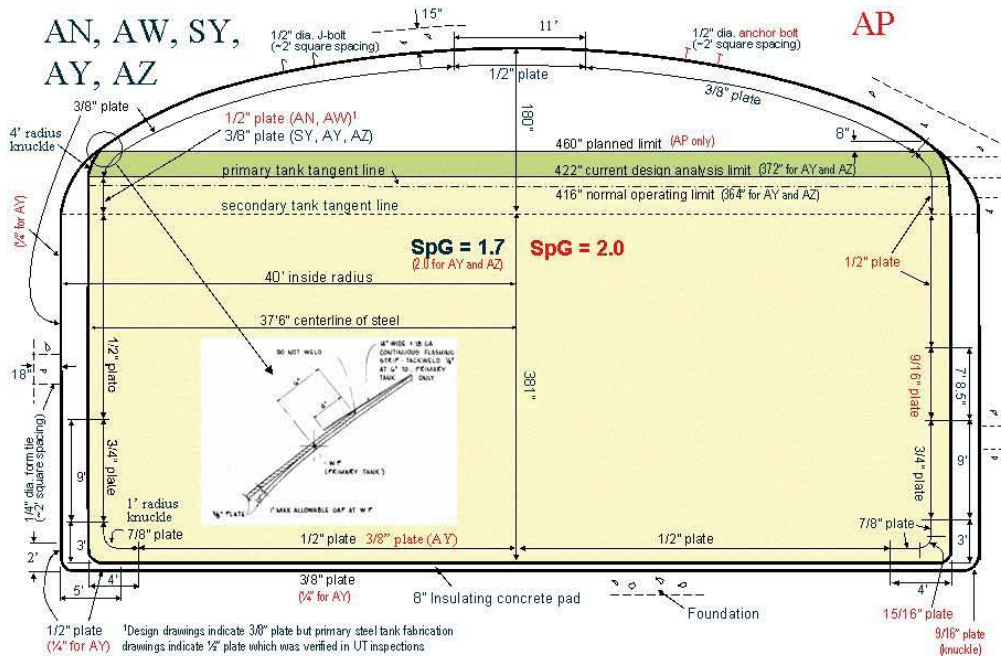


Figure F-1. Cross-Section View of the Hanford DST Primary Tank Designs

Table F-1. Summary of Design Data and Operating Limits for the DST Primary Tanks

Design Data and Operating Limits	The Different Tank Farm Designs			
	AY/AZ	SY	AW/AN	AP
Primary Tank Thickness, inches				
Upper Haunch	0.375	0.375	0.375	0.5
Vertical Wall, Top	0.375	0.375	0.5	0.5
Vertical Wall, Mid	0.5	0.5	0.5	0.563
Vertical Wall, Bottom	0.75	0.75	0.75	0.75
Lower Knuckle	0.875	0.875	0.875	0.9375
Max Allowable Waste Temp., F	350	250	350	210
Max Historical Waste Temp, F	247/263	155	135/150	118
Yield Strength @ Room Temp, ksi	32	35	50	45
Ultimate Strength, ksi	60	65	70	70
Sm at Max. Allow Temp, ksi	18.6	21	21.3	21.7
Sm at Max Hist Temp, ksi	19.2	21.4	21.7	21.7
Specified Max. Waste Height, inch	370	422	422	422
Maximum Specific Gravity	1.77	1.7	1.7	2

Therefore, the present buckling analysis used large displacement finite element analysis to predict the limiting vacuum load for the specific DST primary tank geometries under combined axial and vacuum loads. The detailed finite element analysis included models of the AY and the AP tanks. The AY results are also representative of the AZ, SY, AW, and AN tanks because they have very similar wall thickness

distributions (Table F-1). The current buckling evaluation method uses the ASME NB-3213.25 stiffness reduction method to conservatively estimate the vacuum and axial load limits on the primary tank. Comparison with N-284-1 calculations showed that the large displacement finite element method better accounts for the effect of the wall thickness variation on the limiting vacuum and axial loads. The finite element analysis also predicts that the tank deformations are small at the limit loads and they increase stably at loads beyond the limit loads. A large matrix of analyses was run that covers the expected range of axial forces and vacuum loads on the primary tanks.

F.1.1 The N-284-1 Factors of Safety to Protect Against Buckling

The buckling evaluation was conducted for four different service levels defined in ASME Code Case N-284-1. Each service level has required factors of safety for local and global buckling.

	Factors of Safety	
	Local Buckling	Global Buckling
Level A = Normal operating conditions	2.0	2.4
Level B = Upset conditions	2.0	2.4
Level C = Emergency conditions	1.67	2.0
Level D = Faulted conditions	1.34	1.61

Attachment B of Julyk (2002) makes the argument that axial compression in the tank cylinder will be relieved by local bowing of the wall before the onset of general instability. This position is justified since the meridional (axial) compressive stresses are displacement controlled as a result of differential thermal expansion and concrete creep induced loads on the primary tank. The load deflection response of the large displacement finite element models used in the current buckling analysis confirm that the axial stress in the tank is self-limited by the deformation of the primary tank geometry. This rationale leads to the following buckling criteria when combining the effects of axial and hoop loads on the allowable vacuum:

The allowable vacuum (net negative pressure) in the double-shell tanks is controlled by the minimum of two cases,

- A. Local Buckling (with *local* buckling safety factors imposed) evaluated considering the interaction of the net internal vacuum load (Δp) combined with the meridional compressive stress (σ_ϕ).
- B. General Instability (with *global* buckling safety factors imposed) evaluated considering the net internal vacuum load (Δp) acting alone. No interaction with the meridional compressive stress shall be considered ($\sigma_\phi = 0$).

These criteria were used by Julyk (2002) and they are also used in the current buckling evaluation. It is further assumed that the design basis loads used in the thermal and operating loads analysis conservatively represent Service Levels A, B, and C. This is consistent with the loading conditions assumed by Julyk (2002). Service Level D, however, requires that the incremental seismic stresses be added to the design basis stresses for evaluating the faulted condition.

F.1.2 Justification for Classifying Limit Level Vacuum loads as a Service Level C Emergency Occurrence

Julyk (2002) states that activation of the tank relief valves at the limiting vacuum load should be classified as an ASME Service Level C (emergency) load condition. Service Level C loads are defined by the ASME Code, Section III, Division 1, NB-3113 (ASME 2004a) as:

“The total number of postulated occurrences for all specified service conditions for which Level C Limits are specified shall not cause more than 25 stress cycles having an S_a value greater than that for 10^6 cycles from the applicable fatigue design curves of Figures I-9.0.”

Evidence is provided below that the alternating stress associated with these vacuum cycles is well below the allowable, S_a , and also that the total number of vacuum cycles between normal operating vacuum and the limit vacuum are expected to be less than the maximum number of 25 cycles.

The AY primary tanks were constructed with A515 grade 60 steel, which has a minimum ultimate tensile strength, S_{ult} , of 60 ksi. The allowable alternating stress, S_a , at 10^6 cycles is 12,500 psi for carbon steels with $S_{ult} \leq 80$ ksi (ASME 2004b). The alternating stress due to tank vacuum is the hoop stress corresponding to the limiting vacuum load. The maximum alternating stresses for the different tank designs are:

AY, SY, AN, AY, AZ: Tank Radius = 450 inch, Pressure = -6 inch w.g. (-0.217 psi)
 Minimum Wall Thickness = $0.375 - 0.060 = 0.315$ inch
 Hoop Stress = $pr/t = (-0.217)(450)/0.315$ $S_a = 310$ psi

AP: Tank Radius = 450 inch, Pressure = -12 inch w.g. (-0.434 psi)
 Minimum Wall Thickness = $0.375 - 0.060 = 0.315$ inch
 Hoop Stress = $pr/t = (-0.434)(450)/0.315$ $S_a = 620$ psi

These alternating stresses are factors of 40 and 20 lower than the limiting value of 12,500 psi.

Tank farms operations staff recently reviewed all of the Occurrence Reports from 1990 to the present. This summary information will be released in the next revision of RPP-11413, *Technical Basis for the Ventilation Requirements Contained in Tank Farm Operating Specifications Documents*, authored by L. Payne. No incidents were found where the primary tank differential vacuum has exceeded the 6-inch w.g. maximum. There was a report of reaching a vacuum of 4-inch w.g. in the SY tank ventilation system, but the exhauster shut down on interlock. There was one incident in AW, but it was also limited to 4-inch w.g. or less. The incident that people remembered where a vacuum limit was exceeded was in the AN annulus system in 2005 (PER-2005-072). Note that this occurred in the annulus and not in the primary tank.

This review shows that there is no recorded evidence that the primary tank vacuum limits have ever been achieving during tank operation and even if they had the resulting cyclic stress would be insignificantly small. Therefore, it is very appropriate to define the occurrence of the maximum operating vacuum as an ASME Service Level C emergency load condition.

F.2 Evaluation of Tank Buckling for Variable Waste Height

The buckling evaluations described in Chapter 7 of this report calculate the unfactored vacuum limits for the total range of waste heights. Figures F-2 through F-5 show the relationship of unfactored vacuum limit versus waste height for each of the different tank farms at the design limit loads of waste temperature, waste height, and specific gravity. These plots show that the unfactored vacuum limit increases dramatically as the waste height increases. The increased hydrostatic pressure provides increased hoop stability plus the associated Poisson's effect reduces the meridional compressive stress in the wall of the primary tank as the hoop stress increases. However, to establish conservative vacuum limits for the tanks, the unfactored limit vacuums at the minimum waste height were used when applying the N-284-1 safety factors in Chapter 7. Therefore, from a tank buckling standpoint Figures F-2 through F-5 show that the full tanks could withstand vacuum loads that are more than double the current limits based on the minimum waste height condition. Section F.3 evaluates the J-bolts and their ability to withstand a higher downward load due to increased vacuum.

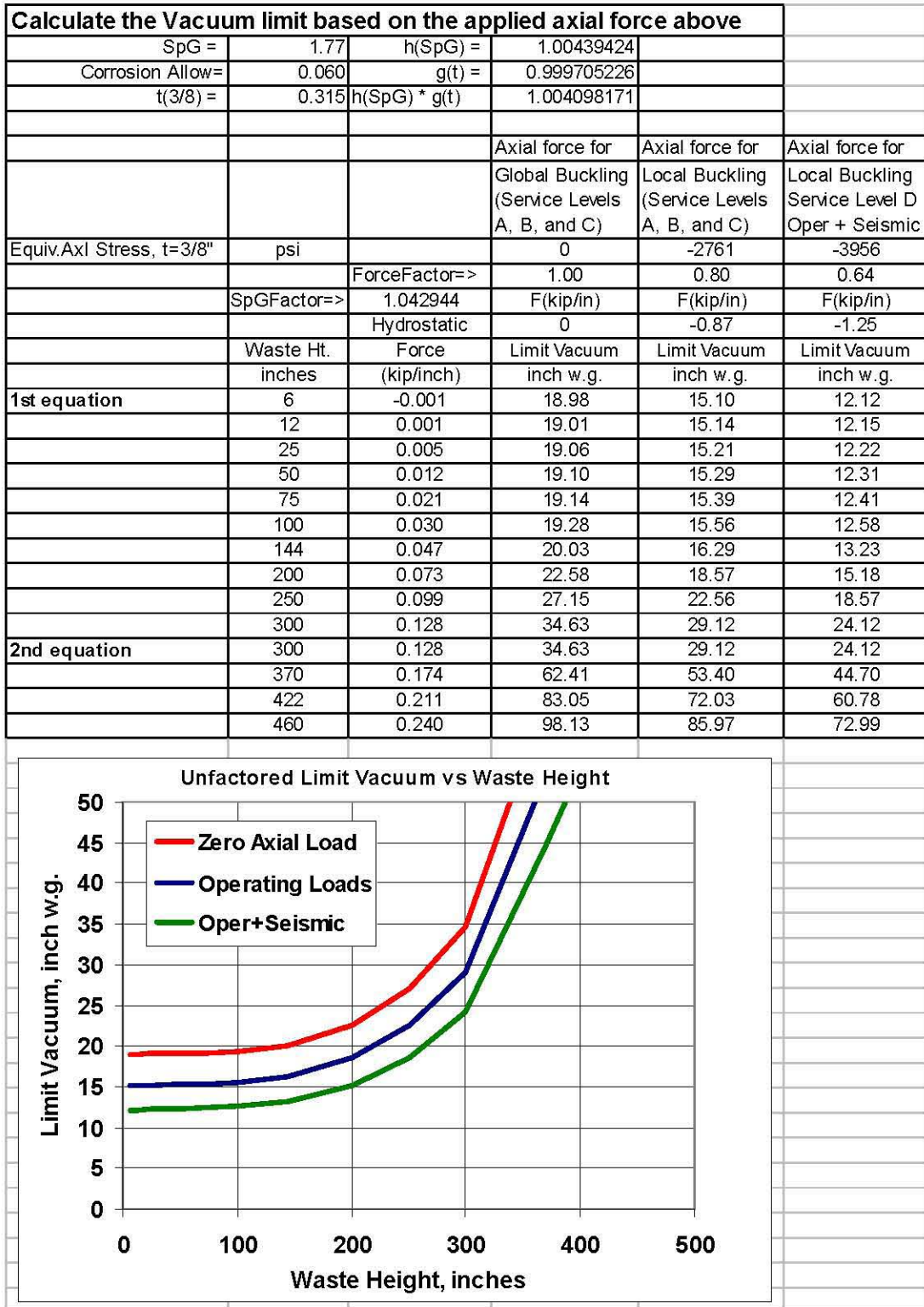


Figure F-2. Unfactored Buckling Limit Vacuum as a Function of Waste Height for the AY and AZ DSTs (Note: To calculate the factored vacuum limits, one must divide by the appropriate safety factors in the table in Section F.1.1.)

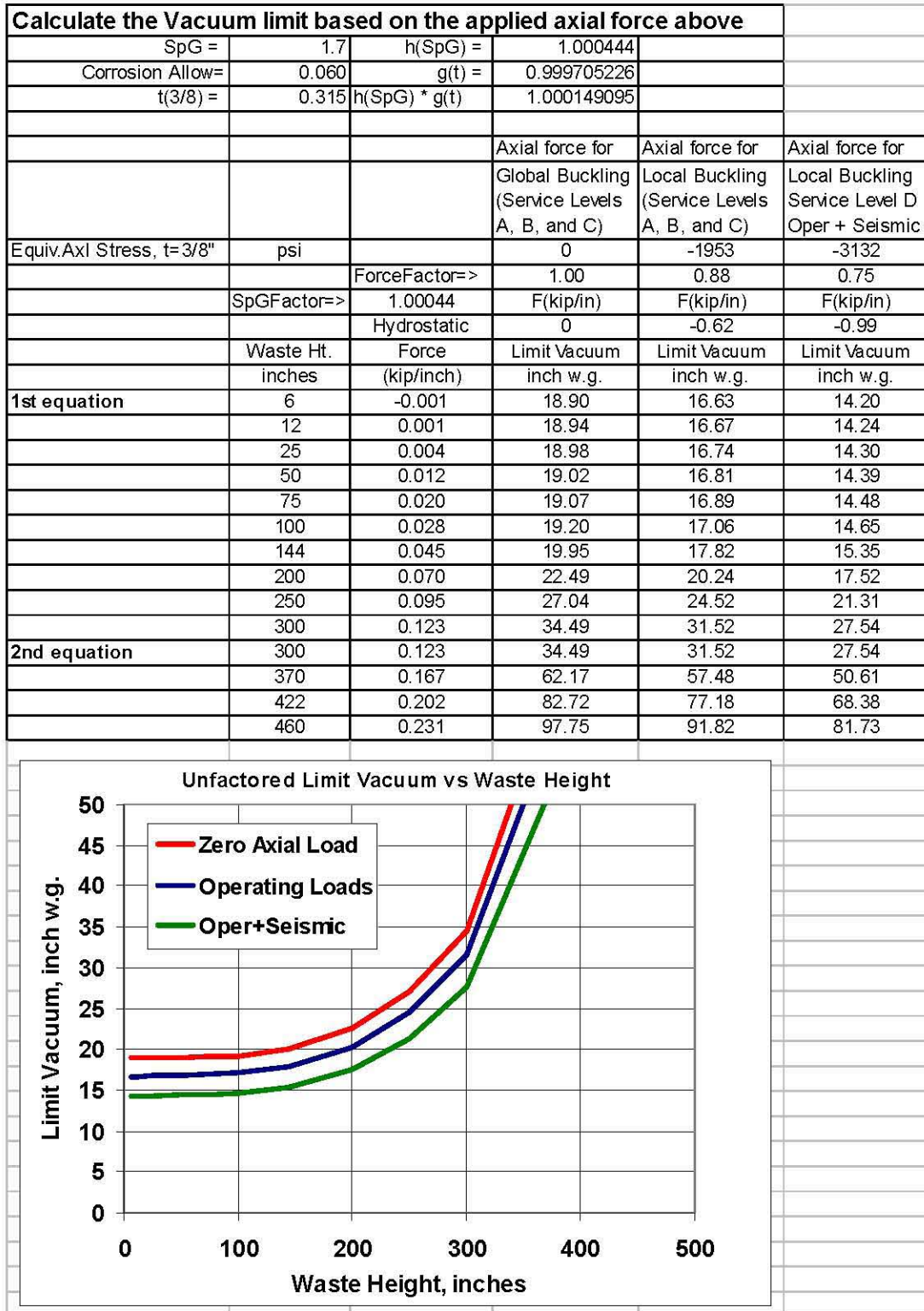


Figure F-3. Unfactored Buckling Limit Vacuum as a Function of Waste Height for the SY DSTs (Note: To calculate the factored vacuum limits, one must divide by the appropriate safety factors in the table in Section F.1.1.)

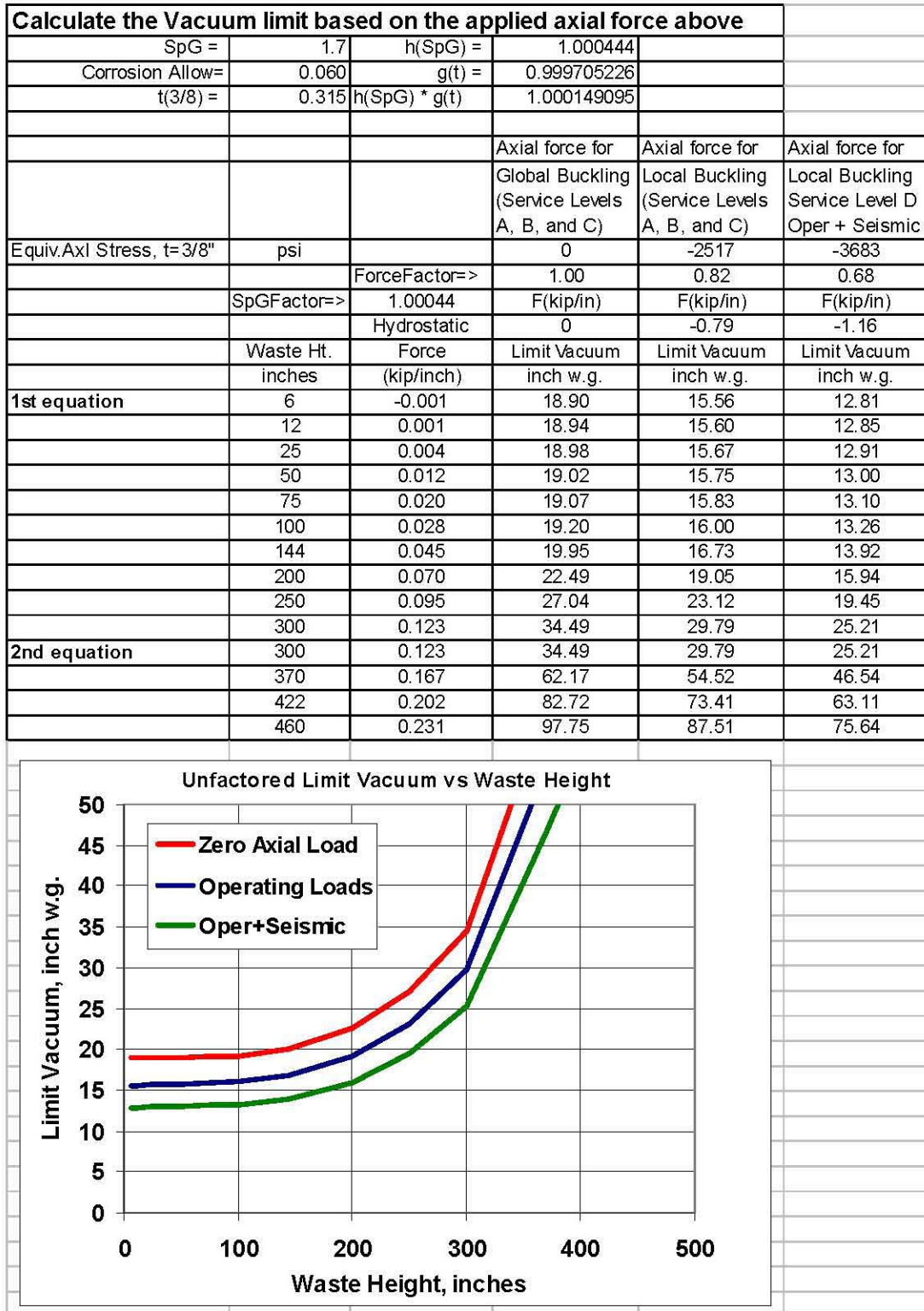


Figure F-4. Unfactored Buckling Limit Vacuum as a Function of Waste Height for the AN and AW DSTs (Note: To calculate the factored vacuum limits, one must divide by the appropriate safety factors in the table in Section F.1.1.)

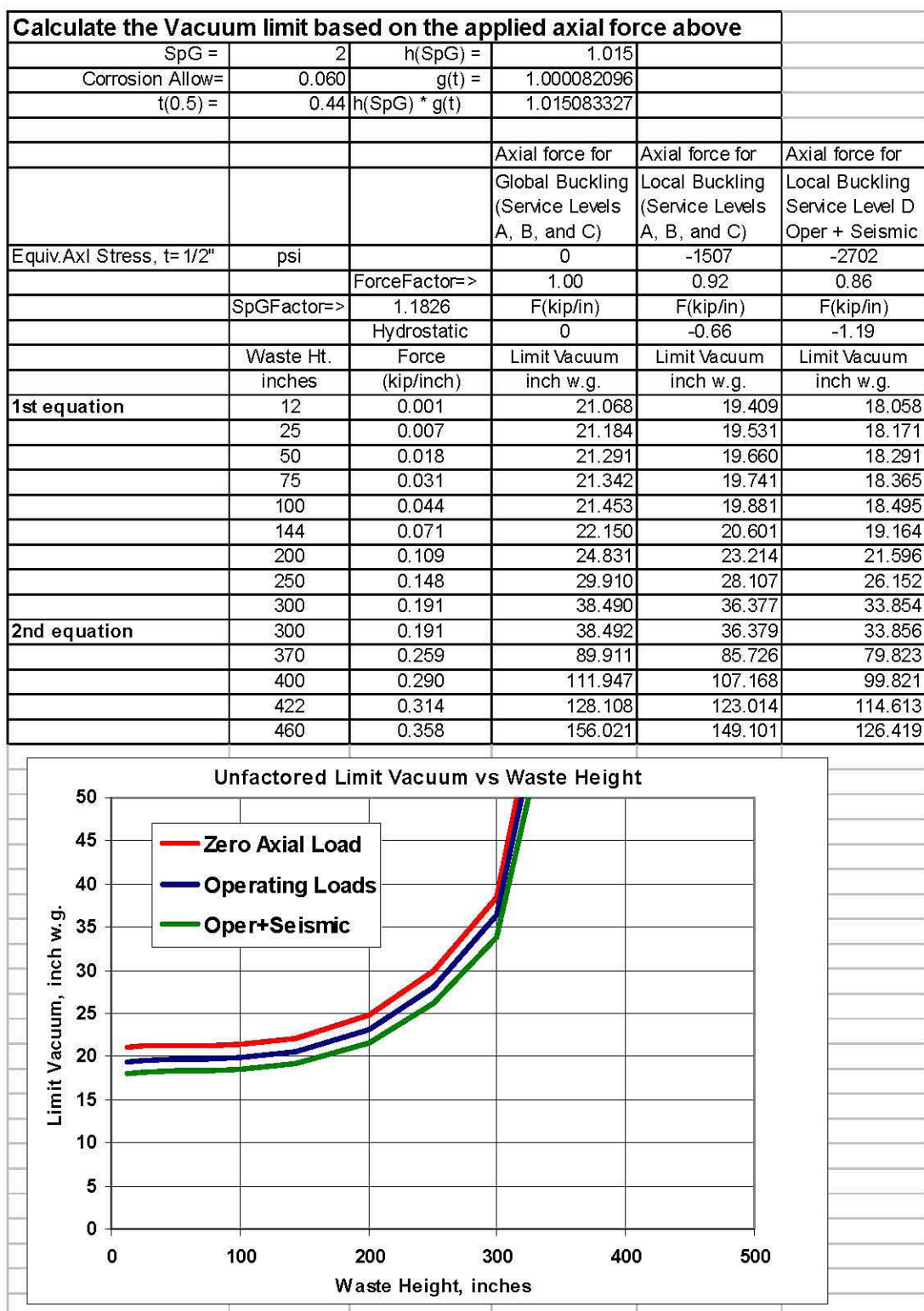


Figure F-5. Unfactored Buckling Limit Vacuum as a Function of Waste Height for the AP DSTs (Note: To calculate the factored vacuum limits, one must divide by the appropriate safety factors in the table in Section F.1.1.)

F.3 Evaluation of the J-Bolts for a Full Tank with Increasing Vacuum

As a bounding case, the buckling evaluation described in the main report considered the AY primary tank with zero axial compression and a waste height of 400 inches. This is bounding from the point of J-bolt tension, because it omits the typical axial compression in the tank wall due to differential thermal expansion between the steel and concrete plus the creep down of the concrete tank structure over the primary tank. The analysis showed that the axial and shear forces in the J-bolts increase with increasing vacuum and waste height. However, Figure F-6 shows that these loads are still a small fraction of the tensile and shear allowable forces. Figure F-6 shows that the combined loading case (J-bolt tension plus shear) is less than 20% of the combined allowables, $(P/F_{ap})^{5/3} + (S/F_{as})^{5/3}$, for vacuum loads up to 20-inch w.g. The calculations were not run for vacuum loads higher than 20-inch w.g.

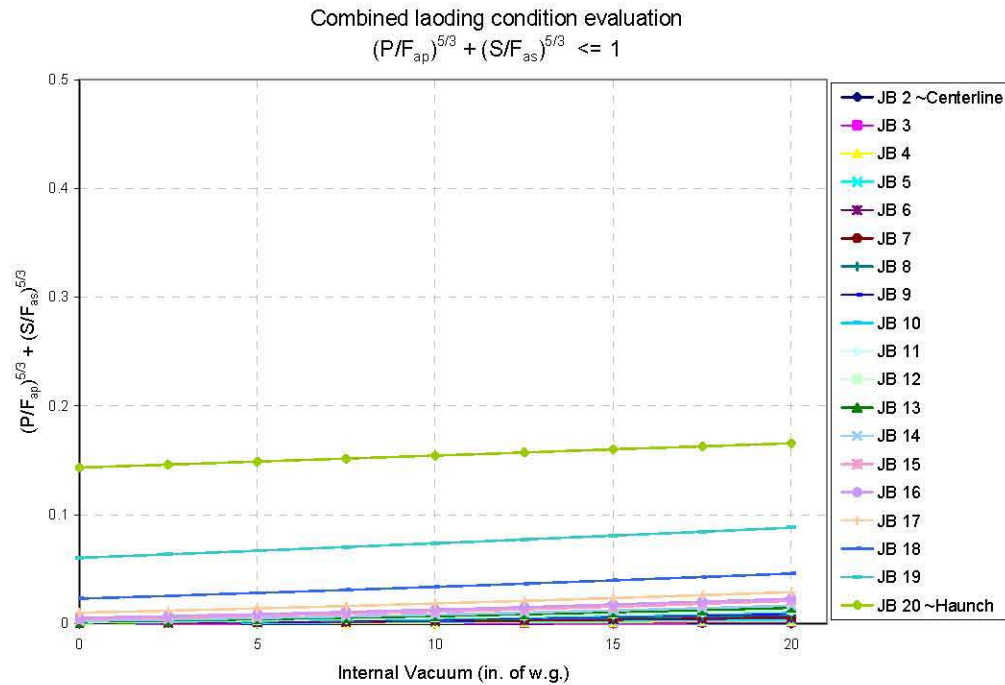


Figure F-6. Combined Tensile and Shear J-Bolt Force Evaluation (for J-bolts from the dome centerline to the haunch) for the Case with Zero Axial Compression, 400-Inch Waste Height, and Increasing Vacuum Load (loads are compared to the factored allowables for J-Bolt shear and tension)

F.4 References

American Society of Mechanical Engineers. 1994. *Code Case N-530, Provisions for Establishing Allowable Axial Compressive Membrane Stresses in the Cylindrical Walls of 0-15 psi Storage Tanks, Classes 2 and 3, Section III, Division 1*. ASME Boiler and Pressure Vessel Code, American Society of Mechanical Engineers, New York, New York.

American Society of Mechanical Engineers. 1995. *Code Case N-284-1, 1995, Metal Containment Shell Buckling Design Method, Class MC, Section III, Division 1*. ASME Boiler and Pressure Vessel Code, American Society of Mechanical Engineers, New York, New York.

American Society of Mechanical Engineers. 2004a. Section III, Division 1, Subsection NB-3113 Service Conditions. ASME Boiler and Pressure Vessel Code, American Society of Mechanical Engineers, New York.

American Society of Mechanical Engineers. 2004b. Section III, Division 1, Mandatory Appendix I, Design Stress Intensity Values, Allowable Stresses, Material Properties, and Design Fatigue Curves, Table I-9.1. ASME Boiler and Pressure Vessel Code, American Society of Mechanical Engineers, New York.

Bandyopadhyay K, A Cornell, C Costantino, R Kennedy, C Miller, and A Veletsos. 1995. *Seismic Design and Evaluation Guidelines for the Department of Energy High Level Waste Tanks and Appurtenances*. BNL 52361, Brookhaven National Laboratory. Associated Universities, Inc., Upton, New York.

CH2M HILL. 2004. *Operability/Technical Evaluation for DST Primary Tank Ventilation Systems. OE-04-0002*. CH2M HILL Hanford Group, Inc., Richland, Washington.

Julyk LJ and HH Ziada. 2002. *Assessment of Double-Shell Tank Internal Vacuum Specification Limits on Primary Tanks*. HNF-1838, Rev. 0-A, CH2M HILL Hanford Group, Inc., Richland, Washington.